PO Box 2345, Beijing 100023, China
Fax: +86-10-85381893
E-mail: wjg@wjgnet.com www.wjgnet.com

World J Gastroenterol 2004;10(9):1233-1237
World Journal of Gastroenterology
Copyright ©2004 by The WJG Press ISSN 1007-9327

• EDITORIAL •

A total of 484 articles published in *World Journal of Gastroenterology* are cited by 361 ISI-SCI covered journals distributed in 38 countries during 1998-2003

Lian-Sheng Ma, Bo-Rong Pan

Lian-Sheng Ma, Bo-Rong Pan, The WJG Press, PO Box 2345, Beijing 100023, China
Supported by the National Natural Science Foundation of China, No.30224801
Correspondence to: Lian-Sheng Ma, M.D., The WJG Press, PO Box 2345, Beijing 100023, China. wjg@wjgnet.com
Telephone: +86-10-85381901 **Fax:** +86-10-85381893
Received: 2004-03-20 **Accepted:** 2004-04-11

Abstract

Articles published in the *World Journal of Gastroenterology* (WJG) have been cited by 361 SCI covered journals, 44.59% of which are journals in the USA and 3.60% in China. Authors from 484 institutions have cited WJG, in which 22.58% of them are in the USA and 18.84% in China. The highest impact factor of SCI journals that have cited WJG is 28.740 (*Nature Medicine*), with 52.95% (n=170) of journals with an impact factor over 2.0. The total citation times of articles published in WJG during 1998-2003 were 484. The total citation times in 2003 were 2736 with 73.24% (2004) self-citation, 1486 in 2002 with 94.27% (1401) self-citation, 537 in 2001 with 92.92% (499) self-citation, 238 in 2000 with 92.43% (220) self-citation and 24 in 1999 with 33.33% (8) self-citation. Articles published in WJG in 2002 were cited 85 times by other SCI covered journals, and 82 articles were cited. The number was increased to 372 and 332 for articles published in 2003, respectively, with increase rates of 337.64% and 304.87%, respectively. Authors who have cited WJG are from 37 countries, and the journals that have cited WJG are from 21 countries. A total of 1 020 (57.46%) articles published in WJG were supported by international or national grants. Authors of WJG articles are from 40 countries. Articles published in issues 5-12 in 2003 have been downloaded 53 476 times online. In 2002, WJG was awarded a special grant from National Natural Science Foundation of China. Generally, the percentage of the self-citation times of articles published in WJG declined from 94.27% in 2002 to 73.24% in 2003. Meanwhile, article numbers and times cited by other SCI covered journals rose to 304.87% and 337.64% respectively. The above data suggested that the WJG underwent rapid development in 2003 with a significant increase in both numbers of cited articles and times of citation.

Ma LS, Pan BR. A total of 484 articles published in *World Journal of Gastroenterology* are cited by 361 ISI-SCI covered journals distributed in 38 countries during 1998-2003. *World J Gastroenterol* 2004; 10(9): 1233-1237
http://www.wjgnet.com/1007-9327/10/1233.asp

INTRODUCTION

World Journal of Gastroenterology (WJG ISSN-1007-9327) is an international academic journal in digestology published in China. The WJG was established in 1995 under the name of China National Journal of New Gastroenterology, and adapted its present title in 1998[1]. The WJG, now published semimonthly by the WJG Press, is a 210×297 mm-sized journal with 160 pages in each issue. The Journal is distributed by the Beijing Newspaper and Periodical Subscription and Distribution Bureau (Postal Issuance Code 82-261). In response to continuing growth in both basic and clinical studies on digestive diseases and the increasing demands for the international exchange in science and technology, the WJG will be published weekly from January 2005, with 160 pages in each issue. The publication dates are on the 7th, 14th, 21th and 28th of each month. Center for Information Analysis, Institute of Scientific and Technical Information of China conducted a general assessment on the SCI citation, source of manuscripts, and grant support of the articles published in the WJG during 1998-2004(issues 1-6), based on the information from ISI SCI, ISI JCR and Citation Report of Chinese Journals of Science and Technology. The assessment report is as follows.

CITATIONS OF ARTICLES PUBLISHED IN WJG BY SCI COVERED JOURNALS

Articles published in WJG have been cited 5 021 times, of which the total citation times in 2003 were 2 736 with 73.24% (2004) self-citation, 1 486 in 2002 with 94.27% (1 401) self-citation, 537 in 2001 with 92.92% (499) self-citation, 238 in 2000 with 92.43% (220) self-citation and 24 in 1999 with 33.33% (8) self-citation. Citations have been consistently increasing. However, the increase in self-citations is significantly lower than the increase in total citations (Figure 1).

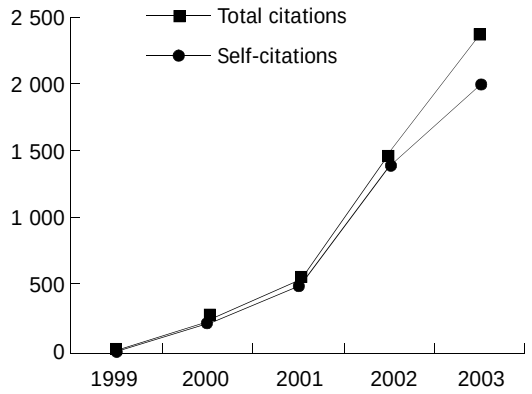

Figure 1 Increase in self-citations is significantly lower than the increase in total citations.

CHANGING TREND IN OVERALL TIMES AND NUMBERS OF ARTICLES PUBLISHED IN WJG CITED BY SCI COVERED JOURNALS

Articles published in WJG in 2002 were cited by other SCI covered journals 85 times, and 82 articles were cited. The numbers were increased to 372 and 332 for articles published in 2003, respectively, with an increase rate of 338% and 305%, respectively (Figure 2, Table 1).

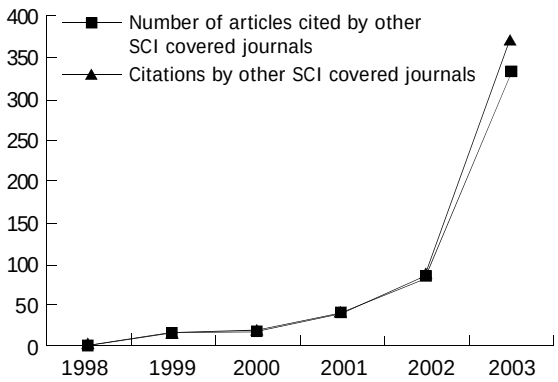

Figure 2 Changing trend in overall times and numbers of articles published in WJG between 1998 and 2003 cited by other SCI covered journals.

Table 1 Overall times and numbers of articles cited by other SCI covered journals

Year	2003	2002	2001	2000	1999	1998
Number of cited articles	332	82	38	17	16	0
Number of citations	372	85	38	18	16	0

GEOGRAPHIC DISTRIBUTION AND NUMBERS OF SCI COVERED JOURNALS THAT HAVE CITED ARTICLES PUBLISHED IN WJG

Overall, 361 SCI covered journals in 21 countries including 161 (44.59%) journals in the USA have cited articles published in WJG (Table 2).

Table 2 Geographic distribution and numbers of SCI covered journals that have cited articles published in WJG between 1998 and February 2004

List	Country	Number of journals
1	USA	161
2	UK	78
3	Netherlands	24
4	Germany	15
5	China	13
6	Switzerland	8
7	Denmark	7
8	France	7
9	Greece	6
10	Australia	5
11	Japan	5
12	Ireland	4
13	Poland	3
14	Italy	3
15	Spain	3
16	Norway	2
17	Brazil	2
18	South Korea	2
19	Singapore	1
20	India	1
21	Austria	1

Of the 361 journals, 10 journals' publishing countries are unknown.

IMPACT FACTORS OF SCI COVERED JOURNALS THAT HAVE CITED ARTICLES PUBLISHED IN WJG

Overall, 361 SCI covered journals have cited articles published in WJG between 1998 and February 2004 (Table 3). Of these journals 321 (88.92%) with an impact factor ranged from 0.160 (*Progress in Biochemistry and Biophysics*) to 28.740 (*Nutare Medicine*). The impact factor was not available for other 40 journals. The impact factors of the 321 journals are shown in Figure 3.

Table 3 Impact factors of SCI covered journals that have cited articles published in WJG

Impact factor	Number of journals (%)
20.699-28.740	4 (1.24)
10.321-18.772	12 (3.73)
6.073-9.825	20 (6.23)
5.095-5.991	14 (6.30)
4.039-4.974	19 (7.88)
3.008-3.991	46 (14.33)
2.013-2.980	55 (17.13)
1.000-1.990	78 (24.29)
0.160-0.996	73 (22.74)

GEOGRAPHIC DISTRIBUTION OF AUTHORS AND ARTICLES IN OTHER SCI COVERED JOURNALS THAT HAVE CITED ARTICLES PUBLISHED IN WJG

Overall, 484 articles by authors of SCI covered journals from 37 countries have cited articles published in WJG, of which 133 (22.58%) were from the USA and 111 (18.84%) from China (Figure 3 and Table 4).

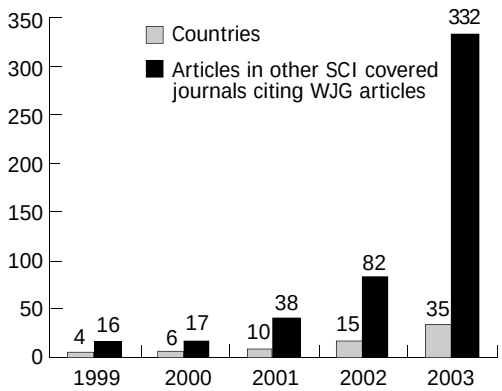

Figure 3 Geographic distribution of authors and articles in other SCI covered journals that have cited articles published in WJG.

Table 4 Geographic distribution of authors and articles in other SCI covered journals that have cited articles published in WJG

List	Country of authors	Number of articles
1	USA	133
2	China	111
3	Japan	38
4	Germany	35
5	UK	35
6	Italy	17
7	France	15
8	Australia	11
9	Spain	10
10	Sweden	8
11	Poland	7
12	South Korea	7
13	Netherlands	7
14	Canada	7
15	Belgium	5
16	Singapore	4
17	Austria	3

18	Greece	3
19	Hungary	3
20	Ireland	2
21	Brazil	2
22	Finland	2
23	Norway	2
24	Switzerland	2
25	Turkey	2
26	India	2
27	Czech Republic	1
28	Croatia	1
29	Slovakia	1
30	Argentina	1
31	Pakistan	1
32	Denmark	1
33	Cuba	1
34	Malaysia	1
35	South Africa	1
36	Thailand	1
37	New zealand	1

DISTRIBUTION OF INSTITUTIONS OF AUTHORS WHO HAVE CITED ARTICLES PUBLISHED IN WJG

The authors who have cited articles published in WJG between 1998 and 2003 are from 484 institutions, including the world famous universities and institutes such as Washington University, Yale University, Cornell University, University of Minnesota, Stanford University, University of California, National Institute of Health and University of London (Table 5).

CITING STATUS OF ARTICLES PUBLISHED IN WJG

Self-citations have been decreased from 6.19 per article published in WJG in 2002 to 3.16 in 2003 and 3.15 in February 2004. The rate decreased from 12.68% in 2001 to 8.84% and 8.61%, respectively, in 2003 and 2004 (Figure 4 and Table 6).

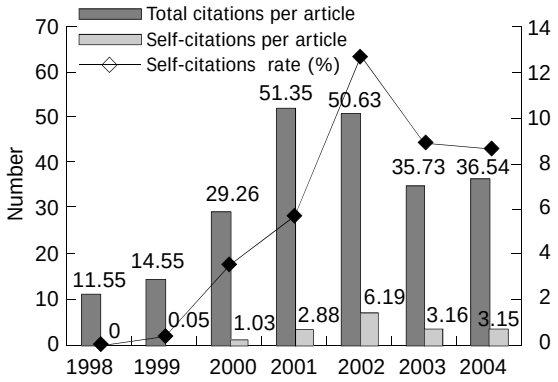

Figure 4 Citing status of articles published in WJG.

GEOGRAPHIC DISTRIBUTION AND GRANT INFORMATION OF MANUSCRIPTS ACCEPTED FOR PUBLICATION IN WJG

Of the 1775 articles published from 1998 to issue 6, 2004, 1020 (57.46%) were supported by various international and national research grants (Figures 5-7).

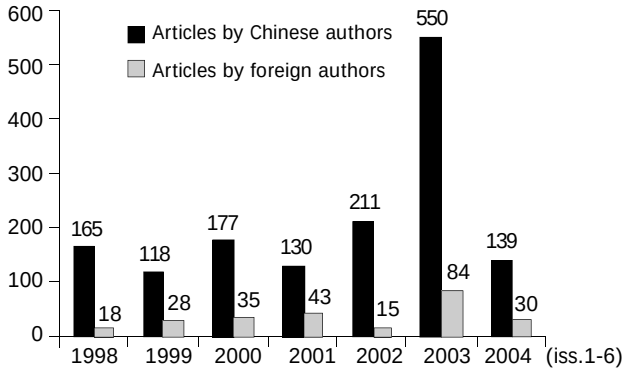

Figure 5 Geographic distribution of authors of manuscripts accepted for publication in WJG.

Table 5 Distribution of institutions of authors who have cited articles published in WJG

List	Country	Higher educational institutions	Research institutions	Medical institutions	Companies	Number of articles
1	USA	91	13	18	11	133
2	China	89	13	6	3	111
3	Japan	30	4	2	2	38
4	Germany	27	4	3	1	35
5	UK	24	2	3	4	33
6	Italy	13	3	0	1	17
7	France	5	5	5	0	15
8	Australia	7	1	3	0	11
9	Spain	7	1	2	0	10
10	Canada	2	2	1	2	7

Table 6 Citing status of articles published in WJG

Year	Volume	Issue	Articles	Total citations	Average citations per article	Self citations	Average self citation per article	Self citation rate (%)
1998	4	1-6	183	2 115	11.55	0	0	0
1999	5	1-6	146	2 125	14.55	8	0.05	0.37
2000	6	1-6	212	6 205	29.26	220	1.03	3.54
2001	7	1-6	173	8 884	51.35	499	2.88	5.61
2002	8	1-6	226	11 444	50.63	1 401	6.19	12.68
2003	9	1-12	634	22 657	35.73	2 004	3.16	8.84
2004	10	1-6	201	7 309	36.54	630	3.15	8.61

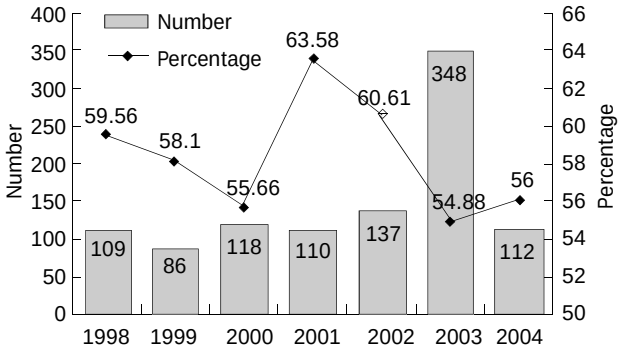

Figure 6 Numbers and percentage of articles with research grants published in WJG.

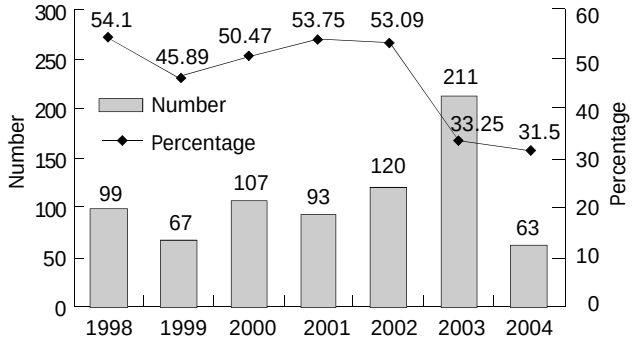

Figure 7 Number and percentage of the National Natural Science Foundation of China articles supported by published in WJG.

Table 7 Online visiting and downloading of articles published in WJG

Total articles	Articles visited	Articles downloaded	Total visits	Total downloads	Average visits per article	Average downloads per article
603	582	582	127 760	64 145	219.51	110.21

Table 8 Geographic distribution and numbers of authors of articles published in WJG

List	Country	Number
1	China	8 232
2	Japan	198
3	USA	190
4	Germany	125
5	Turkey	116
6	Italy	106
7	UK	69
8	Singapore	50
9	South Korea	39
10	Hungary	35
11	Australia	32
12	Poland	29
13	Belgium	23
14	India	21
15	South africa	20
16	Netherlands	17
17	Brazil	16
18	Greece	16
19	Sweden	15
20	Finland	14
21	Thailand	14
22	Canada	13
23	Iran	13
24	Pakistan	11
25	Yugoslavia	11
26	Spain	11
27	Israel	11
28	Argentina	9
29	Russia	9
30	Croatia	8
31	Ireland	6
32	Saudi Arabia	5
33	France	4
34	Norway	4
35	Switzerland	3
36	New Zealand	2
37	Egypt	1
38	Estonia	1
39	Denmark	1
40	Dominica	1

ONLINE VISITING AND DOWNLOADING OF ARTICLES PUBLISHED IN WJG

A total of 436 articles published in issues 5-12, 2003 have been downloaded online with a total downloading number of 53 476 times. One article has been downloaded 2 255 times[2] (Table 7).

GEOGRAPHIC DISTRIBUTION OF AUTHORS OF ARTICLES PUBLISHED IN WJG

Authors of WJG are from 40 countries (Table 8).

HONORS AWARDED TO WJG

The WJG is nationally recognized as a core journal in national natural science and an outstanding journal in science and technology, with an honor of the 2nd National Journal Award, and was listed as one of the 100 most important journals in China. In 2001, it was selected into the China Journal Square consisting of “200” journals. It was awarded a specific project grant as one of the key academic journals by the National Natural Science Foundation of China in 2002 (Project Grant No. 30224801).

OVERALL ASSESSMENT COMMENTS

- Total citation times of articles published in WJG in January and February 2004 by SCI covered journals were 560, in which self-citation rate was 77.67% (435). The total citation times in 2003 were 2736 with 73.24% (2004) self-citation, 1486 in 2002 with 94.27% (1401) self-citation, 537 in 2001 with 92.92% (499) self-citation, 238 in 2000 with 92.43% (220) self-citation and 42 in 1999 with 33.33% (8) self-citation. No data were available in 1998.
- Article number and times cited by other SCI covered journals were 82 and 85 in 2002, 332 and 372 in 2003, and 104 and 125 in January and February 2004, respectively.
- Overall, 361 SCI covered journals in 21 countries including 161 (44.59%) journals in the USA have cited articles published in WJG.
- Journals that have cited WJG include 11 SCI covered journals with a high impact factor; i.e. *Nature Medicine* (IF 28.740), *Cell* (IF 27.254), *Nature Reviews Neuroscience* (IF 24.047), *Nature Cell Biology* (IF 20.699), *Gene and Development* (IF 18.772), *Lancet* (IF 15.397), *Nature Neuroscience* (IF 14.857), *Neuron* (IF 13.846), *Nature Reviews*

Cancer (IF 13.625), *Gastroenterology* (IF 13.440) and *Hepatology* (IF 9.825). The impact factors of the journals that have cited WJG are as follows: 20.699-28.740 (4, 1.24%), 10.321-18.772 (12, 3.73%), 6.073-9.825 (20, 6.23%), 5.095-5.991 (14, 6.30%), 4.039-4.974 (19, 7.88%), 3.008-3.991 (46, 14.33%), 2.013-2.980 (55, 17.13%), 1.000-1.990 (78, 24.29%) and 0.160-0.996 (73, 22.74%).

- Overall, 484 articles by authors of SCI covered journals from 37 countries have cited articles published in WJG; 133 (22.58%) from the USA and 111 (18.84%) from China.
- The authors who have cited WJG are from 484 research institutions, including the world famous universities and institutes, such as Washington University School of Medicine, Yale University, Cornell University, University of Minnesota, Stanford University Center of Medicine, University of California at San Francisco, National Institute of Health and Imperial College, University of London.
- Self-citations have decreased from 6.19 per article published in WJG in 2002 to 3.16 in 2003 and 3.15 in February 2004.
- Of the 1 775 articles published from 1998 to issue 6, 2004, 1 020 (57.46%) were supported by various international and national research grants.
- Authors of WJG are from 40 countries.
- A total of 436 articles published in issues 5-12, 2003 have been downloaded online with a total downloading number of 53 476 times. One article has been downloaded 2 255 times[2].
- In 2002, WJG was awarded a special grant (No. 30224801) from National Natural Science Foundation of China.

In conclusion, WJG has been established its position as a regional and international English journal in gastroenterology, with increasing international influence. Despite high self citations over the past years, it appears that both self citations and self citation rate are rapidly decreasing.

REFERENCES

1 **Ma LS**, Pan BR, Ma JY, Xu JY, Wu XN, Wang XL, Lu HM, Xia HHX, Liu HX, Zhang JZ, Su Q, Ren SY, Zhu L, Zhu LH, Lu YY. Towards a higher international standard - *World Journal of Gastroenterology* will be published semimonthly in 2004. *World J Gastroenterol* 2004; **10**: 1-4

2 **Wang QC**, Nie QH, Feng ZH. RNA interference: Antiviral weapon and beyond. *World J Gastroenterol* 2003; **9**: 1657-1661

Edited by Xia HHX, Wang XL and Zhang JZ **Proofread by** Xu FM

PO Box 2345, Beijing 100023, China
Fax: +86-10-85381893
E-mail: wjg@wjgnet.com www.wjgnet.com

World J Gastroenterol 2004;10(9):1238-1239
World Journal of Gastroenterology
Copyright ©2004 by The WJG Press ISSN 1007-9327

• EDITORIAL •

Wireless capsule video endoscopy: Three years of experience

Rami Eliakim

Rami Eliakim, Department of Gastroenterology, Rambam Medical Center, Technion School of Medicine, Haifa, Israel
Correspondence to: Rami Eliakim, M.D., Department of Gastroenterology, Rambam Medical Center, Bat Galim, Haifa, PO Box 9602, Israel 31096. r_eliakim@rambam.health.gov.il
Telephone: +972-4-8542504 **Fax:** +972-4-8543058
Received: 2004-03-06 **Accepted:** 2004-04-01

Abstract

AIM: To review and summerize the current literatue regarding M2A wireless capsule endoscopy.

METHODS: Peer reviewed publications regarding the use of capsule endoscopy as well as our personal experience were reviewed.

RESULTS: Review of the literature clearly showed that capsule endoscopy was superior to enteroscopy, small bowel follow through and computerized tomography in patients with obscure gastrointestinal bleeding, iron deficiency anemia, or suspected Crohn's disease. It was very sensitive for the diagnosis of small bowel tumors and for survailance of small bowel pathology in patients with Gardner syndrome or familial adenomatous polyposis syndrome. Its role in celiac disease and in patients with known Crohn's disease was currently being investigated.

CONCLUSION: Capsule video endoscopy is a superior and more sensitive diagnostic tool than barium follow through, enteroscopy and entero- CT in establishing the diagnosis of many small bowel pathologies.

Eliakim R. Wireless capsule video endoscopy: Three years of experience. *World J Gastroenterol* 2004; 10(9): 1238-1239
http://www.wjgnet.com/1007-9327/10/1238.asp

INTRODUCTION

The M2A video capsule endoscope (CE) (Given Imaging LTd; Yokneam,Israel) is a wireless capsule (11 mm×27 mm) comprised of a light source, lens, CMOS imager, battery and a wireless transmitter. The slippery out side coating of the capsule allows easy ingestion and prevents adhesion of intestinal contents, while the capsule moves via peristalsis from mouth to anus. The battery provides 7-8 h of work in which the capsule photographs 2 images per second (between 50 000-60 000 images all together), which are transmitted to a recorder which is worn on the belt. The recorder is downloaded into a computer and seen as a continous video film. Since its development additional support systems have been added- a localization system, a blood detector and a double picture viewer. All ment to assist the interpretor of the film and to shorten the reviewing period.

INDICATIONS

The full range of indications for CE became apperant with time. The initial device was invented to address a need for a better diagnostic tool for small bowel pathologies.

Obscure gastrointestinal bleeding

The most obvious and the first indication to be tested was obscure gastrointestinal bleeding (OGIB), which occurred in 5-10% of patients with any type of gastrointestinal (GI) bleeding. Several peer reviewed articles and many abstracts have compared the diagnostic yield of CE to push enteroscopy and other modalities in patients with OGIB[1-4]. The added diagnostic yield of enteroscopy was in the range of 25-30%, while that of CE was significantly better (50-67%). This led Cave to propose an algorithm in which the first method to evaluate the small bowel in a patient with gastrointestinal bleeding with negative gastroscopy and colonoscopy would be CE, and then according to its results, the evaluation was continued with either push enteroscopy, angiography or intra-operative enteroscopy[5]. Cave suggested that the closer the study was performed to the time of actual bleeding, the greater the diagnostic yield of CE.

Crohn's disease

The 2nd obvious indication was in patients with suspected Crohn's disease. Three peer reviewed studies published in journal and some more in abstract form demonstrated the superiority of CE compared to small bowel follow through and entero CT in these patients[6-8]. The diagnostic yield of CE in these patients ranged between 43-71%, significantly better than small bowel follow through or entero CT (<30%). Moreover CE diagnosed Crohn's disease in 6-9% of patients that had OGIB[9]. In patients with undetermined colitis the use of CE changed the diagnosis into Crohn's disease in 50% of patients (5/10)[9].

Costamagna *et al.* compared CE and small bowel radiographs in patients with any suspected small bowel disease, another indication for CE[10]. CE was diagnostic in 45% patients, and suspicious in another 40% patients, while X- ray was diagnostic in only 20% patients.

Other indications for CE

Diagnosis of celiac disease, extent of Crohn's disease, GI tumors, NSAID induced small bowel damage and survailance of polyposis syndromes were currently investigated.

We have recently looked at CE in real life. We looked at the charts of the first 160 patients reffered for CE by various doctors to 4 centers in Israel. We found that CE was of value in patients with OGIB (65%), Crohn's disease (55%) and chronic diarrhea (100%), but not in patients with chronic abdominal pain.

Future probable indications

These indications may include monitoring of small bowel damage due to drugs and chemicals (NSAID, *etc.*), monitoring of mucosal healing after various treatments (Crohn's for example), assessing the extent of diseases (Crohn's, celiac) and monitoring/survailance of upper or lower GI damage (esophagitis, Barrett's, polyps).

CONTRAINDICATIONS

The only definite contraindication for CE was a patient with a history of intestinal obstruction or known stricture, or a patient who was a non surgical candidate.

Severe motility problems, or swallowing abnormalities could also preclude the use of CE. Initialy patients with pacemakers were excluded from CE trials, but recent data mostly in abstract form, revealed that CE could be safely performed in patients with pacemakers.

COMPLICATIONS

The major complication with CE was capsule retention or non natural excretion (NNE) which was usually proximal to a stricture. This happened many times despite normal small bowel X-rays. History of NSAID usage, ischemic bowel event or known Crohn' s disease, carried higher risk for NNE. NNE that neccesitated surgery occurred in less than 1% of all patients and in 1.25% of patients with Crohn' s disease[9]. Usually, there were no clinical signs or symptoms and NNE was found when doing a plain abdominal film. Retrieval of the capsule and ressection of narrowed segment via surgery, usually resolved the medical problem which was detected by the retained capsule.

CONCLUSIONS

M2A CE is a safe, valuable, non-invasive, innovative tool for the diagnosis and management of small bowel lesions like OGIB, Crohn' s disease, chronic diarrhea and probably other small bowel diseases.

Newer versions of CE softwear allow us to get better localization and blood detection. Advanced versions will allow us to get therapeutic modalities and a shorter reading time.

REFERENCES

1 **Lewis BS**, Swain P. Capsule endoscopy in the evaluation of patients with suspected small intestinal bleeding: Results of a pilot study. *Gastrointest Endosc* 2002; **56**: 349-354

2 **Scapa E**, Jacob HJ, Lewkowicz S, Migdal M, Gat D, Glukhovsky A, Guttman N, Fireman Z. Initial experience of wireless capsule endoscopy for evaluating occult gastrointestinal bleeding and suspected small bowel pathology. *Amer J Gastroenterol* 2002; **97**:2776-2779

3 **Ell C**, Remke S, May A, Helou L, Henrich R, Mayer G. The first prospective controlled trial comparing wireless capsule endoscopy with push enteroscopy in chronic gastrointestinal bleeding. *Endoscopy* 2002; **34**: 685-689

4 **Saurin JC**, Delvaux M, Gaudin JL, Fassler I, Villarejo J, Vahedi K, Bitoun A, Canard JM, Souquet JC, Ponchon T, Florent C, Gay G. Diagnostic value of endoscopic capsule in patients with obscure digestive bleeding: Blinded comparison with video push-enteroscopy. *Endoscopy* 2003; **35**: 576-584

5 **Cave DR**. Wireless video capsule endoscopy. *Clin Perspectives Gastroenterol* 2002; **5**: 203-207

6 **Eliakim R**, Fischer D, Suissa A, Yassin K, Katz D, Migdal M, Guttman N. Wireless capsule video endoscopy is a superior diagnostic tool compared to barium folloew through and CT in patients with suspectrd Crohn's disease. *Europ J Gastroenterol Hepatol* 2003; **15**: 363-367

7 **Fireman Z**, Mahajna E, Broude E, Shapiro M, Fich L, Sternberg A, Kopelman Y, Scapa E. Diagnosing small bowel Crohn's disease with wireless capsule endoscopy. *Gut* 2003; **52**: 390-392

8 **Herrerias JM**, Caunedo A, Rodriguez-Tellez M, Pellicer F, Herrerias JM Jr. Capsule endoscopy in patients with suspected Crohn's disese in negative endoscopy. *Endoscopy* 2003; **35**: 1-5

9 **Eliakim R**, Adler SN. Capsule endoscopy in Crohn's disease – the European experience. *Gastrointest Endoscopy Clin N Amer* 2004; **14**: 129-137

10 **Costamagna G**, Shah SK, Riccioni ME, Foschia F, Mutignani M, Perri V. A prospective trial comparing small bowel radiographs and video capsule endoscopy for suspected small bowel disease. *Gastroenterology* 2002; **123**: 999-1005

Edited by Xu XQ and Wang XL **Proofread by** Xu FM

PO Box 2345, Beijing 100023, China
Fax: +86-10-85381893
E-mail: wjg@wjgnet.com www.wjgnet.com

World J Gastroenterol 2004;10(9):1240-1245
World Journal of Gastroenterology
Copyright ©2004 by The WJG Press ISSN 1007-9327

• GASTRIC CANCER •

GSTT1, *GSTM1* and *CYP2E1* genetic polymorphisms in gastric cancer and chronic gastritis in a Brazilian population

Jucimara Colombo, Andréa Regina Baptista Rossit, Alaor Caetano, Aldenis Albaneze Borim, Durval Wornrath, Ana Elizabete Silva

Jucimara Colombo, Ana Elizabete Silva, Departamento de Biologia, UNESP-Campus de São José do Rio Preto-SP, Brazil
Andréa Regina Baptista Rossit, Departamento de Doenças Dermatológicas, Infecciosas e Parasitárias, Faculdade de Medicina, FAMERP, São José do Rio Preto, SP, Brazil
Alaor Caetano, Aldenis Albaneze Borim, Hospital de Base, Faculdade de Medicina, FAMERP, São José do Rio Preto, SP, Brazil
Durval Wohnrath, Fundação Pio XII, Barretos, Brazil
Supported by the Brazilian Agency CAPES
Correspondence to: Ana Elizabete Silva, Departamento de Biologia, UNESP - Campus de São José do Rio Preto, Rua Cristovão Colombo, 2265, 15054-000 - São José do Rio Preto, SP-Brazil. anabete@bio.ibilce.unesp.br
Telephone: +55-17-2212384 **Fax:** +55-17-2212390
Received: 2003-09-23 **Accepted:** 2003-12-30

Abstract

AIM: To test the hypothesis that, in the Southeastern Brazilian population, the *GSTT1*, *GSTM1* and *CYP2E1* polymorphisms and putative risk factors are associated with an increased risk for gastric cancer.

METHODS: We conducted a study on 100 cases of gastric cancer (GC), 100 cases of chronic gastritis (CG), and 150 controls (C). Deletion of the *GSTT1* and *GSTM1* genes was assessed by multiplex PCR. *CYP2E1/Pst*I genotyping was performed using a PCR-RFLP assay.

RESULTS: No relationship between *GSTT1/GSTM1* deletion and the *c1/c2* genotype of *CYP2E1* was observed among the three groups. However, a significant difference between CG and C was observed, due to a greater number of *GSTT1/GSTM1* positive genotypes in the CG group. The *GSTT1* null genotype occurred more frequently in Negroid subjects, and the *GSTM1* null genotype in Caucasians, while the *GSTM1* positive genotype was observed mainly in individuals with chronic gastritis infected with *H pylori*.

CONCLUSION: Our findings indicate that there is no obvious relationship between the *GSTT1*, *GSTM1* and *CYP2E1* polymorphisms and gastric cancer.

Colombo J, Rossit ARB, Caetano A, Borim AA, Wornrath D, Silva AE. *GSTT1*, *GSTM1* and *CYP2E1* genetic polymorphisms in gastric cancer and chronic gastritis in a Brazilian population. *World J Gastroenterol* 2004; 10(9): 1240-1245
http://www.wjgnet.com/1007-9327/10/1240.asp

INTRODUCTION

In Brazil, gastric cancer occupies the fifth position, with an estimates of 20 640 new cases and 11 145 deaths in 2003, as a consequence of late diagnosis, and also of its high recurrence rate[1]. Gastric carcinogenesis is a multi-step process, involving both genetic and environmental factors[2]. Among the latter, the most outstanding are dietary factors[3], smoking[4]; drinking[5]; *Helicobacter pylori* infection[6], and the occurrence of previous gastric injuries[7]. Correa[8] and Stemmermann[9] suggested, in separate studies, a general hypothesis of pre-cancerous sequences for gastric carcinogenesis, especially for the intestinal types, namely superficial gastritis, chronic atrophic gastritis, intestinal metaplasia, dysplasia, and cancer.

Over the last decades, several studies have revealed the participation of polymorphisms in metabolic and DNA repair enzymes, that might confer different degrees of susceptibility to cancer. Among these metabolic enzyme polymorphisms, the most outstanding are those of cytochrome P-450 (CYPs), glutathione-S-transferases (GSTs), and N-acetyltransferases (NATs)[10-12].

Concerning the superfamily of metabolic enzymes, both *CYP2E1* gene, a member of the cytochrome P-450 superfamily, and the *GSTT1* and *GSTM1* genes, that catalyze the conjugation reaction of glutathione with electrophilic compounds, exhibit polymorphisms which have been considered as potentially important modifiers of the individual risk for environmentally induced cancers, including cancer of stomach[13-17]. Subjects with null *GSTT1* and *GSTM1* have a decreased capability of detoxifying some carcinogens, among wich N-nitrous compounds are involved in stomach carcinogenesis[14].

Previous studies have shown inconclusive or controversial findings on associations between polymorphism of these genes and cancer susceptibility, due to the different types of cancer investigated and the diverse ethnic origin of the populations studied. Increased risk for oral[18], nasopharyngeal[19], and pulmonary[20] cancer was observed in carriers of the rare allele *CYP2E1*, while an increased risk for esophageal cancer was observed in carriers of the common allele[21]. On the other hand, *GSTT1* and *GSTM1* null genotypes have been linked to an increased risk for cancer of the lung, bladder and colon, and other specific sites[11,17].

The relationship between *GSTT1*, *GSTM1* and *CYP2E1* gene polymorphisms and the risk for gastric cancer is not obvious. Many investigations were conducted on Asian populations[22-36]. The Brazilian population is characterized by heterogeneous ethnic groups, emphasizing the need to investigate the frequency of these metabolizing genes and their association with gastric cancer.

We performed a case-control study to evaluate the association between the *GSTT1*, *GSTM1* and *CYP2E1* polymorphisms in patients from the Brazilian Southeast with gastric cancer or chronic gastritis, a lesion that increases the risk for gastric cancer by 10%[37]. We also explored the potential interactions between the *GSTT1*, *GSTM1* and *CYP2E1* polymorphisms and demographic risk factors.

MATERIALS AND METHODS

Subjects

We conducted a simultaneous case-control study for gastric cancer and chronic gastritis. The case groups comprised 100 patients with histopathologically confirmed diagnosis of gastric

adenocarcinoma (73 men and 27 women) with a mean age of 60 years (ranging from 28 to 93 years), and 100 patients with histopathologically confirmed diagnosis of chronic gastritis (54 men and 46 women) with a mean age of 53 years (ranging from 19 to 86 years), respectively. These subjects were recruited from the "Hospital de Base", São José do Rio Preto, SP, and from the Pio XII Foundation, Barretos, SP, Brazil. The pathological diagnoses of gastric cancer and chronic gastritis were made according to criteria proposed by Lauren[38] and the Sidney classification[39], respectively. *H pylori* infection was histologically established by Giemsa staining. The control group consisted of 150 healthy volunteers (90 men and 60 women), with a mean age of 54 years (ranging from 20 to 93 years), with no previous history of gastric disease, matched to the patients with respect to age, gender and ethnicity. Most controls were blood donors. Epidemiological data on the study population were collected through a standard interviewer-administered questionnaire, which included questions about current and past occupation, ethnicity, life-long smoking habits and alcohol consumption, and family history of cancer.

The human subject protocol was approved by the Research Ethics Committee of the IBILCE-UNESP, and written informed consent was obtained from all subjects.

Blood sampling and DNA extraction

Whole blood was collected and put into EDTA-coated tubes. Lymphocytes were isolated, transferred to tubes, and assigned a unique identifier code. DNA was then extracted using a non-organic extraction procedure, and stored at -20 ℃ until use for genotyping[40].

Cenotype analysis

The *GSTT1* and *GSTM1* genes were determined simultaneously in a single assay, using a PCR multiplex protocol, where part of exon 7 of the constitutional gene *CYP1A1* was co-amplified as an internal control.

PCR was performed in 25 μL reaction buffer containing 0.5 mmol/L of dNTPs, 2.0 mmol/L of $MgCl_2$, 12.5 pmol of each primer, about 150 ng DNA, and 1.25 U of thermostable Taq DNA polymerase, using a programmable thermocycler. The primers used for *GSTM1* were 5'- GAACTCCCTGAAAAGCTA AGC and 5'- GTTGGGGCTCAAATATACGGTGG. The primers used for *GSTT1* were 5'-TTCCTTACTGGTCCTCACATCTC and 5' TCACCGGATCAGGCCAGCA. The primers used for *CYP1A1* were 5' GAACTGCCACTTCAGCTGTCT and 5' CAGCTGCATT TGGAAGTGCTC.

PCR conditions were 94 ℃ for 5 min, followed by 40 denaturation cycles of 2 min at 94 ℃, 1 min annealing at 59 ℃, and 1 min extension at 72 ℃. The PCR products were then analyzed by electrophoresis on ethidium bromide-stained 20 g/L agarose gel.

The presence or absence of *GSTT1* and *GSTM1* genes was detected by the presence or absence of a band at 480 bp and at 215 bp, respectively. A band at 312 bp (CYP1A1) was documented successful amplification[41].

This technique could not distinguish between heterozygote and homozygote positive genotypes, but it could conclusively identify the null genotypes.

PCR-RFLP was performed to investigate the *CYP2E1*c2* allele. PCR was used to amplify the transcription regulation region of *CYP2E1* that includes the *Pst*I enzyme recognition site. PCR was performed in 25 μL reaction buffer containing 0.28 mmol/L of dNTPs, 1.5 mmol/L of $MgCl_2$, 10 pmol of each primer, about 200 ng DNA, and 1.5 units of thermostable Taq DNA polymerase, using a programmable thermocycler. The *CYP2E1* primers were 5' CCAGTCGACTCTACATTGTCA and 5' TTCATTCTGTCTTCTAACTGG. After 5 min of pretreatment at 94 ℃, 35 denaturation cycles of 1 min at 94 ℃, 30 s annealing at 60 ℃, and 1 min extension at 72 ℃ were performed. After amplification, the PCR products were subjected to restriction digestion by enzyme *Pst*I for 16 h at 37 ℃. The PCR-RFLP fragments were then analyzed by electrophoresis on ethidium bromide-stained 20 g/L agarose gel[42].

All the experiments included positive and negative controls for each studied polymorphism.

Statistical analysis

Statistical analyses were performed using Statidisk, Statistica, Minitab Release 10.1 computer software programs. The probability level (*P*) of 0.05 was used as significance criterion . Student' s *t*-test and ANOVA *F*-test tests were used to compare continuous variables between the groups. Chi-square test or Fisher' s exact test was utilized as appropriate to compare the groups with regard to genotype frequencies and putative risk factors such as gender, ethnicity, smoking, drinking, *H pylori* infection, occupational pesticide exposure, and histological type of adenocarcinoma. In order to investigate gene-environment interactions, we also calculated the odds ratios (OR) and their 95% confidence intervals (95% CI), according to combinations of the *GSTT1*, *GSTM1* and *CYP2E1* polymorphisms with putative risk factors.

RESULTS

Figure 1 (PCR) and Figure 2 (PCR-PFLP) show the genotype analysis results. Table 1 shows the frequency distributions of the *GSTT1* and *GSTM1* genotypes among the groups. With respect to the genotype frequencies, considering the combinations between the *GSTT1*/*GSTM1* genes, no statistically significant differences were observed between the gastric cancer and chronic gastritis patients (*P*=0.189), nor between gastric cancer patients and controls (*P*=0.448). However, a significant difference (*P*=0.048) was observed between chronic gastritis patients and controls, due to a higher frequency of combination *GSTT1*/*GSTM1* positive genotypes in the chronic gastritis patients.

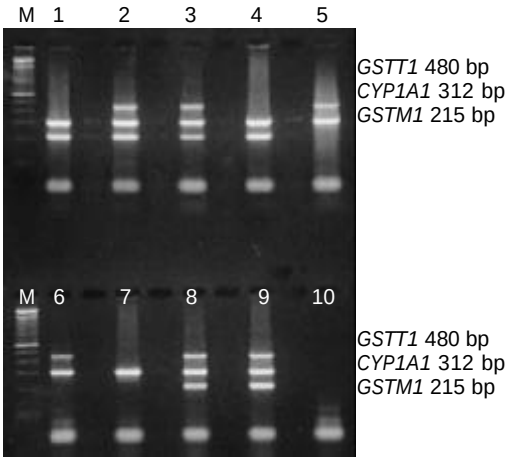

Figure 1 Polymerase chain reaction of the *GSTT1* and *GSTM1* genes. Lanes M: molecular weight maker; Lanes 1 and 4 : patients homozygously null for *GSTT1*; Lanes 2, 3, 8 and 9: patients with positive *GSTT1* and *GSTM1* genotypes; Lanes 5 and 6: patients homozygously null for *GSTM1*; Lane 7: patient homozygously null for *GSTT1*and *GSTM1*; Lane 10 negative control.

The associations of the different genotypes with demographic risk factors (gender, ethnicity, smoking, drinking, pesticide-exposure, *H pylori* infection and histological type of gastric cancer) in each group evidenced that the *GSTT1* null genotype occurred more frequently in Negroid controls (*P*=0.003), and

Table 1 *GSTT1* and *GSTM1* genotype frequencies among gastric cancer (GC) and chronic gastritis (CG) patients and controls (C)

Groups	*n*	*GSTT1* Null (%)	*GSTM1* Null (%)	*GSTT1/GSTM1*			
				+/+ (%)	+/0 (%)	0/+ (%)	0/0 (%)
GC	100	17 (17.0)	47 (47.0)	43 (43.0)	40 (40.0)	10 (10.0)	7 (7.0)
CG	100	12 (12.0)	38 (38.0)	57 (57.0)	31 (31.0)	5 (5.0)	7 (7.0)
C	150	28 (18.6)	62 (41.3)	64 (42.7)	58 (38.7)	24 (16.0)	4 (2.6)

+/+=presence of *GSTT1* and *GSTM1*, +/0=presence of *GSTT1* and absence of *GSTM1*, 0/+=absence of *GSTT1* and presence of *GSTM1*, 0/0=absence of *GSTT1* and *GSTM1*.

Table 2 Associations of *GSTT1* and *GSTM1* genotypes with demographic risk factors in gastric cancer (GC) and chronic gastritis (CG) cases and controls (C)

Groups	Categories	Genotype			
		GSTM1 positive (%)	*GSTM1* null (%)	*GSTT1* positive (%)	*GSTT1* null (%)
C	Ethnicity				
	Caucasian	75 (55.6)	60 (44.4)	114 (84.4)	21 (15.6)
	Negroid	13 (86.7)	2 (13.3)	8 (53.3)	7 (46.7)
		P=0.020		*P*=0.003	
GC	Ethnicity				
	Caucasian	42 (46.3)	45 (51.7)	73 (83.9)	14 (16.1)
	Negroid	11 (84.6)	2 (15.4)	10 (76.9)	3 (23.1)
		P=0.017		*P*=0.690	
CG	*H pylori* Infection				
	No	43 (71.7%)	17 (28.3%)	54 (90.0%)	6 (10.0%)
	Yes	19 (48.7%)	20 (51.3%)	34 (87.2%)	5 (12.8%)
		P=0.032		*P*=0.748	

the *GSTM1* null genotype in Caucasian controls (*P*=0.020) and gastric cancer patients (*P*=0.017). The *GSTM1* positive genotype was observed mainly in chronic gastritis cases with *H pylori* infection (*P*=0.032) (Table 2).

The frequencies of the *GSTT1* and *GSTM1* polymorphisms were compared among the groups by χ^2 tests and estimated OR (data not shown), according to the pattern of the gastric cancer risk factors represented by gender, ethnicity, smoking, drinking, pesticide-exposure, and *H pylori* infection. Thus, comparing the GC and CG groups, multivariate analysis revealed that smoking was not associated with increased OR's for stomach cancer in the *GSTM1* positive subjects (1.54, 95% CI=0.71-3.33), whereas it was associated with elevated OR's in the *GSTM1* null subjects (2.7, 95% CI=1.04-7.14).

Table 3 shows the frequency distributions of *CYP2E1* genotypes among the groups. The frequencies of *CYP2E1* (*c1/c2*) variant genotypes in the gastric cancer, chronic gastritis and control groups were 11.0%, 9.0% and 10.7%, respectively. The rare homozygous genotype (*c2/c2*) was not found. The results showed no statistical difference (*P*=0.878) between the groups, nor was there any relationship with the investigated etiological factors, according to the χ^2 test and estimated OR's (data not shown).

Table 3 *CYP2E1* genotype frequencies among gastric cancer (GC) and chronic gastritis (CG) patients and controls (C)

Groups	Genotype	
	c1/c1 (%)	*c1/c2* (%)
GC	89 (89.0)	11 (11.0)
CG	91 (91.0)	9 (9.0)
C	134 (89.3)	16 (10.7)

c1/c1=homozygote for the common allele, *c1/c2*=heterozygote.

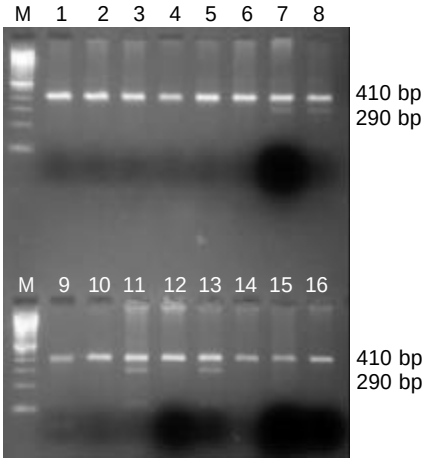

Figure 2 PCR-RFLP of *CYP2E1*/PstI. Lanes M: molecular weight maker; Lanes 1, 2, 3, 4, 5, 6, 10 ,12, 14, 15 and 16 patients homozygote for the common allele of *CYP2E1/Pst*I; Lanes 7, 8, 9, 11 and 13 heterozygote for the rare allele of *CYP2E1/Pst*I.

DISCUSSION

Interindividual differences in the cellular mechanisms of activation and detoxification of carcinogenic chemicals could confer different degrees of susceptibility to cancer[43]. However, the results have not always been consistent, due to a number of possible reasons for anomalous findings, such as interaction between environmental and genetic factors, which is a complicating factor that needs to be taken into account[32].

GSTT1, *GSTM1* and *CYP2E1* genetic polymorphisms have shown pronounced interethnic variations[10]. Brazil is a large country with a very heterogeneous population, resulting from the cross-mating of the native population with immigrants from

Europe, Africa and Asia. Therefore, descriptive studies of the frequencies of genetic polymorphisms in the Brazilian population could be useful in verifing genetic variability in relation to xenobiotic metabolism, since this variability may influence cancer susceptibility. This is the first study that simultaneously evaluated the *GSTT1*, *GSTM1* and *CYP2E1* polymorphisms in Brazilian patients with gastric cancer and chronic gastritis.

The *GSTM1* genotype was absent in 35-65% of individuals[44], while *GSTT1* was deleted in 10-65% of the human population[17]. The prevalence of the *CYP2E1 c2* allele was shown to be 2-8% in both Caucasians and African Americans[13], but higher in Asian populations, ranging from 17 to 26%[45].

The frequencies of *GSTT1* (18.6%) and *GSTM1* (41.3%) null genotypes and the CYP2E21/*Pst*I (10.7%) polymorphism observed in the control group were not different from other studies in Brazilian populations[46-49]. We showed that the frequency of the *GSTT1* null genotype was higher in Negroid subjects, and that the *GSTM1* null genotype was higher in Caucasians. Other studies described similar results in Brazilian[46,50] and also in American populations[51].

Although studies of the *GSTT1* and *GSTM1* polymorphisms were performed previously, their association with gastric cancer susceptibility has not been established. Most of them showed no association between the *GSTT1* null genotype and risk for gastric cancer[25,32,36,52,53]. However, two others suggested that the *GSTT1* null genotype might confer an increased risk for gastric cancer[39,54].

The correlation between the *GSTM1* null genotype and gastric cancer appeared to be more consistent[22,25,27,28,30,53]. On the other hand, other authors failed to demonstrate any statistically significant difference in the *GSTM1* polymorphism distribution of gastric cancer patients and controls[24,26,32,36,52,55,56].

Several case-control studies also failed to find a significant association between the *CYP2E1*/*Pst*I polymorphism and gastric cancer[23,24,26,34]. However, while Nishimoto *et al*.[51] observed that the rare variant *c2/c2* was associated with a reduced risk for gastric cancer in non-Japanese Brazilians, Wu *et al*.[35] observed that the distribution of the *c2/c2* genotype, detected by *Pst*I or *Rsa*I digestion, differed significantly between gastric cancer cases and controls. These authors suggested that the *CYP2E1* genotype could be a determinant of gastric cancer. The reason for these inconsistent results is not clear, but one problem is the lack of sufficient investigation of the gene-environment interactions. Thus, Cai *et al*.[31] and Gao *et al*.[33] suggested that gene-environment interactions between the *CYP2E1* polymorphism and smoking might have the potential to alter the susceptibility for cancer development in the stomach.

Our current data corroborate the hypothesis of there being no association between *GSTT1* and *GSTM1* deletions and *CYP2E1*/*Pst*I polymorphism with gastric cancer and chronic gastritis. However, smoking raised the OR's for stomach cancer in *GSTM1* null subjects. Our findings suggest that *GSTM1* null carriers may be more susceptible to the action of tobacco with regard to stomach cancer. Polycyclic aromatic hydrocarbons and N-nitrosamines found in cigarette smoke are potential human carcinogens. Thus, a deficiency of the detoxifying enzymes may affect the metabolic fates of these chemicals and raise cancer risk in subjects with a *GSTM1* null genotype. Cai *et al*.[30] reported an increased frequency of the *GSTM1* null genotype in smokers with gastric cancer, that may modulate tobacco-related gastric carcinogenesis .

We also observed that a *GSTM1* positive genotype was more prevalent in chronic gastritis patients with *H pylori* infection. In the multi-step carcinogenesis of the stomach, chronic gastritis preceded the formation of gastric cancer, and a great proportion of the clinical tumors occurred in connection with advanced forms of this pathology[57]. *H pylori* has been reported to be a Class I human carcinogen[58], and chronic *H pylori* infection was shown to increase the risk for gastric carcinoma from 2.8 to 9 fold[59-64]. Ng *et al*.[27] observed that the absence of the *GSTM1* enzyme might increase the risk of developing gastric cancer in patients with *H pylori* infection. Thus, chronic gastritis patients with *H pylori* infection, but with a *GSTM1* positive genotype, might benefit from a protective effect and exhibit a smaller predisposition to developing gastric cancer.

In this study, no association between the *CYP2E1*/*Pst*I polymorphism and overall risk for gastric cancer was observed. Different from the study of Nishimoto *et al*.[51] in a Brazilian population, the rare variant *c2/c2* was not observed. Moreover, the risk for gastric cancer as related to demographic risk factors was also not affected by the *CYP2E1*/*Pst*I polymorphisms.

In conclusion, the present work does not show any obvious relationship between *GSTT1*, *GSTM1* and *CYP2E1* polymorphisms and the development of gastric cancer in a Brazilian population. However, smoking and the *GSTM1* null genotype may be associated with an increased OR for stomach cancer. We emphasize that studies with negative findings also need to be reported, so as to avoid a publication bias leading to an overestimate of positive findings. We also suggest that the investigation of a greater number of biometabolism genes associated with DNA repair genes might bring a broader view of the process.

ACKNOWLEDGEMENTS

We wish to thank Dr. Adriana Barbosa Santos and Dr. Antônio José Manzato for their help in the statistical analysis.

REFERENCES

1 **INCA** - Instituto Nacional do Câncer, Ministério da Saúde. Estimativa da incidência e mortalidade por câncer no Brasil, Rio de Janeiro, 2003. Disponível em http://www.inca.org.br.

2 **Stadtländer CT**, Waterbor JW. Molecular epidemiology, pathogenesis and prevention of gastric cancer. *Carcinogenesis* 1999; **20**: 2195-2208

3 **Galanis DJ**, Kolonel LN, Lee J, Nomura A. Intakes of selected foods and beverages and the incidence of gastric cancer among the Japanese residents of Hawaii: a prospective study. *Int J Epidem* 1998; **27**: 173-180

4 **Brenner H**, Arndt V, Bode G, Stegmaier C, Ziegler H, Stümer T. Risk of gastric cancer among smokers infected with *Helicobacter pylori*. *Int J Cancer* 2002; **98**: 446-449

5 **Zaridze D**, Borisova E, Maximovitch D, Chkhikvadze V. Alcohol consumption, smoking and risk of gastric cancer: case-control study from Moscow, Russia. *Cancer Causes Control* 2000; **11**: 363-371

6 **Pakodi F**, Abdel-Salam OM, Debreceni A, Mózsik G. *Helicobacter pylori.* One bacterium and a broad spectrum of human disease! An overview. *J Physiol Paris* 2000; **94**: 139-158

7 **Sipponen P**, Hyvärinen H, Seppaälä K, Blaser MJ. Review article: pathogenesis of transformation from gastritis to malignancy. *Aliment Pharmacol Ther* 1998; **12**: 61-71

8 **Correa P**. A human model of gastric carcinogenesis. *Cancer Res* 1988; **48**: 3554-3560

9 **Stermmermann GN**. Intestinal metaplasia of the stomach. A status report. *Cancer* 1994; **74**: 556-564

10 **Wormhoudt LW**, Commandeur JN, Vermeulen NP. Genetic polymorphisms of human N-acetyltransferase, cytochrome P450, glutathione S-transferase, and epoxide hydrolase enzimes: relevance to xenobiotic metabolism and toxicity. *Crit Rev Toxicol* 1999; **29**: 59-124

11 **Autrup H**. Genetic polymorphisms in human xenobiotica metabolizing enzymes as susceptibility factors in toxic response. *Mutat Res* 2000; **464**: 65-76

12 **Rothman N**, Wacholder S, Caporaso NE, Garcia-Closas M,

Buetow K, Fraumeni JF. The use of common genetic polymorphisms to enhance the epidemiologic study of environmental carcinogens. *Biochim Biophys Acta* 2001; **1471**: 1-10

13 **Liu S**, Park JY, Schantz SP, Stern JC, Lazarus P. Elucidation of *CYP2E1* 5'regulatory *RsaI/Pst*I allelic variants and their role in risk for oral cancer. *Oral Oncol* 2001; **37**: 437-445

14 **Pavanello S**, Clonfero E. Biological indicators of genotoxic risk and metabolic polymorphisms. *Mutat Res* 2000; **63**: 285-308

15 **AICR** - American Institute for Cancer Research. World Cancer Research Fund. Food, Nutrition and the Prevention of Cancer: a Global Perspective. Washington: *Banta Book Group* 1997: 670p

16 **Sheweita SA**, Tilmisany AK. Cancer and phase II drug-metabolizing enzymes. *Curr Drug Metab* 2003; **4**: 45-58

17 **Landi S**. Mammalian class theta GST and differential susceptibility to carcinogens: a review. *Mutat Res* 2000; **463**: 247-283

18 **Hung HC**, Chuang J, Chien YC, Chern HD, Chiang CP, Kuo YS, Hi Desheim A, Chen CJ. Genetic polymorphisms of *CYP2E1*, *GSTM1* and *GSTY1*: environmental factors and risk of oral cancer, *Cancer Epidemiol Biomarkers Prev* 1997; **6**: 901-905

19 **Hildesheim A**, Chen CJ, Caporaso NE, Cheng YJ, Hoover RN, Hsu MM, Levine PH, Chen IH, Chen JY, Yang CS, Daly AK, Idle JR. Cytochrome P450IIE1 genetic polymorphisms and risk of nasopharyngeal carcinoma, Results from a case-control study conducted in Taiwan. *Cancer Epidemiol Biomarkers Prev* 1995; **4**: 607-610

20 **Le Marchand LL**, Sivaraman L, Pierce L, Seifried A, Lum A, Wilkens LR, Lau AF. Association of *CYP1A1, GSTM1* and *CYP2E1* polymorphisms with lung cancer suggest cell type specificities to tobacco carcinogens. *Cancer Res* 1998; **58**: 4858-4863

21 **Lin DX**, Tang YM, Peng Q, Lu SX, Ambrosone CB, Kadlubar FF. Susceptibility to esophageal cancer and genetic polymorphisms in Glutathione S-Transferases T1, P1 and M1 and Cytochrome P4502E1. *Cancer Epidemiol Biomarkers Prev* 1998; **7**: 1013-1018

22 **Harada S**, Misawa S, Nakamura T, Tanaka N, Ueno E, Nozoe M. Detection of *GST1* gene deletion by the polymerase chain reaction and its possible correlation with stomach cancer in Japanese. *Hum Genet* 1992; **90**: 62-64

23 **Kato S**, Onda M, Matsukura N, Tokunaga A, Tajiri T, Kim DY, Tsuruta H, Matsuda N, Yamashita K, Shields PG. Cytochrome P4502E1 (CYP2E1) genetic polymorphism in a case-control study of gastric cancer and liver disease. *Pharmacogenetics* 1995; **5**: 141-144

24 **Kato S,** Onda M, Matsukura N, Tokunaga A, Matsuda N, Yamashita K, Shields PG. Genetic polymorphisms of the cancer related gene and *Helicobacter pylori* infection in Japonese gastric cancer patients: An age and gender matched case-control study. *Cancer* 1996; **77**(8 Suppl): 1654-1661

25 **Katoh T**, Nagata N, Kuroda Y, Itoh H, Kawahara A, Kuroki N, Ookuma R, A'bell D. Glutathione S-transferase M1 (GSTT1) and T1 (GSTT1) genetic polymorphism and susceptibility to gastric and colorectal adenocarcinoma. *Carcinogenesis* 1996; **17**: 1855-1859

26 **Kato S**, Onda M, Matsukura N, Tokunaga A, Matsuda N, Yamashita K, Shields GP. *Helicobacter pylori* infeccion and genetic polymorphisms to cancer related genes in gastric carcinogenesis. *Biomed Pharmacother* 1997; **51**: 145-149

27 **Ng EK**, Sung JJ, Ling TK, Ip SM, Lau JY, Chan AC, Liew CT, Chung SC. *Helicobacter pylori* and the null genotype of glutathione-S-transferase-m in patients with gastric adenocarcinoma. *Cancer* 1998; **82**: 268-273

28 **Oda Y**, Kobayashi M, Ooi A, Muroishi Y, Nakanishi I. Genotypes of glutathione S-transferase M1 and N-acetyltransferase 2 in Japanese patients with gastric cancer. *Gastric Cancer* 1999; **2**: 158-164

29 **Setiawan VW**, Zhang ZF, Yu GP, Li ML, Tsai CJ, Cordova D, Wang MR, Guo CR, Yu SZ, Kurtz RC. GSTT1 and GSTM1 null genotypes and the risk of gastric cancer: a case-control study in a chinese population. *Cancer Epidemiol Biomarkers Prev* 2000; **9**: 73-80

30 **Cai L**, Yu SZ, Zhang ZF. Glutathione S-transferase M1, T1 genotypes and the risk of gastric cancer: A case-control study. *World J Gastroenterol* 2001; **7**: 506-509

31 **Cai L**, Yu SZ, Zhang ZF. Cytochrome P450 2E1 genetic polymorphism and gastric cancer in Changle, Fujian Province. *World J Gastroenterol* 2001; **7**: 792-795

32 **Gao CM**, Takezaki T, Wu JZ, Li ZF, Liu YT, Li SP, Ding JH, Su P, Hu X, Xu TL, Sugimura H, Tajima K. Glutathione-S-transferases M1 (GSTM1) and GSTT1 genotype, smoking, consumption of alcohol and tea and risk of esophageal and stomach cancers: a case-control study of a high-incidence area in Jiangsu Province, China. *Cancer Lett* 2002; **188**: 95-102

33 **Gao CM**, Takezaki T, Wu JZ, Li ZY, Wang J, Ding J, Liu YT, Hu X, Tajima K, Sugimura H. Interation between Cytochrome P-450 2E1 polymorphisms and environmental factors with risk of esophageal and stomach cancers in chinese. *Cancer Epidemiol Biomarkers Prev* 2002; **11**: 29-34

34 **Tsukino H**, Kuroda Y, Qiu D, Nakao H, Imai H, Katoh T. Effects of cytochrome P450 (CYP) 2A6 gene deletion and CYP2E1 genotypes on gastric adenocarcinoma. *Int J Cancer* 2002; **100**: 425-428

35 **Wu MS**, Chen CJ, Lin MT, Wang HP, Shun CT, Shen JC, Liu JT. Genetic polymorphisms of cytochrome p450 2E1, glutathione S-transferase M1 and T1, and susceptibility to gastric carcinoma in Taiwan. *Int J Colorectal Dis* 2002; **17**: 338-343

36 **Choi SC**, Yun KJ, Kim TH, Kim HJ, Park SG, Oh GT, Chae SC, Oh GJ, Nah YH, Kim JJ, Chung HT. Prognostic potential of glutathione S-transferase M1 and T1 null genotypes for gastric cancer progression, *Cancer Lett* 2003; **195**: 169-175

37 **Genta RM**. Gastric atrophy and atrophic gastritis – nebulous concepts in search of a definition. *Aliment Pharmacol Ther* 1998; **12**: 17-23

38 **Lauren J**. The two histological main types of gastric carcinoma: diffuse and so-called intestinal type carcinoma: na attemp at a histo clinical classification. *Acta Pathol Microbiol Scand* 1965; **64**: 31-49

39 **Price AB**. The Sydney system: histological division. *J Gastroenterol Hepatol* 1991; **6**: 209-222

40 **Abdel-Rahman SZ**, Nouraldeen AM, Ahmed AE. Molecular interaction of [2,3-14C] acrylonitrile with DNA in gastric tissue of rat. *J Biochem Toxicol* 1994; **9**: 191-198

41 **Abdel-Rahaman SZ**, El-Zein RA, Anwar WA, Au WW. A multiplex PCR procedure for genetic polymorphism of the *GSTM1* and *GSTT1* genes in human. *Cancer Lett* 1996; **107**: 229-233

42 **Kato S**, Shields PG, Caporaso NE, Hoover RN, Trump BF, Sugimura H, Weston A, Harris CC. Cytochrome P450IIE1 genetic polymorphisms, racial variation, and lung cancer risk. *Cancer Res* 1992; **52**: 6712-6715

43 **van Iersel ML**, Verhagen H, van Bladeren PJ. The role of biotransformation in dietary (anti) carcinogenesis. *Mutat Res* 1999; **443**: 259-270

44 **Mizoue T**, Tokui N, Nishisaka K, Nishisaka S, Ogimoto I, Ikeda M, Yoshimura T. Prospective study on the relation of cigarette smoking with cancer of the liver and stomach in an endemic region. *Int J Epidemiol* 2000; **29**: 232-237

45 **De Stefani E**, Boffetta P, Carzoglio J, Mendilaharsu S, Deneo-Pellegrini H. Tobacco smoking and alcohol drinking as risk factors for stomach cancer: a case-control study in Uruguay. *Cancer Causes Control* 1998; **9**: 321-329

46 **Ekström AM**, Eriksson M, Hansson LE, Lindgren A, Signorello LB, Nyrén O, Hardell L, Occupational exposures and risk of gastric cancer in a population-base case-control study. *Cancer Res* 1999; **59**: 5932-5937

47 **Mikelsaar AV**, Tasa G, Parlist P, Uuskula M. Human glutathione S-transferase GSTM1 genetic polymorphism in Estonia. *Hum Hered* 1994; **44**: 248-251

48 **Persson I**, Johansson I, Lou YC, Yue QY, Duan LS, Bertilsson L, Ingelman-Sundberg M. Genetic polymorphism of xenobiotic metabolizing enzymes among Chinese lung cancer patients. *Int J Cancer* 1999; **81**: 325-329

49 **Gattas GJ**, Soares-Vieira JA. Cytochrome P450-2E1 and glutathione S-transferase mu polymorphisms among caucasians and mulattoes from Brazil. *Occup Med* 2000; **50**: 508-511

50 **Hatagima A**, Klautau-Guimarães MN, Silva FP. Glutathione S-transferase M1 (GSTM1) polymorphism in two Brazilian populations. *Genet Mol Biol* 2000; **23**: 709-713

51 **Nishimoto IN**, Hanaoka T, Sugimura H, Nagura K, Ihara M, Li XJ, Arai T, Hamada GS, Kowalski LP, Tsugane S. Cyto-

chrome P450 2E1 polymorphism in gastric cancer in Brazil: case-control studies of Japanese Brasilians and non-Japanese Brasilians. *Cancer Epidemiol Biomarker Prev* 2000; **9**: 675-580

52 **Losi-Guembarovski R**, D'Arce LPG, Cólus IMS. Glutathione S-transferase Mu (GSTM1) null genotype in relation to gender, age and smoking status in a healthy Brazilian population. *Genet Mol Biol* 2002; **25**: 357-360

53 **Arruda VR**, Grignolli CE, Gonçalves MS, Soares MC, Menezes R, Saad ST, Costa FF. Prevalence of homozygosity for the deleted alleles of glutathione S-transferase um (GSTM1) and theta (GSTT1) among distinct ethinic groups from Brazil: relevance to environmental carcinogenesis? *Clini Genet* 1998; **54**: 210-214

54 **Chen CL**, Liu Q, Relling WV. Simultaneons characterization of glutathioneS-transferase M1 and T1 polymorphisms by polymerase chain reation in American whites and blacks. *Pharmacogenetics* 1996; **6**: 187-191

55 **Deakin M**, Elder J, Hendrickse C, Peckham D, Baldwin D, Pantin C, Wild N, Leopard P, Bell DA, Jones P, Duncan H, Brannigan K, Alldersea J, Fryer A, Strange ARC. Glutathione S-transferase GSTT1 genotypes and suscetibility to cancer: studies of interations with GSTM1 in lung, oral, gastric and colorectal cancers. *Carcinogenesis* 1996; **17**: 881-884

56 **Saadat I**, Saadat M. Glutathione S-transferase M1 and T1 null genotypes and the risk of gastric and colorectal cancers. *Cancer Lett* 2001; **169**: 21-26

57 **Lan Q**, Chow WH, Lissowska J, Hein DW, Buetow K, Engel LS, Ji B, Zatonski W, Rothman N. Glutathione S-transferase genotypes and stomach cancer in a population-based case-control study in Warsaw, Poland. *Pharmacogenetics* 2001; **11**: 655-661

58 **Martins G**, Alves M, Dias J, Santos R, Costa-Neves J, Mafra M, Marins AP, Ramos S, Ramos M, Mexia J, Quina M, Rueff J, Montero C. Glutathione S-transferase mu polymorphism and gastric cancer in the portuguese population. *Biomarkers* 1998; **3**: 441-447

59 **Conde AR**, Martins G, Saraiva C, Rueff J, Monteiro C. Association of p53 genomic instability with the glutathione S-transferase null genotype in gastric cancer in the portuguese population. *Mol Pathol* 1999; **52**: 131-134

60 **Sipponen P**, Hyvärinen H, Seppalä K, Blaser MJ. Review article: pathogenesis of transformation from gastritis to malignancy. *Aliment Pharmacol Ther* 1998; **12**: 61-71

61 International Agency for Research on Cancer. World Health Organization. The evaluation of carcinogenic risks to humans, Monograph Nº 61. Lyon, France, 1994

62 **Kuipers EJ**. Exploring the link between *Helicobacter pylori* and gastric cancer. *Aliment Pharmacol Ther* 1999; **13**: 3-11

63 **El-Omar EM**, Oien K, Murray LS, El-Nujumi A, Wirz A, Gillen D, Williams G, Fullarton G, Mccoll KEL. Incresased prevalence of precancerous changes in relatives of gastric cancer patients: critical role of *H pylori*. *Gastoenterology* 2000; **118**: 22-30

64 **Uemura N**, Okamoto S, Yamamoto S, Matsumura N, Yamaguchi S, Yamakido M, Taniyama K, Sasaki N, Schlemper RJ. *Helicobacter pylori* infection and the development of gastric cancer. *N Engl J Med* 2001; **345**: 784-789

Edited by Wang X L **Proofread by** Xu FM

PO Box 2345, Beijing 100023, China
Fax: +86-10-85381893
E-mail: wjg@wjgnet.com www.wjgnet.com

World J Gastroenterol 2004;10(9):1246-1249
World Journal of Gastroenterology
Copyright ©2004 by The WJG Press ISSN 1007-9327

• GASTRIC CANCER •

Role of nucleostemin in growth regulation of gastric cancer, liver cancer and other malignancies

Si-Jin Liu, Zi-Wei Cai, Ya-Jun Liu, Mei-Yu Dong, Li-Qiu Sun, Guo-Fa Hu, Ying-Yun Wei, Wei-De Lao

Si-Jin Liu, Guo-Fa Hu, Ying-Yun Wei, Wei-De Lao, Institute of Genetics and Developmental Biology, Chinese Academy of Sciences, Beijing 100080, China
Zi-Wei Cai, Li-Qiu Sun, Institute of Biology of Self-protection, Mudanjiang Medical College, Mudanjiang 157011, Heilongjiang Province, China
Ya-Jun Liu, Department of Spine, Beijing Jishuitan Hospital, Peking University, Beijing 100035, China
Mei-Yu Dong, Tianjin Institute of Urologic Surgery, Tianjin Medical University, Tianjin 300211, China
Correspondence to: Professor Wei-De Lao, No. 3 Zhongguancun Road, Haidian District, Beijing 100080, China. wdlao@genetics.ac.cn
Telephone: +86-10-62552956 **Fax:** +86-10-62551951
Received: 2003-12-23 **Accepted:** 2004-01-15

Abstract

AIM: To examine the role of nucleostemin in the growth regulation of gastric cancer, liver cancer and other cancers.

METHODS: RT-PCR was used to clone the fragment of nucleostemin cDNA from HEK 293 cells. Eighteen kinds of malignant tumor tissues including gastric adenocarcinoma and liver cancer tissues, 3 kinds of benign tumor tissues, 3 kinds of benign hyperplastic tissues and normal tissues were employed to examine nucleostemin gene expression by RT-PCR, Slot blot, Northern blot and *in situ* hybridization.

RESULTS: We successfully cloned a 570 bp fragment of nucleostemin-cDNA from HEK-293 cells. All detected malignant tumor tissues, benign tumor tissues, and benign hyperplastic tissues had high levels of nucleostemin expression. Nucleostemin was also expressed in human placenta tissue at a high level. In terminally differentiated normal human adult kidney and mammary gland tissues, no nucleostemin expression could be detected.

CONCLUSION: Nucleostemin can help regulate the proliferation of both cancer cells and stem cells. It might play an important role in the growth regulation of gastric cancer, liver cancer and other cancers.

Liu SJ, Cai ZW, Liu YJ, Dong MY, Sun LQ, Hu GF, Wei YY, Lao WD. Role of nucleostemin in growth regulation of gastric cancer, liver cancer and other malignancies. *World J Gastroenterol* 2004; 10(9): 1246-1249
http://www.wjgnet.com/1007-9327/10/1246.asp

INTRODUCTION

Perhaps the most important and useful property of stem cells is self-renewal. Through this property, striking parallels can be found between stem cells and cancer cells: tumor may originate from the transformation of normal stem cells. Similar signaling pathways may regulate self-renewal in stem cells, and cancer cells[1]. McKay and Tsai found a novel gene nucleostemin (NS) in rat embryo stem cells, the rat central nervous system (CNS) stem cells and rat primitive bone marrow cells. NS gene was apparently involved in regulating the proliferation of both stem cells and at least some types of cancer cells[2]. The protein encoded by NS was abundantly expressed while the cells were proliferating in an early multipotential state, but it abruptly and almost entirely disappeared at the start of differentiation. The fact that NS expressed in stem cells and several cancer cell lines, but not in the differentiated cells of adult tissues, suggested its role in maintaining self-renewal of stem cells and cancer cells. Our recent data also showed that NS expressed in human gastric cancer (SGC-7901) cells, human hepatocarcinoma (HepG2) cells, human cervical cancer (Hela) cells, human osteosarcoma (OS-732) cells, human mammary (MMK-7) cells and human embryo kidney (HEK-293) cells[3]. Coordinated control of self-renewal and commitment to differentiation is key to maintaining the homeostasis of the stem cell compartment[4,5], when deregulated it may contribute to cancer pathogenesis[6,7]. The identification of stem-cell-specific proteins and the elucidation of novel regulatory pathways that ensure the integration of these processes, are therefore of fundamental importance[8,9]. It seems that NS is involved in the regulatory pathways, but the fundamentals about NS are still unknown. For example, why does NS express in stem cells and cancer cells but not in differentiated cells? What are the tumor types that misexpress NS and the underlying mechanism? And what is the timing of NS reactivation in cancer cells.

Gastric cancer is common in China, and its early diagnosis and treatment are difficult[10,11]. To investigate the mechanism of carcinogenesis of gastric cancer would facilitate its diagnosis and treatment. Therefore, NS may take part in the growth regulation of tumor tissues and hyperplastic tissues. So we employed a number of malignant tumor tissues, benign tumor tissues, benign hyperplastic tissues and normal tissues to examine the expression of NS gene by RT-PCR, Slot blot, Northern blot and *in situ* hybridization, which would help illuminate the mechanism of self-renewal of cancer cells.

MATERIALS AND METHODS

Materials

We collected tens of tumor tissue samples including gastric adenocarcinoma, liver cancer, bladder carcinoma, pancreatic cancer and esophagus squamous carcinoma samples. We also collected several kinds of normal tissue samples such as normal kidney tissues and muscle tissues. Human embryo kidney (HEK-293) cells were cultured in DMEM containing 100 mL/L FCS at 37 ℃ in 50 mL/L CO_2[12,13]. The cells were kept in logarithmic growth phase by trypsin digestion and reinoculation every 2-4 d [14,15]. DMEM cell culture medium was purchased from Gibco Corporation; fetal calf serum (FCS) and trypsin from Hyclone Corporation; restriction enzymes and T4 DNA ligase from Promega Corporation. PCR primers were synthesized by Shanghai Shenyou Company and DNA sequencing was also performed by this company.

Cloning of NS cDNA fragment

Total RNA in HEK 293 cells was isolated using total RNA

isolation kit (Promega Corporation). A 2 μg total RNA was used in reverse transcription (RT) reaction. Up-stream primer, 5' -ggatccatgaaaaggcctaagttaaagaaagc (*Bam*HI site underlined); Down-stream primer, 5' -aagcttgctctccaaattctcctttggta (*Hin*dIII site underlined). PCR protocol (94 ℃ 30 s→50 ℃ 30 s→72 ℃ 30 s) was run for 30 cycles and PCR product was about 570 bp. PCR product was separated by agrose gel electrophoresis, recovered with gel extraction kit (Omega Corporation), and ligated with pGEM-T vector. The ligate was transformed into competent *E.coli* JM 109 cells. The correct transformant was identified by restriction enzyme analysis and DNA sequencing.

Isolation of total RNA in tissue samples and RT-PCR

About 100 mg tissues of each sample was used to isolate total RNA using total RNA isolation kit (Promega Corporation). RT protocol and PCR protocol including PCR primers are the same as the above. GAPDH was used as a loading control, its up-stream primer, 5' -ggtggacctgacctgccgtctaga, and its down-stream primer, 5' -ttactccttggaggccatgtggg. PCR protocol (94 ℃ 30 s→55 ℃ 30 s→72 ℃ 20 s) was run for 25 cycles.

Analysis of slot blot

Twenty μg total RNA of each sample was added into slots, and transferred onto nylon membrane. Slot blot analysis was carried out using ^{32}P-labeled NS fragments and human 18S RNA as probes in the hybridization.

Analysis of Northern blot

Equal volume of total RNA of each sample was used in denaturing agarose gel electrophoresis, and after that RNA was transferred onto nylon membrane. Northern blot analysis was made using ^{32}P labeled NS fragments and human 18S RNA as probes in the hybridization.

Preparation of cRNA probes

Nucleostemin cDNA fragment was inserted into pGEM-T vector, and large quantities of plasmid was harvested with Plasmid Extraction Kit (Promega Corporation). After linearization by *Nco*I restriction enzyme, SP6 promoter was used to drive the transcription of NS-cRNA probes *in vitro* and in this system Biotin labeled rUTPs was introduced into NS-cRNA probes. In the same way, after linearization by Not I restriction enzyme, T7 promoter was used to drive the transcription of sense NS-cRNA probes *in vitro*, which acted as the negative control.

Detection of in situ hybridization histochemistry

The expression of NS mRNA was detected *in situ* by Biotin SP-HRP method[16,17]. Pretreatment of paraffin-embedded specimens referred to the previously used methods[13]. In brief, before *in situ* hybridization, sections were deparaffinized in xylene (7.5 min, twice) and rehydrated in graded ethanol. Sections were then rinsed in 2 changes of diethylpyrocarbonate-treated distilled water and rinsed in 10 mmol/L citrate buffer, pH 6.0. Sections were placed in glass racks (20 slides/rack) and submerged in approximately 250 mL citrate buffer in covered glass tubes. Sections were then microwaved in a 900-watt microwave (Panasonic Matsushita Electric, Danville, MA) 3 times for 5 min each time at full power, topped up with additional citrate buffer to compensate for evaporation. Slides were allowed to cool slightly, then were rinsed in 2 changes of diethylpyrocarbonate-treated distilled water, dehydrated in graded ethanol, and dried. Hybridization of the labeled probes to the tissue sections was carried out using a previously described method[18]. Sense NS-cRNA probes and SP-HRP solution were used as negative controls. And the tissue sections were counterstained by hematoxylin.

RESULTS

Gain of NS-cDNA fragment

We successfully cloned a 570 nt fragment by RT-PCR in HEK-293 cells. Then the fragment was ligased with pGEM-T vector and the recombinant vector was named pGEM-T-NS. pGEM-T-NS was digested by BamH I and HindIII enzymes, yielding a 3.0 kb fragment of vector and a 570 bp fragment of NS cDNA (Figure 1). The result of sequencing indicated our sequence of NS cDNA was completely identical to the sequence in Genebank. Sequencing revealed that no base mutation occurred in the sequence of our cloned NS-cDNA fragment.

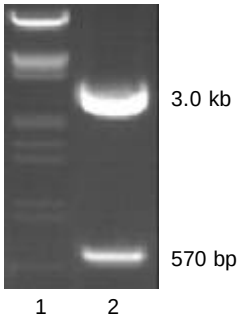

Figure 1 Molecular cloning of nucleostemin cDNA fragment. 1.DNA marker: λDNA, *Eco*RI+ *Hin*d III. 2. pGEM-T-NS, *Bam*HI+*Hin*d III.

NS expression detected by RT-PCR

According to the results of RT-PCR, all above malignant tumor tissues, benign tumor tissues, and benign hyperplastic tissues had high levels of NS expression, so did the normal human placenta tissues. And a lower level of NS expression in normal human adult muscle tissues could also be detected. However, no NS expression could be detected in normal human adult kidney tissues and mammary gland tissues. Partial results of RT-PCR are shown in Figure 2.

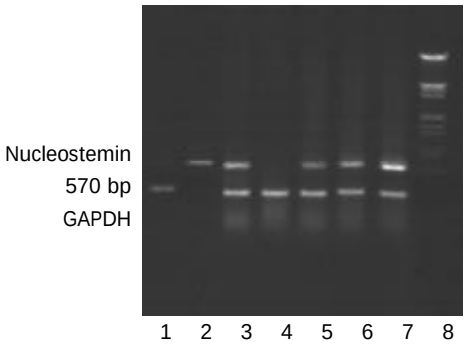

Figure 2 Detection of NS expression in various tumor tissues and normal human adult kidney tissues using RT-PCR. 1. GAPDH cDNA-fragment sample. 2. NS-cDNA fragment sample. 3. Renal carcinoma tissue. 4. Normal human adult kidney tissue. 5. Bladder carcinoma tissue. 6. Liver cancer tissue. 7. Gastric adenocarcinoma tissue. 8. DNA marker: λDNA, *Eco*R I+*Hin*d III.

NS expression by slot blot

Slot blot analysis indicated that NS expressed in all above malignant tumor tissues, benign tumor tissues, and benign hyperplastic tissues, which was in agreement with the results of RT-PCR. However, no NS expression could be detected in normal human adult kidney tissues, mammary gland tissues and muscle tissues. Partial results of Slot blot analysis are shown in Figure 3.

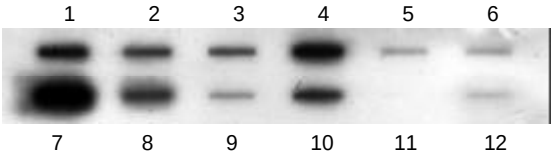

Figure 3 Detection of NS expression in various tumor tissues and normal human adult kidney tissues by Slot blot. 1. Liver cancer tissue. 2. Bladder carcinoma tissue. 3. Pancreatic cancer tissue. 4. Cardia adenocarcinoma tissue. 5. Gastric adenocarcinoma tissue. 6. Esophagus squamous carcinoma tissue. 7. Denatured NS-cDNA sample. 8. Ovary serous cystadenocarcinoma. 9. Ampulle carcinoma tissue.10. Renal carcinoma tissue. 11. Normal human adult kidney tissue. 12. Benign hyperplasia tissue of prostate.

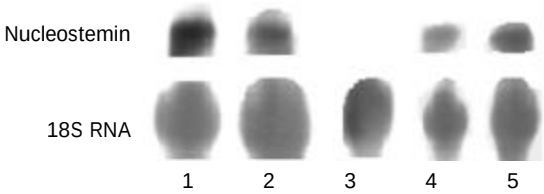

Figure 4 Detection of NS expression in various tumor tissues and normal human adult kidney tissues by Northern blot. 1. Gastric adenocarcinoma tissue. 2. Renal carcinoma tissue. 3. Normal human adult kidney tissue. 4. Liver cancer tissue. 5. Bladder carcinoma tissue.

Detection of NS expression by Northern blot

The results of Slot blot were further confirmed by Northern blot analysis. NS misexpressed in all these malignant tumor tissues, benign tumor tissues, and benign hyperplastic tissues. But the results of Northern blot analysis showed NS did not express in normal human adult kidney tissues, mammary gland tissues and muscle tissues. Partial results of Northern blot analysis are shown in Figure 4.

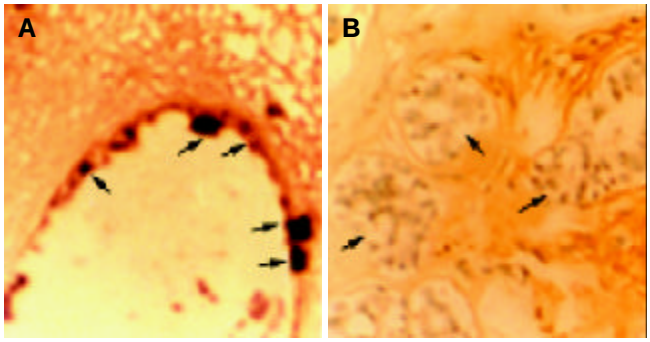

Figure 5 *In situ* hybridization detection of nucleostemin mRNA in invasive ductal breast carcinoma and normal mammary gland tissue by SP-HRP method. Counterstained with hematoxylin. A: Ductal carcinoma cells showed strong staining *in situ* (arrows). B: Normal mammary glandular epithelial cells showed no positive staining, only with azury nuclear counterstaining (arrows).

NS expression in tumor tissues confirmed by in situ hybridization

The Biotin SP-HRP (streptavidin-biotin-peroxidase-DAB) system reacted with 0.05% DAB (3-3' , 4-4' -diaminobenzidine tetrahydrochloride) containing 0.1 mL/L H_2O_2, producing brown positive staining. And counterstain was performed by hematoxylin, producing azury nuclear staining. The results of *in situ* hybridization conformed to those of Slot blot analysis and Northern blot analysis. Positive staining was located in cytoplasm of cancer cells, but no positive staining in cytoplasm of normal adult tissue cells such as normal kidney cells and mammary gland cells. The results of *in situ* hybridization detection of nucleostemin mRNA in invasive ductal breast carcinoma and normal mammary gland tissue are indicated in Figure 5**.** Ductal carcinoma cells showed strong staining in cytoplasm **(**Figure 5A), while normal mammary glandular epithelial cells showed no positive staining, only with azury nuclear counterstaining (Figure 5B).

DISCUSSION

Nucleostemin (NS) is a newly found p53-binding protein, which exists mainly in the nucleoli of stem cells and some various cancer cells, but does not express in committed and terminally differentiated cells[2]. The expression level of NS declined obviously during embryo and adult development due to the differentiation of stem cells. For example, it was expressed preferentially in neuroepithelial precursors during embryogenesis and diminished during the central nervous system (CNS) differentiation. The expression of NS was also found in adult bone marrow hematopoietic stem cells, however could not be found in committed B-lymphocytes and granulocytes. *In vivo* experiments displayed that the NS expression could not even be detected after CNS stem cells were induced to differentiate. Recently, it was confirmed that NS expression also existed in ES cells and mesenchymal stem cells of mice[19]. *In vivo*, NS expression disappeared before the changes of cell cycle markers during the development of CNS, which indicated the disappearance of NS expression induced the cell cycle arrest, but not the reverse. Moreover, non-cycling cells increased by silencing NS expression with small interfering RNA (siRNA) in CNS stem cells and U2OS cancer cells[2].

We successfully cloned a 570 bp fragment of NS-cDNA from HEK-293 cells. The full length of NS-cDNA was 1 650 bp and the cloned fragment was located in the 5' -terminal of the full length. The fragment had high specificity and non-homology with other genes by BLAST analysis, so it was equal to probes in the screening of gene expression. From the results of RT-PCR, Northern blot and Slot blot analysis, we found that all these malignant tumor tissues, benign tumor tissues, and benign hyperplastic tissues had high levels of NS expression, which indicated that NS played an important role in the self-renewal of these cancer cells and hyperplastic cellls. At the same time, NS expressed in human placental tissues also at a high level, possibly due to the existence of a mass of placental stem cells[20-23]. A small quantity of NS expression could be found in normal human muscle tissues by RT-PCR, however no expression could be detected by Slot blot and Northern blot analysis. The reason might be that a few of myoblasts with the characteristic of stem cells existed in muscle tissues[24,25], so only by the sensitive RT-PCR technique could a very small volume of NS expression be detected (figures not provided). In terminally differentiated normal human adult kidney tissues and mammary gland tissues, no NS expression could be detected as no cells possess the characteristics of stem cells or cancer cells in these tissues. The analysis of *in situ* hybridization indicated that NS gene expressed in cancer cells, but not in normal adult tissue cells, such as normal kidney cells and mammary gland cells. These results were in agreement with McKay' s[2].

All these results displayed that NS might play an important role in the proliferation regulation of cancer cells and stem cells. A working hypothesis of NS deduced from all information involved displayed that NS accumulated predominantly in the nucleolus and NS localized into nucleoplasm after binding with GTP[26]. In the nucleoplasm, NS and p53 existed in a protein complex, and subsequently the growth-suppressive function of p53 was inhibited. During cell differentiation, when NS expression was downregulated, p53 was released from the protein complex, which allowed the stabilization or activation of p53 and induction of target genes critical for cell cycle exit

and differentiation, such as $p21^{CIP}$. Members of the E2F family of transcription factors play a crucial role in cell proliferation control by regulating the expression of genes important for DNA synthesis and cell cycle progression[27]. A functional E2F factor is composed of a heterodimer between an E2F polypeptide (E2F1- E2F6) and a DP polypeptide(DP1 and DP2). The transcriptional activities of E2F factors are regulated through association with the Rb(retinoblastoma) tumor suppressor protein and the other pocket proteins, p107 and p130. Binding of a pocket protein inhibits the transcriptional activation capacity of E2F factors and, in at least some cases, can convert E2F to repressors of transcription. The activity of Rb is regulated during the cell cycle by cdks(cyclic dependent kinase), primarily by cdk4 and cdk6, in association with D-type cyclin and cyclin E in association with cdk2. Phosphorylation of Rb by these cdks results in the dissociation of Rb from E2F and the depression/activation of E2F-regulated genes. The E2F-DP transcription complex determined the start of S phase and induced the expression of some genes which were necessary to the progress of S phase, such as Cyclin E, Cyclin A, proliferating cell nuclear antigen (PCNA) and dihydrofolate reductase (DHFR). The product of Cip1, $p21^{CIP1}$, blocked the process of phosphorylation of Rb by cdks and Cyclin complex, so E2F-DP in non-phosphorylation state still bound with RB and could not be freed. Only freed E2F-DP could gain its activity to promote the expression of these genes, and as a result, DNA synthesis was carried out and cells would pass through S phase.

Our results were in agreement with the working hypothesis mentioned above. There were high levels of NS expression in cancer cells, hyperplastic tissue cells and stem cells, so NS inhibited the p53-induced cell differentiation or apoptosis and these cells could easily pass through cell cycles. NS helped regulate the proliferation of both cancer cells and stem cells, although the precise mechanism was not yet clear. The focus on NS has potential therapeutic implications. For example, the growth of gastric cancer may be suppressed by silencing the NS expression with some molecular techniques, which would greatly improve the validity of its treatment.

ACKNOWLEDGEMENT

We want to thank Dr. Hong Gao and Dr. Siguo Liu in our group for their helpful discussions and research suggestions. We also thank Ms. Lin Hou from pathological center of Peking University for her help with *in situ* hybridization experiments and Professor. Hongwei Zhang and her colleagues from Beijing Haidian Hospital for their help with the pathological analysis.

REFERENCES

1 **Reya T**, Morrison SJ, Clarke MF, Weissman IL. Stem cells, cancer, and cancer stem cells. *Nature* 2001; **414**: 105-111
2 **Tsai RY**, McKay RD. A nucleolar mechanism controlling cell proliferation in stem cells and cancer cells. *Genes Dev* 2002; **16**: 2991-3003
3 **Liu SJ**, Cai ZW, Liu YJ, Dong MY, Zhang HW, Hu GF, Liu SG, Gao H, Zhang ZH, Liu XL, Wei YY, Xue Y, Lao WD. The effect of Knocking-down Nucleostemin Gene Expression on the *in vitro* Proliferation and *in vivo* tumorigenesis of HeLa cells. *J Exp Clin Canc Res* 2004; in press
4 **Sperger JM**, Chen X, Draper JS, Antosiewicz JE, Chon CH, Jones SB, Brooks JD, Andrews PW, Brown PO, Thomson JA. Gene expression patterns in human embryonic stem cells and human pluripotent germ cell tumors. *Proc Natl Acad Sci U S A* 2003; **100**: 13350-13355
5 **Goldschmidt-Clermont PJ**. Loss of bone marrow-derived vascular progenitor cells leads to inflammation and atherosclerosis. *Am Heart J* 2003; **146**: S5-12
6 **Hori Y**, Rulifson IC, Tsai BC, Heit JJ, Cahoy JD, Kim SK. Growth inhibitors promote differentiation of insulin-producing tissue from embryonic stem cells. *Proc Natl Acad Sci U S A* 2002; **99**: 16105-16110
7 **Wang N**, Liu ZH, Ding F, Wang XQ, Zhou CN, Wu M. Down-regulation of gut-enriched Kruppel-like factor expression in esophageal cancer. *World J Gastroenterol* 2002; **8**: 966-970
8 **Fiorini M**, Ballaro C, Sala G, Falcone G, Alema S, Segatto O. Expression of RALT, a feedback inhibitor of ErbB receptors, is subjected to an integrated transcriptional and post-translational control. *Oncogene* 2002; **21**: 6530-6539
9 **Zhou J**, Gurates B, Yang S, Sebastian S, Bulun SE. Malignant breast epithelial cells stimulate aromatase expression via promoter II in human adipose fibroblasts: an epithelial-stromal interaction in breast tumors mediated by CCAAT/enhancer binding protein beta. *Cancer Res* 2001; **61**: 2328-2334
10 **Lu JB**, Sun XB, Dai DX, Zhu SK, Chang QL, Liu SZ, Duan WJ. Epidemiology of gastroenterologic cancer in Henan Province, China. *World J Gastroenterol* 2003; **9**: 2400-2403
11 **Zhang C**, Liu ZK. Gene therapy for gastric cancer: A review. *World J Gastroenterol* 2003; **9**: 2390-2394
12 **Nadeau I**, Sabatie J, Koehl M, Perrier M, Kamen A. Human 293 cell metabolism in low glutamine-supplied culture: interpretation of metabolic changes through metabolic flux analysis. *Metab Eng* 2000; **2**: 277-292
13 **Liu SJ**, Hu GF, Liu YJ, Liu SG, Gao H, Zhang CS, Wei YY, Xue Y, Lao WD. The effect of human osteopontin on the proliferation, transmigration and expression of matrix metallproteinase-2 and 9 of osteosarcoma cells *in vitro*. *Chin Med J* 2004; **117**: 235-240
14 **Christoffers AB**, Kreisler M, Willershausen B. Effects of esradiol and progesterone on the proliferation of human gingival fibroblasts. *Eur J Med Res* 2003; **8**: 535-542
15 **Song J**, Rolfe BE, Hayward IP, Campbell GR, Campbell JH. Effects of collagen gel configuration on behavior of vascular smooth muscle cells *in vitro*: association with vascular morphogenesis. *In Vitro Cell Dev Biol Anim* 2000; **36**: 600-610
16 **Palumbo A**, Napolitano A, Carraturo A, Russo GL, d'Ischia M. Oxidative conversion of 6-nitrocatecholamines to nitrosating products: a possible contributory factor in nitric oxide and catecholamine neurotoxicity associated with oxidative stress and acidosis. *Chem Res Toxicol* 2001; **14**: 1296-1305
17 **Duran N**, Bromberg N, Kunz A. Kinetic studies on veratryl alcohol transformation by horseradish peroxidase. *J Inorg Biochem* 2001; **84**: 279-286
18 **Busuttil BE**, Frauman AG. Extrathyoidal manifestations of Graves disease: the thyrotropin receptor is expressed in extraocular, but not cardiac, muscle tissues. *J Clin Endocrinol Metab* 2001; **86**: 2315-2319
19 **Baddoo M**, Hill K, Wilkinson R, Gaupp D, Hughes C, Kopen GC, Phinney DG. Characterization of mesenchymal stem cells isolated from murine bone marrow by negative selection. *J Cell Biochem* 2003; **89**: 1235-1249
20 **Chambers I**, Colby D, Robertson M, Nichols J, Lee S, Tweedie S, Smith A. Functional expression cloning of Nanog, a pluripotency sustaining factor in embryonic stem cells. *Cell* 2003; **113**: 643-655
21 **Bernatchez R**, Belkacemi L, Rassart E, Daoud G, Simoneau L, Lafond J. Differential expression of membrane and soluble adenylyl cyclase isoforms in cytotrophoblast cells and syncytiotrophoblasts of human placenta. *Placenta* 2003; **24**: 648-657
22 **Dhot PS**, Nair V, Swarup D, Sirohi D, Ganguli P. Cord blood stem cell banking and transplantation. *Indian J Pediatr* 2003; **70**: 989-992
23 **Alvarez-Silva M**, Belo-Diabangouaya P, Salaun J, Dieterlen-Lievre F. Mouse placenta is a major hematopoietic organ. *Development* 2003; **130**: 5437-5444
24 **Berendse M**, Grounds MD, Lloyd CM. Myoblast structure affects subsequent skeletal myotube morphology and sarcomere assembly. *Exp Cell Res* 2003; **291**: 435-450
25 **Chen JC**, Goldhamer DJ. Skeletal muscle stem cells. *Reprod Biol Endocrinol* 2003; **1**: 101-107
26 **Bernardi R**, Pandolfi PP. The nucleolus: at the stem of immortality. *Nat Med* 2003; **9**: 24-25
27 **Nevins JR**. Toward an understanding of the functional complexity of the E2F and retinoblastoma families. *Cell Growth Differ* 1998; **9**: 585-593

Edited by Ma JY **Proofread by** Xu FM

PO Box 2345, Beijing 100023, China
Fax: +86-10-85381893
E-mail: wjg@wjgnet.com www.wjgnet.com

World J Gastroenterol 2004;10(9):1250-1255
World Journal of Gastroenterology
Copyright ©2004 by The WJG Press ISSN 1007-9327

• GASTRIC CANCER •

Significance of vascular endothelial growth factor expression and its correlation with inducible nitric oxide synthase in gastric cancer

Zhen-Ya Song, Shu-Qun Wen, Jia-Ping Peng, Xuan Huang, Ke-Da Qian

Zhen-Ya Song, Xuan Huang, Ke-Da Qian, Department of Digestive Medicine, Second Affiliated Hospital of Medical College of Zhejiang University, Hangzhou 310009, Zhejiang Province, China
Shu-Qun Wen, Department of Neurology, Second Affiliated Hospital of Medical College of Zhejiang University, Hangzhou 310009, Zhejiang Province, China
Jia-Ping Peng, Cancer Institute, Zhejiang University, Hangzhou 310009, Zhejiang Province, China
Supported by Science and Technology Fund of Medicine and Health of Zhejiang Province, No.2000A116
Correspondence to: Dr. Zhen-Ya Song, Department of Digestive Medicine, Second Affiliated Hospital of Medical College of Zhejiang University, Hangzhou 310009, Zhejiang Province, China. sz2700@hzcnc.com
Telephone: +86-571-87783715
Received: 2003-10-15 **Accepted:** 2003-12-06

Abstract

AIM: To investigate the clinical significance of the expression of $VEGF_{165}$mRNA and the correlation with vascular endothelial growth factor (VEGF) protein and inducible nitric oxide synthase (iNO) in human gastric cancer.

METHODS: We tested $VEGF_{165}$mRNA expression in 31 cases of resected gastric cancer specimens and normal paired gastric mucosae by RT-PCR. Total RNA was extracted with TRIzol reagents, transcribed into cDNA with oligo (dT_{15}) priming, inner controlled with β-actin expression and agarose gel isolated after PCR. VEGF expression was quantitated with IS1000 imaging system. Meanwhile we also examined expression levels of VEGF protein and iNOS in 85 cases of gastric cancer. All paraffin-embedded samples were immunohistochemically stained by streptavidin -peroxidase method (SP).

RESULTS: The mean expression of $VEGF_{165}$mRNA in gastric cancer was 1.125±0.356, significantly higher than that of normal paired mucosae, which was 0.760±0.278. The data indicated that the expression level of $VEGF_{165}$mRNA was well related to lymph node metastasis and TNM stages of UICC. The expression levels in patients with lymph node metastasis and without lymph node metastasis were 1.219±0.377 and 0.927±0.205 respectively ($P<0.05$). The expression in stages I, II, III, IV was 0.934±0.194, 1.262±0.386 respectively ($P<0.01$). Further analysis showed the lymph node metastasis rate in the group with over-expression of VEGF was higher than that in the group with low expression of VEGF (83.3% *vs* 46.2%), and the ratio of stage III+IV in the group with over-expression of VEGF was also higher than that in the group with low expression with VEGF (77.8% *vs* 33.8%) ($P<0.05$). The positive rates of expression of VEGF protein and iNOS in 85 cases of gastric cancer were 75.4% and 58.8% respectively, and 50.1% of the patients showed positive staining both for iNOS and VEGF, the correlation with the two factors was significant ($P=0.018$). But more intensive analysis showed the immunoreactive grades of VEGF were not associated with that of iNOS.

CONCLUSIONS: The expression of $VEGF_{165}$mRNA is well related with lymph node metastasis and TNM stages of UICC in gastric cancer, and is concerned with the invasiveness and metastasis of gastric cancer. The relationship can be observed between the expression of VEGF and iNOS in gastric cancer.

Song ZY, Wen SQ, Peng JP, Huang X, Qian KD. Significance of vascular endothelial growth factor expression and its correlation with inducible nitric oxide synthase in gastric cancer. *World J Gastroenterol* 2004; 10(9): 1250-1255
http://www.wjgnet.com/1007-9327/10/1250.asp

INTRODUCTION

Many observations have shown that angiogenesis plays an important role in the growth, progression and metastasis of solid tumors. Several potential angiogenic factors have been identified, vascular endothelial growth factor (VEGF) is known as one of the most powerful and specific molecules in vascularization. $VEGF_{165}$ is the major isoform among the five different VEGF species[1,2]. Studies have demonstrated that tumor cells could produce and secrete VEGF periodically by themselves, which binding with the VEGF receptor in the vascular endothelial cells and then promote the angiogenesis in tumors[3]. Inducible nitric oxide synthase (iNOS) is one of the isofroms of nitric oxide synthase that catalyzes the formation of nitric oxide, a regulator of vascular permeability. Expression of VEGF protein and iNO has been shown by immunohistochemistry in gastric cancer[4-8]. However, the relationship has not been well evaluated between the $VEGF_{165}$mRNA and the clinical pathological features, and between VEGF and iNO, the two angiogenic regulators in gastric cancer.

The present study detected the expression of $VEGF_{165}$mRNA by RT-PCR and the expression of VEGF protein and iNO by immunohistochemistry in surgically resected human gastric cancer specimens, and characterized the correlation that mentioned above.

MATERIALS AND METHODS

Materials

Specimens of cancer tissue from 85 cases of gastric cancer were confirmed pathologically and at the second Affiliated Hospital of Medical College of Zhejiang University from August 1998 to January 2002. Of these, 54 patients were male, and 23 female, with a median age of 54 (31-77) years. All the cases were classified by WHO criteria histologically and TNM staging of UICC. Fresh cancerous and normal paired gastric mucosae obtained from 31 cases of them were frozen quickly by liquid nitrogen and stored at -80 ℃ until used for RT-PCR. All the specimens from 85 cases were fixed in 40 g/L buffered formaldehyde and embedded in paraffin for immunohistochemistry.

RT-PCR

Total RNA was extracted from 100 mg each frozen tissue using TRIzol reagents according to the manufacturer's instructions (GIBCO BRL) and the purity and quality were identified by an ultraviolet spectrotometer and denatural gel electrophoresis.

First-strand cDNA was synthesized from 2 μg of total RNA in a 40 μL reaction volume by reverse transcription (RT) using 50 pmol oligo $(dT)_{15}$ 2 μL, RNasin 40 U, 10 mmol/L dNTP 2 μL, M-MLV reverse transcriptase 10 U (PROMEGA). The RNA template and oligo $(dT)_{15}$ were incubated at 65 ℃ for 10 min first, and were then added to the total reaction system at 37 ℃ for 1 h, stored at -20 ℃ for PCR. cDNA of 5 μL was amplified by PCR in a 25 μL reaction volume, containing 10 mmol/L dNTP 0.5 μL, Taq 1.5 U, per primer 10 pmol, and was inner controlled with β-actin. VEGF primers according to Tishcer's design[9] were the upper primer: 5'-CAAGGATCCATGAAC TTTCTGCTGTCTT-3', the lower primer: 5'-CTTAAGCTTGC TCCTTCC TCCTGCCCCGGC-3'. The upper primer of β-actin: 5'-TCGACAACGGCTCCGGCA-3', the lower primer of β-actin: 5'-CGTACATGGCTGGGGTGT-3'. The recombined plasmid pGEM- T-$VEGF_{165}$ was used as positive control (provide by the Surgery Laboratory in our hospital). PCR condition of $VEGF_{165}$: pre-denaturation 94 ℃ for 5 min, then 30 cycles of amplification at 94 ℃ for 45 s, at 60 ℃ for 45 s, and at 72 ℃ for 45 s, extension at 72 ℃ for 10 min.

Aliquots of the PCR products (10 μL) were separated and visualized with ethidium bromide staining after electrophoresis in a 15 g/L agarose gel in Tris acetate ethylenediaminetetraacetic acid buffer at 100 V for 20 min, and quantitated with IS 1000 imaging system (Alpha Inotech). The expression of $VEGF_{165}$mRNA was expressed as follow: numeral value of $VEGF_{165}$=scanning data of $VEGF_{165}$ band/ scanning data of β-actin band. The value greater than 1 was regarded as higher expression of $VEGF_{165}$mRNA, and the value less than 1 was regarded as lower expression of $VEGF_{165}$mRNA. Statistical analysis was performed by means of SPSS10.0.

Immunohistochemical analysis

Paraffin-embedded samples were serially sectioned at 4 μm, and mounted onto the histosticked-coated slides. Sections were dewaxed in xylene, and dehydrated in ethanol, and then heated at 98 ℃ in EDTA retrieved solution for the antigens. Endogenous peroxidase was blocked by incubation of samples in hydrogen peroxide blocking reagent (Maixin Bio, Fuzhou). After washed with phosphate-buffered saline solution, the samples were incubated for 60 min with the primary antibodies. The anti-VEGF antibody is a polyclonal mouse anti-serum against VEGF of human origin and recognizes an amino-terminal epitope found in $VEGF_{121,165,189}$, and the anti-iNOS antibody is a monoclonal mouse anti-serum against the C-terminal domain of iNOS of human origin (The two antibodies were from Santa Cruz Biotechnology, Inc., CA). Location of the primary antibodies was achieved by subsequent application of a biotinylated anti-primary antibody, an avidin-biotin complex conjugated to horseradish peroxidase. The reaction products were visualized with diamino- benzidine. The slides were counter-stained by hematoxylin. Negative controls were established by replacing the primary antibody with PBS and normal rabbit serum. Known immunostaining-positive slides were used as positive controls. Immunoreactivity was diagnosed depending on the shade of cells staining assigned to 0-3 scores (0: negative reaction, 1: weak brown-color staining, 2: moderate brown-color staining, 3: strong brown-color staining), and the percent of positive staining cells, the average percentage of positive cells was determined in at least 5 areas at ×400 and assigned to 0-3 scores (0: negative or equivocal staining, 1: weakly positive expression, cells were staining in 1-25%, 2: moderately positive expression, cells were staining in 25-50%, 3: strongly positive expression, the cells were stained over 50%). The diagnosed grades accorded to the sum of two scores, - : 0-1, +: 2, ++: 3-4, +++: >5. Statistical analysis was performed by means of SPSS10.0.

RESULTS

Expression of $VEGF_{165}$mRNA in gastric cancer

As shown by RT-PCR, the amplification products of VERF and β-actin were 655 bp and 370 bp, respectively. Over-expression of $VEGF_{165}$ was detected in gastric cancer mucosae, and the over-expression rate was 58%, whereas 16% in normal paired mucosae. The mean value of the $VEGF_{165}$mRNA expression in gastric cancer tissues was significantly higher than that in normal paired tissues, which was 1.125±0.356 and 0.760±0.278 respectively (Figure 1 and Table 1).

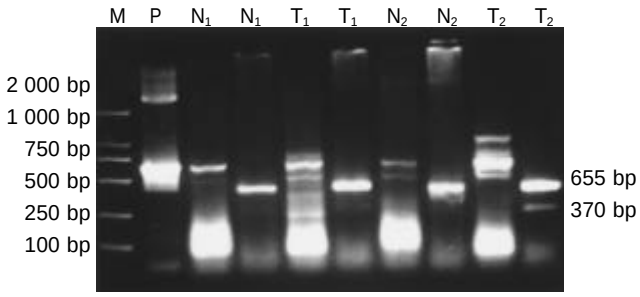

Figure 1 RT-PCR products of $VEGF_{165}$mRNA by 20 g/L agarose gel electrophoresis. M, marker; P, recombined plasmid of $VEGF_{165}$; T, gastric cancer mucosae; N, non-gastric cancer mucosae; ', β-actin. The product of $VEGF_{165}$ mRNA was 655 bp, and the product of β-actin was 370 bp.

Relationship between expression of $VEGF_{165}$mRNA and clinical pathological features of gastric cancer

As shown in Table 2, the expression level of $VEGF_{165}$mRNA in the group of positive lymph node metastasis was higher than that in the group of negative lymph node metastasis (P<0.05), and the expression level in stages III and IV was also higher than that in stages I and II (P<0.05). The expression levels had no correlation with age, sizes of tumors and degree of histological differentiation.

Another observation shown in Table 3 and Table 4 was that the rate of lymph node metastasis and the ratio of stages III and IV in the group with over-expression of $VEGF_{165}$ mRNA were also higher than those in the group with low-expression of $VEGF_{165}$ mRNA (83.3% *vs* 46.2%, 77.8% *vs* 30.8% respectively, P<0.05).

Correlation between VEGF and iNOS in gastric cancer

Positive immmunostaining for iNOS and VEGF was observed in cancer cells, and weakly positive or negative staining was observed in the normal gastric epithelial tissues. VEGF and iNOS immunoreactivity was located mainly in the cytoplasm and cell membrane (Figure 2). The positive expression rate of iNOS was 58.8% (50/85), and that of VEGF was 75.4% (64/85). There were 50.1% (43/85) patients showing positive staining both for iNOS and VEGF, 16.5% (14/85) showing negative staining both for iNOS and VEGF. Correlation with the two factors was significant (P<0.05). But more intensive analysis by Kendall test showed that the immunoreactive grades of VEGF had no association with that of iNOS (P>0.05, see Table 5).

Table 1 Expression of $VEGF_{165}$mRNA in gastric cancer and non-cancerous mucosa by RT-PCR

No.	Sex	Age (yr)	Histological type	Depth of invasion	Lympho node metastasis	Stage of TNM	VEGFmRNA	
							T	N
1	M	67	PD	musclaris	-	I	1.286	0.782
2	M	67	WD	extraserosa	+	III	1.568	1.086
3	F	41	PD	serosa	+	III	1.624	0.925
4	M	54	PD	extraserosa	+	IV	0.815	0.729
5	M	35	PD	extraserosa	+	III	1.204	0.627
6	M	50	MD	extraserosa	+	III	1.111	0.335
7	F	34	WD	extraserosa	+	III	1.347	0.845
8	M	46	MD	serosa	+	III	0.785	0.701
9	M	60	WD	submucosae	-	I	0.833	0.807
10	F	70	WD	serosa	-	I	0.627	0.525
11	M	62	WD	serosa	+	IV	0.850	0.646
12	F	31	WD	mucosae	-	I	0.815	1.136
13	M	55	MD	extraserosa	+	IV	1.545	0.872
14	M	70	WD	serosa	+	II	0.765	0.577
15	M	64	MD	serosa	-	III	1.082	0.842
16	M	66	MD	serosa	+	III	1.069	0.422
17	M	77	PD	serosa	+	IV	1.383	10.28
18	M	40	PD	serosa	+	II	1.156	1.381
19	F	50	PD	serosa	+	II	0.989	0.874
20	M	52	PD	serosa	+	III	1.895	0.356
21	F	38	PD	extraserosa	+	III	1.667	0.759
22	F	68	WD	mucosae	-	I	0.884	0.682
23	F	53	WD	extraserosa	+	III	1.456	0.682
24	M	61	MD	extraserosa	+	III	1.574	0.098
25	M	43	PD	serosa	-	I	1.198	0.429
26	M	43	PD	serosa	+	III	0.368	0.994
27	M	57	PD	serosa	+	II	1.052	0.661
28	F	44	PD	mucosae	-	I	0.952	0.793
29	M	71	WD	extraserosa	-	II	0.750	0.728
30	M	77	PD	extraserosa	+	IV	1.375	10105
31	F	50	PD	mucosae	-	I	0.842	0.794
Mean value							1.125	0.760

Table 2 Relationship between expression of $VEGF_{165}$mRNA and clinical pathological features in gastric cancer tissue

Variable	No	Expression of VEGF (mean±SD)	
Age (yr)			
<55	16	1.139±0.393	P>0.05
>55	15	1.139±0.393	
Sizes of tumor			
≤2 cm	2	0.993±0.271	P>0.05
2-3 cm	6		
>3 cm	23	1.171±0.375	
Histological type			
Well differentiated	10	0.979±0.339	P>0.05
Moderate or poorly differentiated	21	1.1937±0.350	
Lymph node metastasis			
Positive	21	1.219±0.377	P=0.03
Negative	10	0.927±0.205	
Stage of UICC			
I	8	0.934±0.194	P=0.009
II	5		
III	13	1.262±0.386	
IV	5		

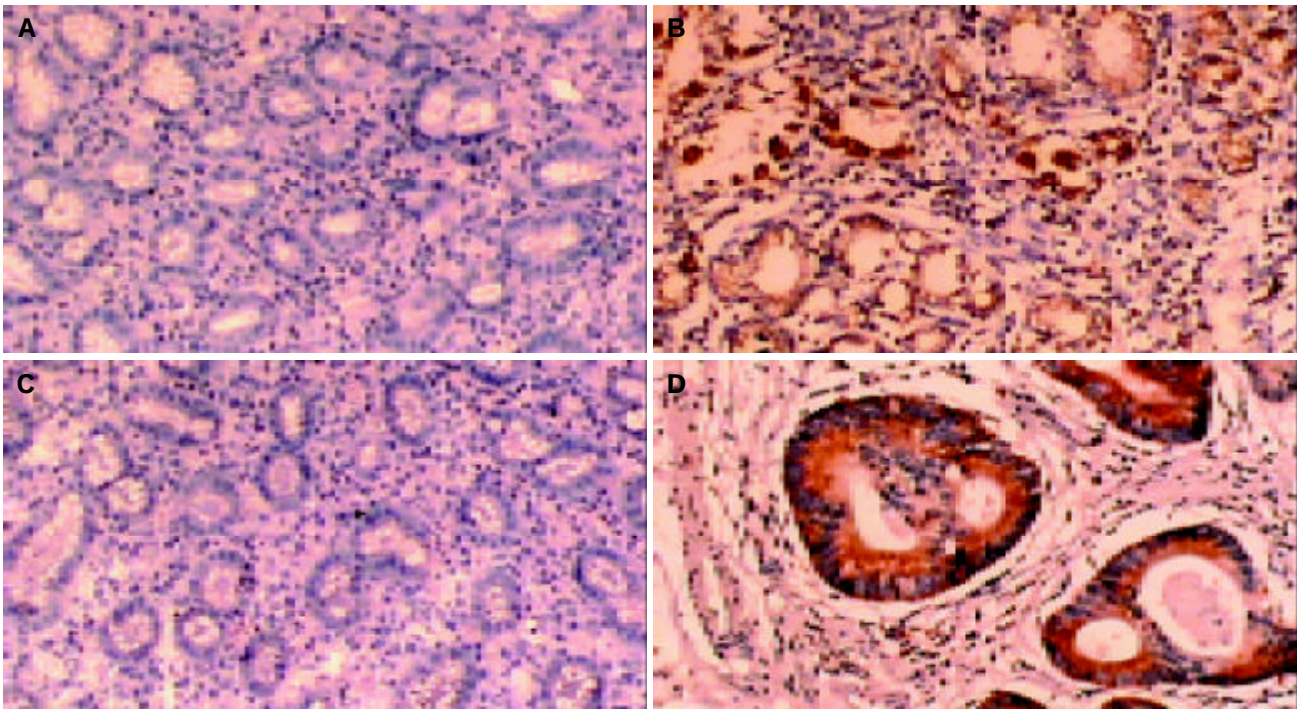

Figure 2 Immmunostaining of VEGF and iNOS in gastric cancer and normal paired tissues. A: Negative staining of VEGF in normal paired gastric mucosae (×100), B: Positive staining of VEGF in gastric cancer (×100), C: Negative staining of iNOS in normal paired gastric mucosae (×100), D: Positive staining of iNOS in gastric cancer (×100).

Table 3 Relationship between level of $VEGF_{165}$mRNA expression and lymph node metastasis

Variable	Lymph node metastasis			
	Positive cases	Negative cases	Total rate	Metastasis
Over-expression	15	3	18	83.3%
Low-expression	6	7	13	46.2%
Total	19	10	31	

χ^2=4.775, *P*=0.02.

Table 4 Relationship between level of $VEGF_{165}$mRNA expression and stages of UICC

Variable	Stages of UICC		Total	Ratio of III+IV
	I+II	III+IV		
Over-expression	4	14	18	77.8%
Low-expression	9	4	13	30.8%
Total	13	18	31	

χ^2=6.85, *P*=0.009.

Table 5 Association with immunoreactive grades of VEGF protein and iNOS in gastric cancer

	VEGF (N)				
iNOS (N)	-	+	++	+++	Total
-	14	12	6	3	35
+	5	9	8	2	24
++	2	5	11	1	19
+++	0	2	3	2	7
Total	21	28	28	8	85

χ^2=5.615, *P*=0.132.

DISCUSSION

VEGF is well characterized by its potent, specific angiogenesis-promoting effect. Native VEGF is a basic, heparin-binding, homodimeric glycoprotein of M_r 43 000-46 000. Five human VEGF mRNA species encoding VEGF isoforms of 121, 145, 165, 189, and 206 amino acids have been identified by alternative splicing of VEGFmRNA. An important biological property that distinguishes the different VEGF isoforms is their heparin and heparin-sulfate binding ability. $VEGF_{165}$ is the predominant form. VEGF has been found to be a highly specific mitogen for endothelial cells, and a prime regulator of angiogenesis and vasculogenesis, and could also contribute to the development of tumors because of its ability to induce permeabilization of blood vessels[1,2,10,11]. Numerous studies have demonstrated that the high expression level of VEGF in many kinds of tumor cells[12-14]. The same observations have also been seen in gastric cancer cells by *in vitro* and *in vivo*[3-6,15,16]. We tested $VEGF_{165}$mRNA expression in 31 cases of resected gastric cancer specimens and normal paired gastric mucosae by RT-PCR, the results showing that the mean expression of $VEGF_{165}$mRNA in gastric cancer was significantly higher than that of normal paired mucosae. VEGF in high expression could combine with its receptors Flt-1 or KDR to exert its powerful function of promoting angiogenesis[1,2,10]. Furthermore, some studies showed the high expression of Flt-1 and KDR in gastric tumor specimens by RT-PCR and immunohistochemistry, and exogenous $VEGF_{165}$ stimulated the growth of KDR positive carcinoma cells[17,18]. These findings indicate there is a possible autocrine pathway for VEGF in gastric cancer, which is very important in the development of gastric cancer.

VEGF induces the formation of fenestrations in blood vessels and vesiculo -vocuolar organelles that form channels through which blood-borne proteins can extravasate. This could lead to the formation of an extravascular fibrin gel, which provides a matrix that supports the growth of endothelial cells and tumor cells and allows invasion of stromal cells into the development of tumors[2]. A substantial number of studies have demonstrated a strong association between elevated tumor

expression of VEGF and advanced disease or poor prognosis in various cancers[1,2]. In our study, the expression of $VEGF_{165}$mRNA was well related with lymph node metastasis and TNM stage, $VEGF_{165}$mRNA elevated in lymph node positive or stages III and IV patients, and was consistent with many immunohistochemical results. Kakeji *et al*.[4] also revealed VEGF to be an independent prognostic factor and independent risk factor for liver metastasis. Karayiannakis *et al*.[19] showed there was a significant association between serum VEGF levels and disease stage, as well as invasion depth of the tumor and the presence of distant metastasis. It was concerned with the invasiveness and metastasis of gastric cancer, and might be predictive of tumor status and prognosis in advanced gastric cancer patients, and could provide new prognostic information not afforded by conventional clinicopathologic prognostic indicators[20-24].

Early gastric cancer patients have high survival rates, but there is lymph node metastasis in early gastric cancer, especially in submucosa, the rate of lymph node metastasis was about 20%, resulting in the decrease of 5-year survival of early gastric cancers. In our study, the expression of $VEGF_{165}$mRNA in the 5 cases of early gastric cancer had no difference with the normal paired mucosae, which the mucosae or submucosae were invaded, and lymph node metastasis was negative in the 5 cases. Recently Amioka *et al*. demonstrated VEGF was associated with lymphatic invasion and lymph node metastasis in early gastric cancer[25-27]. The clinical significance of VEGF expression in early gastric cancer should be intensively studied.

VEGF production has been found to be regulated by growth factors, cytokines, oncogenes, anti-oncogenes and other extra cellular molecules, such as hypoxia, p53 gene, TGF-α[28-32]. But few investigations have been concerned with relationship between VEGF and iNOS. Nitric oxide produced through iNOS induction could enhance vasodilation, increase vascular permeability and accelerate nutrient supply of tumor tissues and promote neovascularization, thereby facilitating tumor growth[7,8]. It has been shown that the expression of iNOS in most tumor tissues was higher than that in normal tissues. There were many reports concerning the high expression of iNOS in gastric cancer, which increased with the stage of the cancer and lymph node metastasis[7,8,33]. We found the expression rate of iNOS in gastric cancer was 58.8%, and iNOS and VEGF had co-expressions in 50.1% of the patients, there was a correlation between the two factors. According to some reports[34], VEGF could induce the release of NO from endothelial cells, on the other hand, endogenous NO enhanced VEGF synthesis in rat vascular smooth muscle cells; Host expression of NOS could contribute to induction of NOS in tumor and melanoma growth in mice, possibly by regulating the amount and aviality of VEGF. The positive interaction between endogenous NO and VEGF might have implications for endothelial regeneration[35]. Kisley *et al*.[36] examined the effect of iNOS deficiency on VEGF protein concentration in mouse lung tumors, and showed VEGF concentration was lower than 54% in lung tumors isolated from iNOS(-/-)mice versus controls(wild-type +/+). NO enhanced the transcription of VEGF gene by inducing HIF-1 (hypoxia -inducible factor-1) binding activity in glioblastoma A-172 cells and hepatoma Hep3B cells. HIF was the best-characterized regulator of VEGF gene transcription[37]. The high coincidental expression of iNOS and VEGF protein accumulation may be important events to enhance gastric carcinogenesis and poor clinical features. But in our present work, more intensive analysis showed that the immunoreactive grades of VEGF were no association with that of iNOS, indicating that many other factors may induce the production and angiogenesis of VEGF besides iNOS in gastric cancer.

REFERENCES

1 **Ferrara N**. Role of Vascular Endothelial Growth Factor in the Regulation of Angiogenesis. *Kidney International* 1999; **56**: 794-814

2 **Neufeld G**, Cohen T, Gaengrinovitch S, Poltorak AZ. Vascular endothelial growth factor (VEGF) and its receptors. *The FASEB Journal* 1999; **13**: 9-22

3 **Tian X**, Song S, Wu J, Meng L, Dong Z, Shou C. Vascular endothelial growth factor: acting as an autocrine growth factor for human gastric adenocarcinoma cell MGC803. *Biochem Biophys Res Commun* 2001; **286**: 505-512

4 **Kakeji Y**, Koga T, Sumiyoshi Y, Shibahara K, Oda S, Maehara Y, Sugimachi K. Clinical significance of vascular endothelial growth factor expression in gastric cancer. *J Exp Clin Cancer Res* 2002; **21**: 125-129

5 **Liu DH**, Zhang XY, Fan DM, Huang YX, Zhang JS, Huang WQ, Zhang YQ, Huang QS, Ma WY, Chai YB, Jin M. Expression of vascular endothelial growth factor and its role in oncogenesis of human gastric carcinoma. *World J Gastroenterol* 2001; **7**: 500-505

6 **Ichikura T**, Tomimatsu S, Ohkura E, Mochizuki H. Prognostic significance of the expression of vascular endothelial growth factor (VEGF) and VEGF-C in gastric cancer. *J Surg Oncol* 2001; **78**: 132-137

7 **Rajnakova A**, Moochhala S, Goh PM, Ngoi S. Expression of nitric oxide synthase,cyclooxygenase, and p53 in different stages of human gastric cancer. *Cancer Lett* 2001; **172**: 177-185

8 **Feng CW**, Wang LD, Jiao LH, Liu B, Zheng S, Xie XJ. Expression of p53, inducible nitric oxide synthase and vascular endothelial growth factor in gastric precancerous lesion:correlation with clinical features. *BMC Cancer* 2002; **2**: 8-15

9 **Tisher E**, Mitchell R, Hartman T, Silva M, Gospodarowicz D, Fiddes JC, Abraham JA. The human gene for vascular endothelial growth factor. Multiple protein forms are encoded through alternative exon splicing. *J Biol Chem* 1991; **266**: 11947-11954

10 **Ferrara N**, Gerber H, LeCouter J. The biology of VEGF and its recetors. *Nat Med* 2003; **9**: 669-676

11 **Bates DO**, Harper SJ. Regulation of vascular permeability by vascular endothelial growth factors. *Vascul Pharmacol* 2002; **39**: 225-237

12 **Whang YE**, Godley PA. Renal cell carcinoma. *Curr Oin Oncol* 2003; **15**: 213-216

13 **Shinkaruk S**, Bayle M, Lain G, Deleris G. Vascular endothelial growth factor (VEGF), an emerging target for cancer chemotherapy. *Curr Med Chem Anti Canc Agents* 2003; **3**: 95-117

14 **Mesters RM**. Angiogenesis in hematologic malignancies. *Ann Hematol* 2002; **81**: S72-74

15 **Song ZY**, Pang JP, Zhu YL, Qian KD, Zheng S. O-chloroacetylcarbamoyl fumagillol combined with 5-fluorouracil in suppression of the growth of gastric cancer. *Chin J Pharmacol Toxicol* 2003; **17**: 24-28

16 **Du JR**, Jiang Y, Zhang YM, Fu H. Vascular endpthelial growth factor and microvascular density in esophageal and gastric carcinomas. *World J Gastroenterol* 2003; **9**: 1604-1606

17 **Ren J**, Dong L, Xu CB, Pan BR. The role of KDR in the interations between human gastric carcinoma cell and vascular endothelial cell. *World J Gastroenterol* 2002; **8**: 596-601

18 **Zhang H**, Wu J, Meng L, Shou CC. Expression of vascular endothelial growth factor and its receptors KDR and Flt-1 in gastric cancer cells. *World J Gastroenterol* 2002; **8**: 994-998

19 **Karayiannakis AJ**, Syrigos KN, Polychronidis A, Zbar A, Kouraklis G, Simopoulos C, Karatzas G. Circulating VEGF levels in the serum of gastric cancer patients: correlation with pathological variables, patient survival, and tumor surgery. *Ann Surg* 2002; **236**: 37-42

20 **Kimura H**, Konishi K, Nukui T, Kaji M, Maeda K, Yabushita K, Tauji M, Miwa A. Prognostic significance of expression of thymidine phosphorylase and vascular endothelial growth factor in human gastric carcinoma. *J Surg Oncol* 2001; **76**: 31-36

21 **Maehara Y**, Kabashima A, Koga T, Tokunaga E, Takeuchi H, Kakeji Y, Sugimachi K. Vascular invasion and poential for tumor angiogenesis and metastasis in gastric carcinoma. *Surgery* 2000; **128**: 408-416

22 **Saito H**, Tsujitani S, Kondo A, Ikeguchi M, Maeta M, Kaibara N. Expression of vascular endothelial growth factor correlated with hematogenous recurrence in gastric carcinoma. *Surgery* 1999; **125**: 195-201
23 **Ohta M**, Konno H, Tanaka T, Baba M, Kamiya K, Syouji T, Kondoh K, Watanabe M, Terada M, Nakamura S. The significance of circulating vascular endothelial growth factor (VEGF) protein in gastric cancer. *Cancer Lett* 2003; **192**: 215-225
24 **Poon RT**, Fan ST, Wong J. Clinical significance of angiogenesis in gastrointestinal cancers: a target for novel prognostic and therapeutic approaches. *Ann Surg* 2003; **238**: 9-28
25 **Amioka T**, Kitadai Y, Tanaka S, Haruma K, Yoshihara M, Yasui W, Chayama K. Vascular endothelial growth factor-C expression predicts lymph node metastasis of human gastric carcinomas invading the submucosa. *Eur J Cancer* 2002; **38**: 1413-1419
26 **Maeda K**, Kang SM, Onoda N, Ogawa M, Kato Y, Sawada T, Chung KH. Vascular endothelial growth factor expression in preoperative biopsy specimens correlates with disease recurrence in patients with early gastric carcinoma. *Cancer* 1999; **86**: 566-571
27 **Konno H**, Baba M, Tanaka T, Kamiya K, Ota M, Oba K, Shoji A, Kaneko T, Nakamura S. Overexpression of vascular endothelial growth factor is responsible for the hematogenous recurrence of early-stage gastric cancinoma. *Eur Surg Res* 2000; **32**: 177-181
28 **Kim YB**, Han JY, Kim TS, Kim PS, Chu YC. Overexpression of c-H-ras p21 is correlated with vascular endothelial growth factor expression and neovascularization in advanced gastric carcinoma. *J Gastroenterol Hepatol* 2000; **15**: 1393-1399
29 **Saito H**, Tujitani S, Ikeguchi M, Ikeguchi M, Maeta M, Kaibara N. Neoagogenesis and relationship to nuclear p53 accumulation and vascular endothelial growth factor expression in advanced gastric carcinoma. *Oncology* 1999; **57**: 164-172
30 **Yamakawa M**, Liu LX, Date T, Belanger AJ, Vincent KA, Akita GY, Kuriyama T, Cheng SH, Gregory RJ, Jiang C. Hypoxia-inducible factor-1 mediates activation of cultured vascular endothelial cells by inducing multiple angiogenic factors. *Circ Res* 2003; **93**: 664-673
31 **Joo TE**, Sohn YH, Joo SY, Lee WS, Min SW, Park CH, Rew JS, Choi SK, Park CS, Kim YJ, Kim SJ. The role of vascular endothelial growth factor (VEGF) and p53 status for angiogenesis in gastric cancer. *Korean J Intern Med* 2002; **17**: 211-219
32 **Joo YE**, Rew JS, Seo YH, Choi SK, Kim YJ, Park CS, Kim SJ. Cyclooxygenase-2 overexpression correlates with vascular endothelial growth factor expression and tumor angiogenesis in gastric cancer. *J Chin Gastroenterol* 2003; **37**: 28-33
33 **Song ZJ**, Gong P, Wu YE. Relationship between the expression of iNOS, VEGF, tumor angiogenesis and gastric cancer. *World J Gastroenterol* 2002; **8**: 591-595
34 **DulaK J**, Jozkowicz A, Dembinska KA, Guevara I, Zdzienicka A, Zmudzinska GD, Florek I, Wojtowicz A, Szuba A, Cooke JP. Nitric oxide induces the synthesis of vascular endothelial growth factor by rat vascular smooth muscle cells. *Arterioscler Thromb Vasc Biol* 2000; **20**: 659-666
35 **Konopka TE**, Barker JE, Bamford TL, Guida E, Anderson RL, Stewart AG. Nitric oxide synthase II gene disruption–Implications for tumor growth and vascular endothelial growth factor production. *Cancer Res* 2001; **61**: 3182-3187
36 **Kisley LR**, Barrett BS, Bauer AK, Dwyer Nield LD, Barthel B, Meyer AM, Thompson DC, Malkinson AM. Genetic ablation of inducible nitric oxide synthase decreases mouse lung tumorigenesis. *Cancer Res* 2002; **62**: 6850-6856
37 **Kimura H**, Weisz A, Kurashima Y, Hashimoto K, Ogura T, D'Acquisto F, Addeo R, Makuuchi M, Esumi H. Hypoxia response element of the human vascular endothelial growth factor gene mediates transcriptional regulation by nitric oxide: control of hypoxia-inducible factor-1 activity by nitric oxide. *Blood* 2000; **95**: 189-197

Edited by Zhao M and Wang XL **Proofread by** Xu FM

PO Box 2345, Beijing 100023, China
Fax: +86-10-85381893
E-mail: wjg@wjgnet.com www.wjgnet.com

World J Gastroenterol 2004;10(9):1256-1261
World Journal of Gastroenterology
Copyright ©2004 by The WJG Press ISSN 1007-9327

• GASTRIC CANCER •

Association of tumor necrosis factor genetic polymorphism with chronic atrophic gastritis and gastric adenocarcinoma in Chinese Han population

Bao-Ying Fei, Bing Xia, Chang-Sheng Deng, Xiao-Qing Xia, Min Xie, J Bart A Crusius, A Salvador Pena

Bao-Ying Fei, Department of Gastroenterology, Zhejiang Provincial People's Hospital, Hangzhou 310014, Zhejiang Province, China
Bing Xia, Chang-Sheng Deng, Department of Gastroenterology, Wuhan University Zhongnan Hospital, Wuhan 430071, Hubei Province, China
Xiao-Qing Xia, Min Xie, Department of Tumor Surgery, Hubei Provincial Tumor Hospital, Wuhan 430071, Hubei Province, China
J Bart A Crusius, A Salvador Pena, Laboratory of GI immunogenetics Vrije Universiteit Medical Center, Amsterdam, The Netherlands
Supported by a grant from provincial public health bureau, Hubei Province, No. 97420
Correspondence to: Dr Bao-Ying Fei, Department of Gastroenterology, Zhejiang Provincial People's Hospital, Hanzhou 310014, Zhejiang Province, China. feibaoying6924@tom.com
Telephone: +86-571-85239988 **Fax:** +86-571-85131448
Received: 2003-11-18 **Accepted:** 2003-12-16

Abstract

AIM: To investigate the association of TNF polymorphisms with chronic atrophic gastritis (CAG) and gastric adenocarcinoma in Chinese Han patients.

METHODS: The TNFa-e 5 microsatellites and 3 RFLP sites were typed using PCR technique, followed by high-voltage denaturing PAGE with silver staining and restriction enzyme digestion respectively in specimens from 53 patients with CAG and 56 patients with gastric adenocarcinoma and 164 healthy controls. The PCR products were cloned and sequenced.

RESULTS: The frequency of TNF-β NcoI*1/2 genotype was higher in patients with chronic atrophic gastritis than in healthy controls, but no significant difference was observed (60.38% *vs* 46.34%, P=0.076). The frequency of TNa10 allele was significantly higher in patients with chronic atrophic gastritis than in healthy controls (19.81% *vs* 11.89%, P=0.04). However, it did not relate to age, gender, atrophic degree or intestinal metaplasia in patients with chronic atrophic gastritis. The frequency of TNF-β NcoI*1/2 and d2/d6 genotypes were significantly higher in patients with gastric adenocarcinoma than in healthy individuals(P>0.05). However, TNF-β NcoI*1/2 and d2/d6 genotypes did not relate to age, gender, grade of differentiation and clinicopathologic stage in patients with gastric adenocarcinoma. The frequency of TNFa6b5c1 haplotype homozygote was significantly lower in patients with gastric adenocarcinoma than in healthy controls (1.79% *vs* 15.85%, P=0.006).

CONCLUSION: TNFa10 allele may be a risk factor for chronic atrophic gastritis. TNF-β NcoI*1/2 and d2/d6 genotypes are associated with the susceptibility to gastric adenocarcinoma, whereas TNFa6b5c1 haplotype homozygote may contribute to the resistance against gastric adenocarcinoma.

Fei BY, Xia B, Deng CS, Xia XQ, Xie M, Crusius JBA, Pena AS. Association of tumor necrosis factor genetic polymorphism with chronic atrophic gastritis and gastric adenocarcinoma in Chinese Han population. *World J Gastroenterol* 2004; 10(9): 1256-1261
http://www.wjgnet.com/1007-9327/10/1256.asp

INTRODUCTION

Gastric adenocarcinoma is one of the most frequent malignant diseases in the world, but the causes of gastric cancer remains unclear. The crude mortality rate of stomach cancer in China was 25.2 per 10^5 (32.8 per 10^5 for males and 17.0 per 10^5 for females), which comprised 23.2% of the total death of cancer from 1990 to 1992, making stomach cancer the leading cause of the death among cancers[1].

Tumor necrosis factor (TNF) is a multifunctional cytokine and its anti-tumor effect has attracted particular attention. TNF was found at a higher concentration in patients with malignant tumor. Forones *et al*.[2] reported increased TNF-α expression in the sera of patients with advanced gastric cancer. TNF-α mRNA was markedly increased in gastric carcinoma tissue[3]. Recombinant TNF has been demonstrated to have considerable treatment effect on gastric cancer *in vitro*[4,5].

The gene for TNF-α and lymphotoxin-α (TNF-β), referred to as the TNF locus, are tandemly arranged within a 7-kilobase region in the HLA on the short arm of chromosome 6. HLA has recently been found to contribute to cancer development[6-9]. Several RFLP sites and 5 microsatellites within the TNF gene have been identified. Some studies have shown that TNF individual alleles were correlated to secretion from activated monocytes[10-13]. Furthermore, some experiments found that TNF secretion was also associated with TNF haplotypes, not only individual alleles[14]. These findings suggest that TNF polymorphisms may play a role in the pathogenesis of several autoimmune, infectious and neoplastic diseases.

Chronic atrophic gastritis (CAG) is believed to be the precancerous lesion of gastric adenocarcinoma. In the present study, we examined whether TNF genetic polymorphisms were associated with CAG and gastric adenocarcinoma in Chinese Han population. Additionally, we determined whether the associations between TNF genetic polymorphisms and CAG and gastric adenocarcinoma varied with clinicopathologic features of the 2 diseases.

MATERIALS AND METHODS

Patients and genomic DNA extraction

The subjects of this study included 56 patients with gastric adenocarcinoma (43 males, 13 females; mean age 55.6±12.2 years), 53 patients with CAG (32 males, 21 females; mean age 53.5±11.4 years), and 164 unrelated healthy individuals (113 males, 51 females; mean age 52.5±11.3 years) from Chinese Han population in Hubei province of China. The diagnoses of gastric adenocarcinoma and CAG were confirmed by histopathology examinations. Genomic DNA was extracted

from venous blood by a salting out procedure with minor modifications.

TNF polymorphism typing

Five microsatellites were amplified using a single step PCR reaction with primers described by Pociot *et al*.[15]. TNF microsatellite alleles were typed by a 60 g/L polyacrylamide, 0.4-mm sequencing gel, followed by silver nitrate staining. Fragments were sized using DNA markers and simultaneously typed with known alleles derived from the cloned PGEM-T vector.

The sites in the first intron of TNF-β marked by AspH1 and *Nco*1 were analyzed using PCR and endonuclease digestion. BSIHKA1, an isoschizomer of AspH1 (New England Biolabs, Beverley, MA) was used instead of AspH1. The digested products were electrophoresed in 1 g/L ethidium bromide-stained 15 g/L agarose gels. Similarly, the TNF-308 polymorphism was examined by PCR amplification and *Nco1* digestion. The digested products were separated on a 100 g/L non-denaturing polyacrylamide gel. Alleles were visualized as described for TNF microsatellite typing.

Cloning and sequencing

The PCR products of 5 microsatellites were purified and ligated with PGEM-T vector. High efficiency JM 109 competent cells were used in the process of transformation. Needed transformants were obtained by blue/white color screening and standard ampicillin selection. Recombinant plasmid DNA were isolated and identified. Sequencing was done on ABI 377 DNA sequencer.

Statistical analysis

Allele frequencies in patients and control groups were calculated by direct counting. The Chi-square test and Fisher's exact test were used for statistical analysis. Hardy-Weiberg equilibrium was tested in a 2×n analysis using Chi-Square.

RESULTS

The frequencies of the various alleles at 8 TNF polymorphic sites in 3 groups are shown in Table 1. The frequency of TNFa10 allele was significantly higher in patients with CAG than in healthy controls (19.81% *vs* 11.89%, *P*=0.04, OR=1.83, 95%CI

Table 1 Distribution frequency of TNF alleles at 8 polymorphic loci in CAG, gastric adenocarcinoma and healthy controls

TNF locus	Allele	Size (bp)	Controls (*n*=164)	CAG (*n*=53)	Gastric adenocarcinoma (*n*=56)	*P*
TNFa	a1	97	0.0183	0.0094	0.0089	
	a2	99	0.1583	0.1698	0.2054	
	a3	101	0.0000	0.0094	0.0268	
	a4	103	0.0061	0.0094	0.0178	
	a5	105	0.0396	0.0378	0.0089	
	a6	107	0.3811	0.3585	0.3928	
	a7	109	0.0793	0.0378	0.0536	
	a8	111	0.0061	0.0094	0.0000	
	a9	113	0.0335	0.0566	0.0152	
	a10	115	0.1189	0.1981*	0.1161	0.040
	a11	117	0.0945	0.0660	0.0803	
	a12	119	0.0091	0.0000	0.0000	
	a13	121	0.0549	0.0378	0.0152	
TNFb	b1	125	0.1006	0.0755	0.1339	
	b2	126	0.0000	0.0000	0.0000	
	b3	127	0.1128	0.0943	0.0536	
	b4	128	0.3293	0.3585	0.3482	
	b5	129	0.4512	0.4717	0.4643	
	b6	130	0.0000	0.0000	0.0000	
	b7	131	0.0061	0.0000	0.0000	
TNFc	c1	159	0.2104	0.7264	0.7679	
	c2	161	0.7896	0.2736	0.2321	
TNFd	d1	124	0.0061	0.0094	0.0000	
	d2	126	0.0548	0.0755	0.0536	
	d3	128	0.0457	0.0566	0.0446	
	d4	130	0.3537	0.3774	0.3393	
	d5	132	0.1341	0.1226	0.1786	
	d6	134	0.3018	0.2925	0.2857	
	d7	136	0.0000	0.0000	0.0000	
	d8	138	0.1037	0.0660	0.0982	
TNFe	e1	99	0.0640	0.0755	0.0000	
	e3	103	0.8110	0.8302	0.7768	
	e4	105	0.1159	0.0660	0.1250	
TNF-α 308	1		0.9329	0.9434	0.9732	
	2		0.0671	0.0566	0.0268	
TNF-β Nco1	1		0.4817	0.4528	0.4464	
	2		0.5183	0.5472	0.5536	
TNF-β AspH1	1		0.3079	0.3302	0.3571	
	2		0.6921	0.6698	0.6429	

1.02-3.27). However, it was not related to age, gender, atrophic degree and intestinal metaplasia in patients with CAG (Table 2). The frequency of TNF-β NcoI*1/2 genotype was higher in patients with chronic atrophic gastritis than in healthy controls (Table 3). However no significant difference was observed (60.38% *vs* 46.34%, *P*=0.076).

The frequency of TNF-β NcoI*1/2 genotype was significantly higher in patients with gastric adenocarcinoma than in healthy controls (64.29% *vs* 46.34%, *P*=0.020, OR=2.08, 95%CI 1. 12-3.86). The frequency of d2/d6 genotype was also significantly higher in patients with gastric adenocarcinoma than in healthy individuals (10.71% *vs* 2.44%, *P*=0.028, OR=4.8, 95%CI 1.18-19.47). However, TNF-β NcoI*1/2 and d2/d6 genotypes were not related to age, gender, grade of differentiation and clinicopathologic stage in patients with gastric adenocarcinoma (Table 4).

Based on maximum likelihood estimate, 4 most frequent 3-locus haplotypes have been described in 4 European populations: TNFa11b4c1, TNFa2b1c2, TNFa6b5c1, TNFa10b4c1. These haplotypes have also been observed in our study. By analysis of 2 locus association, we established 5 extended haplotypes which integrated alleles across the TNF locus in our population: TNFa6b5c1d8e4TNF308-1TNF β Nco1-1TNFAspH1-2, TNFa2b1c2d5e1TNF308-1TNF β Nco1-2TNFAspH1-2, TNFa11b4c1d4e3TNF308-1TNF β Nco1-2TNFAspH1-1, TNFa10b4c1d4e3TNF308-1TNF β Nco1-2TNFAspH1-1, TNFa2b3c1d2e3TNF308-2TNFAspH1-2. There were no significant differences in haplotype frequencies between CAG, gastric adenocarcinoma, and control groups for these haplotypes. However the frequency of TNFa6b5c1 haplotype homozygote was significantly lower in patients with gastric adenocarcinoma than in healthy individuals (1.79% *vs* 15.85%, *P*=0.006). It was not related to age, gender, grade of differentiation and clinicopathologic stage in patients with gastric adenocarcinoma.

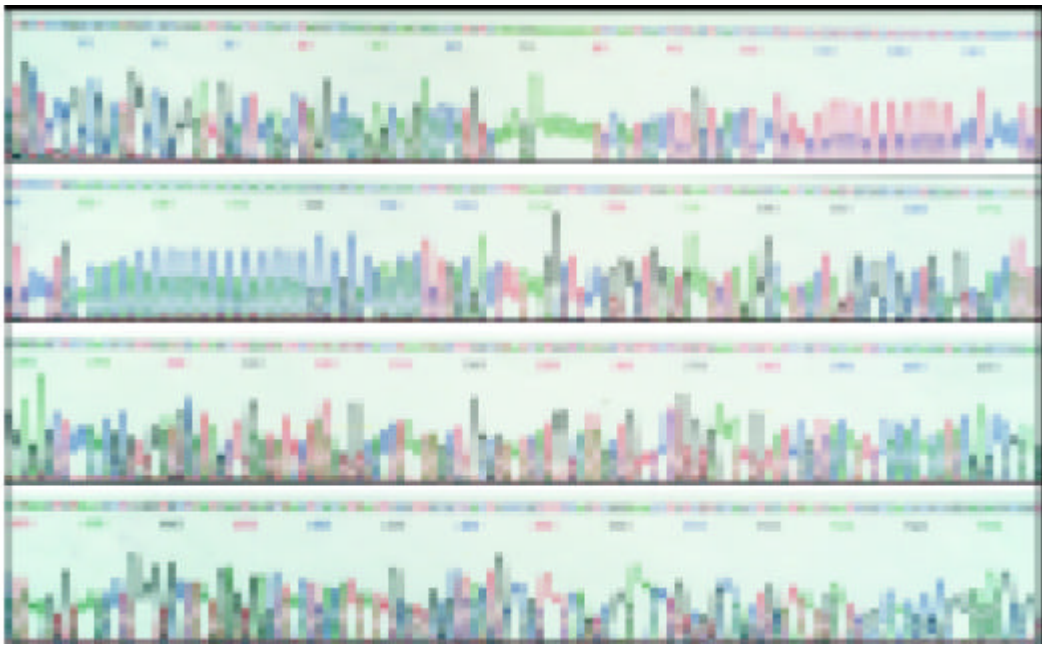

Figure 1 Nucleotide sequence of the cloned PGEM-T vector comprising TNFa6 allele (135→241) and TNFb5 allele (29→157), 150→179 fragment is 15 (AC / GT) repeats, 107→127 fragment is 10.5 (TC / GA) repeats.

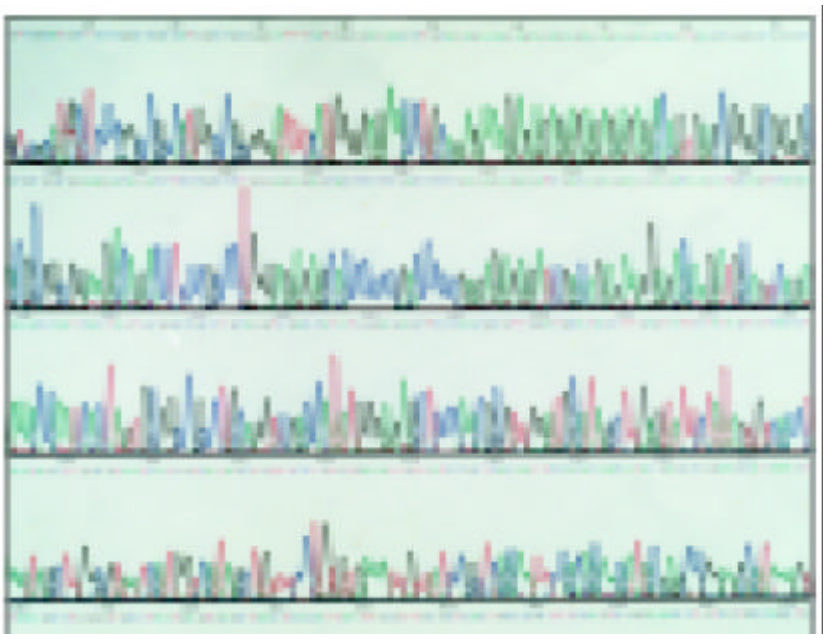

Figure 2 Nucleotide sequence of the cloned PGEM-T vector comprising TNFc1 allele (35→193), 59→76 fragment is 9 (TC / GA) repeats.

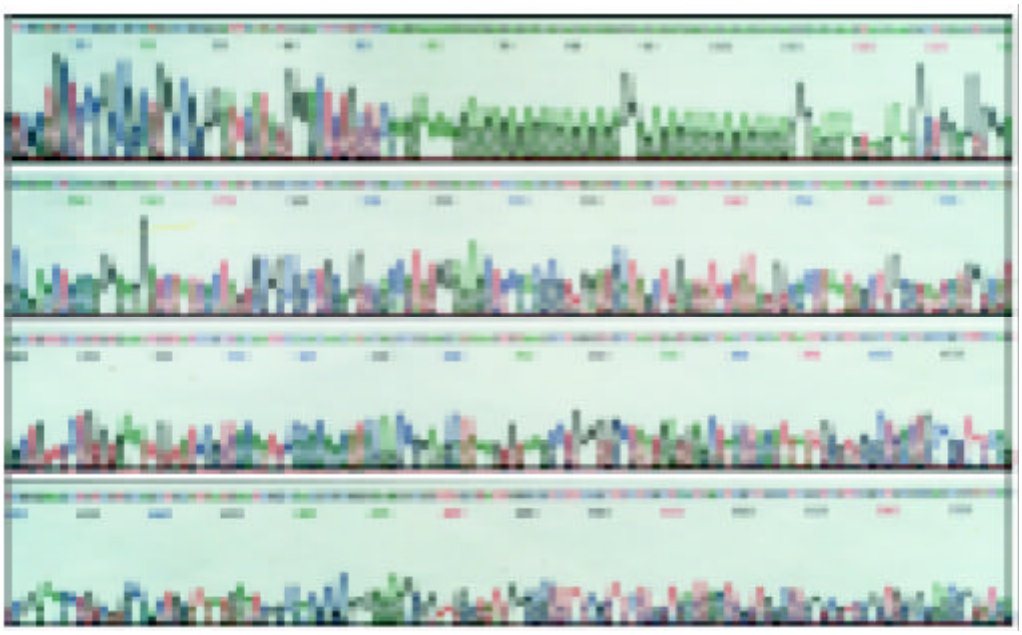

Figure 3 Nucleotide sequence of the cloned PGEM-T vector comprising TNFd4 allele (34→163), 64→85 fragment is 11 (TC / GA) repeats.

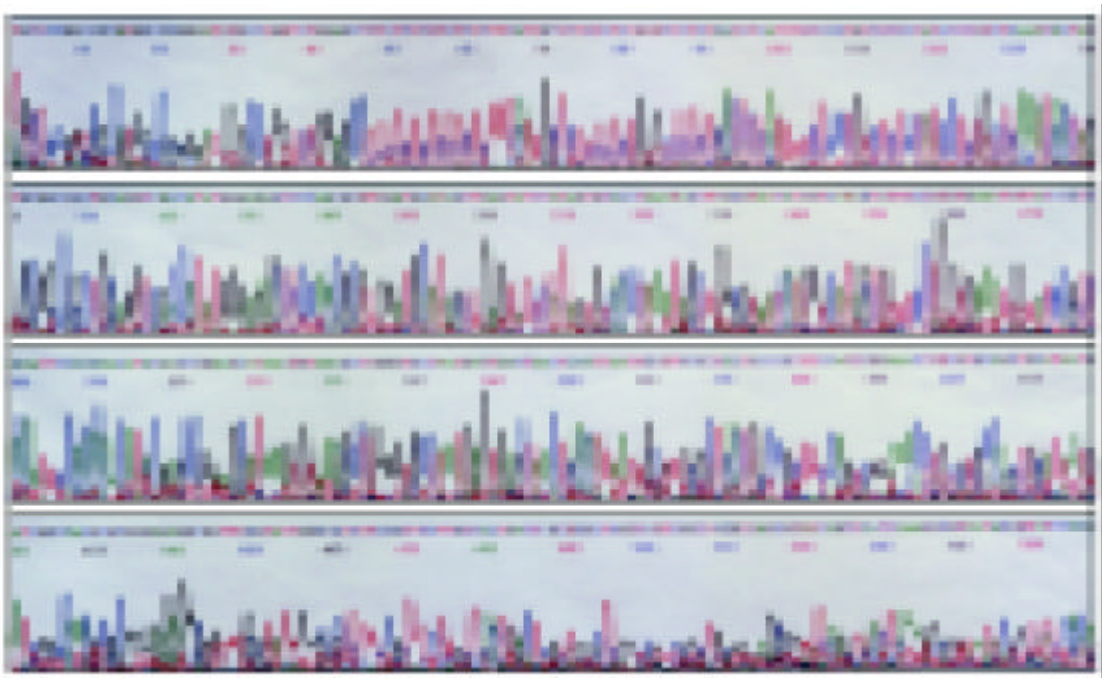

Figure 4 Nucleotide sequence of the cloned PGEM-T vector comprising TNFe3 allele (29→131), 47→62 fragment is 8 (TC / GA) repeats.

Table 2 Association between TNFa10 allele and clinical features of CAG

Groups	Age	Gender		Atrophic degree			Intestinal metaplasia	
	(yr)	M	F	Mild	Moderate	Severe	Positive	Negative
TNFa10+	53.9±9.6	13	8	3	12	6	14	7
TNFa10-	53.2±12.5	19	13	6	18	8	22	10

Table 3 Distribution frequency of TNF TNF-β Ncol*1 / 2 and TNFd2 / d6 genotypes in CAG, gastric adenocarcinoma and healthy controls

Group	TNF-β Ncol*1 / 2		TNFd2 / d6	
	+	-	+	-
Controls	76	88	4	160
CAG	32	21	2	51
Gastric adenocarcinoma	36[a]	20	6[c]	50

[a]$P<0.05$ *vs* compared with control group of TNF-β Ncol*1 / 2, [c]$P<0.05$ *vs* compared with control group of TNFd2 / d6.

Table 4 Association between d2/d6 and TNF-β Ncol*1/2 genotypes and clinical features of gastric adenocarcinoma

Group	Age	Gender		Grade of differentiation		Clinicopathologic stage	
	(yr)	M	F	High and moderate	Low	I-II	III-IV
d2/d6+	59.7±9.5	5	1	0	6	4	2
d2/d6-	55.1±12.5	38	12	13	37	21	29
1/2+	56.7±12.2	26	10	9	27	15	21
1/2-	53.6±11.5	17	3	4	16	10	10

The sequences of five TNF microsatellites (Figures 1-4) were consistent with that from a GeneBank database. However, several base exchanges were noted as following: TNFa at position 218 T→G, TNFc at 129 G→C, 170 A→G, TNFd at 87 G→A, 91 A→G, and TNFe at 81 C→T.

DISCUSSION

Genetic predisposition appears to be important in the pathogenesis of gastric adenocarcinoma. Genetic factors determining cancer risk have been postulated for the last decades and seem to be more apparent for gastric adenocarcinoma[16-21]. The relevant genes mediating the risk of gastric adenocarcinoma have not been identified until now. Progress of CAG towards gastric adenocarcinoma seems to be influenced by genetic factors[22,23].

A diallelic TNF-β polymorphism detected using the enzyme Ncol influences the TNF-α and/or -β secretion of peripheral blood mononuclear cells[24]. Park *et al*.[25] found that TNF-β Ncol*1/1 genotypes showed an increased risk for colorectal cancer, and that TNF-β*1 allele played some role in the initial step of tumorigenesis or activation of dormant tumor cells, whereas TNF-β*2 allele mediated some functions associated with cytotoxicity of tumor cells. Our result showed that the frequency of TNF-β Ncol*1/2 genotype was significantly higher in patients with gastric adenocarcinoma than in healthy individuals. It suggested that TNF-β Ncol*1/2 genotype was related to the pathogenesis of gastric cancer. At the same time we found the frequency of TNF-β Ncol*1/2 genotype was also high in patients with CAG. However, the association between TNF-β Ncol*1/2 genotype and CAG did not show a significant difference. Further studies are necessary to elucidate If TNF-β Ncol*1/2 genotype is a risk factor for CAG. The frequency of d2/d6 genotype was also significantly higher in patients with gastric adenocarcinoma than in healthy individuals. It indicated that d2/d6 genotype might have some effect on pathogenesis of gastric adenocarcinoma.

Azuma *et al*.[23] reported that the DQA1*0102 might contribute to resistance against *H pylori* associated gastric atrophy and immunogenetic factors were important in the etiology of *H pylori* associated gastric atrophy. Proinflammatory IL-1beta polymorphisms are associated with hypochlorhydria and atrophic gastritis in Japan[24]. The presence of the IL-1*C allele may also indicate a risk of mucosal atrophy of the stomach in the Japanese population[26]. Our study has shown an association between TNFa10 allele and CAG, but not between TNFa10 allele and gastric adenocarcinoma. It suggested that TNFa10 allele might be a host risk factor for CAG. However, it was not related to age, gender, atrophic degree and intestinal metaplasia in patients with CAG.

A significant reduction in high expressing haplotypes was found in patients with follicular lymphoma[27]. Hajeer *et al*.[28] reported the TNF a2-b4-d5 haplotype was significantly associated with the number of basal cell carcinoma (BCC) lesions. It provides the evidence that TNF microsatellite haplotype may influence the pathogenesis of multiple BCC. We found negative association between TNFa6b5c1 haplotype homozygote and gastric adenocarcinoma. The frequency of TNFa6b5c1 haplotype homozygote was lower in patients with gastric adenocarcinoma. It suggested that TNFa6b5c1 haplotype homozygote might contribute to the resistance against gastric adenocarcinoma. The absence of TNFa6b5c1 haplotype homozygote might increase the risk of gastric adenocarcinoma.

The TNF-α 308A allele has been associated with enhanced TNF-α expression[10]. Machado *et al*. proposed that individuals carrying TNF-α 308A allele had an increased risk for gastric cancer with an OR of 1.9[29]. However our results showed that there was no association between TNF-α 308 allele and gastric adenocarcinoma. Similarly, Wu *et al*. reported no association was noted between gastric cancer and controls in the distribution of TNF-α genotypes in Taiwanese Chinese population[30]. The discrepancy may be attributable to ethnic difference.

Onishi *et al*.[31] demonstrated a significantly favorable prognosis in the renal carcinoma patients with TNF-β1/1 homozygote compared with other zygotes of TNF-beta polymorphism. The patients with TNF-β1/1 homozygote showed much lower stage and/or grade than those of other zygotes. TNF polymorphisms TNF+488A and TNF-859T were associated with grade of tumour in patients with bladder cancer[32]. However, in our study TNF-β Ncol*1/2 and d2/d6 genotypes and TNFa6b5c1 haplotype were not related to age, gender, grade of differentiation and clinicopathologic stage in patients with gastric adenocarcinoma. Patients with d2/d6 genotype were present with a lowly differentiated tumor, however the difference did not reach statistical significance. Larger sample studies are needed.

The association between TNF genetic polymorphisms and CAG and gastric adenocarcinoma is not clear. However, 2 distinct potential mechanisms can be proposed. First, TNF alleles may be involved in genetically controlled variations in TNF production as previously described. Another possible explanation is that these genes are not responsible for the pathophysiological mechanisms but are linked closely to other responsible genes. TNF has been reported to be in linkage disequilibrium with HLA genes[33-35]. The negative association of TNFa3-e1 with rheumatoid arthritis may be secondary to the negative linkage disequilibrium between TNFa3-e1 and HLA-DR4[36]. Additional studies will be necessary to investigate whether TNF genes are independent of other linked genes to play a role.

With regard to several base exchanges in our sequencing result, more studies should be done to verify whether they are caused by ethnic difference or other factors.

REFERENCES

1 **Sun X**, Mu R, Zhou Y, Dai X, Qiao Y, Zhang S, Huangfu X, Sun J, Li L, Lu F. 1990-1992 mortality of stomach cancer in China. *Zhonghua Zhongliu Zazhi* 2002; **24**: 4-8

2 **Forones NM**, Mandowsky SV, Lourenco LG. Serum levels of interleukin-2 and tumor necrosis factor-alpha correlate to tumor progression in gastric cancer. *Hepatogastroenterology* 2001; **48**: 1199-1201

3 **Izutani R**, Katoh M, Asano S, Ohyanagi H, Hirose K. Enhanced expression of manganese superoxide dismutase mRNA and increased TNF alpha mRNA expression by gastric mucosa

in gastric cancer. *World J Surg* 1996; **20**: 228-233
4 **Wei XC**, Wang XJ, Chen K, Zhang L, Liang Y, Lin XL. Killing effect of TNF-related apoptosis inducing ligand regulated by tetracycline on gastric cancer cell line NCI-N87. *World J Gastroenterol* 2001; **7**: 559-562
5 **Buell JF**, Reed E, Lee KB, Parker RJ, Venzon DJ, Amikura K, Arnold S, Fraker DL, Alexander HR. Synergistic effect and possible mechanisms of tumor necrosis factor and cisplatin cytotoxicity under moderate hyperthermia against gastric cancer cells. *Ann Surg Oncol* 1997; **4**: 141-148
6 **Ghaderi M**, Nikitina Zake L, Wallin K, Wiklund F, Hallmans G, Lenner P, Dillner J, Sanjeevi CB. Tumor necrosis factor A and MHC class I chain related gene A (MIC-A) polymorphisms in Swedish patients with cervical cancer. *Hum Immunol* 2001; **62**: 1153-1158
7 **Juszczynski P**, Kalinka E, Bienvenu J, Woszczek G, Borowiec M, Robak T, Kowalski M, Lech-Maranda E, Baseggio L, Coiffier B, Salles G, Warzocha K. Human leukocyte antigens class II and tumor necrosis factor genetic polymorphisms are independent predictors of non-Hodgkin lymphoma outcome. *Blood* 2002; **100**: 3037-3040
8 **Gelder CM**, Williams OM, Hart KW, Wall S, Williams G, Ingrams D, Bull P, Bunce M, Welsh K, Marshall SE, Borysiewicz L. HLA class II polymorphisms and susceptibility to recurrent respiratory papillomatosis. *J Virol* 2003; **77**: 1927-1939
9 **Matsumoto K**, Yasugi T, Nakagawa S, Okubo M, Hirata R, Maeda H, Yoshikawa H, Taketani Y. Human papillomavirus type 16 E6 variants and HLA class II alleles among Japanese women with cervical cancer. *Int J Cancer* 2003; **106**: 919-922
10 **Wilson AG**, Symons JA, McDowell TL, McDevitt HO, Duff GW. Effects of a polymorphism in the human tumor necrosis factor α promoter on transcriptional activity. *Proc Natl Acad Sci U S A* 1997; **94**: 3195-3199
11 **Kaluza W**, Reuss E, Grossmann S, Hug R, Schopf RE, Galle PR, Maerker-Hermann E, Hoehler T. Different transcriptional production in psoriasis patients carrying the TNF-α 238A promoter polymorphism. *J Invest Dermatol* 2000; **114**: 1180-1183
12 **Fargion S**, Valenti L, Dongiovanni P, Scaccabarozzi A, Fracanzani AL, Taioli E, Mattioli M, Sampietro M, Fiorelli G. Tumor necrosis factor alpha promoter polymorphisms influence the phenotypic expression of hereditary hemochromatosis. *Blood* 2001; **97**: 3707-3712
13 **Baseggio L**, Bienvenu J, Charlot C, Picollet J, Felman P, Coiffier B, Salles G. Higher LPS-stimulated TNF-alpha mRNA levels in peripheral blood mononuclear cells from non-Hodgkin's lymphoma patients. *Exp Hematol* 2001; **29**: 330-338
14 **Bouma G**, Crusius JB, Oudkerk Pool M, Kolkman JJ, von Blomberg BM, Kostense PJ, Giphart MJ, Schreuder GM, Meuwissen SG, Pena AS. Secretion of tumor necrosis factor alpha and lymphotoxin alpha in relation to polymorphisms in the TNF genes and HLA-DR alleles. Relevance for inflammatory bowel disease. *Scand J Immunol* 1996; **43**: 456-463
15 **Pociot F**, Briant L, Jongeneel CV, Molvig J, Worsaae H, Abbal M, Thomsen M, Nerup J, Cambon-Thomsen A. Association of tumor necrosis factor (TNF) and class II major histocompatibility complex alleles with the secretion of TNF-α and TNF-β by human mononuclear cells: a possible link to insulin-dependent diabetes mellitus. *Eur J Immunol* 1993; **23**: 224-231
16 **Artunedo Pe P**, Moreno Azcoita M, Alonso A, Fernandez-Peralta A, Gonzalez-Aguilera JJ. Prognostic significance of high microsatellite instability in a Spanish series of gastric adenocarcinomas. *Anticancer Res* 2000; **20**: 4009-4014
17 **Cai L**, Yu SZ, Zhang ZF. Glutathione S-transferases M1, T1 genotypes and the risk of gastric cancer: A case-control study. *World J Gastroenterol* 2001; **7**: 506-509
18 **El-Omar EM**, Carrington M, Chow WH, McColl KE, Bream JH, Young HA, Herrera J, Lissowska J, Yuan CC, Rothman N, Lanyon G, Martin M, Fraumeni JF Jr, Rabkin CS. Interleukin-1 polymorphisms associated with increased risk of gastric cancer. *Nature* 2000; **404**: 398-402
19 **Machado JC**, Pharoah P, Sousa S, Carvalho R, Oliveira C, Figueiredo C, Amorim A, Seruca R, Caldas C, Carneiro F, Sobrinho-Simoes M. Interleukin 1B and interleukin 1RN polymorphisms are associated with increased risk of gastric carcinoma. *Gastroenterology* 2001; **21**: 823-829
20 **Oue N**, Matsumura S, Nakayama H, Kitadai Y, Taniyama K, Matsusaki K, Yasui W. Reduced expression of the TSP1 gene and its association with promoter hypermethylation in gastric carcinoma. *Oncology* 2003; **64**: 423-429
21 **El-Omar EM**, Rabkin CS, Gammon MD, Vaughan TL, Risch HA, Schoenberg JB, Stanford JL, Mayne ST, Goedert J, Blot WJ, Fraumeni JF Jr, Chow WH. Increased risk of noncardia gastric cancer associated with proinflammatory cytokine gene polymorphisms. *Gastroenterology* 2003; **124**: 1193-1201
22 **Furuta T**, El-Omar EM, Xiao F, Shirai N, Takashima M, Sugimura H, Sugimurra H. Interleukin 1beta polymorphisms increase risk of hypochlorhydria and atrophic gastritis and reduce risk of duodenal ulcer recurrence in Japan. *Gastroenterology* 2002; **123**: 92-105
23 **Azuma T**, Ito S, Sato F, Yamazaki Y, Miyaji H, Ito Y, Suto H, Kuriyama M, Kato T, Kohli Y. The role of the HLA-DQA1 gene in resistance to atrophic gastritis and gastric adenocarcinoma induced by Helicobacter pylori infection. *Cancer* 1998; **82**: 1013-1018
24 **Whichelow CE**, Hitman GA, Raafat I, Bottazzo GF, Sachs JA. The effect of TNF*B gene polymorphism on TNF-alpha and -beta secretion levels in patients with insulin-dependent diabetes mellitus and healthy controls. *Eur J Immunogenet* 1996; **23**: 425-435
25 **Park KS**, Mok JW, Rho SA, Kim JC. Analysis of TNFB and TNFA NcoI RFLP in colorectal cancer. *Mol Cells* 1998; **8**: 246-249
26 **Kato S**, Onda M, Yamada S, Matsuda N, Tokunaga A, Matsukura N. Association of the interleukin-1 beta genetic polymorphism and gastric cancer risk in Japanese. *J Gastroenterol* 2001; **36**: 696-699
27 **Fitzgibbon J**, Grenzelias D, Matthews J, Lister TA, Gupta RK. Tumour necrosis factor polymorphisms and susceptibility to follicular lymphoma. *Br J Haematol* 1999; **107**: 388-391
28 **Hajeer AH**, Lear JT, Ollier WE, Naves M, Worthington J, Bell DA, Smith AG, Bowers WP, Jones PW, Strange RC, Fryer AA. Preliminary evidence of an association of tumour necrosis factor microsatellites with increased risk of multiple basal cell carcinomas. *Br J Dermatol* 2000; **142**: 441-445
29 **Machado JC**, Figueiredo C, Canedo P, Pharoah P, Carvalho R, Nabais S, Castro Alves C, Campos ML, Van Doorn LJ, Caldas C, Seruca R, Carneiro F, Sobrinho-Simoes M. A proinflammatory genetic profile increases the risk for chronic atrophic gastritis and gastric carcinoma. *Gastroenterology* 2003; **125**: 364-371
30 **Wu MS**, Wu CY, Chen CJ, Lin MT, Shun CT, Lin JT. Interleukin-10 genotypes associate with the risk of gastric carcinoma in Taiwanese Chinese. *Int J Cancer* 2003; **104**: 617-623
31 **Onishi T**, Ohishi Y, Goto H, Asano K, Makino H, Hatano T, Tomita M, Abe K, Imagawa K, Kinoshita M, Fukui T. Study on the relationship between tumour necrosis factor gene polymorphism and prognosis in the patients with renal cell carcinoma. *Nippon Hinyokika Gakkai Zasshi* 1998; **89**: 413-420
32 **Marsh HP**, Haldar NA, Bunce M, Marshall SE, le Monier K, Winsey SL, Christodoulos K, Cranston D, Welsh KI, Harris AL. Polymorphisms in tumour necrosis factor (TNF) are associated with risk of bladder cancer and grade of tumour at presentation. *Br J Cancer* 2003; **89**: 1096-1101
33 **Oturai A**, Larsen F, Ryder LP, Madsen HO, Hillert J, Fredrikson S, Sandberg-Wollheim M, Laaksonen M, Koch-Henriksen N, Sawcer S, Fugger L, Sorensen PS, Svejgaard A. Linkage and association analysis of susceptibility regions on chromosomes 5 and 6 in 106 Scandinavian sibling pair families with multiple sclerosis. *Ann Neurol* 1999; **46**: 612-616
34 **Louka AS**, Lie BA, Talseth B, Ascher H, Ek J, Gudjonsdottir AH, Sollid LM. Coeliac disease patients carry conserved HLA-DR3-DQ2 haplotypes revealed by association of TNF alleles. *Immunogenetics* 2003; **55**: 339-343
35 **Di Somma C**, Charron D, Deichmann K, Buono C, Ruffilli A. Atopic asthma and TNF-308 alleles: linkage disequilibrium and association analyses. *Hum Immunol* 2003; **64**: 359-365
36 **Yen JH**, Chen CJ, Tsai WC, Lin CH, Ou TT, Lin SC, Dai ZK, Liu HW. Tumor necrosis factor microsatellite alleles in patients with rheumatoid arthritis in Taiwan. *Immunol Lett* 2002; **81**: 177-182

Edited by Zhu LH and Xu FM

PO Box 2345, Beijing 100023, China
Fax: +86-10-85381893
E-mail: wjg@wjgnet.com www.wjgnet.com

World J Gastroenterol 2004;10(9): 1262-1267
World Journal of Gastroenterology
Copyright ©2004 by The WJG Press ISSN 1007-9327

• GASTRIC CANCER •

Significance of effector protease receptor-1 expression and its relationship with proliferation and apoptotic index in patients with primary advanced gastric adenocarcinoma

Xue-Quan Yao, Fu-Kun Liu, Jie-Shou Li, Xiao-Ping Qi, Bo Wu, Hong-Lin Yin, Heng-Hui Ma, Qun-Li Shi, Xiao-Jun Zhou

Xue-Quan Yao, Fu-Kun Liu, Jie-Shou Li, Xiao-Ping Qi, Bo Wu, Hong-Lin Yin, Heng-Hui Ma, Qun-Li Shi, Xiao-Jun Zhou, School of Medicine, Nanjing University. Department of General Surgery, Jinling Hospital, 305 Zhongshangdong Road, Nanjing, 210002, Jingsu Province, China
Correspondence to: Xue-Quan Yao, Department of General Surgery, Jinling Hospital, 305 Zhongshangdong Road, Nanjing, 210002, Jingsu Province, China. yaoxuequan@yahoo.com
Telephone: +86-25-84826808-860005
Received: 2003-04-02 **Accepted:** 2003-06-07

Abstract

AIM: To investigate the expression of effector protease receptor-1 (EPR-1), proliferative index ki-67 and apoptosis index in patients with primary advanced gastric adenocarcinoma and to clarify the significance of EPR-1 expression and its correlationship with the proliferation and apoptosis indexes.

METHODS: Using immunohistochemical staining and terminal deoxynucleotidyl transferase mediated nick end labelling (TUNEL) technique, we determined the expression of EPR-1, proliferative index (Ki-67) and apoptotic index (AI) in 120 paraffin-embedded specimens of primary advanced gastric adenocarcinoma as well as lymph node metastasis and adjacent normal tissues.

RESULTS: EPR-1 expression was distributed in the cytoplasm of normal gastric mycoderma, carcinoma cells and smooth muscle cells. The positive rate of EPR-1 expression in the primary gastric adenocarcinomas, invasion tumor node and lymph node metastasis was 65.83%, 55.29% and 68%, respectively. While the positive rate in normal gastric mycoderma and smooth muscle cells was 46.7% and 53.3%, respectively. The average positive rate of ki-67 in EPR-1-positive tumors was 7.00% which was significantly lower than that of 8.53% in EPR-1-negative tumors, but the average AI in EPR-1-positive tumors was 1.25%, which was significantly higher than that of 1.00% observed in EPR-1-negative tumors. On the other hand, the average positive labeling index for Ki-67 (ki-67) in EPR-1-positive lymph node metastasis was 7.65%, which was significantly lower than that of 9.44% observed in EPR-1-negative lymph node metastasis. However, the average AI in EPR-1-positive lymph node metastasis tumors was 0.99%, which was significantly higher than that of 0.67% observed in EPR-1-negative lymph node metastasis.

CONCLUSION: The frequency of EPR-1 expression was significantly higher in primary gastric adenocarcinoma and in its lymph node metastasis than that in normal gastric mucosa. Expression of EPR-1 was significantly correlated with tumor histological subtypes and tumor differentiation. Weighted EPR-1 Score is positively correlated with apoptosis index, but is negatively related with proliferative index. Thus, Weighted EPR-1 Score and EPR-1 expression in gastric adenocarcinoma cells maybe a potential marker in clinical setting.

Yao XQ, Liu FK, Li JS, Qi XP, Wu B, Yin HL, Ma HH, Shi QL, Zhou XJ. Significance of effector protease receptor-1 expression and its relationship with proliferation and apoptotic index in patients with primary advanced gastric adenocarcinoma. *World J Gastroenterol* 2004; 10(9): 1262-1267
http://www.wjgnet.com/1007-9327/10/1262.asp

INTRODUCTION

Gastric cancer is the second most common malignancy worldwide. Approximately 95% of all malignant gastric neoplasmas are adenocarcinoma. This study aimed to investigate the correlationship among expression of EPR-1, proliferative index (PI, also referred to as ki-67) and apoptosis index (AI) in patients with primary advanced gastric adenocarcinoma and to clarify the significance of EPR-1 expression in human primary gastric adenocarcinoma, its lymph node metastasis and adjacent non-tumor tissues.

MATERIALS AND METHODS

Patients and tissue samples

Primary gastric adenocarcinoma specimens from 120 patients who had undergone gastrectomy in the period of January 1991 and December 1995 were selected from the files of the Pathology Department, Nanjing Jinling Hospital. None of the patients had received chemotherapy or radiotherapy before surgery. There were 72 males and 48 females, with a median age of 64.8 years (range, 45-78 years). Samples were taken from the representative cancerous lesions as well as lymph node metastasis and adjacent non-cancerous mucosa.

Specimens of the adenocarcinoma were classified into papillary adenocarcinoma, tubular adenocarcinoma, mucinous adenocarcinoma and signet-ring cell carcinoma. Each subclass had 30 cases.

For fomalin-fixed and paraffin-embedded tissue specimens, consecutive 4-μm thick sections were cut and representative sections were used for immunohistochemistry (IHC) and haematioxylin-eosin (H&E) staining as well as the terminal deoxynucleotidyl transferase (TdT)-mediated dUTP-biotin nick end-labeling (TUNEL) for apoptostic index. Using the H&E-stained sections, the tumor histology according to Lauren's grade of tumor differentiation and criteria of the World Health Organization were reassessed. Tumors were staged according to TNM classification.

Immunohistochemistry

The deparaffinized and rehydrated slides were boiled in a 10 mmol/L EDTA buffer (pH 8.0) for 5 min in an autoclave at 121℃. The sections were immunohistochemically stained by

the labeled streptavidin-biotin peroxidase method (LSAB2 Kit; Dako Japan Inc., Kyoto, Japan) with the following primary antibodies: monoclonal antibodies EPR-1(ADI, Alpha Diagnostic International, dilution 1:100), and Ki-67 (Maxim, China, dilution 1:50). The slides were immersed for 10 min in 3 mL/L hydrogen peroxide/methanol to deplete endogenous peroxidase. Then, nonspecific binding sites were blocked with 3 mL/L normal goat serum for 10 min. The primary antibody was then applied, and the sections were incubated overnight at 4 ℃. After washed with PBS (0.01 mol/L pH7.4), biotinylated goat antimouse IgG was applied onto the tissue sections and incubated at room temperature for 10 min. After washed with PBS, a streptavidin peroxicase reagent was applied and incubated at room temperature for 10 min. Finally, the reaction product was visualized using developing color by incubating the slides in a solution of 3 mL/L hydrogen peroxide and AEC chromogen. The sections were counterstained slightly with hematoxylin. Negative controls included parallel sections treated without the primary antibody, in addition to negat an adjacent section of the same block in which the primary antibody was replaced by phosphate-buffered saline (PBS).

TUNEL staining

For detection of apoptotic cells, apoptotic index was examined by the terminal deoxynucleotidyl transferase-mediated deoxyuridine triphosphate fluorescence nick end labeling (TUNEL) method. TUNEL: *In situ* cell death detection *kit* POD (ISCDD, Boehringer Mannheim, Germany) was used to detect the apoptotic cell. The procedures was according to the protocol of the kit and other references. Briefly, the sections were deparaffinized, rehydrated, and washed in distilled water (DW). The tissues were digested with 20 g/mL proteinase K (Boehringer Mannheim, Mannheim, Germany) at room temperature for 15 min. Endogenous peroxidase activity was blocked by incubating it in 3 mL/L hydrogen peroxide/methanol in PBS at 37 ℃ for 30 min. The sections then were incubated with terminal deoxynucleotidyl transferase at 37 ℃ for 60 min, and dioxigenin-conjugatd dUTP was added to the 3' -OH ends of fragmented DNA. Anti-digoxigenin antibody peroxidase was applied to the sections to detect the labeled nucleotides. The sections were stained with DAB and counterstained slightly with hematoxylin. The positive cells were identified, counted and analyzed under the light microscope.

Evaluation of EPR-1 expression

Two experienced pathologists in a blinded fashion (without knowledge of the clinico-pathological features of the tumors) examined the expression of EPR-1 and Ki-67 independently in terms of intensity and positive rate of the immunostaining in each specimen tissue section. The positive staining for EPR-1 protein was expressed as red brown granules, which were mainly located in cell cytoplasm at microscopy. At least 5 high-power (×400 field) fields were chosen randomly and 1 000 cells were counted. The ratio of EPR-1-positive cells was calculated by dividing the number of positive cells over the total number of cells, and was expressed as percentage.

For quantitation of the EPR-1 expression in various samples examined, a semi-quantitative scoring system was used as previously described[1]. An average percentage of positive tumor cells was determined in at least five areas at×400 magnification and assigned to one of the five categories: (a) 0⩽5%, (b) 1=5-25%, (c) 2=25-50%, (d) 3=50-75%, and (e) 4⩾75%. The intensity of EPR-1 immunostaining was scored on a scale of 1-3 as following: (a) weak, 1+; (b) moderate, 2+; and (c) intense, 3+. The percentage of positive tumor cells and the staining intensity were multiplied to produce a weighted score for each case. The case with the weighted score less than 1 was defined as negative, otherwise as positive.

Ki-67-positive cells showed a distinct brown staining of the nuclei with strong intratumoral heterogeneity (Figure 1) The percentages of Ki-67-positive tumor cells were evaluated with a light microscope holding a ×100 oil immersion objective by scoring a minimum of 1 000 tumor cells in randomly selected fields.

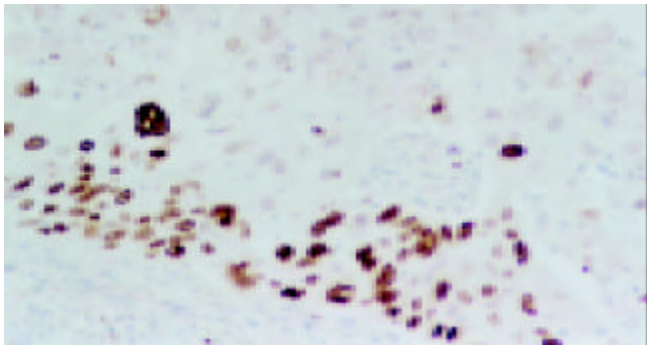

Figure 1 Immunohistochemical staining patterns of Ki-67 in gastric adenocarcinomas. Positive nuclear staining in LSAB, ×200. Poorly-differentiated adenocarcinoma, demonstrated cell proliferative activity.

The percentage of apoptotic cells was calculated as the number of TUNEL-positive cancer cells per 1 000 cancer cells in the most frequently identified areas, and determined as the apoptotic index (AI). Under microscopy, morphological evidences of cell shrinkage, nuclear chromatin condensation, formation of cytoplasmic blebs and apoptotic bodies were frequently observed as the characteristic changes of apoptosis cells (Figure 2).

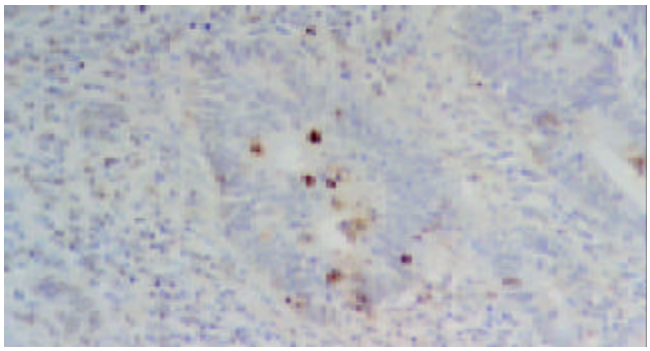

Figure 2 Apoptotic cancer cells in well-differentiated adenocarcinoma detected by TUNEL method. LSAB, ×200.

Statistical analysis

Data were expressed as mean±SD. The two-tailed χ^2 test was used to examine the correlation between various clinical or pathologic parameters and the expression of EPR-1. Statistical significance between different groups was determined by independent Student's *t*-test (two-tailed). The Pearson test was used to examine linear correlation between Weighted EPR-1 Score and proliferative or apoptotic indexes. A *P* value less than 0.05 was considered statistically significant. All the calculations were performer by SPSS 10.0 for windows.

RESULTS

Correlation between EPR-1 protein expression and clinicopathological parameters

No significant relation was found between the expression of EPR-1 and patient age, sex, tumor location, lymph node metastasis or depth of invasion (Table 1, *P*>0.05).

Table 1 No Correlation between EPR-1 protein expression and clinicopathological parameters

Clinico-pathological parameters	Cases	EPR-1 positive cases (%)	*P* value
Age (yr)			
<60	37	21 (56.8)	
⩾60	83	56 (67.5)	0.258
Sex			
Male	72	43 (59.7)	
Female	48	34 (70.8)	0.214
Tumor location			
Upper 1/3	39	22 (56.4)	
Middle 1/3	32	20 (62.5)	
Lower 1/3	19	11 (57.9)	
More than 2 locaitons	30	24 (80.0)	0.199
Differentation			
Well	60	46 (76.7)	
Poorly	60	31 (51.7)	0.004
Subtypes			
Papillary	30	24 (80.0)	
Tubular	30	22 (73.3)	
Mucinous	30	13 (43.3)	
Signet-ring cell	30	18 (60.0)	0.017
Invasion mucosa			
No	66	40 (60.6)	
Yes	54	37 (68.5)	0.369
Lymph node metastasis			
No	70	43 (61.4)	
Yes	50	34 (68.0)	0.459

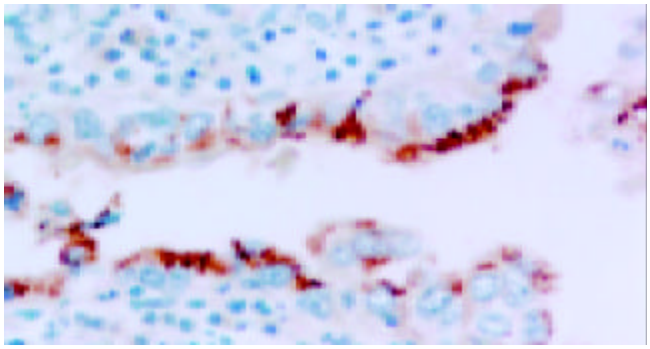

Figure 3 Strong Positive cytoplasma staining of EPR-1 in gastric adenocarcinomas (LSAB×400).

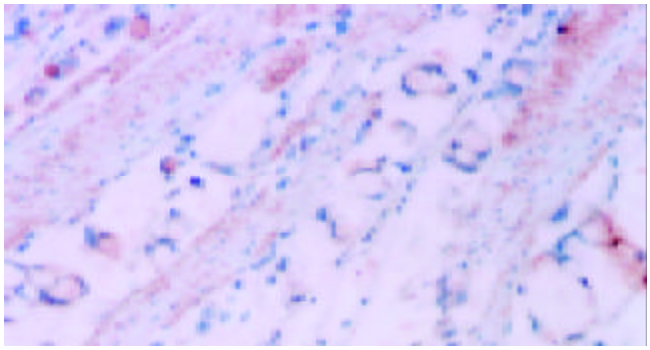

Figure 4 Positive staining of EPR-1 in signet-ring cell carcinoma invasion in smooth muscle and smooth muscle cells (LSAB×200).

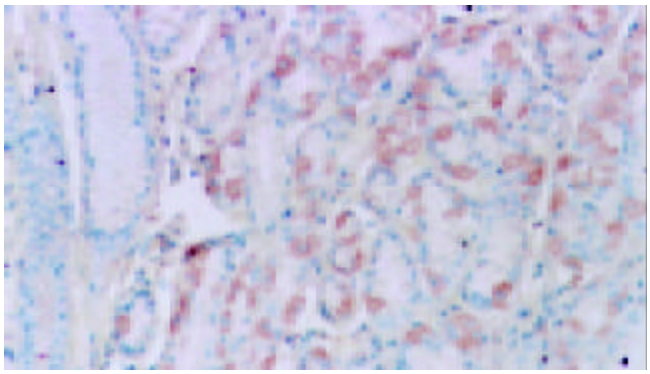

Figure 5 Moderate positive nuclear staining in benign gastric adenocytes (LSAB×200).

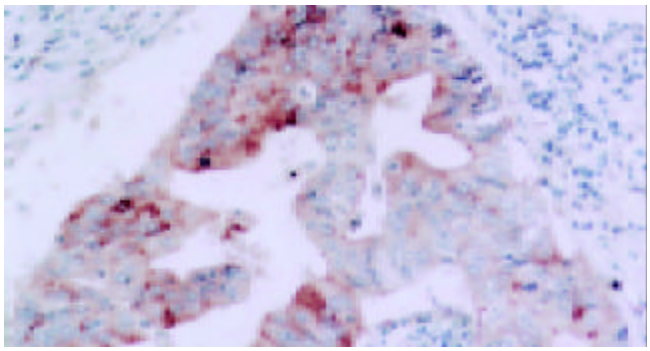

Figure 6 Positive cytoplasma staining in well-differentiated lymph node metastasis (LSAB×200).

Expression of EPR-1 between histological subtypes

There were a variety of positive rates of EPR-1 protein in different histological subtypes (Figures 3, 4, 5, 6 and Table 2). The positive rate of EPR-1 expression nodes was significantly different in the invasive tumor (P=0.007), while it was differently expressed among the 4 subtypes and adjacent non-tumor tissues in the primary carcinoma and its lymph node metastasis (P<0.05). But there was no difference of EPR-1 expression in the adjacent normal gastric mucosa cells and smooth muscle cells among the 4 histological subtypes (P=0.849 and 0.720).

Expression of EPR-1 in the highly-differentiated adenocarcinomas

The positive rate of EPR-1 expression in the primary gastric adenocarcinoma was significantly higher than that in normal gastric mucosa (Table 3, P=0.006), while no significant difference was found in the invasion tumor nodes, lymph node metastasis and smooth muscle (P=0.20, 0.632, 0.088), respectively. However, in the primary highly-differentiated gastric adenocarcinomas, the positive expression rate of EPR-1 was significantly different from that of normal gastric mucosa, invasive tumor node, lymph node metastasis and smooth muscle while no significant difference was found in the poorly-differentiated adenocarcinomas.

Relation of EPR-1 expression with AI and PI in primary adenocarcinoma

The apoptotic index for EPR-1 positive in primary adenocarcinoma group was 1.25% and was, 1.00% for EPR-1 negative group, while the proliferative index for the two group was 7.00% and 8.53%, respectively. The difference of the two indexes between the EPR-1 positive and negative groups was statistically significant (Table 4, P<0.05). The relation of EPR-1 score with AI and PI is shown in Figure 7.

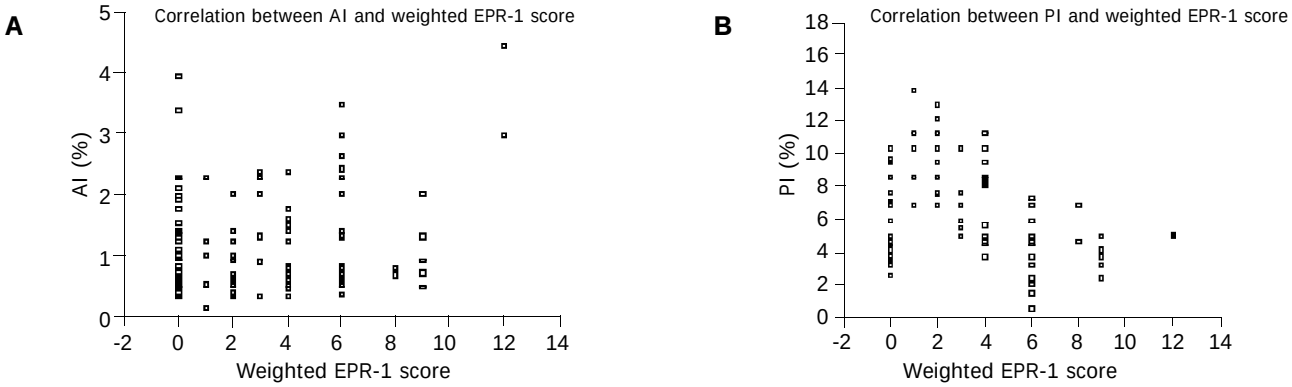

Figure 7 Significant difference of AI and PI with EPR-1 score in primary adenocarcinoma. A: The results of Pearson correlation coefficient, r=0.296, P=0.001<0.05; B: The results of pearson correlation coefficient, r=-0.204, P=0.025<0.05 Weighted EPR-1 Score was positively correlated with apoptotic index, but negatively related with proliferative index in primary adenocarcinoma.

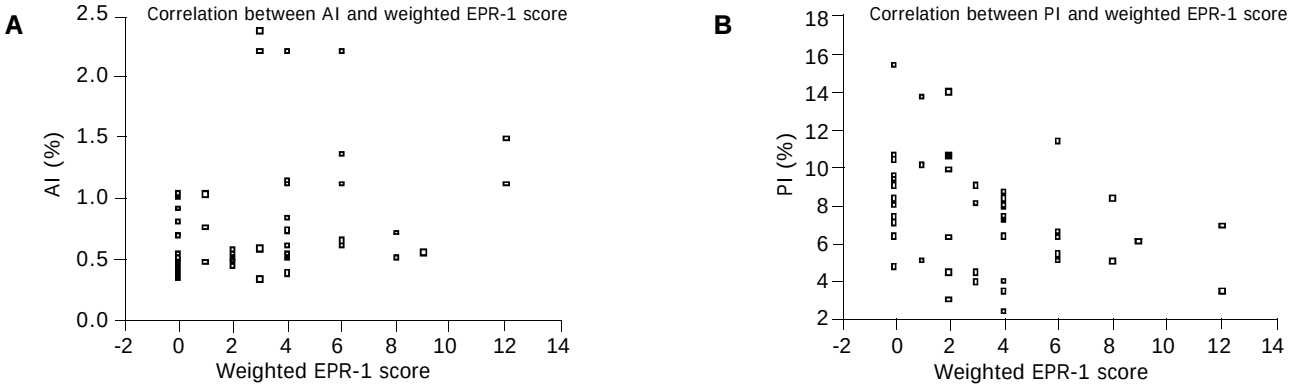

Figure 8 Significant difference of AI and PI with EPR-1 score in lymph node metastasis. A: The results of pearson correlation coefficient, r=0.332, P=0.019<0.05. B: The results of pearson correlation coefficient, r=-0.336, P=0.017<0.05. Weighted EPR-1 score is positively correlated with apoptosis index, but negatively related with proliferative index in lymph node metastasis.

Table 2 Different expression of EPR-1 between histological subtypes

Subtypes	Primary carcino ma	*P* value	Normal gastric mucos a	*P* vlaue	Invasion node	*P* value	Lymph node metastasis	*P* value	Smooth muscle cell	*P* value
Papillary	24/30 (80.0)		14/30 (46.7)		14/17 (82.4)		11/13 (84.6)		17/30 (56.7)	
Tubular	22/30 (73.3)		15/30 (50.0)		12/16 (75.0)		11/15 (73.3)		15/30 (50.0)	
Mucinous	13/30 (43.3)		12/30 (40.0)		10/24 (41.7)		3/10 (30.0)		14/30 (46.7)	
Signet-ring cell	18/30 (60.0)	0.017	15/30 (50.0)	0.849	11/28 (39.3)	0.007	9/12 (75.0)	0.033	18/30 (60.0)	0.720

Table 3 Different expression of EPR-1 in the highly-differentiated adenocarcinomas

Differentation	Primary gastric adenocar cinoma	Normal gastric mucosa cells	Invasion node adenocarcinoma	Lymph node metastasis	Smooth muscle cell	*P* value
Well	46/60 (76.7)	29/60 (48.3)	26/33 (78.8)	22/28 (78.6)	32/60 (53.3)	0.002
Poorly	31/60 (51.7)	27/60 (45.0)	21/52 (40.4)	12/22 (54.5)	32/60 (53.3)	0.594

Table 4 Significant expression difference of the AI and PI between EPR-1 positive and negative groups in primary adenocarcinomas

	n	AI (%)	*P* value	PI (%)	*P* value
EPR-1		mean±SD		mean±SD	
+	77	1.25±0.86		7.00±3.28	
-	43	1.00±0.80	0.024	8.53±2.70	0.010

Relation of EPR-1 expression with AI or PI in cancer with lymph node metastasis

The apoptotic index for EPR-1 positive lymph node metastasis group was 0.99% and was 0.67% for EPR-1 negative lymph node metastasis group, while the proliferative index for the two groups was 7.65% and 9.44%, respectively. The difference of the two indexes between the EPR-1 positive and negative groups was statistically significant (P<0.05). The EPR-1 score was showed with the AI and PI in (Table 5, Figure 8).

Table 5 Significant expression difference of the AI and PI between EPR-1 positive and negative groups in lymph node metastasis

	n	AI (%)	*P*	PI (%)	*P*
EPR-1					
+	34	0.99±0.58		7.65±2.60	
-	16	0.67±0.24	0.010	9.44±3.05	0.037

DISCUSSION

Effector cell Protease Receptor-1 (EPR-1) has been recognized as a receptor of the transmembane glycoprotein coagulation factor Xa and its transcripts are present in terminally differentiated adult tissues[2-9]. Survivin gene was identified by Ambrosini *et al*. during hybridization screening of a human EPR-1 genomic library with the cDNA of EPR-1[10,11]. The gene spanand nearly 15 kb and was co-located at 17q25 with EPR-1[12]. Survivin has been found to be a new member of the inhibitors of apoptosis proteins (IAP) family[13-16], and is selectively overexpressed in common human cancers but not in normal adult tissues.

Transfecting with EPR-1 mRNA into cells could inhibit endogenous expression of survivin gene and induce apoptosis as well as inhibit cell proliferation[17]. Shinozawa *et al*.[18] used RT-PCR method to detect the expression of Survivin and EPR-1 in leukemia and lymphoma, and found that the abnormality of the expression ratio of EPR-1 and Survivin might exert anti-colon tumor proliferation functions. Yamamoto *et al*.[19] reported that EPR-1 in a human colon cancer cell line downregulated survivin expression, with a similar decrease in cell proliferation and an increase in apoptosis. This antitumour efficacy was further enhanced in combination with anticancer agents 5-Fu and CDDP. These findings suggest that regulation of survivin by induction of EPR-1 may have a significant potential as a therapy for human cancer. But to our knowledge, EPR-1 expression in gastric adenocarcarcinaoma has not been report.

In order to gain insight into the role of EPR-1 in gastric adenocarcarcinaoma, we investigated the expression of EPR-1 in a group of gastric adenocarcarcinaomas, and examined the relationship of its expression with cell proliferation and apoptosis index. By immunohistochemical analysis performed in 120 cases, our study shows that positive staining for EPR-1 protein was expressed as red brown granules, which were mainly located in cell cytoplasm. There was no significant relationship between the expression of EPR-1 and patient age, sex, tumor location, lymph node metastasis or depth of invasion. However, a significantly differences expressions of EPR-1 was found between histological subtypes.

Our study also explored the potential relationship between the Weighted EPR-1 expression score and apoptotic, proliferative indexes. Ki-67 has been regarded as a parameter of tumor proliferation[20-29] and the TUNEL method has become a popular way to detect apoptotic cells[30-32]. Using these two reliable methods, we found that the positive rate of EPR-1 expression in the primary gastric adenocarcinoma was significantly higher than that in normal gastric mucosa and in terms with degree of differentiation, the positive expression rate of EPR-1 was significantly different among the primary gastric adenocarcinoma, normal gastric mucosa, tumor invasive node, lymph node metastasis and smooth muscle in the highly-differentiated adenocarcinomas while no significant difference was found in the poorly-differentiated adenocarcinomas.

In conclusion, EPR-1 can influence the biological behaviors of tumor cells not only by inducing their apoptosis, but by inhibiting their proliferation. Whether EPR-1 can be used as a new anti-cancer therapeutics strategy is still waiting for more evidence.

REFERENCES

1 **Lu CD**, Altieri DC, Tanigawa N. Expression of a novel antiapoptosis gene, survivin, correlated with tumor cell apoptosis and p53 accumulation in gastric carcinomas. *Cancer Res* 1998; **58**: 1808-1812

2 **Altieri DC**. Molecular cloning of effector cell protease receptor-1, a novel cell surface receptor for the protease factor Xa. *J Biol Chem* 1994; **269**: 3139-3142

3 **Bouchard BA**, Silveira JR, Tracy PB. On the role of EPR-1 or an EPR-1-like molecule in regulating factor Xa incorporation into platelet prothrombinase. *Thromb Haemost* 2001; **86**: 1133-1135

4 **McLean K**, Schirm S, Johns A, Morser J, Light DR. FXa-induced responses in vascular wall cells are PAR-mediated and inhibited by ZK-807834. *Thromb Res* 2001; **103**: 281-297

5 **Blanc-Brude OP**, Chambers RC, Leoni P, Dik WA, Laurent GJ. Factor Xa is a fibroblast mitogen via binding to effector-cell protease receptor-1 and autocrine release of PDGF. *Am J Physiol Cell Physiol* 2001; **281**: C681-689

6 **Cirera S,** Fredholm M. Isolation and mapping the pig homologs survivin (BIRC5) and effector cell protease receptor 1 (EPR1) genes. *Cytogenet Cell Genet* 2001; **92**: 351-352

7 **Kawabata A**, Kuroda R, Nakaya Y, Kawai K, Nishikawa H, Kawao N. Factor Xa-evoked relaxation in rat aorta: involvement of PAR-2. *Biochem Biophys Res Commun* 2001; **282**: 432-435

8 **Monno R**, Grandaliano G, Faccio R, Ranieri E, Martino C, Gesualdo L, Schena FP. Activated coagulation factor X: a novel mitogenic stimulus for human mesangial cells. *J Am Soc Nephrol* 2001; **12**: 891-899

9 **Shinozawa I**, Inokuchi K, Wakabayashi I, Dan K. Disturbed expression of the anti-apoptosis gene, survivin, and EPR-1 in hematological malignancies. *Leuk Res* 2000; **24**: 965-970

10 **Altieri DC**. Splicing of effector cell protease receptor-1 mRNA is modulated by an unusual retained intron. *Biochemistry* 1994; **33**: 13848-13855

11 **Altieri DC**. Molecular cloning of effector cell protease receptor-1, a novel cell surface receptor for the protease factor Xa. *J Biol Chem* 1994; **269**: 3139-3142

12 **Ambrosini G**, Adida C, Sirugo G, Altieri DC. Induction of apoptosis and inhibition of cell proliferation by survivin gene targeting. *J Biol Chem* 1998; **273**: 11177-11182

13 **Zaffaroni N**, Daidone MG. Survivin expression and resistance to anticancer treatments: perspectives for new therapeutic interventions. *Drug Resist Updat* 2002; **5**: 65-72

14 **Takai N**, Miyazaki T, Nishida M, Nasu K, Miyakawa I. Survivin expression correlates with clinical stage, histological grade, invasive behavior and survival rate in endometrial carcinoma. *Cancer Lett* 2002; **184**: 105-116

15 **Fortugno P**, Wall NR, Giodini A, O'Connor DS, Plescia J, Padgett KM, Tognin S, Marchisio PC, Altieri DC. Survivin exists in immunochemically distinct subcellular pools and is involved in spindle microtubule function. *J Cell Sci* 2002; **115** (Pt 3): 575-585

16 **Kanwar JR**, Shen WP, Kanwar RK, Berg RW, Krissansen GW. Effects of survivin antagonists on growth of established tumors and B7-1 immunogene therapy. *J Natl Cancer Inst* 2001; **93**: 1541-1552

17 **Adida C**, Crotty PL, McGrath J, Berrebi D, Diebold J, Altieri DC. Developmentally regulated expression of the novel cancer anti-apoptosis gene survivin in human and mouse differentiation. *Am J Pathol* 1998; **152**: 43-49

18 **Shinozawa I**, Inokuchi K, Wakabayashi I, Dan K. Disturbed expression of the anti-apoptosis gene, survivin, and EPR-1 in hematological malignancies. *Leuk Res* 2000; **24**: 965-970

19 **Yamamoto T**, Manome Y, Nakamura M, Tanigawa N. Downregulation of survivin expression by induction of the effector cell protease receptor-1 reduces tumor growth potential and results in an increased sensitivity to anticancer agents in human colon cancer. *Eur J Cancer* 2002; **38**: 2316-2324

20 **Scholzen T**, Gerdes J. The Ki-67 protein: from the known and the unknown. *J Cell Physiol* 2000; **182**: 311-322

21 **Aoki T**, Inoue S, Imamura H, Fukushima J, Takahashi S, Urano T, Hasegawa K, Ogushi T, Ouchi Y, Makuuchi M. EBAG9/RCAS1 expression in hepatocellular carcinoma: correlation with tumour dedifferentiation and proliferation. *Eur J Cancer* 2003; **39**: 1552-1561

22 **Nieto A**, Perez-Alenza MD, Del Castillo N, Tabanera E, Castano M, Pena L. BRCA1 expression in canine mammary dysplasias and tumours: relationship with prognostic variables. *J Comp Pathol* 2003; **128**: 260-268

23 **Friedrich RE**, Hagel C, Brehme Z, Kluwe L, Mautner VF. Ki-67 proliferation-index (MIB-1) of neurofibromas in neurofibro-

matosis type 1 patients. *Anticancer Res* 2003; **23**: 953-955
24 **Sredni ST**, Alves VA, Latorre Mdo R, Zerbini MC. Adrenocortical tumours in children and adults: a study of pathological and proliferation features. *Pathology* 2003; **35**: 130-135
25 **Grabsch H**, Takeno S, Parsons WJ, Pomjanski N, Boecking A, Gabbert HE, Mueller W. Overexpression of the mitotic checkpoint genes BUB1, BUBR1, and BUB3 in gastric cancer–association with tumour cell proliferation. *J Pathol* 2003; **200**: 16-22
26 **Furuya Y,** Kawauchi Y, Fuse H. Cell proliferation, apoptosis and prognosis in patients with metastatic prostate cancer. *Anticancer Res* 2003; **23**: 577-581
27 **Watanabe J**, Sato H, Kanai T, Kamata Y, Jobo T, Hata H, Fujisawa T, Ohno E, Kameya T, Kuramoto H. Paradoxical expression of cell cycle inhibitor p27 in endometrioid adenocarcinoma of the uterine corpus - correlation with proliferation and clinicopathological parameters. *Br J Cancer* 2002; **87**: 81-85
28 **Rudolph P**, Bonichon F, Gloeckner K, Collin F, Chassevent A, Schmidt D, Coindre JM, Parwaresch R, Kloppel G. Comparative analysis of prognostic indicators for sarcomas of the soft parts and the viscerae. *Verh Dtsch Ges Pathol* 1998; **82**: 246-252
29 **Janicke F.** Value of tumor biological prognostic factors in adjuvant therapy of node-negative breast cancer. *Zentralbl Gynakol* 1994; **116**: 449-455
30 **Kase S**, Osaki M, Honjo S, Adachi H, Ito H. Tubular adenoma and intramucosal intestinal-type adenocarcinoma of the stomach: what are the pathobiological differences? *Gastric Cancer* 2003; **6**: 71-79
31 **Uysal H**, Cevik IU, Soylemezoglu F, Elibol B, Ozdemir YG, Evrenkaya T, Saygi S, Dalkara T. Is the cell death in mesial temporal sclerosis apoptotic? *Epilepsia* 2003; **44**: 778-784
32 **Bendardaf R**, Ristamaki R, Kujari H, Laine J, Lamlum H, Collan Y, Pyrhonen S. Apoptotic index and bcl-2 expression as prognostic factors in colorectal carcinoma. *Oncology* 2003; **64**: 435-442

Edited by Zhang JZ and Wang XL **Proofread by** Xu FM

PO Box 2345, Beijing 100023, China
Fax: +86-10-85381893
E-mail: wjg@wjgnet.com www.wjgnet.com

World J Gastroenterol 2004;10(9):1268-1275
World Journal of Gastroenterology
Copyright ©2004 by The WJG Press ISSN 1007-9327

• LIVER CANCER •

1α, 25-dihydroxyvitamin D_3 prevents DNA damage and restores antioxidant enzymes in rat hepatocarcinogenesis induced by diethylnitrosamine and promoted by phenobarbital

Mahendrakumar Chandrasekharappa Banakar, Suresh Kanna Paramasivan, Mitali Basu Chattopadhyay, Subrata Datta, Prabir Chakraborty, Malay Chatterjee, Kalaiselvi Kannan, Elayaraja Thygarajan

Mahendrakumar Chandrasekharappa Banakar, Suresh Kanna Paramasivan, Mitali Basu Chattopadhyay, Subrata Datta, Prabir Chakraborty, Malay Chatterjee, Division of Biochemistry, Department of Pharmaceutical Technology, Jadavpur University, Kolkata 700032, India
Kalaiselvi Kannan, Elayaraja Thygarajan, Department of Environmental Science, PSG College of Arts and Science, Coimbatore 641014, Tamilnadu, India
Supported by: All India Council for Technical Education (AICTE), Govt of India and Veerasaiva Vidya Vardhaka Sangha (VVS), Bellary Karnataka, India
Correspondence to: Malay Chatterjee, PO 17028, Division of Biochemistry, Department of Pharmaceutical Technology, Jadavpur University, Kolkata-700032, India. mcbiochem@yahoo.com
Telephone: +91-33-24146393 **Fax:** +91-33-24146393
Received: 2003-10-31 **Accepted:** 2003-12-30

Abstract

AIM: To investigate the chemopreventive effects of 1α, 25-dihydroxyvitamin D_3 in diethylnitrosamine induced, phenobarbital promoted rat hepatocarcinogenesis.

METHODS: The rats were randomly divided into 6 different groups (A-F). Groups A, C and E rats received a single intraperitoneal (i.p) injection of diethylnitrosamine (DEN) at a dose of 200 mg/kg body mass in 9 g/L NaCl solution at 4 wk of age, while group B served as normal vehicle control received normal saline once. After a brief recovery of 2 wk, all the DEN treated rats were given phenobarbital (PB) at 0.5 g/L daily in the basal diet till wk 20. Group A was DEN control. Treatment of 1α, 25-$(OH)_2D_3$ in group C was started 4 wk prior to DEN injection and continued thereafter till wk 20 at a dose of 0.3 μg/100 μL propylene glycol per one single dose (*os*) twice a week. Group E received the treatment of 1α, 25-$(OH)_2D_3$ at the same dose mentioned as above for 15 wk. The rats in group D and F received 1α, 25-$(OH)_2D_3$ alone as in group C without DEN injection.

RESULTS: The comet assay showed statistically higher mean values for length to width ratios (L: W) of DNA mass and tailed cells ($P<0.01$; $P<0.01$ respectively) in DEN treated rats as compared to their normal controls. Continuous supplementation of 1α, 25-dihydroxyvitaminD_3 showed a significant ($P<0.01$) decrease in L:W ratio of DNA mass tailed cells. Furthermore, 1α, 25-$(OH)_2D_3$ supplementations elevated the super oxide dismutase (SOD) activity, hepatic malondialdehyde (MDA) level, reduced glutathione (GSH) and glutathione S-transferase (GST) activity ($P<0.01$, $P<0.05$, $P<0.05$ and $P<0.05$ respectively). As an endpoint marker histological changes were observed to establish the chemopreventive effects of 1α, 25-dihydroxyvitaminD_3.

CONCLUSION: Supplementations of 1α, 25-$(OH)_2D_3$ has a marked protection against hepatic nodulogenesis, antioxidant enzymes and DNA damages in DEN induced rat hepatocarcinogenesis promoted by phenobarbital.

Banakar MC, Paramasivan SK, Chattopadhyay MB, Datta S, Chakraborty P, Chatterjee M, Kannan K, Thygarajan E. 1α, 25-dihydroxyvitamin D_3 prevents DNA damage and restores antioxidant enzymes in rat hepatocarcinogenesis induced by diethylnitrosamine and promoted by phenobarbital. *World J Gastroenterol* 2004; 10(9): 1268-1275
http://www.wjgnet.com/1007-9327/10/1268.asp

INTRODUCTION

1α, 25dihydroxyvitaminD_3 plays an important role in reducing the incidence of carcinomas of breast, prostate and colon in human as well as in experimental animals[1,2]. 1α, 25$(OH)_2D_3$ has been shown to promote the differentiation of cancer cells and cell lines *in vitro*[3,4]. Little information is available for the antioxidant property of 1α, 25$(OH)_2D_3$ in the inhibition of chemical rat hepatocarcinogenesis[5]. A number of micronutrients, macronutrients and non-nutrients have been reported as the chemopreventive agents in the carcinogenesis[6]. Vitamin D_3 treatment of mice with GM-CSF-secreting tumors can interrupt the myelopoiesis-associated immunosuppressor cascade and reduce tumor metastasis[7]. Various new vitamin D analogues are developed with increased growth inhibitory and reduced calcemic activity, but significant antiproliferative and differentiation-inducing agents have now been synthesized and may be used as anticancer drugs[8,9]. Polychlorinated biphenyls, phenobarbital and many other compounds that induce hepatic biotransformation enzymes promote experimental hepatocarcinogenesis in rodents previously exposed to initiating carcinogens[10]. Several mechanisms for liver tumor promotion by PB and other inducing xenobiotics have been documented[11].

Number of methods are available for detecting DNA damage, as opposed to the biological effects of DNA damaging agents (*e.g.*, micronuclei, mutations, structural chromosomal aberrations) have been used to identify substances with genotoxic activity. The alkaline elution assay ignores the critical importance of intercellular differences in DNA damage and requires relatively large numbers of cells. The full approach for assessing DNA damage is the single-cell gel electrophoresis (SCG) or comet assay[12]. Identification of different cell populations can be made by a modified alkaline comet assay[13,14]. Comet assay can be used to identify possible human mutagens and carcinogens[15] and DNA damage of human hepatoma cells irradiated by heavy ions[16]. The alkaline comet assay has been very popular for the analysis of DNA damage caused by various chemical and physical agents[17-20]. The genetic damages in leprosy patients undergoing multidrug treatment are also measured by comet assay[21].

Free radical species are involved in carcinogenesis, superoxide dismutases catalyze the dismutation of super-oxide

radical to hydrogen peroxide and oxygen[22]. Chemical induction of liver carcinoma is associated with changes in the oxygen radical metabolism in liver. The changes in hepatic oxygen radical metabolism were demonstrated by measurement of the antioxidant enzymes SOD. Tumour cells have abnormal activities of antioxidant enzymes, and decreased activities of SOD in tumour cells[23,24]. The influence of oxygen-derived free radicals on survival in advanced colonic cancer was assessed in a prospective randomized controlled double-blind trial using the radical scavengers[25]. Compounds that can scavenge excessive free radicals in the body are suggested to hinder the process of carcinogenesis.

The present study was undertaken to investigate the effectiveness of 1α, $25(OH)_2D_3$ on the development of hepatic nodules, the cytogenetic effects of DEN induced rat hepatocarcinogenesis determined by comet assay and the antioxidant enzymes in diethylnitrosamine induced rat hepatocarcinogenesis promoted by phenobarbital.

MATERIALS AND METHODS

Chemicals

All the reagents and biochemicals, unless otherwise mentioned, were obtained from Sigma Chemical Co. (St. Louis, MO, USA).

Animals

Male Sprague-Dawley rats (80-100 g) were purchased from the Indian Institute of Chemical Biology (CSIR), Kolkata, India. They were given the standard laboratory diet purchased from Lipton, India. The animals were housed in an air-conditioned room (22±1 ℃, relative humidity 50±10%) with a 12-h light/dark cycle in Tarson cages (4 rats per cage) and were acclimatized for 1 wk before the start of the experiment. Guidelines for the care and use of the laboratory animals (National Institute of Health, USA) were followed during the experiment and approved by the Institutional Animal Ethics Committee (IAEC), Jadavpur University, Kolkata.

Experimental regime

The rats were randomly divided into 6 different groups with 10 rats in each as illustrated in Figure 1. Groups A, C and E rats received a single intraperitoneal (i.p) injection of DEN (Sigma) at a dose of 200 mg/kg body mass in 9 g/L NaCl solution at 4 wk of age while group B served as normal vehicle control (received normal saline once). After a brief recovery of 2 wk, all the DEN treated rats were given PB at 0.05% daily in the basal diet till wk 20. Group A was DEN control. Treatment of 1α, $25(OH)_2D_3$ in group C was started 4 wk prior to DEN injection and continued thereafter till wk 20 at a dose of 0.3 μg/100 μL propylene glycol per *os* (*opus sit*) twice a week. In group E 1α, $25(OH)_2D_3$ treatment at the same dose mentioned as above was started 1 wk after DEN injection and continued thereafter till the completion of the experiment. The animals of groups D and F served as 1α, $25(OH)_2D_3$ controls for groups C and E that received 1α, $25(OH)_2D_3$ (Sigma, MO.USA) at a dose of 0.3 μg/100 μL propylene glycol per os twice weekly for 20 wk. All the treatments were withdrawn at wk 20 and the rats were sacrificed at wk 21 under proper ether anaesthesia.

Comet assay

Comet assay was performed on liver tissue under alkaline conditions following the procedure of Ward *et al*.[26], with minor modifications. All the steps of comet assay were conducted under yellow light to prevent the occurrence of additional DNA damage. After sacrifice, liver of either lobe was excised, minced and homogenized in 50 μL of phosphate-buffered saline (PBS; pH 7.5). Briefly, 4 μL of homogenized tissue samples was diluted with 50 μL of PBS and mixed with 150 μL of 10 g/L low melting point agarose (37 ℃) prepared in PBS and pipetted onto an 10 g/L normal melting agarose precoated slide, which had been dried overnight, and covered with a coverslip. After the slide was kept on a chilled plate for 10 min, the coverslip was removed and the slide was lowered into freshly made ice-cold lysis solution (2.5 mol/L NaCl, 100 mmol/L EDTA, 10 mmol/L Tris, 100 g/L DMSO, 10 g/L Triton X-100, pH 10) and kept at 4 ℃ in the dark for 60 min. After draining the lysis solution, the slide was rinsed with distilled water for 15 min. After washed twice in the prepared distilled water, the slide was placed in a horizontal electrophoresis tank containing freshly made buffer (300 mmol/L NaOH and 1 mmol/L EDTA, pH>13) for 30 min. Electrophoresis was performed in the same buffer for 20 min by applying an electric field of 25 V (0.8 V/cm) and adjusting the current to 300 mA by slowly changing the buffer level in the tray. After electrophoresis the slide was rinsed gently with 0.4 mol/L Tris-Hcl buffer (pH 7.5) for 5 min, this step was again repeated. Then the slide was dried at room temperature and kept in a refrigerator in a sealed container until analysis. Duplicate slides were prepared for all the samples.

The slides were immersed in distilled water for 30 min, then stained with 100 μL of ethidium bromide (5 μg/mL) and read at 250× using a Zeiss fluorescence microscope equipped with a green excitation filter and a 590 nm barrier filter. All slides were coded and examined blindly. Routinely 100 cells (50 cells/slide) were screened per sample. In selecting cells for measurements, straight line scanning of a slide was begun at an arbitrary point and cells were measured as they came into the field, provided there was no overlap with patterns from other cells. The length and width of the DNA mass were measured using an ocular micrometer disk. Under these conditions a DNA pattern with a ratio of one had a DNA length of -25 μm and a ratio of four had a DNA length of -100 μm. The length: width ratios of the DNA mass and the frequency of tailed (damaged) cells were used in all comparisons.

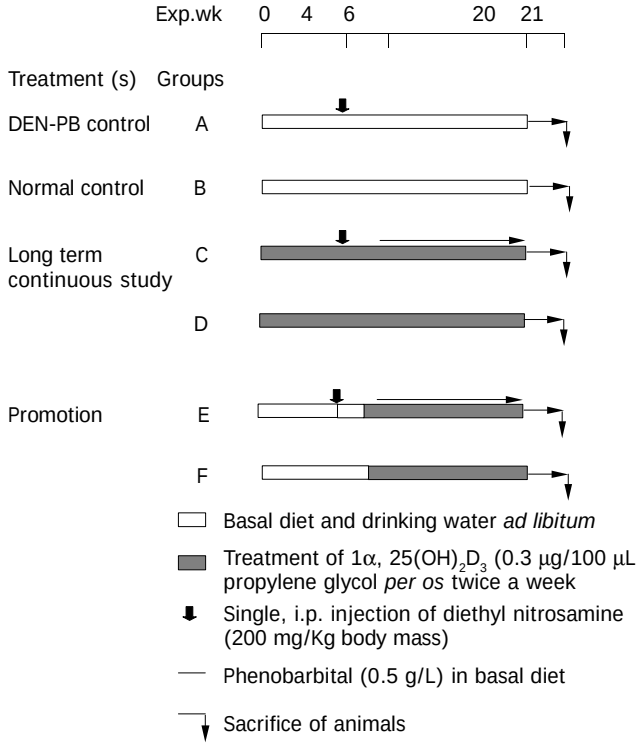

Figure 1 Basic experimental protocol.

Morphology and morphometry of liver tissue

After the rats were sacrificed, their livers were excised from all

treated and control rats, weighed and examined on the surface for subcapsular macroscopic lesions (hyperplastic nodules; HNs). The nodules with approximate spheres were measured in 2 perpendicular directions to the nearest millimeter into three categories namely ≥3, <3 - >1 and ≤1 mm[27].

Histopathological examination

For histopathological examination and morphometric analysis, tissues were fixed in 40 g/L buffered formaldehyde and the fixed paraffin embedded sections were stained with hematoxylin and eosin (H&E).

Histochemical detection of γ-glutamyl transpeptidase-positive foci

After sacrifice of the rats, each liver was examined of the right, left and caudate lobes. They were fixed in an ice-cold mixture of dehydrated ethanol and glacial acetic acid (19:1) for 4 h followed by an overnight incubation in 995 mL/L ethanol at 4 ℃ and then embedded in soft paraffin (melting point 47 ℃). Two contiguous paraffin sections were made from each liver section for γ-glutamyl transpeptidase (GGT) histochemistry according to the method of Rutenberg[28]. Quantitative evaluation of GGT-positive foci (lesions smaller than a liver lobule mainly visible microscopically) was performed according to the method of Campbell[29].

Biochemical assays

The animals were sacrificed with proper anaesthesia. Liver of either lobes was minced and homogenized with 0.25 mol/L sucrose and the homogenate was centrifuged at 9 000 g (33 000 r/min) for 15 min in refrigerated centrifuge (Megafuge 1.0R). The pellet was discarded and an aliquot of supernatant was kept for the assay of cytosolic enzyme activities. The left portion was recentrifuge at 105 000 g for 90 min in refrigerated centrifuge (Megafuge 1.0R). The microsomal fraction was prepared separately from hyperplastic nodule (HNs) and non-nodular surrounding parenchyma (NNSP) liver area and untreated normal control liver. All the operations were done at 0-4 ℃.

The activity of superoxide dismutase (SOD) was measured by following the method of Beyer and Fridovich[30]. Hepatic cytosolic enzymatic lipid peroxidation was estimated according to the method of Okhaw *et al*.,[31] based on the formation of malondialdehyde (MDA). The reduced glutathione (GSH) level was quantified by the method of Ellman[32]. Hepatic cytosolic glutathione S-transferase (GST) activity was determined with 1-chloro 2,4-dinitrobenzene as the substrate according to the method of Habig *et al*.[33].

Statistical analysis

Data were analyzed statistically for differences between the means using Dunnett's *t*-test when more than one group was compared against a control group. *P*-value <0.05 was considered statistically significant.

RESULTS

Dietary intake

Daily food and water intake of all the groups of rats was same. Daily intake of water was measured with a measuring cylinder and it was found that each rat took on an average of 8-10 mL water per day.

Body and liver mass

The effect of 1α, $25(OH)_2D_3$ on body and liver mass of different group of rats sacrificed after 20 wk is shown in Table 1. Body mass of DEN control group rats (group A) were slightly lower ($P<0.05$) than that of the normal control rats (group B). Treatment with 1α, $25(OH)_2D_3$ increased the final body mass of the animals in groups C, D, E and F which received 1α, $25(OH)_2D_3$ as compared with group A carcinogen control. This suggested that treatment with 1α, $25(OH)_2D_3$ had no adverse effect on the growth response of rats. Liver masses of rats in various groups showed no significant differences. The relative liver mass of DEN control group rats (group A) was found to be significantly increased ($P<0.01$) than that of normal control rats (group B). Treatment with 1α, $25(OH)_2D_3$ significantly ($P<0.05$) reduced the relative liver masses of rats in groups C, D, E and F compared with group A. 1α, $25(OH)_2D_3$ supplied rats showed a better resistance against hepatocarcinogenesis.

Table 1 Body and liver masses in each group of rats at end of the study (after 20 wk) (mean±SE)

Group	No of rats	Body mass (g)	Liver mass (g)	Relative liver mass (g) (Liver/100 g body mass)
A	6	282.5±15.8[a]	14.6±2.6	5.16±0.47[b]
B	10	338.0±18.3	10.8±1.9	3.19±0.21
C	8	334.3±13.8[c]	12.3±1.8	3.67±0.36[e]
D	10	348.9±21.6	11.9±1.5	3.41±0.29
E	8	308.1±19.1	13.1±2.2	4.25±0.45
F	10	336.6±22.2	12.1±1.8	3.59±0.42

Statistical level of significance by using Dunnett's *t*-test. [a]$P<0.05$, [b]$P<0.01$, significantly different from normal control (group B), [c]$P<0.05$, [e]$P<0.05$, significantly different from DEN control (group A).

Effect of 1α, $25(OH)_2D_3$ on induction of GGT-positive foci

Table 2 shows that GGT-positive foci developed in all the DEN treated groups (Groups A, C and E), while the livers of rats in normal as well as 1α, $25(OH)_2D_3$ control groups (groups B, D and F respectively) were found to be normal in terms of histochemical observations of GGT-positive foci. In group E supplementation of 1α, $25(OH)_2D_3$ inhibited the appearance of GGT-positive foci (45.25%). But 1α, $25(OH)_2D_3$ treatment which was started 4 wk before DEN administration and continued till the end of the experiment minimized the appearance of GGT-positive foci most significantly in group C (68.80%) than in DEN treatment. Thus 1α, $25(OH)_2D_3$ decreased significantly ($P<0.01$) GGT-positive foci in group C compared to the DEN control (group A).

Table 2 Effect of 1α, $25(OH)_2D_3$ on inhibition of GGT-positive foci in DEN induced rat hepatocarcinogenesis promoted by phenobarbital (mean±SE)

Group	No. of rats	No. of GGT-positive foci/cm^2	Decrease (%)
A	06	26.16±2.16	
C	08	8.16±0.59[b]	68.80
E	08	14.32±1.23[d]	45.25

Statistical level of significance by using Dunnett's *t*- test, [b]$P<0.01$, [d]$P<0.01$ compared with group A.

Effect of 1α, $25(OH)_2D_3$ on hepatic histopathology

Histopathological examination of liver sections from normal untreated group B (Figure 5) revealed normal liver parenchymal cells with granulated cytoplasm and small uniform nuclei radially arranged around the altered cell foci with granulated cytoplasm and small uniform nuclei radially arranged around the central vein. In the DEN treated groups A, C and E, phenotypically altered hepatocytes in altered liver cell foci and nodules at varying extent were noticeable throughout the hepatic parenchyma. The hepatocellular architecture of DEN control (group A) was found to be grossly altered and the hepatocytes became oval

in shape. The altered liver cells in foci and nodules were considerably enlarged, vesiculated and binucleated (Figure 4). A substantial irregularity (enlargement) in the shape of nucleus and chromatin pattern (chromatin condensation) were also observed. The nucleo-cytoplasmic ratio was increased in sinuses and greatly dilated with hyperplastic Kupffer cells. The cytoplasm was extensively vacuolated, continued masses of acidophilic material were observed. Supplementation of 1α, $25(OH)_2D_3$ for the entire period study (group C) elicited a maximum protection against DEN induced hepatocarcinogenesis, which was reflected in almost normal hepatocellular architecture. In group C liver cells were found to contain compact cytoplasmic material with only clear cell foci (Figure 6). The nucleocytoplasmic ratio was decreased considerably as compared to group A. The configuration of sinuses appeared normal with normal Kupffer cells. The size of nuclei resembled that of normal cells and binucleated cells were extremely less. A moderate improvement of hepatic histological picture was observed in 1α, $25(OH)_2D_3$ supplemented group C in comparison to group E. A considerable vacuolation was still observed in the cytoplasm and the compactness of hepatocytes was somewhat disturbed in group C. The liver sections from these groups presented a predominance of clear cell foci rather than eosinophilic or basophilic foci. There was a slight decrement in nucleocytoplasmic ratio in the cells with respect to group A with slightly dilated sinuses. The number of binucleated cells was less as compared to group A with normal size nuclei.

Effect of 1α, $25(OH)_2D_3$ on incidence, number and size of hepatocellular lesions

The carcinogen treated rats showed 100% nodule incidence in group A as compared to the normal control rats (group B). The incidence of HNs was lower in the rats that received 1α, $25(OH)_2D_3$ and DEN in groups C and E (Table 3). The average number of nodules/nodule–bearing livers (nodule multiplicity) was also found to be less in 1α, $25(OH)_2D_3$ supplemented group C (60%) as compared to group A. The result was statically significant ($P<0.01$) in group C compared with group A. The total number of nodule 22 and the average nodule bearing livers (3.66±0.68) in group C were compared with the DEN control (group A). Group C rats showed the lowest value in each range compared with the other groups (groups A and E). In the present study the relative size distribution of nodules revealed that supplementation of 1α, $25(OH)_2D_3$ characteristically reduced the appearance of HNs more than 3 mm in size in group C compared to group A.

Effect of 1α, $25(OH)_2D_3$ on comet Assay

The results of comet assay based on mean tailed cells (TC) (%) and mean length: width ratios (L: W) in hepatic cells of rats treated with DEN are shown in Table 4. The mean length to width ratio of the DNA mass observed in DEN control rats (group A) was significantly greater ($P<0.01$) compared with the normal control group B. Similarly, the mean frequency of tailed cells was (84±0.020) in DEN control rats and significantly different ($P<0.01$) from the normal control (29±0.008). Figures 2 and 3 illustrate the distribution of L: W and TC in DEN control (group A), normal (group B), long term study (group C), and promotion study (group E). For length: width ratio and tailed cells, the median values were higher in DEN control (group A) compared with the normal control (group B). The distribution of damage cells was also wider and the lengths of the boxes were greater in DEN control rats, indicating larger interquartile ranges than that of the normal controls rats. The median line in normal control rats (group B) were tailing towards smaller values. In group C and group E the median lines were in the middle of the boxes, the distribution of TC was more or less symmetrical. In group C 1α, $25(OH)_2D_3$ offered more than 54.09% in the length and width ratio and 53.37% of tailed cells compared to group A.

Table 4 Effect of 1α, 25dihydroxyvitamin D_3 on DNA damage [based on mean tailed cells (%) and mean length: width ratios ± SEM of DNA pattern] in hepatic cells of rats during DEN induced rat hepatocarcinogenesis promoted by phenobarbital (mean±SE, n=100)

Groups	Length and width ratio of DNA mass	Decrease (%)	Tailed cells (%)	Decrease (%)
A	2.44±0.0681		84±0.020	
B	1.029±0.005		29±0.008	
C	1.12±0.025[b]	54.09	39±0.014[d]	53.57
D	1.02±0.0005		29±0.008	
E	1.63±0.026[g]	33.19	62±0.026[f]	26.19
F	1.02±0.005		29±0.008	

Group A: DEN control; Group B: Normal control; Group C: Long term study; Groups D, F 1α, $25(OH)_2D_3$ control; Group E: promotion. Statistical level of significance by using Dunnett's t-test, [b]$P<0.01$, [g]$P<0.01$, [d]$P<0.01$ and [f]$P<0.01$ compared to group A.

Effect of 1α, $25(OH)_2D_3$ on hepatic super oxide dismutase activity

Table 5 depicts the SOD activity. A significant decrease ($P<0.01$) was found in SOD activity in HNs and NNSP tissues in DEN control (group A) compared with the normal control (group B). A significant increase ($P<0.05$) in SOD level was observed in both HNs and NNSP tissues in group C rats, where 1α, $25(OH)_2D_3$ treatment started 4 wk before DEN administration and continued till the end of the experiment. In group E 1α, $25(OH)_2D_3$ was supplemented only for 15 wk, starting the treatment 1 wk after DEN administration showed no statistical significance in SOD activity.

Table 5 Changes in activities of superoxide dismutase (units / mg protein) in different groups of rats treated with 1α, $25(OH)_2D_3$ during DEN induced rat hepatocarcinogenesis promoted by phenobarbital (mean±SE, n=5)

Groups	Nodules	Surrounding	Control
A	4.38±0.56[b]	5.28±0.57[a]	8.64±0.87
C	6.84±0.81[c]	7.60±0.73	8.84±0.80
E	4.88±0.66	5.64±0.53	8.52±0.77

Statistical level of significance by using Dunnett's t -test. [b]$P<0.01$, [a]$P<0.05$, compared with control. [c]$P<0.05$ compared with group A.

Table 3 Effect of 1α, $25(OH)_2D_3$ on incidence, number and size of hepatocellular lessions during DEN induced rat hepatocarcinogenesis promoted by phenobarbital (mean±SE)

Group	No. of rats with nodules	Nodule incidence (%)	Total No. of nodule	Average No. of nodules per nodule bearing liver	Relative size <1mm	>1mm<3mm	>3mm
A	10 / 10	100	168	16.80±1.33	94 (55.95)	48 (28.57)	26 (15.47)
C	6 / 10	60[b]	22	3.66±0.88	11 (50.0)	6 (27.27)	05 (22.72)
E	8 / 10	80[d]	72	8.00±1.05	28 (38.88)	24 (33.33)	20 (27.77)

Statistical level of significance by using Dunnett's t-test, [b]$P<0.01$, [d]$P<0.01$ compared with group A.

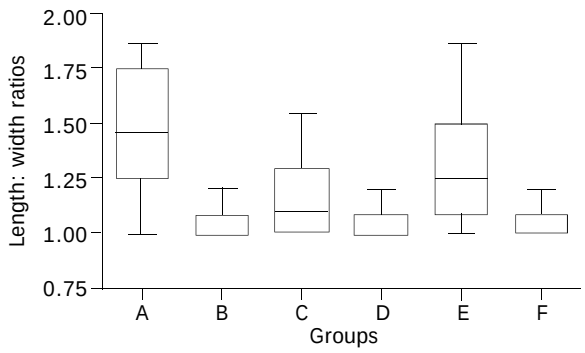

Figure 2 Box-and-whisker plot of the distribution of DNA damage treated with 1alpha, 25(OH)$_2$D$_3$ in DEN induced rat hepatocarcinogenesis promoted by phenobarbital.

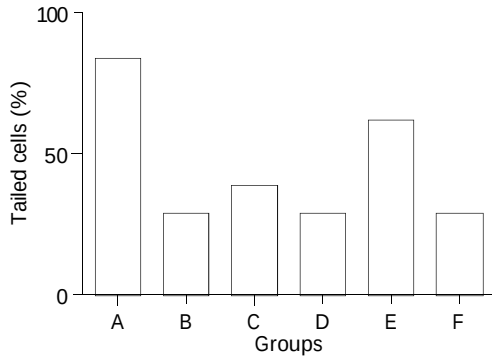

Figure 3 Tailed cells (%) in hepatic cells of rats treated with 1alpha, 25(OH)$_2$D$_3$ in DEN induced rat hepatocarcinogenesis promoted by phenobarbital.

Effect of 1α, 25(OH)$_2$D$_3$ on hepatic cytosolic lipid peroxidation

1α, 25(OH)$_2$D$_3$ had effect on hepatic cytosolic lipid peroxidation (Table 6) in different groups of rats treated with DEN, which was promoted by phenobarbital. A significant increase in the total content of MDA (P<0.01) was observed in DEN control rats (group A), both HNs and NNSP liver area in group A were compared with normal control. A significant decrease (P<0.05) in elevated hepatic MDA level was found in group C when compared with DEN control. Supplementation of 1α, 25(OH)$_2$D$_3$ led to a significant reduction in total MDA production in DEN treated rats. The maximum effect was observed in group C rats whose 1α, 25(OH)$_2$D$_3$ treatment was started 4 wk before DEN administration and continued till 20 wk, which offered a better protection in group E, in which 1α, 25(OH)$_2$D$_3$ was supplemented for only 15 wk, starting 1 wk after DEN administration.

Table 6 Changes in total hepatic lipid peroxidation (nmol MDA/100 mg protein) level in different groups of rats treated with 1α, 25(OH)$_2$D$_3$ during DEN induced rat hepatocarcinogenesis promoted by phenobarbital (mean±SE, n=5)

Groups	Nodules	Surrounding	Control
A	18.72±1.59^b	17.4±1.34^d	2.44±0.84
C	8.80±1.02^a	7.6±0.88	3.16±0.94
E	13.16±1.23	12.32±1.03	2.8±0.79

Statistical level of significance by using Dunnett's t-test. ^{b}P<0.01, ^{d}P<0.01 compared with control; ^{a}P<0.05 compared with group A.

Effect of 1α, 25(OH)$_2$D$_3$ on hepatic cytosolic glutathione (GSH)

Table 7 shows the GSH content in different experimental groups. GSH content was found to be increased both in HNs and NNSP liver areas (P<0.01) in DEN control rats (group A) compared with normal control (group B). GSH content was decreased significantly (P<0.05) in group C. GSH levels were marginally increased in groups D and F when compared with the normal control.

Table 7 Changes in total hepatic reduced glutathione (GSH) (mg/100 g tissue) level in different groups of rats treated with 1α, 25(OH)$_2$D$_3$ during DEN induced rat hepatocarcinogenesis promoted by phenobarbital (mean±SE, n=5)

Groups	Nodules	Surrounding	Control
A	367.6±25.5^b	310.0±24.9^c	226.0±22.5
C	268.0±21.5^a	254.0±20.1	248.0±21.7
E	303.2±22.5	284.0±21.6	256.0±22.5

Statistical level of significance by using Dunnett's t-test. ^{b}P<0.01, ^{c}P<0.05 compared with control. ^{a}P<0.05 compared with group A.

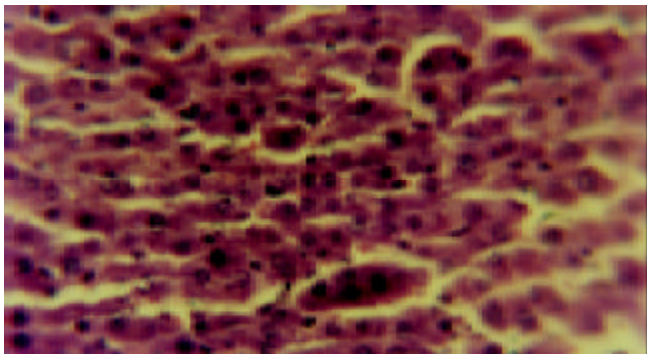

Figure 4 Shows the section of the rat liver (group A) showing abnormal hepatic architecture after a single i.p. Injection of DEN (200 mg/kg b.m.) (HE ×325).

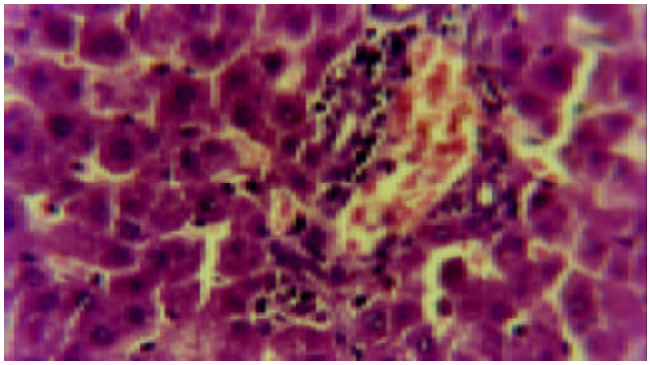

Figure 5 Shows the thin section of normal rat liver untreated (group B) showing hepatocellular architecture (HE ×325).

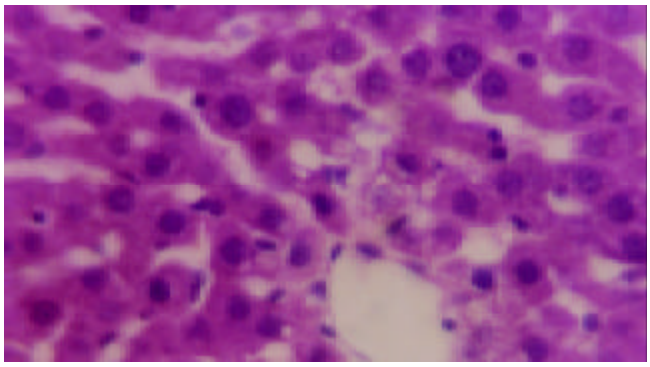

Figure 6 Shows section of rat liver (group C) initiated with DEN and supplemented with 1α, 25(OH)$_2$D$_3$ [0.3 μg/100 μL propylene glycol per os twice a week for 20 wk] showing almost normal hepatic architecture (HE ×325).

Effect of 1α, 25(OH)$_2$D$_3$ on 1-chloro-2, 4-dinitro benzene (CDNB) conjugated hepatic cytosolic glutathione S-transferase (GST) activity in different groups

Table 8 depicts the GST activity with CDNB in different experimental groups. DEN control rats showed (group A) a significantly increase (P<0.01) more than 2-fold in NNSP compared with the normal control, but HNs showed a significantly decrease in value. Altered activity of 1α, 25(OH)$_2$D$_3$ was found in group B. Groups C and E also showed higher altered activity of 1α, 25(OH)$_2$D$_3$ than the normal control rats. 1α, 25(OH)$_2$D$_3$ was found to be more effective in the inhibition of rat liver carcinogenesis (P<0.05) in abating the GST activity. 1α, 25(OH)$_2$D$_3$ control groups (groups D and F) had no statistical significance in the GST activity when compared with normal control.

Table 8 Changes in activity of 1-chloro-2, 4-dinitro benzene (CDNB) conjugated (μmol CDNB conjugated / mg protein / mL) hepatic cytosolic glutathione S-transferase (GST) in different groups of rats treated with 1α, 25(OH)$_2$D$_3$ during DEN induced rat hepatocarcinogenesis promoted by phenobarbital (mean±SE, n=5)

Groups	Nodules	Surrounding	Control
A	2.52±0.23^b	1.54±0.23^c	0.9±0.10
C	1.45±0.27^a	1.24±0.11	1.12±0.13
E	1.76±0.29	1.48±0.19	1.10±0.11

Statistical level of significance by using Dunnett's t-test. ^bP<0.01, ^cP<0.05 compared with control. ^aP<0.05 compared with group A.

DISCUSSION

The results of our present investigation clearly demonstrated that long term supplementation of 1α, 25(OH)$_2$D$_3$ (at a dose of 0.3 μg/100 μL propylene glycol twice a week) greatly reduced the incidence of hepatic nodulogenesis, antioxidant enzymes and genetic damage in DEN induced rat hepatocarcinogenesis promoted by phenobarbital. Previous studies in our laboratory have shown that long term supplementation of 1α, 25(OH)$_2$D$_3$ in combination with vanadium could effectively inhibit DEN-induced rat liver carcinogenesis[34-36].

DEN is a well-known hepatocarcinogen in rats, forming DNA-carcinogen adducts in the liver and inducing hepatocellular carcinomas without cirrhosis through the development of putative preneoplastic enzyme-altered hepatocellular focal lesions[37]. After limited treatment with DEN, the rats ended up with a large benign hepatomas[35,38], which were equivalent to neoplastic nodules and highly differentiated hepatocarcinomas. The preneoplastic lesions were thought to be the possible precursors of hepatic cancer in experimental animals and humans[39]. Treatment with hepatocarcinogen could result in the proliferation of oval cells. These cells have been shown to have the ability to differentiate into hepatocytes[40]. The results of our present investigation clearly indicated that long term supplementation of 1α, 25(OH)$_2$D$_3$ could reduce the incidence, multiplicity and size of visible HNs more than 3 mm in size. Preneoplasia (γ-glutamyl transpeptidase -positive and glucose 6-phosphate negative) appeared in 1α, 25(OH)$_2$D$_3$ treated animals 1 wk after carcinogen withdrawal, but livers from 1α, 25(OH)$_2$D$_3$ depleted rats exhibited an increase in the number of GGT-positive foci. There was no change in the body masses among the groups under study. This is particularly important because nutritional deprivation causing body mass loss might result in a decrease in tumor volume[41]. Thus 1α, 25(OH)$_2$D$_3$ had the maximum effect in reducing the number and nodule growth, which were not mediated through the impairment of nutritional status in the experimental animals. 1α, 25(OH)$_2$D$_3$ effect observed in this study might be important for cancer prevention.

Comet assay is sensitive, a small number of cells and substances are required. It is inexpensive, and easy to apply to any tissues. The tissue selection in our study was based on a recent data analysis of the mice and rats[42]. Comet assay can be applied to any tissues *in vivo*. In comet assay DNA is organized as loops, retaining the super coils and circular structure that are contained in the nucleosome. Epidemiological studies showed that comet tail was made up of relaxed loops and that the number of loops in the tail could indicate the number of DNA damages and tailed cells consisting of fragments of DNA[43]. This study indicated a significantly higher incidence of DNA damage in the DEN-PB control compared with the normal control. In the present investigation, 1α, 25(OH)$_2$D$_3$ protected against the DNA damage in DEN induced rat hepatocarcinogenesis.

SOD is the first line of defense of the cellular antioxidant system against the oxidative damage mediated by superoxide radicals. Life is continuously exposed to oxidative stress, cells are equipped with gene regulatory mechanism that can sense a high oxidative stress potential and consequently induce higher levels of several enzymes capable of reducing reactive oxygen species and repairing oxidative damage. The antioxidant enzymes are thus a major cell defense against acute oxygen toxicity. Their function is to protect membrane and cytosolic components against damage caused by free radicals. SOD, catalase and glutathione peroxidase (GPx) exemplify some of the most important ones. SOD, catalase could convet oxygen into hydrogen peroxides and water, SOD could diminish the damage caused by superoxide-producing agents as long as the generated hydrogen peroxide was removed by glutathione peroxidase and catalase does not become rate limiting[44,45]. The enzyme GPx and glutathione reductase were then destroyed either by catalase or by enzyme system, these 2 systems could convert hydrogen peroxide into water at the expense of NADPH, using reduced GSH as an electron donor[46]. Differences were found between normal and cancer cell superoxide dismutase activity in the treatment of cancer[47]. The SOD ratio was lower in liver cells, and this might provide an explanation for the higher susceptibility of tumor cells to treatments likely to involve oxygen radicals[48,49]. Our present results showed that 1α, 25(OH)$_2$D$_3$ supplementation in group C inclined towards normal and in group E no change was found. Decreased antioxidant activity could cause the accumulation of free radicals. However, there was no change in SOD activities in group E rats, which might be due to the inactivated gene not reactivated by 1α, 25(OH)$_2$D$_3$ supplementation, the physiological characterization and the genetic mapping of the mutant should identify the gene.

Lipid peroxidation plays an important role in carcinogenesis, treatment with inhibitors of lipid peroxidation, such as vitamins D, E, C, as well as selenium and vanadium and beta-carotene are protective agents[36,50-52]. Stimulation of NADPH- dependent microsomal lipid peroxidation was proposed to be mediated by ADP/Fe^{2+}, NADPH-cytochrome P-450 reductase and cytochrome P-450[53]. Therefore, the increase of one of these modulators in the liver could explain the reduced lipid peroxidation. Previous studies in our laboratory showed that a significant increase in the total content of MDA was observed in DEN control compared to normal control[50,54]. In our present study a significant increase in lipid peroxidation was observed in DEN PB-treated rats (group A) when compared with normal control rats (group B). But it was found in group C most significant (P<0.05) compared to DEN-PB control. Treatment with 1α, 25(OH)$_2$D$_3$ abated the production of MDA in different DEN-PB treated rats (groups C and E). The ability of 1α, 25(OH)$_2$D$_3$ to inhibit iron dependent lipid peroxidation in liposomes might be important in protecting the membranes of normal cells against free radical induced oxidative damage[55]. Thus, the oxygen

radical formation and detoxification, which result in lipid peroxidation and tissue damage, may be prevented.

GSH occurred primarily in the soluble phase, part of it conjugated with foreign compounds or their metabolites for detoxification and transport from body in the precancerous stage, GSH concentration in rat liver increased[56-58]. From our study increased level of GSH in DEN control rats (group A), might be that GGT catalysed the degradation of extracellular GSH that can be used in the intracellular GSH synthesis[59]. 1α, $25(OH)_2D_3$ supplemented groups C and F rats showed decrease in GSH levels. The significantly decreased GSH level in group C reflected the chemopreventive mechanism, by promoting the formation of additional pyridine nucleotides to provide hepatocytes with reduced properties and to inhibit the growth and spread of neoplastic nodules.

GST catalyzes the reaction of compounds with -SH group and thus neutralizes their electrophilic sites and produces more water soluble products. The evolution of thiol dependent detoxification pathways was initially the result of the availability of molecular oxygen[60]. The cellular defence against oxygen free radicals and peroxides is of considerable importance to cell survival. Since the initial report of elevated expression of GST activity in nitrogen mustard resistant cell line[61], a number of different tumors have been found to overexpress GST isoenzymes. In MCF-7 human breast cancer cell line, there appeared to have a coordinately increased expression of both GST-$_{II}$ and other enzymes including selenium dependent glutathione peroxidase and SOD[62]. An increased GST activity was observed in metabolic inactivation and resistance to several anticancer drugs[63]. In the present study, an increased activity of GST was observed in DEN control rats (group A). Decreased activity of GST was observed in groups C and F. But the significant decrease ($P<0.05$) in GST activity was found in group C supplemented with 1α, $25(OH)_2D_3$. The increased anti-cancer drug resistance of one or more of the GST isoenzymes in resistant cells was compared with normal cells[64].

1α, $25(OH)_2D_3$ is very much effective in preventing DEN-PB induced changes in hepatocytes possibly through the inhibition of nodular growth, GGT-positive foci development, normalization of DEN induced changes in enzyme activities and prevention DNA damages in DEN-induced rat hepatocarcinogenesis. The results of our present study strongly suggest that 1α, $25(OH)_2D_3$ may be important for caner prevention.

ACKNOWLEDGEMENTS

Mr. Mahendrakumar C.B is highly indebted to All India Council for Technical Education (AICTE), Government of India, and New Delhi for financial assistance to carry out this work and Veerasaiva Vidhya Vardhaka Sangha's T V M College of Pharmacy (VVS) Bellary, Karnataka, India. Mr. P Suresh Kanna is highly indebted to Department of Science & Technology, Government of India.

REFERENCES

1 **Blutt SE**, Allegretto EA, Pike JW, Weigel NL. 1,25-dihydroxyvitamin D_3 and 9-cis-retinoic acid act synergistically to inhibit the growth of LNCaP prostate cells and cause accumulation of cells in G1. *Endocrinology* 1997; **138**: 1491-1497

2 **Beaty MM**, Lee EY, Glauert HP. Influence of dietary calcium and vitamin D on colon epithelial cell proliferation and 1,2-dimethylhydrazine-induced colon carcinogenesis in rats fed high fat diets. *J Nutr* 1993; **123**: 144-152

3 **Welsh J**. Induction of apoptosis in breast cancer cells in response to vitamin D and antiestrogens. *Biochem Cell Biol* 1994; **72**: 537-545

4 **Chouvet C**, Vicard E, Devonec M, Saez S. 1,25-Dihydroxyvitamin D_3 inhibitory effect on the growth of two human breast cancer cell lines (MCF-7, BT-20). *J Steroid Biochem* 1986; **24**: 373-376

5 **Sardar S**, Chakraborty A, Chatterjee M. Comparative effectiveness of vitamin D_3 and dietary vitamin E on peroxidation of lipids and enzymes of the hepatic antioxidant system in Sprague-Dawley rats. *Int J Vitam Nutr Res* 1996; **66**: 39-45

6 **Wattenberg LW**. Inhibition of carcinogenesis by minor dietary constituents. *Cancer Res* 1992; **52**(7 Suppl): 2085s-2091s

7 **Young MR**, Ihm J, Lozano Y, Wright MA, Prechel MM. Treating tumor-bearing mice with vitamin D_3 diminishes tumor-induced myelopoiesis and associated immunosuppression, and reduces tumor metastasis and recurrence. *Cancer Immunol Immunother* 1995; **41**: 37-45

8 **Vink-Van Wijngaarden T**, Pols HA, Buurman CJ, van den Bemd GJ, Dorssers LC, Birkenhager JC, van Leeuwen JP. Inhibition of breast cancer cell growth by combined treatment with vitamin D_3 analogues and tamoxifen. *Cancer Res* 1994; **54**: 5711-5717

9 **James SY**, Mackay AG, Binderup L, Colston KW. Effects of a new synthetic vitamin D analogue, EB1089, on the oestrogen-responsive growth of human breast cancer cells. *J Endocrinol* 1994; **141**: 555-563

10 **Goldsworthy TL**, Pitot HC. The quantitative analysis and stability of histochemical markers of altered hepatic foci in rat liver following initiation by diethylnitrosamine administration and promotion with Phenobarbital. *Carcinogenesis* 1985; **6**: 1261-1269

11 **Kolaja KL**, Stevenson DE, Walborg EF Jr, Klaunig JE. Dose dependence of phenobarbital promotion of preneoplastic hepatic lesions in F344 rats and B6C3F1 mice: effects on DNA synthesis and apoptosis. *Carcinogenesis* 1996; **17**: 947-954

12 **Ostling O**, Johanson KJ. Microelectrophoretic study of radiation-induced DNA damages in individual mammalian cells. *Biochem Biophys Res Commun* 1984; **123**: 291-298

13 **Godard T**, Gauduchon P, Debout CA. First step in visual identification of different cell populations by a modified alkaline comet assay. *Mutation Res* 2002; **520**: 207-211

14 **McNamee JP**, McLean JR, Ferrarotto CL, Bellier PV. Comet assay: rapid processing of multiple samples. *Mutat Res* 2000; **466**: 63-69

15 **Anderson D**, Yu TW, McGregor DB. Comet assay responses as indicators of carcinogen exposure. *Mutagenesis* 1998; **13**: 539-555

16 **Qiu LM**, Li WJ, Pang XY, Gao QX, Feng Y, Zhou LB, Zhang GH. Observation of DNA damage of human hepatoma cells irradiated by heavy ions using comet assay. *World J Gastroenterol* 2003; **9**: 1450-1454

17 **Li WJ**, Gao QX, Zhou GM, Wei ZQ. Micronuclei and cell survival in human liver cancer cells irradiated by 25MeV/u (40) Ar14(+). *World J Gastroenterol* 1999; **5**: 365-368

18 **Mohankumar MN**, Paul SF, Venkatachalam P, Jeevanram RK. Influence of in vitro low-level gamma-radiation on the UV-induced DNA repair capacity of human lymphocytes–analysed by unscheduled DNA synthesis (UDS) and comet assay. *Radiat Environ Biophys* 1998; **37**: 267-275

19 **Koppen G**, Angelis KJ. Repair of X-ray induced DNA damage measured by the comet assay in roots of Vicia faba. *Environ Mol Mutagen* 1998; **32**: 281-285

20 **Mayer C**, Popanda O, Zelezny O, von Brevern MC, Bach A, Bartsch H, Schmezer P. DNA repair capacity after gamma-irradiation and expression profiles of DNA repair genes in resting and proliferating human peripheral blood lymphocytes. *DNA Repair* 2002; **1**: 237-250

21 **Kalaiselvi K**, Rajaguru P, Palanivel M, Usharani MV, Ramu G. Re: Chromosomal aberration, micronucleus and Comet assays on peripheral blood lymphocytes of leprosy patients undergoing multidrug treatment. *Mutagenesis* 2003; **18**: 309-312

22 **McCord JM**, Fridovich I. The utility of superoxide dismutase in studying free radical reactions. I. Radicals generated by the interaction of sulfite, dimethyl sulfoxide, and oxygen. *J Biol Chem* 1969; **244:** 6056-6063

23 **Halliwell B**, Gutteridge JMC. Free Radicals in Biology and medicine (2nd edn). Clarendon Press: oxford, UK, 1989: 543

24 **Oberley LW**, Oberley TD. Free radicals, cancer and aging. In free radicals, aging and denegenerative Diseases Johnson Jr JE, Walford R, Harman D, Miques J (eds). *Alan R Liss, Inc: New*

York 1986: 325-371
25 **Salim AS**. Scavengers of oxygen-derived free radicals prolong survival in advanced colonic cancer. A new approach. *Tumour Biol* 1993; **14**: 9-17
26 **Ward TH**, Butler J, Shahbakhti H, Richards JT. Comet assay studies on the activation of two diaziridinylbenzoquinones in K562 cells. *Biochem Pharmacol* 1997; **53**: 1115-1121
27 **Moreno FS**, Rizzi MB, Dagli ML, Penteado MV. Inhibitory effects of beta-carotene on preneoplastic lesions induced in Wistar rats by the resistant hepatocyte model. *Carcinogenesis* 1991; **12**: 1817-1822
28 **Rutenburg AM**, Kim H, Fischbein JW, Hanker JS, Wasserkrug HL, Seligman AM. Histochemical and ultrastructural demonstration of gamma-glutamyl transpeptidase activity. *J Histochem Cytochem* 1969; **17**: 517-526
29 **Campbell HA**, Pitot HC, Potter VR, Laishes BA. Application of quantitative stereology to the evaluation of enzyme-altered foci in rat liver. *Cancer Res* 1982; **42**: 465-472
30 **Beyer WF Jr,** Fridovich I. Assaying for superoxide dismutase activity: some large consequence of minor changes in conditions. *Anal Biochem* 1987; **161**: 559-566
31 **Okhawa H**, Ohishi N, Yagi K. Assay for lipid peroxides in animal tissues by thiobarbituric acid reaction. *Anal Biochem* 1979; **95**: 351-358
32 **Ellman GL**. Tissue sulfhydryl groups. *Arch Biochem Biophys* 1959; **82**: 70-77
33 **Habig WH**, Pabst MJ, Jakoby WB. Glutathione S-transferase: the first enzymatic step in mercapturic acid formation. *J Biol Chem* 1974; **249**: 7130-7139
34 **Bishayee A**, Chatterjee M. Inhibitory effect of vanadium on rat liver carcinogenesis initiated with diethylnitrosamine and promoted by Phenobarbital. *Br J Cancer* 1995; **71**: 1214-1220
35 **Bishayee A**, Chatterjee M. Inhibition of altered liver cell foci and persistent nodule growth by vanadium during diethylnitrosamine induced hepatocarcinogenesis in rats. *Anticancer Res* 1995; **15**: 455-462
36 **Basak R**, Basu M, Chatterjee M. Combined supplementation of vanadium and 1α, $25(OH)_2D_3$ inhibit diethylnitrosamine-induced rat liver carcinogenesis. *Chem Biol Interact* 2000; **128**: 1-18
37 **Singer B**, Crunderger D. Molecular Biology and Mutagens and Carcinogens, Plenum Press, New York**,** 1984
38 **Scherer P**, Van Dijk WF, Emmelot P. Effect of antilymphocytic and normal serum on growth of precancerous foci and development of tumors induced by diethyl nitrosamine. *Eur J Cancer* 1976; **12**: 25-31
39 **Farber E**. Clonal adaptation during carcinogenesis. *Biochem Pharmacol* 1990; **39**: 1837-1846
40 **Sell S**. Is there a liver stem cell? *Cancer Res* 1990; **50**: 3811-3815
41 **Waitzberg DL**, Goncalves EL, Faintuch J, Bevilacqua LR, Rocha CL, Cologni AM. Effect of diets with different protein levels on the growth of Walker 256 carcinosarcoma in rats. *Braz J Med Biol Res* 1989; **22**: 447-455
42 **Sasaki YF**, Sekihashi K, Izumiyama F, Nishidate E, Saga A, Ishida K, Tsuda S. The comet assay with multiple mouse organs: comparison of comet assay results and carcinogenicity with 208 chemicals selected from the IARC monographs and U.S. NTP Carcinogenicity Database. *Crit Rev Toxicol* 2000; **30**: 629-799
43 **Collins AR**, Dobson VL, Dusinska M, Kennedy G, Stetina R. The comet assay: what can it really tell us? *Mutation Res* 1997; **375**: 183-193
44 **Fridovich I**. Superoxide radical: an endogenous toxicant. *Annu Rev Pharmacol Toxicol* 1983; **23**: 239-257
45 **Fridovich I**. Superoxide dismutases. *Adv Enzymol Relat Areas Mol Biol* 1986; **58**: 61-97
46 **Gaetani GF**, Galiano S, Canepa L, Ferraris AM, Kirkman HN. Catalase and glutathione peroxidase are equally active in detoxification of hydrogen peroxide in human erythrocytes. *Blood* 1989; **73**: 334-339
47 **Oberley LW**, Buettner GR. Role of superoxide dismutase in cancer. *Cancer Res* 1979; **39**: 1141-1149
48 **Bozzi A**, Mavelli I, Finazzi A, Strom R, Wolf AM, Mondovi B, Rotilio G. Enzyme defense against reactive oxygen derivatives. II. Erythrocytes and tumor cells. *Mol Cell Biochem* 1976; **10**: 11-16
49 **Thirunavukkarasu C**, Sakthisekaran D. Effect of selenium on N-nitrosodiethylamine-induced multistage hepatocarcinogenesis with reference to lipid peroxidation and enzymic antioxidants. *Cell Biochem Funct* 2001; **19**: 27-35
50 **Sarkar A**, Bishayee A, Chatterjee M. Beta-carotene prevents lipid peroxidation and red blood cell membrane protein damage in experimental hepatocarcinogenesis. *Cancer Biochem Biophys* 1995; **15**: 111-125
51 **Appel MJ**, Roverts G, Woutersen RA. Inhibitory effects of micronutrients on pancreatic carcinogenesis in azaserine treated rats. *Carcinogenesis* 1991; **2**: 2157–2161
52 **Eskelson CD**, Odeleye OE, Watson RR, Earnest DL, Mufti SI. Modulation of cancer growth by vitamin E and alcohol. *Alcohol Alcohol* 1993; **28**: 117–125
53 **Cajelli E**, Ferraris A, Brambilla G. Mutagenicity of 4-hydroxynonenal in V79 Chinese hamster cells. *Mutat Res* 1987; **190**: 169-171
54 **Basak R**, Bhattacharya R, Chatterjee M. 1alpha, 25-Dihydroxyvitamin D(3) inhibits rat liver ultrastructural changes in diethylnitrosamine-initiated and phenobarbital promoted rat hepatocarcinogenesis. *J Cell Biochem* 2001; **8**: 357-367
55 **Wiseman H**. Vitamin D is a membrane antioxidant. Ability to inhibit iron-dependent lipid peroxidation in liposomes compared to cholesterol, ergosterol and tamoxifen and relevance to anticancer action. *FEBS Lett* 1993; **326**: 285-288
56 **Fiala S**. Intracellular changes in levels of polarographically active sulphydryl groups in rat liver during carcinogenesis. *Nature* 1958; **182**: 257-258
57 **Neish WJ**, Rylett A. effect of alpha-tocopheryl acetate on liver glutathione of male rats injected with 3'-methyl-4-dimethylaminoazobenzene. *Biochem Pharmacol* 1963; **12**: 1147-1150
58 **Dijkstra J**. The contents of trichloroacetic acid-soluble sulphydryl compounds and ascorbic acid in the liver of rats fed aminoazo dyes: the effect of a single large dose of dye. *Br J Cancer* 1964; **13**: 608-617
59 **Reiners JJ Jr**, Kodari E, Cappel RE, Gilbert HF. Assessment of the antioxidant/prooxidant status of murine skin following topical treatment with 12-O-tetradecanoylphorbol-13-acetate and throughout the ontogeny of skin cancer. Part II: Quantitation of glutathione and glutathione disulfide. *Carcinogenesis* 1991; **12**: 2345-2352
60 **Boyland E**, Chasseaud LF. The role of glutathione and glutathione S-transferases in mercapturic acid biosynthesis. *Adv Enzymol Relat Areas Mol Biol* 1969; **32**: 173-219
61 **Wang AL**, Tew KD. Increased glutathione-S-transferase activity in a cell line with acquired resistance to nitrogen mustards. *Cancer Treat Rep* 1985; **69**: 677-682
62 **Mimnaugh EG**, Dusre L, Atwell J, Myers CE. Differential oxygen radical susceptibility of adriamycin-sensitive and -resistant MCF-7 human breast tumor cells. *Cancer Res* 1989; **49**: 8-15
63 **Kulkarni AA**, Kulkarni AP. Retinoids inhibit mammalian glutathione transferases. *Cancer Lett* 1995; **91**: 185-189
64 **Fahey RC**. Biologically important thiol-disulfide reactions and the role of cyst(e)ine in proteins: an evolutionary perspective. *Adv Exp Med Biol* 1977; **86**: 1-30

Edited by Wang XL and Xu FM

PO Box 2345, Beijing 100023, China
Fax: +86-10-85381893
E-mail: wjg@wjgnet.com www.wjgnet.com

World J Gastroenterol 2004;10(9):1276-1280
World Journal of Gastroenterology
Copyright ©2004 by The WJG Press ISSN 1007-9327

• LIVER CANCER •

Association of low p16INK4a and p15INK4b mRNAs expression with their CpG islands methylation with human hepatocellular carcinogenesis

Yang Qin, Jian-Yu Liu, Bo Li, Zhi-Lin Sun, Ze-Fang Sun

Yang Qin, Jian-Yu Liu, Zhi-Lin Sun, Ze-Fang Sun, Department of Biochemistry and Molecular Biology, School of Preclinical and Forensic Medicine, West China Medical Center, Sichuan University, Chengdu, 610041, Sichuan Province, China
Bo Li, Department of General Surgery, West China Hospital, Sichuan University, Chengdu, 610041, Sichuan Province, China
Supported by the National Natural Science Foundation of China. No. 39670702
Correspondence to: Yang Qin, Department of Biochemistry and Molecular Biology, School of Preclinical and Forensic Medicine, West China Medical Center, Sichuan University, Chengdu, 610041, Sichuan Province, China. qin_1@sina.com
Telephone: +86-28-85501265 **Fax:** +86-28-85501257
Received: 2003-11-27 **Accepted:** 2003-12-22

Abstract

AIM: To study the significance of p16 and p15 transcription suppression with hypermethylation of their genes' 5'CpG islands during human hepatocellular carcinogenesis.

METHODS: The mRNA expression levels of p16 and p15 genes were evaluated in cancerous, para-cancerous and non-cancerous tissues of 20 HCC, 3 normal liver tissues from 3 accidentally died healthy adults using semi-quantitatively Northern blot. The methylation status was also assessed with methylation specific PCR.

RESULTS: p16 mRNA expression level was decreased in the cancerous tissues in 60% (12/20) of HCC patients, of which 2 cases had no p16 mRNA detected, 5 cases (25%) displayed variation in the order of cancerous<para-cancerous<non-cancerous liver tissues. p15 mRNA expression level was decreased in the cancerous tissues in 50% (10/20) HCC patients, of which one case had no p15 mRNA detected, 4 cases (20%) displayed variation in the order of cancerous <para-cancerous<non-cancerous liver tissues. In cancerous, para-cancerous and non-cancerous tissues, p16 promoter CpG islands hypermethylation occurred 65%, 60% and 35%, while p15 promoter CpG islands hypermethylation occurred 50%, 40% and 25%. Of 12 HCCs with lower p16 mRNA expression level, 11 cases showed p16 promoter CpG islands methylation (91.6%). Hundred percent (10/10) HCCs with lower p15 mRNA expression level showed p15 promoter CpG islands methylation. Significant correlation between 5'CpG islands methylation and p16/p15 mRNA expression suppression was found. The decreased expression of p16/p15 mRNA or methylation of p16/p15 promoters 5'CpG island was significantly correlate with poor differentiation of HCC (P=0.0083, 0.0102, 0.00271, 0.0218, respectively, P<0.05).

CONCLUSION: p16 and p15 genes transcriptional inactivation might play an important role in hepatocarcinogenesis. 5'CpG islands methylation might be the major mechanism of p16 and p15 genes inactivation in primary HCC in the studied population. 5'CpG islands methylation of p16 and p15 genes might be an early event in hepatocarcinogenesis.

Qin Y, Liu JY, Li B, Sun ZL, Sun ZF. Association of low p16INK4a and p15INK4b mRNAs expression with their CpG islands methylation with human hepatocellular carcinogenesis. *World J Gastroenterol* 2004; 10(9): 1276-1280
http://www.wjgnet.com/1007-9327/10/1276.asp

INTRODUCTION

Hepatocellular carcinoma (HCC) is one of the most common causes of death from cancer in China. The mechanisms of hepatocellular carcinogenesis are not yet expounded although alterations of some cell cycle tumor suppressor genes have been revealed to be involved in hepatocellular carcinogenesis. p16INK4a and p15INK4b are homologous cell cycle tumor suppressors, which are within 30 kb of one another on chromosome 9p21 region and in the same transcription orientation. p16INK4a has 3 exons whereas p15INK4b is encoded by 2 exons. They act as competitive inhibitors by binding directly to CDK4 and CDK6 and prevent their association with a cyclin, which in turn arrest the cells in late G1 phase of the cycle with pRB in a hypophosphorylated state[1-4].

Although the high frequency of P16 protein expression deficiency or low expression in HCC was reported, the rate of p16 gene homozygous deletion and mutation is much lower than P16 protein expression deficiency. This suggested that there might be another mechanism inactivating p16 and p15 genes in human primary hepatocarcinoma[5-9].

It has been demonstrated that aberrant methylation of CpG islands, which are CpG dinucleotide rich region located mainly in the promoter regions of many gene, serves as an alternative mechanism for inactivation of the tumor suppressor gene in cancers[10]. Recently, aberrant methylation of the p16 and p15 promoters has been reported[11-16]. The discordant events in which low P16 protein expression was not companied with deletion or mutation could be resulted from the low mRNA expression level of p16 gene due to hypermethylation of its CpG islands. To further study the association of hypermethylation of CpG islands in p16 and p15 genes with disrupted transcription of the corresponding genes in hepatocarcinogenesis, and to address the question whether the expression of p16 and p15 genes, as well as CpG island methylation of p16 and p15 genes is related to the differentiation degrees of HCC, the mRNA expression of p16 and p15 genes, as well as their CpG island methylation status in 20 HCCs was studied.

MATERIALS AND METHODS

Samples and extraction of total RNA and DNA

With informed consent of patients and ethics committee approval, surgically resected tumor, adjacent cancerous as well as non-cancerous tissue samples from 20 HCC patients, and

normal liver tissues from 3 accidentally died healthy adults were collected in West China Hospital of Sichuan University. The diagnosis of HCC was confirmed histologically in all cases.

Total RNA was extracted from 100 mg frozen tissue specimen with one-step guanidine thiocyanate-phenol method and dissolved in 5 g/L SDS solution. Genomic DNA was isolated from 100 mg frozen tissue specimen by digestion with proteinase K, followed by standard phenol-chloroform extraction and ethanol precipitation. The concentration of RNA and DNA was calculated according to their A_{260} values.

The genomic DNA of human plasmacytoma cell line HS-Sultan, which had p16 and p15 CpG islands methylation, was kindly gifted by Dr. Lo YM in Chinese University of Hong Kong. It was used as a methylation control for methylation specific PCR.

Northern blot hybridization

The plasmid that contained complete sequences of p16 cDNA or p15 cDNA was kindly gifted by Dr. D Beach in Cold Spring Harbor Laboratory. The 0.8 kb cDNA fragment of p16 and 2 kb cDNA fragment of p15 were nick translated with non-radiated digoxinin using Boehring Mannheim random primer DNA labeling kit. A 0.9 kb cDNA fragment of γ-actin was used as control probe. The total RNA (20-30 μg) was fractionated on 1% agarose-formaldehyde gel and blotted onto nylon membrane (Bio-Rad) by capillary transfer. The hybridization was carried out in a solution containing 70 g/L SDS, 500 g/L formamide, 20 mL/L blocking reagent, 50 mmol/L sodium phosphate, pH7.0, 1 g/L sarcosyl, 5×SSC, 80 ng/mL probe. The hybridization and the subject signal chemil-luminineceent imaging were performed according to the manufacturer' s manual. Every membrane was sequentially hybridized with p16, p15 and γ-actin cDNA probe after the bound probe was washed with 5 g/L SDS.

The intensity of the hybridization signal was scanned with UVP GDS8000 and quantited with Gelworks of UVP. To calculate the relative expression level of p16 or p15 gene, the hybridization signal intensity of γ-actin was employed as internal control to correct the unidentical amount of RNA loaded in electrophoresis, because γ-actin gene has a stable expression in various tissues.

Bisulfite conversion of DNA

Bisulfite modification and methylation specific PCR were conducted based on the principle that bisulfite treatment of DNA would convert unmethylated cytocine residues into uracil, whereas methylated cytocine residues would remain unmodified. Thus, the sequence-specific primers would distinguish the bisulfite converted unmethylation sequences and the unmodified methylation sequences by U and C.

The chemical modification was performed essentially as described previously with minor modification[17]. DNA (1-2 μg) in a volume of 50 μL was denatured by NaOH (final concentration, 0.2 mol/L) for 10 min at 37 ℃. Totally 520 μL of 3 mol/L sodium bisulfite at pH5.0 and 30 μL of 10 mmol/L hydroquinone, both freshly prepared, were added. After being mixed, the samples were incubated under the cover of mineral oil at 56 ℃ for 16 h. The modified DNA was desalted with the Wizard DNA purification resin and eluted in 50 μL of water. For alkali desulphonation, an equal volume of 0.6 mol/L NaOH was added to an eluted DNA and incubated for 5 min at room temperature, modified DNA was precipitated with sodium acetate and ethanol and resuspended in 30 μL of water. The DNA was stored at -70 ℃.

Methylation specific PCR

The primers were designed for the CpG islands in promoter and the first exon region of both p16 and p15 genes. All bisulfite-converted DNA samples were amplified with primers specific for methylated p16 or p15 sequence, and also amplified with primers specific for unmethylated p16 or p15 sequence. The sense and antisense primers for methylated p16 sequence were 5' TTATTAGAGGGTGGGGCGGATCGC3' and 5' GACCCCGAACCGCGACCGTAA 3' . The sense and antisense primers for unmethylated p16 sequence were 5' TTATTAGAG GGTGGGGTGGATTGT 3' and 5' CAACCCCAAACCACA ACCATAA3' . The sense and antisense primers for methylated p15 sequence were 5' GCGTTCGTATTTTGCGGTT3' and 5' CGTACAATAACCGAACGACCGA 3' . The sense and antisense primers for the unmethylated p15 sequence were 5' TGTGATGTGTTTGTATTTTGTGGTT 3' and 5' CCATACAATAACCAAACAACCAA 3' . The 25 μL of PCR mixture contained 50 ng of modified DNA, 200 μmol/L each dATP, dGTP, dCTP and dTTP, 1 μmol/L each primer, 50 g/L DMSO, 2.5 mmol/L $MgCl_2$, 1×reaction buffer and 1.5 U Taq polymerase. The PCR conditions were as follows: one cycle of at 95 ℃ for 5 min, 35 cycles of at 95 ℃ for 30 s, at 65 ℃ for 30 s (p16 methylation primers) or at 60 ℃ for 30 s (p16 unmethylation primers, p15 methylation and unmethylation primers), at 72 ℃ for 45 s, and 1 cycle of at 72 ℃ for 7 min. A 10 μL of PCR products was then electrophoresed on a 25 g/L agarose gel, stained with ethidium bromide, and visualized under UV illumination in UVP GDS8000 gel imaging system[17].

Statistical analysis

The difference in the p16 and p15 mRNA expression between cancer and noncancer tissue was analyzed using *t* test. The correlation of p16 or p15 gene mRNA expression level with its corresponding methylation of CpG islands was analyzed using Fisher' s exact test. The correlation of between mRNA expression, and methylation of p16 and p15 genes with pathologic characteristics was also analyzed with Fisher' s exact test. A P value <0.05 was considered statistically significant.

RESULTS

p16 and p15 mRNA expression in human hepatocarcinoma

After Northern blot hybridization, the 1.3 kb transcriptof p16 mRNA, 3.8 kb transcript of p15 mRNA, 2.1 kb transcript of γ-actin mRNA were detected.

As shown in Figure 1, there was a decrease in p16 mRNA expression level in the cancerous tissues in 60%(12/20) of HCC compared with their corresponding para-cancerous and non-cancerous liver tissues, and p16 mRNA signal was not detected in 2 cases (10%). Five cases (25%) displayed variation in the order of cancerous <para-cancerous<non-cancerous tissues. The mRNA expression level of p16 gene in cancerous tissues was significantly lower than that of non-cancerous liver tissues (P<0.05).

p15 mRNA expression level was decreased within the cancerous tissues in 50%(10/20) of HCC, and p15 mRNA was not detected in 1 case. Four cases displayed variation in the order of cancerous<para-cancerous<non-cancerous tissue. The mRNA expression level of p15 gene in cancerous tissues was significantly lower than that of non-cancerous liver tissues (P<0.05).

Methylation status of the 5'CpG islands of p16 and p15 genes

Hypermethylation of p16 promoter CpG islands occurred in cancerous tissues (65%, 13/20), and also in para-cancerous tissues (60%, 11/20,) and non-cancerous tissues (35%, 7/20). Four cancerous tissues exhibited only the methylation band,

while the others showed methylation and unmethylation bands, suggesting partial methylation (Figure 2)[11,13,18].

Aberrant promoter methylation of p15 gene was detected in 50%(10/20) of patients with HCC. Among them, the methylation was found only in cancerous tissues in 2 cases, in both cancerous and para-cancerous tissues in 3 cases, in all of cancerous, para-cancerous and non-cancerous tissues in 5 cases. The partial methylation occurred in all of the non-cancerous tissues. None of the 3 healthy subjects displayed p16 or p15 methylation, whereas they displayed unmethylated p16 and p15 alleles (Figure 3).

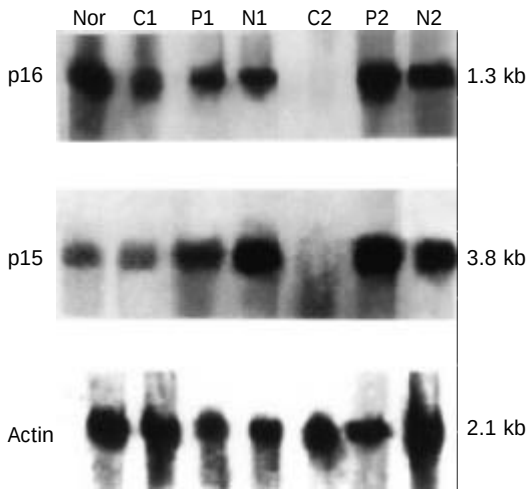

Figure 1 Northern blot analysis of the p16 and p15 genes in human primary heparocarcinoma. Total RNA from tissues of human primary heparocarcinoma was hybridized with cDNA fragment probes of p16, p15 and γ-actin labeled with non-radiated digoxinin. N: Normal liver tissue control; C, P, N represent RNA from cancerous, para-cancerous, non-cancerous liver tissues respectively; 1, 2 represent the No. of HCC patient.

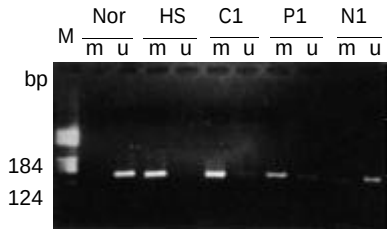

Figure 2 Methylation analysis of p16 gene in human primary heparocarcinoma. MSP product of p16 gene from HCC tissues was electrophoresed on a 25 g/L agarose gel. M: pBR322/HeaIII DNA molecular marker; N: Normal liver tissue DNA; HS: HS-Sultan DNA (positive control); C, P, N represent RNA from cancerous, para-cancerous, non-cancerous liver tissue respectively; 1, 2 mark the HCC patient number; m: PCR products from methylation specific primers, u: PCR products from unmethylation specific primers.

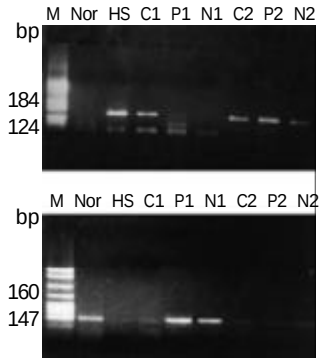

Figure 3 Methylation analysis of p15 gene in human primary heparocarcinoma. MSP product of p15 gene from HCC tissues was electrophoresed on a 2.5% agarose gel. M: pBR322/HeaIII DNA molecular marker (in graph m) or PBR322/Msp I DNA marker (in graph u); N: Normal liver tissue DNA; HS: HS-Sul-

Table 1 CpG island methylation status and expression of p16 and p15 genes and clinical information of 20 HCC patients

Cases	p16 methylation[1]	p16 expression	p15 methylation[1]	p15 expression	HBsAg[4]	Cirrhosis[5]	Differentiation[6]
1	±	D	+	D	+	Y	L
2	+	D	+	D	+	Y	L
3	±	D	+	D	+	N	M
4	±	N	±	D	+	Y	M
5	±	D	+	D	+	N	L
6	+	D	-	N	+	N	L
7	-	N	-	N	-	N	H
8	±	N	±	D	-	N	M
9	±	D	±	D	+	Y	M
10	-	N	-	N	-	N	H
11	+	D	N[2]	N	+	Y	L
12	±	D	-	I	+	Y	M
13	-	D	±	D	+	Y	M
14	-	N	-	I	-	N	M
15	+	D	-	N	+	N	L
16	±	N	±	D	-	Y	L
17	-	D	-	N	-	N	H
18	-	I	-	I	+	N	H
19	±	D	±	D	-	Y	L
20	-	N	-	N	+	N	H

[1]+Positively amplified with methylation primers only; - positively amplified with unmethylation primers only; ± positively amplified with methylation and unmethylation primers; [2]N: Negatively amplified with methylation or unmethylation primers, [3]D: Decreased; I: Increased; N: No significant difference; compared with non-cancer tissue, [4]+: Positive; -: Negative; [5]Y: Cirrhosis; N: No cirrhosis, [6]H: High differentiation; M: moderate differentiation; L: Low differentiation.

tan DNA(positive control); C, P, N represent RNA from cancerous, para-cancerous, non-cancerous liver tissue respectively; 1, 2 mark the HCC patient number; m: PCR products from methylation specific primers, u: PCR products from unmethylation specific primers.

Reciprocal relationship between mRNA expression of p16/p15 and their promoter methylation status

Significant correlation between 5' CpG island methylation and low mRNA expression of p16/p15 was found in the 20 HCCs ($P<0.05$). Among 12 HCCs, which displayed lower p16 mRNA expression level in cancerous tissue, 11 cases showed p16 promoter 5' CpG island methylation (91.6%). Similar event took place in p15 gene. All of 10 HCCs with decreased p15 mRNA expression in cancerous tissue had 5' CpG island hypermethylation (100%), while unmethylation occurred in non-cancerous liver tissue. Interestingly, 1 case displayed no detectable transcript p15 gene in cancerous tissue with hypermethylation (Table 1).

The relationship between mRNA expression, or methylation and pathologic characteristics

Significant correlation either between decreased p16/p15 mRNA expression and poor cellular differentiation of HCC, or between p16/p15 promoters 5' CpG islands methylation and poor differentiation of HCC was found (P=0.0083, 0.0102, 0.00271, 0.0218, respectively, $P<0.05$). However, there was no significant correlation between p16/p15 mRNA expression and HBV infection or cirrhosis, or between their promoter methylation and HBV infection or cirrhosis (Table 1).

DISCUSSION

Our study showed that a decreased p16 mRNA expression level was detected within cancerous tissues in 60% of HCCs compared with their corresponding non-cancerous tissues, 5 of which displayed in turn variation in cancerous tissue less than in para-cancerous tissue, then in non-cancerous liver tissues. It was interesting that among the 12 cases with lower p16 mRNA expression, 9 cases were companied with p16 gene promoter partial methylation in cancerous tissues, while 2 cases were companied with complete methylation. In contrast, methylation was not detected in normal liver tissues from 3 accidentally died subject. The partial methylation of p16 gene promoter may explain why the p16 mRNA expression just decreased but not loss in majority of HCCs. It has been reported that partial loss of expression of p16 was associated with low level of methylation rather than complete loss[11,19,20]. The relationship between p16 mRNA expression and its promoter CpG island methylation has been demonstrated in other studies. Kaneto *et al*, using methylation specific PCR and immunohistochemistry, had detected methylation of p16 promoter in HCC (72.6%, 16/22) and loss of expression in all methylation positive HCC[13]. Roncalli *et al* reported that methylation of p16 promoter with complete loss of immunoreactivity occurred in 27 of 33 HCC (82%)[15]. Thus, our result, which was consistent with other reports, suggested that association of p16 gene 5' CpG island methylation with transcription inactivation might play an important role in hepatocarcinogenesis, and 5' CpG island methylation was the major mechanism of p16 gene inactivation.

Like the alteration of p16 gene, a decreased p15 mRNA expression level was found within cancerous tissue in 50% of HCC compared with their corresponding non-cancerous liver tissues. All cases that had a lower transcription level of p15 were in conjunction with the hypermethylation of p15 promoter CpG island. Roncalli *et al* detected methylation of p15 islands in 42% of HCC (14/33), and methylation positive HCC had a complete loss of immunocytochemical expression of p15. Wong *et al* reported a high frequency of p15 methylation (64%, 15/25) in HCC. Yang *et a*l showed methylation of p15 in 49% of HCC[14-16]. Based on Northern blot analysis, our study found that a complete loss of p15 mRNA expression accounted for a small portion of the p15 methylation positive cases, while the majority had decreased transcription level. This discrepancy of our result with other studies might be due to the high sensitivity of Northern blot analysis. Nevertheless, our result provided further evidence from different aspect for the contribution of the epigenetic alteration to inactivation of p15 gene in hepatocarcinogenesis.

In our present study, partial methylation of p16 and/or p15 promoter was detected in 50% of non-cancerous liver tissues (10/20). However, the p16/p15 positive liver tissue still expressed mRNA of p16/p15 genes. It was very interesting to note that a complete methylation of p16 promoter CpG island was present in cancerous tissue while partial methylation in non-cancerous tissues. A similar phenomenon of p15 gene alteration occurred in 2 cases. This supported the hypothesis that methylation of cell cycle inhibitor gradually accumulate in the transition from cirrhosis or chronic hepatitis to HCC[13, 15]. Yu *et al* detected that hypermethylation of the p16 promoter CpG islands occurred overwhelmingly in HCC samples (56.6%, 17/29) and less frequently in adjacent non-cancerous tissues (21.9%, 6/29) after analyzing the methylation profiling of 20 promoter-CpG islands of genes in human primary hepatocellular carcinoma. Therefore, they thought that hypermethylation of p16 promoter CpG islands may occur at very late stage of the hepatocarcinogenesis[21]. Edamoto *et al* showed that higher rate of promoter methylation of p16 in HCCs (59%) than in cirrhotic liver (21%) or chronic hepatitis lesions (0/10)[22].

Our study also showed that in the non-cancerous liver tissues, the frequency of p15 partial methylation was higher in cirrhosis (44%, 4/9) than non-cirrhosis (9%, 1/11). Also the rate of p16 partial methylation was higher in cirrhosis (44%, 4/9) than non-cirrhosis 27%, 3/11), although these results had no statistical significance probably due to the few studied cases (Data not shown). The percentage of p16 methylation in cirrhosis was reported 29.4% by Kaneto *et al*, and 39% by Roncalli *et al*[13,15]. The frequency of p15 methylation reported by Roncalli et al was 33%[15]. Roncalli *et al* noted that p15 was responsible for the early methylation pattern in cirrhosis but not in HCC. They proposed that p15 but not p16 was necessary for the inactivation of other genes in the transition from cirrhosis to HCC[15]. Nevertheless, the methylation of p16 and p15 might be the major mechanism to inactive cell-cycle inhibitor in preneoplastic stage.

The correlation between either decreased p16/p15 mRNA expression or p16/p15 promoter CpG island methylation and poor differentiation of HCC was determined in our present study. Interestingly, the correlation of loss of p16 protein expression with the cellular differentiation of HCC and gastric cancer has been reported[23,24]. Park *et al* also noted that inactivation of p16 exon 1 by DNA hypermethylation occurred during the progression of tumor cells to poorly differentiated HCC, which was induced by diethylnitrosamine plus thioacetamide in Fischer 344 rats[25]. These studies suggested that the aberrant alteration of mRNA expression and methylation of p16 and p15 genes might be not only involved HCC carcinogenesis but also associated with its progress.

Although the mechanism of methylation in cancers remains to be explained clearly, it has been generally recognized that two methyltransferases, Dnmt1 and Dnmt3b cooperatively maintain DNA methylation and gene silencing in human cancer cells[26-28]. It has been reported that higher expression of methyltransferases was associated with methylation of p16

and p15 genes in HCC[29]. It has been noted that either the inhibitors of methyltransferase, such as 5-aza-2' -deoxycytidine and tea-polyphenol (-)-epigallocatechin-3-gallate or antisense inhibitors of DNA methyltransferases, reactivated silenced tumor suppressor genes and inhibited the growth of cancer cells[30-33].

Thus, methylation of 5' CpG islands of p16 and p15 genes might be an early event in hepatocarcinogenesis. The methylation of p16 and p15 genes could be a biomarker for monitoring HCC and other tumors, which was demonstrated by recent studies[14,34,35,36]. It also provides an insight into therapy of the high risky patients and prevention of HCC.

REFERENCES

1 **Ortega S**, Malumbres M, Barbacid M. Cyclin D-dependent kinase, INK4 inhibitors and cancer. *Biochim Biophys Acta* 2002; **1602**: 73-87

2 **Serrano M,** Hannon GJ, Beach D. A new regulatory motif in cell-cycle control causing specific inhibition of cyclin D/CDK4. *Nature* 1993; **366**: 704-707

3 **Hannon GJ,** Beach D. p15INK4B is a potential effector of TGF-beta-induced cell cycle arrest. *Nature* 1994; **371**: 257-261

4 **Weinberg RA.** The retinoblastoma protein and cell cycle control. *Cell* 1995; **81**: 323-330

5 **Hui AM,** Sakamoto M, Kanai Y, Ino Y, Gotoh M, Yokota J, Hirohashi S. Inactivation of p16INK4 in hepatocellular carcinoma. *Hepatology* 1996; **24**: 575-579

6 **Kita R,** Nishida N, Fukuda Y, Azechi H, Matsuoka Y, Komeda T, Sando T, Nakao K, Ishizaki K. Infrequent alterations of the p16INK4A gene in liver cancer. *Int J Cancer* 1996; **67**: 176-180

7 **Bonilla F**, Orlow I, Cordon-Cardo C. Mutational study of p16CDKN2/MTS1/INK4A and p57KIP2 genes in hepatocellular carcinoma. *Int J Oncol* 1998; **12**: 583-588

8 **Qin Y**, Li B, Tan YS, Sun ZL, Zho FQ, Sun ZF. Polymorphism of p16INK4a gene and rare mutation of p15INK4b gene exon2 in primary hepatocarcinoma. *World J Gastroenterol* 2000; **6**: 411-414

9 **Huang J**, Shen W, Li B, Luo Y, Liao S, Zhang W, Cheng N. A study on the inactivation of p16 and the expression of P16 protein in primary hepatocellular carcinomas. *Huaxi Yike Daxue Xuebao* 2000; **31**: 306-309

10 **Baylin SB,** Herman JG. DNA hypermethylation in tumorigenesis: epegenetics joins genetics. *Trends Genet* 2000; **16**: 168-174

11 **Matsuda Y,** Ichida T, Matsuzawa J, Sugimura K, Asakura H. p16 (INK4) is inactivated by extensive CpG methylation in human hepatocellular carcinoma. *Gastroenterology* 1999; **116**: 394-400

12 **Liew CT,** Li HM, Lo KW, Leow CK, Chan JY, Hin LY, Lau WY, Lai PB, Lim BK, Huang J, Leung WT, Wu S, Lee JC. High frequency of p16INK4A gene alterations in hepatocellular carcinoma. *Oncogene* 1999; **18**: 789-795

13 **Kaneto H**, Sasaki S, Yamamoto H, Itoh F, Toyota M, Suzuki H, Ozeki I, Iwata N, Ohmura T, Satoh T, Karino Y, Toyota M, Satoh M, Endo T, Omata M, Imai K. Detection of hypermethylation of the p16(INK4A) gene promoter in chronic hepatitis and cirrhosis associated with hepatitis B or C virus. *Gut* 2001; **48**: 372-377

14 **Wong IH**, Lo YM, Yeo W, Lau WY, Johnson PJ. Frequent p15 promoter methylation in tumor and peripheral blood from hepatocellular carcinoma patients. *Clin Cancer Res* 2000; **6**: 3516-3521

15 **Roncalli M**, Bianchi P, Bruni B, Laghi L, Destro A, Gioia SD, Gennari L, Tommasini M, Malesci A, Coggi G. Methylation framework of cell cycle gene inhibitors in cirrhosis and associated hepatocellular carcinoma. *Hepatology* 2002; **36**: 427-432

16 **Yang B**, Guo M, Herman JG, Clark DP. Aberrant promoter methylation profiles of tumor suppressor genes in hepatocellular carcinoma. *Am J Pathol* 2003; **163**: 1101-1107

17 **Herman JG,** Graff JR, Myohanen S, Nelkin BD, Baylin SB. Methylation-specific PCR: a novel PCR assay for methylation status of CpG islands. *Proc Natl Acad Sci U S A* 1996; **93**: 9821-9826

18 **Baek MJ**, Piao Z, Kim NG, Park C, Shin EC, Park JH, Jung HJ, Kim CG, Kim H. p16 is a major inactivation target in hepatocellular carcinoma. *Cancer* 2000; **89**: 60-68

19 **Gonzalgo ML,** Hayashida T, Bender CM, Pao MM, Tsai YC, Gonzales FA, Nguyen HD, Nguyen TT, Jones PA. The role of DNA methylation in expression of the p19/p16 locus in human bladder cancer cell lines. *Cancer Res* 1998; **58**: 1245-1252

20 **Herman JG.** p16(INK4): involvement early and often in gastrointestinal malignancies. *Gastroenterology* 1999; **116**: 483-485

21 **Yu J**, Ni M, Xu J, Zhang H, Gao B, Gu J, Chen J, Zhang L, Wu M, Zhen S, Zhu J. Methylation profiling of twenty promoter-CpG islands of genes which may contribute to hepatocellular carcinogenesis. *BMC Cancer* 2000; **2**: 29

22 **Edamoto Y**, Hara A, Biernat W, Terracciano L, Cathomas G, Riehle HM, Matsuda M, Fujii H, Scoazec JY, Ohgaki H. Alterations of RB1, p53 and Wnt pathways in hepatocellular carcinomas associated with hepatitis C, hepatitis B and alcoholic liver cirrhosis. *Int J Cancer* 2003; **106**: 334-341

23 **Wang ZW**, Peng ZH, Li K, Qiu GQ, Zhang Y, Gu W. Effect of p16 gene on carcinogenesis of hepatitis B virus related hepatocellular carcinoma. *Zhonghua Zhongliu Zazhi* 2003; **25**: 356-358

24 **Rocco A**, Schandl L, Nardone G, Tulassay Z, Staibano S, Malfertheiner P, Ebert MP. Loss of expression of tumor suppressor p16(INK4) protein in human primary gastric cancer is related to the grade of differentiation. *Dig Dis* 2002; **20**: 102-105

25 **Park TJ,** Kim HS, Byun KH, Jang JJ, Lee YS, Lim IK. Sequential changes in hepatocarcinogenesis induced by diethylnitrosamine plus thioacetamide in Fischer 344 rats: induction of gankyrin expression in liver fibrosis, pRB degradation in cirrhosis, and methylation of p16(INK4A) exon 1 in hepatocellular carcinoma. *Mol Carcinog* 2001; **30**: 138-150

26 **Rhee I**, Bachman KE, Park BH, Jair KW, Yen RW, Schuebel KE, Cui H, Feinberg AP, Lengauer C, Kinzler KW, Baylin SB, Vogelstein B. DNMT1 and DNMT3b cooperate to silence genes in human cancer cells. *Nature* 2002; **416**: 552-556

27 **Kim GD,** Ni J, Kelesoglu N, Roberts RJ, Pradhan S. Co-operation and communication between the human maintenance and de novo DNA (cytosine-5) methyltransferases. *EMBO J* 2002; **21**: 4183-4195

28 **Robert MF**, Morin S, Beaulieu N, Gauthier F, Chute IC, Barsalou A, MacLeod AR. DNMT1 is required to maintain CpG methylation and aberrant gene silencing in human cancer cells. *Nat Genet* 2003; **33**: 61-65

29 **Saito Y,** Kanai Y, Sakamoto M, Saito H, Ishii H, Hirohashi S. Expression of mRNA for DNA methyltransferases and methyl-CpG-binding proteins and DNA methylation status on CpG islands and pericentromeric satellite regions during human hepatocarcinogenesis. *Hepatology* 2001; **33**: 561-568

30 **Fang MZ**, Wang Y, Ai N, Hou Z, Sun Y, Lu H, Welsh W, Yang CS. Tea polyphenol (-)-epigallocatechin-3-gallate inhibits DNA methyltransferase and reactivates methylation-silenced genes in cancer cell lines. *Cancer Res* 2003; **63**: 7563-7570

31 **Liu LH**, Xiao WH, Liu WW. Effect of 5-Aza-2'-deoxycytidine on the P16 tumor suppressor gene in hepatocellular carcinoma cell line HepG2. *World J Gastroenterol* 2001; **7**: 131-135

32 **Stewart DJ,** Donehower RC, Eisenhauer EA, Wainman N, Shah AK, Bonfils C, MacLeod AR, Besterman JM, Reid GK. A phase I pharmacokinetic and pharmacodynamic study of the DNA methyltransferase 1 inhibitor MG98 administered twice weekly. *Ann Oncol* 2003; **14:** 766-774

33 **Zhang H,** Xiao W, Liang H, Fang D, Yang S, Luo Y. Demethylation in the promoter area by the antisense of human DNA MTase gene. *Zhonghua Zhongliu Zazhi* 2002; **24**: 444-447

34 **Wong IH**, Zhang J, Lai PB, Lau WY, Lo YM. Quantitative analysis of tumor-derived methylated p16INK4a sequences in plasma, serum, and blood cells of hepatocellular carcioma patients. *Clin Cancer Res* 2003; **9**: 1047-1052

35 **Deligezer U**, Yaman F, Erten N, Dalay N. Frequent copresence of methylated DNA and fragmented nucleosomal DNA in plasma of lymphoma patients. *Clin Chim Acta* 2003; **335**: 89-94

36 **Siu LL**, Chan JK, Wong KF, Choy C, Kwong YL.Aberrant promoter CpG methylation as a molecular marker for disease monitoring in natural killer cell lymphomas. *Br J Haematol* 2003; **122**: 70-77

Edited by Zhu LH and Xu FM

PO Box 2345, Beijing 100023, China
Fax: +86-10-85381893
E-mail: wjg@wjgnet.com www.wjgnet.com

World J Gastroenterol 2004;10(9):1281-1285
World Journal of Gastroenterology
Copyright ©2004 by The WJG Press ISSN 1007-9327

• LIVER CANCER •

Correlation of expression of multidrug resistance protein and messenger RNA with ^{99m}Tc-methoxyisobutyl isonitrile (MIBI) imaging in patients with hepatocellular carcinoma

Hai Wang, Xiao-Ping Chen, Fa-Zu Qiu

Hai Wang, Xiao-Ping Chen, Fa-Zu Qiu, Hepatic Center of Tongji Hospital, Tongji Medical College, Huazhong University of Science and Technology, Wuhan 430030, HuBei Province, China
Supported by the Clinical Focal Point Subject Foundation of Ministry of Public Health, No.3212001
Correspondence to: Dr. Xiao-Ping Chen, Hepatic Surgery Center of Tongji Hospital, Tongji Medical College, Huazhong University of Science and Technology, Wuhan 430030, Hubei Province, China. chenxp53@sina.com
Telephone: +86-27-83662599 **Fax:** +86-27-83662851
Received: 2003-03-12 **Accepted:** 2003-08-16

Abstract

AIM: To explore whether P-glycoprotein (Pgp) and other pumps, multidrug resistance-associated protein (MRP) and lung resistance protein (LRP), could affect tumor accumulation and efflux of ^{99m}Tc-MIBI in liver cancer.

METHODS: Surgically treated 78 liver cancer patients were included in this study. Before surgery, ^{99m}Tc-MIBI SPECT was performed 15 min and 120 min after injection of 20 mCi ^{99m}Tc-MIBI, respectively. Early uptake, delayed uptake (L/Nd), and washout rate (L/Nwr) of ^{99m}Tc-MIBI were obtained. Expressions of Pgp, MRP and LRP were investigated with Western blotting and immunohistochemistry. Messenger RNA (mRNA) level of Pgp, MRP and LRP was determined by RT-PCR.

RESULTS: No ^{99m}Tc-MIBI uptakes in tumor lesions of 68 of 78 (87.2%) patients with hepatocellular carcinoma were found on ^{99m}Tc-MIBI SPECT. P-gp expression was observed in tumor tissues of the patients with no uptake of ^{99m}Tc-MIBI ($P<0.017$). No appreciable correlation was found between liver cancer ^{99m}Tc-MIBI images and expression of MRP or LRP on the level of protein or mRNA.

CONCLUSION: ^{99m}Tc-MIBI SPECT is noninvasive, and useful in predicting the presence of MDR1 gene-encoded Pgp in patients with hepatocellular carcinoma.

Wang H, Chen XP, Qiu FZ. Correlation of expression of multidrug resistance protein and messenger RNA with ^{99m}Tc-methoxyisobutyl isonitrile (MIBI) imaging in patients with hepatocellular carcinoma. *World J Gastroenterol* 2004; 10 (9): 1281-1285
http://www.wjgnet.com/1007-9327/10/1281.asp

INTRODUCTION

Multidrug resistance (MDR) is the main barrier to efficient chemotherapy of human malignancies. MDR has been closely associated with overexpression of multidrug resistance genes (MDRI)[1] and has been observed in hepatocellular carcinomas (HCC)[2]. The MDR phenotype has been defined on the basis of cellular drug targets involved Pgp, MRP, LRP and atypical MDR (mediated through altered expression of topoisomerase type II)[3-6]. Pgp, encoded by MDRI gene, is a 170-ku transmembrane glycoprotein and acts as an adenosine triphosphate (ATP)-driven drug efflux pump to reduce drug accumulation[7]. MRP is a 190-ku membrane-bound glycoprotein and can act as a glutathione S-conjugate efflux pump by transporting drugs that are conjugated or cotransported with glutathione[8,9]. Both Pgp and MRP are integral membrane proteins belonging to the ATP-binding cassette (ABC) superfamily of transporter proteins, which appear to confer resistance by decreasing intracellular drug accumulation[10]. In contrast, LRP is not an ABC transporter protein. LRP has recently been identified as a vault protein, which is a typical multisubunit structure involved in nucleocytoplasmic transporter[11]. Determination of these MDR proteins at the time of diagnosis is imperative to the development of rational therapeutic strategies for preventing drug resistance.

^{99m}Tc-MIBI is a cationic lipophilic agent, widely used for myocardial perfusion imaging to detect various tumors[12-18]. Recent evidence has shown that ^{99m}Tc-MIBI is a suitable transport substrate for Pgp and may provide additional information about the Pgp status of tumor cells[19,20]. It has been reported that MIBI is accumulated within mitochondria and cytoplasm of cells based on transmembrane electrical potentials. Malignant tumors show increased transmembrane potential as a result of increased metabolic requirements that induce increased accumulation of MIBI in tumors[21]. The potential advantage of ^{99m}Tc-MIBI imaging lies in its superiority in detecting the presence of Pgp overexpression *in vivo* noninvasively[22,23]. Recently, ^{99m}Tc-MIBI efflux has been shown to be a substrate for MRP *in vivo*[24].

^{99m}Tc-MIBI imaging or SPECT was performed in various cancers[25,26], but no clinical studies in HCC have been found. The aim of this study was to determine whether Pgp and other pumps, MRP and LRP, could affect tumor accumulation and efflux of ^{99m}Tc-MIBI in hepatocellular carcinoma.

MATERIALS AND METHODS

Patients

Seventy-eight patients (30 women, 48 men, aged 24-71 years, mean 54±11.6 years) with HCC were enrolled in the study, 70 of 78 (89.7%) patients were hepatitis B surface antigen positive, 2 (2.6%) were anti-hepatitis C virus positive, and the remaining had no known cause of HCC. No patients previously received chemotherapy. All patients underwent ^{99m}Tc-MIBI SPECT prior to surgery. All tumor samples were analyzed with RT-PCR, Western blotting and immunohistochemistry.

^{99m}Tc-MIBI SPECT

Liver imaging was performed with a double-head gamma camera equipped with a high-resolution parallel-hole collimator (PRISM 2000; Marconi Medical Systerms, Cleveland, OH). Images were obtained 15 and 120 min after injection of 20 mCi ^{99m}Tc-MIBI, respectively. Early and delayed SPECT of the liver was performed

on all patients. For SPECT of the liver, 72 projections were obtained using 64×64 matrix at 45 s per view. Image reconstruction was performed using filtered back projection with Butter-worth and ramp filters. Transverse, coronal, and sagittal sections were reconstructed. Attenuation correction was not applied.

SPECT images were compared with liver CT images, and accumulation in liver tumors was interpreted by nuclear medicine physicians. The findings on ^{99m}Tc-MIBI livers were measured semiquantitatively. Regions of interest (ROIs) were manually defined on the transaxial tomograms showing the lesion's highest uptake in center of the tumor. ROIs placed on the lesions (L) encompassed all pixels that had uptake values of >90% of the maximum uptake in that slice, and the average rate in each ROI was calculated. Another ROI of the same size was then drawn over the normal lung (N) on the same transverse section. The early uptake (L/Ne) and the delayed uptake (L/Nd) were obtained. The washout rate (L/Nwr) was calculated using the following formula: L/Nwr = (L/Ne-L/Nd)×100 (L/Ne).

Immunohistochemical study

After resection of HCC, immunohistochemiscal study of the biopsy or resected tumor tissues and surrounding nontumorous liver parenchyma was performed. Four-micrometer-thick, formalin-fixed, paraffin-embeded tissue sections were cut from the specimens and mounted on poly-L-lysine-coated glass slides (Sigma Chemical Co., St. Louis, MO). The standard avidin-biotin-peroxidase complex (ABC) technique was used for immunostaining using a LSAB kit (Dako Co., Carpinteria, CA).

After deparaffinization and rehydration, the sections were treated with 1 mL/L methanol hydrogen peroxide for 20 min to block endogenous peroxidase activity, incubated with normal horse serum for 30 min at 37 ℃, and with primary antibody, JSB-1 (1:20), MRP1 (1:10), LRP-56 (1:10) overnight in a moist chamber at 4 ℃. The tissue sections were incubated with avidin-biotin-peroxidase complex. The final reaction product was revealed by exposure to 0.3 g/L diaminobenzidine, and the nuclei were counterstained with Mayer's hematoxylin.

A negative control was obtained by staining the sample with secondary antibody and a positive control by inclusive of a normal liver. The results of immunostaining were interpreted independently by two pathologists who were unaware of the imaging studies. Expressions of Pgp, MRP and LRP were scored as follows: -, negative; +, ≤10% positive tumor cells; ++, ≤30% positive tumor cells; +++, >30% positive tumor cells.

Quantitative RT-PCR

RT was performed with random primers with a complementary DNA (cDNA) synthesis kit (Promega, Madison, WI). RT-reaction reagents were added as follows: 2 μL of $MgCL_2$ (50 mmol/L), 2 μL of reverse transcription buffer (Tris-HCL [PH8.3], 100 mmol/L, KCL 500 mmol/L and Triton X-10 010 g/L), 2 μL of deoxynucleotide mixture (10 mmol/L), 0.5 μL of RNase inhibitor (20U), 2 (15U) of avian myeliblastoma virus reverse transcriptase, 1 μL of random primers (500 μg/mL) and 5 μg substrate RNA. The final volume of the reaction (20 μL) was completed with RNase free water. First strand cDNA synthesis was carried out at 42 ℃ for 30 min in the DNA thermal cycler (PTC-100, MJ Reserch Inc., Watertown, MA). Afterwards, the tubes were incubated at 99 ℃ for 5 min to stop the reaction. Then each tube was kept at 4 ℃ until PCR was performed. Expression of the target genes (MDR1, MRP and LRP) and endogenous reference β-actin was quantified using the primers and standards. The primers were designed using the software Primer Express (Applied Biosystems) (Table1).

RT -PCR

Expressions of the target genes (MDR1, MRP and LRP) and GAPDH gene were quantified using the primers and standards. The primers were designed using the software Primer Express (Applied Biosystems) (Table2).

RT-PCR was performed according to the TaqMan 2-step

Table 1 MDR1, MRP, LRP primers for RT-PCR amplifications

Gene	Quantification method	Sequence	cDNA
MDR1	Forward primer	5- CATTGGTGTGGTGAGTCAGG-3	1523-1542
	Reverse primer	5- CTCTCTCTCCAACCAGGGTG-3	1679-1698
MRP	Forward primer	5- CTACCGAGAGGACCTGGACT-3	4099-4118
	Reverse primer	5- GTCTAGCTTGTCAGGAAGGG-3	4437-4456
LRP	Forward primer	5- TAAGGGCTTCCAGCACCAAC-3	148-167
	Reverse primer	5- GGAGTTCTCGCTTCTCGTCC-3	520-539
β-actin	Forward primer	5- GTGTTTGGCCGAGTCCTCACC-3	
	Reverse primer	5- CTCCTGCAAGGAAAAGCTCTG-3	

Table 2 Oligonucleotides used for PCR amplifications

Gene	Quantification method	Sequence	cDNA
MDR1	Forward primer	5'- CCCAGGAGCCCATCCTGT-3'	3774-3791
	Revease primer	5'- CCCGGCTGTTGTCTCCATA-3'	3838-3821
	Probe	5'-(FAM)TGACTGCAGCATTGCTGAGAACATTGC(TAMRA)-3'	3793-3819
MRP	Forward primer	5'- AAGCGCCTCGAGTCGGT-3'	3617-3633
	Revease primer	5'- TCGAATGACGCTGACCCC-3'	3694-3677
	Probe	5'-(FAM)AGCCGCTCCCCGGTCTATTCCC-(TAMRA)-3'	3635-3656
LRP	Forward primer	5'- TTTCGATGACTTCCATAAGAACTCA-3'	1881-1905
	Reverse primer	5'- TTCCGAGGTCTCAAAGCCAA-3'	1950-1931
	Probe	5'(FAM)-CCCGCATCATTCGCACTGCTGT- (TAMRA)3'	1907-1928
GAPDH	Forward primer	5'- GAAGGTGAAGGTCGGAGTCA-3'	
	Revease primer	5'- GAAGATGGTGATGGGA-3'	
	Probe	5'-(JOE)CAAGCTTCCCGTTCTCAGCC(TAMRA)-3'	

method using the ABI PRISM 7 700 sequence detection system (Applied Biosystems). The nontemplate controls, standard dilutions, and samples were assayed. A 25-mm volume of PCR reaction mixture was used, containing 200 ng of the sample cDNA, TaqMan buffer, 200 mmol/L deoxy-ATP, deoxycytidine triphosphate, and deoxy-guanosine triphosphate, 400 mmol/L deoxyuridine triphosphate, 5.5 mmol/L magnesium chloride, 0.025 U/mL AmpliTaq Gold DNA polymease (Applied Biosystems), 0.01 U/mL AmpErase uracil N-glycosylase (Applied Biosystems), 200 nmol/L forward and reverse primers, and 100 nmol/L probe. PCR cycling conditions included an initial phase at 50 ℃ for 2 min, followed by at 95 ℃ for 10 min for AmpErase, 40 cycles at 95 ℃ for 15 s, and at 60 ℃ for 1 min. Quantification of the PCR products was based on the TaqMan 5' nuclease assay using the ABI PRISM 7 700 sequence detection system. The starting quantity of a specific mRNA in an unknown sample was determined by preparing a standard cDNA. The standard curve was generated on the basis of the linear relationship between CT value (corresponding to the cycle number at which a significant increase in fluorescence signal was first detected) and logarithm of the starting quantity. The unknown samples were quantified by the software of the ABI PRISM 7 700 sequence detector system, which calculated the CT value for each sample and then determined the initial quantity of the target using the standard curve. The amount of expressed target gene was normalized to that of GAPDH.

Western blotting

Liver cancer samples were analyzed for the presence of Pgp, MRP and LRP protein. Samples were washed in PBS and homogenized in a lysis buffer[27], Protein supernatants were quantitated using the Lowry assay, and equal amounts of protein from each sample were separated by SDS-PAGE and electroblotted onto nitrocellulose membranes. Membranes were probed with mAb recognizing Pgp, MRP and LRP (Sigma, Co), respectively. Enhanced chemiluminescence was used for protein detection.

Statistical analysis

The results of L/Ne, L/Nd, and L/Nwr were expressed as mean±SD. The differences in L/Ne, L/Nd, and L/Nwr between patients with (-), (+), and (++) Pgp, MRP, and LRP expressions were determined using Student *t* test. The differences in L/Ne, L/Nd, and L/Nwr between patients with high and low Pgp mRNA, MRP mRNA, and LRP mRNA expressions were determined using Student *t* test. If P was <0.05, the difference was considered statistically significant.

RESULTS

All the 78 surgically obtained tissue samples were assessed to estimate the levels of Pgp, MRP, and LRP expression on protein and mRNA. Table 3 summarizes the immunohistochemical results and RT PCR data.

Correlation of ^{99m}Tc-MIBI results with immunohistochemical results

Significant MIBI uptake on ^{99m}Tc-MIBI SPECT was noted in tumor lesions of 10 (12.8%) patients with HCC, but not in tumor lesions of 68 (87.2%) patients with HCC. In patients with MIBI uptake, immunohistochemical analysis of tumor tissues showed no detectable P-glycoprotein-positive cells. But immunohistochemical analysis of tumor lesions in patients without MIBI uptake revealed uniformly distributed P-gp-positive cells. We noted a significant correlation between ^{99m}Tc-MIBI SPECT findings and P-gp expression in tumors of patients with HCC.

MRP and LRP protein expression was found in tumor lesions of 7 and 4 patients, respectively, and no correlation was found with ^{99m}Tc-MIBI.

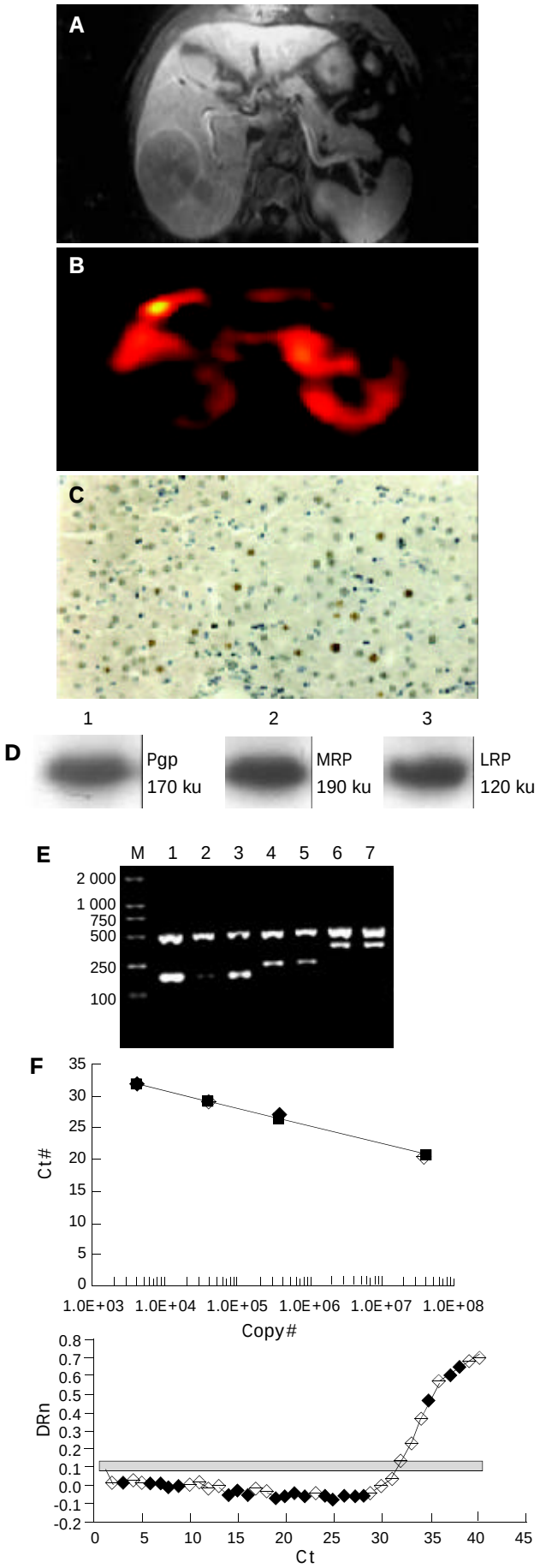

Figure 1 A: CT image of one patient with liver carcinoma. B: ^{99m}Tc-MIBI SPECT Liver image of the patient. C: Immunohistochemical expression of Pgp. D: Western blotting images of Pgp, MRP and LRP. E: MDR1 176 bp, MRP 358 bp, LRP 492 bp shown by RT-PCR image. F: Real time RT-PCR image of Pgp.

Table 3 Patient characteristics and radionuclide imaging

Group	Cases	Tumor size (cm)	^{99m}Tc-MIBI SPECT			Immunohistochemistry			RT-PCR		
			L/Ne	L/Nd	L/Nwr(%)	Pgp	MRP	LRP	mdr1	MRP	LRP
I	68	2.5-15	2.09±0.67	1.25±0.42	54.94±10.23	68 (+)	4 (+)	3 (+)	0.38±0.16	0.04±0.02	0.02±0.01
II	10	1.5-7	1.98±0.56	2.78±0.53	3.07±0.57	10 (-)	3 (+)	1 (+)	0	0.06±0.03	0.03

Correlation of ^{99m}Tc-MIBI with RT-PCR results

No correlation was found between L/Ne and the level of Pgp mRNA, MRP mRNA, and LRP mRNA. The mean L/Nd (2.78±0.64) of the Pgp mRNA low expression group was significantly higher than that (1.25±0.43) of the Pgp high-expression group (P=0.0115, Figure 1). L/Nd was not related to the level of MRP mRNA or LRP mRNA. Statistical support was found toward a significant difference in L/Nwr between the Pgp mRNA high-expression group and the Pgp mRNA low-expression group. L/Nwr was not related to the level of MRP mRNA or LRP mRNA.

The grouping was according to the positive mmunohistochemistry of Pgp, there were 4 cases positive of MRP and 3 cases positive of LRP in group I, there were 3 cases positive of MRP and 1case positive of LRP in group II.

DISCUSSION

The resistance of tumors to multiple drugs is a major problem in cancer chemotherapy. Pgp, a transmembrane ATP-dependent efflux pump encoded by MDR1 gene, has a central role in multidrug resistance. Increased amounts of Pgp may confer multidrug resistance to cells by preventing intracellular accumulation of a variety of cytotoxic drugs. A unique feature of multidrug resistance is the apparent capacity of Pgp for recognizing and transporting a large group of cytotoxic compounds sharing little structural or functional similarity other than being relatively small hydrophobic and cationic agents, including anthracyclines, Vinca alkaloids, and actinomycin D. Evidence has shown that Pgp as a drug efflux pump extrudes ^{99m}Tc-MIBI and other drugs from cells and that Pgp expression and enhanced efflux of ^{99m}Tc-MIBI from these cells are closely connected[28,29]. In animal models, faster clearance of ^{99m}Tc-MIBI was observed in tumors with or without Pgp expression[30,31]. Our study revealed that the mean L/Nd in Pgp (-) patients was significantly higher than that in Pgp (++) patients (P=0.035). Pgp (++) patients had a higher L/Nwr than Pgp (-)patients (P=0.027). No correlation was found between L/Ne and Pgp expression. The same results were obtained from mRNA level. Moreover, no correlation was found between MRP and ^{99m}Tc-MIBI SPECT. The same result was obtained from LRP protein and mRNA level. ^{99m}Tc-MIBI uptake by tumor is associated with many factors, including direct mechanisms such as negative transmembrane potential and drug efflux pump and indirect mechanisms such as blood flow and capillary permeability. We considered L/Ne to be more affected by blood flow. In contrast, L/Nd and L/Nwr clearly reflected Pgp expression of intrinsic properties of the tumor.

Until now, there have been some reports about the expression of Pgp in tumor tissues of patients with HCC[32,33]. Resistance to cancer chemotherapy in HCC resulted from Pgp expression. The specific localization of Pgp and the incidence of Pgp expression in each histological type of HCC were observed. The analysis indicated that the incidence was the lowest in the compact type of HCC, and it was significantly lower than that in the pseudo glandular and trabecular types[34]. But in our study, mRNA and protein level of Pgp revealed no significant difference in the incidence of Pgp expression in each histological type.

It has been established that MRP belongs to the superfamily of ABC transmembrane transporter proteins and can act as a glutathione S-conjugate efflux pump[35]. ^{99m}Tc-MIBI was shown to be a substrate for MRP *in vitro*[36]. The abilities of Pgp and MRP transporters to wash out ^{99m}Tc-MIBI have been reported to be similar in cell lines, in spite of different possible mechanisms of transport[37]. However, cardiac muscle showed a low L/Nwr of ^{99m}Tc-MIBI and a low level of Pgp expression but a high level of MRP expression[38]. In our study, we did not observe any correlation between tumor accumulation or efflux of ^{99m}Tc-MIBI and expression of MRP on protein level or mRNA level in liver cancer. The mechanisms are also unclear.

LRP has been identified as the vault protein involved in nucleocytoplasmic transport. Recently, subcellular accumulation of drugs was found to be localized in cytoplasm and minimally in nuclei in LRP overexpression cells[39]. As increased cytoplasm concentration of the drug could intensify its contact with the membrane, we proposed that efflux of the drug might be enhanced in LRP overexpression cells. However, we did not find a correlation between tumor accumulation or efflux of ^{99m}Tc-MIBI and expression of LRP. Subcellular accumulation of ^{99m}Tc-MIBI within mitochondria and cytoplasm of cells has been reported to be based on transmembrane electric potentials[40]. Therefore, efflux of ^{99m}Tc-MIBI was rarely affected by expression of LRP.

Until now, there have been few clinical studies on the relation between Pgp expression and ^{99m}Tc-MIBI uptake in HCC. As ^{99m}Tc-MIBI is cleared through the liver, and it is not easy to detect liver tumors. To the best of our knowledge, our study was the first to show an inverse correlation in MDR1/Pgp expression and ^{99m}Tc-MIBI uptake in HCC. But ^{99m}Tc-MIBI SPECT has some limitations, because it depends on the optimal perfusion of tumor tissues. Poor MIBI penetration could be attributable to poor tumor perfusion in tumors larger than 2.5 cm, where tumor necrosis would be expected. Therefore, perfusion studies such as a Tl-201 scan could be used to eliminate the possibility of poor penetration.

In conclusion, our results suggest that L/Nd and L/Nwr of ^{99m}Tc-MIBI are noninvasive and useful in detecting the expression of Pgp in patients with HCC

REFERENCES

1 **McGrath MS**, Rosenblum MG, Philips MR, Scheinberg DA. Immunotoxin resistance in multidrug resistant cells. *Cancer Res* 2003; **63**: 72-79

2 **Huesker M**, Folmer Y, Schneider M, Fulda C, Blum HE, Hafkemeyer P, Huesker M, Folmer Y, Schneider M, Fulda C, Blum HE, Hafkemeyer P. Reversal of drug resistance of hepatocellular carcinoma cells by adenoviral delivery of anti-MDR1 ribozymes. *Hepatology* 2002; **36**(4Pt 1): 874-884

3 **Ogiso Y**, Tomida A, Tsuruo T. Nuclear localization of proteasomes participates in stress-inducible resistance of solid tumor cells to topoisomerase II-directed drugs. *Cancer Res* 2002; **62**: 5008-5012

4 **Masanek U**, Stammler G, Volm M. Modulation of multidrug resistance in human ovarian cancer cell lines by inhibition of P-glycoprotein 170 and PKC isoenzymes with antisense oligonucleotides. *J Exp Ther Oncol* 2002; **2**: 37-41

5 **Volm M**. Multidrug resistance and its reversal. *Anticancer Res* 1998; **18**: 2905-2918

6 **Scaglioui GV**, Novello S, Selvaggi G. Multidrug resistance in non-small-cell lung cancer. *Ann Oncol* 1999; **10**(Suppl 5): 583-586

7 **Molinari A**, Calcabrini A, Meschini S, Stringaro A, Crateri P, Toccacieli L, Marra M, Colone M, Cianfriglia M, Arancia G. Subcellular detection and localization of the drug transporter.

Curr Protein Pept Sci 2002; **3**: 653-670

8 **Sharma KG**, Mason DL, Liu G, Rea PA, Bachhawat AK, Michaelis S. Localization, regulation, and substrate transport properties of Bpt1p, a Saccharomyces cerevisiae MRP-type ABC transporter. *Eukaryot Cell* 2002; **1**: 391-400

9 **Jin J**, Huang M, Wei HL, Liu GT. Mechanism of 5-fluorouracil required resistance in human hepatocellular carcinoma cell line Bel(7402). *World J Gastroenterol* 2002; **8**: 1029-1034

10 **Hsia TC**, Lin CC, Wang JJ, Ho ST, Kao A. Relationship between chemotherapy response of small cell lung cancer and P-glycoprotein or multidrug resistance-related protein expression. *Lung* 2002; **180**: 173-179

11 **Damiani D**, Michelutti A, Michieli M, Masolini P, Stocchi R, Geromin A, Ermacora A, Russo D, Fanin R, Baccarani M. P-glycoprotein, lung resistance-related protein and multidrug resistance-associated protein in de novo adult acute lymphoblastic leukaemia. *Br J Haematol* 2002; **116**: 519-527

12 **Vergote J**, Moretti JL, Kouyoumdjian JC, Garnier-Suillerot A. MRP1 modulation by PAK-104P: detection with technetium-99m-MIBI in cultured lung tumor cells. *Anticancer Res* 2002; **22** (1A): 251-256

13 **Zhou J**, Higashi K, Ueda Y, Kodama Y, Guo D, Jisaki F, Sakurai A, Takegami T, Katsuda S, Yamamoto I. Expression of multidrug resistance protein and messenger RNA correlate with ^{99m}Tc-MIBI imaging in patients with lung cancer. *J Nucl Med* 2001; **42**: 1476-1483

14 **Kim YS**, Cho SW, Lee KJ, Hahm KB, Wang HJ, Yim H, Jin YM, Park CH. ^{99m}Tc-MIBI SPECT is useful for noninvasively predicting the presence of MDR1 gene-encoded P-glycoprotein in patients with hepatocellular carcinoma. *Clin Nucl Med* 1999; **24**: 874-879

15 **Andrews DW**, Das R, Kim S, Zhang J, Curtis M. Technetium-MIBI as a glioma imaging agent for the assessment of multidrug resistance. *Neurosurgery* 1997; **40**: 1323-1332

16 **Fukumoto M**, Yoshida D, Hayase N, Kurohara A, Akagi N, Yoshida S. Scintigraphic prediction of resistance to radiation and chemotherapy in patients with lung carcinoma: technetium 99m-tetrofosmin and thallium-201 dual single photon emission computed tomography study. *Cancer* 1999; **86**: 1470-1479

17 **Bom HS**, Kim YC, Song HC, Min JJ, Kim JY, Park KO. Technetium-99m-MIBI uptake in small cell lung cancer. *J Nucl Med* 1998; **39**: 91-94

18 **Cayre A**, Cachin F, Maublant J, Mestas D, Feillel V, Ferriere JP, Kwiaktowski F, Chevillard S, Finat-Duclos F, Verrelle P, Penault-Llorca F. Single static view 99mTc-sestamibi scintimammography predicts response to neoadjuvant chemotherapy and is related to MDR expression. *Int J Oncol* 2002; **20**: 1049-1055

19 **Ramachandran C**, Khatib Z, Escalon E, Fonseca HB, Jhabvala P, Medina LS, D'Souza B, Ragheb J, Morrison G, Melnick SJ. Molecular studies in pediatric medulloblastomas. *Brain Tumor Pathol* 2002; **19**: 15-22

20 **Capella LS**, Gefe MR, Silva EF, Affonso-Mitidieri O, Lopes AG, Rumjanek VM, Capella MA. Mechanisms of vanadate-induced cellular toxicity: role of cellular glutathione and NADPH. *Arch Biochem Biophys* 2002; **406**: 65-72

21 **Vergote J**, Moretti JL, de Vries EG, Garnier-Suillerot A. Comparison of the kinetics of active efflux of ^{99m}Tc-MIBI in cells with P-glycoprotein-mediated and multidrug-resistance phenotypes. *Eur J Biochem* 1998; **252**: 140-146

22 **Heiba SI**, Santiago J, Mirzaitehrane M, Jana S, Dede F, Abdel-Dayem HM. Transient postischemic stunning evaluation by stress gated Tl-201 SPECT myocardial imaging: Effect on systolic left ventricular function. *J Nucl Cardiol* 2002; **9**: 482-490

23 **Yuksel M**, Cermik F, Doganay L, Karlikaya C, Cakir E, Salan A, Berkarda S. 99mTc-MIBI SPET in non-small cell lung cancer in relationship with Pgp and prognosis. *Eur J Nucl Med Mol Imaging* 2002; **29**: 876-881

24 **Kao A**, Shiun SC, Hsu NY, Sun SS, Lee CC, Lin CC. Technetium-99m methoxyisobutylisonitrile chest imaging for small-cell lung cancer. Relationship to chemotherapy response (six courses of combination of cisplatin and etoposide) and p-glycoprotein or multidrug resistance related protein expression. *Ann Oncol* 2001; **12**: 1561-1566

25 **Blocklet D**, Schoutens A, Kentos A, Feremans W. Bone marrow uptake of 99mTc-MIBI in patients with multiple myeloma. *Eur J Nucl Med* 2001; **28**: 1430-1432

26 **Ceriani L**, Giovanella L, Bandera M, Beghe B, Ortelli M, Roncari G. Semi-quantitative assessment of ^{99m}Tc-sestamibi uptake in lung cancer: relationship with clinical response to chemotherapy. *Nucl Med Commun* 1997; **18**: 1087-1097

27 **Wiest R**, Shah V, Sessa WC, Groszmann RJ. Nitric oxide overproduction by eNOS precedes hyperdynamic splanchnic circulation in portal hypertensive rats. *Am J Physiol* 1999; **276**: G1043-G1051

28 **Kostakoglu L**, Elahi N, Kiratli P. Clinical validation of the influence of P-glycoprotein on technetium-99m-sestamibi uptake in malignant tumors. *J Nucl Med* 1997; **38**: 1003-1008

29 **Kostakoglu L**, Kiratli P, Ruacan S. Association of tumor washout rates and accumulation of ^{99m}Tc-MIBI with the expression of P-glycoprotein in lung cancer. *J Nucl Med* 1998; **39**: 228-234

30 **Vecchio SD**, Ciarmiello A, Potena MI, Carriero MV, Mainolfi C, Botti G, Thomas R, Cerra M, D'Aiuto G, Tsuruo T, Salvatore M. *In vivo* detection of multidrug resistant (MDR1) phenotype by technetium-99m-sestamibi scan in untreated breast cancer patients. *Eur J Nucl Med* 1997; **24**: 150-159

31 **Hendrikse NH**, Franssen EJ, van der Graaf WT, Meijer C, Piers DA, Vaalburg W, de Vries EG. ^{99m}Tc-sastamibi is a substrate for P-glycoprotein and the multidrug resistance associated protein. *Br J Cancer* 1998; **77**: 353-358

32 **Nagasue N,** Dhar DK, Makino Y, Yoshimura H, Nakamura T. Overexpression of P-glycoprotein in adenomaous hyperplasia of human liver with cirrhosis. *J Hepatol* 1995; **22**: 197-201

33 **Soini Y**, Virkajarvi N, Raunio H, Paakko P. Expression of P-glycoprotein in hepatocellular carcinoma: a potential marker of prognosis. *J Clin Pathol* 1996; **49**: 470-473

34 **Itsubo M**, Ishikawa T, Toda G, Tanaka M. Immunohistochemical study of expression and cellular localization the multidrug resistance gene product P-glycoprotein in primary liver carcinoma. *Cancer* 1994; **73**: 298-303

35 **Versantvoort CH**, Broxterman HJ, Bagrij T, Schepere RJ, Twentyman PR. Regulation by glutathione of drug trasport in multidrug-resistant human lung cell lines overexpressing multidrug resistant-associated protein. *Br J Cancer* 1995; **72**: 82-89

36 **Hendrikse NH**, Franssen EJ, van der Graaf WT, Meijer C, Piers DA, Vaalburg W, de Vries EG. ^{99m}Tc-sestamibi is a substrate for P-glycoprotein and the multidrug resistance associated protein. *Br J Cancer* 1998; **77**: 353-358

37 **Vergote J**, Morreti JL, de Vries EG, Garnier-Suillcrot A. Comparison of the kinetics of active efflux of ^{99m}Tc-MIBI in cells with P-glycoprotein-mediated and multidrug-resistance protein-associated phenotypes. *Eur J Biochem* 1998; **252**: 140-146

38 **Flens MJ**, Zaman GJ, van der Valk P, Izquierdo MA, Schroeijers AB, Scheffer GL, van der Groep P, de Haas M, Meijer CJ, Scheper RJ. Tissue distribution of the multidrug resistance protein. *Am J Pathol* 1996; **148**: 1237-1247

39 **Cheng SH**, Lam W, Lee ASK, Fung KP, Wu RS, Fong WF. Low-level doxorubicin resistance in benzo[α] pyrene-treated κB-3-1 cells is associated with increased LRP expression and altered subcellular drug distribution. *Toxicol Appl Pharmacol* 2000; **164**: 134-142

40 **Piwnica-Worms D**, Kronauges JF, Chiu ML. Uptake and retention of hexakis (2-methoxyisobutyl isonitrile) technetium (1) in cultured chick myocardial cells: mitochondrial and plasma membrane potential dependence. *Circulation* 1990; **82**: 1826-1838

Edited by Ren SY and Wang XL **Proofread by** Xu FM

PO Box 2345, Beijing 100023, China
Fax: +86-10-85381893
E-mail: wjg@wjgnet.com www.wjgnet.com

World J Gastroenterol 2004;10(9):1286-1291
World Journal of Gastroenterology
Copyright ©2004 by The WJG Press ISSN 1007-9327

• LIVER CANCER •

Differential gene expression in human hepatocellular carcinoma Hep3B cells induced by apoptosis-related gene *BNIPL-2*

Li Xie, Wen-Xin Qin, Xiang-Huo He, Hui-Qun Shu, Gen-Fu Yao, Da-Fang Wan, Jian-Ren Gu

Li Xie, Wen-Xin Qin, Xiang-Huo He, Hui-Qun Shu, Gen-Fu Yao, Da-Fang Wan, Jian-Ren Gu, National Laboratory for Oncogenes and Related Genes, Shanghai Cancer Institute, Shanghai 200032, China
Wen-Xin Qin, Da-Fang Wan, Jian-Ren Gu, Cancer Institute, Shanghai Jiaotong University, Shanghai 200032, China
Supported by a grant from the National Key Basic Research Program (973) of China, No. 2002CB513100 and grants from the National 863 High Technology Research and Development Program of China, No. 2001AA221141, 2002BA711A02, and 2001AA227121
Co-correspondents: Da-Fang Wan
Correspondence to: Dr. Wen-Xin Qin, National Laboratory for Oncogenes and Related Genes, Shanghai Cancer Institute, Shanghai Jiaotong University, Shanghai 200032, China. nlorg@public.sta.net.cn
Telephone: +86-21-64177401 **Fax:** +86-21-64177401
Received: 2003-09-06 **Accepted:** 2003-10-27

Abstract

AIM: Bcl-2/adenovirus E1B 19 ku interacting protein 2-like (BNIPL-2) is a novel protein recently identified in our laboratory. BNIPL-2 is homologous to human BNIP-2, a potentially proapoptotic protein, and can interact with Bcl-2 and Cdc42GAP and promote apoptosis in BEL-7402 cells. Here we report the gene-expression profile regulated by BNIPL-2 in human hepatocarcinoma Hep3B cells and the analysis of its potential roles in cell apoptosis.

METHODS: BNIPL-2 was overexpressed in Hep3B cells using tetracycline inducible or Tet-on system. Screened by Western blot, the cells with low background and high induction fold of BNIPL-2 were obtained. We performed Atlas human cDNA expression array hybridization on these cells and analyzed the data with Quantarray® software to identify *BNIPL-2*-regulated genes and their expression profile. RT-PCR was used to confirm the altered expression level of part of genes identified by the Atlas array hybridization.

RESULTS: Fifteen of 588 genes spotted on the Atlas membrane showed altered expression levels in BNIPL-2-transfected Hep3B-Tet-on cells, in which 8 genes involved in cell apoptosis or growth inhibition were up-regulated and 7 genes involved in cellular proliferation were down-regulated following overexpression of BNIPL-2.

CONCLUSION: cDNA array is a powerful tool to explore gene expression profiles under inducible conditions. The data obtained using the cDNA expression microarray technology indicates that BNIPL-2 may play its roles in apoptosis through regulating the expression of genes associated with cell apoptosis, growth inhibition and cell proliferation.

Xie L, Qin WX, He XH, Shu HQ, Yao GF, Wan DF, Gu JR. Differential gene expression in human hepatocellular carcinoma Hep3B cells induced by apoptosis-related gene *BNIPL-2*. *World J Gastroenterol* 2004; 10(9): 1286-1291
http://www.wjgnet.com/1007-9327/10/1286.asp

INTRODUCTION

Bcl-2/adenovirus E1B 19 ku interacting protein 2-like (BNIPL) is recently identified and characterized as an apoptosis-associated protein[1-3]. BNIPL shares 72% homology (46% identity) with BNIP-2[4] and has 2 variants BNIPL-1 and BNIPL-2. Full-length amino acid sequence of BNIPL-1 is shorter by 82 amino acids at N-terminus than that of BNIPL-2. Our previous experiment showed that BNIPL-1 could inhibit MIF-mediated proliferation of BEL-7402 cells and BNIPL-2 could inhibit cell growth and promote apoptosis in BEL-7402 cells. However, the molecular mechanisms by which BNIPL-1 suppresses the cell growth and BNIPL-2 commits the cell to die are not known[1,2].

In 1992, Gossen and Bugard developed the tetracycline (or doxycycline)-induced gene expression (Tet-on) system, which is useful for controlling the expression of targeted genes in a quantitative manner and for determining the roles of gene products in cellular functions[5,6]. In the present study, Hep3B-Tet-on cells were transfected with *BNIPL-2* using lipofectamine transfection reagent. In order to obtain cells with low background and high induction fold of *BNIPL-2*, transfected cells were screened by Western blot. Using this system, we established Hep3B cell line with doxycycline-regulated BNIPL-2 expression.

The microarray technique was first reported in 1995 by Schena *et al*.[7] and allows simultaneous parallel expression analysis of thousands of genes. Information provided by cDNA microarray analysis might be useful for tumor classification, elucidation of key factor in tumors, and identification of genes which might be applied to diagnostic purposes or as therapeutic targets[8,9]. The Atlas human cDNA expression system provides a convenient and quick method for profiling the expression of 588 genes at the same time. In this study, we used cDNA expression microarray technology to analyze the differentially expressed genes regulated by cell apoptosis-related gene *BNIPL-2*.

MATERIALS AND METHODS

Materials

cDNA microarray Atlas human cDNA expression array membranes (#7740-1) were purchased from Clontech Laboratories Inc (Palo Alto, California, USA). The membrane contained 10 ng of each gene-specific cDNA from 588 known genes and 9 housekeeping genes. Several plasmid and bacteriophage DNAs and blank spots were also included as negative and blank controls to confirm hybridization specificity. The 588 known genes spotted on the Atlas memberane consist of cDNAs for cell-cycle control proteins, stress response proteins, apoptosis-associated proteins, DNA transcription factors, cell receptors, extracellular cell signaling and communication proteins, *etc*. A complete list of the genes with the array positions and GeneBank accession numbers spotted on the array is available at Clontech's web site (http://www.clontech.com).

Enzyme and other reagents

Restriction endonucleases *Bam*HI and *Cl*aI were purchased from New England Biolabs Inc (Beverly, Maryland, USA).

Lambda DNA/*Hin*dIII Markers were from Sino-American Biotechnology Company (Shanghai, China). Tet system approved fetal bovine serum, doxycycline, hygromycin, pTRE2hyg, and Atlas human cDNA expression array trial kit were from BD Biosciences Clontech (Palo Alto, California, USA). Lipofectamine and SuperScript™ first strand synthesis system for RT-PCR were from Invitrogen™ Life Technologies (Carlsbad, California, USA). High glucose Dulbecco's modified Eagle's medium (DMEM) was from Gibco/BRL (Carlsbad, California, USA). Monocolonal antibody actin pan Ab-5, horseradish peroxidase-coupled second antibodies anti-rabbit IgG, and anti-mouse IgG were from Santa Cruz Biotechnology (Santa Cruz, California, USA). SuperSiganl west femto maximum sensitivity substrate and T-PER™ tissue protein extraction reagent was from Pierce Chemical Company (Rockford, Illinois, USA). PROTRAN nitrocellulose transfer membrane was from Schleicher & Schuell (Keene, New Hampshire, USA). Hep3B-Tet-on cell line was constructed by Wang *et al*.[10].

Methods

Plasmid construction For construction of plasmid pTRE2hyg-BNIPL-2, human *BNIPL-2* DNA fragment encoding the full-length protein was amplified by PCR using the primers containing *Bam*HI *and Cla*I restriction sites and HA-tag sequence (Table 1). The PCR product was subcloned into the Tet-on expression vector pTRE2hyg which contains hygromycin-resistance gene. The recombinant plasmid construct, pTRE2hyg-BNIPL-2, was confirmed by *Bam*HI/*Cla*I digestion and DNA sequencing.

Cell culture and transfection

Hep3B-Tet-on cells were cultured in DMEM containing 150 mL/L tetracycline-free fetal bovine serum at 37 ℃ in a 50 mL/L CO_2 incubator. They were grown in 6-well plates to 70% confluence and transfected with pTRE2hyg-BNIPL-2 plasmid DNA using lipofectamine reagents under conditions recommended by the manufacturer. After 48 h, the medium was replaced with fresh DMEM containing 100 mg/L hygromycin to select the stable cell lines. Two weeks later, hygromycin-resistant clones were obtained. Thirty-seven clones were selected and cultured continuously. After further selection in the medium containing 25 mg/L hygromycin for more than 3 wk, they were analyzed by Western blot using anti-BNIPL-2 polyclonal antibody (the rabbit anti-BNIPL-2 polyclonal antibody was prepared by National Laboratory for Oncogenes and Related Genes, Shanghai Cancer Institute, Shanghai, China). BNIPL-2 expression in the cell line was induced by incubating cells with doxycycline (Dox), which is a tetracycline analogue.

Western blot

Cells were washed twice with ice-cold PBS and lysed with T-PER™ tissue protein extraction reagent. Equal amounts of protein (10 μg) were electrophoresed on 100 g/L SDS–PAGE and blotted to PROTRAN nitrocellulose transfer membrane by a semi-dry transfer unit (Amersham Pharmacia Biotech AB, Piscataway, New Jersey, USA). The transferred membranes were blocked with 50 g/L non-fat milk in PBST buffer (20 mmol/L Tris-HCl, pH 7.6; 130 mmol/L NaCl, 1 g/LTween 20) for 1 h at room temperature and subsequently incubated with the primary antibody anti-BNIPL-2 at 1:500 dilutions in PBST containing 40 g/L non-fat milk for 2 h. After several washes with PBST, the membranes were incubated with the corresponding horseradish peroxidase-coupled secondary antibody anti-rabbit IgG in the same buffer. The immunocomplexes were visualized using SuperSignal west femto maximum sensitivity substrate. For standardization and quantification, β-actin was used as an internal control.

cDNA synthesis, labeling and purification

Hep3B-Tet-on-BNIPL-2/13 cells were cultured in DMEM containing 150 mL/L tetracycline-free fetal bovine serum at 37 ℃ in a 50 mL/L CO_2 incubator. They were grown in 4 10-cm dishes to 80% confluence and 2 dishes were treated with Dox (2 mg/mL) for 24 h. Then total RNA samples were extracted from 1×10^7 cells using TRIzol reagent. They were reverse-transcribed into cDNA and labeled with [α-^{32}P] dATP. Before labeling, total RNA of each sample was treated with DNase I (TaKaRa, Dalian, Shenyang, China) at 37 ℃ for 30 min to remove contaminated DNA. For each labeling, the treated 5 μg of total RNA was dissolved in 2 μL of diethyl pyrocarbonate (DEPC)-treated H_2O, incubated with 1 μL CDS Primer Mix at 70 ℃ for 2 min, and continued to incubate at 50 ℃ for 2 min. Then, 2 μL 5× reaction buffer, 0.5 μL 0.1 mol/L DTT, 1 μL dNTP mixture (containing dCTP, dGTP, and dTTP), 3.5 μL [α-^{32}P] dATP (10 μCi/μL), and 1 μL MMLV reverse transcriptase were added to each sample and incubated at 50 ℃ for 25 min. The reaction was stopped by adding 1 μL of 10× Termination Mix. The labeled first strand cDNA probes were purified by NucleoSpin extraction spin column to remove the unincorporated nucleotides. After purification, labeled cDNAs were denatured before use.

Membrane hybridization and exposure

Five milliliters ExpressHyb hybridization solution and 0.5 mg heat-denatured sheared salmon testes DNA were added to the tube containing Atlas human cDNA expression array membrane, which was pre-hybridized at 68 ℃ for 3 h. The different probes were then added to different tubes and hybridization was performed at 68 ℃ for 18 h in a rolling bottle. The membrane was washed twice at 68 ℃ in 2×SSC, 10 g/L SDS for 20 min, once at 68 ℃ in 0.1×SSC, 5 g/L SDS for 20 min, and once at room temperature in 2×SSC for 5 min, followed by exposure to x-ray films at -70 ℃ for 2-5 d.

Image analysis

The images were scanned with Cyclone™ storage phosphor system (Packard Bioscience Company, Meriden, Connecticut, USA) and saved as TIFF format files. The TIFF images were imported into the Quantarray® image system (Packard Bioscience Company) and analyzed. Housekeeping genes *ubiquitin* and *b-actin* were selected for normalization. The normalized intensity of each spot representing a unique gene expression level was acquired. Genes were considered to be up-regulated when the intensity ratio was >2 and down-regulated when the intensity ratio was <0.5.

Semi-quantitative RT-PCR

To confirm the cDNA array results, semi-quantitative RT-PCR was performed for 4 genes (*Rad*, *CLK-1*, *p38 MAP Kinase* and *p21*) that displayed expression alterations. Five micrograms of total RNA was reverse-transcribed into 20 μL of the first strand cDNA with SuperScript™ first strand synthesis system, then 2 μL of the product was used as the template to amplify each specific gene fragment in a 25 μL reaction mixture with corresponding primers (Table 1) under the following conditions: denaturation at 94 ℃ (3 min); 26 cycles at 94 ℃ (30 s), at 60 ℃ (30 s), and at 72 ℃ (30 s); then extension at 72 ℃ (3 min). In each PCR reaction, primers for the human *b–actin* gene were used as an internal control. PCR primer pairs were designed using Primer3 Internet software program. Their specificity was confirmed by a BLAST Internet software assisted search for a nonredundant nucleotide sequence database (National Library of Medicine, Bathesda, Maryland, USA). Ten microliters PCR reaction product was analyzed by electrophoresis on a 20 g/L agarose gel and visualized by ethidium bromide staining.

Table 1 Gene specific primers for PCR

Gene	GenBank accession number	Orientation	Sequence
BNIPL-2	AY033000	Forward	5' CGGGATCCACCATGTACCCATACGATGTTCCAGATT-ACGCTCTTGGAACTATACAAGAG 3'
		Reverse	5' CCATCGATCTATGTCCCTCCTGAGCCATGGAGATCCC-GGTCCAGCTGTCTGACAGC 3'
β-actin	NM_001101	Forward	5' AAGTACTCCGTGTGGATCGG 3'
		Reverse	5' TCAAGTTGGGGGACAAAAAG 3'
Rad	L24564	Forward	5' GCTGCCCTGCGAAGTGGCTC 3'
		Reverse	5' TCCCTCCAGGGCAGGCACAC 3'
CLK-1	L29222	Forward	5' GGGTGGTCCCAACCATGTGA 3'
		Reverse	5' CCGGCAGAACTGTGTTCATCCCA 3'
p38 MAP kinase	L35253	Forward	5' GTTGGAACCCCAGGGGCTGA 3'
		Reverse	5' GGCATGTGCAAGGGCTTGGG 3'
p21	U09579	Forward	5' CTGTGGGGGTGAGGGTCCCA 3'
		Reverse	5' TGGGGAGGGATGGGGTGGAT 3'

Underlined sequences are restriction endonuclease recognition sites (single line) and HA-tag (double lines).

Table 2 Up-regulated genes in BNIPL-2-transfected Hep3B-Tet-on cells

Location	Gene description	Induction-fold
C5n	Rad (Ras associated with diabetes)	5.886
F3e	Insulin-like growth factor binding protein 1 (IGFBP-1)	2.594
D6f	p21; Cdk-interacting proteins (Cip1); mda-6/WAF1/SDI1	2.574
E2m	Interleukin-2 receptor	2.5
D3n	Transcription factor (E2A)	2.115
F7m	Estrogen sulfotransferase (EST)	2.112
F1e	Transforming growth factor-beta (TGF-beta)	2.018
E7k	lfa-1 alpha subunit	2.012

RESULTS

Construction and identification of pTRE2hyg-BNIPL-2 plasmid

Tet-on expression plasmid pTRE2hyg-BNIPL-2 was successfully constructed. Restriction endonucleases *Bam*HI and *Cl*a I digestion showed that *BNIPL-2* gene was correctly inserted into the multicloning site. The *BNIPL-2* fragment and pTRE2hyg vector were about 1.1 kb and 5.3 kb, respectively (Figure 1).

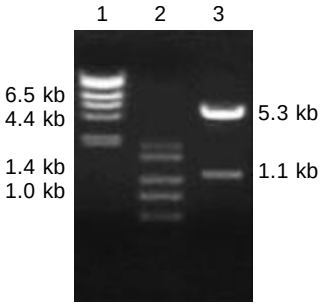

Figure 1 Agarose gel (10 g/L) electrophoresis analysis of recombinant pTRE2hyg-BNIPL-2 digested with *BamH I* and *Cla I* Lane 1: Lambda DNA/Hind III markers, Lane 2: SD 006 markers, Lane 3: pTRE2hyg-BNIPL-2 digested with *BamH I* and *Cla I*.

Screening of stable Hep3B-Tet-on-BNIPL-2 cell line

After screening in the medium containing hygromycin for more than 8 wk, a total of 37 independent Hyg-resistant cell lines were obtained from the Hep3B-Tet-on cells, transfected with pTRE2hyg-BNIPL-2. Of the 37 clones, clone Hep3B-Tet-on-BNIPL-2/13 showed a low background and high induction fold expression of BNIPL-2 by Dox and was selected as the cell line for further investigations. The amount of BNIPL-2 induced in the Hep3B-Tet-on-BNIPL-2/13 cells treated with Dox (2 000 μg/L) was 12-fold higher than that in the cells without Dox treatment (Figure 2A).

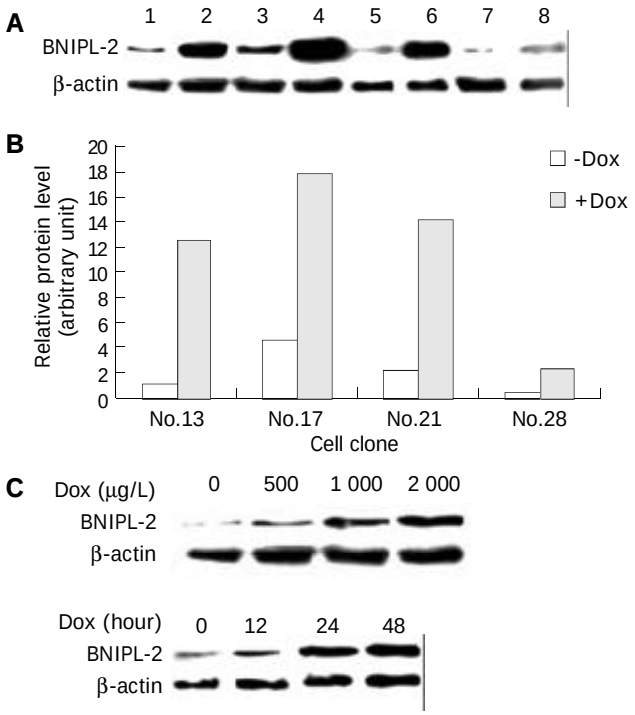

Figure 2 Western blot analysis of BNIPL-2 expression after Dox induction, A: Different cell protein was gotten from 37 clones after hygromycin selection. The clone Tet-on-BNIPL-2/13 showed a low background and high induction fold of BNIPL-2 regulated by Dox. The intensity of each band was quantified by densitometry. Lane 1: lysate of Tet-on-BNIPL-2/13, Lane 2: lysate of Tet-on-BNIPL-2/13+Dox, Lane 3: lysate of Tet-on-BNIPL-2/17, Lane 4: lysate of Tet-on-BNIPL-2/17+Dox, Lane 5: lysate of Tet-on-BNIPL-2/21, Lane 6: lysate of Tet-on-BNIPL-2/21+Dox, Lane 7: lysate of Tet-on-BNIPL-2/28, Lane

8: lysate of Tet-on-BNIPL-2/28+Dox. B: Hep3B-Tet-on-BNIPL-2/13 cells were treated with Dox at different concentrations (0, 500, 1 000, 2 000 μg/L) for 24 h. C: Hep3B-Tet-on-BNIPL-2/13 cells were treated with Dox (2 000 μg/L) for different time as indicated (0, 12, 24, 48 h). Equal amount of total cell protein was analyzed using BNIPL-2 antibody. β-actin was used as an internal control.

Hep3B-Tet-on-BNIPL-2/13 cells were amplified and passaged (1.0×10^5 cells) into 35-mm dishes, and treated with varying amounts of Dox for different times. Equal amounts of total cell protein were detected by Western blot with BNIPL-2 antibody. The level of BNIPL-2 expression increased significantly after exposing the cells to Dox for 24 h over a range of Dox concentrations from 500 μg/L to 2 000 μg/L (Figure 2B). However, the level of BNIPL-2 expression did not increase when Dox concentration was over 2 000 μg/L (data not shown). On the other hand, after the cells were treated with Dox (2 000 μg/L) for 0, 12, 24, or 48 h, the level of the induction increased with the treatment time and apparent increased induction was seen at 24 h (Figure 2C). Therefore, there was a direct correlation between the concentrations of Dox added to the cells or the time of treatment with Dox and the level of BNIPL-2 induction. The above results obtained by Western blot screening with anti-BNIPL-2 polyclonal antibody were confirmed by anti-HA McAb (data not shown).

Microarray analysis

Using a cDNA expression microarray technique we established the expression profile of 588 genes regulated by *BNIPL-2* (Figure 3) in Hep3B-Tet-on-BNIPL-2/13 cells. No signals were visible in the blank spots and negative control spots, indicating that Atlas human cDNA array hybridization was highly specific. The density of housekeeping genes was very similar between samples, indicating that the results were reliable. We used the housekeeping genes *Ubiquitin* and *b-actin* to normalize the intensities. The comparison results analyzed by Quantarray®

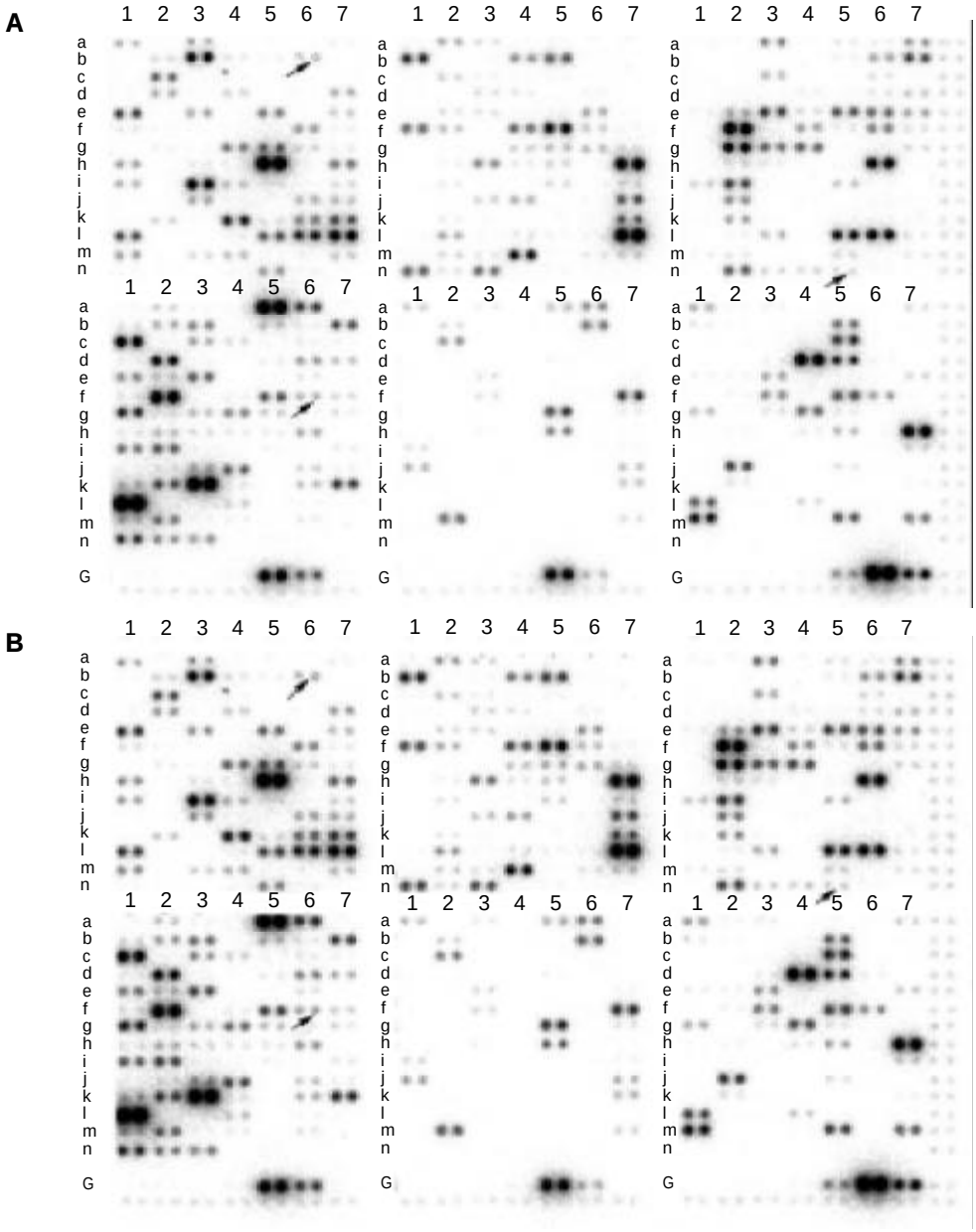

Figure 3 Parallel analysis of gene expression profiles in Hep3B-Tet-on-BNIPL-2/13 cells before or after BNIPL-2 overexpression, Total RNA samples were purified from 1×10^7 cells using TRIzol reagent before (A) or after (B) BNIPL-2 overexpression. They were reverse-transcribed into cDNA, labeled with [α-^{32}P] dATP, and hybridized to Atlas human cDNA expression array (#7740-1) according to the manufacturer's protocol. Notes: The genes in the row G are housekeeping genes. Arrows indicate the three examples of differentially expressed genes (*A6b, p120 antigen*; *C5n, Rad*; *D6f, p21*).

image system showed that there were 15 genes altered in terms of their expression levels, of which 8 were up-regulated (Table 2) and 7 were down-regulated (Table 3) following overexpression of BNIPL-2 in Hep3B cells.

Table 3 Down-regulated genes in BNIPL-2-transfected Hep3B-Tet-on cells

Location	Gene description	Induction-fold
B4f	Transducin beta-1 subunit 3'end	0.429
B1b	MAL protein	0.431
B5f	p38 MAP kinases/CSBP/Mxi2	0.442
A7e	Tob	0.447
A7h	CLK-1	0.457
B4b	GTP binding protein (RAB5)	0.48
A6b	p120 antigen	0.496

Semi-quantitative RT-PCR

Four genes were measured for their transcript levels by RT-PCR to verify the accuracy and universality of the hybridization data. The RT-PCR results were consistent with hybridization data in each of the genes measured (Figure 4), *i.e. Rad* and *p21* were up-regulated, *p38 MAPK* and *CLK-1* were down-regulated in BNIPL-2 overexpressed cells.

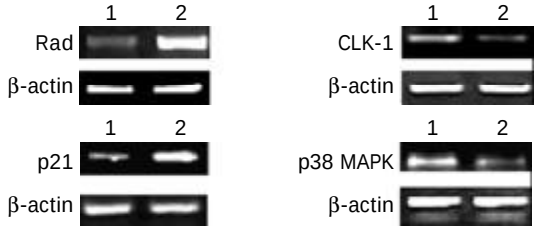

Figure 4 Semi-quantitative RT-PCR assays of *Rad, CLK-1, p21,* and *p38 MAPK* before or after BNIPL-2 overexpression, β–*actin* was also amplified as an internal control. The figure was consisted with the hybridization results. Lane 1: Before BNIPL-2 inducible expression, Lane 2: After BNIPL-2 inducible expression.

DISCUSSION

The Tet-on system, which utilizes an *E. coli* gene regulatory system[11], has been found to have several advantages[12-14]. Namely gene expression is easily regulated by administration of Dox, Dox is minimally toxic, and Dox acts specifically on the target gene, and does not activate other cellular genes. In the present study, we established a cell line Hep3B-Tet-on-BNIPL-2/13 in which *BNIPL-2* gene could be expressed conditionally by Dox treatment. Dox activated the Tet-response element and significantly enhanced the expression of *BNIPL-2* gene in Hep3B cells in a dose-dependent manner. The strategy used here, by which a stable cell line with a low background and high fold Dox-induced expression of BNIPL-2 was generated, seemed to be more efficient and rapid for regulating *BNIPL-2* gene expression.

The cDNA array technology was used to examine simultaneously the expression of specific genes on a single hybridization. Although expression analysis techniques such as differential display polymerase chain reaction (DD-PCR), Northern blot, serial analysis of gene expression (SAGE), and RT-PCR have been widely used, these studies are time-consuming and can only be used to deal with a limited number of genes. Thus a systematic approach to the examination of a large number of genes simultaneously is required. We therefore explored the gene expression profiles in human hepatocarcinoma cell line Hep3B regulated by BNIPL-2 overexpression using Atlas human cDNA array.

Following overexpression of BNIPL-2 in Hep3B cells, the expression level of 15 genes was altered, of which 8 were up-regulated and 7 were down-regulated. Genes involved in growth inhibition (*IGFBP-1, TGF-b)* or cell apoptosis (*p21, E2A*) were up-regulated. IGFBP-1 is thought to be the major short-term modulator of IGF bioavailability. In most clinical studies, circulating IGFBP-1 has been associated with growth inhibition[15]. Insulin-like growth factor I promotes muscle cell survival as an early event in differentiation through a pathway that involves Akt-dependent induction of p21[16]. Transforming growth factor-β (TGF-β) is a potent growth inhibitor for a wide variety of cells, controlling growth, differentiation and apoptosis of cells, and having important functions during embryonic development[17]. It has been found that Cdk inhibitor p21 is often responsible for stress-induced p53-dependent and p53-independent cell cycle arrest, and p21 plays an essential role in growth arrest after DNA damage and its overexpression leads to G1 and G2 or S-phase arrest. In addition, p21 is a negative regulator of p53-dependent apoptosis[18]. Human gastric cells were initially arrested in G1 by TGF-β and then driven to apoptosis after caspase-3-induced cleavage of p21[19]. Overexpression of E2A protein activity has been shown to induce either growth arrest or apoptosis, indicating that these proteins may regulate cell proliferation and survival[20,21]. Genes involved in cellular proliferation (*p38 MAPK, Tob, CLK-1*) were down-regulated in Hep3B cells when BNIPL-2 was overexpressed. P38 MAPK participates in not only inflammatory responses but also stress-induced signaling, cell proliferation and apoptosis. The p38 MAPK pathway participates in p21 induction, which consequently leads to decrease of cyclin D1/cdk4 and cyclinE/cdk2 complexes[22]. Tob is a member of the Tob and BTG anti-proliferative protein family. Recently, one report indicated that Tob functioned as a molecular switch that regulates cell cycle progression through early G1[23]. In *CLK-1* mutants, the affected features included cell cycle, embryonic and post-embryonic development, rhythmic behaviors, reproduction, and life span, all of which were lengthened or slowed down on average[24,25].

In conclusion, cDNA array is a powerful tool to explore gene expression profiles and the present results provide the basis for elucidating previous findings that BNIPL-2 might inhibit cell growth and promote apoptosis in BEL-7402 cells[2]. Although the mechanism of this interaction between BNIPL-2 and other proteins is not clear, we suggest that BNIPL-2 maybe inhibited growth by inducing cell cycle arrest at the G1 phase by TGF-β and p21 and affecting G2/M checkpoint through the p38 MAP kinase pathway.

REFERENCES

1 **Shen L**, Hu J, Lu H, Wu M, Qin W, Wan D, Li YY, Gu J. The apoptosis-associated protein BNIPL interacts with two cell proliferation-related proteins, MIF and GFER. *FEBS Lett* 2003; **540**: 86-90

2 **Qin W**, Hu J, Guo M, Xu J, Li J, Yao G, Zhou X, Jiang H, Zhang P, Shen L, Wan D, Gu J. BNIPL-2, a novel homologue of BNIP-2, interacts with Bcl-2 and Cdc42GAP in apoptosis. *Biochem Biophys Res Commun* 2003; **308**: 379-385

3 **Zhou YT**, Soh UJ, Shang X, Guy GR, Low BC. The BNIP-2 and Cdc42GAP homology/Sec14p-like domain of BNIP-Salpha is a novel apoptosis-inducing sequence. *J Biol Chem* 2002; **277**: 7483-7492

4 **Boyd JM**, Malstrom S, Subramanian T, Venkatesh LK, Schaeper U, Elangovan B, D'Sa-Eipper C, Chinnadurai G. Adenovirus E1B 19 kDa and Bcl-2 proteins interact with a common set of cellular proteins. *Cell* 1994; **79**: 341-351

5 **Lottmann H**, Vanselow J, Hessabi B, Walther R. The Tet-On

system in transgenic mice: inhibition of the mouse pdx-1 gene activity by antisense RNA expression in pancreatic beta-cells. *J Mol Med* 2001; **79**: 321-328

6 **Milo-Landesman D**, Surana M, Berkovich I, Compagni A, Christofori G, Fleischer N, Efrat S. Correction of hyperglycemia in diabetic mice transplanted with reversibly immortalized pancreatic beta-cells controlled by the tet-on regulatory system. *Cell Transplant* 2001; **10**: 645-650

7 **Schena M**, Shalon D, Davis RW, Brown PO. Quantitative monitoring of gene expression patterns with a complementary DNA microarray. *Science* 1995; **270**: 467-470

8 **Selaru FM**, Zou T, Xu Y, Shustova V, Yin J, Mori Y, Sato F, Wang S, Olaru A, Shibata D, Greenwald BD, Krasna MJ, Abraham JM, Meltzer SJ. Global gene expression profiling in Barrett's esophagus and esophageal cancer: a comparative analysis using cDNA microarrays. *Oncogene* 2002; **21**: 475-478

9 **Rew DA**. DNA microarray technology in cancer research. *Eur J Surg Oncol* 2001; **27**: 504-508

10 **Wang JR**, Qin WX, Shu HQ, Pan Y, Zhang YY, Wan DF. Establishment of Hep3B cell line controlled by the Tet-On regulatory system. *Tumor* 2002; **22**: 191-193

11 **Sonntag KC**, Haller GW, Giauffret D, Germana S, Reeves SA, Levy J, Sachs D, LeGuern C. Regulated expression of an MHC class II gene from a promoter-inducible retrovirus. *Hum Gene Ther* 2000; **11**: 1961-1969

12 **Kashima Y**, Miki T, Minami K, Seino S. Establishment of a tet-on gene expression system in glucose-responsive and -unresponsive MIN6 cells. *Diabetes* 2001; **50**(Suppl): S133

13 **Wang D**, Grammer JR, Cobbs CS, Stewart JE Jr, Liu Z, Rhoden R, Hecker TP, Ding Q, Gladson CL. P125 focal adhesion kinase promotes malignant astrocytoma cell proliferation *in vivo*. *J Cell Sci* 2000; **113**(Pt 23): 4221-4230

14 **Kobayashi T**, Sawa H, Morikawa J, Zhang W, Shiku H. Bax inducetion activates apoptotic cascade via mitochondrial cytochrome crelease and Bax overexpression enhances apoptosis induced by chemotherapeutic agents in DLD-1 colon cancer cells. *Jpn J Cancer Res* 2000; **91**: 1264-1268

15 **Kajantie E**, Hytinantti T, Koistinen R, Risteli J, Rutanen EM, Seppala M, Andersson S. Markers of type I and type III collagen turnover, insulin-like growth factors, and their binding proteins in cord plasma of small premature infants: relationships with fetal growth, gestational age, preeclampsia, and antenatal glucocorticoid treatment. *Pediatr Res* 2001; **49**: 481–489

16 **Lawlor MA**, Rotwein P. Insulin-like growth factor-mediated muscle cell survival: central roles for Akt and cyclin-dependent kinase inhibitor p21. *Mol Cell Biol* 2000; **20**: 8983–8995

17 **Derynck R**, Akhurst RJ, Balmain A. TGF-β signaling in tumor suppression and cancer progression. *Nat Genet* 2001; **29**: 117-129

18 **Zhang Y**, Fujita N, Tsuruo T. Caspase-mediated cleavage of p21Waf1/Cip1 converts cancer cells from growth arrest to undergoing apoptosis. *Oncogene* 1999; **18**: 1131–1138

19 **Kim DK**, Cho ES, Lee SJ, Um HD. Constitutive hyperexpression of p21(WAF1) in human U266 myeloma cells blocks the lethal signaling induced by oxidative stress but not by Fas. *Biochem Biophys Res Commun* 2001; **289**: 34–38

20 **Park ST**, Nolan GP, Sun XH. Growth inhibition and apoptosis due to restoration of E2A activity in T cell acute lymphoblastic leukemia cells. *J Exp Med* 1999; **189**: 501–508

21 **Engel I**, Murre C. Ectopic expression of E47 or E12 promotes the death of E2A-deficient lymphomas. *Proc Natl Acad Sci U S A* 1999; **96**: 996–1001

22 **Moon SK**, Jung SY, Choi YH, Lee YC, Patterson C, Kim CH. PDTC, metal chelating compound, induces G1 phase cell cycle arrest in vascular smooth muscle cells through inducing p21Cip1 expression: involvement of p38 mitogen activated protein kinase. *J Cell Physiol* 2004; **198**: 310-323

23 **Suzuki T**, K-Tsuzuku J, Ajima R, Nakamura T, Yoshida Y, Yamamoto T. Phosphorylation of three regulatory serines of Tob by Erk1 and Erk2 is required for Ras-mediated cell proliferation and transformation. *Genes Dev* 2002; **16**: 1356-1370

24 **Gems D**. Nematode ageing: Putting metabolic theories to the test. *Curr Biol* 1999; **9**: R614-616

25 **Levavasseur F**, Miyadera H, Sirois J, Tremblay ML, Kita K, Shoubridge E, Hekimi S. Ubiquinone is necessary for mouse embryonic development but is not essential for mitochondrial respiration. *J Biol Chem* 2001; **276**: 46160-46164

Edited by Liu HX and Wang XL **Proofread by** Xu FM

PO Box 2345, Beijing 100023, China
Fax: +86-10-85381893
E-mail: wjg@wjgnet.com www.wjgnet.com

World J Gastroenterol 2004;10(9):1292-1296
World Journal of Gastroenterology
Copyright ©2004 by The WJG Press ISSN 1007-9327

• LIVER CANCER •

Effects of recombinant human growth hormone on remnant liver after hepatectomy in hepatocellular carcinoma with cirrhosis

Shi-Min Luo, Li-Jian Liang, Jia-Ming Lai

Shi-Min Luo, Li-Jian Liang, Jia-Ming Lai, Department of Hepatobiliary Surgery, The First Affiliated Hospital of Sun Yat-Sen University, Guangzhou 510080, Guangdong Province, China
Correspondence to: Dr. Li-Jian Liang, Department of Hepatobiliary Surgery, The First Affiliated Hospital of Sun Yat-Sen University, 56 Zhongshan Er Lu, Guangzhou 510080, Guangdong Province, China. liangpw@gzsums.edu.cn
Telephone: +86-20-87755766 Ext 8096
Fax: +86-20-87755766 Ext 8663
Received: 2003-11-17 **Accepted:** 2003-12-16

Abstract

AIM: To explore the effects of recombinant human growth hormone (rhGH) on the remnant liver after hepatectomy in hepatocellular carcinoma with liver cirrhosis.

METHODS: Twenty-four patients with hepatocellular carcinoma who underwent hepatectomy were randomly divided into 2 groups: parenteral nutrition (PN) group (n=12) and rhGH+PN group (n=12). Liver function, blood glucose, AFP, serum prealbumin and transferrin were detected before operation, at post-operative d 1 and d 6. Albumin (ALB) mRNA in liver biopsy specimens was detected by RT-PCR at post-operative d 6. Liver Ki67 immunohistochemical staining was studied.

RESULTS: On post-operative d 6, compared with PN group, the levels of blood glucose, serum prealbumin, transferrin, the expression of hepatic ALB mRNA and liver Ki67 labeling index were higher in rhGH+PN group.

CONCLUSION: rhGH can improve protein synthesis and liver regeneration after hepatectomy in hepatocellular carcinoma with liver cirrhosis.

Luo SM, Liang LJ, Lai JM. Effects of recombinant human growth hormone on remnant liver after hepatectomy in hepatocellular carcinoma with cirrhosis. *World J Gastroenterol* 2004; 10(9): 1292-1296
http://www.wjgnet.com/1007-9327/10/1292.asp

INTRODUCTION

Hepatocellular carcinoma (HCC) is one of the most common malignant tumors of mankind. Since 1990s HCC has become the second killer among various cancers in China[1]. Surgical resection of the tumor is considered the only potentially curative therapy, and is regarded as the first choice of treatment of HCC. However, 80% of HCC are complicated with liver cirrhosis in China. After partial hepatectomy, the risk of hemorrhage, infection, and liver failure is very high, as the liver function is usually impaired before surgery in patients with cirrhosis. For safer hepatic resection in patients with cirrhosis, the reserve of hepatic function and rapid regeneration of the remnant liver are crucial. Because liver function is usually impaired in patients with cirrhosis, and because cirrhotic livers are less able to regenerate, it is important to stimulate both the regeneration and function of the remnant cirrhotic liver after hepatectomy.

The prognosis of severe liver failure depends on the ability of the remaining hepatocytes to regenerate. Improvement of hepatic tissue repair can increase the survival rate of patients suffering from acute hepatic failure and reduce the recovery period after massive liver resection. Nutritional support is undoubtedly the most physiologic manner of treatment and it is clear that adequate nutrition should significantly speed up liver regeneration and patient recovery. The composition of parenteral nutrition (PN) for the postoperative nutritional management of patients with liver cirrhosis might be extremely important because of their metabolic disorders and hemodynamic disturbance following surgical intervention.

Considering that the provision of branched-chain amino acids (BCAA) may improve nutritional status and liver regeneration and ameliorate hepatic encephalopathy, increased provision of BCAA in patients with liver disease seems to be a reasonable approach to various forms of liver injury[2-4]. While a decline in liver protein synthesis was induced by the surgical procedure[5]. In patients given short-term PN, plasma insulin concentrations were increased 5-fold compared with control, but no effect on liver protein synthesis rates was observed[6]. Growth hormone (GH) has important direct and indirect effects on protein, carbohydrate and lipid metabolism. Potential areas of further research may include the combination of BCAA supplements with other anabolic factors (*e.g.* GH) in managing patients with catabolic disease states[7]. The aim of this study was to investigate the effects of treatment with amino acids enriched BCAA and recombinant human GH (rhGH) for 5 d on the remnant liver after hepatectomy in HCC with liver cirrhosis.

MATERIALS AND METHODS

Patients

All the patients were from our department who underwent curative resection for HCC with liver cirrhosis between September 2002 and June 2003. Curative resection was defined as complete resection of all macroscopically detectable tumors with histological tumor clearance (the entire tumor mass was included in the surgical specimen without exposure of tumor cells on the cut edge). At the time of entry, the inclusion criteria were no evidence of endocrine disease. The study protocol conformed to the ethical guidelines and the patients were enrolled after informed consent was obtained. Twenty-four patients were recruited and were randomly using sealed envelopes divided into 2 groups: PN group (n=12) and rhGH+PN group (n=12) using sealed envelopes. Between the 2 groups, there were no differences in age, sex, body mass, operative methods, operation time, intraoperative blood loss and intraoperative blood transfusion (Table 1). At the same time, 12 patients with cholelithiasis or hemangioma who underwent operation served as normal controls. None had liver cirrhosis or endocrine disease.

Nutritional support and rhGH administration

Nutritional support and rhGH administration were started on the first day after surgery and continued until d 5. PN was

initiated through a percutaneously placed subclavian vein catheter threaded into the superior vena cava. The formula provided non-protein calorie 25 kcal/kg· d. Each patient was provided 250 mL 200 mL/L MCT/LCT lipid emulsion (Guangzhou Qiaoguang Pharmaceutical Co. Ltd) and 750 mL 100 g/L aminoplasmal Hepa (Braun Co. Ltd) containing 20 kinds of amino acids, 330 g/L branched-chain amino acids and 15.3 g/L nitrogen. Nonprotein calories were provided 310 mL/L as lipid emulsion. The formula provided nitrogen 0.19 g/kg· d. The ratio of nonprotein calories to nitrogen was 132:1. The ratio of glucose (g) to insulin (IU) was 6:1. Vitamins, trace minerals, and electrolytes were supplied according to the daily requirement. This parenteral nutrition was tolerated by all patients without complications, and no patient showed symptoms of sepsis during the treatment period.

Patients in the rhGH+PN group received 10 U rhGH (Saizen, Serono Biotech&Beyond) additionally per day subcutaneously.

Table 1 Patient characteristics

	PN group (n=12)	rhGH+PN group (n=12)
General conditions		
Age (years)	46.1±13.6	50.3±10.6
Sex (M/F)	11/1	10/2
Body weight (kg)	59.7±9.3	64.3±7.7
Operative methods		
Hepatic left lateral lobectomy	0	1
Left hemihepatectomy	2	2
Right hemihepatectomy	1	1
Tumor or segmentectomy	9	8
Intraoperative information		
Operation time (min)	250.8±126.4	203.3±73.2
Intraoperative blood loss (mL)	1 331.7±1 704.8	966.7±1031.4
Intraoperative blood transfusion (mL)	1 100.0±1 334.2	408.3±609.7

Collection of samples

Blood samples were collected from antecubital veins in the morning after an overnight fast prior to operation in the normal, PN and rhGH+PN groups, on postoperative day (POD) 1 and 6 in the PN and rhGH+PN groups. Aliquots were transferred into different tubes placed for the determination of liver function, blood glucose, prealbumin, transferrin and α-fetoprotein (AFP). Blood samples were centrifuged at 4 ℃ and then frozen at -70 ℃ until assay.

Liver specimens from PN and rhGH+PN group, including hepatocellular carcinomas and adjacent non-tumor tissues were excised at the operation and percutaneous liver biopsies were taken on d 6 after operation in the PN group and rhGH+PN group, immediately frozen with liquid nitrogen, and stored at -70 ℃ for analysis of ALB mRNA. Liver biopsy specimens were obtained with Tru-Cut biopsy needles. The needle-biopsy specimens ranged in length from 15 to 20 mm. For histological examination, some liver specimens were fixed in 40 g/L neutrally-buffered formaldehyde and embedded in paraffin.

Biochemical examinations

Liver function, including serum aspartate aminotransferase (AST), alanine aminotransferase (ALT), alkaline phosphatase (ALP), total bilirubin (TBIL), albumin (ALB) and blood glucose were analyzed by an autoanalyzer. Serum prealbumin and transferrin were detected quantitatively by immunoturbidity assay.Serum AFP was detected quantitatively by micropartical enzyme immunoassay. The normal values were <20 μg/L.

Measurement of ALB mRNA in liver tissue

RT-PCR was performed to measure the expression levels of ALB mRNA in liver tissue. The primers used were deduced from the cDNA sequence. The sequences of the primers for ALB sense and antisense were as 5'-CCCAAGTGTCAACTCCAACT-3' (sense) and 5'- GCAGGTCTCCTTATCGTCAG-3' (antisense), a 456-bp long fragment was amplified. The sequences of the primers for β-actin sense and antisense were as 5'-ACTCTTCCAGCCTTCCTTCCT-3' (sense) and 5'-TCACCTTCACCGTTCCAGTTT-3' (antisense), a 513-bp long fragment was amplified.

Total RNA was extracted from frozen liver specimens by the guanidinium isothiocyanate method. The RNA was quantified and checked for purity by spectrophotometry at 260 and 280 nm. Aliquots of total RNA were reversely transcribed using SperSriptII Reverse Transcriptase (Invitrogen Corp) and subsequently amplified by PCR using the Taq DNA polymerase (Promega).

The PCR was carried out in 25 mL of reaction mixture containing 0.5 μL cDNA template, 2.5 μL 10×PCR-Buffer, 1.5 μL 25 mmol/L $MgCl_2$, 0.5 μL 10 mmol/L dNTPs, 0.5 μL 10 μmol/L ALB, 0.15 μL 10 μmol/L β-actin primers, 0.5 μL 5 U/μL Taq DNA polymerase. The mixture was heated for 5 min. at 94 ℃ for initial DNA denaturation, followed by 30 cycles of denaturation at 94 ℃ for 45 s, annealing at 50 ℃ for 45 s, polymerization at 72 ℃ for 1 min. and then a final extension of 10 min at 7 ℃. PCR reactions were stored frozen until analysis by agarose gel electrophoresis.

PCR reactions were electrophoresed on 15 g/L agarose gel, stained with ethidium bromide and quantitated using the interactive build analysis system (IBAS). The band intensity of the ALB was compared with the band intensity of the β-actin, and the amount of ALB mRNA was estimated.

Immunohistochemical staining of Ki67 in liver tissue

Two-step immunohistochemical staining technique was used. Main reagents included rabbit polyclonal antibody Ki67 Ab-4 (Neomarkers) and PV-6000 PicTure™ kits. Briefly, sections were deparaffinized, rehydrated, and then immersed in 0.1 mol/L citric acid buffer (pH 6.0) and boiled for 5-10 min in a microwave oven. The slides were then rinsed gently with phosphate buffered saline (PBS) at pH 7.2-7.4, and treated with 3 mL/L hydrogen peroxide in absolute methanol for 1 h at room temperature (RT) to remove endogenous peroxidase. The sections were then incubated with the primary antibody Ki67 Ab-4 (1:200 dilution) for 30 min at 37 ℃. After rinsed with PBS for 3 times, each for 2 min, the sections were incubated with PV-6000 for 30 min at 37 ℃. They were then rinsed 3 times with PBS for 2 min each and visualized with DAB. Finally, the sections were counterstained with hematoxylin.

On each slide, Ki67-positive nuclei were estimated by means of light microscopy at 400 magnifications. At least 1 000 cells were evaluated in 5 different fields each containing a minimum of 200 cells. The Ki67 labeling index (Ki67 LI) is the percentage (%) of positive cells.

Recording doses of albumin infusions within 5 d after operation

Plasma contained 4.5 g/L albumin. Doses of plasma infusion were converted into doses of albumin.

Statistical analysis

Data were expressed as mean±SD. The statistical software SPSS 10.0 was used. Statistical significance was set at P<0.05.

RESULTS

Surgery outcome and albumin doses within 5 d after operation

There was no surgical mortality in this series. The postoperative

hospital stay showed no difference between the PN group and rhGH+PN group (14.7±6.2 d *vs* 13.5±4.5 d, $P>0.05$). In the PN group, 2 patients had right pleural effusion. In the rhGH+PN group, 1 patient had right pleural effusion, another patient had subcutaneous fat liquefaction. The postoperative complication related morbidity was not different between the 2 groups ($P>0.05$). Albumin doses within 5 d after operation were not different between the PN and rhGH+PN group (57.0±48.8 g *vs* 52.4±24.4 g, $P>0.05$).

The decreased percentage of serum AFP within 5 d after operation

The decreased percentage of serum AFP within 5 d after operation were calculated by (POD 1 serum AFP- POD 6 serum AFP)/POD 1 serum AFP. In the PN group, 6 patients had preoperative serum AFP<20 μg/L. In the rhGH+PN group, 3 patients had preoperative serum AFP<20 μg/L and at POD 6, 3 patients whose preoperative serum AFP were <50 μg/L had their serum AFP<20 μg/L. Those patients were excluded from the statistics. For the other 6 patients in the 2 groups, the decrease percentage of serum AFP within 5 d after operation was not different between the PN group and rhGH+PN group (0.536±0.182 *vs* 0.579±0.193, $P>0.05$).

The changes of liver function and blood glucose

Compared with normal control group, serum AST, ALT of HCC patients with cirrhosis were significantly increased, while serum ALP, TBIL, ALB, blood glucose were not different. Serum AST, ALT, ALP, TBIL, ALB, blood glucose on preoperative day and POD 1 were not different between the PN group and rhGH+PN group. Compared with PN group, serum AST, ALT, ALP, TBIL, ALB on POD 6 in the rhGH+PN group were not different, but blood glucose was significantly increased (Table 2).

The changes of serum prealbumin and transferrin

In HCC patients with cirrhosis, serum prealbumin and transferrin were lower than the normal control group. Serum prealbumin and transferring on preoperative day and POD 1 were not different between PN group and rhGH+PN group, but serum prealbumin and transferring on POD 6 in the rhGH+PN group were significantly increased compared with the PN group (Table 2).

The changes of hepatic ALB mRNA and liver Ki67 labeling index

In HCC patients with cirrhosis, hepatic ALB mRNA of tumor tissues was lower than in adjacent non-tumor tissues, while in adjacent non-tumor tissues it was lower than the normal liver tissues. Compared with the PN group, hepatic ALB mRNA on POD 6 was significantly increased in the rhGH+PN group. Liver Ki67 labeling index in tumor tissues was higher than adjacent non-tumor tissues. Liver Ki67 labeling index on POD 6 in the rhGH+PN group was higher than the PN group (Table 3).

DISCUSSION

The prevalence of malnutrition in patients with liver cirrhosis is high[8]. Nutritional status affects prognosis, and cirrhotic patients with malnutrition are prone to develop major complications and infections. A poor nutritional status negatively influences survival, while appropriate nutritional intervention has been found to improve liver function and survival. Because the liver is the metabolic workhouse of the body, alteration in liver function clearly affects the whole body metabolism. In addition, the goals of nutritional support should include maintenance of adequate nutrition and prevention and/or amelioration of liver damage. Major resection of portions of the liver for primary hepatic or metastatic malignancy and the repair of hepatic injury associated loss of liver tissue are performed with such a frequency as to require careful consideration of the consequences of the postoperative nutritional care of the patients. Often, the recovery from such surgery involves a prolonged period of delayed oral intake.

Table 2 Comparison of liver function, blood glucose, serum prealbumin and transferrin

	Normal control group (n=12)	PN group (n=12)			rhGH+PN group (n=12)		
		Preoperative	POD 1	POD 6	Preoperative	POD 1	POD 6
AST (IU/L)	26.0±5	56.0±27[a]	761.0±578	62.0±32	55.0±25[a]	578.0±206	56.0±25
ALT (IU/L)	27.0±17	60.0±36[a]	749.0±571	153.0±95	42.0±17[a]	590.0±273	154.0±71
ALP (IU/L)	94.0±55	151.0±87	145.0±80	148.0±65	105.0±27	100.0±33	113.0±46
TBIL (μmol/L)	17.4±6.4	22.6±9.0	52.5±48.1	43.1±37.4	20.5±9.3	42.1±41.6	30.2±21.0
ALB (g/L)	42.8±4.0	39.8±4.7	31.5±3.3	34.0±3.4	40.7±3.5	32.4±3.6	37.1±5.0
Blood glucose (mmol/L)	4.6±0.6	4.8±0.9	7.3±3.5	5.3±1.5	4.5±0.6	7.0±3.2	8.8±5.2[c]
Serum prealbumin (mg/L)	279.8±43.0	202.4±32.3[a]	158.3±25.4	127.2±13.4	204.5±31.9[a]	157.2±23.0	156.4±20.0[c]
Serum transferrin (g/L)	3.5±0.5	2.5±0.2[a]	2.1±0.3	1.8±0.2	2.5±0.2[a]	2.2±0.3	2.2±0.3[c]

[a]$P<0.05$, preoperative *vs* normal control group; [c]$P<0.05$, between rhGH+PN group and PN group.

Table 3 Comparison of hepatic ALB mRNA and liver Ki67 labeling index

	Normal control group (n=12)	PN group (n=12)			rhGH+PN group (n=12)		
		Tumor tissues	Adjacent non-tumor tissues	Liver biopsy specimens POD 6	Tumor tissue	Adjacent non-tumor tissues	Liver biopsy specimens POD 6
ALB mRNA	0.69±0.05	0.38±0.01[a]	0.50±0.06[a,c]	0.63±0.05	0.38±0.01[a]	0.50±0.06[a,c]	0.71±0.06[e]
Liver Ki67 LI(%)	0	17.4±6.1[a]	0.20±0.1[a,c]	4.60±0.5	17.2±5.9[a]	0.20±0.1[a,c]	5.50±0.5[e]

[a]$P<0.05$, tumor tissues or adjacent non-tumor tissues *vs* normal control group; [c]$P<0.05$, adjacent non-tumor tissues *vs* tumor tissues in the same group,[e]$P<0.05$, of the same tissues comparison between the PN group and rhGH+PN group.

Although the liver normally has considerable reserve function and regeneration potential, an acute reduction in hepatic mass can significantly affect liver function, its metabolic activity, and substrate metabolism. The trauma caused by moderate or large operation may result in disturbance of glucose, lipid and protein metabolism including hypermetabolism and increased catabolism, which may lead to acute protein malnutrition, decline of immunological function and dysfunction of multiple organs[9-11]. Postoperative maintenance of protein synthesis is one measure to preserve a satisfactory quality of life after hepatectomy[12].

The amino acids that comprise the various parenteral feeding formulations are the important components of these regimens, because they provide the precursors for the synthesis of numerous structural and functional body proteins. BCAA appears to act favorably in albumin metabolism. Early oral supplementation of BCAA for HCV-related cirrhosis with serum albumin level between 3.5 and 3.9 g/dL and branched-chain tyrosine ratio (BTR) less than 4.0, improves serum albumin levels and thus might improve prognosis[13].

Liver protein synthesis is usually estimated in humans by measuring the synthesis rates of major exported liver proteins. Albumin is a ubiquitous protein synthesized only by hepatocytes. Albumin is a polypeptide chain of 580 amino acids that is produced by hepatocytes[14]. The expression of ALB gene is reduced in various liver deseases and the degree of reduction in the hepatic ALB mRNA level is generally correlated with the severity of the disease[15]. This study showed that hepatic ALB mRNA in tumor tissues was lower than in adjacent non-tumor tissues, and it was lower in adjacent non-tumor tissues than normal liver tissues. Serum ALB whose long half-life of approximately 20 d makes it a late index of nutritional status, and its exclusive use may delay implementation of appropriate nutritional interventions. Serum prealbumin and transferrin have been proposed as earlier nutritional markers. Clinically significant changes in albumin can be reliably predicted by earlier changes in serum transferrin and prealbumin[16]. In this study, serum AST, ALT, ALP, TBIL, ALB on POD 6 were not different between the PN group and rhGH+PN group, but blood glucose, serum prealbumin, transferrin, hepatic ALB mRNA, and liver Ki67 labeling index were significantly increased in the rhGH+PN group. Thus, rhGH can promote liver protein synthesis and liver regeneration. Moreover, liver function recovered faster in the rhGH+PN group. It has been demonstrated that PN is not able to support protein synthesis sufficiently in patients with or without malnutrition[17]. Long-term conventional PN is unable to increase or even maintain body protein; the anabolic response to PN is often suboptical because of the concomitant presence of catabolism and/or alterations in the hormonal regulation of metabolism[18,19]. GH is anabolic in protein metabolism. Gu and Wu also demonstrated that the administration of rhGH could result in significant anabolic effects on body growth and improve the efficiency of PN[20].

An important but unresolved question is intrahepatic recurrence after resection of HCC[21-26]. Metastasis and recurrence of HCC after surgical removal is still high.The frequency of 5-year recurrence after radical resection was 61.5% overall[27]. The recurrence, especially at an early period after hepatectomy, is the major cause of poor prognosis in patients with HCC[28]. This is of relevance in determining preventive and therapeutic strategies for recurrence. Although all patients in this study underwent curative tumor resection, the potential tumor-promoting effect of GH must be addressed. This study showed that the decreased percentage of serum AFP within 5 d after operation was not different between the PN group and rhGH+PN group. Furthermore, liver function recovered faster in the rhGH+PN group. However, hepatic functional damage immediately after hepatectomy is a significant risk factor for early intrahepatic recurrence in cirrhotic HCC. Careful perioperative management of hepatic function may therefore be important in preventing early recurrence and prolonging survival[29]. Tacke *et al* demonstrated no evidence for an increased risk of tumor recurrence after rhGH treatment for a short period of time after removal of a gastrointestinal adenocarcinoma[30]. Moreover, rhGH attenuated the depression in cellular immunity following surgical stress[31]. Therefore, short-term use of rhGH in HCC patients with cirrhosis after operation may be safe.

In conclusion, rhGH+PN can promote liver recovery, liver protein synthesis and liver regeneration after hepatectomy in HCC with liver cirrhosis. It may not promote HCC recurrance, but may increase blood glucose.

REFERENCES

1 **Tang ZY.** Hepatocellular carcinoma-cause, treatment and metastasis. *World J Gastroenterol* 2001; **7**: 445-454

2 **Holecek M.** Nutritional modulation of liver regeneration by carbohydrates, lipids, and amino acids: a review. *Nutrition* 1999; **15**: 784-788

3 **Freund HR,** Hanani M. The metabolic role of branched-chain amino acids. *Nutrition* 2002; **18**: 287-288

4 **James JH.** Branched chain amino acids in heptatic encephalopathy. *Am J Surg* 2002; **183**: 424-429

5 **Barle H,** Essen P, Nyberg B, Olivecrona H, Tally M, McNurlan MA, Wernerman J, Garlick PJ. Depression of liver protein synthesis during surgery is prevented by growth hormone. *Am J Physiol* 1999; **276**(4 Pt 1): E620-627

6 **Barle H,** Nyberg B, Andersson K, Essen P, McNurlan MA, Wernerman J, Garlick PJ. The effects of short-term parenteral nutrition on human liver protein and amino acid metabolism during laparoscopic surgery. *J Parenter Enteral Nutr* 1997; **21**: 330-335

7 **Platell C,** Kong SE, McCauley R, Hall JC. Branched-chain amino acids. *J Gastroenterol Hepatol* 2000; **15**: 706-717

8 **Donaghy A**. Issues of malnutrition and bone disease in patients with cirrhosis. *J Gastroenterol Hepatol* 2002; **17**: 462-466

9 **Antonio J,** Sanders MS, Ehler LA, Uelmen J, Raether JB, Stout JR. Effects of exercise training and amino-acid supplementation on body composition and physical performance in untrained women. *Nutrition* 2000; **16**: 1043-1046

10 **Wang SJ,** Wen DG, Zhang J, Man X, Liu H. Intensify standardized therapy for esophageal and stomach cancer in tumor hospitals. *World J Gastroenterol* 2001; **7**: 80-82

11 **Dionigi P,** Alessiani M, Ferrazi A. Irreversible intestinal failure, nutrition support, and small bowel transplantation. *Nutrition* 2001; **17**: 747-750

12 **Ueno S,** Tanabe G, Nuruki K, Yoshidome S, Kubo F, Kihara K, Aoki D, Aikou T. Quality of life after hepatectomy in patients with hepatocellular carcinoma: implication of change in hepatic protein synthesis. *Hepatogastroenterology* 2002; **49**: 492-496

13 **Habu D,** Nishiguchi S, Nakatani S, Kawamura E, Lee C, Enomoto M, Tamori A, Takeda T, Tanaka T, Shiomi S. Effect of oral supplementation with branched-chain amino acid granules on serum albumin level in the early stage of cirrhosis: a randomized pilot trial. *Hepatol Res* 2003; **25**: 312-318

14 **Yamaguchi K,** Nalesnik MA, Carr BI. *In situ* hybridization of albumin mRNA in normal liver and liver tumors: identification of hepatocellular origin. *Virchows Arch B Cell Pathol Incl Mol Pathol* 1993; **64**: 361-365

15 **Ozaki I,** Motomura M, Setoguchi Y, Fujio N, Yamamoto K, Kariya T, Sakai T. Albumin mRNA expression in human liver diseases and its correlation to serum albumin concentration. *Gastroenterol Jpn* 1991; **26**: 472-476

16 **Neyra NR,** Hakim RM, Shyr Y, Ikizler TA. Serum transferrin and serum prealbumin are early predictors of serum albumin in chronic hemodialysis patients. *J Ren Nutr* 2000; **10**: 184-190

17 **Warnold I,** Eden E, Lundholm K. The inefficiency of total parenteral nutrition to stimulate protein synthesis in moderately malnourished patients. *Ann Surg* 1988; **208**: 143-149

18 **Ziegler TR**, Rombeau JL, Young LS, Fong Y, Marano M, Lowry SF, Wilmore DW. Recombinant human growth hormone enhances the metabolic efficacy of parenteral nutrition: a double blind, randomized controlled study. *J Clin Endocrinol Metab* 1992; **74**: 865-873

19 **Wilmore DW.** Growth factors and nutrients in the short bowel syndrome. *J Parenter Enteral Nutr* 1999; **23**(5 Suppl): S117-120

20 **Gu Y,** Wu ZH. The anabolic effects of recombinant human growth hormone and glutamine on parenterally fed, short bowel rats. *World J Gastroenterol* 2002; **8**: 752-757

21 **Qin LX**, Tang ZY. The prognostic significance of clinical and pathological features in hepatocellular carcinoma. *World J Gastroenterol* 2002; **8**: 193-199

22 **Ezaki T**, Yamamoto K, Yamaguchi H, Sasaki Y, Ishida T, Mori M, Aimitsu S. Hepatic resection for hepatocellular carcinoma existing with liver cirrhosis. *Hepatogastroenterology* 2002; **49**: 1363-1368

23 **Sun HC**, Tang ZY. Preventive treatments for recurrence after curative resection of hepatocellular carcinoma-a literature review of randomized control trials. *World J Gastroenterol* 2003; **9**: 635-640

24 **Takada Y**, Otsuka M, Todoroki T, Fukao K. Accompanying liver cirrhosis as a risk factor for recurrence after resection of solitary hepatocellular carcinoma. *Hepatogastroenterology* 2003; **50**: 1991-1995

25 **Grazi GL**, Cescon M, Ravaioli M, Ercolani G, Gardini A, Del Gaudio M, Vetrone G, Cavallari A. Liver resection for hepatocellular carcinoma in cirrhotics and noncirrhotics. Evaluation of clinicopathologic features and comparison of risk factors for long-term survival and tumour recurrence in a single centre. *Aliment Pharmacol The* 2003; **17**(Suppl): 119-129

26 **Imamura H**, Matsuyama Y, Tanaka E, Ohkubo T, Hasegawa K, Miyagawa S, Sugawara Y, Minagawa M, Takayama T, Kawasaki S, Makuuchi M. Risk factors contributing to early and late phase intrahepatic recurrence of hepatocellular carcinoma after hepatectomy. *J Hepatol* 2003; **38**: 200-207

27 **Niu Q,** Tang ZY, Ma ZC, Qin LX, Zhang LH. Serum vascular endothelial growth factor is a potential biomarker of metastatic recurrence after curative resection of hepatocellular carcinoma. *World J Gastroenterol* 2000; **6**: 565-568

28 **Shimada M,** Takenaka K, Gion T, Fujiwara Y, Kajiyama K, Maeda T, Shirabe K, Nishizaki T, Yanaga K, Sugimachi K. Prognosis of recurrent hepatocellular carcinoma: a 10-year surgical experience in Japan.*Gastroenterology* 1996; **111**: 720-726

29 **Hanazaki K,** Wakabayashi M, Sodeyama H, Kajikawa S, Amano J. Hepatic function immediately after hepatectomy as a significant risk factor for early recurrence in hepatocellular carcinoma. *Hepatogastroenterology* 1999; **46**: 3201-3207

30 **Tacke J,** Bolder U, Herrmann A, Berger G, Jauch KW. Long-term risk of gastrointestinal tumor recurrence after postoperative treatment with recombinant human growth hormone. *J Parenter Enteral Nutr* 2000; **24**: 140-144

31 **Liu W,** Jiang Z, Wang X, Shu H, Cui W, Wilmore DW. Impact of perioperative treatment of recombinant human growth hormone on cell immune function and intestinal barrier function: randomized, double-blind, controlled trial. *World J Surg* 2003; **27**: 412-415

Edited by Zhu LH and Xu FM

PO Box 2345, Beijing 100023, China
Fax: +86-10-85381893
E-mail: wjg@wjgnet.com www.wjgnet.com

World J Gastroenterol 2004;10(9):1297-1300
World Journal of Gastroenterology
Copyright ©2004 by The WJG Press ISSN 1007-9327

• COLORECTAL CANCER •

Amino acid uptake in arterio-venous serum of normal and cancerous colon tissues

Lin-Bo Wang, Jian-Guo Shen, Su-Zhan Zhang, Ke-Feng Ding, Shu Zheng

Lin-Bo Wang, Jian-Guo Shen, Department of Surgical Oncology, Sir Run Run Shaw Hospital, Zhejiang University Medical College, Hangzhou 310016, Zhejiang Province, China
Su-Zhan Zhang, Ke-Feng Ding, Shu Zheng, Department of Surgical Oncology, the Second Hospital, Zhejiang University Medical College, Hangzhou 310016, Zhejiang Province, China
Supported by Oncology Research Institute, Medical College, Zhejiang University
Correspondence to: Dr. Lin-Bo Wang, Department of Surgical Oncology, Sir Run Run Shaw Hospital, Zhejiang University Medical College, Hangzhou 310016, Zhejiang Province, China. wanglinbo@medmail.com.cn
Telephone: +86-571-86090073 **Fax:** +86-571-86044817
Received: 2003-08-02 **Accepted:** 2003-10-12

Abstract

AIM: To investigate the difference of amino acid uptake between normal and cancerous colon tissues.

METHODS: Sixteen patients with colon cancer were enrolled in our study. Blood samples were taken during operations, serum amino acid concentrations of blood from cancerous or normal colon were analyzed. Amino acid uptake rate was calculated by the A-V difference and evaluated statistically.

RESULTS: Except for methionine, the uptake rate of amino acids in cancer was higher than that in normal colon (25.01% *vs* -2.29%, $P<0.01$). The amino acid uptake rate did not correlate to the size of tumor mass ($P>0.05$). There was no statistical significance in the amino acid uptake rate according to the Dukes stage, though it was higher in patients with Dukes stage C or D than that with Dukes stage B ($P>0.05$).

CONCLUSION: Abnormal synthetic metabolism of colon cancer may contribute to its higher amino acid uptake rate than that of normal colon.

Wang LB, Shen JG, Zhang SZ, Ding KF, Zheng S. Amino acid uptake in arterio-venous serum of normal and cancerous colon tissues. *World J Gastroenterol* 2004; 10(9): 1297-1300
http://www.wjgnet.com/1007-9327/10/1297.asp

INTRODUCTION

Studies note the significance of amino acid metabolism in neoplasms, though there are lots of questions that remain to be answered[1-5]. It is helpful to improve the life quality if we take patients' nutrition into account according to their characteristic amino acid metabolism before we treat cancer patients. Studies[6,7,8,9] demonstrated that the amino acid concentrations in serum, especially essential amino acids (EAAs) but not leucine, were decreased in colon cancer patients with weight loss, but not in patients without weight changes, of which the non-essential amino acids (NEAAs), like asparagic acid, glutamine, glycine, alanine, taurine and ornithine, were slightly elevated in serum. Zheng[10] studied the changes of free amino acids in colon cancer tissue and revealed that the serum concentration of most EAAs (leucine, isoleucine, phenylalanine, threonine, lysine) and some NEAAs (tyrosine, proline, glutamine) in cancer tissue were obviously higher than those in normal tissue ($P<0.01$), while the serum concentration of most NEAAs and some EAAs (methionine, valine, histamine) was slightly elevated. There was no statistical significance. The ammonia serum concentration in cancer tissue decreased significantly ($P<0.05$). To make further investigations of the amino acid metabolism in colon cancer, we analyzed the arteral and venous (A-V) serum free amino acid uptake rates in tumor region, and tried to find the difference of amino acid metabolism between normal and cancerous colon tissue.

MATERIALS AND METHODS

Clinical materials

Sixteen patients were enrolled in this study from Department of Surgical Oncology, Sir Run Run Shaw Hospital, Zhejiang University Medical College. Patients with a median age of 57 years (range from 37 to 77) were diagnosed having colon cancer pathologically. Nine (66.7%) patients were males and in 9 patients, the mass was larger than 5 cm in size. According to Dukes stage, 10 patients were in stage B, 5 in stage C, and 1 in stage D. Before operation, hormone, blood, albumin and amino acid intake were prohibited. Five-day doses of sulfaguanidine and metronidazol were given for bowel preparations.

Sample collection and processing

A 3 mL arterial blood as sample A was collected before making division of the mesentery vessels during laparotomy, and 3 mL reflux venous blood from the tumor region was collected as sample C, another 3 mL mesentery venous blood in normal colon tissue, which was about 7 cm from the tumor margin, was collected as sample E. After incubation at 37 ℃ for an hour, the serum was collected by centrifugation, and 1mL serum mixed with 50 mg sulfosalicylic acid was placed for an hour at 4 ℃, then centrifuged at 16 000 *g* for 6 min. The supernatant was diluted with 0.02 mol/L hydrochloric acid before analysis. Each sample was analyzed twice with automatic amion-acid analyzer (Japan 835-50) 18 standard amino acids including ammonia were placed as control.

Statistical analysis

The A-V amino acid uptake rate in colon cancer (R1) was calculated by the following formula (R1=(A-C)/A×100%) and that in normal tissue (R2) was calculated as the following: R2= (A-E)/A×100% [A, C and E refer to the amino acid concentrations of samples A, C and E]. The rate was compared by means of *t* test, statistical significance was defined as $P<0.05$.

RESULTS

We measured 16 patients with 48 samples. The uptake rates of amino acids in normal and cancerous colon tissue were calculated. As is shown in Table 1, except for methionine, the uptake rates of all amino acids in cancer were higher than those

in normal colon (25.01% *vs* -2.29%, $P<0.01$). The EAAs uptake rates in cancer tissue were between 25.44% and 39.75% with a mean of 31.7% and between -8.01% and 13.5% in normal colon tissue ($P<0.01$). Methionine was 11.55% in cancer tissue but -0.13% in normal tissue. The ketogenic or ketogenic and glucogenic amino acid uptake rates had a mean of 30.86%, which was higher than that of glucogenic acids (18.7%). Sulfur-bearing amino acid uptake rates in colon cancer tissue, which were comparatively lower than the other amino acids, were higher than those in normal tissue, though there was no statistical significance. The uptake rates of some amino acids (lysine, arginine, proline, glutamine, glycine, alanine, cystine, methionine and ammonia) were negative in normal tissue, and the serum concentration of asparagic acid could not be detected in more than 10 patients.

Table 1 A-V amino acid uptake rates in normal and cancerous colon tissue

Amino acid	Sample number	R2 (%)	R1 (%)	*P* value
Threonine [1,3]	16	13.50±3.76	39.25±7.59	<0.01
Phenylalanine [1,3]	16	6.37±1.77	26.26±4.31	<0.01
Leucine [1,4]	16	8.21±2.13	36.55±6.11	<0.01
Isoleucine [1,3]	15	11.39±3.55	30.63±5.50	<0.01
Methionine [1]	16	-0.13±1.20	11.55±5.22	>0.05
Valine [1]	16	7.67±2.42	33.46±5.56	<0.01
Lysine [1,4]	16	-8.01±1.85	25.44±4.41	<0.01
Histidine [1]	16	1.06±0.94	29.83±6.37	<0.01
Proline [2]	11	-26.86±8.36	6.49±1.69	<0.02
Glutamine [2]	16	-12.42±3.12	18.70±5.23	<0.01
Ammonia [2]	16	-23.61±4.58	4.70±1.97	<0.05
Alanine [2]	16	-9.65±2.47	18.16±2.29	<0.01
Glycine [2]	16	-1.50±0.98	29.18±4.41	<0.01
Cystine [2]	13	-10.01±3.37	8.89±1.58	<0.01
Arginine [2]	16	-1.74±0.88	29.02±4.93	<0.01
Serine [2]	16	2.39±1.02	37.26±5.67	<0.01
Tyrosine [2,3]	16	6.57±1.45	26.33±3.39	<0.01

[1]Refers to essential amino acids, [2]refers to non-essential amino acids, [3]refers to ketogenic and glucogenic amino acids, [4]refers to ketogenic amino acids.

Table 2 Relationship between A-V amino acid uptake rates and tumor size in colon cancer

Amino acid	Tumor size<5.0 cm		Tumor size>5.0 cm		*P* value
	Sample number	R1 (%)	Sample number	R1 (%)	
Threonine	7	35.25±10.13	9	42.37±7.81	0.580
Phenylalanine	7	25.44±10.63	9	26.89±3.81	0.889
Leucine	7	33.02±12.85	9	39.30±6.53	0.648
Isoleucine	6	30.09±16.48	9	30.99±4.34	0.950
Methionine	7	13.53±7.47	9	9.99±8.79	0.772
Valine	7	27.63±8.37	9	37.99±8.50	0.408
Lysine	7	21.17±14.07	9	28.76±7.36	0.618
Histidine	7	25.41±10.03	9	33.26±7.26	0.528
Proline	4	10.05±9.81	7	4.45±7.19	0.653
Glutamine	7	25.45±8.69	9	13.44±11.93	0.455
Ammonia	7	13.92±9.08	9	2.47±7.08	0.179
Alanine	7	14.97±1.56	9	20.64±7.72	0.679
Glycine	7	30.04±1.14	9	28.52±11.24	0.926
Cystine	7	20.82±0.69	8	7.23±10.54	0.329
Arginine	7	21.68±7.09	9	34.73±9.06	0.485
Serine	7	25.40±3.22	9	38.71±9.36	0.836
Tyrosine	7	24.90±0.66	9	27.44±4.56	0.815

Table 3 Relationship between A-V amino acid uptake rates and Dukes stage in colon cancer

Amino acid	Dukes stage B		Dukes stage C or D		*P* value
	Sample number	R1 (%)	Sample number	R1 (%)	
Threonine	10	35.75±8.85	6	45.10±7.10	0.476
Phenylalanine	10	24.26±7.02	6	29.60±6.47	0.616
Leucine	10	29.73±9.68	6	47.93±4.07	0.184
Isoleucine	9	22.74±10.23	6	42.47±4.41	0.158
Methionine	10	2.44±6.39	6	26.72±8.30	0.036
Valine	10	34.85±9.53	6	31.15±3.37	0.776
Lysine	10	20.10±11.03	6	34.34±4.90	0.356
Histidine	10	25.32±8.83	6	37.35±5.08	0.341
Proline	6	-2.70±6.43	5	17.50±7.25	0.066
Glutamine	10	26.30±9.92	6	6.02±10.95	0.209
Ammonia	10	5.44±7.74	6	3.47±10.07	0.879
Alanine	10	21.57±9.65	6	12.50±6.66	0.516
Glycine	10	29.37±8.65	6	28.87±15.91	0.976
Cystine	9	11.46±10.67	6	16.73±6.03	0.715
Arginine	10	23.12±13.84	6	38.85±4.80	0.409
Serine	10	34.32±9.75	6	42.16±12.82	0.632
Tyrosine	10	23.08±7.78	6	31.74±4.30	0.432

Relationships between the uptake rates of amino acids and the size of tumor mass or the Dukes stage are shown in Table 2 and Table 3.

DISCUSSION

Studies have noted the amino acid uptake changes in blood and tumor tissue, but the results were controversial[8,11-13]. More factors, such as ages, food intake, consumption and digestion, liver and kidney functions, could influence the amino acid concentrations in serum, and different sample treatment was also confirmed as an important factor[14-17]. In our study, we compared the amino acid concentrations in cancer tissue with those in normal colon as self-control to eliminate the factors that influenced the results.

Tumor cells needed more glucose and amino acids than normal body cells[1]. Limited data were found in *in vivo* studies. We analyzed the amino acid uptake rates in cancer tissue and revealed that the uptake rates of amino acids, especially EAAs, ketogenic, ketogenic and glucogenic amino acids, but not methionine, were significantly higher than those in normal tissue, suggesting that colon cancer might need more of these amino acids.

Protein synthesis was more active in tumor tissue[18-21], and enzymes such as protein kinase were more active in hepatic cancer cells than those in normal cells. Michael *et al*. demonstrated that the protein concentration in cancer tissue (hepatic cancer, digestive cancer and breast cancer) was elevated continuously with tumor progression. Hagmuller *et al*.[22] revealed that, not only the protein synthesis, but the uptake of EAAs and branched-chain amino acids (BAAs) in cancer tissue were more significant than those in arm tissue, as in our study. Khirallah *et al*. suggested that the sources of amino acids in cell protein synthesis came from the plasma and cell protein degradation, though it was not clear which would be the major source. According to our study, amino acids, especially EAAs, might come from the plasma because colon cancer cells were inadequate to synthesize EAAs.

Asparagic acid, glycine, glutamine, folinic acid and ammonia were the basic substrates in pyrimidine and purine nucleosides

synthesis[23]. Our data showed that asparagic acid was too low to be detected in most patients, which might be due to its total utilization in nucleosides synthesis, as was reported by Norton[6]. Methionine is one of the important amino acids in cancer metabolism, and total parenteral nutrition (TPN) with cystine and methionine deficiency has been shown to decrease the tumor growth by inhibiting DNA and RNA synthesis in cancer cells[24,25]. Our data showed that the cystine and methionine uptake rates in cancer tissue were not higher than those in normal tissue, it might be resulted from its repetitive utilization in methylation by s-ademethionine circulation. On the other hand, lower methylation in nucleosides metabolism might also decrease the cystine/methionine requirement in tumor.

Tumor growth consumes a large amount of energy. Glycolysis was ascertained as the major source of energy especially in archaeocytes and poorly differentiated cells because the enzymes in glycolysis in tumor tissue were elevated, which increased the lactic acid concentration and reduced the pH value. Because a little adenosine triphosphate (ATP) could be released by glycolysis, a lot of glucose should be consumed to get adequate energy. Most studies showed that alanine, glycine and glutamine might be involved in glyconeogenesis for their concentrations in blood were higher than the other amino acids. On the other hand, liver glyconeogenesis increased in tumor tissue, and the enzymes involved in glyconeogenesis were more activated, though they were lower in liver cancer than in normal tissue in some studies[1,26]. The glucogenic amino acid concentrations were not obviously changed in tumor tissue in our study, though the uptake rates were higher than those in normal tissue, suggesting these amino acids were utilized during glyconeogenesis.

Aerobic metabolism was present in tumor tissue. Whether any enzyme deficiency occurs in tumor aerobic metabolism is still controversial. Kern *et al*.[27] reported that the fat, but not the liver starch, was the primary substrate in energy metabolism when fasting. Compared with anaerobic metabolism, it could produce eighteen to nineteen times of ATP. The amino acid concentrations in colon cancer tissue (threonine, isoleucine, leucine, phenylalanine, proline, tyrosine and lysine) were higher than those in normal tissue in our study, suggesting that tumor colon tissue utilized these amino acids as a fuel to get more energy in Krebs cycle. There might be a more active and flawless aerobic metabolism in colon cancer tissue, and further studies should be conducted.

It seems that the poorer the cell differentiation, the more elevated ability the more amino acid uptake in tumor. The samples we selected in our study were moderately differentiated globular adenocarcinomas. It was difficult to reveal the differences according to their differentiation, and more samples are needed in further study. Several studies[28-32] demonstrated that there was a correlation between the amino acid concentrations and the tumor volume. On the contrary, in our study, there was no obvious correlation between the size of tumor and the uptake rates of amino acids in tumor tissue, which might probably due to tumor necrosis or lower metabolism. The amino acid uptake rates of patients in Dukes stage C or D were higher than those in Dukes stage B, but only methionine had statistical significance.

The uptake rates of EAAs (methionine and lysine) and NEAAs (glutamine, glycine, alanine, cystine, arginine, proline and ammonia) were negative in normal colon tissue, suggesting that normal colon tissue has the ability to synthesize these amino acids or produce them by tissue protein degradation. Studies[26,33] demonstrated that malignant neoplasms had the ability to enhance the degradation of proteins in surrounding normal tissue or muscles and absorb some part of amino acids to glyconeogenesis, though its function was ignored in general conditions. Whether it is significant in short gut patients needs further studies.

REFERENCES

1 **Shrivastava GC**, Quastel JH. Malignancy and tissue metabolism. *Nature* 1962; **196**: 876-880

2 **Christensen HN**. Interorgan amino acid nutrition. *Physiol Rev* 1982; **62**(4 Pt 1): 1193-1233

3 **Heys SD**, Park KG, McNurlan MA, Keenan RA, Miller JD, Eremin O, Garlick PJ. Protein synthesis rates in colon and liver: stimulation by gastrointestinal pathologies. *Gut* 1992; **33**: 976-981

4 **Smith TK**, Gibson CL, Howlin BJ, Pratt JM. Active transport of amino acids by gamma-glutamyl transpeptidase through Caco-2 cell monolayers. *Biochem Biophys Res Commun* 1991; **178**: 1028-1035

5 **Johnstone RM**, Scholefield PG. Amino acid transport in tumor cells. *Adv Cancer Res* 1965; **9**: 143-226

6 **Norton JA**, Gorschboth CM, Wesley RA, Burt ME, Brennan MF. Fasting plasma amino acid levels in cancer patients. *Cancer* 1985; **56**: 1181-1186

7 **Liu HL**, Wang YB, Nie L. The amino acids difference between cancer and normal gastric tissue: a 22 cases study. *Acad J PLA Postgrad Med Sch* 2001; **22**: 105-108

8 **Zhang PC**, Pang CP. Plasma amino acid patterns in cancer. *Clin Chem* 1992; **38**: 1198-1199

9 **Tamemasa O**, Goto R, Takeda A, Maruo K. High uptake of 14C-labeled D-amino acids by various tumors. *Gann* 1982; **73**: 147-152

10 **Wang LB**, Zhang SZ, Ding KF, Zheng S. A study of the free amino acids uptake in colon cancer. *Zhejiang Yixue* 1997; **19**: 208-209

11 **Becker W**, Konstantinides F, Eyer S, Ward H, Fath J, Cerra F. Plasma amino acid clearance as an indicator of hepatic function and high-energy phosphate in hepatic ischemia. *Surgery* 1987; **102**: 777-783

12 **Sahai S**, Uhlhaas S. Stability of amino acids in human plasma. *Clin Chim Acta* 1985; **148**: 255-259

13 **Watanabe A**, Higashi T, Sakata T, Nagashima H. Serum amino acid levels in patients with hepatocellular carcinoma. *Cancer* 1984; **54**: 1875-1882

14 **Yang H**, Jiang J, Hu P. Metabolism of protein and amino acids during chronic renal failure. *Zhongguo Linchuang Yingyang Zazhi* 2001; **9**: 175-177

15 **Garibotto G**, Deferrari G, Robaudo C, Saffioti S, Salvidio G, Paoletti E, Tizianello A. Effect of amino acid ingestion on blood amino acid profile in patients with chronic renal failure. *Am J Clin Nutr* 1987; **46**: 949-954

16 **Upton JD**, Hindmarsh P. More pitfalls in human plasma amino acid analysis. *Clin Chem* 1990; **36**: 157-158

17 **Rattenbury JM**, Townsend JC. Establishment of an external quality-assessment scheme for amino acid analyses: results from assays of samples distributed during two years. *Clin Chem* 1990; **36**: 217-224

18 **Smith SR**, Pozefsky T, Chhetri MK. Nitrogen and amino acid metabolism in adults with protein-calorie malnutrition. *Metabolism* 1974; **23**: 603-618

19 **Steiger E**, Oram-Smith J, Miller E, Kuo L, Vars HM. Effects of nutrition on tumor growth and tolerance to chemotherapy. *J Surg Res* 1975; **18**: 455-466

20 **Torosian MH**, Mullen JL, Stein TP, Miller EE, Zinsser KR, Buzby GP. Enhanced tumor response to cycle-specific chemotherapy by pulse total parenteral nutrition. *J Surg Res* 1985; **39**: 103-113

21 **Heys SD**, Park KG, McNurlan MA, Calder AG, Buchan V, Blessing K, Eremin O, Garlick PJ. Measurement of tumour protein synthesis *in vivo* in human colorectal and breast cancer and its variability in separate biopsies from the same tumour. *Clin Sci* 1991; **80**: 587-593

22 **Hagmuller E**, Kollmar HB, Gunther HJ, Holm E, Trede M. Protein metabolism in human colon carcinomas: *in vivo* investigations using a modified tracer technique with L-[1-13C] leucine. *Cancer Res* 1995; **55**: 1160-1167

23 **Cascino A**, Muscaritoli M, Cangiano C, Conversano L, Laviano A, Ariemma S, Meguid MM, Rossi Fanelli F. Plasma amino acid imbalance in patients with lung and breast cancer. *Anticancer Res* 1995; **15**: 507-510
24 **He YC**, Wang YH, Cao J, Chen JW, Pan DY, Zhou YK. Effect of complex amino acid imbalance on growth of tumor in tumor-bearing rats. *World J Gastroenterol* 2003; **9**: 2772-2775
25 **He YC**, Cao J, Chen JW, Pan DY, Zhou YK. Influence of methionine/valine-depleted enteral nutrition on nucleic acid and protein metabolism in tumor-bearing rats. *World J Gastroenterol* 2003; **9**: 771-774
26 **Waterhouse C**, Jeanpretre N, Keilson J. Gluconeogenesis from alanine in patients with progressive malignant disease. *Cancer Res* 1979; **39**(6 Pt 1): 1968-1972
27 **Kern KA**, Norton JA. Cancer cachexia. *J Parenter Enteral Nutr* 1988; **12**: 286-298
28 **Wang L**, Tong XQ, Li QR. The study on interrelation between colonic carcinoma tissue free amino acid and tumor volume. *Parenteral Enteral Nutrition* 2001; **8**: 221-223
29 **Wang L**, Li BY, Li QR. The study on interrelation between gastric cancer tissue free amino acid and tumor volume. *Parenteral Enteral Nutrition* 2000; **7**: 41-44
30 **Yamanaka H**, Kanemaki T, Tsuji M, Kise Y, Hatano T, Hioki K, Yamamoto M. Branched-chain amino acid-supplemented nutritional support after gastrectomy for gastric cancer with special reference to plasma amino acid profiles. *Nutrition* 1990; **6**: 241-245
31 **Nishizaki T**, Matsumata T, Taketomi A, Yamamoto K, Sugimachi K. Levels of amino acids in human hepatocellular carcinoma and adjacent liver tissue. *Nutr Cancer* 1995; **23**: 85-90
32 **Ye SL**, Tang ZY, Liu H, Zhao QC. The changes of amino acids concentration in hepatocellular carcinoma. *Zhonghua Yixue Zazhi* 1989; **69**: 319-320
33 **Goodlad GA**, Clark CM. Leucine metabolism in skeletal muscle of the tumour- bearing rat. *Eur J Cancer* 1980; **16**: 1153-1162

Edited by Wang XL and Zhang JZ **Proofread by** Xu FM

PO Box 2345, Beijing 100023, China
Fax: +86-10-85381893
E-mail: wjg@wjgnet.com www.wjgnet.com

World J Gastroenterol 2004;10(9):1301-1305
World Journal of Gastroenterology
Copyright ©2004 by The WJG Press ISSN 1007-9327

• COLORECTAL CANCER •

Construction of a metastasis-associated gene subtracted cDNA library of human colorectal carcinoma by suppression subtraction hybridization

Li Liang, Yan-Qing Ding, Xin Li, Guang-Zhi Yang, Jun Xiao, Li-Chun Lu, Jin-Hua Zhang

Li Liang, Yan-Qing Ding, Xin Li, Guang-Zhi Yang, Li-Chun Lu, Jin-Hua Zhang, Department of Pathology, the First Military Medical University, Guangzhou 510515, Guangdong Province, China
Jun Xiao, Department of Tropic Medicine, the First Military Medical University, Guangzhou 510515, Guangdong Province, China
Supported by the Military Medical Foundation of China, No. 01MA128
Correspondence to: Professor Yan-Qing Ding, Department of Pathology, the First Military Medical University, Guangzhou 510515, Guangdong Province, China. wcjd@public.bta.net.cn
Telephone: +86-20-61642148 **Fax:** +86-20-61642148
Received: 2002-08-26 **Accepted:** 2003-04-11

Abstract

AIM: To construct a differentially-expressed gene subtracted cDNA library from two colorectal carcinoma (CRC) cell lines with different metastatic phenotypes by suppression subtractive hybridization.

METHODS: Two cell lines of human CRC from the same patient were used. SW620 cell line showing highly metastatic potential was regarded as tester in the forward subtractive hybridization, while SW480 cell line with lowly metastatic potential was treated as tester in the reverse hybridization. Suppression subtractive hybridization (SSH) was employed to obtain cDNA fragments of differentially expressed genes for the metastasis of CRC. These fragments were ligated with T vectors, screened through the blue-white screening system to establish cDNA library.

RESULTS: After the blue-white screening, 235 white clones were picked out from the positive-going hybridization and 232 from the reverse. PCR results showed that 200-700 bp inserts were seen in 98% and 91% clones from the forward and reverse hybridizations, respectively.

CONCLUSIONS: A subtractive cDNA library of differentially expressed genes specific for metastasis of CRC can be constructed with SSH and T/A cloning techniques.

Liang L, Ding YQ, Li X, Yang GZ, Xiao J, Lu LC, Zhang JH. Construction of a metastasis-associated gene subtracted cDNA library of human colorectal carcinoma by suppression subtraction hybridization. *World J Gastroenterol* 2004; 10 (9): 1301-1305
http://www.wjgnet.com/1007-9327/10/1301.asp

INTRODUCTION

CRC is one of the most common malignant tumors in the world and its metastasis is the major cause of mortality in patients with colorectal carcinoma. More than hundreds of genes have been reported to be involved in the regulations of metastasis in colorectal carcinoma. However, they are still not sufficient for fully explaining the complexity and diversity of metastasis. Besides, current investigations of these genes that mostly focused on the expression analysis of one or several genes make it difficult to understand the genes' interactions and find the new genes. Cloning and identification of metastasis-associated genes have been hypothesized to be beneficial to the elucidation of the molecular mechanisms underlying the metastasis and finding gene targets for metastatic forecast, therapy and prognosis of CRC patients. In our study, SSH and bacterial culture PCR screening were used to construct a differentially-expressed gene subtracted cDNA library specific for metastasis of human CRC with the hope to screen new metastasis associated genes.

MATERIALS AND METHODS

Cell lines

Highly metastatic cell line SW620 and lowly metastatic cell line SW480 from human colorectal carcinoma were purchased from ATCC with the number of CCL-227 and CCL-228 respectively. Both of the paired cell lines were from one colonic adenocarcinoma patient and had the same genetic backgrounds. Cell lines were routinely cultured with DMEM supplemented with 10% bovine serum under the atmosphere containing 50 mL/L CO_2 at 37 ℃.

PCR primers and adaptors

cDNA synthesis primer (5' -TTTTGTACAAGCTT$_{30}$N$_1$N-3') was used for the first-strand cDNA synthesis. Adaptor1 (5' -CTAATACGACTCACTATAGGGCTCGAGCGGCCGCCCGGGCAGGTACCTGCCCGG-3') and adaptor2R (5' CTAATACGACTCACTATAGGGCAGCGTGGTCGCGGCCGAGGTACCTCGGCCG-3') have the same sequence of the 5' region and the different palindromic structures in the 3' end. Only the differentially expressed fragments digested by RsaI restriction enzyme could be ligated with two adaptors. Primary PCR was performed to amplify these fragments with primer1 (5' -CTAATACGACTCACTATAGGGC-3') that corresponds to the outer common sequence of the adaptors. After that, nested primer1 (5' -TCGAGCGGCCGCCCGGGCAGGT-3') and nested primer2R (5' -AGCGTGGTCGCGGCCGAGGT-3') designed from the inner sequences of the adaptors respectively were used for the further enrichment of these fragments in secondary PCR. The underlines in the sequences indicated the sites of RsaI restriction enzyme. The above primers and adaptors were provided by PCR-Select ™cDNA Subtraction Kit (Clontech Laboratories Inc, USA).

mRNA isolation

Total mRNA was isolated from the two cell lines respectively using QuickPrep micro mRNA purification kit (Pharmacia, USA) following the recommendations of the manufacturer.

Suppression subtractive hybridization

SSH was performed by using PCR-Select ™cDNA subtraction kit (Clontech Laboratories Inc, USA) according to the

recommendations of the manufacturer. The highly metastatic cell line SW620 was used as the tester while the lowly metastatic cell line SW480 was used as the driver in the forward hybridization, and vice versa in the reverse hybridization.

Double strand cDNA synthesis

A total of 2 μg (4 μL) mRNA with 1 μL oligo (dT_{30}) primer was heated to 70 ℃ for 2 min and rapidly cooled on ice. The reaction mixture was made up to 10 μL by adding 1 μL cDNA synthesis primer (10 μmol/L), 2 μL 5×the first strand reaction buffer, 1 μL dNTP mix (10 mmol/L each) and 1 μL sterile H_2O. Reverse transcription was started by adding 1 μL AMV reverse transcriptase (20 U/μL). The reaction mixture was incubated at 42 ℃ for 1.5 h to synthesize the first strand cDNA. The second strand cDNA synthesis was performed by immediately adding 48.4 μL sterile H_2O, 16 μL 5×the second strand buffer, 1.6 μL dNTP mix, 4 μL 20×the second strand enzyme cocktail. The reaction mixture was incubated at 16 ℃ for 2 h. Double strand cDNA was blunted by adding of 2 μL T4 DNA polymerase and incubated at 16 ℃ for 20 min. The reaction was stopped by adding 20×EDTA/glycogen mix into the reactive mixture. cDNAs were then extracted, precipitated, and resuspended in 50 μL of deionized water.

Ligation of cDNA fragments

For the ligation of cDNA fragments, 43.5 μL of ds cDNA from the tester and driver was digested respectively with 1.5 μL of RsaI (10 U/μL) at 37 ℃ for 1.5 h. The reaction was terminated by adding 20×EDTA/glycogen mix. The resulting fragments of cDNAs were extracted, precipitated and finally resuspended in 5.5 μL of deionized water. Adaptor1 and adaptor2R were ligated separately to 2 μL of RsaI digested tester cDNA with 1:6 dilution in the presence of T4 DNA ligase at 16 ℃ overnight followed by heating at 70 ℃ for 5 min to inactivate the ligase. In order to determine whether the ligation efficiency was high or not, 1 μL of adaptor1-ligated and adaptor2R-ligated cDNAs of the tester was diluted into 200 μL H_2O respectively and amplified in two separate 50 μL reactions. One reaction used G3PDH3' , 5' primer, while the other used G3PDH3' primer and PCR primer1. PCR parameters were as follows: 30 cycles at 94 ℃ for 30 s, at 65 ℃ for 30 s and at 68 ℃ for 2.5 min. The products were examined by electrophoresis on a 20 g/L agarose/EB gel.

Two subtractive hybridizations

In the first hybridization, 1.5 μL of RsaI digested driver cDNA was mixed with 1.5 μL of diluted adaptor1- or adaptor2R-ligated tester cDNA. The samples were denatured at 98 ℃ for 1.5 min and immediately incubated in a thermal cycler at 68 ℃ for 8 h. In the second hybridization, two kinds of sample resulting from the first hybridization were mixed in the presence of a freshly denatured driver cDNA. The samples were incubated at 68 ℃ for 18 h. After 200 μL of dilution buffer was added, the samples were incubated for an additional 7 min. Analysis of the subtraction efficiency was carried out using PCR amplification of G3PDH in diluted subtracted cDNA versus unsubtracted cDNA. PCR was performed for 33 cycles at 94 ℃ for 30 s, at 60 ℃ for 30 s and at 68 ℃ for 2 min. The products were monitored on a 20 g/L agarose/EB gel for an aliquot which was removed from each reaction after 18, 23, 28, 33 cycles.

Two suppression PCRs (nested PCR)

A 1 μL of diluted subtraction mixture was amplified with PCR primer1 in the primary PCR. The reaction mixture was incubated at 75 ℃ for 5 min to extend the adaptors and followed in turn at 94 ℃ for 25 s, 30 cycles at 94 ℃ for 10 s, at 64 ℃ for 30 s and at 71 ℃ for 1.5 min. The primary PCR mixture was diluted 10-fold and 1 μL from that was used in secondary PCR with nested PCR primer1 and primer2R. The conditions of the reaction were 15 cycles at 94 ℃ for 10 s, at 68 ℃ for 30 s and at 72 ℃ for 1.5 min. Eight μL products from each PCR reaction of the secondary PCR was analyzed on a 20 g/L agarose/EB gel.

Screening for subtraction library

The second PCR products were purified and their concentrations were measured by a spectrophotometer. The T/A cloning method was performed by using pGEM-T vector system I (Promega, USA) according to the recommendations of the manufacturer. The PCR product was cloned into the vector with a molar ratio of 6:1(insert: vector). A 2 μL purified PCR products(25 ng/μL) was used in a 10 μL-ligation-reaction system including 5 μL 2×Rapid ligation buffer, 1 μL pGEM-T Easy Vector (50 ng/μL), 1 μL T4 DNA ligase (3Weiss units/μL) and 1 μLdeionized water. The mixture was incubated at 4 ℃ overnight. The positive control was made by using the control insert DNA from the kit instead of the PCR products. The background control was made without inserting any fragments. The recombinant plasmids were transformed respectively into the competent JM109 E-coli cell with the $CaCl_2$ method. A 100 μL of transformants was grown on 8 cm×8 cm agar plates containing 100 μg/mL ampicillin, 100 μmoL/L IPTG and 100 μg/mL X-gal at 37 ℃ for 20 h when the blue/white staining could be clearly distinguished. White clones were counted, inoculated into 3 mL of LB liquid medium containing ampicillin and shaken overnight at 37 ℃. The resulting bacterial culture was directly used as PCR templates to amplify the inserts in 50 μL reaction mixture containing 10×PCR buffer 5.0 μL, Mg^{2+} (25 mmol/L) 3 μL, nested primer 1 (20 μmol/L) 1 μL, nested primer 2R (20 μmol/L) 1 μL, dNTP mix (10 mmol/L) 1 μL, Taq enzyme mix (5 U/μL) 0.5 μL and bacterial culture 0.5 μL. PCR consisted of an initial denaturation step at 94 ℃ for 5 min, followed by 25 cycles at 94 ℃ for 30 s, at 68 ℃ for 30 s and at 72 ℃ for 2 min each. The PCR products were analyzed on an 10 g/Lagarose/EB gel.

RESULTS

Quality identification of extracted mRNA

The extracted mRNA that was electrophoresed on 10 g/L agarose gel exhibited as a clear smear with over 0.5 kb length (Figure 1). Their absorbances(A_{260}/A_{280}>1.8) in spectrophotometry suggested that extracted mRNAs were in a highly purified quality.

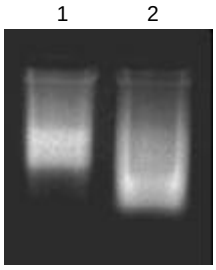

Figure 1 Quality identification of mRNA extracted from two cell lines, Lane 1: SW480 cell line, Lane 2: SW620 cell line.

RsaI digestion analysis of synthesized cDNA

The results of 10 g/L agarose electrophoresis showed that cDNA before digested with RsaI, displayed a zonal smear with a length from 0.5 kb to 10 kb. After the digestion, the cDNA length became shorter with fragments from 0.1 kb to 2 kb, suggesting that cDNAs were completely digested (Figure 2).

Analysis of ligation efficiency

The high ligation efficiency was the most important factor for

success of SSH. Figure 3 shows that the intensity of band 2/ band1, band4/ band3 was over 80%, indicating that subtracted cDNA library had the high ligation efficiency, 80% of the tester' ds cDNA fragments were ligated with adaptors1 or 2R.

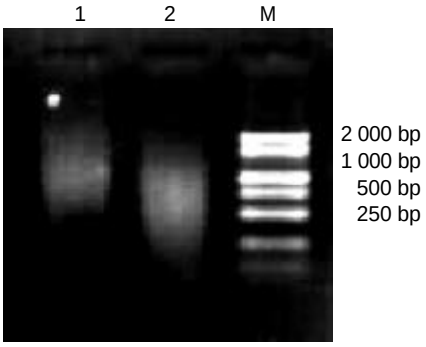

Figure 2 RsaI digestion analysis of synthesized cDNA, Lane 1: Synthesized cDNA digested with RsaI, Lane 2: Synthesized cDNA, Lane M: Marker DGL2000.

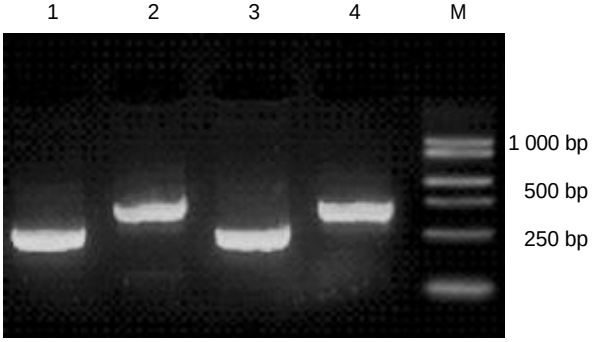

Figure 3 Ligation efficiency analysis of ds cDNA, Lane 1: PCR products using tester1-1 (adaptor1-ligated-cDNA fragment) as the template and the G3PDH3', 5' primer; Lane 2: PCR products using tester1-1 as the template and the G3PDH3' primer, PCR primer1; Lane 3: PCR products using tester1-2 (adaptor2R-ligated-cDNA fragments) as the template and the G3PDH3', 5' primer; Lane 4: PCR products using tester1-2 as the template and the G3PDH3' primer, PCR primer1; Lane M: Marker DGL2000.

Analysis of secondary PCR products

Nested primers from the inner sequences of adaptors were used to amplify the primary PCR products, and the smear was increased obviously after 15 cycles, in which some obscure bands with the lengths between 0.2 and 1.5 kb were observed (Figure 4).

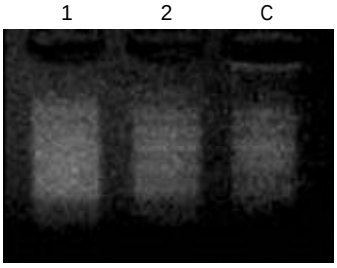

Figure 4 Electrophoresis of secondary PCR products, Lane C: Positive control cDNA supplied with the kit, Lane 1: Unsubtracted cDNA, Lane 2: Subtracted cDNA.

Subtractive efficiency

Figure 5 shows that obvious bands were seen after 23 cycles in unsubtracted cDNA and after 33 cycles in diluted subtracted cDNA. The amount of G3PDH was significantly decreased after subtraction, indicating that the subtracted cDNA library had the high subtraction efficiency.

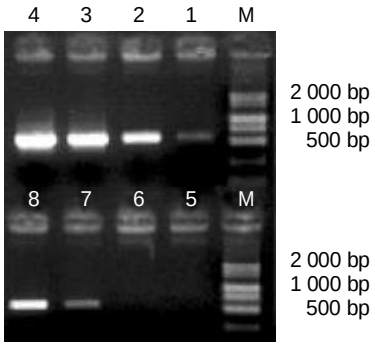

Figure 5 Reduction of G3PDH by PCR subtraction, Lanes 1-4: Unsubtracted secondary PCR products, Lanes 5-8: Subtracted secondary PCR products, Lanes 1, 5: 18 cycles Lane 2, 6: 23 cycles, Lanes 3, 7: 28 cycles, Lane 4, 8: 33 cycles, Lane M: Marker DGL2000.

Screening for subtraction cDNA library

On the agar plates with 100 μL of transformants, 235 white clones were obtained in the forward hybridization (group A) while 232 white clones were obtained in the reverse hybridization (group R) (Figure 6). White clones accounted for more than 80% of the total clones. Ninety-eight percent and 91% of the white clones were demonstrated by PCR having the inserts with a length of 200-700 bp in groups A and R, respectively (Figure 7), indicating that a subtracted cDNA library specific for metastasis in CRC was successfully constructed.

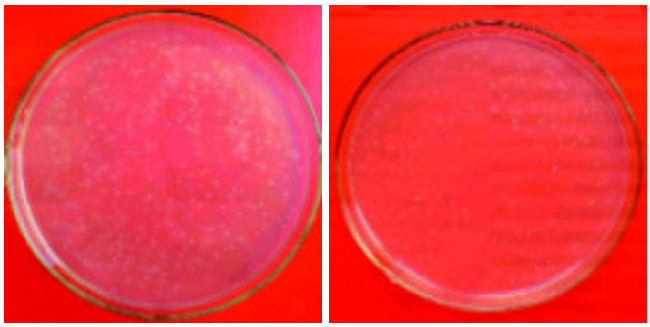

Figure 6 Blue / white screening for target clones, Two hundred and thirty-five white clones (86%) and 37 blue clones were seen on the agar plates in group A, and 232 white clones (91%) and 21 blue clones were seen in group R.

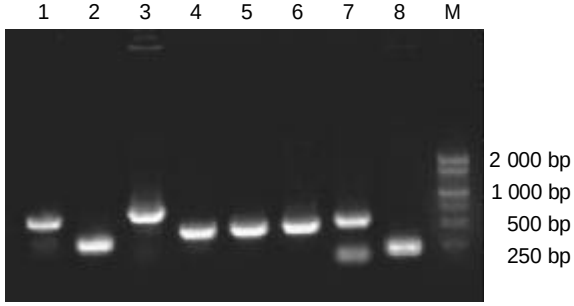

Figure 7 Different lengths of cDNA fragments from white clones amplified by PCR, Lanes 1-8: Randomly-selected white clones, Lane M: Marker DGL2000.

DISCUSSION

Metastasis is the major cause of mortality in CRC patients. The molecular basis for metastasis has not been fully elucidated yet. Available studies have shown that many specific genes are involved in the process of metastasis, which may accelerate or suppress metastasis by a mechanism of cooperative or inhibitive interactions between genes[1]. Till now hundreds of genes have been reported to be involved in the regulation of metastasis in colorectal carcinoma. However, the existent methods for investigating the molecular mechanism of metastasis are mostly limited to the analysis of expressions of only one or several genes, which makes it difficult to understand the genes' interactions and their relations to the metastasis.

One of the most important ways to understand the carcinogenesis and development of tumors is to clone and identify the differentially expressed genes. In recent years several cloning techniques for the differentially expressed genes have been established, including differential display PCR (DD-PCR), representational difference analysis (RDA), SSH and cDNA microarray. Until now, these techniques have been widely applied in the study of pathology[2], immune[3], embryo development[4], as well as the specific expression of tissue protein[5]. Although it is rapid, easy to perform and sensitive, DD-PCR has also some limitations, such as the higher false positive rate and the truncated length of obtained specific cDNA that is usually located in non-translated regions of 3' poly(A). Likewise, RDA needs less amount of mRNAs samples and has lower false positive rate. But it is troublesome to perform more complicated steps of hybridization or PCR. Microarray-based methods have the potentials to revolutionize the study of differential gene expression under parallel conditions with higher automation. While a number of drawbacks of this approach have been found such as the higher expense and less sensitive than that of PCR-based techniques.

SSH was first put forward by Diatchenko *et al.* in 1996. The basic principle was that common cDNAs in the paired materials were subtracted by subtractive hybridization and then suppressive PCR was carried out to amplify cDNA fragments specially expressed in tester. The advantage of SSH was the design of two different adaptors and the introduction of suppression PCR with the result that the differentially expressed cDNA fragments were amplified. It allows two subtractive hybridizations in the forward or reverse direction. Some mRNA expressed with low abundance could be detected, which provided clues for the further gene sequencing and identification[6-9]. With the development and improvement of SSH technique, it has become one of the most effective techniques for cloning differentially expressed genes. Since it was established, more than two hundred papers have been published concerning about carcinogenesis[10], tumor metastasis[11], signal transduction[12], apoptosis[13] and tumor therapy[14]. Combined with other molecular biological techniques such as DNA chip, it could clone tumor associated genes[15] and metastasis-associated genes in lung carcinoma, breast carcinoma and other malignancies[16-20]. Zhang *et al.*[21] carried out SSH in human NCI-H69 cell line and its variant, a more aggressive NCI-N417 SCLC cell line, to characterize the variable expression of genes between the two cell lines, in which 42 genes were screened by the forward and reverse hybridizations. Wang *et al.*[22] have identified five cDNA fragments with SSH that were expressed at much higher levels in the poorly metastatic cancer cell clone than in the highly metastatic variety. Until now studies on separating metastasis-associated genes in human CRC have not been reported.

In our study, SSH and bacterial culture PCR were performed to construct a subtracted cDNA library specific for the metastasis-related genes of human CRC, in which a pair of human colorectal carcinoma cell lines SW620 and SW480 was used. The SW480 cell line was derived from a Dukes' stage B colon carcinoma that arose in a 50-year-old male patient with liver and mesenteric lymph node metastases. The SW620 cell line was derived from one of the lymph node metastases. The monoclonal origin of the two cell lines that was confirmed by the presence of shared maker chromosomes on cytogenetic analysis makes it suitable to study the genetic basis of their phenotypic differences. Hewitt *et al.*[23] have also found that the phenotypic differences of both SW620 and SW480 cell lines were retained, despite long-term culture *in vitro*.

Both the forward and reverse hybridizations were performed in this study. In the forward hybridization (group A), the highly metastatic cell line SW620 was treated as the tester, while the lowly metastatic cell line SW480 was treated as the tester in the reverse hybridization (group R). As a result, the total cDNAs in the tester and driver were subtracted efficiently. cDNA fragments appearing only in SW620 cells were amplified specially in group A and those only in SW480 cells were amplified in group R. After that, the second PCR products were inserted into T vectors and then screened by the blue/white screening system. Two hundred and thirty-five or 232 white clones were obtained in group A or group R respectively. The resultant subtractive cDNA library that was rich in metastasis-associated gene fragments of CRC was superior to that obtained by other methods for 4 reasons: (1) High specificity. Two subtractive hybridizations and two suppressive PCR were carried out to amplify the differentially expressed cDNA fragments, and suppress the amplification of unspecific cDNA fragments. Thus, the specificity of the subtractive library was greatly increased. (2) High sensitivity. The normalization of tester ss cDNA by SSH could make the differentially expressed genes with high or low abundance separated efficiently. (3) High efficiency. One SSH reaction could separate hundreds and thousands differentially expressed genes simultaneously. (4) More information. The differentially expressed fragments in the forward hybridization might have a role in accelerating metastasis, and those in the reverse hybridization might be metastasis suppressor genes. The forward and reverse hybridizations could provide more information of the screening results.

However, the subtracted cDNA library constructed by SSH had some limitations. One of them was the requirement of large quantities of mRNA samples. The other was that differentially expressed cDNAs obtained from SSH were cDNA fragments digested by restrictive enzyme and needed to be amplified to get the full length. These drawbacks could be overcame by other methods such as the multi-cycle linear amplification based on cDNA synthesis and templet-guided *in vitro* transcription, in which enough mRNA for the continual research could be amplified with less than 1-50 ng RNA samples[24]. Thus, it is especially suitable for tissues that are hard to get or too little to provide enough RNAs. In addition, the full length of differential fragments could be obtained by the rapid amplification of cDNA ends (RACE) [25].

After the blue/ white screening, bacterial culture PCR was used in the present study to screen the positive recombinants. Compared with the routine methods, bacterial culture PCR was not only simple but also helpful for the further identifications. Our results showed that there were 98% clones with 200-700 bp inserts in group A and 91% positive clones of recombinants in group R, suggesting that these clones may contain metastasis-related cDNA fragments. The construction of this library is therefore of significance in screening and identifying the genes associated with metastasis of CRC, which would be beneficial to the elucidation of the molecular mechanism of metastasis and provide new gene targets for metastasis forecast, gene therapy and prognosis estimation in clinical practice.

REFERENCES

1 **Welch DR**, Rinker-Schaeffer CW. What defines a useful marker of metastasis in human cancer? *J Natl Cancer Inst* 1999; **91**: 1351-1353

2 **Sharma R**, Samantaray S, Shukla NK, Ralhan R. Transcriptional gene expression profile of human esophageal squamous cell carcinoma. *Genomics* 2003; **81**: 481-488

3 **Dunphy JL**, Balic A, Barcham GJ, Horvath AJ, Nash AD, Meeusen EN. Isolation and characterization of a novel inducible mammalian galectin. *J Biol Chem* 2000; **275**: 32106-32113

4 **Li P**, Li JL, Hou R, Han QD, Zhang YY. Changes in the gene expression profile of the left heart ventricle during growth in the rat. *Shengli Xuebao* 2003; **55**: 191-196

5 **Ito H**, Akiyama H, Iguchi H, Iyama K, Miyamoto M, Ohsawa K, Nakamura T. Molecular cloning and biological activity of a novel lysyl oxidase-related gene expressed in cartilage. *J Biol Chem* 2001; **276**: 24023-24029

6 **Sandhu H**, Dehnen W, Roller M, Abel J, Unfried K. mRNA expression patterns in different stages of asbestos-induced carcinogenesis in rats. *Carcinogenesis* 2000; **21**: 1023-1029

7 **Zhu NX**, Zheng S, Xu RZ, Gao RL, Shen JP, Yu RX. Identification of multidrug resistance related genes in leukemia by suppression subtractive hybridization. *Zhonghua Yexue Zazhi* 2003; **24**: 14-17

8 **Ai JK**, Huang X, Wang YJ, Bai Y, Lu YQ, Ye XJ, Xin DQ, Na YQ, Zhang ZW, Guo YL. Screening of novel genes differentially expressed in human renal cell carcinoma by suppression subtractive hybridization. *Aizheng* 2002; **21**: 1065-1069

9 **Shen C**, Hui-Zhao, Wang D, Jiang G, Wang J, Zhang G. Molecular cloning, identification and analysis of lung squamous cell carcinoma-related genes. *Lung Cancer* 2002; **38**: 235-241

10 **Hufton SE**, Moerkerk PT, Brandwijk R, de Bruine AP, Arends JW, Hoogenboom HR. A profile of differentially expressed genes in primary colorectal cancer using suppression subtractive hybridization. *FEBS Lett* 1999; **463**: 77-82

11 **Asai T,** Tomita Y, Nakatsuka S, Hoshida Y, Myoui A, Yoshikawa H, Aozasa K. VCP (p97) regulates NFkappaB signaling pathway, which is important for metastasis of osteosarcoma cell line. *Jpn J Cancer Res* 2002; **93**: 296-304

12 **Kostic C**, Shaw PH. Isolation and characterization of sixteen novel p53 response genes. *Oncogene* 2000; **19**: 3978-3987

13 **Sakamoto H**, Mashima T, Kizaki A, Dan S, Hashimoto Y, Naito M, Tsuruo T. Glyoxalase I is involved in resistance of human leukemia cells to antitumor agent-induced apoptosis. *Blood* 2000; **95**: 3214-3218

14 **Zhang Z**, DuBois RN. Detection of differentially expressed genes in human colon carcinoma cells treated with a selective COX-2 inhibitor. *Oncogene* 2001; **20**: 4450-4456

15 **Schlingemann J**, Hess J, Wrobel G, Breitenbach U, Gebhardt C, Steinlein P, Kramer H, Furstenberger G, Hahn M, Angel P, Lichter P. Profile of gene expression induced by the tumour promotor TPA in murine epithelial cells. *Int J Cancer* 2003; **104**: 699-708

16 **Yin J**, Fan Q, Hao X, Fan D. Identification of genes associated with human osteosarcoma metastasis suppression using suppression subtractive hybridization. *Zhonghua Yixue Yichuanxue Zazhi* 2002; **19**: 213-217

17 **Yin JN**, Fan QY, Hao XB, Yang N. Apoptosis antagonizing transcription factor is a gene highly expressed in highly metastatic human osteosarcoma cell lines. *Aizheng* 2002; **21**: 127-131

18 **Koo TH**, Lee JJ, Kim EM, Kim KW, Kim HD, Lee JH. Syntenin is overexpressed and promotes cell migration in metastatic human breast and gastric cancer cell lines. *Oncogene* 2002; **21**: 4080-4088

19 **Goldberg SF**, Miele ME, Hatta N, Takata M, Paquette-Straub C, Freedman LP, Welch DR. Melanoma metastasis suppression by chromosome 6: evidence for a pathway regulated by CRSP3 and TXNIP. *Cancer Res* 2003; **63**: 432-440

20 **Devoogdt N**, Hassanzadeh Ghassabeh G, Zhang J, Brys L, De Baetselier P, Revets H. Secretory leukocyte protease inhibitor promotes the tumorigenic and metastatic potential of cancer cells. *Proc Natl Acad Sci U S A* 2003; **100**: 5778-5782

21 **Zhang L**, Cilley RE, Chinoy MR. Suppression subtractive hybridization to identify gene expressions in variant and classic small cell lung cancer cell lines. *J Surg Res* 2000; **93**: 108-119

22 **Wang T**, Lu Y, Liu S. Suppression subtractive hybridization in the cloning of gene fragments in relation to lung cancer metastasis. *Zhonghua Zhongliu Zazhi* 2001; **23**: 296-300

23 **Hewitt RE**, McMarlin A, Kleiner D, Wersto R, Martin P, Tsokos M, Stamp GW, Stetler-Stevenson WG, Tsoskas M. Validation of a model of colon cancer progression. *J Pathol* 2000; **192**: 446-454

24 **Wang E**, Miller LD, Ohnmacht GA, Liu ET, Marincola FM. High-fidelity mRNA amplification for gene profiling. *Nat Biotechnol* 2000; **18**: 457-459

25 **Xu CS**, Li YC, Lin JT, Zhang HY, Zhang YH. Cloning and analysizing the up-regulated expression of transthyretin-related gene (LR1) in rat liver regeneration following short interval successive partial hepatectomy. *World J Gastroenterol* 2003; **9**: 148-151

Edited by Wang XL and Zhu L **Proofread by** Xu FM

PO Box 2345, Beijing 100023, China
Fax: +86-10-85381893
E-mail: wjg@wjgnet.com www.wjgnet.com

World J Gastroenterol 2004;10(9):1306-1309
World Journal of Gastroenterology
Copyright ©2004 by The WJG Press ISSN 1007-9327

• *H pylori* •

Helicobacter pylori L-form and patients with chronic gastritis

Ke-Xia Wang, Lin Chen

Ke-Xia Wang, Lin Chen, School of Medicine, Anhui University of Science & Technology Huainan 232001, Anhui Province, China
Supported by The Education Department of Anhui Province, China No.2003kj111
Correspondence to: Dr. Ke-Xia Wang , School of Medicine, Anhui University of Science & Technology, Huainan, 232001, Anhui Province, China. kexiawang2003@yahoo.com.cn
Telephone: +86-554-6658770 **Fax:** +86-554-6662469
Received: 2003-10-20 **Accepted:** 2003-12-08

Abstract

AIM: To study the relationship between infection with *Helicobacter pylori* L-forms and chronic gastritis and its association with possible changes of cellular immune function.

METHODS: Gastric mucosal biopsies were taken from 428 patients with chronic gastritis to detect *H pylori* L-form by Gram staining and immunohistochemistry staining. Peripheral venous blood samples of patients were taken to detect the percentage of CD3+, CD4+ and CD8+ by the biotin-streptavidin (BSA) assay and the levels of IL-2, IL-6and IL-8 by ELISA.

RESULTS: The rate of infection with *H pylori* L-forms was 48.83% (209/428). The rate was 50.47% (216/428) and 52.80% (226/428), respectively, as detected by immunohistochemistry staining and Gram staining (P>0.05). The rate of *H pylori* L-forms in males and females was 57.8% (136/235) and 37.28% (73/193), respectively, (χ^2=17.05, P<0.01). Furthermore, the rate increased with age, with the rate being significantly greater in patients ⩾40 years old than in those <40 years old (P<0.01). The percentage of CD3+, CD4+, CD8+, the ratio of CD4+ / CD8+, and the levels of IL-2, IL-6, IL-8 in *H pylori*-positive patients were 47.58±4.44%, 25.51±4.74%, 22.77±7.46%, 1.44±0.51%, 1.56±0.47 mg/L, 103.62±5.85 ng/L, and 109.79±7.18 ng/L, respectively. Compared with *H pylori*-negative patients, the percentage of CD3+, CD4+ and the ratio of CD4+ / CD8+ and the IL-2 level decreased, but the levels of IL-6, IL-8 increased (P<0.001-P<0.01). Moreover, the percentage of CD3+, CD4+, CD8+, the ratio of CD4+ / CD8+, and the levels of IL-2, IL-6 and IL-8 in patients infected with both *H pylori* L-forms and vegetative forms were 46.67±5.21%, 30.75±4.89%, 22.15±6.45%, 1.32±0.47%, 1.16±0.38 mg/L, 116.45±5.44 ng/L, and 118.64±6.24 ng/L, respectively. Compared with patients infected with only vegetative forms, the percentage of CD_4^+, the ratio of CD4+ / CD8+and IL- 2 level decreased, but the levels of IL-6 and IL-8 increased (P<0.001 or P<0.01).

CONCLUSION: L-form variation often occurs in patients with chronic gastritis and is commonly found in male patients and associates with ages. The L-form variation may be an important factor causing disorder of cellular immune function in the patients with *H pylori*-induced chronic gastritis.

Wang KX, Chen L. *Helicobacter pylori* L-form and patients with chronic gastritis. *World J Gastroenterol* 2004; 10(9): 1306-1309
http://www.wjgnet.com/1007-9327/10/1306.asp

INTRODUCTION

Helicobacter pylori infection of the gastric mucosa can be found in approximately 50% of the world's population, and is associated with a range of pathologies, including chronic gastritis, peptic ulcer, atrophic gastritis, and gastric cancer[1-6]. Infection of *H pylori* is life-long that elicits a marked host inflammatory response[7-9]. However, natural infection fails to yield protective immunity[10,11]. *H pylori* is a gram-negative, spiral and microaerophilic bacterium that colonizes the gastric epithelium of humans[12-15]. Under some hostile conditions, *H pylori* changes from vegetative forms into L-forms by which *H pylori* can escape the body's immune response and live in the body for a long time. Once conditions return to normal *H pylori* reverts into vegetative forms, which further deteriorates the pathological changes. Therefore, *H pylori* L-forms appear to be more pathogenic and virulent than vegetative forms[16-18]. Animal experiments and clinical studies have demonstrated that damages induced by *H pylori* are associated with Th1 cell-mediated immune response[19-23]. The aim of this study was to confirm the occurrence of L-forms variation of *H pylori* vegetative forms, and to determine the relationship between *H pylori* L-form infection and chronic gastritis, and its association with possible changes of cellular immune function in the patients. In the study, gastric mucosal biopsies were taken from 428 patients with chronic gastritis to detect *H pylori* L-form by Gram staining and immunohistochemistry staining, and T lymphocyte subsets and serum levels of IL-2, IL-6 and IL-8 of patients were also detected.

MATERIALS AND METHODS

Patients

A total of 428 patients (aged from 14 to 67 years, 235 males and 193 females) with chronic gastritis diagnosed in our affiliated hospital from September 2000 to December 2002 were included in this study. Patients with other diseases were excluded.

Reagents

Gram staining and immunohistochemistry staining were used in this study. The biotin-streptavidin (BSA) reagents for T lymphocyte subset classification were provided by Jin'an Medical Laboratory Institute in Shanghai. Separating medium for lymphocyte was supplied by The Second Biochemical Reagent Factory in Shanghai (batch No.011215), and the test kits for IL-2 (batch No.1002-21), IL-6 (batch No.1006-32) and IL-8 (batch No.1008-25), were offered by Besancon Company (France).

Detection of H pylori L-forms

Biopsies of gastric antrum and gastric corpus were taken from 428 patients during upper endoscopy, fixed in 40 g/L formaldehyde, then embedded in paraffin and cut into section in 4 μm thickness. The sections were used for Gram staining and immunohistochemistry staining separately. Gram stained slide was observed under oil lens (10×100), and a total of 10-15

fields were randomly counted for *H pylori* L-forms. We regarded it as positive only when the average number was greater than 20. The antigen and antibody used in immunohistochemistry staining for *H pylori* L-forms were made in our laboratory, and the concentration of first antibody is 1:80. Other steps were performed according to the instruction of manufacturer (Dako company), using the known positive slide as a positive control and using PBS instead of first antibody as a negative control. A specimen was defined to be infected with *H pylori* L-forms when both staining methods produced a positive result.

Detection of cellular immune function

To investigate the possible changes of cellular immune function in *H pylori*-infected individuals, including the patients infected by *H pylori* L-forms and vegetative forms, the percentage of CD3+, CD4+, CD8+, ratio of CD4+ / CD8+, and the levels of IL-2, IL-6, IL-8 in peripheral blood of *H pylori*-positive individuals were tested with the biotin-streptavidin (BSA) method. The peripheral venous blood of the subjects was taken, anticoagulated with heparin, and diluted with a solution free of Ca^{2+}, Mg^{2+}. Then, peripheral blood mononuclear cells were separated with lymphocytes separating medium and cleaned, and the number of cells was adjusted to $(1\text{-}3)\times10^9$/L of which 10 μL was taken and smeared in an acidproof varnish circle on the surface of a slide. When it dried naturally, McAb of anti- CD3+, anti- CD4+ and anti- CD8+, and sleep anti-guineapig IgG, and SA-HRP. Cells was regarded as positive when the membrane was stained in brown color. A total of 200 cells were counted, and the positive percentages of cells were calculated. In addition, the serum levels of IL-2, IL-6 and IL-8 were detected by ELISA following the procedures detailed in the product instructions.

Statistical analysis

Data were expressed as mean±SD. Multiple comparison tests were performed with the χ^2 test and *t*-test.

RESULTS

Examination of H pylori L-forms with gram staining

Of the 428 patients studied, 226 (52.80%) were positive for both *H pylori* vegetative forms and L-forms, and other 17 (3.97%) were positive for vegetative forms only by Gram staining. The morphology of *H pylori* L-forms was highly variable, such as spheroid, coccoid form, big body, elementary body, long filament body, as seen on the smears under microscope.

Comparation between gram staining and immunohistochemistry staining

H pylori L-forms was detected in 216 (50.47%) patients by immunohistochemistry staining, of whom 209 (48.83%) were also detected *H pylori* L-forms by Gram staining. There was no significant difference in detection rate of *H pylori* L-forms between the 2 methods ($P>0.05$) (Table 1).

Relationship between infection of H pylori L-forms and gender as well as age of patients with chronic gastritis

H pylori L-forms were present in 57.87% (136/235) of males and 37.82% (73/193) of females ($\chi^2=17.05$, $P<0.01$). Furthermore, the rate of *H pylori* L-forms was significant difference between patients <40 years old and those ⩾40 years old ($P<0.01$) (Table 2).

Detection of cellular immune function

The percentages of CD3+, CD4+ and the ratio of CD4+ / CD8+ and IL-2 decreased, but the levels of IL-6 and IL-8 increased in *H pylori*–positive patients, compared with *H pylori*–negative patients, (Tables 3 and 4). In addition, the percentage of CD_4^+, the ratio of CD4+ / CD8+ and the levels of IL-2 decreased , but the levels of IL-6 and IL-8 increased in the patients infected by both L-forms and vegetative forms of *H pylori*, compared with those only infected by vegetative forms (Tables 3, 4).

Table 1 Comparation of Gram staining and immunohistochemistry staining in detection of *H pylori* L-forms

Gram staining (*n*)	Immunohistochemistry staining (*n*)		Total (*n*)
	Positive	Negative	
Positive	209	17	226
Negative	7	195	202
Total	216	212	428

$\chi^2=0.46779$, $P>0.05$ between the 2 methods.

Table 2 Relationship of infection of *H pylori* L-forms with gender and age of patients with chronic gastritis

Age(yr)	Male		Female		Total	
	n	Detection rate (%)	*n*	Detection rate (%)	*n*	Detection rate (%)
14-	62	31 (50.00)	75	17 (22.67)	137	48 (35.04)[b]
30-	37	14 (37.84)	48	18 (37.50)	85	32 (37.65)[b]
40-	55	35 (63.64)	23	12 (52.17)	78	47 (60.26)[b]
50-	81	56 (69.14)	47	26 (55.32)	128	82 (64.06)[b]
Total	235	136 (57.87)[d]	193	73 (37.82)[d]	428	209 (48.83)

[d]$\chi^2=17.05$, $P<0.01$; [b]$\chi^2=33.74$, $P<0.01$.

Table 3 Detection of T lymphocyte subsets in patients with chronic gastritis in relation to infection with *H pylori* (Hp) and its L-forms

Group	*n*	CD3+ (%)	CD4+ (%)	CD8+ (%)	CD4+ / CD8+
Hp (-)	202	60.72±8.38[b]	36.33±3.68[d]	25.83±6.93	1.55±0.34[j]
Hp (+)	226	47.58±4.44[b]	25.51±4.74[d]	22.77±7.46	1.44±0.51[j]
Hp-L (-)	17	50.81±6.20	33.74±5.34[f]	25.04±10.48	1.68±0.58[h]
Hp-L (+)	209	46.67±5.21	30.75±4.89[f]	22.15±6.45	1.32±0.47[h]
Total	428	52.20±6.21	34.31±4.18	23.49±6.86	1.16±0.466

[b]$P<0.001$, $t=20.61$; [d]$P<0.001$, $t=26.21$; [j]$P<0.001$, $t=4.36$; [f]$P<0.001$, $t=7.78$; [h]$P<0.01$, $t=2.99$.

Table 4 Detection of serum IL-2, IL-6 and IL-8 in patients with chronic gastritis in relation to infection with *H pylori* (Hp) and its L-forms

Group	*n*	IL-2 (mg / L)	IL-6 (ng / L)	IL-8 (ng / L)
Hp (-)	202	6.14±0.65[b]	36.82±3.15[d]	48.35±3.63[f]
Hp (+)	226	1.56±0.47[b]	103.62±5.85[d]	109.79±7.18[f]
Hp-L (-)	17	3.39±0.57[h]	63.35±6.51[j]	82.33±8.45[l]
Hp-L (+)	209	1.16±0.38[h]	116.45±5.44[j]	118.64±6.24[l]
Total	428	3.27±0.52	81.83±4.73	87.53±5.68

[b]$P<0.001$, $t=83.06$; [d]$P<0.001$, $t=145.3$; [f]$P<0.001$, $t=110.3$; [h]$P<0.001$, $t=21.08$; [j]$P<0.001$, $t=38.45$; [l]$P<0.001$, $t=22.61$.

DISCUSSION

Helicobacter pylori was first isolated by Warren and Marshall in 1983 from gastric mucosa of patients with gastritis. It is now accepted to be an etiological agent of chronic gastritis, peptic ulcer and gastric cancer. It is a Gram-negative, spiral-shaped, microaerophilic bacterium that colonizes human gastric epithelium, with a curved, S or arc-like appearance in the stomach. When exposed to factors such as gastric juice, bile,

antibiotics and other hostile conditions, some bacterial cells turn into pleomorphic variations[24-26] of which L-forms (spheroid) is the most common one[27-30]. In this study, gastric mucosal biopsy specimens from 428 patients with chronic gastritis were taken for the detection of *H pylori* L-forms. Gram staining showed that 226 patients were infected with both *H pylori* L-forms and vegetative forms, and 17 patients were infected with *H pylori* vegetative forms only. This indicates that L-forms variation of *H pylori* is common in patients with chronic gastritis. Due to the loss of cell walls, or certain components and antigens of cell walls, *H pylori* L-forms differ from the vegetative forms in antigenicity, which may affect the result of serology diagnoses and, more importantly, enables the bacteria to live in the stomach for a long time by escaping the body's immunity. Moreover, when conditions improve, L-form can revert to typical vegetative forms, which may be an important factor leading to deterioration and relapse of infection. Therefore, *H pylori* L-forms are more adhesive, invasive and pathogenic, and the variation of *H pylori* results in the deferment and recurrence of chronic gastritis[9,31].

In this study, the detection rate of *H pylori* L-forms was significantly greater in males than in female (57.87% *vs* 37.82%). This may be related to some male habits, such as smoking, drinking, irregular diets that might damage gastric mucosa and change the gastric internal environment[9,30-35]. In addition, the presence of *H pylori* L-forms seems to be related to patients' ages, as the detection rate of *H pylori* L-forms increases with age.

Cellular immune function of patients with *H pylori* has been described in recent years. The chronic inflammatory responses associated with natural infection do not provide protection, but contribute to tissue damages and pathogenesis of gastroduodenal diseases, including atrophic gastritis, peptic ulcer, and gastric cancer. These immune responses are likely to attribute to a subject of T helper lymphocytes, so-called Th1 cells, which enhance cell-mediated immunity and induce damage to the gastric epithelium. To investigate the mechanisms for Th1 immune response caused by *H pylori* based on the variation of L forms, T lymphocyte subsets and the levels of IL-2, IL-6, and IL-8 in peripheral blood of the patients were detected. The results showed that in *H pylori*-positive patients, CD3+, CD4+, CD4+/CD8 and IL-2 decreased, but IL-6 and IL-8 increased, compared with those in *H pylori*-negative, indicating that *H pylori* infection may weaken the immune function of the host and cause a predominant Th1 cellular response. Moreover, the percentage of CD4+, the ratio of CD4+/CD8 and the level of IL-2 were lower but the levels of IL-6 and IL-8 were higher in the patients infected with both L-forms and vegetative forms, compared with those infected with vegetative forms only. Thus, *H pylori* L-forms infection may be closely related to disorder of the immune function, and may be one of the crucial factors causing Th1 immune response. We postulate that *H pylori* L-forms may invade into the host cells where they may serve as a pronounced inducer for Th1-type CD4 (+) T cell response, leading to the decrease in the percentage of CD4+ and the ratio of CD4+/CD8. Active CD4+-T cell may also inhibit the activation of Th1 cells cytokines, and the outcome of IL-2 is a risk factor of cellular immune response.

In addition, in this study, the levels of IL-6 and IL-8 in peripheral blood of the patients increased significantly, which is likely to be associated with ulceration inflammation, blood macrophage stimulation and active secretion by the neutrophils and vascular endothelial cells. Once attached to the gastric epithelial cells, *H pylori* incites an immune response characterized by the increased pro-inflammatory cytokine of IL-8, IL-12 and TNF-alpha. Activated inflammatory and immunologically competent cells such as neutrophils, lymphocytes and monocytes release cytokines such as IL-6, IL-8 and IFN-gamma. As a result, the serum levels of IL-6 and IL-8 increase[18].

In conclusion, Co-infection with both *H pylori* vegetative forms and L-forms is common in patients with chronic gastritis. The rate of infection with *H pylori* L-forms in males is higher than in females, and the rate increases with age. Once *H pylori* L-forms occurs, the morphology and microstructure of the organisms change, *i.e.*, the cell walls of the L-forms are partly or completely lost, the charge of the bacterial surface increases, and the adherence and invasiveness of the bacteria become more powerful. All of these changes may play an important role in the deferment and relapse of chronic gastritis and in the disordered cellular immune function in patients with *H pylori* infection.

REFERENCES

1 **Pineros DM**, Riveros SC, Marin JD, Ricardo O, Diaz OO. *Helicobacter pylori* in gastric cancer and peptic ulcer disease in a Colombian population. Strain heterogeneity and antibody profiles. *Helicobacter* 2001; **6**: 199-206

2 **Takeuchi K**, Ohno Y, Tsuzuki Y, Ando T, Sekihara M, Hara T, Kuwano H. *Helicobacter pylori* infection and early gastric cancer. *J Clin Gastroenterol* 2003; **36**: 321-324

3 **So JB**, Yeoh KG, Moochala S, Moochlani N, Ho J, Wong WK, Mack P, Goh PM. Serum pepsinogen levels in gastric cancer patients and their relationship with *Helicobacter pylori* infection: a prospective study. *Gastric Cancer* 2003; **5**: 228-232

4 **Vandenplas Y**. *Helicobacter pylori* infection. *World J Gastroenterol* 2000; **6**: 20-31

5 **Miehlke S**, Yu J, Schuppler M, Frings C. *Helicobacter pylori vacA, iceA*, and *cagA* status and pattern of gastritis in patients with malignant and benign gastroduodenal disease. *Am J Gastroenterol* 2001; **96**: 1008-1013

6 **Ayhan S**, Demir MA, Kandiloglu AR, Saruc M, Kucuketin N. Features of chronic inflammation at the gastric cardia and the relationship with *Helicobacter pylori* infection and oesophagitis. *Acta Gastroenterol Belg* 2003; **66**: 144-149

7 **Atisook K**, Kachinthorn U, Luengrojanakul P, Yanwandee T, Pakdirat P, Pupairoj A. Histology of gastritis and *Helicobacter pylori* infection in Thailand: a nationwide study of 3776 cases. *Helicobacter* 2003; **8**: 132-141

8 **Nguyen TN**, Barkun AN, Fallone CA. Host determinants of *Helicobacter pylori* infection and its clinical outcome. *Helicobacter* 1999; **4**: 185-197

9 **Hahm KB**, Kim DH, Lee KM, Lee JS, Surh YJ, Kim YB, Kim JH, Joo HJ, Cho YK, Nam KT, Cho SW. Effect of long-term administration of rebamipide on *Helicobacter pylori* infection in mice. *Aliment Pharmacol Ther* 2003; **18**(Suppl): 24-38

10 **Kotloff KL**, Sztein MB, Wasserman SS, Losonsky GA, DiLorenzo SC, Walker RI. Safety and immunogenicity of oral inactivated whole-cell *Helicobacter pylori* vaccine with adjuvant among volunteers with or without subc linicalinfection. *Infect Immun* 2001; **69**: 3581-3590

11 **Hwang IR**, Hsu PI, Peterson LE, Gutierrez O, Kim JG, Grahsam DY, Yamaoka Y. Interleukin-6 genetic polymorphisms are not related to *Helicobacter pylori*-associated gastroduodenal diseases. *Helicobacter* 2003; **8**: 142-148

12 **Chatzaki E**, Charalampopoulos I, Leontidis C, Mouzas IA, Tzardi M, Tastsanis C, Margioris AN, Gravanis A. Urocortin in human gastric mucosa: relationship to inflammatory activity. *J Clin Endocrinol Metab* 2003; **88**: 478-483

13 **Holck S**, Norgaard A, Bennedsen M, Permin H, Norn S, Andersen LP. Gastric mucosal cytokine responses in *Helicobacter pylori*-infected patients with gastritis and peptic ulcers. Association with inflammatory parameters and bacteria load. *FEMS Immunol Med Microbiol* 2003; **36**: 175-180

14 **Megraud F**. *Helicobacter pylori*, gastric inflammation and its consequences. *Ann Pharm Fr* 2003; **61**: 282-287

15 **Touati E**, Michel V, Thiberge JM, Wuscher N, Huerre M, Labigne A. Chronic *Helicobacter pylori* infections induce gastric mutations in mice. *Gastroenterology* 2003; **124**: 1408-1419

16 **Schmidtke LM**, Carson J. Induction, characterization and pathogenicity in rainbow trout Oncorhynchus mykiss (Walbaum) of *Lactococcus garvieae* L-forms. *Vet Microbiol* 1999; **69**: 287-300

17 **Dominis M**, Dzebro S, Gasparov S. Morphology of gastritis and *Helicobacter pylori* infection. *Lijec Vjesn* 2002; **124**(Suppl 1): 36-42
18 **Londono-Arcila P**, Freeman D, Kleanthous H, O'Dowd AM, Lewis S, Turner AK, Rees EL, Tibbitts TJ, Greenwood J, Monath TP, Darsley MJ. Attenuated *Salmonella enterica* serovar Typhi expressing urease effectively immunizes mice against *Helicobacter pylori* challenge as part of a heterologous mucosal priming-parenteral boosting vaccination regimen. *Infect Immun* 2002; **70**: 5096-5106
19 **Scheiman JM,** Greenson JK, Lee J, Cryer B. Effect of cyclooxygenase-2 inhibition on human *Helicobacter pylori* gastritis: mechanisms underlying gastrointestinal safety and implications for cancer chemoprevention. *Aliment Pharmacol Ther* 2003; **17**: 1535-1543
20 **Smith MF** Jr, Mitchell A, Li G, Ding S, Fitzmaurice AM, Ryan K, Crowe S, Goldberg JB. Toll-like receptor (TLR) 2 and TLR5, but not TLR4, are required for *Helicobacter pylori*-induced NF-kappa B activation and chemokine expression by epithelial cells. *J Biol Chem* 2003; **278**: 32552-32560
21 **Stromberg E**, Lundgren A, Edebo A, Lundin S, Svennerholm AM, Lindholm C. Increased frequency of activated T-cells in the *Helicobacter pylori*-infected antrum and duodenum. *FEMS Immunol Med Microbiol* 2003; **36**: 159-168
22 **Su B**, Ceponis PJ, Lebel S, Huynh H, Sherman PM. *Helicobacter pylori* activates Toll-like receptor 4 expression in gastrointestinal epithelial cells. *Infect Immun* 2003; **71**: 3496-3502
23 **Ernst PB**, Pappo J. T-cell-mediated mucosal immunity in the absence of antibody: lessons from *Helicobacter pylori* infection. *Acta Odontol Scand* 2001; **59**: 216-221
24 **Kusters JG**. Recent developments in *Helicobacter pylori* vaccination. *Gastroenterol* 2001; **234**(Suppl): 15-21
25 **Nilsson I**, Utt M, Nilsson HO, Ljungh A, Wadstrom T. Two-dimensional electrophoretic and immunoblot analysis of cell surface proteins of spiral-shaped and coccoid forms of *Helicobacter pylori*. *Electrophoresis* 2000; **21**: 2670-2677
26 **Wen M**, Zhang Y, Yamada N, Matsuhisa T, Matsukura N, Sugisaki Y. An evaluative system for the response of antibacterial therapy: based on the morphological change of *Helicobacter pylori* and mucosal inflammation. *Pathol Int* 1999; **49**: 332-337
27 **Khin MM**, Ringner M, Aleljung P, Wadstrom T, Ho B. Binding of human plasminogen and lactoferrin by *Helicobacter pylori* coccoid forms. *J Med Microbiol* 1996; **45**: 433-439
28 **She FF**, Su DH, Lin JY, Zhou LY. Virulence and potential pathogenicity of coccoid *Helicobacter pylori* induced by antibiotics. *World J Gastroenterol* 2001; **7**: 254-258
29 **Brenner H**, Bode G, Adler G, Hoffmeister A, Koenig W, Rothenbacher D. Alcohol as a gastric disinfectant? The complex relationship between alcohol consumption and current *Helicobacter pylori* infection. *Epidemiology* 2001; **12**: 209-214
30 **Guarner J**, Mohar A, Parsonnet J, Halperin D. The association between *Helicobacter pylori* and gastric neoplasia. Epidemiologic evidence. *Rev Gastroenterol Mex* 2000; **65**: 20-24
31 **Bergin IL**, Sheppard BJ, Fox JG. *Helicobacter pylori* infection and high dietary salt independently induce atrophic gastritis and intestinal metaplasia in commercially available outbred Mongolian gerbils. *Dig Dis Sci* 2003; **48**: 475-485
32 **Touati E**, Michel V, Thiberge JM, Wuscher N, Huerre M, Labigne A. Chronic *Helicobacter pylori* infections induce gastric mutations in mice. *Gastroenterology* 2003; **124**: 1408-1419
33 **Genta RM**, Rindi G, Fiocca R, Magner DJ, D'Amico D, Levine DS. Effects of 6-12 months of esomeprazole treatment on the gastric mucosa. *Am J Gastroenterol* 2003; **98**: 1257-1265
34 **Kaise M**, Miwa J, Iihara K, Suzuki N, Oda Y, Ohta Y. *Helicobacter pylori* stimulates inducible nitric oxide synthase in diverse topographical patterns in various gastroduodenal disorders. *Dig Dis Sci* 2003; **48**: 636-643
35 **Jang J**, Lee S, Jung Y, Song K, Fukumoto M, Gould VE, Lee I. Malgun (clear) cell change in *Helicobacter pylori* gastritis reflects epithelial genomic damage and repair. *Am J Pathol* 2003; **162**: 1203-1211

Edited by Xia HHX and Xu FM

PO Box 2345, Beijing 100023, China
Fax: +86-10-85381893
E-mail: wjg@wjgnet.com www.wjgnet.com

World J Gastroenterol 2004;10(9):1310-1314
World Journal of Gastroenterology
Copyright ©2004 by The WJG Press ISSN 1007-9327

• BASIC RESEARCH •

C-kit gene mutation in human gastrointestinal stromal tumors

Ying-Yong Hou, Yun-Shan Tan, Meng-Hong Sun, Yong-Kun Wei, Jian-Fang Xu, Shao-Hua Lu, Su-Jie A-Ke-Su, Yan-Nan Zhou, Feng Gao, Ai-Hua Zheng, Tai-Ming Zhang, Wen-Zhong Hou, Jian Wang, Xiang Du, Xiong-Zeng Zhu

Ying-Yong Hou, Yun-Shan Tan, Jian-Fang Xu, Shao-Hua Lu, Su-Jie A-Ke-Su, Yan-Nan Zhou, Feng Gao, Department of Pathology, Zhongshan Hospital, Fudan University, Shanghai 200032, China
Meng-Hong Sun, Yong-Kun Wei, Ai-Hua Zheng, Tai-Ming Zhang, Wen-Zhong Hou, Jian Wang, Xiang Du, Xiong-Zeng Zhu, Department of Pathology, Cancer Hospital, Fudan University, Shanghai 200032, China
Supported by the National Natural Science Foundation of China, No. 30300152
Correspondence to: Dr. Xiong-Zeng Zhu, Department of Pathology, Cancer Hospital, Fudan University, Shanghai 200032,China
Telephone: 86-21-64175590-3204
Received: 2003-09-09 **Accepted:** 2003-10-22

Abstract

AIM: To investigate the significance of c-kit gene mutation in gastrointestinal stromal tumors (GIST).

METHODS: Fifty two cases of GIST and 28 cases of other tumors were examined. DNA samples were extracted from paraffin sections and fresh blocks. Exons 11, 9 and 13 of the c-kit gene were amplified by PCR and sequenced.

RESULTS: Mutations of exon 11 were found in 14 of 25 malignant GISTs (56%), mutations of exon 11 of the c-kit gene were revealed in 2 of 19 borderline GISTs (10.5%), and no mutation was found in benign tumors. The mutation rate showed significant difference (χ^2=14.39, P<0.01) between malignant and benign GISTs. Most of mutations consisted of the in-frame deletion or replication from 3 to 48 bp in heterozygous and homozygous fashions, None of the mutations disrupted the downstream reading frame of the gene. Point mutations and frame deletions were most frequently observed at codons 550-560, but duplications were most concentrated at codons 570-585. No mutations of exons 9 and 13 were revealed in GISTs, Neither c-kit gene expression nor gene mutations were found in 3 leiomyomas, 8 leiomyosarcomas, 2 schwannomas, 2 malignant peripheral nerve sheath tumors, 2 intra-abdominal fibromatoses, 2 malignant fibrous histiocytomas and 9 adenocarcinomas.

CONCLUSION: C-kit gene mutations occur preferentially in malignant GISTs and might be a clinically useful adjunct marker in the evaluation of GISTs and can help to differentiate GISTs from other mesenchymal tumors of gastrointestinal tract, such as smooth muscle tumors, schwannomas, *etc*.

Hou YY, Tan YS, Sun MH, Wei YK, Xu JF, Lu SH, A-Ke-Su SJ, Zhou YN, Gao F, Zheng AH, Zhang TM, Hou WZ, Wang J, Du X, Zhu XZ. C-kit gene mutation in human gastrointestinal stromal tumors. *World J Gastroenterol* 2004; 10(9): 1310-1314
http://www.wjgnet.com/1007-9327/10/1310.asp

INTRODUCTION

GISTs are the most common mesenchymal tumors of the human gastrointestinal tract, previously uniformly classified as smooth muscle tumors. Recently, GISTs have been defined as cellular spindle cell, epithelioid, or occasionally pleomorphic mesenchymal tumors of the gastrointestinal tract(GI) that express the c-kit protein (CD117), as detected using immunohistochemistry. GISTs are strongly and nearly uniformly CD117 positive[1-4].

Resently, the c-kit mutations in GISTs have been shown to lead to ligand-independent activation of the tyrosine kinase of c-kit[5]. So several questions were suggested: what are the possible relationship of c-kit expression and mutations, the relationship of mutations and malignancy, and the possible specificity of the mutations for GISTs?

A study of larger series of GISTs, revealed that these tumors had a spectrum of clinical behaviors at all sites of their occurrence[6]. Some GISTs are typical benign tumors, and most of them are found incidentally in other conditions, for example, during gall bladder or gynecologic surgery. In constrast, other GISTs metastasize to the liver and disseminate in the peritoneal cavity. Large tumor size, presence of intratumoral necrosis, infiltrative growth pattern in muscularis propria, invasion of mucosa, and high mitotic figures are considered as malignant. However, there is a definite percentage of mitotically inactive tumors that subsequently metastasize, emphasizing the fact that low mitotic count does not rule out a malignant behavior. Therefore, the designation "uncertain malignant potential" applies to a significant number of GISTs.

In this study, we further explored whether the c-kit gene mutations were valuable as an adjunct malignant marker in GISTs and could help to differentiate GISTs from other tumors.

MATERIALS AND METHODS

Cases

Archival paraffin-embedded and frozen tissue samples of 52 GISTs were immunohistochemically analysed for CD117 and CD34. They were mainly obtained from the Department of Pathology, Zhongshan Hospital, Fudan University, and from other pathology departments in Cancer Hospital, Huadong Hospital, and Chongming Center Hospital, etc. Additionally, 28 other tumors were investigated, including 8 leiomyosarcomas of retroperitoneum, 3 leiomyomas of esophagus, 2 schwannomas of stomach, 2 malignant peripheral nerve sheath tumors of intra-abdomen, 2 intra-abdominal fibromatoses of intestine, 2 malignant fibrous histiocytomas of intra-abdomen, and 9 adenocarcinomas of GI (of which, 4 were accompanied by GISTs).

Histologic evaluation

One to 14 hematoxylin and esosin-stained slides (median, 4 slides) were reviewed for each case. The following features were recorded in all cases: type of the majority cells (spindle *vs* epithelioid), skeinoid fibers (extracellular collagen globles), mucosal ulceration. Additionally, other important features included mitoses counted from 50 consecutive high-power fields (HPFs), coagulation necrosis, infiltrative growth pattern, and lymph node involvement. According to the histologic observation, GISTs were divided into 3 groups: small incidental tumors with less 5 cm in diameter or fewer mitoses per 50 HPF

were designated as benign, mitotically inactive tumors larger than 5 cm or cellular tumors which had no necrosis and infiltration were designated as uncertain malignant potential, and tumors with active mitotic counts over five per 50HPF or with necrosis, infiltrative growth pattern were designated as malignant.

Immunohistochemistry

Antibodies to the following antigens were used. CD117 (c-kit prooncogene product, polyclonal, 1:70) was purchased from Santa Cruz Biotechnology, Santa Cruz, CA, USA, CD34 (QBEND-10, monoclonal, 1:150, DAKO), α-SMA (1A4 monoclonal, 1:200), MSA (HHF35 monoclonal, 1:200), desmin (D33, monoclonal, 1:150), S-100 protein (polyclonal, 1:300), and protein gene product 9.5 (PGP9.5, polyclonal, 1:300) were purchased from Dako Corp. Epitope retrieval was used for antibodies. The slides were immersed in 10 mmol/L citrate buffer, pH 6.0 and heated in a microwave oven at a high setting for 5 min. The EnVision staining technique was used followed by incubation with 3,3' -diaminobenzidine tetrahydrochloride and counterstained with hematoxylin.

DNA extraction

Ten micrometers of tissue sections were cut from freshy frozen tumors or paraffin embedded, and then incubated in extraction buffer (50 mmol/L KCl, 10 mmol/L Tris[pH8.3], 2.5 mmol/L $MgCl_2$) containing 60 μg/mL proteinase K overnight at 55 ℃. The proteinase K was inactivated by a 10-min incubation at 95 ℃. The resulting lysate was spun in a microcentrifuge for 5 min to pellet debris, and then stored at -20 ℃.

PCR amplification of exons 11, 9, and 13 of c-kit gene

PCR assays were developed to amplify exons 11, 9, and 13. The 3 primer pairs were designed based on the human c-kit gene. Exons 9, 11 and 13 of the c-kit gene were amplified by PCR using the following oligonucleotide primer pairs: for exon 9, 5' -TCCTAGAGTAAGCCAGGGCTT-3' /5' -TGGTAGACAGAGC CTAAACATCC-3' ; for exon 11, 5' -CCAGAGTGCTCTAATGA CTG-3' /5' -TGACATGG AAAGCCCCTGTT-3' ; and for exon 13,5' -GCTTGACATCAGTTTGCCAG-3' /5' -AAAGGCAGCTT GGACACGGCTTTA-3' . The lengths of PCR products were 261 bp, 225 bp, and 193 bp, respectively. The PCR reaction conditions were the standard ones recommended by Perkin Elmer. The annealing temperature was 55 ℃. The PCR products were size fractionated on 50 g/L polyacrylamide gels and stained with ethidium bromide.

DNA sequencing

Direct sequencing was performed on the ABI Prism 310 DNA sequencer, using the same primers as were used for amplification. Sequencing reactions were conducted with the big dye terminator sequencing ready reaction kit (Perkin-Elmer) according to the manufacturer's instructions.

Statistical analysis

χ^2 test was used.

RESULTS

Clinicopathological features of GISTs

There were 27 gastric, 7 small intestine, 6 rectal, 5 extra-GI, 2 abdominal disseminated primary tumors, with 5 intraabdominal recurrences. Of these tumors, 8 were classified as histologically benign, 19 as histologically uncertain malignant potential of borderline tumor, and 25 as malignant based on high mitotic activity, coagulative necrosis, infiltrative growth pattern. These tumors displayed a wide variety of cell types and histologic patterns, of which, 34 tumors had a predominant spindle cell pattern, 8 were epithelioid, and 10 were spindle/epithelioid mixed. The spindle cells were most often arranged in interlacing fascicles, The epithelioid cells were characterized by sheets. However, they often showed focally a storiform pattern, mimicked large rosettes, or palisaded the nuclei.

Immunohistochemical findings

CD117 positivity was detected in 50 of 52 cases (96.2%), typically in most of tumor cells in a strong membrane of apparently diffuse cytoplasm. CD34 positivity was seen in 38 of 52 cases (73%), including focal reactive cases. Two CD117-negative cases were CD34 positive. A small number were focal positive for α-SMA (10 of 52), MSA (9 of 52), desmin (2 of 52). Additionally, 6 and 3 cases were reactive for S-100 and PGP9.5.

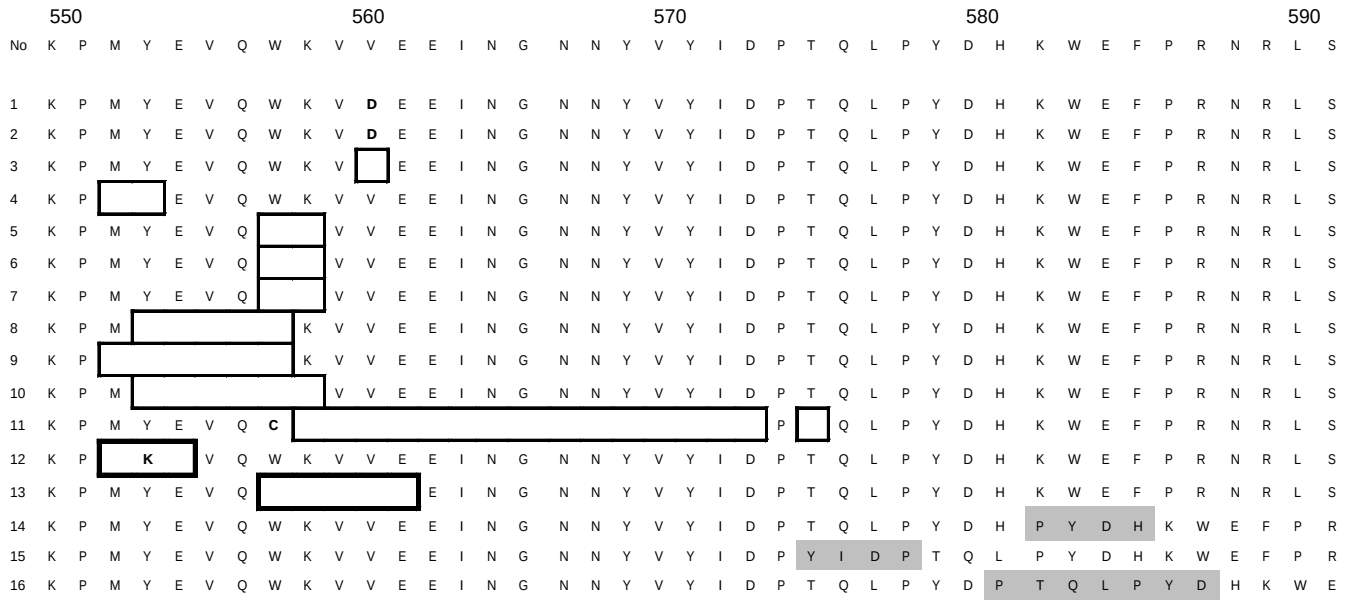

Figure 1 Exon 11 of c-kit mutations in 16 GIST samples. The wild-type sequence of amino acids encoded by exon 11 is shown at the top. The sequence starting at codon 550 and ending at 590. The wide-type sequence is shown above, the numbers are shown at the left. Point mutation is shown in black type, deletion is shown in□the thin line indicates heterozygote mutation and thick line indicates homozygote ones. the shaded areas correspond to insertion or duplication mutations.

Evaluation of mutations in exons 11, 9, and 13 of c-kit gene

PCR amplification and DNA sequencing revealed exon 11 mutation in 14 malignant GISTs, in 2 borderline GISTs, and in no benign GISTs. Sequence analysis showed in-frame deletions of 3 to 48 bp, point mutations, and duplications. Point mutations and deletions were most frequently observed at codons 550-560, but duplications were most concentrated at codon 570-585. Of the 16 mutated GISTs, 2 had a homozygous mutation and 14 heterozygous mutation, which did not result in any amino acid change. The sequence corresponding to these mutations are shown in Figure 1. Figure 2 shows a case of duplication by DNA direct sequencing.

Five non-tumor tissue samples from the stomach or intestine adjacent to mutation-bearing GISTs demonstrated neither deletions nor point mutations.

The conservation of c-kit mutation pattern was observed in a relapse lesion from the same patients (Figure 3).

No exon 9 and exon 13 mutation were detected.

χ^2 test showed that the c-kit mutation of GISTs demonstrated a statistical (χ^2=14.39, P<0.01) significance between the malignant group and the borderline and benign groups.

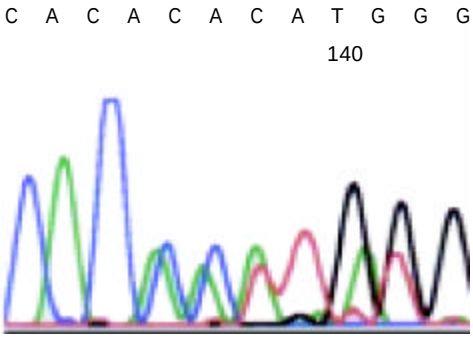

Figure 2 Duplication of codons from 581 to 584 (PYDH) in one case of GIST by direct sequencing of c-kit exon 11.

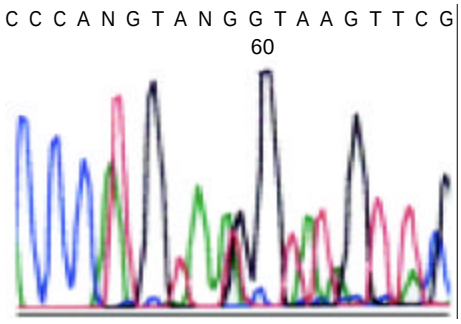

Figure 3 Deletion of codon from 553 to 557 (YEVQW) by direct sequencing of c-kit exon 11.

Other tumors

The three esophageal leiomyomas were histologically paucicellular spindle cell neoplasms with distinctly eosinophilic cytoplasm, and lack of mitotic activity. All cases were positive for α-SMA, MSA and desmin, and negative for CD117 and CD34, and only mast cells in the stroma showed positive CD117.

The 8 retroperitoneal leiomyosarcomas were spindle cell tumors that resembled smooth muscle tumor with oval to mildly elongated nuclei and variably eosinophilic cytoplasm. Four tumors showed focal pleomorphism and high mitotic activity (>50/50HPF). Coagulation necrosis was present in 4 tumors. All cases were positive for α-SMA, MSA, and 7 cases positive for desmin. All cases were negative for CD34 but 1 case was focal weak positive for CD117.

The 2 cases of schwannomas showed slender spindle cells and a characteristic lymphoid cuff. Two cases were diffusely and strongly positive for S-100 and 1 case was positive for PGP9.5. Both of them were negative for CD117 and CD34. The 2 cases malignant peripheral nerve sheath tumor showed spindle cells and active mitosis. Two cases were positive for S-100 and weak positive for PGP9.5 and negative for CD117 and CD34.

The 2 cases of intro-abdominal fibromatosis of intestine and 2 cases of malignant fibrous histiocytoma were negative for all antigens but 1 case of intro-abdominal fibromatosis was focal positive for α-SMA.

There were no mutations of the c-kit gene in the above 28 control tumors and one case of adenocarcinoma accompanied by mutation-bearing GIST also had wild-type c-kit gene.

DISCUSSION

Most of the GISTs examined expressed both CD117 and CD34, which was consistent with the literature reports[7-12]. The rates of CD117 and CD34 expression had no difference between benign, borderline, and malignant GISTs, so the expressions were not useful markers for evaluating malignancy.

In this study, we examined the sequence and expression of c-kit gene in the spectrum of GISTs, including benign, borderline, and malignant variants from different sites. The sequences of c-kit gene were also evaluated in typical smooth muscle tumors, schwannomas and other tumors, especially in 4 adenocarcinmas accompanied by GISTs.

Our series of 52 benign, borderline, and malignant GISTs showed that 96.2% of the GISTs expressed CD117 and only some of the GISTs had mutations. The results indicated a considerable proportion of GISTs expressed CD117 with no mutation. In other words, most of c-kit mutations did not affect the proportion of GISTs with CD117 expression. Mutations in exon 11 of the c-kit gene were observed in 56% of malignant cases. In constrast, only 2 borderline GISTs (10.5%) showed mutations, and no benign GISTs showed mutations, suggesting that the mutations of exon 11 of the c-kit gene may represent a genotypic marker with a correlation to malignancy.

Lasota and colleagues[13] reported the mutation of exons 9 and 13, but the mutation rate seemed to be very low, and they only detected the small portion (8%) of mutations of GISTs in exons 9 and 13, which did not have mutations in exon 11 of the c-kit gene. In our series, no mutations were detected. The result also indicated the rates of mutations in other regions of the c-kit gene were very low.

Our present results were in accordance with those previously reported[14-16]. In hot spot region of exon 11 involving codons 550-560, point mutation and frame deletion were mainly detected at these codons, and 2 cases showed homozygous deletions.

In addition to the change at codons of 550-560, however, the duplication mutation fashion was found in 3 cases to cluster at codons 570 to 585, which was rarely detected in the previously reports.

Analysis of c-kit mutation pattern in relapse lesions showed the persistence of the mutation that remained identical in the primary lesion. Therefore, the c-kit mutation pattern could be tumor-specific.

C-kit mutations were never observed in smooth muscle tumors or nerve sheath tumors or other soft tissue tumors. Furthermore, one adenocarcinoma accompanied by mutation-positive GIST was the wild-type c-kit gene. Therefore, c-kit mutations may also represent a genotypic lineage marker for GISTs.

Previous and present molecular studies have revealed the gain-of-function mutations of the c-kit gene could be observed in mast cell neoplasms[17,18], human germ cell tumors[19] and GISTs, but the location of c-kit mutations differs in them. The particular aspartic acid in the tyrosine kinase domain would

changes into valine in mast cell neoplasms, The aspartic acid at amino acid position 816 would change into histidine, whereas deletion, point mutation, or both in the juxtamembrane domain were observed in GISTs mutations. Specially, the mutations were located within codons 550 to 560 in exon 11, and rare mutations are detectable in other domains of the c-kit gene, such as exons 9, 13. Clustering of c-kit mutations in the same region of GISTs and in different region with mast cell neoplasm supported their specific biological significance.

The occurrence of activating mutations involving exon 11 of the c-kit gene in sporadic GIST and the association of exon 11 germline mutations in familial GISTs indicated they were important in GIST' s tumorigenesis[20]. Especially, c-kit mutations could be detected only in some of GISTs[21,22], so the value of the c-kit gene mutation in GISTs inspired the researchers, but there are no concordant conclusions, reports regarding the frequency of mutations in exon 11 varied widely, and prognostic significance of c-kit mutations with respect to the association between exon 11 mutations and malignant histology and/or aggressive malignant behavior were conflicting, and the reported frequency of these mutations varied over a wide range[23-29]. Taniguchi and colleagues[23] found that c-kit mutation-positive GIST were worse than c-kit mutation-negative GISTs. But other studies showed that c-kit exon 11 mutation analysis did not correlate well with histological assessment of malignant potential, and could not be regarded as a reliable objective marker for poor prognosis in GISTs.

Some malignant GISTs lack of exon 11 mutation suggested that mutations in exon 11 of c-kit gene were not the only mechanisms related to malignancy and there must exist other molecular mechanisms[30-33], which may include mutations in other regions of the c-kit gene. But previous report and our study indicated other region mutation of the c-kit gene was few. Recently, Heihrich and colleagues[34] have made an important finding in GISTs, they reported that 35% (14/40) of GISTs lacking c-kit mutations had intragenic activation mutations in tyrosine kinase, platelet-derived growth factor (PDGFRA). C-kit gene and PDGFRA mutations appeared to be alternative and mutually exclusive in GISTs, further study is needed to understand the role of PDGFRA in GISTs.

In summary, the results showed a consistent c-kit expression in GISTs with or without detectable mutations. The mutations occurred more preferentially in malignant GISTs than versus in benign GISTs, but not in smooth muscle tumor and other tumors. These observations suggest that mutations in exon 11 of the c-kit gene might represent useful molecular genetic markers for malignant GISTs and help to differentiate GIST from other tumors. Whether the c-kit gene mutation can indicate bad prognosis of malignant GISTs needs to be further studied.

ACKNOWLEDGMENTS

We thank Dr. Lu X,Y. and Dr. Yu M. for kindly providing the cases.

REFERENCES

1 **Chan JKC**. Mesenchymal tumors of the gastrointestinal tract: a paradise for acronyms (STUMP, GIST, GANT, and now GIPACT) implication of c-*kit* in genesis, and yet another of the many emerging roles of the interstitial cell of Cajal in the pathogenesis of gastrointestinal disease? *Advances Anatomic Pathol* 1999; **6**: 19-40

2 **Tworek JA**, Goldblum JR, Weiss SW, Greenson JK, Appelman HD. Stromal tumors of the abdominal colon. A clinicopathologic study of 20 cases. *Am J Surg Pathol* 1999; **23**: 937-945

3 **Sircar K**, Hewlett BR, Huizinga JD, Chorneyko K, Berezin I, Riddell RH. Interstitial cells of Cajal as precursors of gastrointestinal stromal tumors. *Am J Surg Pathol* 1999; **23**: 377-389

4 **Miettinen M**, Lasota J. Gastrointestinal stromal tumors-definition, clinical, histological, immunohistochemical, and molecular genetic features and differential diagnosis. *Virchows Arch* 2001; **438**: 1-12

5 **Moskaluk CA**, Tian Q, Marshall CR, Rumpel CA, Franquemont DW, Frierson HF. Mutations of c-*kit* JM domain are found in a minority of human gastrointestinal stromal tumors. *Oncogene* 1999; **18**: 1897-1902

6 **Miettinen M**, Sarlomo-Rikala M, Lasota J. Gastrointestinal stromal tumors: recent advances in understanding of their biology. *Human Pathol* 1999; **30**: 1213-1220

7 **Seidal T**, Edvardsson H. Expression of c-kit (CD117) and ki67 provides information about the possible cell of origin and clinical course of gastrointestinal stromal tumours. *Histopathology* 1999; **34**: 416-424

8 **Robinson TL**, Sircar K, Hewlett BR, Chorneyko K, Riddelll RH, Huizinga JD. Gastrointestinal stromal tumors may originate from a subset of CD34-positive interstitial cells of Cajal. *Am J Pathol* 2000; **156**: 1157-1163

9 **Miettinen M**, Sobin LH, Sarlomo-Rikala M. Immunohistochemical spectrum of GISTs at different sites and their differential diagnosis with a reference to CD117(KIT). *Mod Pathol* 2000; **13**: 1134-1142

10 **Miettinen M**, Furlong M, Sarlomo-Rikala M, Burke A, Sobin LH, Lasota J. Gastrointestinal stromal tumors, Intramural leiomyomas, and leiomyosarcomas in the rectum and anus. A clinicopathologic, immunohistochemical, and molecular genetic study of 144 cases. *Am J Surg Pathol* 2001; **25**: 1121-1133

11 **Smithey BE**, Pappo AS, Hill DA. C-kit expression in pediatric solid tumors. *Am J Surg Pathol* 2002; **26**: 486-492

12 **Hornick JL**, Fletcher CDM. Immunohistochemical staining for KIT(CD117) in soft tissues sarcomas is very limited in distribution. *Am J Clin Pathol* 2002; **117**: 188-193

13 **Lasota J**, Wozniak A, Sarlomo-Rikala M, Rys J, Kordek R, Nassar A, Sobin LH, Miettinen M. Mutations in exons 9 and 13 of KIT gene are rare events in gastrointestinal stromal tumors A study of 200 cases. *Am J Pathol* 2000; **157**: 1091-1095

14 **Allander SV**, Nupponen NN, Ringnér M, Hostetter G, Maher GW, Goldberger N, Chen Y, Carpten J, Elkahloun AG, Meltzer PS. Gastrointestinal stromal tumors with kit mutations exhibit a remarkably homogeneous gene expression profile. *Cancer Res* 2001; **61**: 8624-8628

15 **Miettinen M**, Sarlomo-Rikala M, Sobin LH, Lasota J. Esophageal stromal tumors: a clinicopathologic, immunohistochemical, and molecular genetic study of 17 cases and comparison with esophageal leiomyomas and leiomyosarcomas. *Am J Surg Pathol* 2000; **24**: 211-222

16 **Wardelmann E**, Neidt I, Bierhoff E, Speidel N, Manegold C, Fischer HP, Pferfer U, Pietsch T. c-kit mutations in gastrointestinal stromal tumors occur preferentially in the spindle rather than in the epithelioid cell variant. *Mod Pathol* 2002; **15**: 125-136

17 **Jordan JH**, Fritsche-Polanz R, Sperr WR, Mitterbauer G, Födinger M, Schernthaner GH, Bankl HC, Gebhart W, Chott A, Lechner K, Valent P. A case of 'smouldering' mastocytosis with high mast cell burden, monoclonal myeloid cells, and C-KIT mutation Asp-816-Val. *Leuk Res* 2001; **25**: 627-634

18 **Sotlar K**, Escribano L, Landt O, Möhrle S, Herrero S, Torrelo A, Lass U, Horny HP, Bültmann B. One-step detection of c-kit point mutations using peptide nucleic acid-mediated polymerase chain reaction clamping and hybridization probes. *Am J Pathol* 2003; **162**: 737-746

19 **Tian Q**, Frierson HF Jr, Krystal GW, Moskaluk CA. Activating c-kit gene mutations in human germ cell tumors. *Am J Pathol* 1999, **154**: 1643-1647

20 **Maeyama H**, Hidaka E, Ota H, Minami S, Kajiyama M, Kuraishi A, Mori H, Matsuda Y, Wada S, Sodeyama H, Nakata S, Kawamura N, Hata S, Watanabe M, Lijima Y, Katsuyama T. Familial gastrointestinal stromal tumor with hyperpigmentation: association with a germline mutation of the c-kit gene. *Gastroenterology* 2001; **120**: 210-215

21 **Lasota J**, Jasinski M, Sarlomo-Rikala M, Miettinen M. Mutations in exon 11 of c-kit occur preferentially in malignant *vs* benign gastrointestinal stromal tumors and do not occur in leiomyomas or leiomyosarcomas. *Am J Pathol* 1999; **154**: 53-60

22 **Miettinen M**, Sarlomo-Rikala M, Sobin LH, Lasota J. Gastrointestinal stromal tumors and leiomyosarcomas in the colon. *Am J Surg Pathol* 2000; **24**: 1339-1352
23 **Taniguchi M**, Nishida T, Hirota S, Isozaki L, Ito T, Nomura T, Matuda H, Kitamura Y. Effect of c-*kit* mutation on prognosis of gastrointestinal stromal tumors. *Cancer Res* 1999; **59**: 4297-4300
24 **Rubin BP**, Singer S, Tsao C, Duensing A, Lux ML, Ruiz R, Hibbard MK, Chen CJ, Xiao S, Tuveson DA, Demetri GD, Fletcher CDM, Fletcher JA. KIT activation is ubiquitous feature of gastrointestinal stromal tumors. *Cancer Res* 2001; **61**: 8118-8121
25 **Corless CL**, McGreevey L, Haley A, Town A, Heinrich MC. KIT mutation are common in incidental gastrointestinal stromal tumors one centimeter or less in size. *Am J Pathol* 2002; **160**: 1567-1572
26 **Miettinen M**, El-Rifal W, Sobin LH, Lasota J. Evalution of malignancy and prognosis of gastrointestinal stromal tumors: A review. *Hum Pathol* 2002; **33**: 478-483
27 **Andersson J**, Sjögren H, Meis-Kidblom JM, Stenman G, Aman P, Kindblom LG. The complexity of KIT gene mutations and chromosome rearrangements and their clinical correlation in gastrointestinal stromal (pacemaker cell) tumors. *Am J Pathol* 2002; **160**: 15-22
28 **Miettinen M**, Kopczynski J, Makhlouf H, Sarlomo-Rikala M, Gyorffy H, Burke A, Sobin LH, Lasota J. Gastrointestinal stromal tumors, intramural leiomyomas, and leiomyosarcomas in the duodenum. A clinicopathologic, immunohistochemical, and molecular genetic study of 167 cases. *Am J Surg Pathol* 2003; **27**: 625-641
29 **O'Leary T**, Ernst S, Przygodzki R, Emory T, Sobin L. Loss of heterozygosity at 1p36 predicts poor prognosis in gastrointestinal stromal/smooth muscle tumors. *Lab Invest* 1999; **79**: 1461-1467
30 **O'Leary T**, Berman JJ. Gastrointestinal stromal tumors: answers and questions. *Hum Pathol* 2002; **33**: 456-458
31 **El-Rifai W**, Sarlomo-Rikala M, Andersson LC, Knuutila S, Miettinen M. DNA sequence copy number changes in gastrointestinal stromal tumors: tumor progression and prognostic significance. *Cancer Res* 2000; **60**: 3899-3903
32 **Heinrich M**, Rubin BP, Longley BJ, Fletcher JA. Biology and genetic aspects of gastrointestinal stromal tumors: KIT activation and cytogenetic alterations. *Hum Pathol* 2002; **33**: 484-495
33 **Kim NG**, Kim JJ, Ahn JY, Seong CM, Noh SH, Kim CB, Min JS, Kim H. Putative chromosomal deletions on 9P, 9Q and 22Q occur preferentially in malignant gastrointestinal stromal tumors. *Int J Cancer* 2000; **85**: 633-638
34 **Heinrich MC**, Corless CL, Duensing A, McGreevey L, Chen CJ, Joseph N, Singer S, Griffith DJ, Haley A, Town A, Demetri GD, Fletcher CDM, Fletcher JA. PDGFRA activating mutations in gastrointestinal stromal tumors. *Science* 2003; **299**: 708-710

Edited by Wang XL and Xu FM

PO Box 2345, Beijing 100023, China
Fax: +86-10-85381893
E-mail: wjg@wjgnet.com www.wjgnet.com

World J Gastroenterol 2004;10(9):1315-1320
World Journal of Gastroenterology
Copyright ©2004 by The WJG Press ISSN 1007-9327

• BASIC RESEARCH •

Suppressive effects of 17b-estradiol on hepatic fibrosis in CCl_4-induced rat model

Qing-Hua Liu, Ding-Guo Li, Xin Huang, Chun-Hua Zong, Qin-Fang Xu, Han-Ming Lu

Qing-Hua Liu, Ding-Guo Li, Xin Huang, Chun-Hua Zong, Qin-Fang Xu, Han-Ming Lu, Department of Gastroenterology, Xinhua Hospital of Shanghai Secondary Medical University, Shanghai 200092, China
Supported by the National Natural Science Foundation of China, No. 30170411
Correspondence to: Dr. Ding-Guo Li, Department of Gastroenterology, Xinhua Hospital of Shanghai Secondary Medical University, Shanghai 200092, China. dingguo_li@yahoo.com.cn
Telephone: +86-21-65790000-5316 **Fax:** +86-21-55055127
Received: 2003-08-11 **Accepted:** 2003-10-12

Abstract

AIM: To investigate the pathway via which 17β-estradiol (β-Est) exerts suppressive effects on rat hepatic fibrosis.

METHODS: *In vivo* study was done in CCl_4-induced female hepatofibrotic rats. Fibrosis-suppressive effect of β-Est (20 μg/kg·d) was evaluated in intact and ovariectomized rat models. Six weeks after the treatment, all the rats were sacrificed and specimens of serum or liver tissue were collected for the studies. Serum liver enzymes, fibrosis markers and estradiol levels were determined by standard enzymatic methods, ELISA and RIA, respectively. Degrees of fibrosis and areas of hepatic stellate cells (HSCs) positive for alpha-smooth muscle actin (α-SMA) in the liver were determined by van Gieson (VG) stain and immunohistochemistry. *In vitro* studies, HSCs were isolated by a combination of pronase-collagenase perfusion and density gradient centrifugation. First-passage HSCs were randomly divided into 10 groups, and different concentrations of β-Est, 2-hydroxyestradiol (2OHE) or 2-methoxyestradiol (2MeOE) were separately added to the cell groups. After incubation for 72 h, the degree of cell proliferation, collagen production, α-SMA or estrogen receptor (ER) expression was determined by MTT assay, ELISA and immunohistochemistry, respectively.

RESULTS: β-Est treatment reduced aspartate aminotransferase (AST), alanine aminotransferase (ALT), hyaluronic acid (HA) and type IV collagen (C IV) in sera, suppressed hepatic collagen content, decreased the areas of HSCs positive for α-SMA significantly in both intact and ovariectomized female hepatofibrotic rats. There was a negative correlation between the percentage of fibrotic area of liver tissue and the serum estradiol level; the calculated correlation coefficient was –0.57 (P<0.01). β-Est and its metabolites concentration-dependently (10^{-9} mol/L-10^{-7} mol/L) inhibited HSC proliferation and collagen synthesis. At the concentration of 10^{-7} mol/L, they could inhibit α-SMA expression. The order of potency was 2MeOE>2OHE>β-Est.

CONCLUSION: β-Est may suppress hepatic fibrosis probably via its biologically active metabolites.

Liu QH, Li DG, Huang X, Zong CH, Xu QF, Lu HM. Suppressive effects of 17β-estradiol on hepatic fibrosis in CCl_4-induced rat model. *World J Gastroenterol* 2004; 10(9): 1315-1320
http://www.wjgnet.com/1007-9327/10/1315.asp

INTRODUCTION

Several epidemiological studies demonstrated a lower incidence of hepatic cirrhosis and its complications in women than in men[1-3]. But as menopause comes, the morbidity of the disease increases gradually. So, endogenous estrogen may take part in the protective effects on hepatic fibrosis. *In vivo*, 17β-estradiol (β-Est) is the most active estrogen and can be converted to several metabolites, some of which are known to possess biological activities. Of the various metabolites, 2-hydroxyestradiol (2OHE) and 2-methoxyestradiol (2MeOE) are the biologically active substances, which have been investigated in depth[4,5]. 2OHE is one of the hydroxylated metabolites of β-Est converted by cytochrome P-450 enzymes (CYP450) and can be rapidly catalyzed by enzyme catechol-O-methyl-transferase (COMT) to 2MeOE[6-8]. Recent studies have shown that 2OHE and 2MeOE could inhibit DNA synthesis, cell proliferation, collagen synthesis and mitogen activated protein kinase activity in vascular smooth muscle cells (VSMCs), cardiac fibroblasts (CFs) and glomerular mesangial cells (GMCs) with the potency stronger than β-Est[9-13]. Hence, the fibrosis-suppressive effects of β-Est not only reflect the biological effects of β-Est per se but also those of its biologically active metabolites.

Hepatic stellate cells (HSC), the key cells responsible for hepatic fibrogenesis, are VSMC, CF or GMC analogs and belong to the pericytes generically[14]. So, they may have many properties in common, including a prominent role in fibrosing injury and the same reaction to metabolites of β-Est.

The present study was initiated to investigate the role of β-Est in the female rat model of carbon tetrachloride (CCl_4)-induced hepatic fibrosis. Moreover, the effects of β-Est, 2OHE and 2MeOE on the first-passage rat HSCs were assessed.

MATERIALS AND METHODS

In vivo study

Fifty female Sprague-Dawley rats aged 10 wk (Laboratory Animal Center affiliated to Chinese Academy of Sciences, Shanghai, China) were divided into 5 groups (n=10). All the rats were initiated with either a bilateral ovariectomy (Ovx) or a sham operation 3 wk before the studies. Control group received subcutaneous injection of olive oil (3 mL/kg every 3 d and first dosage doubled), CCl_4 group was given the same dose of 400 g/L CCl_4, Ovx+CCl_4 group was treated with the same dose of 400 g/L CCl_4 after ovariectomy, β-Est+CCl_4 group along with CCl_4 injection described above was treated with 0.002% β-Est (1 mL/kg·d, Sigma-Aldrich Corporation, St Louis, Missouri, USA), Ovx+β-Est+CCl_4 group was treated the same as β-Est +CCl_4 group with the addition of ovariectomy.

At the end of 6 wk, the number of alive rats in the groups was 10, 7, 8, 10, 9 respectively. Several rats died of infection at the site of injection or hepatic crack by unsuitable handling.

After an overnight fast, all the rats were sacrificed. Serum samples obtained were treated with proteinase inhibitor and stored at -20 ℃. Liver tissue specimens were rinsed with normal saline containing 0.1 g/L DEPC, some were stored at -80 ℃, and the others were fixed in neutral formalin and embedded in paraffin.

Serum activities of aspartate aminotransferase (AST) and alanine aminotransferase (ALT) were assayed by standard enzymatic methods, hyaluronic acid (HA) and type IV collagen (C IV) concentrations were measured by enzyme-linked immunosorbent assay (ELISA) using a commercial kit (Navy Medical Institute, Shanghai, China).

The embedded liver specimens were sliced 5 μm in thickness, mounted on slides, deparaffinised in xylene, and dehydrated in alcohol. For histopathological studies, the liver sections were stained with van Gieson (VG). For alpha-smooth muscle actin (α-SMA) immunohistochemistry, the sections were incubated with 3% (v/v) hydrogen peroxide in methanol for 15 min to block endogenous peroxidase, and then with 1 g/L Triton-X plus 1 g/L BSA in phosphate-buffered saline (PBS) to block non-specific antigens. After absorption of surplus liquid, the samples were incubated with a 1:100 dilution of a polyclonal antibody against α-SMA (Boster Biological Technology Corporation, Wuhan, China) at 37 ℃ for 2 h. Then the samples were rinsed and incubated with a 1:100 dilution of biotin-conjugated goat anti-rabbit IgG (Boster Biological Technology Corporation, Wuhan, China) at 37 ℃ for 30 min. Finally, the antigen-antibody complexes were visualized with 3,3'-diaminobenzidine (DAB).

For morphometric analysis, the mean value of collagen content or α-SMA positive cells in six ocular fields per specimen was used as the percentage area at 100x magnification using Zeiss KS400 image analysis system (Kontron Electronics, Eching, Germany).

Serum estradiol concentrations were measured with radioimmunoassay (RIA) using a commercial kit (Diagnostic Products Corporation, Tianjin, China).

In vitro study

HSCs were isolated and purified from the livers of normal female rats weighing about 400 g to 450 g by a combination of pronase-collagenase perfusion and density gradient centrifugation[15-19]. Briefly, the liver was perfused *in situ* through the portal vein, first with Ca^{2+}/Mg^{2+}-free Krebs-Ringer (KR) solution at a flow rate of 20 mL/min, followed by pronase and then with collagenase (Sigma-Aldrich Corporation, St Louis, Missouri, USA) in KR solution. The digested liver was excised, minced with scissors, and incubated in KR solution containing pronase and DNase (Sigma-Aldrich Corporation, St Louis, Missouri, USA) for 30 min. The resulting suspension was filtered through nylon mesh (200 μm in diameter) and then washed 3 times by centrifugation in D-Hanks solution at 1 700 r/min for 7 min. An HSC-enriched fraction was obtained by centrifugation of the filtrate in an 180 g/L nycodenz (Sigma-Aldrich Corporation, St Louis, Missouri, USA) solution with the volume ratio of 1:2 at 3 200 r/min for 17 min. The cells in the upper layer were washed by centrifugation at 1 700 r/min for 7 min and suspended in Dulbecco's modified Eagle medium (DMEM, GIBCO BRL Life Technologies Incorporation, USA) supplemented with 200 mL/L fetal bovine serum (FBS, GIBCO BRL Life Technologies Incorporation, USA). Both cell viability and purity were over 90%, examined by trypan blue (Sigma-Aldrich Corporation, St Louis, Missouri, USA) exclusion and autofluorescence respectively.

Cells were plated at a density of 1×10^6 cells in 1 mL culture medium on uncoated plastic culture dishes. The culture medium was changed after 24 h and then every 3 d. After cultured for 14 d, the cells were passaged.

The first-passage HSCs were plated at a density of 2×10^5 cells in 1 mL DMEM supplemented with 100 g/L FBS on an uncoated plastic culture dish. Subconfluent HSCs were divided into 10 groups, and different concentrations of β-Est, 2OHE, 2MeOE (Sigma-Aldrich Corporation, St Louis, Missouri, USA) or vehicle were added to the cells. After incubated for 24 h, experiments were done to assess the functional state of HSCs.

HSC proliferation was measured by MTT assay. The cells were continually cultivated with 3-(4,5-dimethylthiazol-2yl)-2, 5-diphenyl tetrazolium bromide (MTT, Sigma-Aldrich Corporation, St Louis, Missouri, USA) in a 96-well plate for 4 h. After the supernatant in each well was aspirated and discarded, the cells were agitated with dimethylsulfoxide (DMSO, Sigma-Aldrich Corporation, St Louis, Missouri, USA) 150 μLfor 10 min. Finally, the optical density of each well was read in an auto reader using a 492 nm filter with a reference at 630 nm.

The levels of HA and C IV in the supernatants of cell were messured as afore-metioned.

For immunohistochemical examination of α-SMA, estrogen receptor (ER)α and ERβ, the cells were mounted on slides and fixed with 40 g/L paraformaldehyde for 5 min at 4 ℃. Following incubation with 30 mL/L H_2O_2 for 15 min, the cells were blocked by 1 g/L Triton-X plus 1 g/L BSA in PBS for 15 min at room temperature. They were incubated for 2 h at 37 ℃ with a 1:100 dilution of polyclonal antibody against α-SMA, ERα or ERβ (Santa Cruz Biotechnology Incorporation, California, USA) in a humid chamber. After the samples were rinsed, they were incubated with a 1:200 dilution of biotin-conjugated goat anti-rabbit IgG, and then visualized with DAB. Integral light density (ILD) analysis was performed on 20 cells in up, down, left, right quadrant of each section, data were calculated from average of 4 ILDs.

Statistical analysis

Data are presented as mean±SE unless otherwise indicated. Parametric data were compared using one-way analysis of variance, followed by multiple pair-wise comparisons according to the least-significant difference *t*-test. Pearson's analysis was performed to compare the correlation between serum estradiol and fibrotic area percentage. A *P* value less than 0.05 was accepted as statistically significant.

RESULTS

In vivo effect of β-Est on hepatic fibrosis

Table 1 shows the liver enzymes and fibrosis markers in CCl_4-treated female rats. Treatment with CCl_4 caused a significant increase in the activities of serum ALT and AST compared with the control animals. The enzyme levels in ovariectomized model rats were higher than those in CCl_4 model group, whereas CCl_4 plus β-Est group showed a significant decrease in enzyme levels compared with CCl_4 group. There was no significant difference between CCl_4 group and Ovx+β-Est+CCl_4 group.

The changes of fibrosis markers, HA and C IV, were in parallel with those of the enzyme levels in all groups.

The control livers showed a distinct lobular architecture with collagens only surrounding the central and portal veins (Figure 1A). Administration of CCl_4 induced inflammation, necrosis and collagen deposition in the livers. Ovariectomy significantly increased hepatic fibrosis induced by CCl_4 (Figure 1B), whereas β-Est had the opposite effect. The fibrotic area percentage of Ovx+CCl_4+β-Est group was similar to that of CCl_4 group (Figure 1C).

Immunohistochemistry of α-SMA, an activation marker of rat HSC[20-22], showed strong staining around vascular wall, but not the sinusoids in control female rat livers (Figure 2A). After administration of CCl_4, fibrotic change was evident with significant increases of α-SMA positive cells in centrilobular

and periportal fibrotic bands. Ovariectomy significantly increased the percentage area of staining (Figure 2B), whereas β-Est had the opposite effect. There was no significant difference in the fibrotic area percentage of staining between CCl_4 and Ovx+CCl_4+β-Est groups (Figure 2C).

Figure 3 summarizes the histopathological and immunohistochemical changes in CCl_4-treated female rats.

Figure 4 shows the serum estradiol levels in the rats. The levels did not change in animals treated with CCl_4 alone. Ovariectomy produced significantly lower serum estradiol levels. In rats model treated with exogenous β-Est, the levels increased significantly as compared with those of control or CCl_4 model groups. Twenty μg/kg· d β-Est could rectify the low serum estradiol levels in ovariectomized rats.

Table 1 Change of liver enzymes and serum fibrosis indicators

	ALT (nkat/L)	AST (nkat/L)	HA (μg/L)	C IV (μg/L)
Control	275.50±32.05	84.80±11.83	155.50±10.41	17.10±1.77
CCl_4	1 070.71±82.95^{b}	806.00±82.43^{b}	481.43±24.68^{b}	49.57±2.47^{b}
Ovx+CCl_4	1 403.88±120.30^{ab}	1 102.88±84.91^{bd}	583.75±37.50^{ab}	61.00±3.30^{ab}
CCl_4+β-Est	789.40±58.61^{ab}	606.70±45.68^{ab}	389.30±29.77^{ab}	38.80±2.59^{ab}
Ovx+CCl_4+β-Est	1 008.44±93.07^{b}	794.89±70.93^{b}	474.56±32.57^{b}	46.22±3.06^{b}

$^{a}P<0.05$ *vs* CCl_4, $^{b}P<0.01$ *vs* Control, $^{d}P<0.01$ *vs* CCl_4.

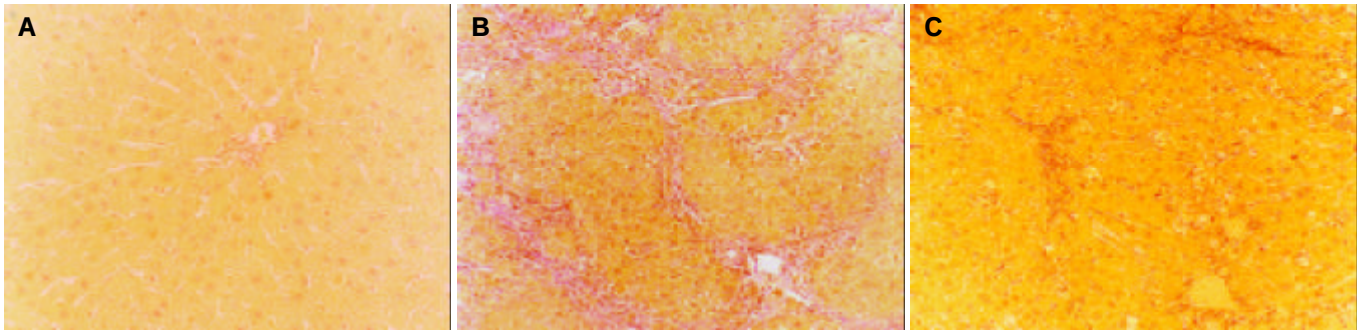

Figure 1 Histopathological findings of representative liver sections from female rats treated with CCl_4, VG staining, original magnification ×100, A: Control group; B: Ovx+CCl_4 group; C: Ovx+CCl_4+β-Est group.

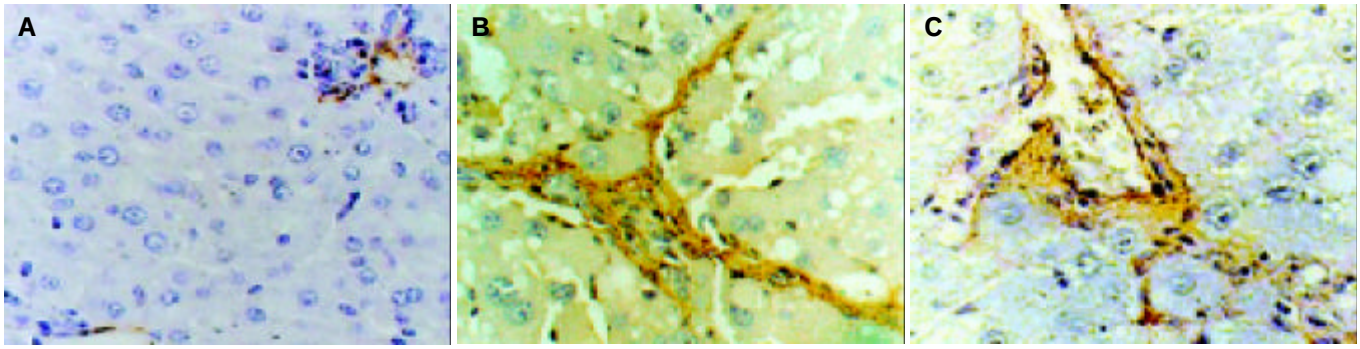

Figure 2 Immunohistochemistry of α-SMA in representative liver sections from female rats treated with CCl_4, DAB staining, A: control group, original magnification ×200; B: Ovx+CCl_4 group, original magnification ×400; C: Ovx+CCl_4+β-Est group, original magnification ×400.

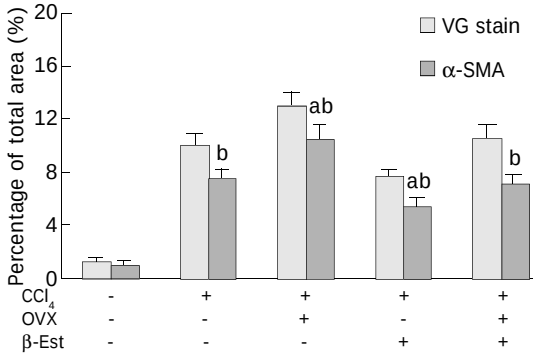

Figure 3 Histopathological and immunohistochemical changes in CCl_4-treated female rats (fibrotic area percentage of total field), $^{a}P<0.05$ *vs* CCl_4; $^{b}P<0.01$ *vs* control.

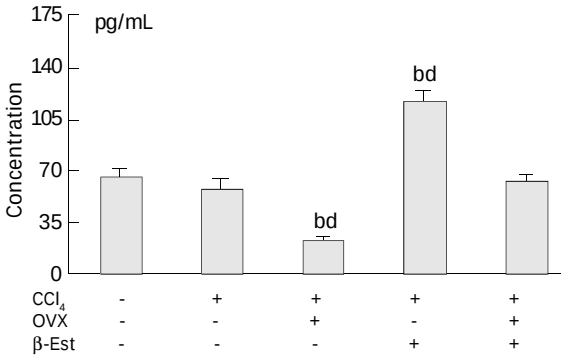

Figure 4 Serum estradiol levels in CCl_4–treated female rats, $^{b}P<0.01$ *vs* control, $^{d}P<0.01$ *vs* CCl_4.

In 34 CCl_4-treated rats, there was a negative correlation between the fibrotic area percentage and serum estradiol level, the calculated correlation coefficient was -0.57 (P<0.01, Figure 5).

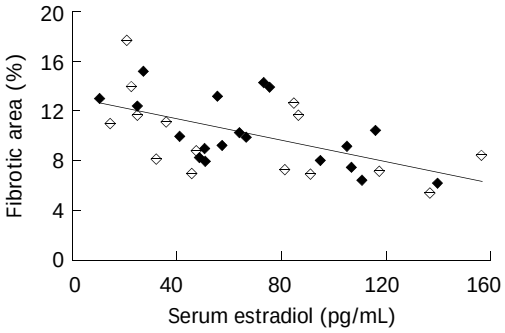

Figure 5 Negative correlation between fibrotic area percentage and serum estradiol level (r=0.57, P<0.01).

In vitro effect of β-Est and its metabolites on activation of rat HSCs

β-Est, 2OHE and 2MeOE (10^{-9}-10^{-7} mol/L) inhibited HSC proliferation (Figure 6A) and ECM secretion (Figures 6B and 6C) in a dose-dependent manner. Only the high concentration (≥10^{-7} mol/L) of β-Est exerted inhibitory effects, while a concentration of 2MeOE as low as 10^{-9} mol/L had a similar effect. The order of potency was 2MeOE>2OHE>β-Est. At a concentration of 10^{-7} mol/L, β-Est, 2OHE and 2MeOE all could inhibit HSCs in expressing α-SMA, and the potency of 2MeOE was significantly stronger than that of β-Est (Figure 6D)

A representative immunohistochemistry showed the expression of ER-β (Figure 7B) but not ER-α (Figure 7A) on rat HSCs.

DISCUSSION

Hepatic fibrosis, which is often associated with hepatocellular necrosis and inflammation, occurs as a repair process in many chronic liver diseases and is considered to be a forerunner of cirrhosis. HSCs are regarded as the primary target cells for inflammatory stimuli in the injured liver. Once activated, HSCs would be transformed into α-SMA positive myofibroblast-like cells, which are responsible for much of the collagen hypersecretion during hepatic fibrogenesis[23-28].

In vivo study showed that β-Est at physiological doses could suppress the development of hepatic fibrosis in CCl_4-

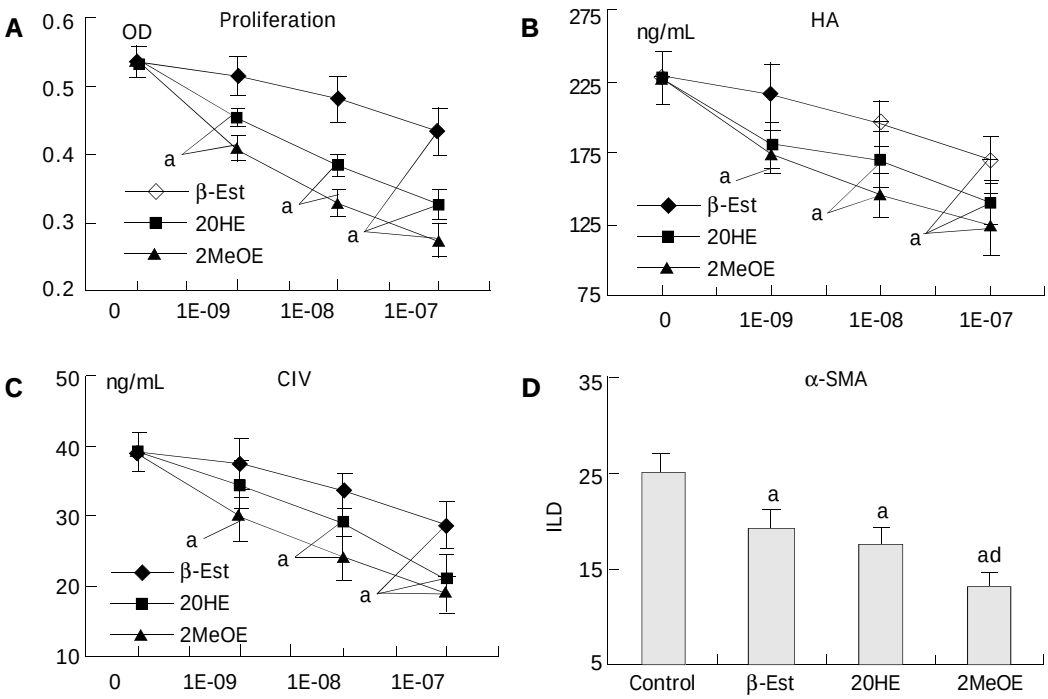

Figure 6 Effects of estradiol metabolites on function of HSCs proliferation (A), HA (B) and C IV (C) secretion in HSCs, effects of 10^{-7} mol/L estradiol metabolites on α-SMA expression (D) of HSCs,Values for each point represent mean±SD from 5 separate experiments, ^aP<0.05 *vs* control, ^dP<0.05 *vs* 10^{-7} mol/L β-Est.

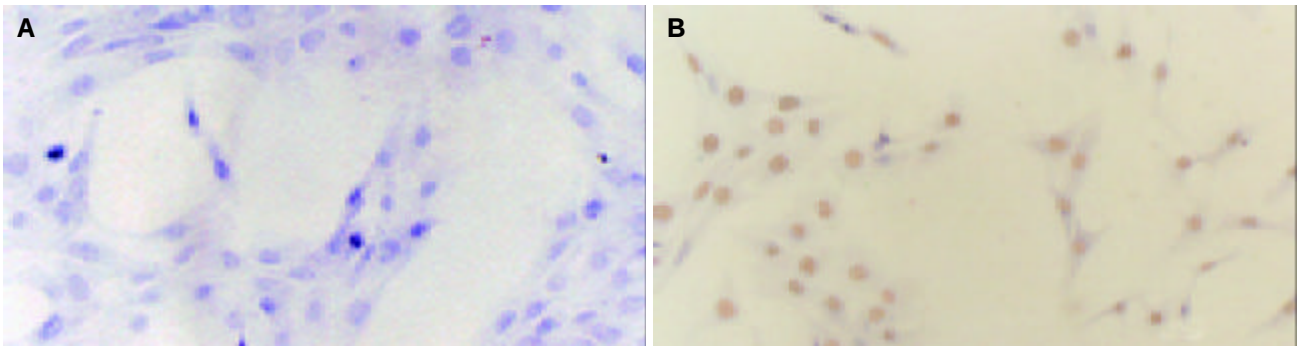

Figure 7 Representative immunohistochemistry showing expression of ER on HSCs used for studies, original magnification ×200, No expression of ER-α(A) but ER-β(B) was observed.

induced hepatofibrotic rat models along with decreased serum liver enzymes, reduced collagen content and smaller areas of fibrosis in the liver. There was a negative correlation between the percentage of fibrotic area and the serum estradiol level with a calculated correlation coefficient of -0.57. Additionally, in cultured rat HSCs, β-Est inhibited cell proliferation, ECM secretion and α-SMA expression in a dose-dependent manner. These findings support β-Est as a potent inhibitor of HSCs transformation, thus, playing an antifibrogenic role in the progression from hepatic fibrosis to cirrhosis.

The pathway by which β-Est inhibits HSC activation is not clear. As HSCs contain ERs, it is presumed that ERs mediate the fibrosuppressive effects of β-Est. However, several lines of evidence do not support the hypothesis. In this regard, high levels of ERβ but low or no levels of ERα expression were observed in normal and fibrotic livers and also in quiescent and activated HSCs from both male and female rats[29], but β-Est in physiological doses was unable to suppress hepatic fibrosis in male rats following dimethylnitrosamine or pig serum administration[30-32]. Our preliminary studies also suggested a sexually dimorphic response pattern of the injured liver to β-Est. Besides, the male patients expressed high serum levels of estradiol parallel to the stage of liver cirrhosis.

HSCs are VSMC, CF or GMC analogs that belong to the pericytes generically, so they may have many properties in common including a prominent role in repairing fibrosis against injury and similar reactions to β-Est. Recent studies by Iafrati *et al*.[33] and Karas *et al*.[34, 35] showed that β-Est inhibited injury-induced VSMC proliferation in arteries of mice that lacked either ERα or ERβ as well as in double knockout mice that lacked both ERα and ERβ, suggesting that the effects might be mediated via an ER-independent pathway. Furthermore, 2OHE and 2MeOE, the biologically active metabolites of β-Est, could inhibit DNA synthesis, cell proliferation, collagen synthesis and mitogen activated protein kinase activity in VSMCs, CFs or GMCs with a potency stronger than β-Est[9-13,36,37]. Liver is the main locus where β-Est metabolizes, so it is possible that the antifibrogenic actions of β-Est are mediated in part by local conversion of β-Est to biologically active metabolites.

In the present study, we attempted to testify this hypothesis by comparing the inhibitory effects of β-Est and its metabolites on the activation of rat HSCs *in vitro*. We found that treatment of HSCs with β-Est or its metabolites differentially inhibited FCS-induced cell proliferation, ECM secretion and α-SMA expression in the following order of potency: 2MeOE>2OHE> β-Est. Only the pharmacological concentration (>10^{-7} mol/L) of β-Est could significantly inhibit HSC proliferation and collagen synthesis, while the concentration of 2MeOE or 2OHE as low as 10^{-9} mol/L gave similar effects. β-Est, 2OHE and 2MeOE at a concentration of 10^{-7} mol/L each inhibited α-SMA expression by 24%, 30% and 47%, respectively.

The findings of this study provided evidence in rat HSC experiments that the metabolites of β-Est with little or no affinity for ERs could mediate the fibrosuppressive effects of β-Est via an ER-independent pathway. The results suggest that β-Est metabolism in the liver may be an important determinant of fibrosuppressive effects of circulating estradiol and that sexual differences in the liver metabolism of β-Est could determine a sexually dimorphic response pattern of liver cirrhosis. Moreover, genetic or acquired differences in β-Est metabolism may determine the fibrosuppressive benefits a patient receives from β-Est replacement therapy. Finally, the results also imply that nonfeminizing β-Est metabolites may afford antifibrogenic protection regardless of gender.

REFERENCES

1 **Poynard T**, Bedossa P, Opolon P. Natural history of liver fibrosis progression in patients with chronic hepatitis C. The OBSVIRC, METAVIR, CLINIVIR, and DOSVIRC groups. *Lancet* 1997; **349**: 825-832

2 **Poynard T**, Ratziu V, Charlotte F, Goodman Z, McHutchison J, Albrecht J. Rates and risk factors of liver fibrosis progression in patients with chronic hepatitis C. *J Hepatol* 2001; **34**: 730-739

3 **el-Serag HB**. Epidemiology of hepatocellular carcinoma. *Clin Liver Dis* 2001; **5**: 87-107

4 **Zhu BT**, Conney AH. Functional role of estrogen metabolism in target cells: review and perspectives. *Carcinogenesis* 1998; **19**: 1-27

5 **Zhu BT**, Conney AH. Is 2-methoxyestradiol an endogenous estrogen metabolite that inhibits mammary carcinogenesis? *Cancer Res* 1998; **58**: 2269-2277

6 **Cheng ZN**, Shu Y, Liu ZQ, Wang LS, Ou-Yang DS, Zhou HH. Role of cytochrome P450 in estradiol metabolism *in vitro*. *Acta Pharmacol Sin* 2001; **22**: 148-154

7 **Lee AJ**, Cai MX, Thomas PE, Conney AH, Zhu BT. Characterization of the oxidative metabolites of 17beta-estradiol and estrone formed by 15 selectively expressed human cytochrome p450 isoforms. *Endocrinology* 2003; **144**: 3382-3398

8 **Goodman JE**, Jensen LT, He P, Yager JD. Characterization of human soluble high and low activity catechol-O-methyltransferase catalyzed catechol estrogen methylation. *Pharmacogenetics* 2002; **12**: 517-528

9 **Dubey RK**, Gillespie DG, Zacharia LC, Barchiesi F, Imthurn B, Jackson EK. CYP450- and COMT-derived estradiol metabolites inhibit activity of human coronary artery SMCs. *Hypertension* 2003; **41**(3 Pt 2): 807-813

10 **Barchiesi F**, Jackson EK, Gillespie DG, Zacharia LC, Fingerle J, Dubey RK. Methoxyestradiols mediate estradiol-induced antimitogenesis in human aortic SMCs. *Hypertension* 2002; **39**: 874-879

11 **Dubey RK**, Gillespie DG, Keller PJ, Imthurn B, Zacharia LC, Jackson EK. Role of methoxyestradiols in the growth inhibitory effects of estradiol on human glomerular mesangial cells. *Hypertension* 2002; **39**(2 Pt 2): 418-424

12 **Dubey RK**, Gillespie DG, Zacharia LC, Rosselli M, Imthurn B, Jackson EK. Methoxyestradiols mediate the antimitogenic effects of locally applied estradiol on cardiac fibroblast growth. *Hypertension* 2002; **39**(2 Pt 2): 412-417

13 **Dubey RK**, Gillespie DG, Zacharia LC, Rosselli M, Korzekwa KR, Fingerle J, Jackson EK. Methoxyestradiols mediate the antimitogenic effects of estradiol on vascular smooth muscle cells via estrogen receptor-independent mechanisms. *Biochem Biophys Res Commun* 2000; **278**: 27-33

14 **Bissell DM**. Sex and hepatic fibrosis. *Hepatology* 1999; **29**: 988-989

15 **Friedman SL**, Rockey DC, McGuire RF, Maher JJ, Boyles JK, Yamasaki G. Isolated hepatic lipocytes and Kupffer cells from normal human liver: morphological and functional characteristics in primary culture. *Hepatology* 1992; **15**: 234-243

16 **Riccalton-Banks L**, Bhandari R, Fry J, Shakesheff KM. A simple method for the simultaneous isolation of stellate cells and hepatocytes from rat liver tissue. *Mol Cell Biochem* 2003; **248**: 97-102

17 **Ratziu V**, Lalazar A, Wong L, Dang Q, Collins C, Shaulian E, Jensen S, Friedman SL. Zf9, a Kruppel-like transcription factor up-regulated *in vivo* during early hepatic fibrosis. *Proc Natl Acad Sci U S A* 1998; **95**: 9500-9505

18 **Reynaert H**, Vaeyens F, Qin H, Hellemans K, Chatterjee N, Winand D, Quartier E, Schuit F, Urbain D, Kumar U, Patel YC, Geerts A. Somatostatin suppresses endothelin-1-induced rat hepatic stellate cell contraction via somatostatin receptor subtype 1. *Gastroenterology* 2001; **121**: 915-930

19 **Williams EJ**, Benyon RC, Trim N, Hadwin R, Grove BH, Arthur MJ, Unemori EN, Iredale JP. Relaxin inhibits effective collagen deposition by cultured hepatic stellate cells and decreases rat liver fibrosis *in vivo*. *Gut* 2001; **49**: 577-583

20 **Ikeda K**, Wakahara T, Wang YQ, Kadoya H, Kawada N, Kaneda K. *In vitro* migratory potential of rat quiescent hepatic stellate cells and its augmentation by cell activation. *Hepatology* 1999; **29**: 1760-1767

21 **Kim KY**, Choi I, Kim SS. Progression of hepatic stellate cell

activation is associated with the level of oxidative stress rather than cytokines during CCl4-induced fibrogenesis. *Mol Cells* 2000; **10**: 289-300

22 **Sato M**, Suzuki S, Senoo H. Hepatic stellate cells: unique characteristics in cell biology and phenotype. *Cell Struct Funct* 2003; **28**: 105-112

23 **Friedman SL**. Molecular regulation of hepatic fibrsis, an integrated cellular response to tissue injury. *J Biol Chem* 2000; **275**: 2247-2250

24 **Gabele E**, Brenner DA, Rippe RA. Liver fibrosis: signals leading to the amplification of the fibrogenic hepatic stellate cell. *Front Biosci* 2003; **8**: D69-D77

25 **Mann DA**, Smart DE. Transcriptional regulation of hepatic stellate cell activation. *Gut* 2002; **50**: 891-896

26 **McCrudden R**, Iredale JP. Liver fibrosis, the hepatic stellate cell and tissue inhibitors of metalloproteinases. *Histol Histopathol* 2000; **15**: 1159-1168

27 **Dooley S**, Delvoux B, Lahme B, Mangasser-Stephan K, Gressner AM. Modulation of transforming growth factor beta response and signaling during transdifferentiation of rat hepatic stellate cells to myofibroblasts. *Hepatology* 2000; **31**: 1094-1106

28 **Brenner DA**, Waterboer T, Choi SK, Lindquist JN, Stefanovic B, Burchardt E, Yamauchi M, Gillan A, Rippe RA. New aspects of hepatic fibrosis. *J Hepatol* 2000; **32**(1 Suppl): 32-38

29 **Zhou Y**, Shimizu I, Lu G, Itonaga M, Okamura Y, Shono M, Honda H, Inoue S, Muramatsu M, Ito S. Hepatic stellate cells contain the functional estrogen receptor beta but not the estrogen receptor α in male and female rats. *Biochem Biophys Res Commun* 2001; **286**: 1059-1065

30 **Yasuda M**, Shimizu I, Shiba M, Ito S. Suppressive effects of estradiol on dimethylnitrosamine-induced fibrosis of the liver in rats. *Hepatology* 1999; **29**: 719-727

31 **Shimizu I**, Mizobuchi Y, Yasuda M, Shiba M, Ma YR, Horie T, Liu F, Ito S. Inhibitory effect of oestradiol on activation of rat hepatic stellate cells *in vivo* and *in vitro*. *Gut* 1999; **44**: 127-136

32 **Xu JW**, Gong J, Chang XM, Luo JY, Dong L, Hao ZM, Jia A, Xu GP. Estrogen reduces CCL4- induced liver fibrosis in rats. *World J Gastroenterol* 2002; **8**: 883-887

33 **Iafrati MD**, Karas RH, Aronovitz M, Kim S, Sullivan TR Jr, Lubahn DB, O'Donnell TF Jr, Korach KS, Mendelsohn ME. Estrogen inhibits the vascular injury response in estrogen receptor alpha deficient mice. *Nat Med* 1997; **3**: 545-548

34 **Karas RH**, Hodgin JB, Kwoun M, Krege JH, Aronovitz M, Mackey W, Gustafsson JA, Korach KS, Smithies O, Mendelsohn ME. Estrogen inhibits the vascular injury response in estrogen receptor β-deficient female mice. *Proc Natl Acad Sci U S A* 1999; **96**: 15133-15136

35 **Karas RH**, Schulten H, Pare G, Aronovitz MJ, Ohlsson C, Gustafsson JA, Mendelsohn ME. Effects of estrogen on the vascular injury response in estrogen receptor α, β (double) knockout mice. *Circ Res* 2001; **89**: 534-539

36 **Dubey RK**, Jackson EK. Cardiovascular protective effects of 17β-estradiol metabolites. *J Appl Physiol* 2001; **91**: 1863-1883

37 **Dubey RK**, Jackson EK. Estrogen-induced cardiorenal protection: potential cellular, biochemical, and molecular mechanisms. *Am J Physiol Renal Physiol* 2001; **280**: F365-F388

Edited by Kumar M and Wang XL **Proofread by** Xu FM

PO Box 2345, Beijing 100023, China
Fax: +86-10-85381893
E-mail: wjg@wjgnet.com www.wjgnet.com

World J Gastroenterol 2004;10(9):1321-1324
World Journal of Gastroenterology
Copyright ©2004 by The WJG Press ISSN 1007-9327

• BASIC RESEARCH •

Hyperammonemia, brain edema and blood-brain barrier alterations in prehepatic portal hypertensive rats and paracetamol intoxication

Camila Scorticati, Juan P. Prestifilippo, Francisco X. Eizayaga, José L. Castro, Salvador Romay, María A. Fernández, Abraham Lemberg, Juan C. Perazzo

Camila Scorticati, Juan P. Prestifilippo, Francisco X. Eizayaga, Salvador Romay, Marí a A Fernández, Abraham Lemberg, Juan C. Perazzo, Cátedra de Fisiopatologí a, Facultad de Farmaciay Bioquí mica, Universidad de Buenos Aires, Buenos Aires, Argentina
José L. Castro, Cátedra de Farmacologí a, Facultad de Farmacia y Bioquí mica, Universidad de Buenos Aires, Buenos Aires, Argentina
Supported by Grant # TB 56 from the University of Buenos Aires, Argentina
Correspondence to: Professor. Dr. J. C. Perazzo, Cátedra de Fisiopatologí a, Juní n 956, 5º Piso, (1113), Ciudad Autónoma de Buenos Aires, Argentina. jperazzo@ffyb.uba.ar
Fax: +54-11-4964 8268
Received: 2003-09-23 **Accepted:** 2003-12-24

Abstract

AIM: To study the blood-brain barrier integrity, brain edema, animal behavior and ammonia plasma levels in prehepatic portal hypertensive rats with and without acute liver intoxication.

METHODS: Adults male Wistar rats were divided into four groups. Group I: sham operation; II: Prehepatic portal hypertension, produced by partial portal vein ligation; III: Acetaminophen intoxication and IV: Prehepatic portal hypertension plus acetaminophen. Acetaminophen was administered to produce acute hepatic injury. Portal pressure, liver serum enzymes and ammonia plasma levels were determined. Brain cortex water content was registered and trypan blue was utilized to study blood brain barrier integrity. Reflexes and behavioral tests were recorded.

RESULTS: Portal hypertension was significantly elevated in groups II and IV. Liver enzymes and ammonia plasma levels were increased in groups II, III and IV. Prehepatic portal hypertension (group II), acetaminophen intoxication (group III) and both (group IV) had changes in the blood brain-barrier integrity (trypan blue) and hyperammonemia. Cortical edema was present in rats with acute hepatic injury in groups III and IV. Behavioral test (rota rod) was altered in group IV.

CONCLUSION: These results suggest the possibility of another pathway for cortical edema production because blood brain barrier was altered (vasogenic) and hyperammonemia was registered (cytotoxic). Group IV, with behavioral altered test, can be considered as a model for study at an early stage of portal-systemic encephalopathy.

Scorticati C, Prestifilippo JP, Eizayaga FX, Castro JL, Romay S, Fernández MA, Lemberg A, Perazzo JC. Hyperammonemia, brain edema and blood-brain barrier alterations in prehepatic portal hypertensive rats and paracetamol intoxication. *World J Gastroenterol* 2004; 10(9): 1321-1324
http://www.wjgnet.com/1007-9327/10/1321.asp

INTRODUCTION

Portal hypertension (PH) is a major syndrome that frequently accompanies chronic liver diseases such as cirrhosis. Prehepatic PH creates a splanchnic hyperdynamic circulation and hyperemia with increased splanchnic resistance and production of collateral vessels that drive splanchnic blood flow to systemic circulation[1].

Portal-systemic encephalopathy (PSE), the most commonly encountered form of hepatic encephalopathy (HE), describes a wide spectrum of reversible and irreversible neuropsychiatric abnormalities that appear as a complication in patients with acute or chronic liver disease. HE is usually found as an overt form or in a mild form with lesser neuropsychiatric symptoms, which can be misdiagnosed[2].

Acetaminophen (APAP) is a non-steroid anti-inflammatory drug (NSAID), frequently used in adults and children. At high concentration of APAP, the gluthation-dependent conjugation system generates a toxic metabolite that binds covalently to cellular proteins and macromolecules followed by cell destruction[3,4].

Finally, ammonia originated from the gut protein metabolism has been implicated as an important factor in the production of HE. In chronic liver disease, ammonia evades liver catabolism to urea through portal systemic shunts and collaterals, and reaches the brain in high blood concentration[5].

In previous experiments we documented different aspects of the relationship between prehepatic PH in rats and central nervous system: alterations in uptake and release of norepinephrine and modification and tyrosine hydroxylase activity in discrete regional mesencephalic nucleus[6,7]. Furthermore, we considered that PH rats underwent a subclinical HE[8].

The aim of this experiment was to study the blood-brain barrier (BBB) integrity, brain cortical edema, ammonia plasma levels and behavior in rats with different liver injuries.

MATERIALS AND METHODS

Animals and surgical procedures

Male Wistar rats (240-260 g of body mass, 12 h of light cycle: 8 a.m.-8 p.m.) were used and animal welfare was in accordance with guidelines of the Faculty of Pharmacy and Biochemistry of Buenos Aires and approved by ethical committee according to Helsinki's Declaration. Animals were placed in individual cages and allowed to recover from surgery. Rats were fed standard laboratory chow and water *ad libitum*.

Group II (chronic PH): Portal hypertensive (PH) animals were obtained by calibrated stenosis of the portal vein according to Chojkier *et al*.[1]. Rats were lightly anesthetized with ether and then midline abdominal incision was made. The portal vein was located and isolated from surrounding tissues. A ligature of 3.0 silk suture was placed around the vein, and snuggly tied to a 20-gauge blunt-end needle placed along the side of the portal vein. The needle was subsequently removed to yield a calibrated stenosis of portal vein, after which the abdomen was sutured. Operations were performed at 2 p.m. to obey circadian rhythm and fourteen days later the animals developed PH.

Group III (acute intoxication): Acetaminophen was injected i.p. at a dose of 750 mg/kg.d per rat on the 13th and 14th day, considering as the start day or day zero, the day of the surgical procedure of group II.

Group IV (chronic PH plus acute intoxication): Rats underwent partial portal vein ligation as in group II and then

received acetaminophen the same dose as in group III.

Group I: Shamly operated rats underwent the same experimental procedure like group II, except that portal vein was isolated but not stenosed.

All groups received a subcutaneous injection (25 mL/Kg of body mass) of a 50 g/L dextrose, 4.5 g/L saline solution, containing 20 mEq/L of potassium chloride, every 12 h after the first injection of APAP, as a supportive therapy to prevent hypoglycemia and renal failure[9]. Rats were sacrificed on d 14, 6 to 8 h after the last acetaminophen injection.

Experimental procedures

Following experiment were performed in four groups of animals (I: SHAM, II: HP, III: APAP and IV: HP+APAP, *n*=6/8 per group).

Portal pressure measurement

Rats were anesthetized with sodium pentobarbital (40 mg/kg, ip). The spleen was cannulated with a polyethylene cannula (PE 50) filled with heparinized saline solution (25 U/mL) to measure portal pressure by Statham Gould P23ID pressure transducer (Statham, Hato Rey, Puerto Rico) coupled to a Grass 79 D polygraph (Grass Instruments, Quincy, MA).

Biochemical determination

Blood samples were obtained by abdominal aortic artery puncture for the determination of biochemical parameters. Plasma aminotransferase activity was determined using standardized and optimized commercial Boheringer-Manenhein kits (Germany). Ammoniac Enzyimatique UV kits (Biomerieux-France) were used to determine plasma ammonia concentration. Plasma levels of urea, glucose and creatinine were measured by current biochemical colorimetric UV methods (Wiener, Argentine).

Microscopy

High resolution optical microscopy (HROM): sections of liver were fixed in buffered formalin and embedded in paraplast. Routine stains were used: hematoxylin-eosin, PAS and Masson' s trichrome for light microscopy and toluidine blue stain for HROM.

Brain water content

Rats were sacrificed by exsanguination under complete ether anesthesia, their brains cortex water content was measured to quantify possible brain edema according to Marmorou[10].

One cerebral hemisphere was quickly removed after rats were sacrificed and stored at 4 ℃ to be processed within 30 min. The hemisphere was cut into coronal slices and eight samples taken from the cerebral cortex, approximately 10 mg in weight, was placed in a bromobenzene-kerosene density gradient column to measure brain water[10]. The column was previously calibrated with varying concentrations of potassium sulfate to ensure a linear relation (>0.997) between the K2 SO4 and readings in the density gradient. The equilibration point of the samples was read at 2 min and averaged, conversion from specific gravity to brain water was done as previously reported[10].

Trypan blue transcardial perfusion

Rats were perfused with trypan blue (TB) solution and then fixed in paraformaldehyde. TB solution (5 g/L) was made by dissolving 1 g of TB in 200 mL of PBS with gentle heat. The solution was allowed to cool room temperature and then added to the filtrate, then the solution was placed on ice and used immediately. The temperature of TB solution was 10-12 ℃ at the time of perfusion. Rats were anesthetized with ethyl urethane (1 mg/kg) and perfused transcardially with 200 mL of TB solution, followed by 300 mL of ice-cold paraformaldehyde (20 g/L in PBS), the low rate of perfusate was maintained at 25 mL/min. Brains were dissected and post-fixed overnight in 0.3 Kg/L sucrose for 2 d. Subsequently, brains were frozen in powdered dry ice and stored at -80 ℃ until processed for microscopic studies. Slices of brain hippocampus were obtained with cryostat in sections of 300 microns according to Watson and Paxinos (Hippocampus fig 24, bregma 4.8, interneuron 4.2). Hippocampal slices were evaluated under light microscopy and the results were expressed as positive (+) or negative (-) for TB staining. Medial eminence and choroids plexus staining were used as control of TB appropriated perfusion[11].

Pharmacological and behavioral test

Corneal, pain-response and right reflexes were performed. Automated open field (Animex) and rota-rod tests (to study motor coordination) were realized. Rota-rod speed was fixed at 25 turns/min. Rats were trained 48 h before the experiment until they fell down less than 3 times in 5 min. The number of falls during the experiment and time elapsed to the first fall were recorded[12,13].

Statistical methods

Results were expressed as mean±SE. Statistical analysis was performed by means of repeated measurement analysis of variance (ANOVA) followed by Newman-Keuls' s test. Dunn´ s test was used for non-parametric data, *P* values less than 0.05 were considered statistically significant.

RESULTS

Portal pressure (PP) was significant higher in groups II and IV ($^aP<0.01$) when compared to control group. There was no significant difference when compared PP of group I (Sham) with group III (APAP) (Table 1).

Table 1 Portal pressure (PP) and plasma aminotranferase levels

	Sham (I)	PH (II)	APAP (III)	PH+APAP (IV)
PP (mmHg)	8.5±0.5	12.1±1^a	8.1±0.2	11.9±0.9^a
AST (UI/L)	155±25	316±23^b	426±36^b	380±34^b
ALT (UI/L)	39±4	63±9	134±20^a	308±27^b

PP was significantly increased in groups II and IV ($^aP<0.05$ *vs* control and APAP group). AST plasma levels were significantly increased in groups II, III and IV ($^bP<0.001$ *vs* sham group). ALT was significantly increased in groups III and IV ($^aP<0.05$ and $^bP<0.001$ *vs* sham group, respectively).

AST plasma levels were significant increased in groups II, III and IV when compared with group I ($^bP<0.001$). ALT plasma levels were significant increased in groups III and IV when compared with control group (Table 1).

Plasma levels of urea, glucose and creatinine were normal in all groups of rats (data not shown).

Ammonia blood concentrations (μmol/L) showed significant increase in PH rats, APAP group and PH plus APAP ($P<0.05$ and $P<0.001$ respectively) (Figure 1).

Light microscopy and HROM showed normal histology in liver parenchyma in group I, minimal focal necrosis in group II; diffuse hemorrhagic necrosis in group III and focal hemorrhage and confluent necrosis in group IV. (Figure 2 A-D).

Brain cortical water content (H_2O/ g brain weight %) showed significant increase in rats injected with APAP ($P<0.001$) and in those with PH+APAP ($P<0.01$) (Figure 3).

In Groups II, III and IV trypan blue was positive in the perivascular space in the hippocampus area (Figure 4).

All reflexes studied including the Animex were normal for all groups except for rota-rod test that showed in group IV a significant difference at the time elapsed to the first fall (not in number of falls), when compared to shamly operated animals (Table 2).

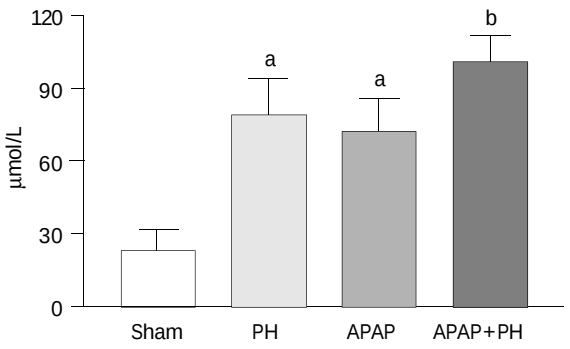

Figure 1 Significantly increased ammonia plasma levels in all groups of rats [a]$P<0.05$ and [b]$P<0.01$ when compared with sham group.

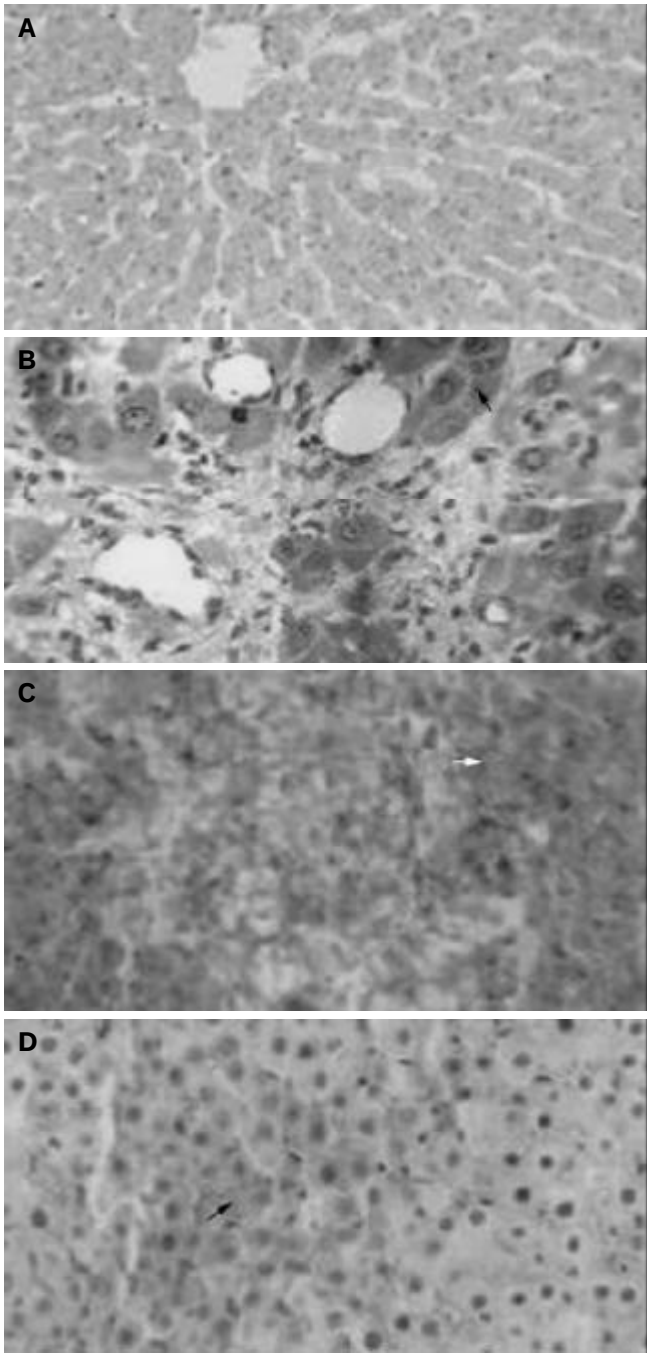

Figure 2 Liver Microscopy. A: Shows a normal liver histology corresponding to a rat in sham group (HE, 100×), B: Minimal focal necrosis in group II (HE, asterisk, 500×), C: Diffuse hemorrhagic necrosis in group III (HE, arrows, 400×), D: Focal hemorrhagic confluent necrosis in group IV (HE, asterisk, 400×).

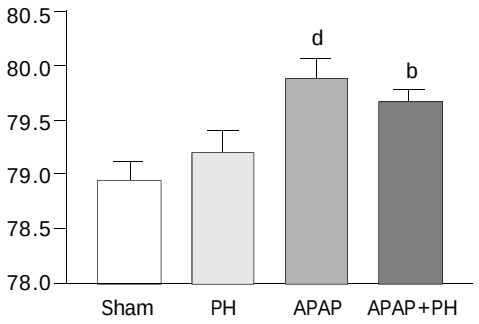

Figure 3 Significantly increased brain water content in groups III and IV [d]$P<0.01$, [b]$P<0.001$ when compared with sham group.

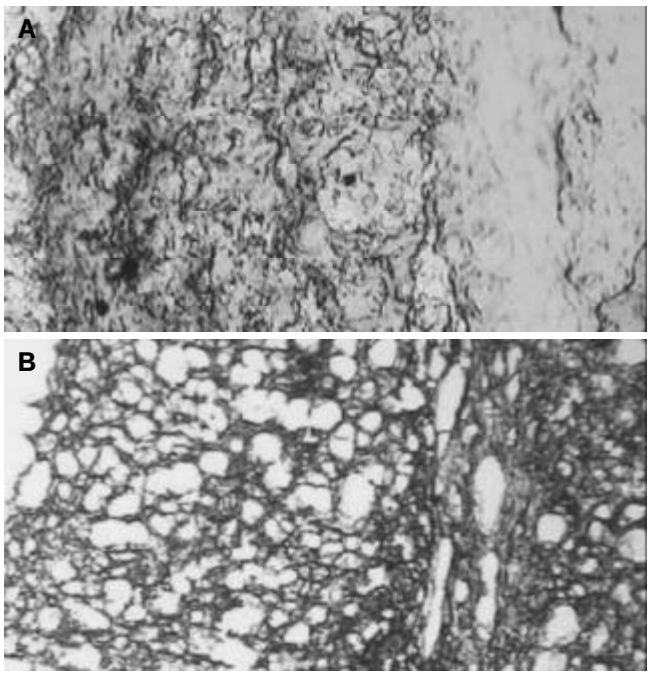

Figure 4 Trypan blue and BBB. A: Trypan blue dye in hippocampus of a sham rat. No breakdown of BBB was observed. Trypan blue was only positive in vascular space (100×), B: Trypan blue dye diffusion due to the breakdown of BBB as an example of what was observed in hippocampus in groups II, III and IV (100×).

Table 2 Rota rod test: First fall time

	Sham (I)	PH (II)	APAP (III)	PH+APAP (IV)
Median	300[a]	300[1]	205[1]	45[1]
Confidence interval (Lower 95%-Upper 95%)	(172-356)	(63-316)	(45-318)	(-13.9-108)[a]

[1]: expressed in seconds. Rota rod test was significantly different in group IV compared with all the others groups ([a]$P<0.05$ Dunnett´s test).

DISCUSSION

Experimental prehepatic portal hypertension produces a hyperdynamic redistribution of splanchnic circulation and minimal liver damage. It could be considered that prehepatic PH is a subclinic PSE stage[8]. In this study APAP was used to produce liver injury because of its aggressive effect on liver parenchyma[3,4]. It was administrated to two groups that reflected different situations, namely an acute form of liver injury (group III) and a chronic liver PH group plus an acute liver intoxication.

Portal pressure (PP) was significantly increased in group II, as it was described elsewhere[8] and in group IV. PP in group III (APAP) had normal values. This agreed with acute intoxications

and specifically with acute APAP intoxication[14]. Group IV and group II had similar PP values, and it might be due to a chronic PH induced shunt (groups II and IV).

Liver enzymes reflected hepatocyte damage. When liver parenchyma was injured, the enzymes increased as it could be seen in early stages of PSE. Plasma enzyme levels were higher in group III than those in APAP induced acute liver damage. In addition, liver histopathology was concordant with these data as a diffuse hemorrhagic necrosis was observed in group III[14].

Ammonia plasma level data showed normal values in group I and significantly increased values in groups II, III and IV. The values registered were remarkably lower than those observed in different models of acute liver failure (ALF). It is important to point out that in group II hyperammonemia was produced by opened shunts due to the splanchnic blood flow redistribution[15]. It is also interesting that in this experimental model the hepatic blood flow was reduced, but not completely shunted as in other models (e.g. porto-caval shunts, PCS). Ammonia was markedly increased as the major responsible molecule related to HE[16] had several pathways, lately the cGMP-NO-glutamate that leads to cytotoxic brain edema characterized by swelling of astrocytes and their processes, raised intracranial pressure and as a consequence, to brain herniation[5]. This was the main cause of mortality in ALF and it could be predicted by increased arterial ammonia plasma levels[17]. Besides this, PSE could lead to increased nNOS activity[18], associated with L-arginine uptake in a PCS model[19].

In this model of PH, brain edema was not correlated with ammonia increase. Furthermore brain edema was documented in group III and ammonia level was lower than that in group II and no cerebral edema was observed. Besides this, brain edema was lower in group IV than in group III and the highest recorded ammonia was recorded. What is the major mechanism involved in the development of brain edema in this experiment? One of the pathways of brain edema is the vasogenic and if that mechanism was involved in groups III and IV, why in group II BBB integrity was broken-down and ammonia plasma levels were increased, and no cortical brain edema was documented? Although a mixed mechanism (vasogenic and cytotoxic) was proposed for brain edema in ALF[20], in this experiment no brain edema was present in the chronic group without acute hepatocyte injury. In the chronic group plus acute liver injury brain edema was registered and the cytotoxic mechanism could be mostly responsible. Under these experimental conditions another mechanism of brain edema might involve aquaporins. The aquaporin-type water channels are integral membrane proteins that have been found to function as conduits for osmotically driven transport of water across cell plasma membranes[21]. In this experiment BBB integrity was altered and thus endothelial cells were involved. AQP4 presented in both, endothelia and astrocytes might play an active role in regulation of astrocyte swelling and the presence of brain edema[22].

TB demonstrated altered integrity of the BBB at the hippocampus areas involved in learning and memory consolidation in groups II, III and IV. Furthermore, the only group with an altered behavioral test, at first fall in rota rod test, was group IV. These might be related with the observation in the only group with PH, elevated enzymes, hepatocyte injury, hyperammonemia, brain edema, positive TB and altered rota rod test. Dixit[23] demonstrated that in rats with galactosamine-induced ALF BBB breakdown evidenced by TB dye infusion studies began in grade III coma. Despite this, under the present experimental conditions no clinical evidence of coma could be registered in any group. Therefore, group IV can be considered as an experimental model of subclinic PSE.

REFERENCES

1 **Chojkier M**, Groszmann RJ. Measurement of portal-systemic shunting in the rat by using gamma-label microspheres. *Am J Physiol* 1981; **240**: G371-375

2 **Watanabe A**. Cerebral changes in hepatic encephalopathy. *J Gastroenterol Hepatol* 1998; **13**: 752-760

3 **Kelly JH**, Koussayes T, Da-hertte HE, Chong MG, Shang TA, Wissenbrot HH, Sussman NC. An improved model of acetaminophen-induced fulminant hepatic failure in dogs. *Hepatol* 1992; **15**: 329-335

4 **Francavilla A**, Makowka L, Polimeno L, Barone M, Demetris J, Prelich J, Van Thiel DH, Starzl TE. A dog model for acetaminophen-induced fulminant hepatic failure. *Gastroenterology* 1989; **96**(2 Pt 1): 470-478

5 **Felipo V**, Butterworth RF. Neurobiology of ammonia. *Prog Neurobiol* 2002; **67**: 259-279

6 **Lemberg A**, Eizayaga F, Vatta M, Dominguez A, Romay S, Bianciotti L, Sanso G, Fernandez B. Prehepatic portal hypertension in rats modifies norepinephrine metabolism in hypothalamus, medulla oblongata and portal vein. *Dig Dis Sci* 1993; **38**: 1259-1262

7 **Lemberg A**, Rubio M, Bengochea L, Romay S, Eizayaga F, Diez A, Perazzo JC. Tyrosine hydroxylase activity in discrete brain regions from prehepatic portal hypertensive rats. *Hepatogastroenterology* 1998; **45**: 547-550

8 **Scorticati C**, Prestifilippo P, Murer G, Lemberg A, Perazzo JC. Functional alterations in central nervous system of prehepatic portal hypertensive rats. *Medicina* 2001; **61**: 673-675

9 **Gammal SH**, Basile AS, Heller D, Skolnick P, Jones LA. Reversal of the behavioral and electrophysiological abnormalities of an animal model of hepatic encephalopathy by benzodiazepines receptor ligands. *Hepatology* 1990; **11**: 371-378

10 **Marmarou A**, Poll W, Shulman K, Banagavem H. A simple gravimetric technique for measurement of cerebral edema. *J Neurosurg* 1978; **49**: 530-537

11 **Reynolds DS**, Morton AJ. Changes in Blood Brain Barrier permeability following neurotic lesions of rat brain can be visualized with Trypan Blue. *J Neurosci Methods* 1998; **79**: 115-121

12 **Dunham NW**, Miya TS. A note on a simple apparatus for detention neurological deficit in rats and mice. *J Am Pharm Assoc* 1957; **46**: 208-209

13 **Maynert EW**. A test group for central depressants. RA Turner (Ed) screening methods in pharmacology. New York: *Academic Press* 1965: 80-86

14 **Bengochea L**, Ghanem C, Perazzo JC, Ghisolfi C, Marabotto L, Acevedo C, Mino J, Lemberg A, Rubio M. Drug glucuronidation and hepatic lipid microsomal membrane profile in cholestatic rats followed paracetamol intoxication. *Pharmacol Res* 1999; **40**: 369-376

15 **MacMathuna P**, Vlavianos P, Westaby D, Williams R. Pathophysiology of Portal Hypertension. *Dig Dis* 1992; **10**(Suppl 1): 3-15

16 **Kramer E**, Tribl B, Gendo A, Zauner C, Schneider B, Ferenci P, Madl C. Partial pressure of ammonia versus ammonia in hepatic encephalopathy. *Hepatology* 2000; **31**: 30-34

17 **Clemmensen JO**, Larsen FS, Kondrup J, Hansen BA, Ott P. Cerebral hermiation in patients with acute liver is correlated with arterial ammonia concentration. *Hepatol* 1999; **29**: 648-653

18 **Rao VL**, Audet RM, Butterworth RF. Increased nitric oxide synthase activities and l- [3 H] arginine uptake in brain following portacaval anastomosis. *J Neurochem* 1995; **65**: 677–678

19 **Rao VL**, Audet RM, Butterworth RF. Portacaval shunting and hyperammonemia stimulate the uptake of l- [3 H] arginine but not of l- [3 H] nitroarginine into rat brain synaptosomes. *J Neurochem* 1997; **68**: 337–343

20 **Swain M**, Butterworth RF, Blei AT. Ammonia and related amino acids in the pathogenesis of brain edema in acute ischemic liver failure in rats. *Hepatol* 1992; **15**: 449-453

21 **Verkman AS**. Role of aquaporin water channels in eye function. *Exp Eye Res* 2003; **76**: 137-143

22 **Papadopoulos MC**, Krishna S, Verkman AS. Aquaporin water channels and brain edema. *Mt Sinai J Med* 2002; **69**: 242-248

23 **Dixit V**, Chang TM. Brain edema and blood brain barrier in galactosamine-induce fulminant hepatic failure rats. An animal model for evaluation of liver support systems. *ASAIO Trans* 1990; **36**: 21-27

Edited by Wang XL **Proofread by** Xu FM

PO Box 2345, Beijing 100023, China
Fax: +86-10-85381893
E-mail: wjg@wjgnet.com www.wjgnet.com

World J Gastroenterol 2004;10(9):1325-1328
World Journal of Gastroenterology
Copyright ©2004 by The WJG Press ISSN 1007-9327

• BASIC RESEARCH •

Modulation of Kupffer cells on hepatic drug metabolism

Hong Ding, Jing Tong, Shi-Cheng Wu, Deng-Ke Yin, Xian-Fen Yuan, Jian-Yuan Wu, Jun Chen, Gang-Gang Shi

Hong Ding, Gang-Gang Shi, Medical College, Shantou University, Shantou 515031, Guangdong Province, China
Jing Tong, Shi-Cheng Wu, Deng-Ke Yin, Xian-Fen Yuan, Jian-Yuan Wu, Jun Chen, Department of Pharmacology, College of Pharmacy, Wuhan University, Wuhan 430072, Hubei Province, China
Supported by the Postdoctor Science Foundation of China, No. 2002032238 the Major State Basic Research Deaelopment Program of China, No. 2002ccc00300
Correspondence to: Jing Tong, College of Pharmacy, Wuhan University, Wuhan 430072, Hubei Province, China. tongjing2002@etang.com
Telephone: +86-27-87682339 **Fax:** +86-27-87682339
Received: 2003-08-26 **Accepted:** 2003-10-07

Abstract

AIM: To observe the effects of Kupffer cells on hepatic drug metabolic enzymes.

METHODS: Kunming mice were ip injected with $GdCl_3$10, 20, 40 mg/kg to decrease the number and block the function of kupffer cells selectively. The contents of drug metabolic enzymes, cytochrome P450, NADPH-cytochrom C redutase (NADPH-C), aniline hydroxylase (ANH), aminopyrine N-demethylase (AMD), erythromycin N-demethylase (EMD), and glutathione s-transferase (mGST) in hepatic microsome and S9-GSTpi, S9-GST in supernatant of 9 000 g were accessed 1 d after the injection. The time course of alteration of drug metabolic enzymes was observed on d 1, 3, and 6 treated with a single dose $GdCl_3$. Mice were treated with *Angelica sinensis* polysaccharides (ASP) of 30, 60, 120 mg/kg, ig, qd ×6 d, respectively and the same assays were performed.

RESULTS: P450 content and NADPH-C, ANH, AMD, and EMD activities were obviously reduced 1 d after Kupffer cell blockade. However, mGST and S9-GST activities were significantly increased. But no relationship was observed between $GdCl_3$ dosage and enzyme activities. With single dose $GdCl_3$ treatment, P450 content, NADPH-C, and ANH activities were further decreased following Kupffer cell blockade lasted for 6 d, by 35.7%, 50.3%, 36.5% after 3 d, and 57.9%, 57.9%, 63.2% after 6 d, respectively. On the contrary, AMD, EMD, mGST, and S9-GST activities were raised by 36.5%, 71.9%, 23.1%, 35.7% after 3 d, and 155%, 182%, 21.5%, 33.7% after 6 d, respectively. Furthermore, the activities of drug metabolic enzymes were markedly increased after 30 mg/kg ASP treatment, and decreased significantly after 120 mg/kg ASP treatment. No change in activity of S9-GSTpi was observed in the present study.

CONCLUSION: Kupffer cells play an important role in the modulation of drug metabolic enzymes. The changes of drug metabolic enzyme activities depend on the time of kupffer cell blockade and on the degree of Kupffer cells activated. A low concentration of ASP increases the activities of drug metabolic enzymes, but a high concentration of ASP decreases the activities of drug metabolic enzymes.

Ding H, Tong J, Wu SC, Yin DK, Yuan XF, Wu JY, Chen J, Shi GG. Modulation of Kupffer cells on hepatic drug metabolism. *World J Gastroenterol* 2004; 10(9): 1325-1328
http://www.wjgnet.com/1007-9327/10/1325.asp

INTRODUCTION

Drug metabolic enzymes can detoxify endogenous and exogenous compounds and also generate potentially carcinogenic or toxic compounds in the process of catalyzing the metabolism of xenobiotics, and inhibition and induction of their activities are also the key mechanisms in drug-drug interactions[1,2]. The induction or inhibition of metabolizing enzyme activities by a great deal of substances (including drugs, foods, inflammatory factors, *etc*.) influences their toxicological or pharmacological outcomes as well as those of other xenobiotics or drugs[3-5].

The role of sinusoidal cells in hepatic metabolism has been greatly underestimated until now. However, Kupffer cells, despite their size represents 80% to 90% of all fixed macrophages in the body and approximately 14% of the hepatic cellular mass, the function in hepatic metabolism of Kupffer cells is unknown. Some reports suggested that Kupffer cells might play an important role in xenobiotic-induced hepatotocixity, which is often dependent on their metabolism. Although hepatotocytes are the major site of xenobiotic metabolism, several enzymatic activities such as glutathione s-transferase, UDP-glucuronosyltransferase and cytochrome P450-dependent oxidase have been found in nonparenchymal cells (mainly Kupffer cells) and may play an important role in the metabolism and cellular effects of paracetamol[6,7]. Only a small number of reports demonstrated the relationship between drug metabolic enzymes and activities of Kupffer cells. The aim of this work was to investigate the effects of kupffer cell mediated metabolism as demonstrated by hepatic drug metabolic enzymes.

MATERIALS AND METHODS

Reagents

Gadolinium chloride ($GdCl_3$), glutathione (GSH), erythromycin, aniline, NADPH, aminophenazone, isocitric acid, isocitric acid dehydrogenase, 1-chloro-2,4-dinitrobenzene (CDNB), ethacrynic acid (EA) were purchased from Sigma, USA. All other reagents used in this study were of AR grade.

Animals and treatment

Kunming strain male mice (aged 4-6 wk) weighing 18-24 g were obtained from the Experimental Animal Center, Wuhan University School of Medicine. The animals were fed with a standard diet in pellets, and allowed free access to water. The mice were randomly divided into 9 groups, 10 per group: control group; $GdCl_3$10-1d group; $GdCl_3$20-1d group; $GdCl_3$40-1d group: mice received ip injection of $GdCl_3$10, 20, 40 mg/kg, respectively, and killed after 1 d; $GdCl_3$20-3 d group; $GdCl_3$20-6 d group: mice were treated with $GdCl_3$ at a single dose of 20 mg/kg, and killed after 3 d, and 6 d, respectively; ASP1 group; ASP2 group; ASP3 group: mice were given ASP 30, 60, and 120 mg/kg, respectively, i.g, qd×7 d, and were then killed on the 7th d. The livers were collected for the assay of drug metabolic enzyme activities.

Preparation of liver sample S9 and microsomal fractions

Microsomal fractions were preparated as previously described[8]. Total protein concentration in mice liver microsomes was determined by the method of Lowry *et al*.[9] (1951) using BSA as the standard. All operations were performed at 4 ℃.

Assays for metabolic enzyme activities

Total cytochrome P450 (P450) content was based on the use of the extinction coefficient of 105 mmol/L· cm for reduced cytochrome P450 minus oxidized P450 with a UV-1601 spectrophotometer[10].

NADPH-cytochrome C reductase (NADPH-C) activity was determined with a spectrophotometer at 550 nm by monitoring the reduction of cytochrome C (0.5 mg /mL) at 37 ℃ in an incubation mixture containing potassium phosphate (300 mmol/L, pH7.7) EDTA (0.1 mmol/L), liver microsomes (20 μg/mL) and NADPH (2 mg/L)[11].

Aminopytine N-demethylase (AMD) and erythomycin N-demethylase (EMD) were detected by measuring the production of formaldehyde. Its reaction system contained Tris-HCl 50 mmol/L, $MgCl_2$ 10 mmol/L, KCl 50 mmol/L and an NADPH-generating system (including $NADP^+$ 0.4 mmol/L, isocitric acid 10 mmol/L, and isocitric acid dehydrogenase 0.6 units). Erythromycin 0.4 mmol/L or aminopyrine 8 mmol/L was added, the reaction was initiated by the NADPH-generating system, the supernatant was incubated with the Nash reagent at 60 ℃ for 20 min and the color absorbance was measured at 415 nm with a UV-1601 spectrophotometer[12].

Aniline hydroxylase (ANH) was assessed with aniline as substrate as previously described[13].

Microsome glutathione s-transferase (mGST) and S9 glutathione s-transferase (S9-GST) activities were measured with CDNB as substrate (ε=9.6 mmol/L· cm)[14]. The assay mixture contained 850 μL of 0.1 mol/L sodium phosphate-1 mmol/L EDTA (pH6.5), 50 μL of 20 mmol/L GSH, 50 μL of 50 mmol/L CDNB, and 50 μL of sample. The absorbance at 340 nm was continuously recorded for 1 min[15]. S9-GSTpi was determined with EA and GSH as substrates (ε=5.0 mmol/L· cm)[14]. The assay mixture contained 850 μL of 0.1 mol/L sodium phosphate, 1 mmol/L EDTA (pH6.8), 50 μL of 50 mmol/L GSH, 50 μL of 50 mmol/L EA, and 50 μL of sample. The absorbance at 340 nm was continuously recorded for 1 minute.

Statistical analysis

The data were presented as mean±SD. Comparisons were performed using one-way analysis of variance (ANOVA) followed by the *posteriori* Student-Newman-Keuls' *t*-test. $P<0.05$ was considered statistically significant.

RESULTS

Influence of different dose of $GdCl_3$ on P450 content and P450 isoform activities

The content of P450 and the activities of NADPH-C, ANH, AMD, and EMD were obviously reduced after 1 d after $Gdcl_3$ treatment, and no relationship was found between the enzyme activities and the dose of $Gdcl_3$ (Table 1).

Time course of alterations of P450 content, activities of P450 isoforms, S9-GSTpi, S9-GST and mGST by Kupffer cell blockade

The content of P450 and activities of NADPH-C and ANH were reduced by 35.7%, 50.3%, 36.8% after Kupffer cell blockade for 3 d, and 57.9%, 57.9%, 63.2% for 6 d, respectively. However, the activities of AMD, EMD were raised by 36.5%, 71.9% after 3 d, and 155%, 181% after 6 d, respectively. S9-GST, mGST were markedly increased by Kupffer cell blockade. However, the changes were not related with the time of Kupffer cell blockade. No changes in S9-GST were observed (Table 2).

Influence of ASP on P450, activities of P450 isoforms, S9-GSTpi, S9-GST and mGST

The content of P450 and the activities of NADPH-C, ANH,

Table 1 Influence of different dose of $GdCl_3$ on P450 content and P450 isoform activities

Group	P-450 (nmol/mg·pro)	NADPH-C (nmol/min·mg·pro)	ANH (nmol/min·mg·pro)	AMD (nmol/min·mg·pro)	EMD (nmol/min·mg·pro)
Control	1.4±0.4	14.5±2.8	0.038±0.009	0.96±0.07	0.89±0.06
$GdCl_3$10-1 d	1.13±0.25	10.9±1.0^b	0.032±0.016	0.76±0.07^b	0.78±0.12
$GdCl_3$20-1 d	0.87±0.28^b	10.5±1.8^b	0.033±0.006	0.82±0.03^a	0.74±0.13^a
$GdCl_3$40-1 d	1.01±0.29^a	6.0±1.0^b	0.036±0.010	0.77±0.17^a	0.74±0.18^a

$GdCl_3$10-1 d, $GdCl_3$20-1 d, $GdCl_3$40-1 d: Mice were intraperitoneally injected with $GdCl_3$ 10, 20, 40 mg/kg, respectively, and sacrificed after 1 d. The hepatic microsome was prepared to assess the content of P450 and the activities of P450 isoforms. P450: cytochrome P450; NADPH-C: NADPH-cytochrome c reductase; ANH: aniline hydroxylase; AMD: aminopytine N-demethylase; EMD: erythomycin N-demethylase (n=8, mean±SD, $^aP<0.05$, $^bP<0.01$ compared with control group).

Table 2 Time course of alterations of P450 content, activities of P450 isoforms, S9-GSTpi, S9-GST and mGST by Kupffer cell blockade

Group	Control	$GdCl_3$20-1 d	$GdCl_3$20-3 d	$GdCl_3$20-6 d
P-450 (nmol/mg·pro)	1.4±0.4	0.87±0.28^b	0.90±0.21^b	0.59±0.24^b
NADPH-C (nmol/min·mg·pro)	14.5±2.8	10.5±1.8^b	7.2±1.0^b	6.1±0.8^b
ANH (nmol/min·mg·pro)	0.038±0.009	0.033±0.006	0.024±0.006^b	0.024±0.006^b
AMD (nmol/min·mg·pro)	0.96±0.07	0.82±0.03^a	1.31±0.24^b	1.31±0.24^b
EMD (nmol/min·mg·pro)	0.89±0.06	0.74±0.13^a	1.53±0.26^b	2.5±0.3^b
S9-GSTpi (nmol/min·mg·pro)	1.07±0.28	0.93±0.17	1.1±0.4	0.98±0.23
S9-GST (nmol/min·mg·pro)	8.3±0.91	0.2±1.5^a	11.4±0.9^b	11.1±1.3^b
mGST (nmol/min·mg·pro)	0.25±0.03	0.28±0.06	0.31±0.04^b	0.305±0.015^b

$GdCl_3$20-1 d, $GdCl_3$20-3 d, $GdCl_3$20-6 d: Mice were intraperitoneally injected with a signal dose of 20 mg/kg of $GdCl_3$, and sacrificed after 1 d, 3 d, and 6 d of $GdCl_3$ treatment. The hepatic microsome was prepared to assay the P450 content, and activities of P450 isoforms, S9-GSTpi, S9-GST and mGST. (n=8, mean±SD, $^aP<0.05$, $^bP<0.01$ compared with control group).

Table 3 Influence of ASP on P450 content, P450 isoform activities and activities of S9-GSTpi, S9-GST and mGST

Group	Control	ASP1	ASP2	ASP3
P-450 (nmol/mg·pro)	1.4±0.4	2.1±0.4[b]	1.2±0.4	0.60±0.13[b]
NADPH-C (nmol/min·mg·pro)	14.5±2.8	19.7±2.2[b]	19.1±4.3[a]	7.6±1.1[b]
ANH (nmol/min·mg·pro)	0.038±0.009	0.045±0.009[b]	0.018±0.006[b]	0.010±0.003[b]
AMD (nmol/min·mg·pro)	0.96±0.07	1.29±0.11[b]	1.11±0.19	0.61±0.16[b]
EMD (nmol/min·mg·pro)	0.89±0.06	1.30±0.21	1.14±0.33	0.41±0.09[b]
S9-GSTpi (nmol/min·mg·pro)	1.07±0.28	1.2±0.3	1.15±0.26	0.78±0.19[a]
S9-GST (nmol/min·mg·pro)	8.3±0.9	0.5±1.9[a]	11.8±1.5[a]	7.9±0.7[a]
mGST (nmol/min·mg·pro)	0.25±0.03	0.29±0.03[a]	0.35±0.08[b]	0.155±0.016[b]

ASP1, ASP2, ASP3: Mice were given 30, 60, and 120 mg/kg ASP, ig, qd×7 d, respectively and sacrificed on day 7. The hepatic microsome was prepared to assay the content of P450, and activities of P450 isoforms, S9-GSTpi, S9-GST and mGST. (n=8, mean± SD, [a]P<0.05, [b]P<0.01 compared with control group).

AMD, EMD were obviously increased by 50.0%, 35.9%, 18.4%, 34.4%, and 46.1% after 30 mg/kg ASP treatment, and obviously decreased by 57.1%, 47.6%, 73.7%, 36.5%, and 53.9% after 120 mg/kg ASP treatment, respectively. Thirty and 60 mg/kg of ASP could increase the activity of S9-GST by 26.5%, 42.3%, respectively. The alterations of mGST activity were similar to those of S9-GST. The activities of S9-GST and mGST were reduced by 4.8%, 38.0% after administration of 120 mg/kg ASP, respectively. No changes in S9-GSTpi were observed (Table 3).

Influence of different dose of $GdCl_3$ on activities of S9-GSTpi, S9-GST and mGST

S9-GST activity was increased by 18.1%, 22.9% after 10 mg and 20 mg/kg of $GdCl_3$ treatment, respectively, and the alterations in mGST activity were similar to those of S9-GST. No changes in S9-GSTpi were observed (Table 4).

Table 4 Influence of different dose of $GdCl_3$ on activities of S9-GSTpi, S9-GST and mGST

Group	S9-GSTpi	S9-GST	mGST
	(nmol/min·mg·pro)		
Control	1.07±0.28	8.3±0.9	0.25±0.03
$GdCl_3$10-1d	1.16±0.0.19	9.8±1.5[a]	0.289±0.026[a]
$GdCl_3$20-1d	0.93±0.17	10.2±1.5[a]	0.28±0.06
$GdCl_3$40-1d	0.91±0.12	7.9±0.8	0.264±0.012

The administration of $GdCl_3$ and the treatment of animals were the same as described in Table 1. S9-GST: glutathione s-transferase in S9; S9-GSTpi: glutathione s-transferase pi in S9; mGST: glutathione s-transferase in microsome. (n=8, mean±SD, [a]P<0.05 compared with control group).

DISCUSSION

Neyrinck *et al*.[16,17] reported that Kupffer cells might play a role of xenobiotic metabolism in hepatocytes *in vitro*, and treatment of $GdCl_3$ could decrease the total hepatic content of cytochrome P450. Kupffer cells were involved in some liver diseases in which the activities of drug metabolic enzymes changed[18,19]. Few studies until now have reported an effect of $GdCl_3$ injection on the activities of specific CYP isoforms and GST, and on the time course of developmental changes of their activities after Kupffer cells blocked by $GdCl_3$ *in vivo*. The present study showed that Kupffer cell blockade indicated a tendency to decrease cytochrome P450 content and its isoform activities, and to increase GST (including S9-GST, and mGST) activities. However, CYP isoforms and GST activities showed different changes following different time of Kupffer cell blockade. The total cytochrome P450 content, NADPH-C and ANH (as marker of CYP2E1) activities had a sustained decrease following prolonged Kupffer cell blockade, but AMD, EMD (as marker of CYP3A) activities obviously raised 3 d after Kupffer cell blockade, and GST activities kept a high level 6d after Kupffer cell blockade. Some authors have already reported that the treatment of $GdCl_3$ causing inactivation of Kupffer cells could protect liver against damage induced by some toxic chemicals (such as ethanol, CCl_4, *etc*.) through inhibiting CYP2E1[20, 21]. The present study offered further support for a relevant role of Kupffer cells through the control of hepatocyte metabolism mediated liver injury. CYP3A contributed significantly to the biotransformation of xenobiotic chemicals such as drugs, and toxic chemicals[22]. GSTs constitute a multigene family of phase II conjugating enzymes broadly distributed phylogenetically. Detoxification of electrophilic compounds by GSTs may occur via catalytic conjugation of electrophilic intermediates with GSH, via GSH-dependent reduction of organic peroxides, or via direct binding to lipophilic compounds. GST might have an important cytoprotective function[23]. The current study showed CYP3A and GST activities were rapidly recovered, which might be a self-regulated and self-protected mechanism of the body.

The changes in CYP and GST activities were related with the state of Kupffer cells activated by Angelica sinensis polysaccharides (ASP). Now, some new functions of ASP have been reported. ASP could promote ulcer healing, protect hepatic injury and might have antitumor effects[24-26]. Immunoactivity is the most important function of ASP. It could enhance the proliferative response of lymphocytes *in vitro* and differential expression of genes in the liver of immunological injury mice[27,28]. In the present study, 30 mg/kg ASP could increase cytochrome P450 content , P450 isoform activities and GST activities. However, 120 mg/kg ASP could obviously decrease the activities of these enzymes. This phenomenon might be concerned with the immunoactivity of ASP. Its mechanism remains to be further studied.

GSTpi, a glutathion s-transferase of placenta type, often presented high expression in tumor tissues related with drug resistance[29]. The present study indicated that GSTpi activity was not influenced by Kupffer cell blockade or activated, suggesting that GSTpi activity is not easily induced in normal tissues.

In conclusion, Kupffer cells and their adjacent hepatocytes capable of regulating interactions could be demonstrated[30], suggesting that Kupffer cells may mediate hepatic functions including drug metabolism.

REFERENCES

1 **Jarin C**, Ute MK, Rachel MM, Lawrence MS, Paul FH. Mechanism-based inactivation of cytochromes P450 2B1 and P450 2B6 by 2-phenyl-2 (1-piperidinyl) propane. *Drug Metab Dispos* 2000; **8**: 905-911

2 **Li AP**, Maurel P, Gomez-lechon MJ, Cheng LC, Jurima-Romet

M. Preclinical evaluation of drug-drug interaction potential: present status of the application of primary human hepatocytes in the evaluation of cytochrome P450 induction. *Chem Biol Interact* 1997; **2**: 5-16

3 **Harris R**, Jang G, Tsunoda S. Dietary effects on drug metabolism and transport. *Clin Pharmacokinet* 2003; **13**: 1071-1088

4 **Paolini M**, Biagi GL, Cantelli-Forti G. The many consequences of chemical- and genetic-based modulation of drug metabolizing enzyme activities. *Life Sci* 1999; **8**: 75-79

5 **Nicholson TE**, Renton KW. Modulation of cytochrome P450 by inflammation in astrocytes. *Brain Res* 1999; **8**: 12-18

6 **Bennis RK**, Bethany K, Yuji I, Ronald GT. Gadolinium chloride blocks alcohol-dependent liver toxicity in rats treated chronically with inytagastric alcohol despite the induction of CYP2E1. *Mol Pharma* 1997; **2**: 944-950

7 **Kim SG**, Choi SH. Gadolinium chloride inhibition of rat hepatic microsomal epoxide hydrolase and glutathione S-transferase gene expression. *Drug Metab Dispos* 1997; **12**: 1416-1423

8 **Lake BG**. Preparation and characterisatuon of microsomal fractions for studies of xenobiotic metabolism. *Biochemical Toxicology: A Practical Approach. IRL Press, Oxford* 1987; 189-215

9 **Lowry OH**, Rosebrough NJ, Farr AL, Randall RJ. Protein measurement with the Folin phenol reagent. *J Biol Chem* 1951; **193**: 265-275

10 **Badger DA**, Sauer JM, Hoglen NC, Jolley CS, Sipes IG. The role of inflammatory cells and cytochrome P450 in the potentiation of CCl4-induced liver injury by a single dose of retinol. *Toxicol Appl Pharmacol* 1996; **2**: 507-519

11 **Williams** CH Jr, Kamin H. Microsomal triphosphopyridine nucleotide-cytochrome c reductase of liver. *J Biol Chem* 1962; **237**: 587-595

12 **Wang H**, Peng RX, Zhang YH, Chen JH, Li QX, Kong R, Ding H, Yu JP. Demethylation capacity of human fetal adrenal mitochrondrial cytochrome P-450 *in vitro*. *Acta Pharmacol Sin* 1999; **4**: 358-367

13 **Badger DA**, Kuester RK, Sauer JM, Sipes IG. Gadolinium chloride reduces cytochrome P450: relevance to chemical-induced hepatotoxicity. *Toxicolgy* 1997; **2**: 143-153

14 **Kim SG**, Chung HC, Cho JY. Molecular mechanism for alkyl sulfide-modulated carbon tetrachloride-induced hepatotoxicity: the role of cytochrome P450 2E1, P45 02B and glutathione S-transferase expression. *J Pharmacol Exp Ther* 1996; **2**: 1058-1066

15 **Sundberg K**, Jernstrom B, Swedmark S. Studies on the differential inhibition of glutathione conjugate formation of (+)-anti-benzo(a) pyren 7,8-dihydrodiol 9,10-epoxide and 1-chloro-2, 4-dinitrobenzene in V79 Chinese hamster cells. *Biochem J* 2000; **349**: 693-696

16 **Neyrinck A**, Eeckhoudt SL, Meunier CJ, Pampfer S, Taper HS, Verbeeck R. Modulation of paracetamol metabolism by Kupffer cells: a study on rat liver slices. *Lif Sci* 1999; **26**: 2851-2859

17 **Milosevic N**, Schawalder H, Maier P. Kupffer cell-mediated differential down-regulation of cytochrome P450 metabolism in rat hepatocytes. *Eur J Pharmacol* 1999; **1**: 75-87

18 **Lee WY**, Lee SM. The roles of Kupffer cells in hepatocellular dysfunction after femur fracture trauma in rats. *Arch Pharm Res* 2003; **1**: 47-52

19 **Niemela O**, Parkkila S, Bradford B, Iimuro Y, Pasanen M, Thurman RG. Effect of Kupffer cell inactivation on ethanol-induced protein adducts in the liver. *Free Radic Biol Med* 2002; **3**: 350-355

20 **Gouillon ZQ**, Miyamoto K, Sonohue TM, Wan YJ, French BA, Nagao Y, Fu P, Reitz RC, hagbjork A, Yap C, Yuan QX, Ingelman-Sundberg M, French SW. Role of CYP2E1 in the pathogenesis of alcoholic liver disease: modifications by cAMP and ubiquitin-proteasome pathway. *Front Biosci* 1999; **4**: A16-25

21 **Badger DA**, Sauer JM, Hoglen NC, Jooey CS, Sipes IG. The role of inflammatory cells and cytochrome P450 in the potentiation of CCl4-induced liver injury by a single dose of retinol. *Toxicol Appl Pharmacol* 1996; **2**: 507-519

22 **Zhang W**, Parentau II, Greenly RL, Metz CA, Affarwal S, Wainer IW, Tracy TS. Effect of protein-calorie malnutrition on cytochromes P450 and glutathione S-transferase. *Eur J Drug Metab Pharmacokinet* 1999; **2**: 141-147

23 **Choi SH**, Kim SG. Lipopolysaccharide inhibition of rat hepatic microsomal epoxide hydrolase and glutathione S-transferase gene expression irrespective of nuclear factor-kappaB activation. *Biochem Pharmacol* 1998; **11**: 1427-1436

24 **Ye YN**, So HL, Liu ES, Shin VY, Cho CH. Effect of polysaccharides from Angelica sinensis on gastric ulcer healing. *Life Sci* 2003; **8**: 925-932

25 **Ye YN**, Liu ES, Li Y, So HL, Cho CC, Sheng HP, Lee SS, Cho CH. Protective effect of polysaccharides-enriched fraction from Angelica sinensis on hepatic injury. *Life Sci* 2001; **6**: 637-646

26 **Shang P**, Qian AR, Yang TH, Jia M, Mei QB, Cho CH, Zhao WM, Chen ZN. Experimental study of anti-tumor effects of polysaccharides from Angelica sinensis. *World J Gastroenterol* 2003; **9**: 1963-1967

27 **Shan JJ**, Wang Y, Wang SC, Liu D, Hu ZB. Effect of Angelica sinensis polysaccharides on lymphocyte proliferation and induction of IFN-gamma. *Yaoxue Xuebao* 2002; **7**: 497-500

28 **Ding H**, Shi GG, Yu X, Yu JP, Huang JA. Modulation of GdCl3 and Angelica sinensis polysaccharides on differentially expressed genes in liver of hepatic immunological injury mice by cDNA microarray. *World J Gastroenterol* 2003; **5**: 1072-1076

29 **Mayr D**, Pannekamp U, Baretton GB, Gropp M, Meier W, Flens MJ, Scheper R, Biebold J. Immunohistochemical analysis of drug resistance-associated proteins in ovarian carcinomas. *Pathol Res Pract* 2000; **7**: 469-475

30 **Milosevic N**, Schawalder H, Maier P. Kupffer cell-mediated differential down-regulation of cytochrome P450 metabolism in rat hepatocytes. *Eur J Pharmacol* 1999; **8**: 75-87

Edited by Zhang JZ and Wang XL **Proofread by** Xu FM

PO Box 2345, Beijing 100023, China
Fax: +86-10-85381893
E-mail: wjg@wjgnet.com www.wjgnet.com

World J Gastroenterol 2004;10(9):1329-1332
World Journal of Gastroenterology
Copyright ©2004 by The WJG Press ISSN 1007-9327

• BASIC RESEARCH •

Peroxisome proliferator activated receptor-g in pathogenesis of experimental fatty liver disease

Cai-Yan Zhao, Ling-Ling Jiang, Li Li, Zhuo-Jun Deng, Bao-Li Liang, Jian-Mei Li

Cai-Yan Zhao, Ling-Ling Jiang, Department of Biochemistry, Hebei Medical University, Shijiazhuang 050017, Hebei Province, China
Li Li, Zhuo-Jun Deng, Bao-Li Liang, Jian-Mei Li, Department of Liver Disease, Third Affiliated Hospital of Hebei Medical University, Shijiazhuang 050051, Hebei Province, China
Correspondence to: Ling-Ling Jiang, Department of Biochemistry, Hebei Medical University, Shijiazhuang 050017, Hebei Province, China. zhaoyy63811@sohu.com
Telephone: +86-13313012898
Received: 2003-10-29 **Accepted:** 2004-01-08

Abstract

AIM: To study the expression of peroxisome proliferator activated receptor-γ (PPARγ) in the liver of rats with fatty liver disease (FLD) and to explore the role of PPARγ in the pathogenesis of FLD to provide the basis for using PPARγ ligand to treat patients with FLD.

METHODS: Forty Wistar rats were divided into 4 groups of ten rats each randomly: normal group (group A), alcohol group (group B), fat-rich diet group (group C), alcohol and fat-rich diet group (group D). The rats were sacrificed at the end of the 16th week from the feeding day. Alanine aminotransferase (ALT), tumor necrosis factor-alfa (TNFα) in serum and malondialdehyde (MDA) in liver homogenate were determined; livers were collected for observing pathologic changes by HE, Sudan IV, Masson stain under microscope. The morphologic results were analyzed by picture quantitative analysis technique. The changes of ultrastructure were also examined under electron microscope. The expression of PPARγ in liver was detected by immunohistochemistry and RT-PCR. The correlations between the expression of PPARγ and biochemical indexes, and liver histology were analyzed.

RESULTS: The steatosis, inflammation, necrosis and fibrosis were present in livers of different experimental groups, especially in livers of alcohol and fat-rich diet group. The content of immunodetectable PPARγ was decreased remarkably in the livers of model rats (group B-D); the level in alcohol and fat-rich diet group (3.43±1.48) was significantly lower than that in normal group (18.34±3.73), alcohol group (8.82±2.52) and fat-rich diet group (11.73±2.51) (all $P<0.01$). The level of PPARγ mRNA was also lower in the livers of model rats (group B-D) than in livers of controls. The expression of PPARγ in rat liver correlated negatively with the degree of its inflammation, necrosis and fibrosis, as well as the level of serum TNFα and the content of MDA in liver homogenates, but not with steatosis or serum ALT.

CONCLUSION: Decreased expression of PPARγ may play an important role in the development of hepatocellular inflammation, necrosis and fibrosis of rats with FLD. Thus, activating PPARγ by its ligand can be anticipated to provide a therapy target for FLD.

Zhao CY, Jiang LL, Li L, Deng ZJ, Liang BL, Li JM. Peroxisome proliferator activated receptor-γ in pathogenesis of experimental fatty liver disease. *World J Gastroenterol* 2004; 10(9): 1329-1332
http://www.wjgnet.com/1007-9327/10/1329.asp

INTRODUCTION

Fatty liver disease (FLD) includes alcoholic liver disease (ALD) caused by alcohol and non-alcoholic fatty liver disease (NAFLD) due to obesity, hypertriglyceridemia and other factors. The pathogenesis is not clear now. Some scholars put forward the tale of two or multiple "hits"[1]. The first hit is steatosis by ethanol or insulin resistance which offers substrates for lipid peroxidation. The second hit is alcoholic hepatitis or nonalcoholic steatohepatitis (NASH) caused by oxidative stress and lipid superoxidation. The release of the inflammation mediator, inflammation and necrosis can be found in hepatocytes[2-6]. Liver fibrosis or cirrhosis is the third hit because the synthesis of extracellular matrix exceeds the decomposition of it or inflammation is continuous. Why excess hepatocellular fat can induce inflammation or even fibrosis in the liver? The pathogenesis is not clarified up now. Peroxisome proliferator-activated receptor-gamma (PPARγ), is one member of the nuclear hormone receptor superfamily that can be activated by various ligands. Recent studies showed that this transcription factor associated not only with adipocyte differentiation, insulin resistance, sugar and lipid metabolism[7-10], but also with the regulation of inflammation, hepatocyte proliferation and the apoptosis in human liver cancer cells[11-17]. The role of PPARγ in FLD has not been well addressed and some studies even showed contrary results. The present study was designed to characterize PPARγ activity in liver of rats with FLD so to explore whether PPARγ ligand could be used as a potential therapeutic agent for FLD.

MATERIALS AND METHODS

Rat model of fatty liver disease

Forty female Wistar rats (from the Animal Center of Hebei Medical University) were divided into 4 groups of ten rats each randomly. Rats in normal group (group A) received standard diet and intragastric saline (1.5 mL/100 g body mass) twice daily. Rats in alcohol group (group B) were intragastrically fed twice a day initially with 400 mL/L ethanol (1.5 mL/100 g body weight) for 4 wk, with 500 mL/L ethanol for 4 wk and then with 60% ethanol for 8 wk on the basis of standard diet. Rats in fat-rich diet group (group C) were fed with high fat diet (standard diet with 10% lard and 2% cholesterin) and given intragastrically with saline twice a day. Rats in alcohol and fat-rich diet group (group D) had the same high fat diet as rats in group C and took the same ethanol as rats in group B.

Preparation of samples

Serum from rats fasted for 12 h was isolated and stored at -70 ℃ for alanine aminotransferase (ALT) and tumor necrosis factor alfa (TNFα) determination. Liver was homogenized in 10 volumes of 0.01 mol/L sucrose containing 10 mmol/L Tris -Cl^-, pH 7.4, and 0.1 mmol/L ethylenediaminotetraacetic acid and

centrifuged at 3 000 r/mim for 10 min at 4 ℃ and the supernatant was stored at -70 ℃ for MDA assay. A small sample of liver was stored in liquid nitrogen for isolation of total RNA. The others were fixed in 40 g/L fomaldehyde for light microscopy or in 40 g/L paraformaldehyde for immunohistochemistry and in 40 g/L glutaraldehyde for electron microscopy.

Biochemical indexes

Serum ALT, TNFα were measured using an auto-biochemical analyzer (Olympus AU 2700) and radio-immuno- assay (Beijing Furui) respectively. MDA in liver homogenates was detected using TBA kit (Nanjing Jiancheng).

Liver histology

Livers were fixed in 40 g/L buffered formaldehyde, embedded in paraffin, sectioned, and stained with hematoxylin-eosin for routine examination and with Sudan IV for steatosis or with Masson for fibrosis. The steatosis and collagen were quantified as the percentage of positive area by multifunctional pathological image analyzer (Beijing Aerospace University). The activity of necro- inflammation was scored between 1 to 4 blindly by an independent pathologist. The ultrastructure of the livers was observed by HITACHI H7500 transmission electron microscope (TEM) after the samples underwent 40 g/L glutaraldehyde-osmic acid fixation, epoxy resin embedding and ultrathin section.

Immunohistochemistry

In brief, paraffin-embedded tissue specimens and controls were sectioned at a thickness of 4 μm, deparaffinized, and rehydrated. The slides were incubated with 30 mL/L hydrogen peroxide in methanol for 10 min to block endogeneous peroxidase activity and then washed twice in phosphate -buffered saline (PBS) for 5 min. Antigen in sections was retrieved by microwave. Sections were then blocked with 10% goat serum and incubated (12 h at 4 ℃) with the primary antibody (mouse anti-rat monoclonal antibody of PPARγ, E-8, 1:100, Santa Cruz). After being washed twice for 15 min in PBS, sections were incubated (30 min at 37 ℃) with the secondary antibody (goat anti -mouse IgG marked by biotin), with streptoavidin marked by horseradish peroxidase, and then with DAB (Beijing Zhongshan). Then, 0.01 mol/L PBS was substituted for primary antibody as the negative control. The positive cells presented brownish yellow. Quantitative analysis was done by a multifunctional pathological image analyzer. Ten high power fields were examined randomly per sample.

Reverse transcriptase-polymerase chain reaction

Total RNA was isolated from liver using a modification of the single -step guanidinium-phenol-chloroform method. cDNA was obtained by reverse transcription (Promega kit) and then subjected to PCR amplification with GAPDH as standard reference (452 bp). A 403 bp PPARγ gene fragment was amplified with the following primers: up 5' -TATCATAAATAAGCTT CAATCGGATG GTTC -3' and down 5' -ACCACAGTCCATG CCATCAC-3' . The primers were designed according to the published sequences[18] and synthesized by Shanghai Biology Engineering Corporation. Thirty-two cycles of amplification were performed at 94 ℃ for 5 min, then at 94 ℃ for 30 s, at 57 ℃ for 45 s, and at 72 ℃ for 1 min, with a final extension at 72 ℃ for 5 min. The PCR reaction mixture was electrophoresed in 5% SDS-polyacrylamide gel, and observed by EB staining under UV light. The optical density of EB-stained DNA bands was analyzed by BIO-PROFIL picture analysis system and the ratio of PPARγ to GAPDH was calculated.

Statistical analysis

SAS8.0 package was used to process all data. Results were expressed as mean±SD. Student's *t*-test was used for the comparison between two groups. Group means were compared by ANOVA followed by the Student-Newman- Keuls test if the former was significant. Differences were considered significant when $P<0.05$. Linear regression analysis was used for relativity analysis.

RESULTS

Biochemistry

The biochemical features are outlined in Table 1. Serum ALT, TNFα and MDA in liver homogenates were elevated significantly, particularly in group D.

Table 1 Biochemical features of rats with fatty liver disease

Group	n^1	ALT (U/L)	TNFα (μg/L)	MDA (μmol/g)
A	10	34±9.02	1.36±0.35	5.71±0.25
B	9	119±17.15[a]	3.39±0.42[a]	7.26±0.32[a]
C	10	103±17.24[a]	3.02±0.37[a]	6.72±0.31[a]
D	9	125±16.51[a]	5.01±0.52[a,b,d]	9.12±0.42[a,b,d]

[a]$P<0.05$ *vs* the normal control; [b]$P<0.01$ *vs* the alcohol group; [d]$P<0.01$ *vs* the fat-rich diet group, [1] One rat died in groups B, D respectively in the process of experiment.

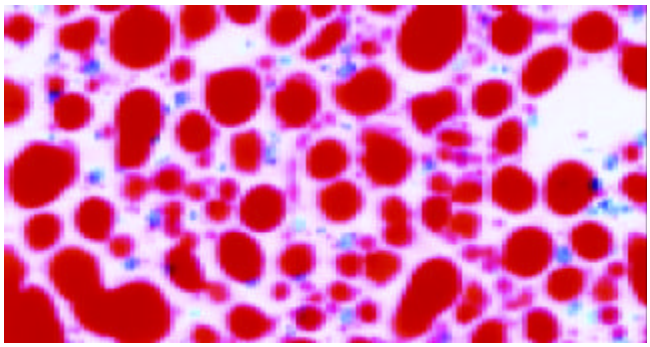

Figure 1 Swelling, diffusive steatosis of hepatocytes (SudanIV 40×).

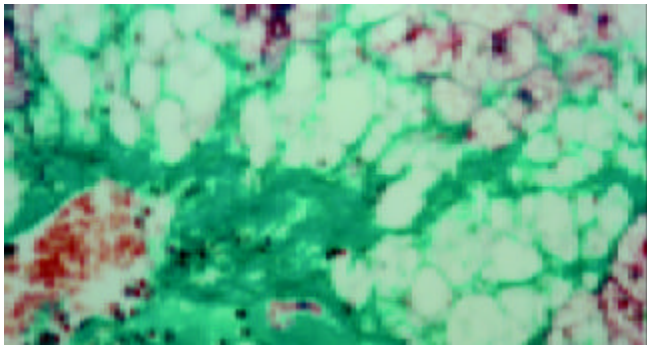

Figure 2 Central vein fibrosis (Masson 40×).

Liver histology

The quantitative evaluation of the liver histology of rats in each group is shown in Table 2. The livers of model rats (group B-D) were engorged with microvesicular and macrovesicular fat, particularly in alcohol and high-fat group (group D) (Figure 1). The hepatocytes of rats in alcohol group presented inflammation, and centrolobular (zone 3) cloudy swelling, ballooning degeneration, spotty necrosis with either pericellular fibrosis or Mallory body. The hepatic sinusoids became narrowed significantly. The infiltration of inflammatory cells, especially

neutrophilic granulocytes could be seen in the portal areas, and there was fibrosis around the hepatic sinusoids. Focal necrosis or piecemeal necrosis (PN) even bridge necrosis (BN) in alcohol and fat-rich diet group could be found. Around these areas there were a large number of inflammatory cells. Perisinusoid fibrosis and central vein fibrosis could be seen (Figure 2) and the vein wall became thick even occluded. The portal area was enlarged, the fibrous tissue proliferated and extended to interlobular area. Under TEM, the nuclear membrane was tortuous, the nuclear chromatin agglutinated into blocks in hepatocytes of the model rats (groups B-D). The cytoplasm was loose and had more or less fat. The mitochondria swelled and proliferated and sometimes huge mitochondria could be seen. Some of the sinusoids were capillarized. Activated stellate cells and perisinusoid fibrosis could be observed distinctly (Figure 3).

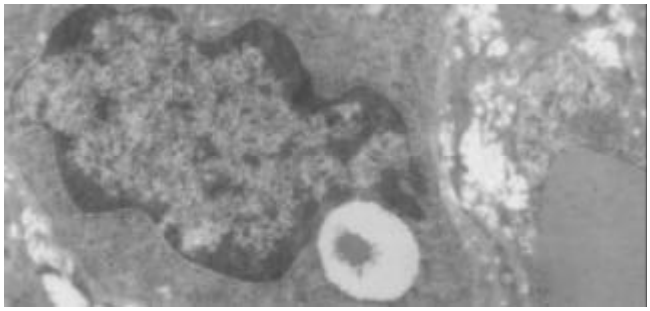

Figure 3 Activated stellate cells and perisinusoid fibrosis (TEM ×8 000).

Table 2 Quantitative evaluation of liver histology of rats (%)

Groups	*n*	Steatosis	Inflammation and necrosis	Collagen
A	10	1.34±0.33	0.67±0.66	2.03±0.87
B	9	12.79±2.73[a]	4.35±0.56[a]	11.85±3.89[a]
C	10	35.82±8.52[a,b]	3.05±0.72[a]	7.90±2.79[a,b]
D	9	37.97±11.48[a,b]	5.71±1.03[a,c]	19.02±4.01[a,b,c]

[a]$P<0.01$ *vs* the normal control; [b]$P<0.05$ *vs* the alcohol group; [c]$P<0.05$ *vs* the fat-rich diet group.

Expression of PPARg

The level of PPARγ protein and mRNA in rat livers detected by immunohistochemistry and RT-PCR respectively is shown in Table 3. The levels of PPARγ expression were decreased significantly in model groups (groups B-D), especially in group D (Figure 4).

Table 3 Level of PPARγ protein and mRNA in rat livers (%)

Group	*n*	PPARγ protein	PPARγ mRNA
A	10	18.34±3.73	0.8097±0.098
B	9	8.82±2.52[a]	0.2530±0.072[a]
C	10	11.73±2.51[a]	0.3647±0.084[a]
D	9	3.43±1.48[a,b,d]	0.1226±0.054[a,b,d]

[a]$P<0.05$ *vs* the normal control; [b]$P<0.01$ *vs* the alcohol group; [d]$P<0.01$ *vs* the fat-rich diet group.

Relationship between levels of PPARg protein and biochemical and histological parameters

The correlation analysis showed that the expression of PPARγ protein in the liver of model rats (group B-D) was associated negatively with the level of serum TNFα, the content of MDA in the liver, the degree of liver inflammation, necrosis, and fibrosis, but not associated with the degree of liver steatosis and the level of serum ALT (Table 4).

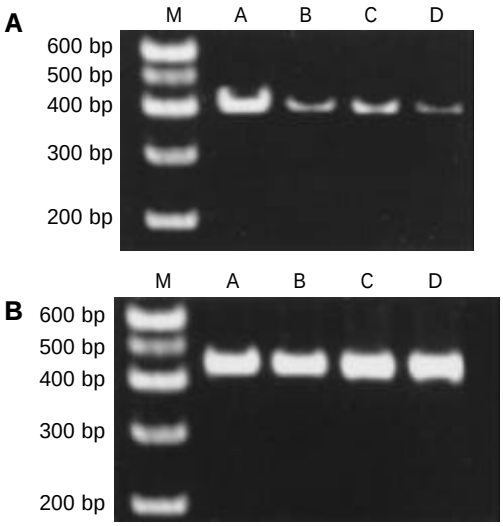

Figure 4 Expression of PPARγ mRNA and GAPDH mRNA in the liver of rats with FLD (Note: from left to right M: PCR marker; lane A: normal control; lane B: alcohol group; lane C: fat-rich diet group. Lane D: alcohol and fat-rich diet group). A: Expression of PPARγ mRNA in the liver of rats with FLD, B: Expression of GAPDH mRNA in the liver of rats with FLD.

Table 4 Correlation between levels of PPARγ protein and biochemical, histological parameters in model rats (*r* value)

Groups	ALT	TNFα	MDA	Steatosis	Inflammation	Fibrosis
B	-0.263	-0.745[b]	-0.560[a]	-0.437	-0.568[b]	-0.728[a]
C	-0.493	-0.662[a]	-0.772[b]	-0.323	-0.671[a]	-0.812[b]
D	-0.352	-0.624[b]	-0.781[b]	-0.329	-0.891[b]	-0.679[b]

[a]$P<0.05$ *vs* the normal control the alcohol group [b]$P<0.01$.

DISCUSSION

It is well known that PPARγ is one of the nuclear transcription factors activated by ligands and belongs to type II nuclear receptor superfamily. It includes 3 subtypes as PPARα, PPARδ and PPARγ. PPARα is expressed abundantly in liver associated with lipid deposition and certain amount of PPARγ could be found in liver possibly related to the inflammation[19-30]. The experiment *in vitro* proved that the activation of PPARγ could inhibit the secretion of cytokines and chemokines. For example, the activation of PPARγ could inhibit the secretion of IL-6, IL-1 and TNFα induced by lipopolysaccharide (LPS)[31]. Kon proved that pioglitazone (1 mg/kg body weight), the ligand of PPARγ could prevent liver from inflammation, necrosis and increase of serum TNFα caused by carbon tetrachloride. At the same time pioglitazone could inhibit the expression of α-SMA and type I precollagenin of primary cultured hepatic stellate cells (HSC_s)[11,32]. The activation of HSC was the basis of liver fibrosis. Everett's research also proved that activation of PPARγ could inhibit the activation of cultured HSC *in vitro*[19]. We speculated that decreased expression and dysfunction of PPARγ might correlate with the release of inflammatory mediator and fibrosis during the process of liver injury due to alcohol and high fat diet.

Our data showed that there were steatosis, inflammation and centrolobular ballooning degeneration, necrosis with fibrosis in the livers of rats fed with either alcohol or high fat diet, especially in the rats fed with both alcohol and high fat. The expression of PPARγ in the liver of rats with FLD (groups

B, C, D) decreased significantly particularly in group D compared to the normal control ($P<0.05$). The correlation analysis indicated that except for steatosis ,the expression of PPARγ correlated negatively with the levels of liver MDA, serum TNFα and the degree of inflammation and fibrosis in livers of rats with FLD. These suggested that the weaker the PPARγ expressed, the more severe the liver would be damaged. High-fat diet could deteriorate liver damage and promote liver fibrosis by increasing the lipid deposition, lipid peroxidation and inhibiting PPARγ expression in the liver. It proved that PPARγ played a very important role in the cascade reaction of lipid peroxidation - release of inflammation cytokines -damage of liver - liver fibrosis of rats with FLD. It might be one of the initiation factors. Therefore, the ligand of PPARγ might block the development of inflammation, necrosis and fibrosis of FLD and be potentially used for FLD treatment.

REFERENCES

1 **Day CP**, James OF. Steatohepatitis: a tale of two "hits". *Gastroenterology* 1998; **114**: 842-845

2 **Chitturi S**, George J. Interaction of iron, insulin resistance, and nonalcoholic steatohepatitis. *Curr Gastroenterol Rep* 2003; **5**: 18-25

3 **Gao ZQ**, Lu FE. Free fatty acid, insulin resistance and nonalcoholic steatohepatitis. *Shijie Huaren Xiaohua Zazhi* 2003; **11**: 1043-1045

4 **Fan JG**. Steat ohepatitis studies. *Shijie Huaren Xiaohua Zazhi* 2001; **9**: 6-10

5 **Chitturi S**, Abeygunasekera S, Farrell GC, Holmes-Walker J, Hui JM, Fung C, Karim R, Lin R, Samarasinghe D, Liddle C, Weltman M, George J. NASH and insulin resistance: Insulin hypersecretion and specific association with the insulin resistance syndrome. *Hepatology* 2002; **35**: 373-379

6 **Wu Q**, Cheng J, Li L. Study on alcoholic fatty liver disease. *Shijie Huaren Xiaohua Zazhi* 2002; **10**: 1037-1038

7 **Bedoucha M**, Atzpodien E, Boelsterli UA. Diabetic KKAY mice exhibit increased hepatic PPAR gamma 1 gene expression and develop hepatic steatosis upon chronic treatment with antidiabetic thiazolidinediones. *J Hepatol* 2001; **35**: 17-23

8 **Kersten S**. Peroxisome proliferator activated receptors and obesity. *Eur J Pharmacol* 2002; **440**: 223-234

9 **Clarke SD**, Thuillier P, Baillie RA, Sha X. Peroxisome proliferator -activated receptors: a family of lipid-activated transcription factors. *Am J Clin Nutr* 1999; **70**: 566-571

10 **Kersten S**, Mandard S, Escher P, Gonzalez FJ, Tafuri S, Desvergne B, Wahli W.The peroxisome proliferator-activated receptor alpha regulates amino acid metabolism. *FASEB J* 2001; **15**: 1971-1978

11 **Kon K**, Ikejima K, Hirose M, Yoshikawa M, Enomoto N, Kitamura T, Takei K, Sato N. Pioglitazone prevents early-phase hepatic fibrogenesis caused by carbon tetrachloride. *Biochem Biophys Res Commun* 2002; **291**: 55-61

12 **Marra F**, Efsen E, Romanelli RG, Caligiuri A, Pastacaldi S, Batignani G, Bonacchi A, Caporale R, Laffi G, Pinzani M, Gentilini P. Ligands of peroxisome proliferator –activated receptor gamma modulate profibrogenic and proinflammatory actions in hepatic stellate cells. *Gastroenterology* 2000; **119**: 466-478

13 **Li MY**, Deng H, Zhao JM, Dai D, Tan XY. Peroxisome proliferator-activated receptor gamma ligands inhibit cell growth and induce apoptosis in human liver cancer BEL-7402 cells. *World J Gastroenterol* 2003; **9**: 1683-1688

14 **Li MY**, Deng H, Zhao JM, Dai D, Tan XY. PPARgamma pathway activation results in apoptosis and COX-2 inhibition in HepG2 cells. *World J Gastroenterol* 2003; **9**: 1220-1226

15 **Kersten S**, Desvergne B, Wahli W. Roles of PPARs in health and disease. *Nature* 2000; **405**: 421-424

16 **Rao MS**, Peters JM, Gonzalez FJ, Reddy JK. Hepatic regeneration in peroxisome proliferator-activated receptor alpha-null mice after partial hepatectomy. *Hepatol Res 2002*; **22**: 52-57

17 **Yu S**, Rao S, Reddy JK. Peroxisome proliferator-activated receptors, fatty acid oxidation, steatohepatitis and hepatocarcinogenesis. *Curr Mol Med* 2003; **3**: 561-572

18 **Braissant O**, Foufelle F, Scotto C, Dauca M, Wahli W. Differential expression of peroxisome proliferator-activated receptors (PPARs): tissue distribution of PPAR-α, - β, and –γ in the adult rat. *Endocrinology* 1996; **137**: 354-366

19 **Everett L**, Galli A, Grabb D. The role of hepatic peroxisome proliferator -activated receptors (PPARs) in health and disease. *Liver* 2000; **20**: 191-199

20 **Reddy JK**, Hashimoto T. Peroxisomal beta-oxidation and peroxisome proliferator-activated receptor alpha: an adaptive metabolic system. *Annu Rev Nutr* 2001; **21**: 193-230

21 **Qi C**, Zhu Y, Reddy JK. Peroxisome proliferator-activated receptors, coactivators, and downstream targets. *Cell Biochem Biophys* 2000; **32**: 187-204

22 **Qi C**, Zhu Y, Pan J, Usuda N, Maeda N, Yeldandi AV, Rao MS, Hashimoto T, Reddy JK. Absence of spontaneous peroxisome proliferation in enoyl-CoA Hydratase/L-3-hydroxyacyl-CoA dehydrogenase-deficient mouse liver. Further support for the role of fatty acyl CoA oxidase in PPARalpha ligand metabolism. *J Biol Chem* 1999; **274**: 15775-15780

23 **Yu S**, Matsusue K, Kashireddy P, Cao WQ, Yeldandi V, Yeldandi AV, Rao MS, Gonzalez FJ, Reddy JK. Adipocyte-specific gene expression and adipogenic steatosis in the mouse liver due to peroxisome proliferator-activated receptor gamma1 (PPARgamma1) overexpression. *J Biol Chem* 2003; **278**: 498-505

24 **Hashimoto T**, Cook WS, Qi C, Yeldandi AV, Reddy JK, Rao MS. Defect in peroxisome proliferator-activated receptor alpha-inducible fatty acid oxidation determines the severity of hepatic steatosis in response to fasting .*J Biol Chem* 2000; **275**: 28918-28928

25 **Kersten S**, Seydoux J, Peters JM, Gonzalez FJ, Desvergne B, Wahli W. Peroxisome proliferator-activated receptor alpha mediates the adaptive response to fasting. *J Clin Invest* 1999; **103**: 1489-1498

26 **Reddy JK**. Nonalcoholic steatosis and steatohepatitis. III. Peroxisomal beta-oxidation, PPAR alpha, and steatohepatitis. *Am J Physiol Gastrointest Liver Physiol* 2001; **281**: G1333-1339

27 **Rao MS**, Reddy JK. Peroxisomal beta-oxidation and steatohepatitis. *Semin Liver Dis* 2001; **21**: 43-55

28 **Fan CY**, Pan J, Usuda N, Yeldandi AV, Rao MS, Reddy JK. Steatohepatitis, spontaneous peroxisome proliferation and liver tumors in mice lacking peroxisomal fatty acyl-CoA oxidase. Implications for peroxisome proliferaror-activated receptor alpha natural ligand metabolism. *J Biol Chem* 1998; **273**: 15639-15645

29 **Clarke SD**. Nonalcoholic steatosis and steatohepatitis. I. Molecular mechanism for polyunsaturated fatty acid regulation of gene transcription. *Am J Physiol Gastrointest Liver Physiol* 2001; **281**: G865-869

30 **Chitturi S**, Farrell GC. Etiopathogenesis of nonalcoholic steatohepatitis. *Semin Liver Dis* 2001; **21**: 27-41

31 **Reginato MJ**, Krakow SL, Bailey ST, Lazar MA. Prostaglandins promote and block adipogenesis through opposing effects on peroxisome proliferator-activated receptor gamma. *J Biol Chem* 1998; **273**: 1855-1858

32 **Miyahara T**, Schrum L, Rippe R, Xiong S, Yee HF Jr, Motonura K, Anania FA, Willson TM, Tsukamoto H. Peroxisome proliferator-activated receptors and hepatic stellate cell activation. *J Biol Chem* 2000; **275**: 35715-35722

Edited by Zhu LH and Wang XL **Proofread by** Xu FM

PO Box 2345, Beijing 100023, China
Fax: +86-10-85381893
E-mail: wjg@wjgnet.com www.wjgnet.com

World J Gastroenterol 2004;10(9):1333-1336
World Journal of Gastroenterology
Copyright ©2004 by The WJG Press ISSN 1007-9327

• BASIC RESEARCH •

Dexamethasone and dextran 40 treatment of 32 patients with severe acute pancreatitis

Zi-Fa Wang, Chang Liu, Yi Lu, Rui Dong, Jun Xu, Liang Yu, Ying-Min Yao, Qing-Guang Liu, Cheng-En Pan

Zi-Fa Wang, Chang Liu, Yi Lu, Rui Dong, Jun Xu, Liang Yu, Ying-Min Yao, Qing-Guang Liu, Cheng-En Pan, Department of Surgery, First Hospital, Xi' an Jiaotong University, Xi' an 710061, Shaanxi Province, China
Zi-Fa Wang, Now is in the Department of Surgery, University of Pittsburgh School of Medicine, Pittsburgh, PA 15213, USA
Correspondence to: Dr. Zi-Fa Wang, Department of Surgery, University of Pittsburgh, NW607, Montefiore University Hospital, 3459 Fifth Avenue, Pittsburgh, PA 15213, United States. ziw3@pitt.edu
Telephone: +1-412-343-9407 **Fax:** +1-412-647-5959
Received: 2003-05-10 **Accepted:** 2004-01-29

Abstract

AIM: Based on the pathogenesis of severe acute pancreatitis and our experimental studies, to investigate the effect of dexamethasone and dextran in treatment of patients with severe acute pancreatitis.

METHODS: Thirty-two patients with severe acute pancreatitis were treated with 0.5-1 mg/kg per day dexamethasone for 3-5 d, and 500-1 000 mL/d of dextran 40 for 7 d, besides the routine therapy.

RESULTS: After 4-8 h of treatment, abdominal pain began to be relieved; range of tenderness began to be localized in 27 patients. They were cured with nonsurgical treatment. Five of them were deteriorated, and treated with surgery. Four patients in this group died.

CONCLUSION: Dexamethasone and dextran 40 block the pathologic process of severe acute pancreatitis through inhibition of inflammatory mediators and improvement of microcirculation disorders respectively.

Wang ZF, Liu C, Lu Y, Dong R, Xu J, Yu L, Yao YM, Liu QG, Pan CE. Dexamethasone and dextran 40 treatment of 32 patients with severe acute pancreatitis. *World J Gastroenterol* 2004; 10 (9): 1333-1336
http://www.wjgnet.com/1007-9327/10/1333.asp

INTRODUCTION

Acute pancreatitis (AP) is usually mild and self-limiting. However, 15-20% of cases deteriorate and develop organ failure or local complications (including necrosis, pseudocyst and abscess)[1]. Many patients with severe AP develop organ failure during the first few days of illness, and this accounts for the majority of early deaths[2]. The rate of severe AP approaches 40 per cent[3]. Although a number of treatments are currently available to treat AP, they have failed to have a significant impact on the overall disease progression[1,4-6]. It is known that the activation of trypsin is the trigger of AP. The key to understand the pathophysiology of AP lies in discovering why a proportion of patients progress from a limited local inflammation to a potentially dangerous systemic inflammatory response. Recent studies[6-21] showed that inflammatory mediators and microcirculation disorders (MCD) play very important roles in the pathogenesis of severe acute pancreatitis. It has been proposed that the systemic sequelae of AP arise from excessive leukocyte activation with the release of secondary inflammatory mediators, such as interleukin (IL)-1α, IL-6, IL-8, IL-10; tumor necrosis factor-α (TNF-α); platelet-activating factor (PAF); nitric oxide (NO); and phospholipase A_2[6-14]. Excessive production of these mediators contributes to the induction of the systemic inflammatory response syndrome, acute phase response, and multiple organ failure[7,14]. On the other hand, the pancreatic microcirculation is impaired in acute pancreatitis[15]. Local release of acinar enzyme, vasoactive mediators, vasoconstriction, increase in vascular permeability, ischaemia, intravascular coagulation, and capillary stasis result in pancreatic edema and hemoconcentration, and impaired capillary and venous drainage consequently lead to hemorrhagic pancreatic necrosis[16-21]. Furthermore, MCD in severe AP are not confined to the pancreas but can also be found in the colon, liver, and lungs; they extend beyond the early stage of AP and persist for 48 h or longer. They not only affect capillary blood flow but also involve prolonged changes of capillary permeability and leukocyte endothelial interaction[22]. There is no strict correlation between necrosis and organ failure in AP. Patients with pancreatic necrosis are not necessarily at risk of having initial organ failure or later organ failure during the total hospital stay and *vice versa*[23].

Therefore, the therapeutic strategy for severe AP should focus on inhibiting inflammatory mediators and improving systemic MCD. Based on our previous experimental studies[24,25], 32 patients with severe AP were treated with the new therapeutic approach.

MATERIALS AND METHODS

General data of patients

According to the definition of the International Symposium on Acute Pancreatitis held in 1992 in Atlanta[26], 32 patients with severe AP were treated in our hospital. Eighteen of them were males and fourteen females. The mean age was 42.8 (range 26-63) years. The treatment began from 8 h to 4 d after the symptoms onset.

Diagnosis

The patients had an epigastric pain of visceral nature that radiated to the back. The pain was constant and at times could be poorly localized. Other clinical findings included fever, nausea, vomiting, ileus, and abdominal distention, hyperamylasemia, and hypotension. Ultrasonography demonstrated edema of the pancreas, retroperitoneal edema, and pancreatic ascites. Sixteen patients represented biliary systemic problems (cholecystitis, cholelithiasis or biliary ductal dilatation). Findings on CT (or contrast-enhanced dynamic CT) included edema of the pancreas, peripancreatic fluid collections, and edema of the surrounding viscera and pancreatic necrosis. Twelve patients had abnormal findings on chest radiographs at the time of diagnosis, including segmental atelectasis, an elevated hemidiaphragm, pleural effusions, or the presence of

early pulmonary parenchyma infiltrates.

Treatment

After severe AP was diagnosed, the patients were treated with following routine methods: (1) Nasogastric tube decompression; (2) Supplemental oxygen, mechanical ventilation instituted in the event of respiratory insufficiency, (3) Aggressive fluid and electrolyte resuscitation to prevent hypovolemia and prerenal azotemia; and (4) Prophylactic antibiotics (Imipenem).

Besides above routine therapy, 0.5-1.0 mg/kg of dexamethasone was administered daily for 3-5 d, and 500-1 000 mL of dextran 40 was daily administered for 7 d.

RESULTS

After for 4-8 h of treatment, the abdominal pain began to be relieved, and the range of tenderness began to be localized in 27 patients. They were cured with nonsurgical treatment. Five patients were deteriorated, and 4 patients were treated with surgery (necrosectomy). The necrotic peripancreatic and pancreatic tissues were removed, and the lesser sac was drained with multiple drains (closed drainage), or lavaged with a large volume of dialysate (closed lavage). Cholecystectomy was performed in 21 patients with biliary pancreatitis, after pancreatitis was completely relieved. Operative cholangiography was performed in 18 patients. Gallstone was found in 5 cases of them, and their common bile ducts were explored. Four cases died, and 2 of them died from acute respiratory distress syndrome, 1 died from postoperative intraabdominal hemorrhage and sepsis and, 1 died from severe intraabdominal infection and organ failure.

DISCUSSION

It is now becoming much better understood that inflammatory mediators and MCD play a dominant role in the pathogenesis of systemic inflammatory response syndrome and organ dysfunction of AP. In addition, there is little doubt that inhibition or blockage of the inflammatory mediators or improvement of MCD can dramatically alter the expected course of experimental AP[30-33]. In our observation, the patients were treated with dexamethasone and dextran 40 for 4-8 h, then, their symptoms and signs began to be improved. Twenty-seven out of 32 patients were cured with this non-surgical approach. The mortality rate was lower (12.5%) compared with literature (40%)[3].

It has been shown in recent studies that inflammatory mediators, including IL-1, IL-6, PAF, and archidonic acid metabolites were excessively produced during AP. These mediators play an active role in initiating or amplifying the cytokines cascade[9,10], and a central role in the progression of AP from a local to a systemic disease[11,27-29]. It is the cumulative effect of each of these mediators that eventually leads to vascular leakage, hypovolemia, systemic inflammatory response syndrome, shock, and organ failure[27,28]. Therefore, recent advances in understanding of the pathophsiology of the early systemic illness have led to the development of a new therapeutic approach in AP. Many specific inhibitors of these mediators have beneficial effects in experimental AP[33-40]. However, few specific inhibitors can be used in clinic. A recent randomized, controlled study showed that antagonist of PAF activity is not sufficient to ameliorate systemic inflammatory response syndrome in severe AP[41]. One of main reasons is that many inflammatory mediators may be involved in the pathophysiology of AP, and any one specific antagonist can not successfully down-regulate this inflammatory response, systemic effects, and organ failure. Dexamethasone is a non-specific anti-inflammatory agent, can inhibit or block several inflammatory mediators' production, including inhibition of synthesis of TNF-α, IL-1α, IL-6, IL-8, and prostaglandins[42-44]. In our previous study, we found that dexamethasone attenuated the inflammatory mediators, 6-keto-$PGI_1\alpha$, TXB_2, and cytokine IL-6, and then improved the survival rate of experimental AP[24]. The mechanism by which dexamethasone inhibits archidonic acid and its metabolites is that dexamethasone can induce phospholipase A_2 inhibitor lipocortin. Other studies also indicated that exogenous glucocorticords have beneficial effects in experimental AP[42-47]. Now it is also clear that, the earlier glucocorticords used, the better the results obtained. However, the optimal dose of glucocorticords is not known. We used a high dose of dexamethasone short time interval, and found significant results. Although glucocorticords have a positive impact on AP, Gomez *et al*[48] found that survival rate decreased and pancreatic necrosis increased in mice after 7 d of pretreatment with hydrocortisone. Therefore, in our clinic, dexamethasone was used for 3-5 d to prevent its potential side reactions.

MCD is another important factor in the pathogenesis of multiple organ dysfunction syndromes in AP[49,50]. MCD involve a series of changes including vasoconstriction, ischaemia, increased vascular permeability, impairment of nutritive tissue perfusion, ischaemia/reperfusion, leukocyte adherence, hemorrheological changes and impaired lymphatic drainage. In addition, MCD in AP is not confined to the pancreas but appear to be a systemic disorder. Increased capillary permeability results in ascites and/or pleural effusion. Above mentioned ultrasonography demonstrated ascites in all patients with severe AP. In our previous experimental study, we found that blood viscosity, plasma viscosity, hematocrit, erythrocyte osmotic fragility elevated, while erythrocyte sedimentation rate and fibrinogen decreased significantly in AP[25]. MCD affect organs other than the pancreas and persist after pancreatic necrosis is manifested and enzyme levels have returned to normal values[22]. Therefore, MCD are not only an initiating or aggravating factor to pancreatic injury, but considered as a systemic reaction that contributes to pancreatitis-associated multiple organ dysfunction syndrome. Dextran 40 has numerous pharmacologic effects when infused intravenously: anti-platelet activity, anti-fibrin activity, and plasma volume expansion in hypovolemia, improvement of microcirculation by decreasing blood viscosity and impeding erythrocyte aggregation. The principal effect of dextran 40 is plasma volume expansion, resulting from the drug's colloidal osmotic effect in the drawing fluid from the interstitial to the intravascular spaces. Plasma volume expansion is accompanied by an increase in central venous pressure, cardiac output, stroke volume, blood pressure, urinary output, capillary perfusion, and pulse pressure, and by a decrease in heart rate, peripheral resistance, blood viscosity, and mean transit time. Dextran 40 also enhances blood flow through correction of hypovolemia and improved microcirculation. Dextran 40 may coat erythrocytes, thus reducing bonding forces and maintaining the erythrocytes in a state of electronegativity, and mutual repellancy; dextran 40 may also coat other formed elements. In addition, the drug may decrease erythrocyte rigidity, thereby facilitating passage of erythrocytes through small blood vessels[51]. In experimental studies, it has been shown that dextran not only limited the progression of pancreatic necrosis by improving pancreatic microcirculation, reduced trypsinogen activation, prevented acinar necrosis, and improved survival in necrotizing rodent pancreatitis[52-56], but also reduced blood viscosity, hematocrit and erythrocyte osmotic fragility, and elevated fibrinogen significantly[25]. The colon, liver, and lungs affected by the AP associated systemic inflammatory response may still benefit from improved microcirculation at a time when pancreatic necrosis can no longer be reversed[22].

In conclusion, treatment of severe AP with dexamethasone and dextran is an effective and practical approach. Dexamethasone can inhibit multiple inflammatory mediators and dextran can improve MCD. We emphasize that high dose of dexamethasone should be used in a short time interval to ensure the pharmacological effect and avoid its potential side reactions. Of course, when patients represent acute respiratory distress syndrome or severe intraabdominal infection, other therapeutic approaches, such as, mechanical ventilation, surgery should be considered.

REFERENCES

1 **Beger HG**, Rau B, Isenmann R. Prevention of severe change in acute pancreatitis: prediction and prevention. *J Hepatobiliary Pancreat Surg* 2001; **8**: 140-147

2 **Mutinga M**, Rosenbluth A, Tenner SM, Odze RR, Sica GT, Banks PA. Does mortality occur early or late in acute pancreatitis? *Int J Pancreatol* 2000; **28**: 91-95

3 **Yousaf M**, McCallion K, Diamond T. Management of severe acute pancreatitis. *Br J Surg* 2003; **90**: 407-420

4 **Slavin J**, Ghaneh P, Sutton R, Hartley M, Rowlands P, Garvey C, Hughes M, Neoptolemos J. Management of necrotizing pancreatitis. *World J Gastroenterol* 2001; **7**: 476-481

5 **Ulrich CD 2cnd**. Medical management of acute pancreatitis: strategies, reality, and potential. *Curr Gastroenterol Rep* 2000; **2**: 115-119

6 **Norton ID**, Clain JE. Optimising outcomes in acute pancreatitis. *Drugs* 2001; **61**: 1581-1591

7 **Wang ZF**, Pan CE, Liu SG. Role of inflammatory mediators in acute pancreatitis. *Huaren Xiaohua Zazhi* 1998; **7**: 170-171

8 **Kingsnorth A**. Role of cytokines and their inhibitors in acute pancreatitis. *Gut* 1997; **40**: 1-4

9 **Makhija R,** Kingsnorth AN. Cytokine storm in acute pancreatitis. *J Hepatobil Pancreat Surg* 2002; **9:** 401-410

10 **Mckay CJ,** Gallagher G, Brooks B, Imrie CW, Baxter JN. Increased monocyte cytokine production in association with systemic complication in acute pancreatitis. *Br J Surg* 1996; **83**: 919-923

11 **Uhl W**, Schrag HJ, Schmitter N, Aufenanger J, Nevallanen TJ, Buchler MM. Experimental study of a novel phospholipase A_2 inhibitor in acute pancreatitis. *Br J Surg* 1998; **85**: 618-623

12 **Uhl W,** Schrag HJ, Schmitter N, Wheatley AM, Büchler MW, Nevalainen TJ, Aufenanger J. Pathophysiological role of secretory type I and II phospholipase A_2 in acute pancreatitis: an experimental study in rats. *Gut* 1997; **40**: 386-392

13 **Abe T,** Shimsegawa T, Satoh A, Abe R, Kikuchi Y, Koizumi M, Toyota T. Nitric oxide modulate pancreatic edema formation in ratcaerulein-induced pancreatitis. *J Gastroenterol* 1995; **30**: 636-642

14 **de Beaux AC,** Goldie AS, Ross JA, Carter DC, Fearon KC. Serum concentrations of inflammatory mediators related to organ failure in patients with acute pancreatitis. *Br J Surg* 1996; **83**: 349-353

15 **Zhou ZG,** Chen YD. Influencing factors of pancreatic microcirculatory impairment in acute panceatitis. *World J Gastroenterol* 2002; **8**: 406-412

16 **Chen HM,** Hwang TL, Chen MF. The effect of gabexate mesilate on pancreatic and hepatic microcirculation in acute experimental pancreatitis in rats. *J Surg Res* 1996; **66**: 147-153

17 **Yuan YZ**, Lou KX, Gong ZH, Tu SP, Zhai ZK, Xu JY. Effects and mechanisms of emodin on pancreatic tissue EGF expression in acute pancreatitis in rats. *Shijie Huaren Xiaohua Zazhi* 2001; **9**: 127-130

18 **Sunamura M,** Yamauchi J, Shibuya K, Chen HM, Ding L, Takeda K, Kobari M, Matsuno S. Pancreatic microcirculation in acute pancreatitis. *J Hepatobil Pancreat Surg* 1998; **5**: 62-68

19 **Zhou ZG,** Chen YD, Sun W, Chen Z. Pancreatic microcirculatory impairment in experimental acute pancreatitis in rats. *World J Gastroenterol* 2002; **8**: 933-936

20 **Schmidt J,** Ebeling D, Ryschich E, Werner J, Gebhard MM, Klar E. Pancreatic capillary blood flow in an improved model of necrotizing pancreatitis in the rat. *J Surg Res* 2002; **106**: 335-341

21 **Bong JJ,** Ammori BJ, McMahon MJ, Kumar A, Turney JH, Norfolk DR. Thrombotic microangiopathy in acute pancreatitis. *Pancreas* 2002; **25**: 107-109

22 **Foitzik T,** Eibl G, Hotz B, Hotz H, Kahrau S, Kasten C, Schneider P, Buhr HJ. Persistent multiple organ microcirculatory disorders in severe acute pancreatitis: experimental findings and clinical implications. *Dig Dis Sci* 2002; **47**: 130-138

23 **Lankisch PG,** Pflichthofer D, Lehnick D. No strict correlation between necrosis and organ failure in acute pancreatitis. *Pancreas* 2002; **20**: 319-322

24 **Wang ZF,** Xu J, Pan CE, Liu SG, Dong R. Dexamethasone inhibits inflammatory mediators and improves the prognosis of severe acute pancreatitis. *Shijie Huaren Xiaohua Zazhi* 2000; **8**: 239

25 **Wang ZF,** Pan CE, Liu SG. Treatment for acute necrotizing pancreatitis with correcting abnormal hemorheology. *Zhonghua Gandan Waike Zazhi* 2000; **6**: 89

26 **Bradley EL 3rd.** A clinically based classification system for acute pancreatitis. Summary of the International symposium on Acute Pancreatitis, Atlanta, Ga, September 11 through 13, 1992. *Arch Surg* 1993; **128**: 586-590

27 **Norman J.** The Role of cytokines in the pathogenesis of acute pancreatitis. *Am J Surg* 1998; **175**: 76-83

28 **Sandoval D,** Gukovskaya A, Reavey P, Gukovsky S, Sisk A, Braquet P, Pandol SJ, Poucell-Hatton S. The role of neutrophils and platelet-activating factor in mediating experimental pancreatitis. *Gastroenterology* 1996; **111:** 1081-1091

29 **Norman JG**, Fink GW, Denham W, Yang J, Carter G, Sexton C, Falkner J, Gower WR, Franz MG. Tissue-Specific cytokine production during experimental acute pancreatitis (a probable mechanism for distant organ dysfunction). *Dig Dis Sci* 1997; **42**: 1783-1788

30 **Hughes CB,** Gaber LW, Mohey el-Din AB, Grewal HP, Kotb M, Mann L, Gaber AO. Inhibition of TNF alpha improves survival in an experimental model of acute pancreatitis. *Am Surg* 1996; **62**: 8-13

31 **Windsor AC,** Mullen PG, Walsh CJ, Fisher BJ, Blocher CR, Jesmok G, Fowler AA 3rd, Sugerman HJ. Delayed tumor necrosis factor a blockade attenuates pulmonary dysfunction and metabolic acidosis associated with experimental gram-negative sepsis. *Arch Surg* 1994; **129**: 80-89

32 **Norman J,** Franz M, Messina J, Riker A, Fabri PJ, Rosemurgy AS, Gower WR Jr. Interleukin-1 receptor antagonist decreases severity of experimental acute pancreatitis. *Surgery* 1995; **117**: 648-655

33 **Guice K,** Oldham KT, Remick DG, Kunkel SL, Ward PA. Anti-tumor necrosis factor antibody augments edema formation in caerulein-induced acute pancreatitis. *J Surg Res* 1991; **51**: 495-499

34 **Osman MO,** Kristensen JU, Jacobsen NO, Lausten SB, Deleuran B, Deleuran M, Gesser B, Matsushima K, Larsen CG, Jensen SL. A monoclonal anti-interleukin 8 antibody (WS-4) inhibits cytokine response and acute lung injury in experimental severe acute necrotizing pancreatitis in rabbits. *Gut* 1998; **43**: 232-239

35 **McKay CJ,** Curran F, Sharples C, Baxter JN, Imrie CW. Prospective placebo-controlled randomized trial of lexipafant in predicted severe acute pancreatitis. *Br J Surg* 1997; **84**: 1239-1243

36 **Kusske AM**, Rongione AJ, Ashley SW, McFadden DW, Reber HA. Interlenkine-10 prevents death in lethal necrotizing pancreatitis in mice. *Surgery* 1996; **120**: 284-288

37 **Norman J,** Franz M, Fink GS, Messina J, Fabri PJ, Gower WR, Carey LC. Decreased mortality of severe acute pancreatitis following proximal cytokines blockade. *Ann Surg* 1995; **221**: 625-631

38 **Hughes CB,** Grewal HP, Gaber LW, Kotb M, El-din AB, Mann L, Gaber AO. Anti- TNF-α therapy improves survival and ameliorates the pathophysiology sequelae in acute pancreatitis in the rat. *Am J Surg* 1996; **171**: 274-280

39 **Kingsnorth AN,** Galloway SW, Formela PJ. Randomized double blind phase trial of lexipafant, a platelet-activating factor antagonist, in human acute pancreatitis. *Br J Surg* 1995; **82**: 1414-1420

40 **Grewal HP,** Mohey el Din A, Gaber L, Kotb M, Gaber AO. Amelioration of the physiologic and biochemical changes of acute pancreatitis using an anti-TNF-alpha polyclonal antibody. *Am J Surg* 1994; **167**: 214-218

41 **Johnson CD,** Kingsnorth AN, Imrie CW, McMahon MJ, Neoptolemos JP, McKay C, Toh SK, Skaife P, Leeder PC, Wilson P, Larvin M, Curtis LD. Double blind, randomized, placebo controlled study of a platelet activating factor antagonist, lexipafant, in the treatment and prevention of organ failure in predicted severe acute pancreatitis. *Gut* 2001; **48:** 62-69

42 **Yao XL,** Cowan MJ, Gladwin MT, Lawrence MM, Angus CW, Shelhamer JH. Dexamethasone alters arachidonate release from human epithelial cells by induction of p11 protein synthesis and inhibition of phospholipase A_2 activity. *J Biol Chem* 1999; **274**: 17202-17208

43 **Wang ZF,** Pan CE, Lu Y, Liu SG, Zhang GJ, Zhang XB. The role of inflammatory mediators in severe acute pancreatitis and regulation of gluccorticords. *Hepatobil Pancreas Dis Int* 2003; **2**: 458-462

44 **Takaoka K**, Kataoka K, Sakagami J. The effect of steroid pulse therapy on the development of acute pancreatitis induced by closed duodenal loop in rats. *J Gastroenterol* 2002; **37**: 537-542

45 **Rakonczay Z,** Duda E, Kaszaki J, Ivanyi B, Boros I, Lonovics J, Takacs T. The anti-inflammatory effect of methylprednisolone occurs down-stream of nuclear factor-kappaB DNA binding in acute pancreatitis. *Eur J Pharmacol* 2003; **464**: 217-227

46 **Osman MO,** Jacobsen NO, Kristensen JU, Larsen CG, Jensen SL. Beneficial effects of hydrocortisone in a model of experimental acute pancreatitis. *Dig Surg* 1999; **16**: 214-221

47 **Gloor B**, Uhl W, Tcholakov O, Roggo A, Muller CA, Worni M, Buchler MW. Hydrocortisone treatment of early SIRS in acute experimental pancreatitis. *Dig Dis Sci* 2001; **46**: 2154-2161

48 **Gomez G,** Townsend CMJ, Green D, Rajaraman S, Uchida T, Thompson JC. Involvement of cholecystokinin receptors in the adverse effect of glucocorticords on diet-induced necrotizing pancreatitis. *Surgery* 1989; **106**: 230-236

49 **Gullo A,** Beriot G. Ingredients of organ dysfunction or failure. *World J Surg* 1996; **20**: 430-436

50 **Eibl G,** Buhr HJ, Foitzik T. Therapy of microcirculatory disorders in severe acute pancreatitis: what mediators should we block? *Intens Care Med* 2002; **28**: 139-146

51 **McEvoy GK.** AHFS Drug Information. 45th ed. *Bethesda: American Society of Health-System Pharmacists, Inc* 2003: 2487-2489

52 **Schmidt J,** Huch K, Mithofer K, Hotz HG, Sinn HP, Buhr HJ, Warshaw AL, Herfarth C, Klar E. Benefits of various dextrans after delayed therapy in necrotizing pancreatitis of the rat. *Intens Care Med* 1996; **22**: 1207-1213

53 **Klar E,** Foitzik T, Buhr H, Messmer K, Herfarth C. Isovolemic hemodilution with dextran 60 as treatment of pancreatic ischemia in acute pancreatitis. Clinical practicability of an experimental concept. *Ann Surg* 1993; **217**: 369-374

54 **Schmidt J,** Fernandez-del Castillo C, Rattner DW, Lewandrowski KB, Messmer K, Warshaw AL. Hyperoncotic ultrahigh molecular weight dextran solutions reduce trypsinogen activation, prevent acinar necrosis, and lower mortality in rodent pancreatitis. *Am J Surg* 1993; **165**: 40-44

55 **Kusterer K,** Enghofer M, Poschmann T, Usadel KH. The effect of somatostatin, gabexate mesilate and dextran 40 on the microcirculation in sodium taurocholate-induced pancreatitis. *Acta Physiol Hung* 1992; **80**: 407-415

56 **Klar E,** Herfarth C, Messmer K. Therapeutic effect of isovolemic hemodilution with dextran 60 on the impairment of pancreatic microcirculation in acute biliary pancreatitis. *Ann Surg* 1990; **211**: 346-353

Edited by Xu CT and Pan BR **Proofread by** Xu FM

PO Box 2345, Beijing 100023, China
Fax: +86-10-85381893
E-mail: wjg@wjgnet.com www.wjgnet.com

World J Gastroenterol 2004;10(9):1337-1340
World Journal of Gastroenterology
Copyright ©2004 by The WJG Press ISSN 1007-9327

• BASIC RESEARCH •

Detection of K-ras point mutation and telomerase activity during endoscopic retrograde cholangiopancreatography in diagnosis of pancreatic cancer

Guo-Xiong Zhou, Jie-Fei Huang, Zhao-Shen Li, Guo-Ming Xu, Feng Liu, Hong Zhang

Guo-Xiong Zhou, Jie-Fei Huang, Hong Zhang, Department of Gastroenterology, Affiliated Hospital of Nantong Medical College, Nantong 226001, Jiangsu Province, China
Zhao-Shen Li, Guo-Ming Xu, Feng Liu, Changhai Hospital, Second Military Medical University, Shanghai 200433, China
Correspondence to: Dr. Guo-Xiong Zhou, Department of Gastroenterology, Affiliated Hospital of Nantong Medical College, Nantong 226001, Jiangsu Province, China. zhouguoxiong@pub.nt.jsinfo.net
Telephone: +86-513-5052079
Received: 2003-06-05 **Accepted:** 2003-08-16

Abstract

AIM: To study the value of monitoring K-ras point mutation at codon 12 and telomerase activity in exfoliated cells obtained from pancreatic duct brushings during endoscopic retrograde cholangiopancreatography (ERCP) in the diagnosis of pancreatic cancer.

METHODS: Exfoliated cells obtained from pancreatic duct brushings during ERCP were examined in 27 patients: 23 with pancreatic cancers, 4 with chronic pancreatitis. K-ras point mutation was detected with the polymerase chain reaction and restriction fragment-length polymorphism (PCR-RFLP). Telomerase activity was detected by PCR and telomeric repeat amplification protocol assay (PCR-TRAP-ELISA).

RESULTS: The telomerase activities in 27 patients were measured in 21 exfoliated cell samples obtained from pancreatic duct brushings. D_{450} value of telomerase activities in pancreatic cancer and chronic pancreatitis were 0.446±0.27 and 0.041±0.0111, respectively. Seventy-seven point eight percent (14/18) of patients with pancreatic cancer and none of the patients with chronic pancreatitis showed telomerase activity in cells collected from pancreatic duct brushings when cutoff value of telomerase activity was set at 2.0. The K-ras gene mutation rate (72.2%) in pancreatic cancer was higher than that in chronic pancreatitis (33.3%) (P<0.05). In considering of both telomerase activities and K-ras point mutation, the total positive rate was 83.3% (15/18), and the specificity was 100%.

CONCLUSION: Changes of telomerase activities and K-ras point mutation at codon 12 may be an early event of malignant progression in pancreatic cancer. Detection of telomerase activity and K-ras point mutation at codon 12 may be complementary to each other, and is useful in diagnosis of pancreatic cancer.

Zhou GX, Huang JF, Li ZS, Xu GM, Liu F, Zhang H. Detection of K-ras point mutation and telomerase activity during endoscopic retrograde cholangiopancreatography in diagnosis of pancreatic cancer. *World J Gastroenterol* 2004; 10(9): 1337-1340
http://www.wjgnet.com/1007-9327/10/1337.asp

INTRODUCTION

Pancreatic cancer has a poor prognosis, its early diagnosis remains unsatisfactory. Even serum tumor markers, such as CA19-9, are associated with pancreatic cancer, but lack sensitivity and tumor specificity. Recent studies have shown that K-ras oncogene is often activated by specific point mutations restricted to codon 12 in human pancreatic ductal adenocarcinoma. In pancreatic adenocarcinoma, K-ras mutations were found in 75% to 100% of the cases[1-8]. We and others previously showed that k-ras analysis from specimens obtained during ERCP was a sensitive (around 80% to 85%) and specific (close to 100%) method in differentiating benign from malignant pancreatic diseases. Therefore, k-ras mutation identification has been claimed as an useful and early marker in diagnosis of pancreatic cancer[9-12]. Telomerase is a key enzyme with regard to immortalization of cancer cells and increased activity has been demonstrated in various human malignant neoplasms[13-16]. We previously detected telomerase activity in 87% of surgically resected human pancreatic cancers. While in adjacent tissues, the positive rate of telomerase activity was only 10%. Detection of telomerase activity was useful in diagnosis of pancreatic cancer[17].

In the present study, we evaluated the diagnostic role of K-ras mutation and telomerase activity in exfoliated cells obtained from pancreatic duct brushings alone and in combination, in differentiating chronic pancreatitis from pancreatic cancer.

MATERIALS AND METHODS

Patients

From April 1999 to December 2000, 27 patients undergoing ERCP were prospectively investigated at Changhai Hospital, 23 of them were patients with pancreatic cancer, 4 were patients with chronic pancreatitis. There were 17 men, 10 women with a mean age of 58.5 years (range: 22 to 75). The diagnosis of pancreatic cancer was confirmed histologically. The locations of the cancer were pancreatic head (n=13), body (n=5) and tail (n=1), and diffusion over the pancreas (n=4). Chronic pancreatitis was diagnosed by clinical history, ERCP and CT findings. All patients with chronic pancreatitis were followed up clinically and radiologically for at least six months.

Sampling technique

ERCP was performed using Olympus JF-240, 230 and TJF200 duodenoscope (Olympus, Japan). Lesions were identified after injection of iodinated contrast agent, a wire (0.035 inch in length) was introduced carefully into the main pancreatic duct and advanced to the suspected abnormal areas under guidance of fluoroscopic monitoring. Then a pancreatic duct brush (BC-24Q, Olympus) was introduced through the guide wire to the suspicious lesion, and the guide wire was withdrawn. The brush was moved rigorously back and forth across the suspicious lesion, brushes were retracted into the guiding catheter tip and removed together with the catheter to avoid losing a portion of the specimen inside the catheter. Specimens were immediately

collected in 5 mL of sterile saline solution at 4 ℃ for analysis of telomerase activity and DNA or smeared on glass slides, fixed in 95% alcohol and stained by HE for cytological examination, the order of brushing samples studied was always kept consistent.

Detection of K-ras point mutations at codon 12

Samples were centrifuged at 2000 r/mim for 15 min and the pellet was collected. Genomic DNA was isolated using DNA lysis buffer and proteinase K digestion, followed by extraction with phenol and chloroform. K-ras point mutations were detected using PCR and restriction fragment-length polymorphism (PCR-RFLP). Primers were synthesized and supplied by Shanghai Bio-Engineering Research Center. The sequences of primers were: P1=5'-CTTGTGGTAGTTGGACCT-3' containing a mismatched base indicated by the underline, P2=5'-GTCAGAGAAACCTTTATCTG-3', P3=5'-TGCACCAGTAATATG-CATAT-3'. The reaction volume was 50 μL containing 5 μL of 10×Ex Taq buffer, 4 μL of dNTP mixture, 0.5 μL of each primer, 0.25 μL (5 U/μL) of Taq DNA polymerase. The primers for the first PCR were P1 (sense) and P2 (antisense) that flanked codon 12 of the K-ras gene. The first PCR amplification was performed for 30 cycles using a DNA thermal cycler, and each cycle consisted of denaturation at 94 ℃ for 30 s, annealing at 52 ℃ for 30 s, and extension at 72 ℃ for 45 s. A 5 μL sample of the first PCR product was digested with 1 μL (10 U/μL) of Mva I at 37 ℃ for 1 h under the conditions recommended by the supplier of mismatched sense primer described above. Subsequently, 5 μL of the reaction mixture was subjected to a second round of PCR and amplified for 30 cycles under the same conditions using the following primers: sense: P1; antisense: P3. The second PCR products were also digested with 1 μL (10 U/μL) of Mva I for 1 h. Mutations were confirmed by electrophoresis of 10 μL of the second digested sample on a 20 g/L agarose gel.

Detection of telomerase activity

Telomerase activity was detected with telomerase PCR-ELISA (Boehringer Mannheim, Germany). Exfoliated cells obtained from pancreatic duct brushings were collected and washed with PBS, and centrifuged at 10 000 g for 10 min. Then the cells in PBS containing 200 μL Lysis reagent were incubated on ice for 30 min, and centrifuged at 16 000 g for 20 min at 4 ℃. Next, the supernatants (175 μL) were transferred to a Eppendorf tube, and tested for telomerase activity assay. Protein concentration was determined by Coomassie protein assay. Each of TRAP reactions contained 2 μL of cell extract (5-6 μg total protein) and sterile water with a final volume of 50 μL. The reaction mixture was incubated at 25 ℃ for 30 min, heated at 94 ℃ for 5 min. Then PCR amplification was performed for 33 cycles using a DNA thermal cycler, and each cycle consisted of denaturation at 94 ℃ for 30 s, annealing at 50 ℃ for 30 s, and extension at 72 ℃ for 90 s followed by 72 ℃ for 10 min. After PCR, 5 μL of the PCR products was dispensed into a reaction tube and incubated with 20 μL of denaturation reagent at room temperature for 10 min, and then mixed thoroughly by overtaxing briefly with 225 μL hybridization buffer per tube. By transferring 100 μL of the mixture per well of percolated MTP modules, MTP modules were incubated at 37 ℃ on a shaker (300 r/min) for 2 h and washed 3 times with PBS, and enzyme reactions were incubated at room temperature on a shaker (300 r/min) for 30 min by addition of 100 μL anti-Dig-POD per well. After washed 5 times with PBS, 100 μL TMB substrate solution was added to each well and incubated for color development at room temperature for 20 min while shaking at 300 r/min. Using a ELISA reader, the absorbance value of samples was measured at 450 nm within 30 min after termination of reaction.

Statistical analysis

Statistical analysis was performed using the unpaired *t* test and χ^2 test or Fisher's exact test. $P<0.05$ was considered statistically significant. Data were expressed as mean±SD.

RESULTS

Detection of K-ras point mutations at codon 12

K-ras point mutations at codon 12 were detected in 21 exfoliated cell samples obtained from pancreatic duct brushings by PCR-RFLP. Normal DNA had a 114 base pair (bp) band and k-ras DNA mutation remained as a 131 bp band since it was not digested by MvaI (Figures 1,2). K-ras gene mutation rate in pancreatic cancer was 72.2%, which was higher than that of chronic pancreatitis (33.3%, $P<0.05$).

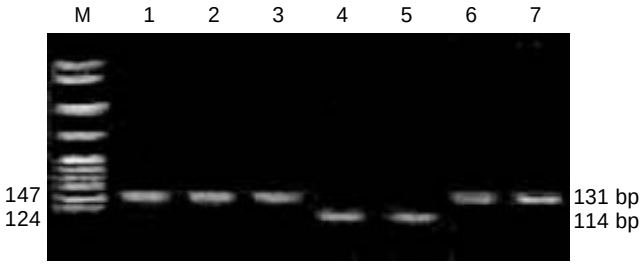

Figure 1 PCR products after restriction enzyme digestion, M: Marker; 1: Positive control; 2-7:Pancreatic cancer.

Detection of telomerase activity

Telomerase activities in 27 patients were measured in 21 exfoliated cell samples obtained from pancreatic duct brushings. D450 values of telomerase activity in carcinoma and chronic pancreatitis were 0.446±0.27 and 0.041±0.0111, respectively. Seventy-seven point eight percent (14/18) of the patients with pancreatic cancer and none of patients with chronic pancreatitis showed telomerase activity in cells from pancreatic duct brushings when cutoff value of telomerase activity was set at 2.0. Both telomerase activity and cytological examination were detected in 66.7% (12/18) of patients.

Table 1 Location of pancreatic cancer and K-ras mutation or telomerase activity

Location	*n*	K-ras mutation		Telomerase activity	
		(+)	%	(+)	%
Head	11	8	72.7	9	81.8
Body	3	2	66.7	2	66.7
Tail	1	1	100	1	100
Diffuse	3	2	66.7	2	66.7
Totol	18	13	72.2	14	77.8

Table 2 Comparison of K-ras point mutations and telomerase activity

	K-ras mutation	Telomerase	Both
Pancreatic cancer (*n*=18)	13	14	12
Chronic pancreatitis (*n*=3)	1	0	0
Sensitivity (%)	72.2	77.8	66.7
Specificity (%)	66.7	100	100

Relationship between K-ras gene or telomerase activity and location of tumors

No significant correlation of positivity of K-ras gene or telomerase activity with tumor location was observed (Table 1).

Comparison of K-ras point mutations with telomerase activity

The total rate of positive telomerase activity and K-ras mutation was 83.3% (15/18). The sensitivity and specificity of K-ras mutation and telomerase in differential diagnosis of pancreatic cancer and chronic pancreatitis was compared (Table 2).

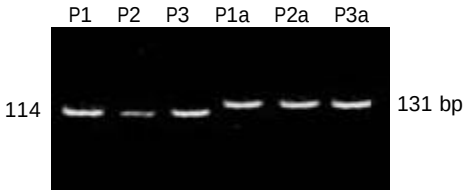

Figure 2 Agarose gel of PCR products, P1, P2, P3 : after restriction enzyme digestion; P1a, P2a, P3a: before restriction enzyme digestion, P1 and P1a, P2 and P2a, P3 and P3a reprent same samples, respectively.

DISCUSSION

Recent application of molecular biologic techniques, such as detection of K-ras mutation, has been proposed for the diagnosis of pancreatic cancer[18-22]. K-ras gene mutation was found in greater than 90% of pancreatic cancers, and detection of K-ras gene mutation-positive cells in pure pancreatic juice or duodenal juice were reported to be useful in the diagnosis of pancreatic cancer[23-26]. K-ras mutation was detected in ERCP brush samples. We used the sensitive RFLP method and found 72.2% of patients with pancreatic cancer had K-ras mutation, which was relatively higher than that in other reports. K-ras mutation was also detected in 1 patient with chronic pancreatitis. Although K-ras mutation has been detected mainly in malignancy, it could be detected in nonmalignant pancreatic lesions[27-29]. However, a recent long-term follow-up report suggested that K-ras mutation in chronic pancreatitis might represent false-positive results[30]. Studies including ours showed that this mutation could also occur in benign condition. Queneau *et al*.[31] found 27.8% (10/36) chronic pancreatitis patients had k-ras mutations. Recently, several investigators failed to detect K-ras mutations in chronic pancreatitis even though they used highly sensitive methods[32,33] and suggested that K-ras mutation was an extremely specific event in pancreatic cancer. Unfortunately, the reason for this discrepancy is not clear.

Telomerase is an enzyme that was found containing an RNA template complementary to the short DNA sequence repeats at chromosomal ends[34]. Telomerase activity has been found in the majority of malignant tissues, such as pancreatic cancers, but not in somatic tissues except for reproductive and hematopoietic cells. Moreover, telomerase activity was detected in an extremely early stage of pancreatic cancer when the tumor could not be detected by other diagnostic methods[35]. Hiyama *et al*.[36] reported that 95% of pancreatic carcinomas but none of 11 benign pancreatic tumors showed telomerase activity. Suehara *et al*.[37] reported that 100% of pancreatic carcinomas had high levels of telomerase activity. None of pancreatitis or normal pancreas extracts had detectable telomerase activity. However, some pancreatic adenomas demonstrated weak telomerase activity. Telomerase activity in pancreatic juice reflected the activity of the enzyme in tissue specimens[38,39]. The telomerase activity in pancreatic juice from patients with pancreatic ductal carcinomas was lower than that in resected tissues. It is possible that various digestive enzymes in pancreatic juice might disturb telomerase assay by inhibiting Taq polymerase[40]. Myung *et al*.[41] and Uehara *et al*.[42]. Have reported their study results in the diagnosis of pancreatic cancer by detecting K-ras mutations and telomerase activity alone and in combination in pancreatic juice. We compared these two methods and evaluated their usefulness alone and in combination for the differentiation of pancreatic cancer from chronic pancreatitis. Using PCR-TRAP-ELISA method, we could give a more accurate diagnosis of pancreatic cancer by evaluating both K-ras mutations and telomerase activity in cells obtained from pancreatic duct brushings, and found that K-ras mutations in cells obtained from pancreatic duct brushings were useful for detecting neoplastic lesions and that telomerase activity was useful for differentiating malignancy from benign lesions of the pancreas, when telomerase activity cutoff was set at 2.0. The sensitivity and specificity of K-ras mutations for the diagnosis of pancreatic cancer were 72.2% and 66.7%, respectively, whereas those of telomerase activity were 77.8% and 100%, respectively. By combining these two methods, the sensitivity was 66.7% and the specificity was 100%.

In conclusion, detection of K-ras mutation and telomerase activity in cells obtained from pancreatic duct brushings may be complementary to each other, and may prove to be a potent tool for the diagnosis of pancreatic cancer.

REFERENCES

1 **Inoue S**, Tezel E, Nakao A. Molecular diagnosis of pancreatic cancer. *Hepatogastroenterology* 2001; **48**: 933-938

2 **Yoshizawa K**, Nagai H, Sakurai S, Hironaka M, Morinaga S, Saitoh K, Fukayama M. Clonality and K-ras mutation analyses of epithelia in intraductal papillary mucinous tumor and mucinous cystic tumor of the pancreas. *Virchows Arch* 2002; **441**: 437-443

3 **Raimondo M**, Tachibana I, Urrutia R, Burgart LJ, DiMagno EP. Invasive cancer and survival of intraductal papillary mucinous tumors of the pancreas. *Am J Gastroenterol* 2002; **97**: 2553-2558

4 **Nakata B**, Yashiro M, Nishioka N, Aya M, Yamada S, Takenaka C, Ohira M, Ishikawa T, Nishino H, Wakasa K, Hirakawa K. Genetic alterations in adenoma-carcinoma sequencing of intraductalpapillary-mucinous neoplasm of the pancreas. *Int J Oncol* 2002; **21**: 1067-1072

5 **Mizumoto K**, Tanaka M. Genetic diagnosis of pancreatic cancer. *J Hepatobiliary Pancreat Surg* 2002; **9**: 39-44

6 **Tada M**, Komatsu Y, Kawabe T, Sasahira N, Isayama H, Toda N, Shiratori Y, OmataM. Quantitative analysis of K-ras gene mutation in pancreatic tissue obtained by endoscopic ultrasonography-guided fine needle aspiration: clinical utility for diagnosis of pancreatic tumor. *Am J Gastroenterol* 2002; **97**: 2263-2270

7 **Pabst B**, Arps S, Binmoeller K, Thul R, Walsemann G, Fenner C, Klapdor R. Analysis of K-ras mutations in pancreatic tissue after fine needle aspirates. *Anticancer Res* 1999; **19**: 2481-2483

8 **Luttges J**, Schlehe B, Menke MA, Vogel I, Henne-Bruns D, Kloppel G. The K-ras mutation pattern in pancreatic ductal adenocarcinoma usually is identical to that in associated normal, hyperplastic, and metaplastic ductal epithelium. *Cancer* 1999; **85**: 1703-1710

9 **Futakawa N**, Kimura W, Yamagata S, Zhao B, Ilsoo H, Inoue T, Sata N, Kawaguchi Y, Kubota Y, Muto T. Significance of K-ras mutation and CEA level in pancreatic juice in the diagnosis of pancreatic cancer. *J Hepatobiliary Pancreat Surg* 2000; **7**: 63-71

10 **Tateishi K**, Tada M, Yamagata M, Isayama H, Komatsu Y, Kawabe T, Shiratori Y, Omata M. High proportion of mutant K-ras gene in pancreatic juice of patients with pancreatic cystic lesions. *Gut* 1999; **45**: 737-740

11 **Watanabe H**, Yamaguchi Y, Ha A, Hu YX, Motoo Y, Okai T, Yoshimura T, Sawabu N. Quantitative determination of K-ras mutations in pancreatic juice for diagnosis of pancreatic cancer using hybridization protection assay. *Pancreas* 1998; **17**: 341-347

12 **Watanabe H**, Sawabu N, Songur Y, Yamaguchi Y, Yamakawa O, Satomura Y, Ohta H, Motoo Y, Okai T, Wakabayashi T. Detection of K-ras point mutations at codon 12 in pure pancreatic juice for the diagnosis of pancreatic cancer by PCR-RFLP analysis. *Pancreas* 1996; **12**: 18-24

13 **Pearson AS**, Chiao P, Zhang L, Zhang W, Larry L, Katz RL, Evans DB, AbbruzzeseJL. The detection of telomerase activity in patients with adenocarcinoma of the pancreas by fine needle aspiration. *Int J Oncol* 2000; **17**: 381-385

14 **Yeh TS**, Cheng AJ, Chen TC, Jan YY, Hwang TL, Jeng LB, Chen MF, Wang TC. Telomerase activity is a useful marker to distinguish malignant pancreatic cystic tumors from benign neoplasms and pseudocysts. *J Surg Res* 1999; **87**: 171-177

15 **Tsutsumi M**, Tsujiuchi T, Ishikawa O, Majima T, Yoshimoto M, Sasaki Y, Fukuda T, Oohigashi H, Konishi Y. Increased telomerase activities in human pancreatic duct adenocarcinomas. *Jpn J Cancer Res* 1997; **88**: 971-976

16 **Mizumoto K**, Suehara N, Muta T, Kitajima S, Hamasaki N, Tominaga Y, Shimura H, Tanaka M. Semi-quantitative analysis of telomerase in pancreatic ductal adenocarcinoma. *J Gastroenterol* 1996; **31**: 894-897

17 **Zhou GX**, Li ZS, Xu GM, Huang JF. Telomerase activity and Telomerase gene expression in pancreatic cancer. *Shiyong Aizheng Zazhi* 2003; **18**: 32-34

18 **Mulcahy H**, Farthing MJ. Diagnosis of pancreatico-biliary malignancy: detection of gene mutations in plasma and stool. *Ann Oncol* 1999; **10**(Suppl 4): 114-117

19 **Wenger FA**, Zieren J, Peter FJ, Jacobi CA, Muller JM. K-ras mutations in tissue and stool samples from patients with pancreatic cancer and chronic pancreatitis. *Langenbecks Arch Surg* 1999; **384**: 181-186

20 **Castells A**, Puig P, Mora J, Boadas J, Boix L, Urgell E, Sole M, Capella G, Lluis F, Fernandez-Cruz L, Navarro S, Farre A. K-ras mutations in DNA extracted from the plasma of patients with pancreatic carcinoma: diagnostic utility and prognostic significance. *J Clin Oncol* 1999; **17**: 578-584

21 **Mulcahy HE**, Lyautey J, Lederrey C, Qi Chen X, Anker P, Alstead EM, Ballinger A, Farthing MJ, Stroun M. A prospective study of K-ras mutations in the plasma of pancreatic cancer patients. *Clin Cancer Res* 1998; **4**: 271-275

22 **Lu X**, Xu T, Qian J, Wen X, Wu D. Detecting K-ras and p53 gene mutation from stool and pancreatic juice fordiagnosis of early pancreatic cancer. *Chin Med J* 2002; **115**: 1632-1636

23 **Kimura W**, Zhao B, Futakawa N, Muto T, Makuuchi M. Significance of K-ras codon 12 point mutation in pancreatic juice in the diagnosis of carcinoma of the pancreas. *Hepatogastroenterology* 1999; **46**: 532-539

24 **Nakamura Y**, Onda M, Uchida E. Analysis of K-ras codon 12 point mutations using duodenal lavage fluid for diagnosis of pancreatic carcinoma. *Pancreas* 1999; **18**: 133-140

25 **Ha A**, Watanabe H, Yamaguchi Y, Ohtsubo K, Wang Y, Motoo Y, Okai T, Wakabayahi T, Sawabu N. Usefulness of supernatant of pancreatic juice for genetic analysis of K-ras in diagnosis of pancreatic carcinoma. *Pancreas* 2001; **23**: 356-363

26 **Wilentz RE**, Chung CH, Sturm PD, Musler A, Sohn TA, Offerhaus GJ, Yeo CJ, Hruban RH, Slebos RJ. K-ras mutations in the duodenal fluid of patients with pancreatic carcinoma. *Cancer* 1998; **82**: 96-103

27 **Tada M**, Ohashi M, Shiratori Y, Okudaira T, Komatsu Y, Kawabe T, Yoshida H, Machinami R, Kishi K, Omata M. Analysis of K-ras gene mutation in hyperplastic duct cells of the pancreas without pancreatic disease. *Gastroenterology* 1996; **110**: 227-231

28 **Rivera JA**, Rall CJ, Graeme-Cook F, Fernandez-del Castillo C, Shu P, Lakey N, Tepper R, Rattner DW, Warshaw AL, Rustgi AK. Analysis of K-ras oncogene mutations in chronic pancreatitis with ductal hyperplasia. *Surgery* 1997; **121**: 42-49

29 **Berndt C**, Haubold K, Wenger F, Brux B, Muller J, Bendzko P, Hillebrand T, Kottgen E, Zanow J. K-ras mutations in stools and tissue samples from patients with malignant and nonmalignant pancreatic diseases. *Clin Chem* 1998; **44**: 2103-2107

30 **Furuya N**, Kawa S, Akamatsu T, Furihata K. Long-term follow-up of patients with chronic pancreatitis and K-ras gene mutation detected in pancreatic juice. *Gastroenterology* 1997; **113**: 593-598

31 **Queneau PE**, Adessi GL, Thibault P, Cleau D, Heyd B, Mantion G, Carayon P. Early detection of pancreatic cancer in patients with chronic pancreatitis:diagnostic utility of a K-ras point mutation in the pancreatic juice. *Am J Gastroenterol* 2001; **96**: 700-704

32 **Hsiang D**, Friess H, Buchler MW, Ebert M, Butler J, Korc M. Absence of K-ras mutations in the pancreatic parenchyma of patients with chronic pancreatitis. *Am J Surg* 1997; **174**: 242-246

33 **Orth M**, Gansauge F, Gansauge S, Beger HG, Adler G, Schmid RM. K-ras mutations at codon 12 are rare events in chronic pancreatitis. *Digestion* 1998; **59**: 120-124

34 **Greider CW**, Blackburn EH. Identification of a specific telomere terminal transferase activity inTetrahymena extracts. *Cell* 1985; **43**: 405-413

35 **Suehara N**, Mizumoto K, Kusumoto M, Niiyama H, Ogawa T, Yamaguchi K, Yokohata K, Tanaka M. Telomerase activity detected in pancreatic juice 19 months before a tumor is detected in a patient with pancreatic cancer. *Am J Gastroenterol* 1998; **93**: 1967-1971

36 **Hiyama E**, Kodama T, Shinbara K, Iwao T, Itoh M, Hiyama K. Telomerase activity is detected in pancreatic cancer but not in benign tumors. *Cancer Res* 1997; **57**: 326-331

37 **Suehara N**, Mizumoto K, Muta T, Tominaga Y, Shimura H, Kitajima S, Hamasaki N, Tsuneyoshi M, Tanaka M. Telomerase elevation in pancreatic ductal carcinoma compared to nonmalignant pathological states. *Clin Cancer Res* 1997; **3**: 993-998

38 **Suehara N**, Mizumoto K, Tanaka M, Niiyama H, Yokohata K, Tominaga Y, Shimura H, Muta T, Hamasaki N. Telomerase activity in pancreatic juice differentiates ductal carcinoma from adenoma and pancreatitis. *Clin Cancer Res* 1997; **3**: 2479-2483

39 **Iwao T**, Tsuchida A, Hiyama E, Kajiyama G. Telomerase activity in pancreatic juice for the preoperative diagnosis of pancreatic cancer. *Nippon Rinsho* 1998; **56**: 1229-1233

40 **Piatyszek MA**, Kim NW, Wwinrich SL, Hiyama K, Hiyama E, Wright WE, Shay JW. Detection telomerase activity in human cells and tumors by a telomeric repeat amplification protocol (TRAP). *Methods Cell Sci* 1995; **17**: 1-15

41 **Myung SJ**, Kim MH, Kim YS, Kim HJ, Park ET, Yoo KS, Lim BC, Wan Seo D, Lee SK, Min YI, Kim JY. Telomerase activity in pure pancreatic juice for the diagnosis of pancreatic cancer may be complementary to K-ras mutation. *Gastrointest Endosc* 2000; **51:** 708-713

42 **Uehara H**, Nakaizumi A, Tatsuta M, Baba M, Takenaka A, Uedo N, Sakai N, Yano H, Iishi H, Ohigashi H, Ishikawa O, Okada S, Kakizoe T. Diagnosis of pancreatic cancer by detecting telomerase activity in pancreatic juice: comparison with K-ras mutations. *Am J Gastroenterol* 1999; **94**: 2513-2518

Edited by Ren SY and Wang XL **Proofread by** Xu FM

PO Box 2345, Beijing 100023, China
Fax: +86-10-85381893
E-mail: wjg@wjgnet.com www.wjgnet.com

World J Gastroenterol 2004;10(9):1341-1344
World Journal of Gastroenterology
Copyright ©2004 by The WJG Press ISSN 1007-9327

• CLINICAL RESEARCH •

Epidemiology and outcome of Crohn's disease in a teaching hospital in Riyadh

Abdullah S. Al-Ghamdi, Ibrahim A. Al-Mofleh, Rashed S. Al-Rashed, Saleh M. Al-Amri, Abdulrahman M. Aljebreen, Arthur C. Isnani, Reda El-Badawi

Abdullah S. Al-Ghamdi, Ibrahim A. Al-Mofleh, Rashed S. Al-Rashed, Saleh M. Al-Amri, Abdulrahman M. Aljebreen, Reda El-Badawi, Gastroenterology Division, Department of Medicine (38), King Khalid University Hospital, Riyadh, Kingdom of Saudi Arabia
Arthur C. Isnani, King Khalid University Hospital, College of Medicine and Research Center (74), PO Box 2925, Riyadh, Kingdom of Saudi Arabia
Correspondence to: Professor Ibrahim A. Al-Mofleh, Gastroenterology Division, Department of Medicine (38), King Khalid University Hospital, PO Box 2925 Riyadh 11461, Kingdom of Saudi Arabia
Telephone:+966-1-4671215 **Fax:** +966-1-4672558
Received: 2003-10-15 **Accepted:** 2004-01-09

Abstract

AIM: To know the epidemiology and outcome of Crohn's disease at King Khalid University Hospital, Riyadh, Saudi Arabia and to compare the results from other world institutions.

METHODS: A retrospective analysis of patients seen for 20 years (between 1983 and 2002). Individual case records were reviewed with regard to history, clinical, findings from colonoscopy, biopsies, small bowel enema, computerized tomography scan, treatment and outcome.

RESULTS: Seventy-seven patients with Crohn's disease were revisited, 13% presented the disease in the first 10 years and 87% over the last 10 years. Thirty-three patients (42.9%) were males and 44 (57.1%) were females. Age ranged from 11–70 years (mean of 25.3±11.3 years). Ninety-two (92%) were Saudi. The mean duration of symptoms was 26±34.7 mo. The mean annual incidence of the disease over the first 10 years was 0.32:100 000 and 1.66:100 000 over the last 10 years with a total mean annual incidence of 0.94:100 000 over the last 20 years. The chief clinical features included abdominal pain, diarrhea, weight loss, anorexia, rectal bleeding and palpable mass. Colonoscopic findings were abnormal in 58 patients (76%) showing mostly ulcerations and inflammation of the colon. Eighty nine percent of patients showed nonspecific inflammation with chronic inflammatory cells and half of these patients revealed the presence of granulomas and granulations on bowel biopsies. Similarly, 69 (89%) of small bowel enema results revealed ulcerations (49%), narrowing of the bowel lumen (42%), mucosal thickening (35%) and cobblestone appearance (35%). CT scan showed abnormality in 68 (88%) of patients with features of thickened loops (66%) and lymphadenopathy (37%). Seventy-eight percent of patients had small and large bowel disease, 16% had small bowel involvement and only 6% had colitis alone. Of the total 55 (71%) patients treated with steroids at some point in their disease history, a satisfactory response to therapy was seen in 28 patients (51%) while 27 (49%) showed recurrences of the condition with mild to moderate symptoms of abdominal pain and diarrhea most of which were due to poor compliance to medication. Seven patients (33%) remained with active Crohn's disease. Nine (12%) patients underwent surgery with resections of some parts of bowel, 2 (2.5%) had steroid side effects, 6 (8%) with perianal Crohn's disease and five (6.5%) with fistulae.

CONCLUSION: The epidemiological characteristics of Crohn's disease among Saudi patients are comparable to those reported from other parts of the world. However the incidence of Crohn's disease in our hospital increased over the last 10 years. The anatomic distribution of the disease is different from other world institutions with less isolated colonic affection.

Al-Ghamdi AS, Al-Mofleh IA, Al-Rashed RS, Al-Amri SM, Aljebreen AM, Isnani AC, El-Badawi R. Epidemiology and outcome of Crohn's disease in a teaching hospital in Riyadh. *World J Gastroenterol* 2004; 10(9): 1341-1344
http://www.wjgnet.com/1007-9327/10/1341.asp

INTRODUCTION

Crohn's disease is a chronic recurrent inflammatory disorder of the bowel of unknown cause that can affect any gastrointestinal site from mouth to the anal canal. It results in long-term morbidity and the need for medical treatment and surgical interventions with resection of bowels. Slight increase in mortality plays significant demands upon healthcare resources[1,2]. Epidemiological studies have shown that Crohn's disease tends to increase[3-5]. These may be due to improvement of diagnostic procedures and practices and increasing awareness of the disease. Crohn's disease varies with geographical location[6-15]. Diet and genetic predisposition triggered by environmental factors may play a significant role[16].

The aim of this study was to know the epidemiology and outcome of Crohn's disease at our institution and to compare the results with reports from other world institutions.

MATERIALS AND METHODS

All patients attending the Gastroenterology Unit of King Khalid University Hospital, Riyadh, Saudi Arabia with a diagnosis of Crohn's disease between 1983 and 2002 were enrolled into the study. Seventy-seven patients with Crohn's disease were qualified (based on completeness of the data). The files of these patients were thoroughly reviewed from the time when the diagnosis of Crohn's disease was made based on history, colonoscopic findings, colonic biopsies, small bowel enema and CT scan of abdomen up to the date of each patient's last follow-up. Significant data collected included epidemiological points of Crohn's disease patients, age and gender at presentation, smoking history, the common clinical features of the disease, diagnostic modalities used for confirmation of the disease and their corresponding results, laboratory tests at initial and last visits, current status of the patient, treatment protocols used, their responses to treatment and outcome of management.

Data were entered systematically into computer with Microsoft Excel. Statistical analyses and correlations were done

using Stat Pac Gold analysis software. *P* values less than 0.05 were considered statistically significant.

RESULTS

A total of 77 patients with Crohn's disease over the last 20 years were reviewed. Ten (13%) patients presented the disease in the first 10 years and 67 (87%) patients over the last 10 years (Figure 1). Thirty-three (42.9%) patients were males and 44 (57.1%) were females. Age ranged from 11 to 70 years with a mean age of 25.3±11.3 years. Seventy-one (92%) were Saudi nationals (Figure 2). The mean duration of symptoms was 26±34.7 mo (range 1-180 mo). Table 1 shows the demographic characteristics of all patients with Crohn's disease.

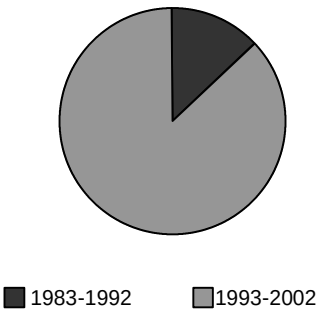

Figure 1 Number of patients with Crohn's disease over the last 20 years.

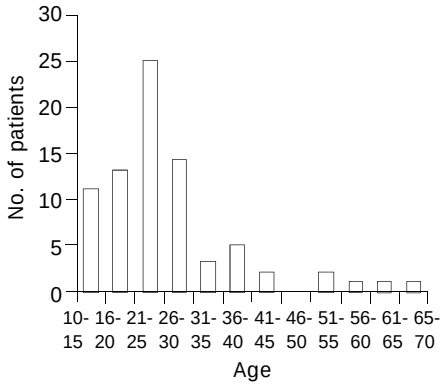

Figure 2 Age of patients at presentation.

Table 1 Demographic characteristics of patients with Crohn's disease in KKUH, Riyadh, Saudi Arabia (*n*=77)

	All patients	Active	On remission
Number	77	34 (44%)	43 (56%)
Total males	33 (42.9%)	15 (44%)	18 (42%)
Total females	44 (57.1%)	19 (56%)	25 (58%)
Age (range)	11-70 years	11-55 years	11-70 years
Mean age	25.3±11.3 years	22.9±8.3 years	27.3±13.2 years
Nationality (Saudi/non-Saudi)	71/6	32/2	39/4

The mean annual incidence of the disease in the first 10 years was 0.32:100 000 and 1.66:100 000 in the last 10 years with total a mean annual incidence of 0.94:100 000 in the last 20 years.

Table 2 illustrates the chief clinical features of patients with Crohn's disease, showing abdominal pain in 67 patients (87%), diarrhea in 60 (78%), weight loss in 41 (53%), anorexia in 22 (29%) and rectal bleeding in 19 patients (25%). Fifty eight percent of patients had abdominal tenderness and 10% had palpable mass while 42% had negative physical examination findings.

Table 2 Clinical features of Crohn's disease in KKUH

	All patients *n*=77 (%)	Active Crohn's *n*=34 (%)	Remission *n*=43 (%)
Abdominal pain	67 (87)	29 (85)	38 (88)
Diarrhea	60 (78)	27 (79)	33 (77)
Weight loss	41 (53)	23 (68)	18 (42)
Anorexia	22 (29)	10 (29)	12 (28)
Fever	20 (26)	8 (24)	12 (28)
Rectal bleeding	19 (25)	5 (15)	14 (32)
Normal physical examination	32 (42)	10 (29)	22 (51)
Abdominal tenderness	45 (58)	24 (71)	21 (49)
Palpable mass	8 (10)	3 (9)	5 (12)

Table 3 shows the colonoscopic, biopsy results, enteroclysis findings and CT scan results. Colonoscopy was abnormal in 58 patients (76%) showing features of ulcerations in 40 patients (52%), inflammation in 25 (33%), thickened mucosa in 18 (24%), pseudopolyps in 13 (17%) and nodularity in 8 (11%). Biopsy showed abnormal results in all patients with chronic inflammatory cell infiltration in 69 patients (90%), ulceration and granuloma in 31 patients (40%), crypt abscess in 19 (25%), edema in 15 (19.5%), granulations in 11 (14%) and goblet cell depletion in 10 (13%). Small bowel enema showed abnormal findings in 69 patients (89%) with ulceration in 34 (49%), narrowed lumen in 29 (42%), mucosal thickening in 24 (35%), nodularity in 18 (23%), loop separation in 15 (19%) and filling defect in 6 (8%). CT scan results showed abnormal findings in 68 patients (88%) with thickened loops in 45 patients (66%), small mesenteric nonspecific lymphadenopathy in 25 (37%), hypervascularity in 18 (23%) and presence of mass in 15 (19%).

Table 3 Colonoscopic, biopsy, small bowel enema findings and CT scan results of Crohn's disease in KKUH

		All patients	Active Crohn's	Remission
Colonoscopy		*n*=76	*n*=33	*n*=43
	Normal	18 (24%)	8 (24%)	10 (23%)
	Abnormal	58 (76%)	25 (76%)	33 (77%)
Biopsy		*n*=77	*n*=34	*n*=43
	Normal	0	0	0
	Abnormal	77 (100%)	34 (100%)	43 (100%)
Enteroclysis		*n*=77	*n*=34	*n*=43
	Normal	8 (11%)	5 (15%)	3 (7%)
	Abnormal	69 (89%)	29 (85%)	40 (93%)
CT scan		*n*=77	*n*=34	*n*=43
	Normal	9 (12%)	9 (26%)	0
	Abnormal	68 (88%)	25 (74%)	43 (100%)

The anatomic distribution of Crohn's disease in our patients was as follows, namely 16% had small bowel disease without colonic involvement, 78% had both small and large bowel disease and 6% had colitis alone.

Of the 77 patients, 55 were treated with steroids. A satisfactory response was seen in 28 patients (51%) while 27 (49%) showed recurrences of the condition, most of which were due to poor compliance to medication. Twenty-one (27%) patients however, did not receive steroids, of them seven (33%) remained with active Crohn's disease.

Nine (12%) patients underwent surgery with resections of parts of their bowel, two (2.5%) with steroid side effects, 6 (8%) with perianal disease (*e.g.* fissure, sinuses or fistulae), and 3 (4%) with fistulae between the bowel and 2 (2.5%) with perianal fistulae.

Table 4 Initial laboratory results of Crohn's disease patients at KKUH (all patients *vs* active *vs* on remission)

	All patients	Active Crohn's	Remission
WBC count	9.06±3.95	8.57±4.43	9.42±3.58
Hemoglobin	10.8±1.89	10.97±1.61	10.72±2.12
Platelets	429.9±161	422.5±145.2	435.4±176.1
ESR	42.8±27.8	34.4±22.9	49.5±26.6
Albumin	30.7±8.9	30.4±9.9	30.97±8.21

Table 5-A Comparison of initial and last follow-up laboratory results of Crohn's disease patients who went into remission

	Initial visit	Last follow-up	*P* value
WBC count	9.42±3.58	8.36±3.4	0.1629
Hemoglobin	10.72±2.12	12.4±1.78	0.0001
Platelets	435.4±176.1	396.4±132.02	0.2485
ESR	49.5±26.6	29.9±26.01	0.0009
Albumin	30.97±8.21	33.5±7.97	0.1508

Table 5-B Comparison of initial and last follow-up laboratory results of Crohn's disease patients who remained active

	Initial visit	Last follow-up	*P* value
WBC count	8.57±4.43	8.35±3.04	0.8120
Hemoglobin	10.97±1.61	11.2±2.3	0.6344
Platelets	422.5±145.2	388.5±122.5	0.3005
ESR	34.4±22.9	33.05±24.4	0.8148
Albumin	30.4±9.9	30.55±7.67	0.9445

Table 4 illustrates the comparison of the initial laboratory results in all patients with active Crohn's disease and those with remission. Of these initial laboratory results, the hemoglobin level in patients with remission was statistically significantly higher than those patients with active Crohn's disease (*P* value =0.0118). Table 5-A shows the comparison of initial and last follow-up laboratory results of 43 patients with remission. In patients with remission, the hemoglobin level was significantly increased from an initial level of 10.72±2.12 g/L to 12.4±1.78 g/L at the last follow-up (*P* value=0.0001). Furthermore, erythrocyte sedimentation rate (ESR) of 49.5±26.6 on the initial visit was significantly dropped to 29.9±26.01 at the last follow-up (*P* value 0.0009). Whereas, in patients with active Crohn's, there was no significant change in their laboratory results from initial to last follow-up (Table 5-B).

DISCUSSION

Before 1982, Kirsner and shorter observed that inflammatory bowel disease was rare or non existent in Saudi Arabia and Morocco[16]. In 1982 Mokhtar and his group from King Abdul-Aziz University in Jeddah reported the first two cases of Crohn's disease in Saudi's[6]. In 1984 Al-Nakib et al in Kuwait reported 14 patients with Crohn's disease and suggested that inflammatory bowel disease was uncommon in our population was wrong[17]. El Sheik et al from Riyadh Armed Force Hospital reported three cases of Crohn's disease between 1979 and 1985[18]. In 1990 Hossain and his group from King Khalid University Hospital in Riyadh reported seven cases of Crohn's disease, three patients were Saudis and the remaining were of different Arab nationalities and concluded that Crohn's disease did exist among Arabs[7]. Hubler and Isbister from King Faisal Specialist and Research Hospital in Riyadh reported 28 patients with Crohn's disease between 1976 and 1994[19]. From the previous reports we noticed that Crohn's disease was present among Saudi nationals in the 1980s but in a few numbers.

The present study was a retrospective study done in a referral, teaching hospital where we noticed an increase in the number of patients with Crohn's disease over the last a few years (Figure 1).

The total number of patients with Crohn's disease in KKUH from1983 till 2002 was seventy-seven. Some of them were diagnosed after admission to the hospital for investigation and management of acute problems and the remaining as outpatients for investigations of chronic problems, *e.g.* diarrhea, abdominal pain and loss of weight.

There was an increase in the number and incidence of patients with Crohn's disease over the last 10 years in comparison to the first 10 years of the study. This is not definitely related to the accuracy of diagnostic tools because the same investigations were applied to all patients, *e.g.* colonoscopy and radiological investigations from the start of the study. These may reflect an actual increase in the number of patients since 1993.

The mean annual incidence of the disease over the last 20 years was 0.94:100 000 and this is more than that in Japan and some other Far East countries, less than that of Western countries and similar to that in the Province of Granada in Spain[8-13,20].

It appeared that there was a slight female preponderance to the disease and the female to male ratio was 1.33. This is similar to that of North American population and some European countries, while in some studies from various areas of Asia and Europe suggested that there was a marked male preponderance, e.g. 1.6:1-2.2:1 in Japan and Korea respectively and 1.3:1 in Italy[1,8-14].

In many European studies, the age distribution showed a bimodal pattern, with peaks at the ages of 20-29 and 60-69 years[12]. Many other studies, however, have demonstrated a unimodal distribution and some a trimodal distribution[15]. The peak age at diagnosis in our study was between 20 and 30 years and this is similar to the results of other institutions (Figure 3).

The clinical manifestations of Crohn's disease are variable depending on the involved part of the bowel and the extent of disease. In our center more than two thirds of our patients presented had abdominal pain and diarrhea, half of all our patients had weight loss and tenderness, less than one third had fever and rectal bleeding and a few percent had a palpable mass. These presentations were investigated and the diagnosis of Crohn's disease was confirmed by endoscopies, biopsies and radiological investigations. The above presentations are the usual manifestations of Crohn's disease in most of the communities.

The worldwide anatomic distribution of Crohn's disease ranged from 30-40% in those with small bowel disease, 40-55% in those with both small and large intestine involvement and 15-25% in those with colitis alone[20,21]. In our study the distribution of the disease was different, most of the patients had small and large intestinal involvement and less than a quarter of patients had small bowel disease, while colonic disease alone represented only 6%.

It is difficult to predict which patients with Crohn's disease will go into remission. Localization of the disease, age, sex or even clinical symptoms did not significantly correlated with outcome of the treatment. Prolonged steroid response could occur in nearly half of patients receiving steroid[22]. In this review, 55 patients (71%) received steroids and 28 of them (51%) went into remission with good response to therapy while the remaining did not, mainly due to poor compliance to treatment. During the long-term follow-up of this study, 42 patients (54.5%) were in remission at any time.

It was estimated that 75% of patients with Crohn's disease require surgery within the first 20 years after onset or appearance of symptoms. The most common operation performed is a resection of a diseased segment of small intestine and colon[23,24]. Only 12% of our patients had surgeries with resections of parts

of their colon and small bowel.

In general, perianal Crohn's disease is present in as many as 25% of patients and develops in 31% to 94% of patients over the course of their illness. Manifestations of perianal disease include skin involvement (maceration, erosions, skin tags, ulceration, and abscesses), lesions of the anal canal (fissures, ulcers, and stenosis), and fistulae. Approximately two thirds of patients with Crohn's colitis have perianal fissures.

Unlike ordinary anal fissure, typical fissures associated with Crohn's disease are multiple, painless, and non-midline in location. Fistulae have been found to develop in 20% to 40% of patients with Crohn's disease and were difficult to be managed medically[25-27]. More than half of patients with colonic involvement will have anal complications, whereas in less than 20% of patients with small-bowel disease, anal symptoms were likely to develop[28,29]. Only 6% of our patients had perianal disease with fissures, sinuses and fistulae, all of them had involvement solely of the colon.

Patients with Crohn's disease who went into remission showed significant improvement in their hemoglobin and erythrocyte sedimentation rate (ESR) while other laboratory results remained statistically insignificant as that before remission.

Those who remained active showed no changes in all laboratory results.

The epidemiological characteristics of Crohn's disease among Saudi patients are comparable to those reported from other parts of the world. There is an increase in the incidence of Crohn's disease in our hospital over the last 10 years. However, the anatomic distribution of the disease is entirely different from other world institutions, with less isolated colonic disease and, all patients with perianal disease have colonic inflammation.

REFERENCES

1 **Loftus EV**, Schoenfeld P, Sandborn WJ. The epidemiology and natural history of Crohn's disease in population-based patient cohorts from North America: a systematic review. *Aliment Pharmacol Ther* 2002; **16**: 51-60

2 **Rubin GP**, Hungin AP, Kelly PJ, Ling J. Inflammatory bowel disease: epidemiology and management in an English general practice population. *Aliment Pharmacol Ther* 2000; **14**: 1553-1559

3 **Loftus EV**, Sandborn WJ. Epidemiology of inflammatory bowel disease. *Gastroenterol Clin North Am* 2002; **31**: 1-20

4 **Loftus EV**. A matter of life or death: mortality in Crohn's disease. *Inflamm Bowel Dis* 2002; **8**: 428-429

5 **Card T**, Hubbard R, Logan RF. Mortality in inflammatory bowel disease: a population-based cohort study. *Gastroenterology* 2003; **125**: 1583-1590

6 **Mokhtar A**, Khan MA. Crohn's disease in Saudi Arabia. *Saudi Med J* 1982; **3**: 207-208

7 **Hossain J**, Al-Mofleh IA, Laajam MA, Al-Rashed RS, Al-Faleh FZ. Crohn's disease in Arab. *Ann Saudi Med* 1991; **11**: 40-46

8 **Yang SK**, Loftus EV Jr., Sandborn WJ. Epidemiology of inflammatory bowel disease in Asia. *Inflammatory bowel disease* 2001; **7**: 260-270

9 **Probert CS**, Jayanthi V, Mayberry JF. Inflammatory bowel disease in Indian migrants in Fiji. *Digestion* 1991; **50**: 82-84

10 **Munkholm P**, Langholz E, Nielsen OH, Kreiner S, Binder V. Incidence and prevalence of Crohn's disease in the country of Copenhagen, 1962-87: a sixfold increase in incidence. *Scand J Gastroenterol* 1992; **27**: 609-614

11 **Loffler A**, Glados M. Data on the Epidemiology of Crohn's disease in the city of Cologne. *Med Klin* 1993; **88**: 516-519

12 **Martinez-Salmeron JF**, Rodrigo M, de Teresa J, Nogueras F, Garcia- Montero M, de Sola C, Salmeron J, Caballero M. Epidemiology of inflammatory bowel disease in the Province of Granada, Spain: aretrospective study from 1979 to 1988. *Gut* 1993; **34**: 1207-1209

13 **Cottone M**, Cipolla C, Orlando A, Oliva L, Salermo G, Pagliaro L. Hospital incidence of Crohn's disease in the province of Palermo. A preliminary report. *Scand J Gastroenterol* 1989; **170**: 27-28

14 **Cottone M**, Cipolla C, Orlando A, Oliva L, Aiala R, Puleo A. Epidemiology of Crohn's disease in Sicily: a hospital incidence study from 1987 to 1989. "The Sicilian Study Group of Inflammatory Bowel Disease." *Eur J Epidemiol* 1991; **7**: 636-640

15 **Kaerleo L**, Teglbjaerg PS, Sabroe S, Kolstad HA, Ahreas W, Eriksson M, Guenel P, Hardell L, Launoy G, Merler E, Merletti F, Stang A. Medical risk factors for small bowel adenocarcinoma with focus on Crohn's disease: a European population-based case-control study. *Scand J Gastroenterol* 2001: **36**: 641-646

16 **Kirsner JB**, Shorter RG. Recent developments in non-specific inflammatory bowel disease. *N Engl J Med* 1982; **306**: 837-848

17 **Al-Nakib B**, Radhakrishnan S, Jacob GS, Al-Liddawi H, Al-Ruwaih A. Inflammatory bowel disease in Kuwait. *Am J Gastroenterol* 1984; **79**: 191-194

18 **El Sheikh MAR**, Dip Ven Al Karawi MA, Hamid MA, Yasawy I. Lower gastrointestinal endoscopy. *Ann Saudi Med* 1987; **7**: 306-311

19 **Hubler M**, Isbister W. Inflammatory bowel disease in Saudi Arabia presentation and initial. *J Gastroenterol Hepatol* 1998; **13**: 1119-1124

20 **Moum B**, Ekbom A. Epidemiology of inflammatory bowel disease-methodological considerations. *Dig Liver Dis* 2002; **34**: 364-369

21 **Nakahara T**, Yao T, Sakurai T, Okada M, Iida M, Fuchigami T, Tanaka K, Okada Y, Sakamoto K, Sata M. Long-term prognosis of Crohn's disease. *Nippon Shokakibyo Gakkai Zasshi* 1991; **88**: 1305-1312

22 **Munkholm P**, Langholz E, Davidsen M, Binder V. Frequency of glucocorticoid resistance and dependency in Crohn's disease. *Gut* 1994; **35**: 360-362

23 **Becker JM**. Surgical therapy for ulcerative colitis and Crohn's disease. *Gastroenterol Clin North Am* 1999; **28**: 371-390

24 **Iida M**, Yao T, Okada M. Long-term follow-up study of Crohn's in Japan. The research committee of Inflammatory Bowel Disease in Japan. *J Gastroenterol* 1995; **30**(Suppl 8): 17-19

25 **Brown MO**. Inflammatory bowel disease. *Prim Care* 1999; **26**: 141-170

26 **Rubesin SE**, Scotiniotis I, Birnbaum BA, Ginsberg GC. Radiologic and endoscopic diagnosis of Crohn's disease. *Surg Clin North Am* 2001; **81**: 39-70

27 **Thuraisingam A**, Leiper K. Medical management of Crohn's disease. *Hosp Med* 2003; **64**: 713-718

28 **McClane SJ**, Rombeau JL. Anorectal Crohn's disease. *Surg Clin North Am* 2001; **81**: 169-183

29 **Tersigni R**, Alessandroni L, Kohn A, Speziale G. Treatment of perianal Crohn's disease (Abstract). *Chir Ital* 2000; **52**: 155-164

Edited by Wang XL **Proofread by** Xu FM

PO Box 2345, Beijing 100023, China
Fax: +86-10-85381893
E-mail: wjg@wjgnet.com www.wjgnet.com

World J Gastroenterol 2004;10(9):1345-1348
World Journal of Gastroenterology
Copyright ©2004 by The WJG Press ISSN 1007-9327

• CLINICAL RESEARCH •

Catheter-related infection in gastrointestinal fistula patients

Ge-Fei Wang, Jian-An Ren, Jun Jiang, Cao-Gan Fan, Xin-Bo Wang, Jie-Shou Li

Ge-Fei Wang, School of Medicine, Nanjing University, Nanjing, 210093, Jiangsu Province, China
Jian-An Ren, Jun Jiang, Cao-Gan Fan, Xin-Bo Wang, Jie-Shou Li, Department of General Surgery, Jinling Hospital, Clinical School of Nanjing University, Nanjing 210002, Jiangsu Province, China
Correspondence to: Dr. Ge-Fei Wang, School of Medicine, Nanjing University, 27 Hankou Road, Nanjing, 210093, Jiangsu Province, China. wang_gefei@hoitmail.com
Telephone: +86-25-4825110 **Fax:** +86-25-4803956
Received: 2003-08-06 **Accepted:** 2003-10-07

Abstract

AIM: To study the incidence, bacterial spectrum and drug sensitivity of catheter-related infection (CRI) in gastrointestinal fistula patients.

METHODS: A total of 216 patients with gastrointestinal fistulae during January 1998 to April 2001 were studied retrospectively. Two hundred and sixteen catheters of the 358 central venous catheters used in 216 gastrointestinal fistula patients were sent for microbiology analysis.

RESULTS: Ninety-five bacteria were cultivated in 88 catheters (24.6%). There were 54 Gram-negative bacteria (56.8%), 35 Gram-positive bacteria (36.8%), and 6 fungi (6.4%). During the treatment of CRI, 20 patients changed to use antibiotics or antifungal, and all patients were cured. The mean time of catheters used was 16.9±13.0 d.

CONCLUSION: CRI is still the common complication during total parenteral nutrition (TPN) treatment in patients with gastrointestinal fistulae, and Gram-negative bacteria are the main pathogens, and bacterial translocation is considered the common reason for CRI.

Wang GF, Ren JA, Jiang J, Fan CG, Wang XB, Li JS. Catheter-related infection in gastrointestinal fistula patients. *World J Gastroenterol* 2004; 10(9): 1345-1348
http://www.wjgnet.com/1007-9327/10/1345.asp

INTRODUCTION

Total parenteral nutrition (TPN) support is one of the main treatments for gastrointestinal fistula patients, and central venous catheters (CVC) are widely used as the major route. Catheter-related infection (CRI) is a serious complication during TPN. This paper retrospectively reviewed patients with gastrointestinal fistulae complicated by CRI during TPN during January 1998 to April 2001, and studied the incidence, bacterial spectrum and drug sensitivity of CRI. There were special characteristics of CRI in gastrointestinal fistula patients.

MATERIALS AND METHODS

Patient data

Patient data were obtained from a retrospective review of 216 CVC of 358 CVC from 216 patients with gastrointestinal fistulae in the surgical unit of Nanjing Jinling Hospital during January 1998 to April 2001.

Intervention

The catheters were removed and sent for microbiological culture and analysis, when the patients were clinically considered as CRI because of infection signs (*e.g.* tremble and fever) during TPN.

Diagnosis of CRI

Patients who had signs of infection and positive culture of CVC were diagnosed as CRI.

Statistical analysis

Patient data, culture of central venous catheters and drug sensitivity were collected and analyzed by the softwares of WHONET 5.0 and SPSS 10.0

RESULTS

Clinical data

In this study, 358 catheters were inserted in 216 gastrointestinal fistula patients. The number of male patients was 129, mean age was 42.5±16.6 years, and that of female was 87, mean age was 43.9±16.5 years. Two hundred and sixteen catheters were removed, and then the catheter tips and concurrent peripheral venous blood were sent for microbiological analysis when the patients had such infection signs as phricasmus, chill and fever. Of the catheters sent for microbiological analysis, 88 (24.6%) were confirmed to have infection by positive culture. Ninety-five bacteria were cultivated, and 8% were polymicrobes. Of the concurrent peripheral venous blood culture, 50 (14.0%) were confirmed to be positive. Fifty-two bacteria were cultivated, and 4% were polymicrobes. Twenty-four bacteria were cultivated from catheters and concurrent peripheral venous blood. The mean time of catheters used was 16.9±13.0 d.

Treatment and outcome

All the 88 patients who were confirmed having CRI were cured. Five patients were self-cured without treatment of any antibiotics after CVC was removed. Among the other 83 patients who were treated by antibiotics, 63 were cured by antibiotics in 1-3 d, 16 changed to use antibiotics, and 4 were treated by antifungal drugs according to the drug sensitivity because of persistent infection.

Microbiological analysis

Ninety five bacteria were cultivated from 88 catheters. The bacterial spectrum is shown in Table 1. There were 54 Gram-negative bacteria (56.8%), 35 Gram-positive bacteria (36.8%), and 6 fungi (6.4%). Drug sensitivity test was performed in 77 of 95 bacteria. Drug sensitivity of 48 Gram-negative bacteria and 29 Gram-positive bacteria is shown in Table 2 and Table 3, respectively. The result of drug sensitivity test indicated severe drug resistance. The preferably sensitive antibiotics for Gram-negative bacteria were imipenem, amikacin, ciprofloxacin, ceftazidime and cefoperazone/sulbactam in turn, and those for Gram-positive bacteria were vancomycin, norfloxacin and ciprofloxacin.

Table 1 Organisms present in 88 catheters

Species of bacteria	No of bacteria	Percent (%)
Gram-negative bacteria		56.8
Enterobacteriaceae		
Enterobacter cloacae	6	6.3
Escherichia coli	5	5.3
Non- identified Gram-negative bacteria	4	4.2
Klebsiella pneumoniae	1	1.1
Non-ferment gram negative rods		
Pseudomonas	20	21.1
Acinetobacter baumannii	7	7.3
Bacterium aeruginosa	5	5.3
Corynebacterium diphtheriae	4	4.2
Acinetobacter lwoffii	2	2.1
Gram-positive bacteria		36.8
Staphylococcus epidermidis	9	9.4
Staphylococcus haemolyticus	7	7.3
Tetrads	4	4.2
Staphylococcus aureus	4	4.2
Enterococcus sp.	4	4.2
Streptococcus viridans	2	2.1
Staphylococcus hominis	2	2.1
Staphylococcus warneri	2	2.1
Staphylococcus simulans	1	1.1
Fungus		6.4
Candida	5	5.3
Saccharomyces	1	1.1
Total	95	100.0

DISCUSSION

Characteristics of CRI in gastrointestinal fistula patients

As the serious complication during TPN support, the incidence of CRI was as high as 23% in simple malnutrition patients in the early years of TPN[1]. Due to the development in nurse technology and catheter materials, the incidence of CRI has gradually decreased to 2-6%[2-4]. However, the CRI incidence in surgical critical patients was still as high as 21.1-34%, and its mortality was increased[5,6]. Based on this report, the CRI incidence in gastrointestinal fistula patients was similar to that in critical patients, and higher than that in simple malnutrition patients. The mean time of catheters used was 16.9±13.0 d, and it was 17 d in other reports [2,5,6]. So it is important to supervise the symptoms of gastrointestinal fistula patients during TPN, especially 17 d after catheters were inserted.

In most literature reports, Gram-positive bacteria like *S. epidermidis* and *S. aureus* were most frequently cultivated from catheters[5-8]. Bacterial skin colonization at the catheter-skin interface at the time of insertion or afterward distal spread of the bacteria along the external catheter surface is the basic pathogenesis. However, Gram-negative bacteria are the most common organisms causing CRI of gastrointestinal fistula patients, and the orderly are Gram-positive bacteria and Fungi. Three reasons were considered for this phenomenon. First, the importance of catheter nursing has been cognized and the means for decreasing bacterial skin colonization, such as disinfection and dressing replacement were performed 3 times per week. Second, gastrointestinal fistula patients always were complicated with inflammation of abdomen, microorganisms especial Gram-negative bacteria could broadcast from abdominal abscess to blood and adhere to catheter-hub and colonize. Third, patient were commonly fasting once gastrointestinal fistula occurred. If long-term lack of food stimulation and direct lumen nutrition, mucous atrophy, height of villus decrease and

Table 2 Drug sensitivity test of 48 Gram-negative bacteria (%S)

Species of bacteria	*n*	AMK	AMP	CFP	CSL	PIP	CAZ	CRO	CXA	CIP	IPM
Pseudomonas	20	75	12.5	0	25	25	70	45	0	70.5	75
Acinetobacter baumannii	7	100	16.7	0	100	0	60	60	0	85.7	100
Enterobacter cloacae	6	75	0	100	75	50	75	80	33.3	50	100
Escherichia coli	5	0	0	0	100	0	0	0	0	0	100
Bacterium aeruginosa	5	40	0	20	80	20	60	20	0	60	80
Corynebacterium diphtheriae	4	75	0	50	100	0	75	50	25	75	100
Klebsiella pneumoniae	1	0	0	0	0	100	0	0	100	100	100
Summary	48	80	7.5	30	69.2	21.1	70.3	55.6	8.9	75.6	90

%S indicates drug sensitivity. AMK: Amikacin, AMP: Ampicillin, CFP: Cefoperazone, CSL: Cefoperazone / Sulbactam, PIP: Piperacillin, CAZ: Ceftazidime, CRO: Ceftriaxone, CXA: Cefuroxime axetil, CIP: Ciprofloxacin, IPM: Imipenem.

Table 3 Drug sensitivity test of 29 Gram-positive bacteria (%S)

Species of bacteria	*n*	AMK	AMP	SAM	CEP	CIP	ERY	NOR	PEN	PIP	VAN
Staphylococcus epidermidis	9	0	0	0	0	66.7	0	66.7	0	0	100
S. haemolyticus	7	50	0	20	25	50	16.7	60	0	0	100
S. aureus	4	100	0	0	0	25	33.3	75	0	0	100
Enterococcus sp.	4	0	0	0	0	100	0	0	0	0	100
S. hominis	2	0	0	0	0	50	0	0	0	60	100
S. warneri	2	0	0	100	0	100	100	0	0	100	100
S. simulans	1	0	0	100	100	0	0	0	0	0	100
Summary	29	50	0	18.2	16.7	56.2	21.4	66.7	11.8	10.2	100

%S indicates drug sensitivity. AMK: Amikacin, AMP: Ampicillin, SAM: Ampicillin / Sulbactam, CEP: cephalothin, CIP: Ciprofloxacin, ERY: Erythromycin, NOR: Norfloxacin, PEN: Penicillin, PIP: Piperacillin, VAN: Vancomycin.

barrier damage would arise, followed by bacterial translocation from gastrointestinal tract to the mesenteric lymph nodes even blood[9-11]. Gram-negative bacterial translocation was considered to be the most common reason for the high incidence of CRI in gastrointestinal fistula patients. Several researches indicated that gut bacterial translocation might be the pathogenesis of catheter-related infection during TPN. Pierro *et al* found that in neonates and infants who were receiving long-term parenteral nutrition, enteric microorganisms including *Escherichia coli, Klebsiella, Candida species* and *enterococci* were the main microorganisms cultured from blood sample, and they figured out that CRI might be a gut-related phenomenon[12]. Pappo *et al*. speculated that Candida sepsis during TPN might be the result of Candida translocation from the gut due to the combination of high-density Candida colonization and favorable local conditions in the gut induced by TPN and bowel rest[13]. Another research indicated that patients with an extremely short remaining small bowel (shorter than 50 cm) receiving home TPN had a higher frequency of catheter-related sepsis, particularly by enteric microorganisms[14]. Based on our research, Gram-negative bacterial translocation was considered to be the pathogenesis of CRI in gastrointestinal fistula patients. Absence of gastrointestinal integrality and extravasations of intestinal succus would induce abdominal or systemic infection once fistula occurs, and the best treatment to deal with fistulae and infection is more effective drainage. Without effective drainage, it is very difficult to control infection, even with antibiotics from low to high grade or narrow to broad spectrum. Abuse of antibiotic would result in arouse increase of drug resistance. Our study demonstrated that drug resistance of gastrointestinal fistula patients was high, and the preferably sensitive antibiotics for Gram-negative bacteria were imipenem, ceftazidime and cefoperazone/sulbactam, and those for Gram-positive bacteria were vancomycin, norfloxacin and ciprofloxacin.

Prevention and treatment of CRI

The methods for prevention of CRI included skin cleanout and antisepsis before catheter inserted, strictly disinfection system and operation during inserting, catheter nursing and dressing replacement after insertion, decreasing manipulation of catheter, and avoiding unnecessary device[15-22]. Catheters must be removed once CRI occurred or clinically suspected to be, subsequently therapies of experiential antibiotics were supposed to utilize, though part of patients could self-cure without treatment of any antibiotics[23-29]. Imipenem, ceftazidime and cefoperazone/sulbactam are the perfect choice for therapy of experiential antibiotics based on the result of drug sensitivity. If the infective symptom persisted after catheters were removed and antibiotics were utilized, drug resistance or Candida infection should be considered, and effective antibiotics or antifungal drugs should apply according to drug sensitivity. Intravenous glutamine or short-chain fatty acids could reduce central venous catheter related infection by reducing bacterial translocation from gut lumen[30,31]. According to the advancement of gastrointestinal physiology, enteral nutrition has been confirmed to improve gut mucosa barrier and liver function and nutrition, reduce bacterial translocation and avoid infection complication of TPN[32-34]. For avoiding CRI, enteral nutrition (EN) should be utilized, and the time of TPN should be reduced in gastrointestinal fistula patients. CRI is a severe complication in gastrointestinal fistula patients, and attention should be paid to its high incidence based on this retrospective study. Gram-negative bacteria with high drug resistance are the most common organisms causing CRI. Catheters must be removed and sent for microbiological analysis once CRI occurs, sensitive antibiotics for Gram-negative bacteria should be utilized. If the infective symptom persists, drug resistance or Candida infection should be considered, and effective antibiotics or antifungal drugs should be applied according to drug sensitivity.

REFERENCES

1 **Adal KA**, Farr BM. Central venous catheter-related infections: a review. *Nutrition* 1996; **12**: 208-213

2 **Peterson KK**. Central line sepsis. *Clin J Oncol Nurs* 2003; **7**: 218-221

3 **Safdar N**, Kluger DM, Maki DG. A review of risk factors for catheter-related bloodstream infection caused by percutaneously inserted, noncuffed central venous catheters: implications for preventive strategies. *Medicine* 2002; **81**: 466-479

4 **Memish ZA**, Arabi Y, Cunningham G, Kritchevsky S, Braun B, Richards C, Weber S, Pereira CR.Comparison of US and non-US central venous catheter infection rates: evaluation of processes and indicators in infection control study. *Am J Infect Control* 2003; **31**: 237-242

5 **Charalambous C**, Swoboda SM, Dick J, Perl T, Lipsett PA. Risk factors and clinical impact of central line infections in the surgical intensive care unit. *Arch Surg* 1998; **133**: 1241-1246

6 **Clarke DE**, Raffin TA. Infectious complication of indwelling long-term central venous catheters. *Chest* 1990; **97**: 966-972

7 **Page S**, Abel G, Stringer MD, Puntis JW. Management of septicaemic infants during long-term parenteral nutrition. *Int J Clin Pract* 2000; **54**: 147-150

8 **Reimund JM**, Arondel Y, Finck G, Zimmermann F, Duclos B, Baumann R. Catheter-related infection in patients on home parenteral nutrition: results of a prospective survey. *Clin Nutr* 2002; **21**: 33-38

9 **Alverdy JC**, Aoys E, Moss GS. Total parenteral nutrition promotes bacterial translocation from the gut. *Surgery* 1988; **104**: 185-190

10 **Odetola FO**, Moler FW, Dechert RE, Van Der Elzen K, Chenoweth C. Nosocomial catheter-related bloodstream infections in a pediatric intensive care unit: Risk and rates associated with various intravascular technologies. *Pediatr Crit Care Med* 2003; **4**: 432-436

11 **Eizaguirre I**, Aldamiz L, Aldazabal P, Garcia Urkia N, Asensio AB, Bachiller P, Garcia Arenzana JM, Ruiz JL, Sanjurjo P, Perez Nanclares G.Tissue antioxidant capacity and bacterial translocation under total parenteral nutrition. *Pediatr Surg Int* 2001; **17**: 280-283

12 **Pierro A**, van Saene HK, Donnell SC, Hughes J, Ewan C, Nunn AJ, Lloyd DA. Microbial translocation in neonates and infants receiving long-term parenteral nutrition. *Arch Surg* 1996; **131**: 176-179

13 **Pappo I**, Polacheck I, Zmora O, Feigin E, Freund HR. Altered gut barrier function to Candida during parenteral nutrition. *Nutrition* 1994; **10**: 151-154

14 **Terra RM**, Plopper C, Waitzberg DL, Cukier C, Santoro S, Martins JR, Song RJ, Gama-Rodrigues J. Remaining small bowel length: association with catheter sepsis in patients receiving home total parenteral nutrition: evidence of bacterial translocation. *World J Surg* 2000; **24**: 1537-1541

15 **Wang FD**, Cheng YY, Kung SP, Tsai YM, Liu CY. Risk factors of catheter-related infections in total parenteral nutrition catheterization. *Zhonghua Yixue Zazhi* 2001; **64**: 223-230

16 **Rijnders BJ**, Vandecasteele SJ, Van Wijngaerden E, De Munter P, Peetermans WE. Use of semiautomatic treatment advice to improve compliance with Infectious Diseases Society of America guidelines for treatment of intravascular catheter-related infection: a before-after study. *Clin Infect Dis* 2003; **37**: 980-983

17 **Bong JJ**, Kite P, Ammori BJ, Wilcox MH, McMahon MJ. The use of a rapid *in situ* test in the detection of central venous catheter-related bloodstream infection: a prospective study. *J Parenter Enteral Nutr* 2003; **27**: 146-150

18 **Kamala F**, Boo NY, Cheah FC, Birinder K. Randomized controlled trial of heparin for prevention of blockage of peripherally inserted central catheters in neonates. *Acta Paediatr* 2002; **91**: 1350-1356

19 **Chang L**, Tsai JS, Huang SJ, Shih CC. Evaluation of infectious complications of the implantable venous access system in a general oncologic population. *Am J Infect Control* 2003; **31**: 34-39

20 **Shin JH**, Kee SJ, Shin MG, Kim SH, Shin DH, Lee SK, Suh SP,

Ryang DW. Biofilm production by isolates of Candida species recovered from nonneutropenic patients: comparison of bloodstream isolates with isolates from other sources. *J Clin Microbiol* 2002; **40**: 1244-1248

21 **Buchman AL**. Complications of long-term home total parenteral nutrition: their identification, prevention and treatment. *Dig Dis Sci* 2001; **46**: 1-18

22 **Widmer AF**. Management of catheter-related bacteremia and fungemia in patients on total parenteral nutrition. *Nutrition* 1997; **13**(4 Suppl): 18S-25S

23 **Dinc L**, Erdil F. The effectiveness of an educational intervention in changing nursing practice and preventing catheter-related infection for patients receiving total parenteral nutrition. *Int J Nurs Stud* 2000; **37**: 371-379

24 **McConnell SA**, Gubbins PO, Anaissie EJ. Do antimicrobial-impregnated central venous catheters prevent catheter-related bloodstream infection? *Clin Infect Dis* 2003; **37**: 65-72

25 **Shorr AF**, Humphreys CW, Helman DL. New choices for central venous catheters: potential financial implications. *Chest* 2003; **124**: 275-284

26 **Kaplan SL**, Deville JG, Yogev R, Morfin MR, Wu E, Adler S, Edge-Padbury B, Naberhuis-Stehouwer S, Bruss JB. Linezolid versus vancomycin for treatment of resistant Gram-positive infections in children. *Pediatr Infect Dis J* 2003; **22**: 677-686

27 **Harbarth S**, Sax H, Gastmeier P. The preventable proportion of nosocomial infections: an overview of published reports. *J Hosp Infect* 2003; **54**: 258-266

28 **Beathard GA**. Catheter management protocol for catheter-related bacteremia prophylaxis. *Semin Dial* 2003; **16**: 403-405

29 **Hanna HA**, Raad II, Hackett B, Wallace SK, Price KJ, Coyle DE, Parmley CL. Antibiotic-impregnated catheters associated with significant decrease in nosocomial and multidrug-resistant bacteremias in critically ill patients. *Chest* 2003; **124**: 1030-1038

30 **Ding LA**, Li JS. Effects of glutamine on intestinal permeability and bacterial translocation in TPN-rats with endotoxemia. *World J Gastroenterol* 2003; **9**: 1327-1332

31 **McAndrew HF**, Lloyd DA, Rintala R, van Saene HK. Intravenous glutamine or short-chain fatty acids reduce central venous catheter infection in a model of total parenteral nutrition. *J Pediatr Surg* 1999; **34**: 281-285

32 **Fatkenheuer G**, Buchheidt D, Cornely OA, Fuhr HG, Karthaus M, Kisro J, Leithauser M, Salwender H, Sudhoff T, Szelenyi H, Weissinger F. Central venous catheter (CVC)-related infections in neutropenic patientsGuidelines of the Infectious Diseases Working Party (AGIHO) of the German Society of Hematology and Oncology (DGHO). *Ann Hematol* 2003; **82**(Suppl 2): S149-157

33 **Alpers DH**. Enteral feeding and gut atrophy. *Curr Opin Clin Nutr Metab Care* 2002; **5**: 679-683

34 **Wang XB**, Ren JA, Li JS. Sequential changes of body composition in patients with enterocutaneous fistula during the 10 days after admission. *World J Gastroenterol* 2002; **8**: 1149-1152

Edited by Wang XL and Kumar M **Proofread by** Xu FM

PO Box 2345, Beijing 100023, China
Fax: +86-10-85381893
E-mail: wjg@wjgnet.com www.wjgnet.com

World J Gastroenterol 2004;10(9):1349-1352
World Journal of Gastroenterology
Copyright ©2004 by The WJG Press ISSN 1007-9327

• CLINICAL RESEARCH •

Capsule endoscopy in diagnosis of small bowel Crohn's disease

Zhi-Zheng Ge, Yun-Biao Hu, Shu-Dong Xiao

Zhi-Zheng Ge, Yun-Biao Hu, Shu-Dong Xiao, Department of Gastroenterology, Renji Hospital, Shanghai Institute of Digestive Disease, Shanghai Second Medical University, Shanghai 200001, China
Correspondence to: Dr. Zhi-Zheng Ge, Department of Gastroenterology, Renji Hospital, Shanghai Institute of Digestive Disease, Shanghai Second Medical University, 145 Shandong Zhong Road, Shanghai 200001, China. gezheng@public8.sta.net.cn
Telephone: +86-21-63260930 **Fax:** +86-21-63200879
Received: 2003-06-05 **Accepted:** 2003-08-16

Abstract

AIM: To evaluate the effectiveness of wireless capsule endoscopy in patients with suspected Crohn's disease (CD) of the small bowel undetected by conventional modalities, and to determine the diagnostic yield of M2A Given Capsule.

METHODS: From May 2002 to April 2003, we prospectively examined 20 patients with suspected CD by capsule endoscopy. The patients had the following features: abdominal pain, weight loss, positive fecal occult blood test, iron deficiency anaemia, diarrhoea and fever. All the patients had normal results in small bowel series (SBS) and in upper and lower gastrointestinal endoscopy before they were examined. Mean duration of symptoms before diagnosis was 6.5 years.

RESULTS: Of the 20 patients, 13 (65%) were diagnosed as CD of the small bowel according to the findings of M2A Given Capsule. The findings detected by the capsule were mucosal erosions (2 patients), aphthas (5 patients), nodularity (1 patient), large ulcers (2 patients), and ulcerated stenosis (3 patients). The distribution of the lesions was mainly in the distal part of the small bowel, and the mild degree of lesions was 54%.

CONCLUSION: Wireless capsule endoscopy is effective in diagnosing patients with suspected CD undetected by conventional diagnostic methods. It can be used to detect early lesions in the small bowel of patients with CD.

Ge ZZ, Hu YB, Xiao SD. Capsule endoscopy in diagnosis of small bowel Crohn's disease. *World J Gastroenterol* 2004; 10 (9): 1349-1352
http://www.wjgnet.com/1007-9327/10/1349.asp

INTRODUCTION

Crohn's disease (CD) is a systemic granulomatous disease that may involve any part of the alimentary tract. The small bowel is the affected site in 30-40% of cases[1]. Recent studies have reported a worldwide rise in the incidence of CD. The "gold standard" for the diagnosis of CD includes the presence of following features: abdominal pain, weight loss, positive fecal occult blood test, iron deficiency anaemia, diarrhoea, fever, and typical evidence of pathological processes on conventional imaging techniques, such as, small bowel X ray, computerized tomography (CT) of the abdomen, enteroscopy, colonoscopy and ileoscopy. The small bowel is the most difficult part to be examined by endoscopy because of its distance from the mouth and anus. Small bowel series (SBS) therefore remains the first line approach in the diagnosis of small bowel Crohn's disease. When the disease is mild, with inflammatory changes confined to the mucosa, CD lesions can be missed by SBS.

Wireless capsule endoscopy (CE)[2-7] has now made painless imaging of the entire small bowel possible. In some trials, CE proved to have a higher diagnostic yield in patients with suspected small bowel diseases[8-19]. It can be used to detect early lesions in the small bowel of patients with CD. The current study represented our initial experience with the M2A Capsule in diagnosing CD in patients undergone conventional investigations in which no characteristic abnormalities were detected.

MATERIALS AND METHODS

Patients

From May 2002 to April 2003, we prospectively examined 20 patients with suspected CD by capsule endoscopy. They were 5 women and 15 men, aged 16-78 years (mean 45.2). The had following manifestions such as abdominal pain, weight loss, positive fecal occult blood test, iron deficiency anaemia, diarrhoea and fever. All patients had normal results in SBS and in upper and lower gastrointestinal endoscopy within 6 mo before they were examined. Exclusion criteria included a history of bowel obstruction, X ray evidence of small bowel stricture, evidence of any pathological abnormalities of the small bowel, any use of non-steroidal anti-inflammatory drugs during the past year.

The pertinent characteristics of the study population are shown in Table 1. The symptoms of the 20 patients enrolled in the study were consistent with suspected CD. Fourteen had abdominal pain, 13 had positive fecal occult blood test, 10 had iron deficiency anaemia (mean 81 g/L haemoglobin), 4 had diarrhoea, 3 had weight loss, and 2 had fever, some had more than one symptoms. Mean duration of the symptoms before diagnosis was 6.5 years (SD6.5).

Table 1 Clinical data of patients with suspected Crohn's disease

	Total patients CD	Patients based on CE
Patients (*n*)	20	13
Age (yr) (mean (range))	45.2 (16-78)	44.2 (16-78)
Sex(%): male / female	75 / 25	85 / 15
Positive fecal occult blood test [1]	13 / 20 (65)	11 / 13 (85)
Anaemia [1] (%)	10 / 20 (55)	9 / 13 (77)
Haemoglobin (g%) (mean (SD))	8.1 (2.0)	7.8 (1.9)
Abdominal pain [1] (%)	14 / 20 (70)	7 / 13 (54)
Diarrhoea [1] (%)	4 / 20 (20)	2 / 13 (15)
Weight loss [1] (%)	3 / 20 (15)	3 / 13 (23)
Fever [1] (%)	2 / 20 (10)	2 / 13 (15)
Duration of disease (y) (mean±SD)	6.5 (6.5)	7.0 (7.8)

[1]Some of the patients had more than one symptoms.

Instrument[2-7]

Wireless capsule endoscope (CE) (Given M2A, Given Imaging Ltd, Yoqneam, Israel) measures 11 mm×26 mm, has a battery life of approximately 6-8 h, and is propelled by peristalsis, not requiring air insufflation. CE is used in conjunction with an imaging system which includes a data recorder and interpretive workstation. CE is disposable and contains a complementary metal-oxide semiconductor (CMOS) chip camera, a transmitter, a light-emitting diode (LED) to provide illumination, and silver oxide batteries. Continuous video images were transmitted from the capsule to an antenna worn over the patient abdomen at a rate of two frames per second during passage of the CE through the gastrointestinal tract. The hemispheric lens yielded a 140-degree field of view. During the procedure, approximately 50 000 images were recorded by a solid-state recorder that was worn as a belt by the patient. The recorder was later connected to a computer workstation, in which the images were processed and then viewed on a monitor using a specifically designed reporting and processing of images and data (RAPID) software package.

Procedures

After an overnight fast for 8-12 h, the patients ingested CE with a small amount of water. They were then free to remain active as outpatients. After the study interval, the patients returned to the clinic and the recorded digital information was then downloaded into a computer. Images from the stomach and the length of small bowel were analyzed using the proprietary RAPID software. The images transmitted by the capsule were interpreted by two independent gastroenterologists. All patients were interviewed after completing the study to evaluate the tolerance or complications.

RESULTS

All the 20 patients described that the capsule was easy to swallow, painless, and preferable to conventional endoscopy. No complications were observed. The images displayed were considered to be good (Figure 1). Retention of the capsule was observed in three patients with small bowel stenosis caused by Crohn's disease (5, 7 and 22 d after capsule ingestion, respectively). One of them had a transient abdominal pain on the third and fourth day after capsule ingestion. None of the three patients with retention of the capsule showed any symptoms of acute or subacute obstruction during the follow-up. The capsule failed to reach the colon in 2 patients during the 8-h acquisition time.

Based on the results of the Given M2A Capsule, we diagnosed CD of the small bowel in 13/20 patients (65%) and normal small bowel mucosa in the remaining 6 of 7 (30%), a jejunal carcinoid confirmed by surgery in the other one. The findings detected by the capsule were mucosal erosions (2 patients), aphthas (5 patients), nodularity (1 patient), large ulcers (2 patients), and ulcerated stenosis (3 patients) (Figure 1). The distribution of the lesions was mainly in the distal part of small bowel (9 in ileum and 2 in the distal part of jejunum) which could not be reached with push endoscopy. The mild lesions or early stages of the disease accounted for 54% (2 mucosal erosions and 5 aphthas). Most of the patients underwent total colonoscopy (16/20), ileoscopy (the ileoscopy succeeded in only five patients) and gastroscopy (20/20). Fourteen out of 20 patients had abdominal CT and all had small bowel X ray series. Some of the patients underwent the procedures more than once. The mean number of procedures undergone previously was 5.4 (SD2.3).

Of the 13 patients who received medications, 11 showed a good clinical improvement after 5-ASA (mean 4 g/d) and a short term steroid treatment while the other two showed some improvement in their clinical symptoms with the same treatment. Follow up ranged from one to eleven months (mean 4 mo).

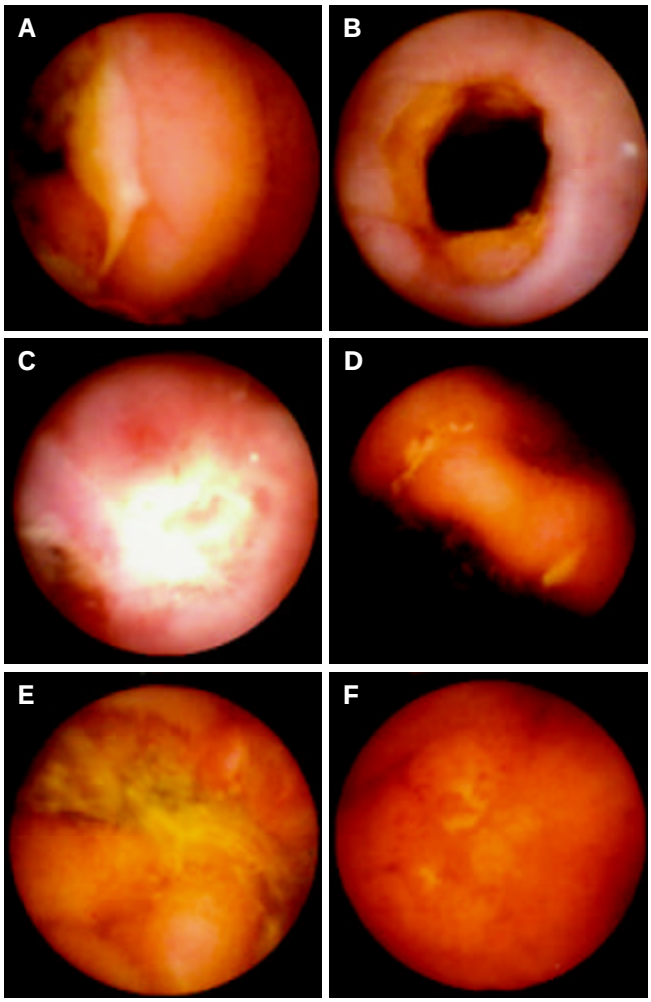

Figure 1 Capsule endoscopic findings of Crohn's disease in small bowel. A: A large ulcer in the distal part of jejunum, B: Ulcerations in a narrow ring caused by Crohn's disease in jejunum, C: A large ulcer in ileum, D: Ileal ulcers, E: Aphthas in the distal part of ileum, F: Ileal mucosal erosions.

DISCUSSION

It is generally accepted that the current visualization and imaging methods available to gastroenterologists in identifying small bowel pathology, particularly inflammatory diseases, were unsatisfactory[19,20].

The reliability of radiological studies is highly influenced by the skill and experience of the operator and how fine is the detail of the mucosa on the film. Neither enteroclysis nor small bowel follow-through (SBFT) X-ray series were able to detect flat mucosal lesions[14,21-23]. CT of the abdomen could not detect mucosal inflammation, it could show transmural thickening and extramural complications but is incapable of discerning CD in early stages of the disease.

Push enteroscopy requires an experienced and skillful endoscopist, the procedure requires between 15 and 45 min and is often uncomfortable for patients. In addition, the instrument could only examine between 80 cm and 120 cm beyond the ligament of Treitz, and occasional complications might occur[24-27].

Sonde endoscopy in theory, has the potential to examine the entire small bowel. The procedure time is often 8 h or longer and can be associated with significant patient discomforts. Among patients referred for Sonde examination, 10% had

complications, and up to 75% of the distal ileum was not reached. For these reasons, Sonde- enteroscopy was seldom performed and available in only a few diagnostic centers worldwide[25-28].

Another approach to small bowel imaging is examination of the entire small bowel by intraoperative endoscopy. The limitations of this option were the drawbacks associated with exploratory laparotomy and general anaesthesia[29].

The alternative solution should be relatively comfortable for patients, easy to use by gastroenterologists, and one that could provide a reasonable level of visual imaging for the detection of small bowel abnormalities. The Given diagnostic imaging system (M2A Capsule)[2-7] is a new modality designed to accommodate these requirements.

Capsule endoscopy has now made imaging of the entire small bowel possible. Its indications[30] are obscure gastrointestinal bleeding, abnormal imaging of small intestine, chronic abdominal pain with reasonable suspicion of organic cause in small intestine, chronic diarrhea, evaluation of extent of Crohn's disease and celiac disease and visualization of surgical anastomoses, surveillance of polyposis syndromes of small intestine.

The cost of the technology per test is about ¥8 500. In order to answer what is the cost of capsule endoscopy in comparison with the cost of traditional examinations, one must consider the diagnostic yield and *cost-effectiveness* of capsule endoscopy compared with traditional diagnostic tools. The diagnostic rate of wireless capsule endoscopy in patients with suspected small bowel diseases was about 70% in our experience[8,9]. It was similar to some other reports and significantly superior to the traditional diagnostic tools[10,19]. The potential for cost savings includes (1) improved diagnostic rate and reduction in reccurrence, conclusive testing associated not only with the clarity of the images obtained by the Capsule, but also with the Capsule's ability to traverse the entire small bowel (whereas endoscopic examinations leave part of the small bowel unexamined); (2) improved diagnostic precision able to confirm the source of bleeding, and/or rule-out certain etiologies; (3) earlier diagnosis of potentially adverse conditions such as malignancies of the small bowel; (4) reduced complications associated with the diagnostic procedure such as intestinal tears resulting from placement of the enteroscope and/or infection; (5) reduced loss in productivity associated with undergoing testing and repetitive examinations, and reduced loss in quality of life associated with both testing and worry; (6) reduced pain and discomfort associated with the diagnostic procedures.

A significant advantage of wireless capsule endoscopy is its ability to detect small bowel abnormalities, including those areas not reached by traditional endoscopy. The current battery life of 8 h could allow a reliable examination of the upper GI tract and small bowel in most patients. This was our experience as well because the complete small bowel could be studied in 18 of the 20 (90%) patients (except for the three patients with small bowel stenosis caused by Crohn's disease). The lesions in the distal jejunum and ileum were identified in 11 of 13 patients (85%) with abnormal capsule endoscopy beyond the reach of push enteroscope.

The only definite contraindication to the procedure is a patient who is a nonsurgical candidate or who refuses to entertain the idea of surgery. A retained capsule then would present the problem of retrieval with laparotomy. Severe motility disorders, including untreated achalasia and gastroparesis, should preclude CE, unless the capsule could be delivered endoscopically to the duodenum[30].

In our study, retention of the capsule occurred in three patients with small bowel stenosis caused by Crohn's disease and delayed passage of the capsule was observed in two CD patients, possibly because of slow transit time due to the inflamed small bowel mucosa. Although the capsule failed to reach the caecum, we could still identify typical lesions of CD from the recordings that emerged before the battery ran out. The information gained was helpful in further treatment planning for all these patients.

Possible complications existed with any procedure, CE was no exception. The major issue was capsule retention proximal to a stricture. The narrowed area might be anticipated or completely unexpected. Even enteroclysis could not preclude the possibility of a stricture. Our initial experience suggests the capsule does not itself cause intestinal obstruction, but proximal to a stricture it would tumble around and either eventually passes or rarely needs surgical retrieval. A retained capsule usually is asymptomatic and can be detected on the video when reviewed. Plain abdominal films could be obtained after several days to see whether the capsule passed spontaneously. The transient abdominal pain usually signals the passage of the capsule. Barkin *et al*.[31] reported that surgical intervention to remove a non-passed capsule was only 0.75% (7/937). Therefore, capsule endoscopy should not be used in patients with a history of small bowel obstruction or evidence of significant bowel stenosis.

Our study demonstrated a high diagnostic rate in patients with clinical symptoms indicative of CD who had previously undergone several diagnostic procedures that showed normal results. The patients had long intervals from the onset of disease to diagnosis. The wireless capsule might have been able to provide a correct diagnosis during early stages of the disease as well as in cases of less severe forms. We propose the wireless capsule as an effective modality for diagnosing patients with suspected CD.

In conclusion, wireless capsule endoscopy is a valuable diagnostic tool in the evaluation of obscure GI bleeding and a variety of other small bowel disorders. It illustrates the power of innovative technology to advance our diagnostic capabilities that can be applied safely to patients in the outpatient setting. In our opinion, CE should become the initial diagnostic choice in patients with suspected small bowel diseases and negative upper and lower gastrointestinal endoscopic studies.

REFERENCES

1 **Delaney CP**, Fazio VW. Crohn's disease of the small bowel. *Surg Clin North Am* 2001; **81**: 137-158

2 **Iddan G**, Meron G, Glukhovsky A, Swain P. Wireless capsule endoscopy. *Nature* 2000; **405**: 417

3 **Gong F**, Swain P, Mills T. Wireless endoscopy. *Gastrointest Endosc* 2000; **51**: 725-729

4 **Swain P**. Wireless capsule endoscopy. *Gut* 2003; **52**: 48-50

5 **Fritscher-Ravens A**, Swain CP. The wireless capsule: new light in the darkness. *Dig Dis* 2002; **20**: 127-133

6 **Bar-Meir S**, Bardan E. Wireless capsule endoscopy–pros and cons. *Isr Med Assoc J* 2002; **4**: 726

7 **Fireman Z**, Glukhovsky A, Jacob H, Lavy A, Lewkowicz S, Scapa E. Wireless capsule endoscopy. *Isr Med Assoc J* 2002; **4**: 717-719

8 **Ge ZZ**, Hu YB, Gao YJ, Xiao SD. Clinical application of wireless capsule endoscopy. *Zhonghua Xiaohua Zazhi* 2003; **23**: 7-10

9 **Ge ZZ**, Hu YB, Xiao SD. An evaluation of capsule endoscopy and push enteroscopy in the diagnosis of obscure gastrointestinal bleeding. *Zhonghua Xiaohua Neijing Zazhi* 2003; **20**: 223-226

10 **Ang TL**, Fock KM, Ng TM, Teo EK, Tan YL. Clinical utility, safety and tolerability of capsule endoscopy in urban Southeast Asian population. *World J Gastroenterol* 2003; **9**: 2313-2316

11 **Appleyard M**, Fireman Z, Glukhovsky A, Jacob H, Shreiver R, Kadirkamanathan S, Lavy A, Lewkowicz S, Scapa E, Shofti R, Swain P, Zaretsky A. A randomized trial comparing wireless capsule endoscopy with push enteroscopy for the detection of small-bowel lesions. *Gastroenterology* 2000; **119**: 1431-1438

12 **Appleyard M**, Glukhovsky A, Swain P. Wireless-capsule diagnostic endoscopy for recurrent small-bowel bleeding (letter). *N Engl J Med* 2001; **344**: 232-233

13 **Lewis BS**, Swain P. Capsule endoscopy in the evaluation of patients with suspected small intestinal bleeding: Results of a pilot study. *Gastrointest Endosc* 2002; **56**: 349-353

14 **Costamagna G**, Shah SK, Riccioni ME, Foschia F, Mutignani M, Perri V, Vecchioli A, Brizi MG, Picciocchi A, Marano P. A prospective trial comparing small bowel radiographs and video capsule endoscopy for suspected small bowel disease. *Gastroenterology* 2002; **123**: 999-1005

15 **Ell C**, Remke S, May A, Helou L, Henrich R, Mayer G. The first prospective controlled trial comparing wireless capsule endoscopy with push enteroscopy in chronic gastrointestinal bleeding. *Endoscopy* 2002; **34**: 685-689

16 **Van Gossum A**, Francois E, Hittelet A, Schmit A, Deviere J. A prospective, comparative study between push enteroscopy and wireless video capsule in patients with obscure digestive bleeding. *Gastroenterology* 2003; **125**: 276

17 **Scapa E**, Jacob H, Lewkowicz S, Migdal M, Gat D, Gluckhovski A, Gutmann N, Fireman Z. Initial experience of wireless-capsule endoscopy for evaluating occult gastrointestinal bleeding and suspected small bowel pathology. *Am J Gastroenterol* 2002; **97**: 2776-2779

18 **Bardan E**, Nadler M, Chowers Y, Fidder H, Bar-Meir S. Capsule endoscopy for the evaluation of patients with chronic abdominal pain. *Endoscopy* 2003; **35**: 688-689

19 **Schreyer AG**, Golder S, Seitz J, Herfarth H. New diagnostic avenues in inflammatory bowel diseases. Capsule endoscopy, magnetic resonance imaging and virtual enteroscopy. *Dig Dis* 2003; **21**: 129-137

20 **Tibble JA**, Bjarnason I. Non-invasive investigation of inflammatory bowel disease. *World J Gastroenterol* 2001; **7**: 460-465

21 **Lewis B**. Radiology versus endoscopy of the small bowel. *Gastrointest Clin North Am* 1999; **9**: 13-27

22 **Chong AK**. Comments regarding article comparing small bowel radiographs and video capsule endoscopy. *Gastroenterology* 2003; **125**: 276

23 **Liangpunsakul S**, Chadalawada V, Rex DK, Maglinte D, Lappas J. Wireless capsule endoscopy detects small bowel ulcers in patients with normal results from state of the art enteroclysis. *Am J Gastroenterol* 2003; **98**: 1295-1298

24 **MacKenzie J**. Push enteroscopy. *Gastrointest Endosc Clin North Am* 1999; **1**: 29-36

25 **Swain CP**. The role of enteroscopy in clinical practice. *Gastrointest Endosc Clin N Am* 1999; **9**: 135–144

26 **Lewis BS**. The history of enteroscopy. *Gastrointest Endosc Clin N Am* 1999; **9**: 1–11

27 **Gay GJ**, Delmotte JS. Enteroscopy in small intestinal inflammatory diseases. *Gastrointest Endosc Clin N Am* 1999; **9**: 115–123

28 **Seensalu R**. The sonde exam. *Gastrointest Endosc Clin N Am* 1999; **9**: 37-59

29 **Delmotte JS**, Gay GJ, Houcke PH, Mesnard Y. Intraoperative endoscopy. *Gastrointest Endosc Clin North Am* 1999; **1**: 61-69

30 **Ge ZZ**, Xiao SD. Prospects for wireless capsule endoscopy. *Wei Chang Bing Xue* 2002; **7**: 326-330

31 **Barkin J**, Friedman S. Wireless capsule endoscopy (WCE) requiring surgical intervention: The world's experience [abstract]. *2nd conference on capsule endoscopy, Berlin* 2003: 171

Edited by Zhang JZ and Wang XL **Proofread by** Xu FM

PO Box 2345, Beijing 100023, China
Fax: +86-10-85381893
E-mail: wjg@wjgnet.com www.wjgnet.com

World J Gastroenterol 2004;10(9):1353-1356
World Journal of Gastroenterology
Copyright ©2004 by The WJG Press ISSN 1007-9327

• BRIEF REPORTS •

Plasma erythropoietin levels in anaemic and non-anaemic patients with chronic liver diseases

Cosimo Marcello Bruno, Sergio Neri, Claudio Sciacca, Gaetano Bertino, Pietro Di Prima, Danila Cilio, Rinaldo Pellicano, Luciano Caruso, Raffaello Cristaldi

Cosimo Marcello Bruno, Sergio Neri, Claudio Sciacca, Gaetano Bertino, Pietro Di Prima, Danila Cilio, Luciano Caruso, Raffaello Cristaldi, Department of Internal Medicine and Sistemic Diseases, University of Catania, Italy
Rinaldo Pellicano, Department of Gastro-Hepatology, Molinette Hospital, Torino, Italy
Correspondence to: Professor C.M. Bruno, Dip. Medicina Interna e Patologie Sistemiche, Osp. S. Marta, via G. Clementi 36, 95124 Catania, Italy. cmbruno@unict.it
Telephone: +39-95-7435706 **Fax:** +39-95-7435706
Received: 2003-10-08 **Accepted:** 2003-12-24

Abstract

AIM: To investigate the serum erythropoietin (Epo) levels in patients with chronic liver diseases and to compare to subjects with iron-deficiency anaemia and healthy controls.

METHODS: We examined 31 anaemic (ALC) and 22 non-anaemic (NALC) cirrhotic patients, 21 non- anaemic subjects with chronic active hepatitis (CAH), 24 patients with iron-deficiency anaemia (ID) and 15 healthy controls. Circulating Epo levels (ELISA; R&D Systems, Europe Ltd, Abingdon, UK) and haemoglobin (Hb) concentration were determined in all subjects.

RESULTS: Mean±SD of Epo values was 26.9±10.8 mU/mL in ALC patients, 12.5±8.0 mU/mL in NALC subjects, 11.6±6.3 mU/mL in CAH patients, 56.4±12.7 mU/mL in the cases of ID and 9.3±2.6 mU/mL in controls. No significant difference (P>0.05) was found in Epo levels between controls, CAH and NALC patients. ALC individuals had higher Epo levels (P<0.01) than these groups whereas ID subjects had even higher levels (P<0.001) than patients suffering from ALC.

CONCLUSION: Increased Epo values in cirrhotics, are only detectable when haemoglobin was lesser than 12 g/dL. Nevertheless, this rise in value is lower than that observed in anaemic patients with iron-deficiency and appears blunted and inadequate in comparison to the degree of anaemia.

Bruno CM, Neri S, Sciacca C, Bertino G, Di Prima P, Cilio D, Pellicano R, Caruso L, Cristaldi R. Plasma erythropoietin levels in anaemic and non-anaemic patients with chronic liver diseases. *World J Gastroenterol* 2004; 10(9): 1353-1356
http://www.wjgnet.com/1007-9327/10/1353.asp

INTRODUCTION

Chronic anaemia is often observed in patients with liver disease, especially in advanced stages, and an inverse relation has been reported between haemoglobin (Hb) concentration or hematocrit value and survivorship[1]. Inapparent gastrointestinal bleeding, folate and vitamin B_{12} deficiency, autoimmune haemolysis, altered oxide-reductive balance and hypersplenism are underlying mechanisms responsible for the anaemic state[2-4].

Moreover, a reduced proliferation of erythroid precursor cells has been described in the bone marrow of these patients[4,5].

Erythropoietin (Epo) is an endogenous glycoprotein stimulating erythrocytosis which interacts with erythroid progenitor cells to promote their proliferation and maintain their viability as they differentiate[6,7]. The regulation of erythropoiesis is a biological feedback loop whereby the degree of tissue oxygenation sets the amount of Epo production, the concentration of erythropoietin in turn drives the bone marrow to produce a level of red cells at which oxygen delivery is sufficient to lower Epo production[8]. The gene codifying for this growth factor has been isolated and a regulatory region involved with oxygen sensing has been defined. Expression in response to hypoxia is mediated via a DNA-binding complex[8].

Since literature data[9,10] suggest an emerging role of this hormone in causing haematological changes in chronic diseases, suboptimal production of, or response to, Epo might contribute to the pathogenesis of chronic anaemia in cirrhotics. Some studies regarding the association between Epo levels and cirrhosis have appeared in literature[11-16] but reported data are controversial.

The aim of this study was to investigate the circulating Epo levels in patients suffering from chronic liver disease of various degrees, with and without concomitant anaemia, compared to subjects with iron-deficiency uncomplicated anaemia as well as to healthy controls, in order to assess the relationship between serum Epo and Hb concentration.

MATERIALS AND METHODS

We examined 74 patients suffering from chronic liver diseases (21 chronic active hepatitis [CAH] and 53 cirrhosis), 24 patients with iron-deficiency (ID) uncomplicated anaemia and 15 healthy control subjects, comparable to sex and age. Haematology, albumin concentration, aspartate aminotransferase (AST) and alanine aminotransferase (ALT) levels, serum bilirubin and prothrombin time (as percentage of prothrombin activity), were measured in all patients and controls.

Diagnosis of patients with liver disease, was based on clinical (medical history, physical examination), instrumental (ultrasonography, endoscopy) and laboratory (liver function tests) data. In 47 out of these cases, hepatic damage was confirmed by liver biopsy (in the remaining subjects the procedure was not necessary, as diagnosis was clinically evident).

In 6 out of 21 CAH patients, the etiological agent was hepatitis B virus (HBV) while in the remaining 15, hepatitis C virus (HCV). Of the 53 cirrhotic subjects, 19 were infected with HBV, 31 with HCV while 3 had a history of alcohol abuse.

According to accepted criteria[8], thirty-one cirrhotic patients had normocromic normocytic anaemia (ALC group, mean±SD Hb 10.2±0.9 gr/dL) and twenty-two were non anemic (NALC group, mean±SD Hb 13.6±0.7 gr/dL).

None of anaemic cirrhotics had signs of iron-deficiency (serum iron ⩾70 μg/dL, serum ferritin ⩾50 ng/mL and transferrin saturation ⩾30%).

Table 1 Main characteristics of investigated subjects

	Controls *n*=15	CAH patients *n*=21	NALC patients *n*=22	ALC patiens *n*=31	ID patients *n*=24
Age (yr, mean ±SD)	52±6	54±8	59±3	60±5	54±5
Males	8	10	9	12	10
Famales	7	11	13	19	14
Albumin (g/dL)	3.6±0.2	3.3±0.3	3.0±0.3	2.9±0.2	3.5±0.3
AST (U/L)	14.2±1.5	73.7±19.2	41.9±12.6	40.6±16.4	16.1±3.5
ALT (U/L)	15.6±2.7	69.7±8.4	39.8±10.1	37.9±12.5	14.2±3.1
Bilirubin (mg/dL)	0.6±0.1	0.8±0.1	1.1±0.2	1.3±0.2	0.7±0.1
Prothrombin time (%)	98.2±5.0	81.1±6.2	72.4±8.9	70.3±10.2	95.1±3.1

In agreement with Child-Pugh's classification[17], 12 of NALC patients were in class B and 10 belonged to class C. In the ALC group, 13 patients were in class B whereas 18 in class C.

Cirrhotic subjects affected by gastrointestinal bleeding in the previous 3 mo (as confirmed by endoscopy and fecal occult blood testing) and those with suspected hepatocellular carcinoma (on the basis of ultrasonography, alpha-foetoprotein and carcinoembryonic antigen levels performed during the screening) were excluded from the study.

Diagnosis in patients with iron-deficiency anaemia, was based on clinical (medical history, physical examination), and laboratory (Hb concentration <12 g/dL, serum ferritin <40 ng/dL and transferrin saturation<16%) data. None of them had clinical or laboratory (C-reactive protein) evidence of inflammatory condition.

All subjects had normal renal function (serum creatinine <1.2 mg/dL, creatinine clearance ⩾70 mL/min). The main characteristics of our study groups are summarised in Table 1.

The study was conformed to Helsinki Declaration and informed consent was obtained from the whole study series.

A blood sample was obtained from all subjects and ethylenediaminetetraacetic acid (EDTA) was added. Samples were centrifuged and plasma was stored at -25 ℃. Erythropoietin was determined by a commercial ELISA kit (R&D Systems Europe Ltd, Abingdon, UK). The sensitivity of assay was less than 0.6 mU/mL. Non specific binding was <1%. Intra and inter-assay variability averaged 3.1% and 3.5%, respectively. Epo concentrations were expressed as mU/mL.

Analysis of variance and Kruskall-Wallis test were used to compare mean±SD between various groups. Relationship between continuous variables was investigated by correlation test or multiple regression test when they were more than two. Covariance analysis was performed to assess the difference in Epo values for adjusted Hb, between ALC and ID patients. The regression lines between Hb concentration and Epo values in these two groups were compared by *t*-test, according to current statistical procedures[18].

RESULTS

No significant difference (P>0.05) in Hb concentration was observed between controls (13.9±0.3 gr/dL), CAH (13.7±0.5 gr/dL) and NALC (13.6±0.7 gr/dL) patients. Subjects suffering from ALC (10.2±0.9 gr/dL) and ID (10.1±0.8 gr/dL) had values significantly lower than others (P<0.05), but Hb concentration was similar in these two groups (P>0.05). Among cirrhotic subjects, Hb concentration was similar (P>0.05) in Child-Pough class B and class C patients both in ALC (10.4±0. 7 gr/dL *versus* 10.1±0.9 gr/dL, respectively) and in NALC (13.8±0.4 gr/dL *versus* 13.5±0.9 gr/dL, respectively) groups.

Mean±SD of plasma Epo was 9.3±2.6 mU/mL in controls, 11.6±6.3 mU/mL in CAH patients, 12.5±8.0 mU/mL in NALC subjects, 26. 9±10.8 mU/mL in ALC patients and 56.4±12.7 mU/mL in ID individuals.

Regarding Child-Pugh related allocation, mean±SD of plasma Epo was 24.18±9.56 mU/mL for patients in class B *versus* 30.71±10.82 mU/mL for those in class C of the ALC group, 12.3±7.8 mU/mL in class B *versus* 12.9±8.1 mU/mL in class C patients of the NALC group, respectively.

Statistical analysis did not show any significant difference between controls, CAH patients and NALC patients (P>0.05). ALC subjects had significantly higher Epo levels than these three groups (P<0.01) and patients suffering from ID had significantly higher Epo levels than ALC patients (P<0.001). In both NALC and ALC groups, no significant difference (P>0.05) was observed between class B and class C patients.

Epo levels were not related (P>0.05) to albumin concentration, AST and ALT values, serum bilirubin and prothrombine time in any group of patients with liver disease.

An inverse significant relationship between Epo and Hb was found in ID patients (r =-0.61, P=0.001) but not in ALC patients (r=-0.22, P>0.05). Covariance analysis revealed a significant difference (P<0.001) in Epo values for adjusted Hb concentration between ALC and ID patients.

Finally, the regression lines between Epo and Hb in ALC and ID patients, were compared and a significant difference was found (ALC patients: slope -2.47, ES 2.02, y-intercept 52.39; ID patients: slope -9.79, ES 2.7, y-intercept 155.48; t=2.23, fd=53, P=0.03).

DISCUSSION

Anaemia is a multifactorial complication of liver cirrhosis[2-5]. Papers regarding abnormalities of circulating Epo in patients with liver diseases were few and results were contradictory[11-18]. Some authors have reported higher Epo levels in cirrhotic patients when compared to healthy controls. An inverse relation between Epo values and the haematological indices has been described by some groups.

We assessed plasma Epo levels in anaemic and non-anaemic patients with chronic liver disease compared to healthy controls and iron-deficiency anaemic subjects.

Our results showed that non-anaemic patients with liver disease and controls had similar Epo values, in cirrhotic patients, circulating Epo was not related to Child-Pugh score. Moreover, multiple regression test documented that Epo levels were not related to concentration of albumin, bilirubin, ALT or AST values and prothrombin time in any of these three groups of patients with liver disease.

This was in part conflicting with the findings of other authors[12,13,15] and suggested that liver damage itself, independent of the degree of dysfunction, was not able to alter circulating Epo levels.

On the other hand, we detected a significant increase in levels of this hormone both in ALC patients and in ID patients.

However, a significant inverse correlation between Epo and Hb was found in ID group (r=-0.61, P<0.05) but not in ALC group (r=-0.22, P>0.05).

Nevertheless, increased Epo level in anaemic patients *versus* healthy controls was not enough to assess Epo production.

In fact, the definition of defective Epo production has relied on a low Epo value in comparison to reference patients with similar Hb[19]. Consequently, circulating Epo cannot be simply compared with normal values and levels found must be evaluated in relation to the degree of anaemia.

As it has been widely accepted that adequate Epo production occur in patients with iron-deficiency anaemia[19], we chosen ID patients as reference group.

Mean±SD of Hb values was similar in the two groups of anaemic patients, but mean±SD of Epo concentrations in ALC group was much lower than that in ID patients.

Analysis of covariance showned a significant difference in Epo values between the two groups (P<0.001). Moreover, we also compared the regression lines between Epo and Hb in ALC and ID patients. The slope and y-intercept of two regression lines (Figure 1) were significantly different (P<0.05).

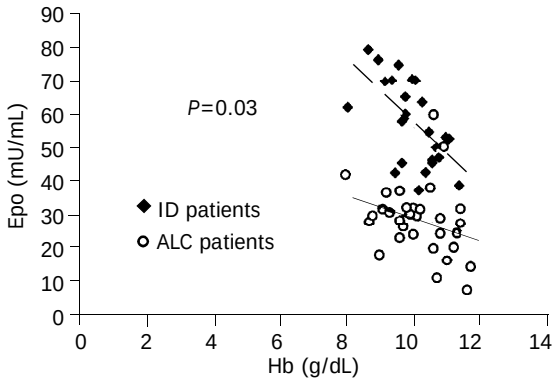

Figure 1 Comparison between regression lines of Epo and Hb in ALC and ID patients.

Therefore, although circulating Epo levels in ALC patients, were higher than that in non anaemic individuals with liver disease, they were significantly lower in healthy subjects, than in ID patients. The reason of this finding is unclear. It seems that an altered Epo clearance did not result in the difference because normal metabolism of this hormone was maintained in cirrhotics[20].

Cazzola *et al*.[21] described an inverse relationship between red blood precursor mass and serum Epo. As in cirrhosis, a reduction of erythroid cells has been reported[4,5], the finding of lower Epo values in our ALC patients than in ID patients was not due to an increased utilization by precursor cells.

Therefore, lower Epo values in ALC subjects, are likely provoked by an impaired synthesis rather than by an increased metabolism.

Consequently, we think that Epo production occurred in different quantitative patterns in these two groups, and other factors besides Hb concentration, could affect its output in cirrhotic patients.

This can explain why no relationship was found between Hb and Epo in our ALC patients.

In adults, Epo has been found to be synthesised by the kidney and to a lesser extent by the liver[22]. Thus, liver failure could endanger the hepatic residual share of Epo synthesis, even though in this study, the absence of relation between Epo values and investigated indices of liver dysfunction did not support this hypothesis. Alternatively, a reduced sensitivity of renal cells to hypoxic stimuli could be hypothesized. Furthermore, the inhibitory action of reactive oxygen species and nitric oxide as well as malnutrition of cirrhotic patients might contribute to reduction in Epo synthesis[23-26].

Finally, inflammatory cytokines, namely interleukin-1, tumor necrosis factor and transforming growth factor, are enhanced in liver diseases and have been found to inhibit hypoxia-induced erythropoietin production *in vitro* and *in vivo*[27-29].

Whatever the cause of blunted and unsuitable rise in circulating Epo is the levels of this hormone in anaemic cirrhotics, appear defective and inadequate with regard to the degree of anaemia.

Even though Epo deficiency is not only the cause of anaemia in cirrhotics, its insufficient concentration could play a role in the persistence of anaemic status, worsening the outcome of cirrhotic patients.

In conclusion, non-anaemic patients with chronic liver disease have normal Epo levels. During cirrhosis, elevated Epo values are detectable in patients with Hb concentration lesser than 12 g/dL and are not related to the degree of both Hb concentration and severity of liver dysfunction. In addition, such an increase is lower than that observed in patients with iron-deficiency anaemia and appears blunted and inadequate in comparison to the degree of anaemia.

REFERENCES

1 **Pignon JP**, Poynard T, Naveau S, MarteauP, Zourabichvili O, Chaput JC. Multidimensional analysis by Cox's model of the survival of patients with alcoholic cirrhosis. *Gastroenterol Clin Biol* 1986; **10**: 461-467

2 **Tymofieiev VV**, Kolomoiets' MIW. The pathogenetic characteristics of the anemic syndrome in liver cirrhosis. *Lik Sprava* 1997; **5**: 66-71

3 **Mehta AB**, McIntyre N. Hematological disorders in liver disease. *Forum* 1998; **8**: 8-25

4 **Sherlok S**, Dooley J. "The haematology of liver disease" in Diseases of the Liver and Biliary System, 11th edition. UK 2002: 47, Oxford: Blackwell Publishing

5 **Korolko IUR**, Sarycheva TG, Kotelnikov VM, Kozinets GI, Zherebtsov LA. Anemic syndrome in chronic hepatitis and liver cirrhosis. *Klin Med* 1993; **71**: 45-48

6 **Spivak JL**, Pham T, Isaacs M, Hankins WD. Erythropoietin is both a mitogen and survival factor. *Blood* 1991; **77**: 1228-1233

7 **Koury MJ**, Bondurant MD. Erythropoietin retards DNA breakdown and prevents programmed death in erythroid progenitor cells. *Science* 1990; **248**: 378-381

8 **Weatherall DJ**, Provan AB. Red cells I: inherited anaemias. *Lancet* 2000; **355**: 1169-1175

9 **Scudla V**, Adam Z, Scudlova M. Diagnosis and therapy of anemia in chronic diseases. *Vnitr Lek* 2001; **47**: 400-406

10 **Spivak JL**. The blood in systemic disorders. *Lancet* 2000; **355**: 1707-1712

11 **Siciliano M**, Tomasello D, Milani A, Ricerca BM, Storti S, Rossi L. Reduced serum levels of immunoreactive erythropoietin in patients with cirrhosis and chronic anemia. *Hepatology* 1995; **22**: 1132-1135

12 **Pirisi M**, Fabris C, Falleti E, Soardo G, Toniutto P, Gonano F, Bartoli E. Evidence for a multifactorial control of serum erythropoietin concentration in liver disease. *Clin Chim Acta* 1993; **219**: 47-55

13 **Mady E**, Wissa G, Khalifa A, el-Sabbagh M. Assessment of erythropoietin levels and some iron indices in chronic renal failure and liver cirrhosis patients. *Dis Markers* 1999; **15**: 229-236

14 **Vasilopoulos S**, Hally R, Caro J, Martin P, Westerberg S, Moritz M, Jarrel B, Munoz S. Erythropoietin response to post-liver transplantation. *Liver Transpl* 2000; **6**: 349-355

15 **Tacke F**, Schoffski P, Gauser A, Manus MP. Erythropoietin plasma levels are elevated in chronic liver disease and correlate with anemia, liver dysfunction, bleeding episodes and interleukin-6 (Abstract). *J Hepatol* 2002; **36**: 65

16 **Oczko-Grzesik B**, Weicek A, Kokot F. Influence of IFN-alpha on plasma erythropoietin levels in patients with hepatitis B virus-

associated chronic active hepatitis. *J Interferon Cytokine Res* 2001; **21**: 669-676

17 **Pugh RNH**, Murray-Lyon IM, Dawson JL, Pietrosi MC, Williams R. "Transection of the esophagus for bleeding esophageal varices". *Br J Surg* 1973; **60**: 646

18 **Colton T**. Statistics in Medicine. *Boston: Little, Brown and Company*, 1973: 201

19 **Cazzola M**, Mercuriali F, Brugnara C. Use of recombinant human erythropoietin outside the setting of uremia. *Blood* 1997; **89**: 4248-4267

20 **Jensen JD**, Jensen LW, Madsen JK, Poulsen L. The metabolism of erythropoietin in liver cirrhosis patients compared with healthy volunteers. *Eur J Haematol* 1995; **54**: 111-116

21 **Cazzola M**, Guarnone R, Cerani P, Centenara E, Rovati A, Beguin Y. Red blood cell precursor mass as an independent determinant of serum erythropoietin level. *Blood* 1998; **91**: 2139-2145

22 **Krantz SB**. Erythropoietin. *Blood* 1991; **77**: 419-434

23 **Canbolat O**, Fandrey J, Jelkmann W. Effects of modulators of the production and degradation of hydrogen peroxide on erythropoietin syntesis. *Respir Physiol* 1998; **114**: 175-183

24 **Fandrey J**, Frede S, Jelkmann W. Role of hydrogen peroxide in hypoxia-induced erythropoietin production. *Biochem J* 1994; **303**: 507-510

25 **Schobersberger W**, Hoffmann G, Fandrey J. Nitric oxide donors suppress erythropoietin production *in vitro*. *Pflugers Arch* 1996; **432**: 980-985

26 **Genius J**, Fandrey J. Nitric oxide affects the production of reactive oxygen species in hepatoma cells: implications for the process of oxygen sensing. *Free Radic Biol Med* 2000; **29**: 515-521

27 **Faquin WC**, Schneider TJ, Goldberg MA. Effect of inflammatory cytokines on hypoxia-induced erythropoietin production. *Blood* 1992; **79**: 1987-1994

28 **Jelkmann WE**, Fandrey J, Frede S, Pagel H. Inhibition of erythropoietin production by cytokines. Implications for the anemia involved in inflammatory states. *Ann N Y Acad Sci* 1994; **718**: 300-309

29 **Poveda Gomez F**, Camacho Siles J, Quevedo Morales E, Fernandez Zamorano A, Codoceo Alquinta R, Arnalich Fernandez F, Sempere Alcocer M. Pattern of blood levels of erythropoietin and proinflammatory cytokines in patients with anemia of chronic disorders secondary to infection. *An Med Interna* 2001; **18**: 298-304

Edited by Wang XL and Xu FM

PO Box 2345, Beijing 100023, China
Fax: +86-10-85381893
E-mail: wjg@wjgnet.com www.wjgnet.com

World J Gastroenterol 2004;10(9):1357-1360
World Journal of Gastroenterology
Copyright ©2004 by The WJG Press ISSN 1007-9327

• BRIEF REPORTS •

Effect of cyclin G2 on proliferative ability of SGC-7901 cell

Jie Liu, Ze-Shi Cui, Yang Luo, Li Jiang, Xiao-Hui Man, Xue Zhang

Jie Liu, Ze-Shi Cui, Experimental Technology Center, China Medical University, Shenyang 110001, Liaoning Province, China
Yang Luo, Li Jiang, Xiao-Hui Man, Xue Zhang, Medical Gene Group of Cell Biology Laboratory, Key Laboratory of the Ministry of Health, China Medical University, Shenyang 110001, Liaoning Province, China
Supported by a grant for Distinguished Young Teachers of Higher Education of the Ministry of Education of the Teaching and Research Encouragement Plan
Correspondence to: Dr. Xue Zhang, Medical Gene Group of Cell Biology Laboratory, Key Laboratory of the Ministry of Health, China Medical University, Shenyang 110001, Liaoning Province, China. zhangxuenew@yahoo.com
Telephone: +86-24-23256666-5532 **Fax:** +86-24-23265492
Received: 2003-10-10 **Acceped:** 2003-12-16

Abstract

AIM: To study the effect of cyclin G2 on proliferation of gastric adenocarcinoma cell line-SGC-7901 cell *in vitro*.

METHODS: By use of cation lipofectamine transfection reagent, the pIRES-G2 and pIRESneo plasmids were transferred into SGC-7901cell line. Anticlones were selected by G418. Positive clones were observed and counted using Giemsa staining. Cell proliferative ability was assayed by MTT.

RESULTS: (1) The clone number of pIRES-G2 group decreased, clone volume reduced. The number of cell clones in pIRESneo group was 87±3, that of pIRES-G2 group was 53±4, occupying 60.1% of pIRESneo group, there was significant difference obviously (P<0.01, t=15.45). (2) The average absorbance of clone cell obtained by stable transfection of pIRES-G2 at 570 nm was 1.6966±0.2125, the average absorbance of clone cell obtained by stable transfection of pIRESneo at 570 nm was 2.1182±0.3675, there was significant difference between them (P<0.01, t=3.412).

CONCLUSION: Cyclin G2 can inhibit SGC-7901cell proliferative ability obviously, it may be a negative regulator in cell cycle regulation.

Liu J, Cui ZS, Luo Y, Jiang L, Man XH, Zhang X. Effect of cyclin G2 on proliferative ability of SGC-7901 cell. *World J Gastroenterol* 2004; 10(9): 1357-1360
http://www.wjgnet.com/1007-9327/10/1357.asp

INTRODUCTION

Cell cycle regulation is the core part in cell proliferation, which has a close relationship with cell carcinogenesis. In recent years, the study of cell cycle regulation is the foreland and hotspot field in cell biology and genetics. At present, research on the formation, activation, inactivation of cyclin-CDK (cyclin-dependent kinase) holo-enzyme complex is the main molecular basis of cell cycle regulation[1,2]. All the 12 type different cyclins found in mammalian cells contain a 100 amino-acid homologous region named cyclin box, which is the molecular structure marker of cyclins[3]. Cyclin G is a new member of cyclin family, which includes cyclin G1 and cyclin G2. Although the identity of amino acid sequence and nucleotide sequence of cDNA of cyclin G1 and cyclin G2 was 53% and 60% respectively, their biological function and distribution in tissue and organ differ greatly[4,5]. Research shows that cyclin G1 is located mainly in nucleus, whose expression is induced by the damage of DNA and depends on the expression level of p53[6,7]. Cyclin G2 is located mainly in cytoplasm, whose expression can be induced by the VHL protein and to some degree is independent of p53[8]. We have known that cyclin G1 is a positive regulator in cell cycle regulation. But we still do not know if cyclin G2 is connected with CDKs and with which kind of CDKs. The expression of cyclin G2 induced by cancer -suppressing gene hints that it may act as a negative regulator in cell proliferation[9]. Moreover, we purified oral squamous carcinoma cell by laser capture micro-dissection, and found that 4 cases showed low expression of cyclin G2 in 5 cases in the gene expression pedigree research with gene chip analysis[10]. Thus, it is much more likely for cyclin G2 to have the negative regulating effect on the cell proliferation.

In this article, we transfected pIRES-G2 into SGC-7901 cell and studied the effect of cyclin G2 expression on the cell proliferation *in vitro*.

MATERIALS AND METHODS

Materials

The eukaryotic plasmid expression vector contains the whole length of cyclin G2 and selective marker gene, neo was constructed by the Medical Gene Group of China Medical University[11]. pIRESneo vector was purchased from Clontech. *E.Coli* JM109 competent cell was the product of TaKaRa, plasmid extraction and purification kits were from Qiagen. Lipofectamine Plus™ and G418 were the products of Invitrogen. MTT was from Huamei. SABC kit and DAB kit were from Boster.

The human gastric adenocarcinoma cell line SGC-7901(Cell Biology Laboratory of China Medical University) was grown in DMEM (Gibco) supplemented with 100 mL/L heat-inactivated fetal calf serum (Hyclone), 100 U/mL of penicillin sodium and 100 μg/mL streptomycin sulfate, cultured at 37 ℃, with 50 mL/L CO_2.

Methods

Plasmid amplification reaction and evaluation E.Coli JM109 competent cells were transformed by pIRES-G2 plasmid, cultured in LB medium supplemented with Amp^+ (100 μg/ mL). The positive clones were selected and cultured. Abundant plasmids were produced and purified by alkaline lysis method, identified by 10 g/L agarose gel electrophoresis after restriction endogenous enzyme digestion. The concentration and purity were determined by ultraviolet scanning spectrophotometer.

Gene transfection Exponentially growing SGC-7901 cells were seeded using 2 mL non-antibiotics culture medium into 6-well plates. After 24 h when cells grew to 60-80% confluence transfection began. Cells were transiently transfected according to the protocol of Lipofectamine Plus™. Briefly, the plasmid DNA was premixed with the Plus reagent by diluting 1 μg DNA into 100 μL transfection DMEM (serum-free, non-antibiotics) and adding 6 μL Plus reagents in polystyrene tubes. Solutions

were combined, gently mixed, and incubated for 15 min at room temperature to allow formation of DNA/Plus complexes. Meanwhile, 4 μL Lipofectamine reagents were diluted in 100 μL transfection DMEM. The DNA/Plus reagent was mixed with the diluted Lipofectamine reagent and incubated for 15 min again at room temperature. The growth medium was removed from the cells and replaced with 800 μL transfection DMEM. The complexes were added to the cells and incubated for 3 h at 37 ℃, with 50 mL/L CO_2. Then 1 mL of non-antibiotics DMEM containing 200 mL/L FCS was added to it. Transfection of the pIRESneo vector into SGC-7901cell was the same.

Cell clone At 24 h after gene transfection, cells were trypsin digested and transferred into 100 mm culture dish, and cultured for another 2 wk in G418 (400 μg/ mL) selective culture medium. The clone formation and cell morphology were observed under an inverted microscope (Olympus IX70). Images were acquired using a cool charge-coulped device (Spot) and transferred into computer. Cells were fixed in methanol/ice acetic acid (3:1) and stained in 50-100 g/L Giemsa. Cell clones were observed and counted.

Immunocytochemistry staining for exogenous cyclin G2 expression Cell transfection and G418 selection were done as above. After fourteen days, cell clones could be seen in pIRES-G2 and pIRESneo group. After PBS washing, the cell clones were circled, separated with sterile tip and cultured in G418 (250 μg/ mL) selective culture medium for another 2 wk. The stably transfected cell lines were obtained after passage by 2-3 generations. Cells were seeded into 6-well culture plates containing coverslips allowed to grow until they were 60-80% confluence and coverslips were picked up, washed with PBS, then fixed in ice cold acetone for 30 min at room temperature, washed 3 times (5 min each) in PBS. Cytochemistry staining was preformed by the avidin-biotin peroxidase complex method using the SABC kit as follows: cells were treated to remove endogenous peroxidase activity, blocked with rabbit serum for 30 min at room temperature, and then incubated in primary goat anti-cyclin G2 polyclonal antibody (American Santa Cruz Company) for 1 h at 37 ℃ or overnight at 4 ℃, washed 3 times with PBS, then incubated with a rabbit-anti-goat secondary antiboby conjugated to horseradish peroxidase for 1 h. Following PBS washing, the coverslips were incubated with SABC elite reagent for 30 min at room temperature and washed 3 times in PBS. The bound horseradish peroxidase complexes were developed using DAB kit. The coverslips were counterstained with hematoxylin, for colored by 10 mL/L hydrochloric acid ethanol, dehydrated by graded ethanol, and enveloped by neutral resin, negative contrast was made by using PBS instead of primary antibody.

MTT assay The stably transfected cells were seeded into 24-well culture plates and cultured for 24 h at 37 ℃, with 50 mL/L CO_2. Cells were seeded into 96-well culture plates at 4 000-6 000 cells/well. After 48 h culture, the culture solution was poured out and washed twice with PBS. 150 μL (0.5 mg/mL) MTT was added at 37 ℃ for 4 h, the culture medium solution was poured out and 150 μL/ each well DMSO was added again, shaken for 10 min in horizontal shaker. The absorbance at 570 nm was read by enzyme-labelling analysis equipment. The average absorbance reflected the cell proliferative ability. Data showed in mean±SD format and statistic significance was analyzed by *t* test.

RESULTS

Plasmid appraisal

The cyclin G2 fragment was inserted between the *Bam*HI and *Bst*XI restriction sites, the restriction enzyme digestion and gel electrophoresis results were the same as predicted.

Selection of the stable transfection cell line and exogenous cyclin G2 gene expression

After 14 d of selection by G418 in transfected cells, several cell clones could be seen in pIRES-G2 and pIRESneo group. After PBS washing, the cell clones were circled, and the larger single cell clones were separated with sterile tip, cultured in G418 (250 μg/ mL) selective culture medium for another 2 wk, the stable transfection cell lines were obtained after passage by 2-3 generations.

Immunocytochemistry staining result showed that a large number of gray positive granules appeared in SGC-7901cell cytoplasma after pIRES-G2 transfection, while pIRESneo cell cytoplasma only appeared blue and no positive granule was seen in negative contrast cell.

The effect of cyclin G2 overexpression on the colony-formation of SGC-7901 cell

Observing the stably transfected SGC-7901 cell obtained by G418 selection under microscope, the clone number of pIRES-G2 group decreased, clone volume reduced and the cells in clone changed irregularly, many granules and bubbles appeared in cytoplasm. The 5 repeated experimental results were the same. The number of pIRESneo group was 87±3, that of pIRES-G2 group was 53±4, occuping 60.1% of pIRESneo group, there was significant difference obviously ($P<0.01$, $t=15.45$) (Figures 1, 2).

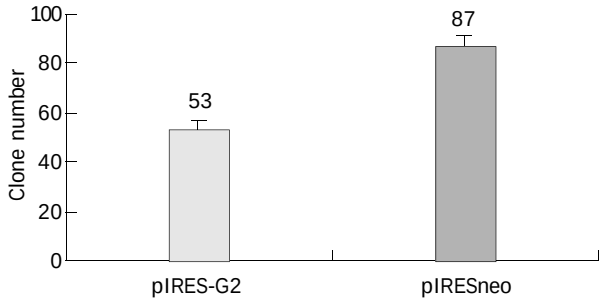

Figure 1 The positive clone number obtained with pIRES-G2 and pIRESneo plasmids after stable transfection in SGC-7901 cell line.

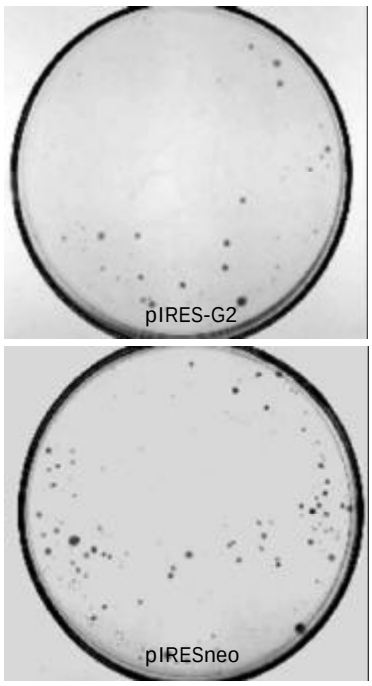

Figure 2 Effect of cyclin G2 overexpression on the colony-formation ability of SGC-7901.

Effects of cyclin G2 overexpression on SGC-7901 proliferative ability

By MTT assay analysis the proliferative ability change of stably transfected SGC-7901 cell obtained by G418 selection was as following: the average absorbance of clone cell obtained by stably transfected pIRES-G2 at 570 nm was 1.6966±0.2125, the average absorbance of clone cell obtained by stably transfected pIRESneo at 570 nm was 2.1182±0.3675, there was statistical difference between them (P<0.01, t=3.412) (Table 1) .

Table 1 The proliferative ability compared between 2 clone-cell

Group	Well number	Average absorbancee
pIRESneo	96	2.1182±0.3675[b]
pIRES-G2	96	1.6966±0.2125

[b]P<0.01, t=3.412 *vs* pIRES-G2.

DISCUSSION

There are many kind of cyclins and CDKs in mammalin cells, which combine with each other forming active cyclin-CDK complex as a triggering factor in the regulation of cell cycle. The expression level of cyclins shows phase specificity, which is obviously regulated by transcription and the rate of protein hydrolysis. Cyclin G, a recent addition to the cyclin family, has homology to fisson yeast Cig1, B-type cyclins, and human cyclin A and I. The molecular structure of cyclin G differs from other cyclins. NH_2 terminus lacks a "destruction box" sequence controlling the ubiquitin-dependent degradation mitotic cyclins, while contains an epidermal growth factor receptor (EGF-R/ ErbB) like autophosphorylation motif in its carboxyl terminus[12]. The structure suggested that a role for cyclin G in signal transduction. Cyclin G has not yet been matched with a CDK binding partner, and its biologic function is still elusive. Cyclin G is the only known cyclin that is transcriptionally activated by the p53 tumor suppressor gene. Cyclins G1 and G2 share the highest sequence identity and similarity to the fission yeast B-type cyclins Cig1 and Cig2 respectively, while cyclin G2 exhibits high sequence identity to the S-phase cyclin Clb-5 of budding yeast. Cloning and sequencing a partial cDNA sequence revealed the cyclin G1 transcript does not encode motifs which resemble known degradation signals. In contrast, the cyclin G2 protein contains a prototypic protein destabilizing (PEST) rich sequences which may be responsible for its potential regulated degradation in cell cycle. The cyclin G1 mRNA expression does not fluctuate with cell cycle phase, whereas the expression of cyclin G2 mRNA oscillated with cell cycle and reached peak in the mid-late S phase. In contrast to cyclin G1, cyclin G2 mRNA weakly expressed in skeletal muscles and heart. It showed high expression in cerebrum, thymus, spleen, prostate gland and kidney[13]. Notably cyclin G2 transcripts are abundant in tissue rich in either terminally differentiated cells or cells reacting to growth inhibitory signals and apoptosis[5]. Cyclin G1 is a positive regulator and prompts cell proliferation, so far, neither the physiological role nor the biochemical function of cyclin G2 has been defined. The mRNA expression of cyclin G1 and cyclin G2 can be induced by DNA-damage drug actinomycin-D, which has the p53 dependency for cyclin G1 but the p53 independency for cyclin G2[14]. Cyclin G2 can be induced by negative growth regulators such as TGF-β1 and dexamethasone. In the growth inhibition state of B cell, the transcription level of cyclin G2 is up-regulated. Re-conducting the VHL cancer-suppressing gene into renal cancer cells with VHL gene defect can induce cyclin G2 expression. The newest research also showed that lack of cyclin G2 plays an important role in the malignant transformation of papillary carcinoma of the thyroid. It may play an adjuvant role in the transformation of follicular adenoma to carcinoma[15]. So cyclin G2 most likely appears to be a negative regulator of the cell cycle.

The result showed that compared with the control group, the clones formed by transfected pIRES-G2 group were smaller and fewer, cells became wrinkled and irregular, which proved that the high expression of cyclin G2 inhibited the cell proliferation. In this research we had the gene transfection experiment through cloning cyclin G2 cDNA into bicistronic eukaryotic expression vector pIRESneo, the 2 open reading frame (ORF) of inserted gene cyclin G2 and selective label gene neo were separated by the inserted brain cardiomyoditis virus IRES[16,17]. So the recombinant plasmid pIRES-G2 in host cells only produced a single transcriptional template, which made the 2 proteins to be translated simultaneously to ensure all positive cells after G418 selection express target genes, overcame the shortcoming that these 2 genes could not be transcribed and translated at the same time when using other eukaryotic expression vectors[18,19]. The positive clones formed by G418 selection in the experimental group of pIRES-G2 should have the expression of cyclin G2. Thus, the difference of clones between the experimental and control groups was only caused by the high expression of cyclin G2. The MTT assay also testified that the average absorbance of pIRES-G2 group cell was lower than that of pIRESneo group, it showed that the proliferative ability decreased after pIRES-G2 transfection. Because by MTT assay, the cell numbers in pIRES-G2 group and pIRESneo group were the same and they also grew at the exponentially growing state, thus the average absorbance difference between them was merely caused by the difference of transfected genes. From this we could draw the conclusion that cyclin G2 overexpression makes the proliferative ability decrease.

Our experiment indicates that cyclin G2 could inhibit the SGC-7901 cell proliferation. Unlike other cyclins, it may be a negative regulating factor of cell cycle.

REFERENCES

1 **Hunter T**, Pines J. Cyclins and cancer. *Cell* 1991; **66**: 1071-1074

2 **Pines J**, Hunter T. Cyclin-dependent kinases : a new cell cycle motif ? *Trends Cell Biol* 1991; **1**: 117-121

3 **Pines J**. Cyclins and cyclin-dependent kinases:theme and variations. *Adv Cancer Res* 1995; **66**: 181-212

4 **Draetta GF**. Mammalian G1 cyclins. *Curr Opin Cell Biol* 1994; **6**: 842-846

5 **Horne MC**, Goolsby GL, Donaldson KL, Tran D, Neubauer M, Wahl AF. Cyclin G1 and cyclin G2 comprise a new family of cyclins with constrasting tissue-specific and cell cycle-regulated expression. *J Biol Chem* 1996; **271**: 6050-6061

6 **Zauberman A**, Lupo A, Oren M. Identification of p53 target genes through immune selection of genomic DNA: the cyclin G gene contains two distinct p53 binding sites. *Oncogene* 1995; **10**: 2361-2366

7 **Kimura SH**, Ikawa M, Ito A, Okabe M, Nojima H. Cyclin G1 is involved in G2/M arrest in response to DNA damage and in growth control after damage recovery. *Oncogene* 2001; **20**: 3290-3300

8 **Wykoff CC**, Pugh CW, Maxwell PH, Harris AL, Ratcliffe PJ. Identification of novel hypoxia dependent and independent target genes of the von Hippel-Lindau(VHL) tumor suppressor by mRNA differential expression profiling. *Oncogene* 2000; **19**: 6297-6305

9 **Horne MC**, Donaldson KL, Goolsby GL, Tran D, Mulheisen M, Hell JW, Wahl AF. Gyclin G2 is up-regulated during growth inhibition and B cell antigen receptor-mediated cell cycle arrest. *J Biol Chem* 1997; **272**: 12650-12661

10 **Alevizos I**, Mahadevappa M, Zhang X, Ohyama H, Kohno Y, Posner M, Gallagher GT, Varvares M, Cohen D, Kim D, Kent R, Donnff RB, Todd R, Yung CM, Warrington JA, Wang DT. Oral cancer *in vivo* gene expression profiling assisted by laser capture microdissection and microarray analysis. *Oncogene* 2001;

20: 6196-6204

11 **Tian YL**, Liu FR, Liu J, Jiang L, Luo Y, Zhang X. Ectopic expression of cyclin G2 inhibits cell proliferation in HeLa cancer cell line. *Aizheng* 2002; **21**: 577-581

12 **Tamura K**, Kanaoka Y, Jinno S, Nagata A, Ogiso Y, Shimizu K, Hayakawa T, Nojima H, Okayama H. Cyclin G: a new mammalian cyclin with homology to fission yeast Cig1. *Oncogene* 1993; **8**: 2113-2118

13 **Jensen MR**, Audolfsson T, Keck CL, Zimonjic DB, Thorgeirsson SS. Gene structure and chromosomal localization of mouse cyclin G2 (Ccng2). *Gene* 1999; **230**: 171-180

14 **Bates S**, Rowan S, Vousden KH. Characterisation of human cyclin G1 and G2: DNA damage inducible genes. *Oncogene* 1996; **13**: 1103-1109

15 **Ito Y**, Yoshida H, Uruno T, Nakano K, Takamura Y, Miya A, Kobayashi K, Yokozawa T, Matsuzuka F, Kuma K, Miyauchi A. Decreased expression of cyclin G2 is significantly linked to the malignant transformation of papillary carcinoma of the thyroid. *Anticancer Res* 2003; **23**: 2335-2338

16 **Rees S**, Coote J, Stables J, Goodson S, Harris S, Lee MG. Bicistronic vector for the creation of stable mammalian cell lines that predisposes all antibiotic-resistant cells to express recombinant protein. *Biotechniques* 1996; **20**: 102-110

17 **Gaines P**, Wojchowski DM. PIRES-CD4t, a dicistronic expression vector for MACS- or FACS- based selection of transfected cells. *Biotechniques* 1999; **26**: 683-688

18 **Felgner PL**. Improvements in cationic liposomes for *in vivo* gene transfer. *Hum Gene Ther* 1996; **7**: 1791-1793

19 **Bennett CF**, Chiang MY, Chan H, Shoemaker JE, Mirabelli CK. Cationic lipids enhance cellular uptake and activity of phosphorothioate antisense oligonucleotides. *Mol Pharmacol* 1992; **41**: 1023-1033

Edited by Zhu LH and Xu FM

PO Box 2345, Beijing 100023, China
Fax: +86-10-85381893
E-mail: wjg@wjgnet.com www.wjgnet.com

World J Gastroenterol 2004;10(9):1361-1364
World Journal of Gastroenterology
Copyright ©2004 by The WJG Press ISSN 1007-9327

• BRIEF REPORTS •

Expression of tumor related gene NAG6 in gastric cancer and restriction fragment length polymorphism analysis

Xiao-Mei Zhang, Shou-Rong Sheng, Xiao-Yan Wang, Liang-Hua Bin, Jie-Ru Wang, Gui-Yuan Li

Xiao-Mei Zhang, Department of Digestive Medicine, Xiangya Hospital, Central South University, Changsha 410008, Hunan Province, China
Shou-Rong Sheng, Xiao-Yan Wang, Department of Digestive Medicine, the Third Xiangya Hospital, Central South University, Changsha 410013, Hunan Province, China
Liang-Hua Bin, Jie-Ru Wang, Gui-Yuan Li, Cancer Research Institute, Xiangya Medical College, Central South University, Changsha 410078, Hunan Province, China
Supported by the atural Science Foundation of Hunan Province, No.02JJY2049 and the National "863" Program of China, No.102-10-01-05
Correspondence to: Dr. Shou-Rong Sheng, Department of Digestive Medicine, the Third Xiangya Hospital, Central South University, Changsha 410013, Hunan Province, China. tangyy@public.cs.hn.cn
Telephone: +86-731-4316667
Received: 2003-04-12 **Accepted:** 2003-09-18

Abstract

AIM: NAG6 gene is a novel tumor related gene identified recently. This study was designed to examine the expression of this gene in gastric cancer and corresponding normal tissues, and to investigate its role in the occurrence and development of gastric cancer, also to study if the genetic structure of NAG6 was altered in gastric cancer.

METHODS: Reverse transcription-polymerase chain reaction (RT-PCR), Northern blot analysis and dot hybridization were used to compare the expression level of NAG6 gene in 42 cases of gastric cancer tissues with their corresponding normal tissues of the same patients respectively. In addition, restriction fragment length polymorphism (RFLP) analysis was adopted to study if the genetic structure of NAG6 was altered in gastric carcinomas.

RESULTS: The expression of NAG6 in 57.1% gastric cancer tissues (25/42) was absent by RT-PCR analysis. The down-regulation rate of NAG6 in gastric cancer tissues was significantly higher than that in corresponding normal tissues ($P<0.01$). However no correlation between the down-regulation of NAG6 and lymph-node and/or distance metastasis was found in this study ($P>0.05$). Dot hybridization confirmed the results of RT-PCR. Furthermore, the results of *Eco*RI RFLP analysis of NAG6 gene demonstrated that 3 of 7 cases of gastric cancer showed loss of 5 kb fragment in comparison with their corresponding normal tissues.

CONCLUSION: NAG6 gene is significantly down regulated in gastric cancer. The loss of genetic materials may be the cause of down-regulation of NAG6 expression. This seems to suggest that NAG6 may represent a candidate of putative tumor suppressor gene at 7q31-32 loci associated with gastric carcinoma. The down-regulation of this gene may play a role in occurrence and development of this disease, however it may not be associated with lymph node and/or distance metastasis.

Zhang XM, Sheng SR, Wang XY, Bin LH, Wang JR, Li GY. Expression of tumor related gene NAG6 in gastric cancer and restriction fragment length polymorphism analysis. *World J Gastroenterol* 2004; 10(9): 1361-1364
http://www.wjgnet.com/1007-9327/10/1361.asp

INTRODUCTION

Gastric cancer (GC) is one of the leading causes of cancer death in the world, although its incidence has gradually declined in recent years[1,2]. However, in the Far East, including China and Japan, gastric cancer remains a prevalent cancer with a high mortality[3,4]. It is well known that carcinogenesis and progression of human gastric cancer are related to multiple genetic aberrations including activation of oncogenes and inactivation of tumor suppressor genes. The latter involves the loss of heterozygosities (LOH) of several chromosomal loci and mutations in tumor suppressor genes, such as *p53* and *DCC* genes. However, the mechanism of the process of multistage carcinogenesis is still not well understood[5-12]. Recently, a number of cytogenetic and molecular genetic studies have revealed that LOH on the long arm of chromosome 7 occurs frequently in many types of primary cancers including nasopharyngeal, gastric, breast, ovarian, and oral carcinomas, and investigators have identified the most common site of LOH as 7q31-32, implying the existence of at least one multi-tissue tumor suppressor gene (TSG) at this locus[13-22]. Based on these findings, in our previous studies, we have cloned a novel tumor related gene from this common deletion region in 7q31-32 by positional candidate cloning strategy, we named it NAG6, and its GenBank accession number was AF156971. It was found to be a potential tumor suppressor gene associated with NPC[23-26]. To investigate whether the expression of NAG6 was also altered in GC and whether NAG6 gene also played a role in the pathogenesis of gastric carcinoma, we analyzed the expression level of NAG6 in 42 cases of human gastric carcinoma and their matched normal tissues by RT-PCR, Northern blot analysis and dot hybridization. Furthermore, to study if the genetic structure alteration of NAG6 was the reason of its abnormal expression in GC, RFLP analysis was adopted. These studies can lead to a better understanding of the molecular mechanism of gastric cancer.

MATERIALS AND METHODS

Tumor specimens

Fresh surgical specimens of forty-two gastric carcinoma (GC) and corresponding normal tissues were obtained from the Affiliated Xiangya Hospital of Central South University from January 2000 to July 2000. All tumor specimens were confirmed by pathological diagnosis. Each freshly resected specimen was frozen immediately and stored in liquid nitrogen until analyzed. Histologically, In the 42 cases of gastric carcinoma, 4 were well-differentiated adenocarcinomas, 30 poorly-differentiated adenocarcinomas, 6 signet ring cell carcinomas and 2 mucoid carcinomas. There were 22 males and 20 females, their age ranged from 30 to 68 years (mean

age, 51.7 years). Six cases had lymph node or distance metastases. No patient had received chemotherapy or radiation therapy before surgery.

RT-PCR

Total RNA was isolated using Trizol reagent (Gibco-BRL, Gaithersburg, MD, USA) according to the protocol provided by the manufacturer. After treated with DNase-I (Promega), 1-2 μg of total RNA was reversely transcribed into complementary DNA (cDNA) with oligo(dT) using cDNA synthesis kit (Promega). Then 1 μL product was used as the template to amplify specific fragments in a 25 μL reaction mixture. The subsequent PCR was performed using Taq polymerase and the buffer (Promega) supplied with 0.2 mmol/L dNTPs and 0.2 μmol/L primers. Primers corresponding to NAG6 sequences were designed with WWW Primer Picking (Primer 3) and synthesized by TaKaRa. Gene-specific forward and reverse primers for NAG6 were designed to produce a PCR product of 680 bp. RT-PCR reaction was carried out with an initial denaturation at 95 ℃ for 5 min, followed by 35 cycles at 94 ℃ for 50 s, annealing at 56 ℃ for 50 s, at 72 ℃ for 60 s, and a final extension at 72 ℃ for 10 min. At the same time, a housekeeping gene, GAPDH was amplified as internal control to normalize the relative levels of cDNA, which generated a PCR product of 475 bp. An aliquot (10 μL) of each reaction product was analyzed by 10 g/L agarose gel electrophoresis.

The sequences of primers were as follows: NAG6F1, 5'-GGCACTGGAGTACAAAGACA-3'; NAG6R1, 5'-TTACTTTTCCCATTTGCTCA-3'; GAPDHF1, 5'-GTCATCCATGACAACTTTGGTATC-3'; GAPDHR1, 5'-CTGTAGCCAAATTCGTTGTCATAC-3'.

Northern blot analysis

Total RNA was isolated from human gastric carcinoma and corresponding normal tissues by Trizol reagent (Gibco-BRL), and hybridization was performed as described. A 30 μg RNA was separated by electrophoresis by denaturing agarose gels and blotted onto nylon membrane (Clontech). RNA was permanently attached to the membrane by UV illumination for 150 s (GS Gene Linker, Bio-Rad, USA), and the membrane was dried in a vacuum at 80 ℃ for 2 h and sealed in a plastic bag for use. The hybridization probes were obtained by RT-PCR amplification. NAG6 cDNA probe was random-prime labeled with [α-^{32}P]dCTP using primer-a-gene random labeling kit (Promega, USA) and following the protocol. Hybridization with the RNA blots was carried out at 68 ℃ overnight in Express Hyb TM hybridization solution (Clontech) in a rolling bottle. The membranes were washed twice at room temperature in 2×saline sodium citrate (SSC), 0.5 g/LSDS for 10 min, once at 42 ℃ in 1×SSC, 1 g/L SDS for 15 min and once at 50 ℃ in 0.1×SSC, 1 g/L SDS for 30 min. Then, they were exposed to film (Eastman Kodak, Rochester, NY, USA) for 4 d at -70 ℃. After exposure, the blot was again hybridized with a GAPDH probe.

Dot blot analysis

GAPDH and NAG6 cDNA fragments containing open reading frames from cDNA of gastric carcinoma samples were obtained by RT-PCR. These cDNAs were reclaimed and purified by using a kit according to the instructions of its manufacturer (Shanghai Huashun Co.). After alkali dissolution, GAPDH and NAG6 cDNA were blotted onto nylon membranes. cDNA was permanently attached to the membrane by UV illumination for 150 s, and the membranes were dried in a vacuum at 80 ℃ for 2 h to fix the cDNA. Ten μg total RNA was isolated from 10 cases of human gastric carcinomas and 10 cases of each corresponding normal tissues, and reversely-transcribed into cDNA probe with oligo (dT) and [α-^{32}P] dCTP using cDNA synthesis kit after treated with DNase I and RNasin at 37 ℃ for 1 h to remove contaminated DNA (1 μg total RNA of each case was used). Then the two cDNA probes were hybridized with GAPDH and NAG6 cDNA blots respectively as Northern hybridization described above.

Southern-based RFLP analysis

Genomic DNA was extracted from gastric cancer and corresponding normal tissues by using sodium dodecyl sulphate (SDS), EDTA, proteinase K, dispelled protein and phenol-chloroform methods, removing RNA with RNA enzyme, precipitating DNA with alcohol of two times in volume, mixed in proper TE buffer solution, and kept for use at 4 ℃. Genomic DNA was digested with the stated restriction endonuclease *Eco*RI and electrophoresed on 7 g/L agarose (TAE) gel. After electrophoresis, DNAs were denatured, neutralized and transferred to nylon membranes. Then DNAs were permanently attached to the membrane by UV illumination and the membrane was dried in a vacuum at 80 ℃ for 2 h. The nylon membrane was hybridized with the radiolabelled NAG6 cDNA probe according to the method of Southern blot. After washed and autoradiographed at - 70 ℃ for 3 to 5 d, hybridizing was carried out.

Statistical analysis

Chi-square test was used. A P value less than 0.05 was considered statistically significant.

RESULTS

Expression of NAG6 in gastric cancer and corresponding normal tissues

In 42 pairs of GC and corresponding normal tissues, NAG6 expression was undetectable in 24 tumors (57.1%), while it was detectable in all corresponding normal tissues. The expression of NAG6 in gastric carcinomas was significantly down-regulated than that in normal tissues (χ^2=33.6, P<0.005). Representative cases of NAG6 expression detected by RT-PCR are shown in Figure 1. The down-regulation rate of NAG6 in patients with lymph node and/or distance metastases and those without lymph-node and/or distance metastases was 66.7%(4/6) and 47.2%(17/36) respectively. There was no apparent relevance between NAG6 down-expression and lymph node and/or distance metastasis of gastric carcinomas (P>0.05).

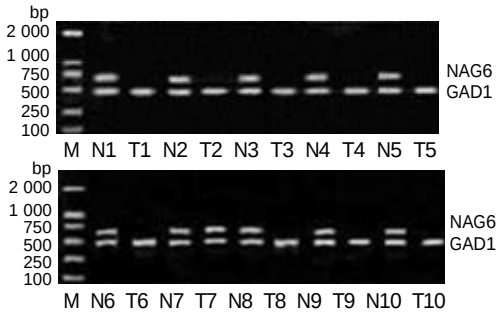

Figure 1 Expression of NAG6 in gastric carcinoma and corresponding normal tissues examined by RT-PCR. The RT products were examined by PCR with NAG6 primers, producing a 680 bp fragment and with GAPDH primers, producing a 466 bp fragment. Lane M: 2 000 bp marker, Lane N: normal epithelium tissues, Lane T: gastric carcinoma tissues.

In order to verify the results of RT-PCR, Northern hybridization was performed. Northern blot analysis did not detect NAG6 expression in both gastric carcinoma and

corresponding normal tissues, whereas GAPDH was strongly expressed in both of them. We speculated that the expression abundance of NAG6 gene in gastric cancer and corresponding normal tissues might be too low to be detected by Northern blot analysis. So, we used dot hybridization analysis to verify the reliability of RT-PCR on the other hand. The results of dot hybridization confirmed the results of RT-PCR that the expression of NAG6 was significantly down-regulated in gastric carcinoma tissues (Figure 2).

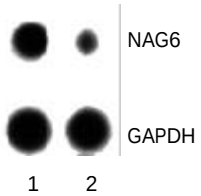

Figure 2 Dot hybridization analysis of NAG6 gene expression profiles in human gastric carcinoma and corresponding normal tissues. NAG6 cDNA obtained by RT-PCR was blotted onto nylon membranes. The membranes were hybridized with ^{32}P-labeled cDNA probes obtained from total RNA of human gastric carcinoma (1) and corresponding normal gastric epithelial (2) tissues. After stringent washes, membranes were exposed to X-ray film for 4 d at-70 ℃. NAG6 was down-regulated in gastric carcinoma tissues.

RFLP analysis

*Eco*RI RFLP analysis of NAG6 gene was performed in 7 cases of gastric cancer and corresponding normal tissues. The results showed that there were two kinds of common allelic fragments (11.5 Kb, 5.0 Kb) in all corresponding normal tissues and 4 cases of gastric cancer, but 3 cases of gastric cancer tissues showed loss of 5 Kb fragment in comparison with their matched normal tissues.

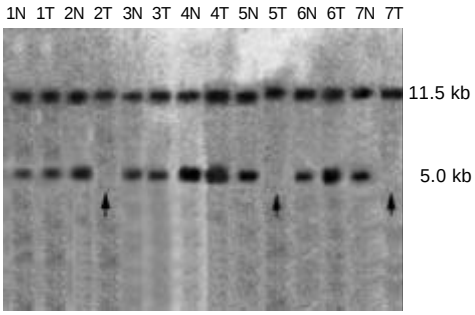

Figure 3 RFLP analysis using Southern hybridization. Gastric cancer and normal epithelium genome DNAs were digested with *Eco*RI and hybridized with NAG6 cDNA probe. Three cases of gastric cancer tissues showed loss of 5Kb fragment (N: normal epithelium tissues, Lane T: gastric carcinoma tissues).

DISCUSSION

NAG6 gene has been recently identified and cloned by our group at chromosome 7q31-32, the common deletion site in various human malignancies. Comparison with GenBank and EMBO database using the BLAST program the cDNA sequence of NAG6 gene was a unique gene with no homology to any previously reported human genes, and its GenBank accession number is AF156971. The predicted NAG6 protein contained four protein kinase C (PKC) phosphorylation sites, suggesting that the activity of NAG6 protein can be regulated by phosphorylation. Its mRNA expression level in NPC biopsies was significantly lower than that in normal nasopharyngeal epithelium, and the down-regulation of NAG6 in NPC was attributable to several factors including loss of genetic materials and hypermethylation. All these findings supported NAG6 as a candidate tumor suppressor gene at 7q31-32. The down-regulation of this gene might play a role in occurrence and development of NPC[23-26].

Cytogenetic and molecular analyses demonstrated that frequent LOH on the long arm of chromosome 7 could also be observed in a high proportion of gastric cancer cases[13-16]. Nishizuka *et al* reported LOH at any locus on 7q occurred in 34% (18 out of 53) of primary gastric carcinomas[14]. Kuniyasu *et al* examined LOH on the long arm of chromosome 7 using 5 polymorphic marker probes in 98 gastric carcinomas[15]. The results showed twenty-six of 82(32%) informative cases showed LOH on 7q at least one locus of 5 loci. Xia *et al* studied a total of 28 primary gastric cancer specimens, and they found that deletion of 7q (21/26) was one of the characteristic structural changes of primary gastric cancer[16]. Furthermore, investigators have identified the most common site of LOH as 7q32-qter, and concluded that in the 7q32-qter segments, at least one tumor suppressor gene probably existed and it might have a close relation to the development and progression of gastric cancer[13-16]. NAG6 gene located at 7q31-32 locus. We were interested in whether expression of NAG6 was altered in GC and whether NAG6 was also a possible tumor suppressor in human gastric carcinoma. In this study, RT-PCR, Northern blot and dot hybridization were used to detect the expression abundance of the gene in gastric carcinoma and corresponding normal tissues. The results of RT-PCR showed that the down-regulation rate of NAG6 in gastric carcinoma tissues was significantly higher than that in corresponding normal tissues ($P<0.005$). Dot hybridization confirmed the results of RT-PCR. However the expression of NAG6 was not relevant to lymph node and/or distance metastasis of gastric carcinomas. This seems to suggest that down-regulation of NAG6 might play a role in the occurrence and progression of GC.

In order to study the possible cause of down-regulation of NAG6 in gastric cancers, we studied on the restriction fragment length polymorphisms (RFLPs) of NAG6 gene in gastric cancer and corresponding normal tissues to detect if the genetic structure of NAG6 was changed in GC. We used restriction enzymes to cut DNA at specific recognition sites, fragments of restricted DNA separated by gel electrophoresis and detected by subsequent Southern blot hybridization to a radiolabeled DNA probe. In recent twenty years, the application value of restriction fragment length polymorphism (RFLP) analysis in the detection of genetic structure change and genetic polymorphisms of candidate gene has called attention of the scholars at home and abroad[27-29]. Polymorphic sequences that result in RFLPs are used as markers on both physical maps and genetic linkage maps. In this study, *Eco*RI RFLP analysis of NAG6 gene was performed in 7 cases of gastric cancer and corresponding normal tissues. The results demonstrated that 3 of 7 cases of gastric cancer showed loss of 5 kb fragment in comparison with their corresponding normal tissues. In the previous study, RFLP analysis also found that 6 of 14 NPC cases lost the fragment of 3 kb in comparison with their matched peripheral blood lymphocytes. These results demonstrated that the genetic structure of NAG6 was changed in both NPC and GC. A preliminary conclusion was drawn that loss of genetic materials might be the cause of down-regulation of NAG6 expression.

To summarize, our data showed that NAG6 was down-regulated in gastric cancer, and loss of genetic materials of NAG6 was also found in GC. It is reasonable to predict that NAG6 may represent a candidate of putative tumor suppressor gene at 7q31-32 locus associated with GC and NPC, and this gene may play an important role in suppressing GC tumorigenesis, losses of its function may contribute to the occurrence and

development of GC. The mechanism of this gene is still unclear. Further studies on a large patient population are needed to verify these initial observations and to characterize the mechanism of down-regulation of NAG6 in tumors. It is important to examine the possible relationship between loss or preservation of NAG6 expression and clinical outcome in patients with tumor.

REFERENCES

1 **Stadtlander CT**, Waterbor JW. Molecular epidemiology, pathogenesis and prevention of gastric cancer. *Carcinogenesis* 1999; **20**: 2195-2208

2 **Palli D**. Epidemiology of gastric cancer: an evaluation of available evidence. *J Gastroenterol* 2000; **35**(Suppl): 84-89

3 **Maehara Y**, Kakeji Y, Oda S, Takahashi I, Akazawa K, Sugimachi K. Time trends of surgical treatment and the prognosis for Japanese patients with gastric cancer. *Br J Cancer* 2000; **83**: 986-991

4 **Deng DJ**. Progress of gastric cancer etiology: Nnitrosamides in the 1999s. *World J Gastroenterol* 2000; **6**: 613-618

5 **Becker KF**, Keller G, Hoefler H. The use of molecular biology in diagnosis and prognosis of gastric cancer. *Surg Oncol* 2000; **9**: 5-11

6 **Boussioutas A**, Taupin D. Towards a molecular approach to gastric cancer management. *Intern Med J* 2001; **31**: 296-303

7 **Yasui W**, Oue N, Kuniyasu H, Ito R, Tahara E, Yokozaki H. Molecular diagnosis of gastric cancer: present and future. *Gastric Cancer* 2001; **4**: 113-121

8 **Maltoni M**, Volpi A, Nanni O, Bajorko P, Belletti E, Vecci AM, Liverani M, Danesi S, Calistri D, Ricotti L, Amadori D. Gastric cancer: epidemiologic and biological aspects. *Forum* 1998; **8**: 199-207

9 **Xu AG**, Li SG, Liu JH, Gan AH. Function of apoptosis and expression of the proteins *Bcl*-2, p53 and C-*myc* in the development of gastric cancer. *World J Gastroenterol* 2001; **7**: 403-406

10 **Liu LX**, Liu ZH, Jiang HC, Qu X, Zhang WH, Wu LF, Zhu AL, Wang XQ, Wu M. Profiling of differentially expressed genes in human gastric carcinoma by cDNA expression array. *World J Gastroenterol* 2002; **8**: 580-585

11 **Meltzer SJ**. Tumor genomics *vs* tumor genetics: a paradigm shift? *Gastroenterology* 2001; **121**: 726-729

12 **Nishizuka S**, Tamura G, Terashima M, Satodate R. Loss of heterozygosity during the development and progression of differentiated adenocarcinoma of the stomach. *J Pathol* 1998; **185**: 38-43

13 **Zenklusen JC**, Conti CJ. Cytogenetic, molecular and functional evidence for novel tumor suppressor genes on the long arm of human chromosome 7. *Mol Carcinog* 1996; **15**: 167-175

14 **Nishizuka S**, Tamura G, Terashima M, Satodate R. Commonly deleted region on the long arm of chromosome 7 in differentiated adenocarcinoma of the stomach. *Br J Cancer* 1997; **76**: 1567-1571

15 **Kuniyasu H**, Yasui W, Yokozaki H, Akagi M, Akama Y, Kitahara K, Fujii K, Tahara E. Frequent loss of heterozygosity of the long arm of chromosome 7 is closely associated with progression of human gastric carcinomas. *Int J Cancer* 1994; **59**: 597-600

16 **Xia J**, Xiao S, Zhang J. Direct chromosome analysis and FISH study of primary gastric cancer. *Zhonghua Zhongliu Zazhi* 1999; **21**: 345-349

17 **Tan G**, Xiao J, Tian Y, Dong L, Jiang N, Zhan F, Li G. Microsatellite analyses of loci at 7q31.3-q36 reveal a minimum of two common regions of deletion in nasopharyngeal carcinoma. *Otolaryngol Head Neck Surg* 2002; **126**: 296-300

18 **Zenklusen JC**, Weintraub LA, Green ED. Construction of a high-resolution physical map of the approximate 1-Mb region of human chromosome 7q31.1-q31.2 harboring a putative tumor suppressor gene. *Neoplasia* 1999; **1**: 16-22

19 **Lin JC**, Scherer SW, Tougas L, Traverso G, Tsui LC, Andrulis IL, Jothy S, Park M. Detailed deletion mapping with a refined physical map of 7q31 localizes a putative tumor suppressor gene for breast cancer in the region of MET. *Oncogene* 1996; **13**: 2001–2008

20 **Koike M**, Takeuchi S, Yokota J, Park S, Hatta Y, Miller CW, Tsuruoka N, Koeffler HP. Frequent loss of heterozygosity in the region of the D7S523 locus in advanced ovarian cancer. *Genes Chromosomes Cancer* 1997; **19**: 1–5

21 **Koike M**, Tasaka T, Spira S, Tsuruoka N, Koeffler HP. Allelotyping of acute myelogenous leukemia: loss of heterozygosity at 7q31.1 (D7S486) and q33-34 (D7S498, D7S505). *Leuk Res* 1999; **23**: 307-310

22 **Wang XL**, Uzawa K, Miyakawa A, Shiiba M, Watanabe T, Sato T, Miya T, Yokoe H, Tanzawa H. Localization of a tumour-suppressor gene associated with human oral cancer on 7q31.1. *Int J Cancer* 1998; **75**: 671-674

23 **Jiang N**, Zhan F, Tan G, Deng L, Zhou M, Cao L, Qiu Y, Xie Y, Li G. A cDNA located on chromosome 7q32 shows loss of expression in epithelial cell line of nasopharyngeal carcinoma. *Chin Med J* 2000; **113**: 650-653

24 **Jiang N**, Zhan F, Xie Y, Zeng Z, Zhou M, Deng L, Li G. Establishment of partial gene expression map of 7q32 in nasopharyngeal carcinoma and primary culture normal nasopharyngeal epithelial cells. *Zhonghua Yixue Yichuanxue Zazhi* 1998; **15**: 267-270

25 **Jiang N**, Deng LW, Tan GL, Zhan FH, Zhou M, Cao L, Qiu YZ, Xie Y, Li GY. A nasopharyngeal carcinoma negatively related EST on 7q32. *Yichuan Xuebao* 1999; **26**: 301-308

26 **Zhang XM**, Sheng SR, Wang XY, Xiang Q, Li J, Tan C. Expression of tumor related gene NAG6, NAG-7, BRD7 in gastric cancer. *Zhonghua Xiaohua Zazhi* 2002; **22**: 733-736

27 **Yuan Y**, Dong M, Lu P, Wang XJ, Jin CL, He AG. Restriction fragment length polymorphism of pepsinogen C gene in patients with stomach carcinoma and in its high risk population. *China Natl J New Gastroenterol* 1996; **2**: 223-225

28 **Byrne M**, Parish TL, Moran GF. Nuclear RFLP diversity in *Eucalyptus nitens*. *Heredity* 1998; **81**: 225-233

29 **Butcher PA**, Moran GF, Perkins HD. RFLP diversity in the nuclear genome of Acacia mangium. *Heredity* 1998; **81**: 205-213

Edited by Zhang JZ and Wang XL **Proofread by** Xu FM

PO Box 2345, Beijing 100023, China
Fax: +86-10-85381893
E-mail: wjg@wjgnet.com www.wjgnet.com

World J Gastroenterol 2004;10(9):1365-1368
World Journal of Gastroenterology
Copyright ©2004 by The WJG Press ISSN 1007-9327

• BRIEF REPORTS •

Establishment of a P-glycoprotein substrate screening model and its preliminary application

Yi Wang, Jiang Cao, Su Zeng

Yi Wang, Su Zeng, College of Pharmaceutical Sciences, Zhejiang University, Hangzhou 310031, Zhejiang Province, China
Jiang Cao, Cancer Institute, Zhejiang University, Hangzhou 310009, Zhejiang Province, China
Supported by the National Natural Science Foundation of China, No. 30225047
Correspondence to: Dr. Su Zeng, College of Pharmaceutical Sciences, Zhejiang University, Hangzhou 310031, Zhejiang Province, China. zengsu@cps.zju.edu.cn
Telephone: +86-571-87217060
Received: 2003-08-11 **Accepted:** 2003-10-12

Abstract

AIM: To establish a high P-glycoprotein (P-gp) expressing cell line as a model for studying drug absorption and distribution, and to explore the preliminary application of this screening model.

METHODS: A full-length MDR1 cDNA fragment in plasmid pMDRA1 was first subcloned into plasmid pET28a(+), then MDR1 cDNA was cut from the recombinant plasmid with double-digestion and ligated into the mammalian expression vector pcDNA3.1(+). The recombinant plasmid pcDNA3.1 (+)/MDR1 was transfected into breast cancer cell line Bcap37 using the Superfect transfection reagent. Several stably transfected clones were obtained after selection with G418. Real-time fluorescent quantitative RT- PCR and Western blot methods were used to detect the expression of P-gp, and the cellular location of the expressed protein was determined by immunohistochemical staining. Drug sensitivity assay was used to evaluate the biological function of expressed P-gp. Concentration of quercetin in cells was determined by high-performance liquid chromatography (HPLC).

RESULTS: The recombinant plasmid was confirmed to be inserted in the correct orientation by restrictive enzyme digestion and DNA sequencing. Real-time fluorescent quantitative RT-PCR showed a higher level of P-gp mRNA in transfected cells compared to that in the control cells, and the Western blot result also indicated that P-gp expression in transfected cells was higher than that in control cells. The immunohistochemical staining showed that the expressed P-gp was localized on cell membranes. Drug sensitivity assay showed that the IC_{50} for adriamycin and colchicine of the transfected cells was higher than that of the control cells. The concentration of quercetin in model cells was lower than that in control cells by HPLC. After P-gp inhibitor verapamil was administered, the concentration of quercetin in model cells was increased.

CONCLUSION: A high P-gp expressing cell line can be established, which could provide a suitable *in vitro* model system for studying drug intestinal absorption mechanism, predicting the drug permeability characteristics and screening new multi-drug resistance reversing agents. With this model, quercetin can be found to be transported by P-gp, and it is a P-gp substrate.

Wang Y, Cao J, Zeng S. Establishment of a P-glycoprotein substrate screening model and its preliminary application. *World J Gastroenterol* 2004; 10(9): 1365-1368
http://www.wjgnet.com/1007-9327/10/1365.asp

INTRODUCTION

P-glycoprotein (P-gp), a product of the multidrug resistance (MDR) gene, is widely distributed in normal tissues of the body, including intestinal mucosa, proximal tubule of the kidneys, placenta, testes, and blood-brain barrier[1]. It is an ATP-dependent efflux transporter that affects the absorption, distribution, and excretion of a number of clinically important drugs[2]. For example, in intestinal mucosa, P-gp serves as a biochemical barrier to drug delivery. Drugs or drug candidates are bound to P-gp and transported back to the apical surface of the tissue, thereby restricting the overall permeability of drugs and drug candidates.

Due to *in vivo* disposition and pharmacokinetics of drug efflux transporters, identification of compounds as P-gp substrates can aid the optimization and screening of new drug candidates. A variety of *in vitro* assays have been used to classify compounds as P-gp substrates[3]. These assays can be classified into three groups. One is transport across polarized cell monolayers expressing P-gp on the apical membrane, the other is drug uptake into cells over-expressing P-gp, the third is direct binding to P-gp using inside-outside membrane vesicles or reconstituted P-gp.

Quercetin, a flavonoid and phytoestrogen, is present in a wide variety of fruits and vegetables [4]. Quercetin is also a potent antioxidant *in vivo* and *in vitro*, and thus quercetin and other flavonoids have been considered as therapeutic agents for a wide range of diseases, including cancer, viral infection, inflammation/allergy, hypertension and atherosclerosis[5-7].

In this study we constructed a P-gp expressing plasmid, established a P-gp high-expression cell model, and identified quercetin as a P-gp substrate with this cell model.

MATERIALS AND METHODS

Cell lines and cell culture

Breast cancer cell line Bcap37 (maintained by the Cancer Institute of Zhejiang University) was cultured in RPMI 1640 medium (Hyclone, USA) containing 100 ml/L heat-inactivated newborn calf serum (GIBCO), 100 U/mL penicillin and 100 μg/mL streptomycin. The cells were incubated at 37 ℃ in a humidified atmosphere with 50 mL/L CO_2 in air.

Construction of expression vector

Plasmid pMDRA1 containing a full-length MDR1 cDNA was kindly provided by Professor Kazumitsu Ueda[8]. The plasmid was digested with *Sac*I and *Xho*I, and the MDR1 cDNA fragment was ligated into pET28a(+) which was pre-cut with *Sac*I and *Xho*I. The recombinant plasmid was digested with *Bam*HI and *Xho*I, and the insert was purified by 0.8% agarose gel electrophoresis and ligated into the mammalian expression vector pcDNA3.1(+) pre-cut with *Bam*HI and *Xho*I. The resulting pcDNA3.1(+)/MDR1 was digested with *Eco*RI to

check the orientation of the insert and DNA sequencing was used to verify the inserted sequence.

Transfection of Bcap37 cells

Bcap37 cells were transfected with the recombinant expression vector pcDNA3.1(+)/MDR1 using Superfect transfection reagent according to the manufacturer's instructions (QIAGEN). After 48 h of transfection, stable transfectants were isolated by selection with 800 μg/mL G418 for 10 d. G418-resistant stable clones were picked for further characterization. The transfectants were maintained in RPMI 1640 containing 100 mL/L newborn calf serum and 400 μg/mL G418. Bcap37 cells were also transfected with pcDNA3.1(+) vector as the control.

Real-time fluorescent quantitative RT-PCR

Total RNAs in Bcap37/MDR1 cells and control cells were extracted using TRIzol™reagent (GIBcoBRL, Life Technologies) according to the user's guide. Real-time fluorescent quantitative RT-PCR was done with the MDR1 mRNA quantification kit (designed by the Cancer Institute of Zhejiang University and manufactured by Shanghai Jiusheng Medical Instrument Company) according to the manufacturer's instructions[9].

Western blot

Total proteins in Bcap37/MDR1 and control cells were extracted with 1 g/L Triton X-100 and protein concentration was determined with a Bio-Rad protein assay kit and standardized with bovine serum albumin. The samples were electrophoresed (SDS-PAGE, 80 g/L) and electroblotted onto PVDF membrane (BioRad). The membrane was blocked in buffer with 50 mL/L fat free dry milk, detected with anti P-gp antibody (monoclonal F4, Sigma).

Immunohistochemical staining

Bcap37/MDR1 cells and control cells were harvested by centrifugation at 2 000 r/min for 5 min, washed twice with PBS, and mounted onto the slides. Immunohistochemical staining was doned with the UltraSensitive™S-P mouse kit (Fuzhou Maxim Biotech, Inc). The protocol was accorded to the user guide. Primary antibody was monoclonal anti-human P-glycoprotein antibody purchased from Fuzhou Maxim Biotech (monoclonal number C494).

Drug sensitivity assay

Sensitivity of cells to anticancer drugs was examined by a colorimetric assay using MTT method. Cells (6×10^3cells/well) were seeded on 96-well plates, and cultured in a humidified atmosphere with 50 mL/L CO_2 at 37 ℃. Twenty- four hours later, drugs were added at various concentrations. Control wells were included for each drug that consisted of the respective solvents. Forty-eight hours later, 50 μL of 1 mg/mL MTT(in PBS) [3-[4,5-dimethylthiazol-2-yl]-2,5-diphenyltetrazolium bromide] was added to each well and incubated in a humidified atmosphere with for 4 h at 37 ℃ 50 mL/L CO_2. The supernatants were aspirated, and 200 μL /well of dimethyl sulfoxide was added to dissolve formazan crystals. Color intensity was measured at 570 nm using an ELISA reader. The 50% inhibitory concentration for a particular agent was defined as the drug concentration which resulted in a 50% reduction in cell number at 48 h relative to the control. Each experiment was performed in triplicate.

Accumulation of quercetin

Bcap37 and Bcap37/MDR1 cells were seeded at the density of 7.5×10^5 to a 35 mm i.d. tissue culture well. After twenty-four hours, the culture medium was aspirated, and replaced by the medium containing 25 μmol/L quercetin. After 10 and 20 min, the medium was aspirated and the cells were washed 3 times with ice-cold PBS (pH7.4) to stop further uptake. A 1 mL of 1 g/L Triton X-100 was added to each well to lyse the cells. Drug concentration in lysis solution was determined by reverse-phase HPLC, and normalized with cellular protein content[10].

Bcap37/MDR1 and control cells were seeded at the density of 7.5×10^5 to a 35 mm i.d. tissue culture well. After twenty-four hours, the culture medium was aspirated, and replaced by the medium containing 25 μmol/L quercetin with/without 6.6 μmol/L verapamil. After 30 min, the media were aspirated and the cells were washed 3 times with ice-cold PBS (pH7.4) to stop further uptake. A 1 mL of 1 g/L Triton X-100 was added to each well to lyse the cells. Drug concentration in lysis solution was determined by reverse- phase HPLC, and normalized with cellular protein content.

The HPLC system used was Agilent 1 100 system (Agilent Technologies). Separation was done on a conLichrospher ODS-C18 (4.6 mm i.d.×250 mm) column. The mobile phase consisted of pH2.0 phosphate buffer-tetrahydrofuran-methanol-isopropanol (65:15:10:20, v:v:v:v) at a flow rate of 0.5 mL/min, and the wavelength of UV detector was 380 nm. Morin was used as internal standard. Cell protein was quantitated by Bio-Rad DC protein assay kit.

RESULTS

Analysis of plasmid expression

After digestion with *Eco*RI, the recombinant plasmid pcDNA3.1 (+)/MDR1 showed three DNA fragments about 1.2 kb, 3.4 kb and 5.4 kb as expected (Figure 1). DNA sequencing result further confirmed the correct construction of this P-gp expression vector.

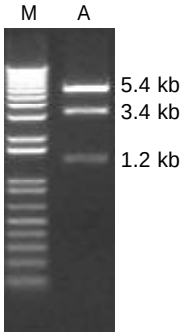

Figure 1 Analysis of pcDNA3.1(+)/MDR1 digested by *Eco*RI. M: DNA ladder; A: pcDNA3.1(+)/MDR1 digested by *Eco*RI.

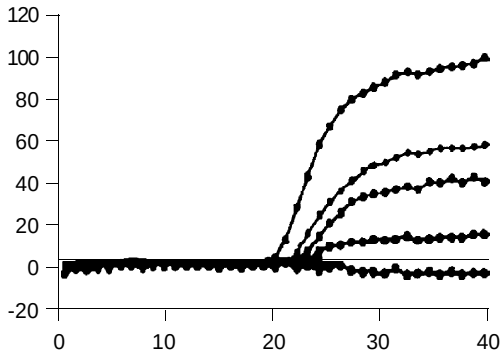

Figure 2 Map of real-time fluorescent quantitative RT-PCR. Blue curve: Bcap37; Other color curves: Bcap37 cell clones transfected with pcDNA3.1(+)/MDR1; Red curve stands for the clone expressing higher P-gp level than others.

Real-time fluorescent quantitative RT-PCR

The C_T of Bcap37/MDR1 and control cells was 19 and 40 cycles (Figure 2). It showed a significant increase of MDR1 mRNA levels in Bcap37/MDR1 than in control cells.

Western blot

The Bcap37/MDR1 cells showed significantly higher level of P-gp at 170 ku compared with control cells (Figure 3).

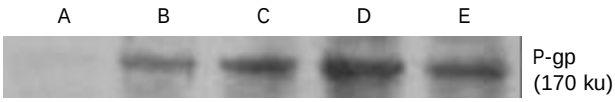

Figure 3 Western blot analysis of P-gp expression in Bcap37 and Bcap37/MDR1 cells. A: Bcap37; B, C, D, E: Bcap37 cell clones transfected with pcDNA3.1(+)/MDR1.

Immunohistochemical staining

The nuclei and plasma of control cells were stained blue (Figure 4A), demonstrating that the cells did not express P-gp. The Bcap37/MDR1 cells showed brown staining on cell membrane (Figure 4B). This indicated that P-gp was expressed on the transfected cell membrane.

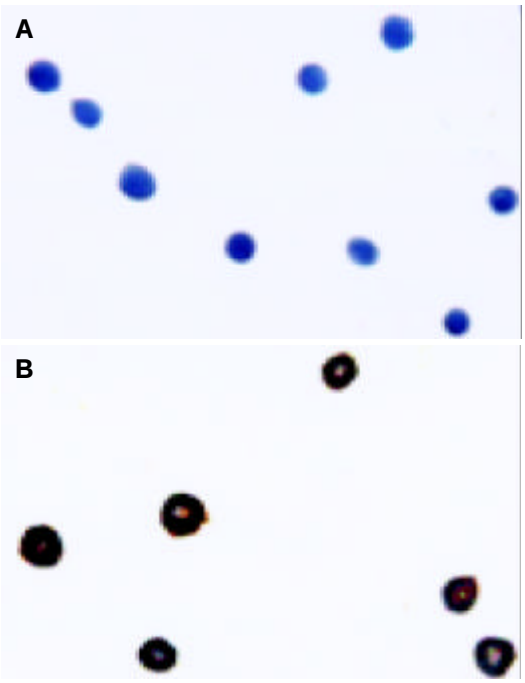

Figure 4 P-gp immunohistochemical staining in Bcap37 (A) and Bcap37/MDR1 (B) cells.

The cells were stained using a human anti-Pgp primary antibody, biotinylated anti-rabbit IgG secondary antibody, followed by the avidin and horseradish containing Vector ABCD reagent. The sections were then stained with 3,3-diaminobenzidine (DAB) and counterstained with hematoxylin. The brown color represented Pgp expression and the blue color was the non-specific counterstaining.

Drug sensitivity assay

Resistance to anticancer drugs was determined using MTT assay.Bcap/MDR1 exhibited multidrug resistant phenotypes characterized by cross-resistance to two unrelated antitumor agents (Table 1) including adriamycin and colchicine. The results confirmed the expressed Pgp in transfected cells played a role as an efflux pump.

Table 1 Relative resistance of multidrug resistant Bcap37 transfected cells

Cell line	IC_{50} (μg/mL)	
	Adriamycin	Colchicine
Bcap37	0.047	0.028
Bcap37/MDR1	2.203	0.391

Logarithmically growing cells were incubated for 48 h in the presence of the drug. IC_{50} referred to the drug concentration that resulted in a 50% reduction in cell number.

Quercetin accumulation in cells

Quercetin was incubated with Bcap37/MDR1 and Bcap37 for 10 min and 20 min, and the drug accumulation in cells is listed in Table 2. After P-gp inhibitor verapamil was administered the concentration of quercetin in model cells was increased (Figure 5). All values were normalized with protein content. The results demonstrated that quercetin was accumulated in Bcap37 much more than in Bcap37/MDR1 ($P<0.05$).

Table 2 Quercetin accumulation over different periods (n=3)

Cell line	10 min	20 min
Bcap37(μmol/L.mg)	2.44	3.33
Bcap37/MDR1(μmoL/mg)	1.47[a]	1.82[a]

[a]$P<0.05$ *vs* Bcap37 cells.

The amount of quercetin accumulation in cells was determined by reverse phase HPLC through a standard curve, and the values were normalized with cellular protein content. There was a significantly higher concentration of quercetin accumulated in MDR1 transgenic cells ($P<0.05$).

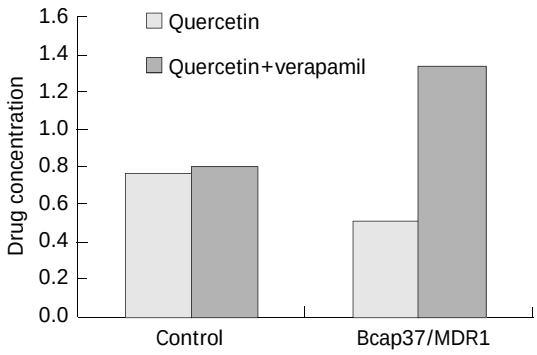

Figure 5 Amount of quercetin accumulation in cells with/without verapamil.

DISCUSSION

In recent years, it has become apparent that transport proteins play a major role in controlling the distribution, elimination and potentially the metabolism of some drugs, including organic cation transporters, organic anion transporters, MRP related transporters, and P-glycoprotein. P-gp has received considerable attention in recent years both as a barrier to drug absorption and distribution, and as a potential source for variability in drug pharmacokinetics and pharmacodynamics. In the intestine, P-gp could actively transport drugs counter-current to the absorptive transport of drugs, thus posing a barrier to absorption of exogenous compounds[11]. This activity has been proposed to act in concert with intestinal cytochrome P-450 3A4 to increase pre-systemic metabolism of drugs, further minimizing systemic exposure to other drugs and xenobiotics[12,13]. For

example, Pgp limited intestinal absorption of digoxin, talinolol, and cyclosporine after oral dosing, limited the central nervous system penetration of human immunodeficiency virus protease inhibitors, and helped excrete paclitaxel into intestine[14-18].

A P-gp over-expressing cell line was established and characterized by Western blot, drug sensitivity assay and flow cytometry (data not shown). The results showed that the P-gp over-expressing cell line had biological functions.

In cellular drug accumulation assays, drug accumulation in P-gp expressing cells was compared with accumulation in cells from the parental cell line. Since the accumulation of P-gp substrates in P-gp over-expressing cells was restricted by P-gp mediated efflux of the compound back into the extracellular fluid, P-gp substrates showed less accumulation in P-gp expressing cells than in P-gp deficient cells. Similarly, drug accumulation was increased under conditions when P-gp was inhibited. In our experiment, quercetin showed less accumulation in Bcap37/MDR1 than in Bcap37. After P-gp inhibitor verapamil was administered, the concentration of this flavonoid in model cells increased. This implied the compound was a P-gp substrate. The result was similar to that of Walgren *et al*[19].

A high P-gp expressing cell line can be established which provides a suitable *in vitro* model system for studying drug intestinal absorption mechanism, predicting the drug permeability characteristics and screening new multi-drug resistant reversing agents.

REFERENCES

1 **Hugger ED**, Novak BL, Burton PS, Audus KL, Borchardt RT. A comparison of commonly used polyethoxylated pharmaceutical excipients on their ability to inhibit P-glycoprotein activity *in vitro*. *J Pharm Sci* 2002; **9**: 1991-2002

2 **Schinkel AH**. P-glycoprotein, a gatekeeper in the blood-brain barrier. *Adv Drug Deliv Rev* 1999; **36**: 179-194

3 **Hochman JH**, Yamazaki M, Ohe T, Lin JH. Evaluation of drug interactions with P-glycoprotein in drug discovery: *in vitro* assessment of the potential for drug-drug interactions with p-glycoprotein. *Curr Drug Metab* 2002; **3**: 257-273

4 **Jovanovic SV,** Simic MG. Antioxidants in nutrition. *Ann N Y Acad Sci* 2000; **899:** 326-334

5 **Wiseman H**. The bioavailability of non-nutrient plant factors: dietary flavonoids and phyto-oestrogens. *Proc Nutr Soc* 1999; **58:** 139-146

6 **Graefe EU**, Derendorf H, Veit M. Pharmacokinetics and bioavailability of the flavonol quercetin in humans. *Int J Clin Pharmacol Ther* 1999; **37:** 219-233

7 **Lamson DW**, Brignall MS. Antioxidants and cancer 3: quercetin. *Altern Med Rev* 2000; **5:** 196-208

8 **Kioka N**, Tsubota J, Kakehi Y, Komano T, Gottesman MM, Pastan I, Ueda K. P-glycoprotein gene (MDR1) cDNA from human adrenal: normal P-glycoprotein carrier Gly^{185} with an altered pattern of multidrug resistance. *Biochem Biophys Res Commun* 1989; **162**: 224-231

9 **Becker K**, Pan D, Whitley CB. Real-time quantitative polymerase chain reaction to assess gene transfer. *Hum Gene Ther* 1999; **10**: 2559-2566

10 **Takara K**, Tanigawara Y, Komada F, Nishiguchi K, Sakaeda T, Okumura K. Cellular pharmacokinetic aspects of reversal effect of itraconazole on P-glycoprotein-mediated resistance of anticancer drugs. *Biol Pharm Bull* 1999; **22**: 1355-1359

11 **Lown KS,** Mayo RR, Leichtman AB, Hsiao HL, Turgeon DK, Schmiedlin-Ren P, Brown MB, Guo W, Rossi SJ, Benet LZ, Watkins PB. Role of intestinal P-glycoprotein (mdr1) in interpatient variation in the oral bioavailability of cyclosporine. *Clin Pharmacol Ther* 1997; **62**: 248-260

12 **Shapiro AB**, Ling V. Stoichiometry of coupling of rhodamine 123 transport to ATP hydrolysis by P-glycoprotein. *Eur J Biochem* 1998; **254**: 189-193

13 **Ambudkar SV,** Dey S, Hrycyna CA, Ramachandra M, Pastan I, Gottesman MM. Biochemical, cellular, and pharmacological aspects of the multidrug transporter. *Annu Rev Pharmacol Toxicol* 1999; **39**: 361-398

14 **Sparreboom A,** van Asperen J, Mayer U, Schinkel AH, Smit JW, Meijer DK, Borst P, Nooijen WJ, Beijnen JH, van Tellingen O. Limited oral bioavailability and active epithelial excretion of paclitaxel (Taxol) caused by P-glycoprotein in the intestine. *Proc Natl Acad Sci U S A* 1997; **94**: 2031-2035

15 **Kim RB**, Fromn MF, Wandel C, Leake B, Wood AJ, Roden DM, Wilkinson GR. The drug transporter P-glycoprotein limits oral absorption and brain entry of HIV-1 protease inhibitors. *J Clin Invest* 1998; **101**: 289-294

16 **Polli JW,** Jarrett JL, Studenberg SD, Humphreys JE, Dennis SW, Brouwer KR, Woolley JL. Role of P-glycoprotein on the CNS disposition of amprenavir (141W94), an HIV protease inhibitor. *Pharm Res* 1999; **16**: 1206-1212

17 **Verschraagen M**, Koks CH, Schellens JH, Beijnen JH. P-glycoprotein system as a determinant of drug interactions: the case of digoxin-verapamil. *Pharmacol Res* 1999; **40**: 301-306

18 **Schwarz UI,** Gramatte T, Krappweis J, Oertel R, Kirch W. P-glycoprotein inhibitor erythromycin increases oral bioavailability of talinolol in humans. *Int J Clin Pharmacol Ther* 2000; **38**: 161-167

19 **Walgren RA**, Walle UK, Walle T. Transport of quercetin and its glucosides across human intestinal epithelial Caco-2 cells. *Biochem Pharmacol* 1998; **55**: 1721-1727

Edited by Zhu LH and Wang XL **Proofread by** Xu FM

PO Box 2345, Beijing 100023, China
Fax: +86-10-85381893
E-mail: wjg@wjgnet.com www.wjgnet.com

World J Gastroenterol 2004;10(9):1369-1371
World Journal of Gastroenterology
Copyright ©2004 by The WJG Press ISSN 1007-9327

• BRIEF REPORTS •

Diagnosis of intestinal acariasis with avidin-biotin system enzyme-linked immunosorbent assay

Rong-Bo Zhang, Yong Huang, Chao-Pin Li, Yu-Bao Cui

Rong-Bo Zhang, Chao-Pin Li, Yu-Bao Cui, Department of Etiology and Immunology, School of Medicine, Anhui University of Science and Technology, Huainan 232001, Anhui Province, China
Yong Huang, Shandong Institute of Parasitic Diseases, Jining 272033, Shandong Province, China
Correspondence to: Dr. Chao-Pin Li, Department of Etiology and Immunology, School of Medicine, Anhui University of Science and Technology, Huainan 232001, Anhui Province, China. cpli @aust.edu.cn
Telephone: +86-554-6658770 **Fax:** +86-554-6662469
Received: 2003-08-02 **Accepted:** 2003-09-18

Abstract

AIM: To explore the value of avidin-biotin system enzyme-linked immunosorbent assay (ABC-ELISA) in diagnosis of intestinal acariasis.

METHODS: Mite-specific IgG levels in serum of 48 patients with intestinal acariasis were measured with ABC-ELISA. The sensitivity of this method was compared with that of staphylococcal protein A enzyme-linked immunosorbent assay (SPA-ELISA).

RESULTS: The positive rate of mite-specific IgG detected with ABC-ELISA and SPA-ELISA was 89.58% (43/48) and 56.25% (27/48), respectively. The positive rate with ABC-ELISA was statistically higher than that with SPA-ELISA (χ^2=13.50, P<0.01).

CONCLUSION: ABC-ELISA is an effective method for the diagnosis of intestinal acariasis.

Zhang RB, Huang Y, Li CP, Cui YB. Diagnosis of intestinal acariasis with avidin-biotin system enzyme-linked immunosorbent assay. *World J Gastroenterol* 2004; 10(9): 1369-1371
http://www.wjgnet.com/1007-9327/10/1369.asp

INTRODUCTION

Mites could live in intestinal tract and cause intestinal acariasis with most frequent symptoms of abdominal pain, diarrhea and pyohemofecia[1-3]. Intestinal acariasis is traditionally diagnosed by identification of adult or larval mites, eggs or hypopus in either single or multiple fecal specimens under microscopy. The detection of the parasites is increased on examination of multiple fecal samples obtained on three different days. However, it is not easy to detect mites technically. Thus, the present study intended to develop and evaluate an enzyme-linked immunosorbent assay for mite-specific antibody detection in serum samples using *Dermatophagoides farinae* extract.

MATERIALS AND METHODS

Serum

A total of 78 serum specimens were collected from 48 patients with intestinal acariasis and 30 health blood donors. All of the subjects investigated were asked to provide stools for detection of mites by saturated saline floatation method. The 48 patients with mites in stools were grouped as experimental group, while the health blood donors without mites as control group.

Reagents

Reagents for ABC-ELISA and SPA-ELISA were provided by Shanghai Institute of Biological Products (Batch No. 990004 and 990012). *Dermatophagoides farinae* extract was made according to NIBSC82/518 approved by World Health Organization (WHO) in 1984. The mites were cultured in the initial medium for several months. A 48-h maceration in a borate buffer (pH 8.5) was centrifuged. The supernatant was neutralized and precipitated with a series of acetone. The precipitated fraction at 800 mL/L acetone was isolated, washed and dried. This purified extract was lyophilized or stored as a solution in the presence of 500 mL/L glycerol and 50 mL/L phenol[4-7].

Methods

ABC-ELISA procedure Initially 0.1 mL *Dermatophagoides farinae* extract with protein concentrations of 62.5 μg/mL was added in each well on a 40-well plate coated with enzyme, and the plate was placed at 4 ℃ overnight. Then the plate was washed with PBS (pH=7.4), sera of the patients with intestinal acariasis were diluted at 1:40 and added in duplicated wells, and incubated in water bath at 37 ℃ for 60 min. Following washing of the plate, bio-SAH IgG at the concentration of 1:40 was added and incubated at 37 ℃ for 60 min, avidin-HRP at the concentration of 1:20 was added for reaction at 37 ℃ for 30 min, and the substrate OPD-H_2O_2 was added and incubated at 37 ℃ for 30 min. Lastly, 2 mol/L H_2SO_4 was added to terminate the reaction. Sera of the control group were detected with the same procedure[8,9].

SPA-ELISA procedure Concentrations of antigen and sera dilution in SPA-ELISA method were similar to those in ABC-ELISA. SPA-ELISA was performed as routine. Values of optic densities (OD) in each well were determined, the value of 2.1 times or more of the negative control was considered as positive.

RESULTS

General data

A total of 48 patients (male 32 and female 16) with intestinal acariasis were selected as mites were found in their stools. The 48 patients consisted of 13 workers in traditional Chinese medical storehouses, 22 workers in rice storehouse or mill, 8 miners, 2 workers in machine factory and 3 with other occupations. The mites in stool samples included *Acarus siro*, *TyroPhagus putrescentiae*, *Dermatophagoides farinae*, *D. pteronyssinus*, *Glycyphagus domesticus*, *G.ornatus*, *Carpoglyphus lactis* and *Tarsonemus granaries*.

ABC-ELISA data

In ABC-ELISA, the mean OD value of mite-specific IgG in sera of the 48 patients was 0.358±0.124 (0.176-0.615), while that in 30 controls was 0.112±0.065 (0.085-0.253). The Absorbent values in 43 of 48 patients were at least 2.1 times of 0.112, the positive

rate of the patients detected by ABC-ELISA was 89.58%. Interestingly, the *A* value of one case in normal control group was 0.253, and the false positive rate was 3.33%.

SPA-ELISA data

In SPA-ELISA, the mean OD value of mite-specific IgG in sera of the 48 patients was 0.225±0.147 (0.133-0.574) and that in the control group was 0.078±0.047 (0.043-0.172). The *A* values in 37 patients were at least 2.1 times of 0.078, the positive rate of the patients detected by SPA-ELISA was 56.25%. However, the *A* values of 2 cases in control group were 0.168 and 0.172, respectively, which were higher than 0.1638. The false positive rate in SPA-ELISA was 6.67%.

Comparison between ABC-ELISA data and SPA-ELISA data

The positive rate of the patients detected by ABC-ELISA and SPA-ELISA was 89.58% (43/48) and 56.25% (27/48) with a significant difference (χ^2=13.50, P<0.01). Although only 25 cases were positive in both ABC-ELISA and SPA-ELISA, the positive number of patients was 45 (93.75%) by ABC-ELISA or SPA-ELISA (Table 1).

Table 1 Intestinal acariasis detected with ABC-ELISA and SPA-ELISA

Methods	ABC-ELISA method (+)	ABC-ELISA method (-)	Total
SPA-ELISA method (+)	25	2	27[b]
SPA-ELISA method (-)	18	3	21
Total	43[b]	5	48

[b]: χ^2=13.50, P<0.01.

DISCUSSION

ABC-ELISA and SPA-ELISA were used to detect mite-specific antibody IgG in serum samples from 48 patients with intestinal acariasis, and the positive rate in ABC-ELISA and SPA-ELISA was 89.58% and 56.25%, respectively. ABC-ELISA had high specificity in diagnosis of intestinal acariasis. Moreover, ABC-ELISA in detection of mite-specific antibody was easy to perform, inexpensive, and numerous samples could be performed simultaneously. The test could be carried out quickly for the diagnosis, particularly for individuals who suffered from recurrent diarrhea, chronic abdominal pain, malabsorption and stunting due to infection.

The occurrence of false positive in two methods in diagnosis of intestinal acariasis might be associated with mites' invasive locus, stool examination techniques and dilution of sera. In addition to gastrointestinal tract, acaroid mites could infest other organs of the human body such as respiratory tract and urinary tract, no matter where they were parasized, mite-specific antibody would occur in peripheral blood[10-18]. Although saturated saline floatation method is useful in examination of feces, some large and heavy mites may be missed because of difficult drift. Sera dilution at 1:40 in the present study was lower than that in routine ELISA with dilution at 1:100 to 1:200. It was suggested that much more times repeating stool examination should be carried out in the normal control group to avoid false positive detection[19-24].

Our study showed 8 species of mites in human stools. We used *Dermatophagoides farinae* extract as coating antigen only, which might decrease the detectable rates of mite-specific antibody, because common antigen might exist in *Dermatophagoides farinae* and other seven species of mites[25-28]. In addition, the number of mites in intestinal tract might affect the levels of mite-specific antibodies and detectable rates. In conclusion, ABC-ELISA method is effective in diagnosis of intestinal acariasis.

REFERENCES

1 **Li CP**, Wang J. Intestinal acariasis in Anhui Province. *World J Gastroenterol* 2000; **6**: 597-600

2 **Li CP**, Cui YB, Wang J, Yang QG, Tian Y. Acaroid mite, intestinal and urinary acariasis. *World J Gastroenterol* 2003; **9**: 874-877

3 **Li CP**, Wang KX. A study on treatment of intestinal acariasis. *Shijie Huaren Xiaohua Zazhi* 2000; **8**: 919-920

4 **Nuttall TJ**, Lamb JR, Hill PB. Characterization of major and minor *Dermatophagoides* allergens in canine atopic dermatitis. *Res Vet Sci* 2001; **71**: 51-57

5 **Basomba A**, Tabar AI, de Rojas DH, Garcia BE, Alamar R, Olaguibel JM, del Prado JM, Martin S, Rico P. Allergen vaccination with a liposome-encapsulated extract of *Dermatophagoides pteronyssinus*: a randomized, double-blind, placebo -controlled trial in asthmatic patients. *J Allergy Clin Immunol* 2002; **109**: 943-948

6 **Akcakaya N**, Hassanzadeh A, Camcioglu Y, Cokugras H. Local and systemic reactions during immunotherapy with adsorbed extracts of house dust mite in children. *Ann Allergy Asthma Immunol* 2000; **85**: 317-321

7 **Hillier A**, Kwochka KW, Pinchbeck LR. Reactivity to intradermal injection of extracts of *Dermatophagoides farinae*, *Dermatophagoides pteronyssinus*, house dust mite mix, and house dust in dogs suspected to have atopic dermatitis: 115 cases (1996-1998). *J Am Vet Med Assoc* 2000; **217**: 536-540

8 **Guo H**, Zhao ZF, Shi DZ. A study on the culture medium antigens of Cystcercus cellulosae for detecting antibodies of cysticercosis by means of ABC-ELISA. *Southeast Asian J Trop Med Public Health* 1997; **28**(Suppl 1): 125-127

9 **Koldas M**, Uras F. Avidin-biotin ELISA for measurement of prothrombin in human plasma. *Thromb Res* 2001; **102**: 221-227

10 **Beco L**, Petite A, Olivry T. Comparison of subcutaneous ivermectin and oral moxidectin for the treatment of notoedric acariasis in hamsters. *Vet Rec* 2001; **149**: 324-327

11 **Hiraoka E**, Sato T, Shirai W, Kimura J, Nogami S, Itou M, Shimizu K. A case of pulmonary acariasis in lung of Japanese macaque. *J Vet Med Sci* 2001; **63**: 87-89

12 **van der Geest LP**, Elliot SL, Breeuwer JA, Beerling EA. Diseases of mites. *Exp Appl Acarol* 2000; **24**: 497-560

13 **Hammerberg B**, Bevier D, DeBoer DJ, Olivry T, Orton SM, Gebhard D, Vaden SL. Auto IgG anti-IgE and IgG x IgE immune complex presence and effects on ELISA-based quantitation of IgE in canine atopic dermatitis, demodectic acariasis and helminthiasis. *Vet Immunol Immunopathol* 1997; **60**: 33-46

14 **Morris DO**, Dunstan RW. A histomorphological study of sarcoptic acariasis in the dog: 19 cases. *J Am Anim Hosp Assoc* 1996; **32**: 119-124

15 **Jungmann P**, Guenet JL, Cazenave PA, Coutinho A, Huerre M. Murine acariasis: I. Pathological and clinical evidence suggesting cutaneous allergy and wasting syndrome in BALB/c mouse. *Res Immunol* 1996; **147**: 27-38

16 **Jungmann P**, Freitas A, Bandeira A, Nobrega A, Coutinho A, Marcos MA, Minoprio P. Murine acariasis. II. Immunological dysfunction and evidence for chronic activation of Th-2 lymphocytes. *Scand J Immunol* 1996; **43**: 604-612

17 **Ponsonby AL**, Kemp A, Dwyer T, Carmichael A, Couper D, Cochrane J. Feather bedding and house dust mite sensitization and airway disease in childhood. *J Clin Epidemiol* 2002; **55**: 556-562

18 **Paufler P**, Gebel T, Dunkelberg H. Quantification of house dust mite allergens in ambient air. *Rev Environ Health* 2001; **16**: 65-80

19 **Gonin P**, Trudel L. Detection and differentiation of Entamoeba histolytica and Entamoeba dispar isolates in clinical samples by PCR and enzyme-linked immunosorbent assay. *J Clin Microbiol* 2003; **41**: 237-241

20 **Molinari JL**, Garcia-Mendoza E, de la Garza Y, Ramirez JA, Sotelo J, Tato P. Discrimination between active and inactive

neurocysticercosis by metacestode excretory/secretory antigens of Taenia solium in an enzyme-linked immunosorbent assay. *Am J Trop Med Hyg* 2002; **66**: 777-781

21 **Levett PN**, Branch SL. Evaluation of two enzyme-linked immunosorbent assay methods for detection of immunoglobulin M antibodies in acute leptospirosis. *Am J Trop Med Hyg* 2002; **66**: 745-748

22 **Van Gool T**, Vetter H, Vervoort T, Doenhoff MJ, Wetsteyn J, Overbosch D. Serodiagnosis of imported schistosomiasis by a combination of a commercial indirect hemagglutination test with Schistosoma mansoni adult worm antigens and an enzyme-linked immunosorbent assay with S. mansoni egg antigens. *J Clin Microbiol* 2002; **40**: 3432-3437

23 **Odashima NS**, Takayanagui OM, Figueiredo JF. Enzyme linked immunosorbent assay (ELISA) for the detection of IgG, IgM, IgE and IgA against Cysticercus cellulosae in cerebrospinal fluid of patients with neurocysticercosis. *Arq Neuropsiquiatr* 2002; **60**: 400-405

24 **Starke-Buzetti WA**, Machado RZ, Zocoller-Seno MC. An enzyme-linked immunosorbent assay (ELISA) for detection of antibodies against Toxocara vitulorum in water buffaloes. *Vet Parasitol* 2001; **97**: 55-64

25 **Varela J**, Ventas P, Carreira J, Barbas JA, Gimenez-Gallego G, Polo F. Primary structure of Lep d I, the main Lepidoglyphus destructor allergen. *Eur J Biochem* 1994; **225**: 93-98

26 **Kemp SF**, Lockey RF, Fernandez-Caldas E, Arlian LG. Skin test and crossreactivity studies with Euroglyphus maynei and Dermatophagoides pteronyssinus. *Clin Exp Allergy* 1997; **27**: 893-897

27 **Garcia-Robaina JC**, Eraso E, De la Torre F, Guisantes J, Martinez A, Palacios R, Martinez J. Extracts from various mite species contain cross-reactive and noncross-reactive IgE epitopes. A RAST inhibition study. *J Investig Allergol Clin Immunol* 1998; **8**: 285-289

28 **Smith W**, Mills K, Hazell L, Hart B, Thomas W. Molecular analysis of the group 1 and 2 allergens from the house dust mite, Euroglyphus maynei. *Int Arch Allergy Immunol* 1999; **118**: 15-22

Edited by Ren SY and Wang XL **Proofread by** Xu FM

PO Box 2345, Beijing 100023, China
Fax: +86-10-85381893
E-mail: wjg@wjgnet.com www.wjgnet.com

World J Gastroenterol 2004;10(9):1372-1374
World Journal of Gastroenterology
Copyright ©2004 by The WJG Press ISSN 1007-9327

• BRIEF REPORTS •

Catheterization-associated complications of intraperitoneal chemotherapy in advanced gastric cancer

Meng Ye, Hong-Ming Pan, Hai-Yun Wang, Fang Lou, Wei Jin, Yu Zheng, Jin-Ming Wu

Meng Ye, Hong-Ming Pan, Hai-Yun Wang, Fang Lou, Wei Jin, Yu Zheng, Jin-Ming Wu, Center for Oncology, Sir Run Run Shaw Hospital, Zhejiang University, Hangzhou 310016, Zhejiang Province, China
Correspondence to: Professor Hong-Ming Pan, Center for Oncology, Sir Run Run Shaw Hospital, Zhejiang University, Hangzhou 310016, Zhejiang Province, China. panhongming@163.net
Telephone: +86-571-86090073-3121 **Fax:** +86-571-86044817
Received: 2003-06-30 **Accepted:** 2003-07-30

Abstract

AIM: To assess the catheterization-associated complications during intraperitoneal chemotherapy (IPCT) for advanced gastric cancer.

METHODS: From 1998 to 2002, 80 patients with advanced gastric cancer received a total of 320 courses of IPCT using a large bore central venous catheter and associated complications were analyzed.

RESULTS: Catheterization-associated complications occurred in 11 of the 80 patients (13.8%), including abdominal pain caused by catheter in 2 cases (0.63%), insertion failure in 2 cases (0.63%), bowel perforation in 1 case (0.31%) and abdominal pain during chemotherapy in 6 cases (1.88%). No serious complications required surgical intervention.

CONCLUSION: IPCT using central venous catheters can be performed safely and simply without severe associated complications.

Ye M, Pan HM, Wang HY, Lou F, Jin W, Zheng Y, Wu JM. Catheterization-associated complications of intraperitoneal chemotherapy in advanced gastric cancer. *World J Gastroenterol* 2004; 10(9): 1372-1374
http://www.wjgnet.com/1007-9327/10/1372.asp

INTRODUCTION

Gastrointestinal tumor is quite common. In China, the morbidity of gastric cancer is the leading cause of malignant tumors. For non-advanced gastric cancer, surgical removal is the first choice, but for advanced gastric cancer, the outcome of surgical resection remains unsatisfactory. Fifty percent of gastric cancer patients have local recurrence or long distance metastasis after radical surgery within 5 years. The common sites of gastric cancer recurrence or metastasis are the resection site, liver and peritoneal surfaces[1-4]. It was reported that intraperitoneal chemotherapy could result in markedly increased local drug concentration, and had favorable clinical results in preventing recurrence and metastasis of gastric cancer after surgical treatment, but some complications were reported by using Tenckhoff catheter in IPCT[5-7]. From March 1998 to June 2002, 80 patients with advanced gastric cancer were treated by central venous catheterization during intraperitoneal chemotherapy (IPCT) after radical gastrectomy in SRRSH Cancer Center. The main purpose of this study was to analyze the complications of central venous catheterization during IPCT.

MATERIALS AND METHODS

Patients

Between March 1998 and June 2002, 80 patients with advanced gastric cancer were treated in SRRSH Cancer Center. Forty-eight cases were males and 31 females aged 29 to 71 years (median 43.5 years). Patients in stage III_A were 18 cases, stage III_B 29 cases, stage IV 33 cases. The patients were treated with a total of 320 courses of IPCT. Each patient received at least 3 courses of IPCT (mean 4 courses for each patient).

Peritoneal catheters and methods

Single cavity central venous catheters were produced by Arrow Raulerson Syring Ltd, USA. Transparent protecting patches and heparin caps were produced by 3 mol/L Health Care Ltd, USA. As there are no large vessels in this site, puncture site is usually chosen at the cross-point of left midclavicular line and navel line, which is located at outer edge of rectus abdominis muscle. Two percent lidocaine was used for local anesthesia, then a conducting needle was put into the peritoneal cavity, after a steel string was put into peritoneal cavity though the conducting needle. The needle was taken out and the central venous catheter was put into the peritoneal cavity following the steel string after the abdominal wall was dilated. Then 100 mL normal saline was administrated though the catheter, if nothing abnormal was observed, and a heparin cap was put on the top of the catheter and the catheter was fixed to the abdominal wall.

The regimen of intraperitoneal chemotherapy was HCPT+5-FU+CF+VP-16, the dose of chemotherapeutic agents was 8 mg/m^2 for HCPT, 375 mg/m^2 for 5-FU, 100 mg for leucovorin (CF), 80 mg/m^2 for etopside (VP-16) for three days. HCPT was administrated though peritoneal cavity, other agents were administrated though peripheral vein. Before chemotherapy started, 1 000 mL warm (42 ℃) normal saline was administrated into the peritoneal cavity together with 10 mg DXM and 20 mL 20 g/L lidocaine. HCPT was dissolved in 500 mL of normal saline and instilled in the peritoneal cavity though the implanted catheter. Then 42 ℃ normal saline was instilled to the peritoneal cavity again, until the total volume reached 1 500 mL/m^2. Patients were asked to change their position every 15 min for 2 h after drug administration. Chemotherapy was given 2 wk after surgery, and repeated every 3 wk with the same regimen. The central venous catheter was taken out after each cycle of chemotherapy, a new catheter was put into peritoneal cavity just before the next cycle of IPCT started.

RESULTS

The complications associated with catheterization during IPCT in this series were common and mild. Moderate to severe pain induced by catheterization occurred in 2 cases (0.63%). Failure in catheterization because of intraabdominal adhesion occurred in 2 cases (0.63%), but the catheter was successfully put into peritoneal cavity through the other side of abdominal wall. Bowel perforation occurred in one case (0.31%) possibly due

to severe intraabdominal adhesion after surgery, and the catheter was put into bowel cavity. This patient received systemic chemotherapy instead of IPCT afterwards, and antibiotics were given to him. He had no signs of peritonitis during the procedure. Moderate pain during chemotherapy occurred in 6 cases (1.88%). There was no incidence of severe complications such as intestinal obstruction, peritonitis, intestinal hemorrhage, leakage of peritoneal fluid and anastomotic stoma fistula (Table 1).

Table 1 Catheterization-associated complications

Complications	Cases (n=320, %)
Pain by catheterization	2 (0.63)
Insertion failure	2 (0.63)
Bowel perforation	1 (0.31)
Pain during chemotherapy	6 (1.88)

DISCUSSION

Postoperative IPCT should be started early[8-11]. Because surgery for gastrointestinal cancer is associated with an extremely high rate of dissemination within the peritoneal cavity and seeding on peritoneum, the resection site and abraded peritoneal surfaces are common sites of tumor cell seeding, early postoperative IPCT lets all intraabdominal surfaces expose to intraperitoneal chemotherapy agents. Because all adhesions are lysed at this time, the response rate of minor metastatic lesions on peritoneal surface to the chemotherapy agents can be 100%. Besides, tumor burden is light at this time according to tumor cell proliferative kinetics, chemotherapy agents can not only kill dissociative tumor cells in peritoneal cavity, but also kill inflammatory cells in peritoneal cavity, thus decreasing the releasing of cellular factors and preventing their effect on tumor cell proliferation. Regional chemotherapy could result in markedly increasd local responses without compromising systemic effects[12-14]. Studies of pharmacokinetics of IPCT also showed advantages. Sugarbaker[15] summarized the pharmacokinetics of 4 kinds of chemotherapy agents often used in IPCT, the area under the curve (AUC) within peritoneal fluid compared with plasma of these agents was as follows, 5-FU 150/1, MMC 72/1, ADM 205/1, and DDP 20/1. There was an obvious difference between AUC within peritoneal fluid and AUC within plasma.

Several methods could be used in IPCT[7,16]. The catheters commonly used are Tenckhoff catheter and single peritoneal cavity catheter. Tenckhoff catheter is popular in Western countries. After completing the surgical procedure and prior to closing the abdominal wall, Tenckhoff catheter is placed through the abdominal wall and then a Dacron cuff is fixed subcutaneously. A needle is inserted into the Dacron cuff during chemotherapy. The disadvantage of this method is that the catheter is left in the peritoneal cavity for a long period, and there are some complications. Esquivel *et al*.[17] reported that in 44 patients who received IPCT during the first day to fifth day after surgery, 13% of the patients had pneumonia, 9% bleeding after surgery, 9% intestinal fistula, 7% a prolonged duration of intubation, 2% biliary fistula, 2% anastomotic stoma fistula, and 2% pancreatitis. The total complication morbidity was 37%, 17% of the complications were related to bowel function. Topuz *et al*.[18] also reported that there were 39 patients in 205 cycles of intraperitoneal chemotherapy, severe abdominal pain was in 4 patients (10.3%), peritonitis and coloperitoneal fistula each in 1 patient (2.6%), catheter obstruction in 3 patients (7.7%) and colon puncture in 4 patients (10.3%). Sakuragi *et al*.[19] did IPCT in 78 patients using Tenckhoff catheter, the total cycles were 365. Among them, 27 (34.6%) experienced IPCT related complications, 17 (21.8%) had extensive intraabdominal adhesion, 13 (16.7%) had local infection around the reservoir, 3 (3.8%) had an abscess at the site of the implanted port of the catheter, 3 (3.8%) had catheter obstruction, one (1.3%) had ilieus, one (1.3%) had perforation of small intestine, one (1.3%) underwent opening of the wound at the site of catheter implantation due to bleeding.

We used central venous catheter in IPCT, the procedure of catheterization was easy to master. Meanwhile it was not necessary to leave the catheter for a long time, the catheter could be taken out 2-3 d after chemotherapy, which could improve the life quality of patients. Moreover, central venous catheter was used only one time with few complications. In fact, our patients had no severe complications such as intestinal perforation, intestinal bleeding, peritonitis, anastomotic stoma fistula and implantation site infection. The morbidity of complications in our group was 13.75%, much lower than reported in other documents. Pain after catheterization was due to the length of catheter into the peritoneal cavity, and the pain could be relieved after pulling out the catheter. The pain during chemotherapy could be relieved by administrating lidocaine and DXM into peritoneal cavity.

The reasons why our group has a low morbidity of complications are as follows. Chemotherapy was started two weeks after surgery instead of 5 d after surgery. Since surgical incision was healed 2 wk after surgery, many complications of IPCT were avoided by starting chemotherapy 2 wk after surgery. Besides, statistical analysis showed that there was no difference in response rate (data not shown). Tenckhoff catheter used by Sakuragi *et al*.[19] had to put in the peritoneal cavity for a long period and there also must be a drainage system or an outflow tube. But we used central venous catheter only one time and did not need an outflow tube and the chemotherapy agents of IPCT were spontaneously absorbed by peritoneum. Clinical observation revealed that intraperitoneal fluid could be absorbed spontaneously 2 or 3 d after chemotherapy. Radical gastrectomy has a great surgical scope and can cause severe intraabdominal adhesion which can limit intraperitoneal fluid to flow freely. Sugarbaker *et al*.[15] thought this would affect the distribution of chemotherapy agents in peritoneal cavity, and would affect chemotherapy agents to contact with peritoneum. If there was not enough fluid in the peritoneal cavity, the fluid could not flow freely in peritoneal cavity because of resistance. Though patients changed their position frequently, chemotherapy agents could not distribute to the whole peritoneal cavity, thus decreasing the response rate. Only a large volume of fluid causing abdominal distension could make chemotherapy agents distribute evenly in peritoneal cavity[20]. Therefore, 1 500-2 000 mL fluid should be given to patients every time during chemotherapy, and the patients should change their position frequently in order to achieve chemotherapeutic effect. Besides, a large volume of fluid can decrease the incidence of complications such as abdominal pain, intestinal perforation, intestinal bleeding, ileus, peritonitis and anastomotic stoma fistula.

In conclusion, it is safe and convenient to use central venous catheters in intraperitoneal chemotherapy and it also has less side effects and fewer complications.

REFERENCES

1 **Earle CC**, Maroun J, Zuraw L. Neoadjuvant or adjuvant therapy for resectable gastric cancer? A practice guideline. *Can J Surg* 2002; **45**: 438-446

2 **Hu JK**, Chen ZX, Zhou ZG, Zhang B, Tian J, Chen JP, Wang L, Wang CH, Chen HY, Li YP. Intravenous chemotherapy for resected gastric cancer: meta-analysis of randomized controlled trials. *World J Gastroenterol* 2002; **8**: 1023-1028

3 **Jeung HC**, Rha SY, Jang WI, Noh SH, Chung HC. Treatment of advanced gastric cancer by palliative gastrectomy,

cytoreductive therapy and postoperative intraperitoneal chemotherapy. *Br J Surg* 2002; **89**: 460-466

4 **Yagi Y**, Seshimo A, Kameoka S. Prognostic factors in stage IV gastric cancer: univariate and multivariate analyses. *Gastric Cancer* 2000; **3**: 71-80

5 **Fu QG**, Meng FD, Shen XD, Guo RX. Efficacy of intraperitoneal thermochemotherapy and immunotherapy in intraperitoneal recurrence after gastrointestinal cancer resection. *World J Gastroenterol* 2002; **8**: 1019-1022

6 **Witkamp AJ**, de Bree E, Van Goethem R, Zoetmulder FA. Rationale and techniques of intra-operative hyperthermic intraperitoneal chemotherapy. *Cancer Treat Rev* 2001; **27**: 365-374

7 **Averbach AM**, Jacquet P. Strategies to decrease the incidence of intra-abdominal recurrence in resectable gastric cancer. *Br J Surg* 1996; **83**: 726-733

8 **Noh SH**, Yoo CH, Chung HC, Roh JK, Shin DW, Min JS. Early postoperative intraperitoneal chemotherapy with mitomycin C, 5-fluorouracil and cisplatin for advanced gastric cancer. *Oncology* 2001; **60**: 24-30

9 **Jeung HC**, Rha SY, Jang WI, Noh SH, Chung HC. Treatment of advanced gastric cancer by palliative gastrectomy, cytoreductive therapy and postoperative intraperitoneal chemotherapy. *Br J Surg* 2002; **89**: 460-466

10 **Maehara Y**, Baba H, Sugimachi K. Adjuvant chemotherapy for gastric cancer: a comprehensive review. *Gastric Cancer* 2001; **4**: 175-184

11 **Tsujitani S**, Fukuda K, Saito H, Kondo A, Ikeguchi M, Maeta M, Kaibara N. The administration of hypotonic intraperitoneal cisplatin during operation as a treatment for the peritoneal dissemination of gastric cancer. *Surgery* 2002; **131**(1Suppl): S98-104

12 **Yu W**, Whang I, Chung HY, Averbach A, Sugarbaker PH. Indications for early postoperative intraperitoneal chemotherapy of advanced gastric cancer: results of a prospective randomized trial. *World J Surg* 2001; **25**: 985-990

13 **Ceelen WP**, Hesse U, de Hemptinne B, Pattyn P. Hyperthermic intraperitoneal chemoperfusion in the treatment of locally advanced intra-abdominal cancer. *Br J Surg* 2000; **87**: 1006-1015

14 **Fujimoto S**, Takahashi M, Mutou T, Kobayashi K, Toyosawa T. Successful intraperitoneal hyperthermic chemoperfusion for the prevention of postoperative peritoneal recurrence in patients with advanced gastric carcinoma. *Cancer* 1999; **85**: 529-534

15 **Sugarbaker PH**. Peritoneal carcinomatosis:natural history and rational therapeutic interventions using intraperitoneal chemotherapy. *Cancer Treat Res* 1996; **81**: 149-168

16 **Yu W**, Whang I, Averbach A, Chang D, Sugarbaker PH. Morbidity and mortality of early postoperative intraperitoneal chemotherapy as adjuvant therapy for gastric cancer. *Am Surg* 1998; **64**: 1104-1108

17 **Esquivel J**, Vidal-Jove J, Steves MA, Sugarbaker PH. Morbidity and mortality of cytoreductive surgery and intraperitoneal chemotherapy. *Surgery* 1993; **113**: 631-636

18 **Topuz E**, Basaran M, Saip P, Aydiner A, Argon A, Sakar B, Tas F, Uygun K, Bugra D, Aykan NF. Adjuvant intraperitoneal chemotherapy with cisplatinum,mitoxantrone,5-fluorouracil, and calcium folinate in patients with gastric cancer : a phase II study. *Am J Clin Oncol* 2002; **25**: 619-624

19 **Sakuragi N**, Nakajima A, Nomura E, Noro N, Yamada H, Yamamoto R, Fujimoto S. Complications relating to intraperitoneal administration of cisplatin or carboplatin for ovarian carcinoma. *Gynecol Oncol* 2000; **79**: 420-423

20 **Sugarbaker PH**. Intraperitoneal chemotherapy and cytor eductive surgery for the prevention and treatment of peritoneal carcinomatosis and sarcomatosis. *Semin Surg Oncol* 1998; **14**: 254-261

Edited by Wang XL **Proofread by** Xu FM

PO Box 2345, Beijing 100023, China
Fax: +86-10-85381893
E-mail: wjg@wjgnet.com www.wjgnet.com

World J Gastroenterol 2004;10(9):1375-1378
World Journal of Gastroenterology
Copyright ©2004 by The WJG Press ISSN 1007-9327

• BRIEF REPORTS •

Protective effect of doxorubicin induced heat shock protein 72 on cold preservation injury of rat livers

Hao Chen, Ying-Yan Yu, Ming-Jun Zhang, Xia-Xing Deng, Wei-Ping Yang, Jun Ji, Cheng-Hong Peng, Hong-Wei Li

Hao Chen, Xia-Xing Deng, Wei-Ping Yang, Cheng-Hong Peng, Hong-Wei Li, Department of Surgery and Center of Organ Transplantation, Ruijin Hospital, Shanghai Second Medical University, Shanghai 200025, China
Ying-Yan Yu, Jun Ji, Center of Organ Transplantation, Ruijin Hospital, Shanghai Second Medical University, Shanghai 200025, China
Ming-Jun Zhang, Animal Laboratory, Ruijin Hospital, Shanghai Second Medical University, Shanghai 200025, China
Correspondence to: Hao Chen, Department of Surgery and Center of Organ Transplantation, Ruijin Hospital, Shanghai Second Medical University, Shanghai 200025, China. chenhaodr@sohu.com
Telephone: +86-21-64370045 **Fax:** +86-21-64333548
Received: 2003-08-26 **Accepted:** 2003-10-22

Abstract

AIM: To observe the protective effect of heat shock protein 72 (HSP 72) induced by pretreatment of doxorubicin (DXR) on long-term cold preservation injury of rat livers.

METHODS: Sprague-Dawley rats were administered intravenously DXR at a dose of 1 mg/kg body mass in DXR group and saline in control group. After 48 h, the rat liver was perfused with cold Linger's and University of Wisconsin (UW) solutions and then was preserved in UW solution at 4 ℃ for 24, 36 and 48 h. AST, ALT, LDH and hyaluronic acid in preservative solution were determined. Routine HE, immunohistochemical staining for HSP 72 and electron microscopic examination of hepatic tissues were performed.

RESULTS: After 24, 36 and 48 h, the levels of AST, ALT and hyaluronic acid in preservative solution were significantly higher in control group than in DXR group ($P<0.05$), while LDH level was not significantly different between the 2 groups ($P>0.05$). Hepatic tissues in DXR group were morphologically normal and significantly injured in control group. HSP 72 was expressed in hepatocytes and sinusoidal endothelial cells in DXR group but not in control group.

CONCLUSION: Pretreatment of DXR may extend the time of rat liver cold preservation and keep liver alive. The expression of HSP 72 in liver can prevent hepatocytes and sinusoidal endothelial cells from long-term cold preservation injury.

Chen H, Yu YY, Zhang MJ, Deng XX, Yang WP, Ji J, Peng CH, Li HW. Protective effect of doxorubicin induced heat shock protein 72 on cold preservation injury of rat livers. *World J Gastroenterol* 2004; 10(9): 1375-1378
http://www.wjgnet.com/1007-9327/10/1375.asp

INTRODUCTION

The term of organ preservation has been extended enormously since Belzer invented University of Wisconsin (UW) solution in 1988[1]. In liver transplantation, the use of UW solution doubles the time of liver cold preservation compared with the use of Euro-Collins solution. But hepatic cold preservation reperfusion injury remains the important reason for the failure of liver transplantation[2-5]. It was reported that cold preservation reperfusion injury in liver, kidney and lung could be prevented by the expression of heat shock protein, which was induced by heat shock reaction (HSR)[6-8]. Kume *et al*[9] reported that doxorubicin (DXR) could induce HSR, which attenuated hepatic warm ischemia reperfusion injury. DXR is a kind of cytotoxic agent and may induce HSR[10]. Being administered intravenously, DXR was accumulated and metabolized in liver. As a result, semiquinone free radicals were produced, which could induce stress oxidative reaction and expression of HSP 72[11]. Hela cells and cardiac cells could express HSP 72 by pretreatment of DXR *in vitro* in experiments[12,13]. The aim of this study was to observe the protective effect of HSR induced by DXR on long-term hepatic cold preservation injury.

MATERIALS AND METHODS

Reagents

Doxorubicin was purchased from Shenzhen Main Luck Pharmaceuticals. Inc., China-Merian Corp., Japan. University of Wisconsin solution was purchased from Dupan Co., USA. HA RIA kit was purchased from Shanghai Ocean Research Biomedical Technology Center, China. Monoclonal antibody of HSP 72 was purchased from Oncogene Co. DAKO Envision™ kit was from Dako Co.

Animals

Male Sprague-Dawley rats weighing 200-300 g were purchased from Sino-British Sippr/BK Lab Animal Ltd. All rats were kept in animal quarters with controlled temperature (18-25 ℃) and light (light on from 7 a.m. to 7 p.m.) and were fed with a standard laboratory chow and water in accordance with institutional animal care policies. Prior to the experimental procedure, the rats were fasted for 12 hours but allowed free access to water.

Experimental design

Thirty-six rats were randomly assigned into DXR group and control group. The rats in DXR group were injected intravenously DXR at a dose of 1 mg/kg body mass 48 h before the operation[9], while those in control group were treated with 1 mL normal saline (NS). After being cold perfused orthotopically, the livers were preserved in UW solution for 24, 36 and 48 h.

Liver procurement and cold storage

Rat orthotopic liver cold perfusion was used according to the method described by Kamada and Calne[14]. Under ether anesthesia, 2 mL of heparinized saline solution (250 units/mL) was injected intravenously. Laparotomy was performed via a midline incision. After the abdominal aorta was cannulated with a 14-gauge angiocatheter, the liver was flushed with 10 mL of Linger's solution at 4 ℃. Simultaneously, the supra and infrahepatic vena cava were cut to enhance flushing of the liver. Then, 5 mL of Linger's solution, followed by 10 mL of

UW solution at 4 ℃ was progressively injected into portal vein. Finally the liver was excised and preserved in 40 mL of UW solution at 4 ℃.

Hepatic enzyme assays of preservative solution

Alanine aminotransferase (ALT), aspartate aminotransferase (AST) and lactic dehydrogenase level (LDH) in the preservative solutions, collected at 24, 36 and 48 h after cold preservation, were determined by a standard biochemistry autoanalyzer (Backman DU 640).

Assessment of hyaluronic acid (HA) of preservative solution

HA in the preservative solutions collected at 24, 36 and 48 h after cold preservation was determined using a HA RIA kit according to the manufacturer' s protocols.

Histology and immunohistochemical analysis for HSP 72

The liver specimens collected at 24, 36 and 48 h after cold preservation were fixed in buffered 10% formalin and embedded in paraffin. Tissue sections (4-μm thick) were stained with hematoxylin-eosin.

Immunohistochemical analysis was performed by using a mouse anti-HSP 72 monoclonal antibody at a dilution of 1:100, and rabbit anti-mouse IgG as a secondary antibody. Then the specimens were incubated with horseradish peroxidase-conjugated streptavidin complex. Diaminobenzidine was used as the substrate. The specimens were counterstained with hematoxylin. All specimens were examined under an optical microscope (Olympus BX51).

Transmission electron microscopical analysis

Liver fragments of approximately 1 mm×1 mm×2 mm were fixed in 20 g/L glutaraldehyde at 4 ℃. After washed in phosphate buffer solution, fragments were postfixed with 10 g/L osmium tetroxide, dehydrated in graded alcohols, replaced in epoxy ethane and stained with uranyl acetate. All specimens were examined under an electron microscope (Hitachi 500).

Statistical analysis

Values are expressed as mean±SE. Intragroup analysis was performed by paired Student' s *t* test. *P* value less than 0.05 was considered statistically significant.

RESULTS

ALT, AST and LDH level

ALT and AST levels were significantly higher in control group after preservation for 24, 36 and 48 h than in DXR group ($P<0.05$), but LDH level was not different between the 2 groups ($P>0.05$) (Table 1).

Table 1 Comparison of ALT, AST and LDH levels between two groups

Group	*n*	Term of storage	ALT (IU/L)	AST (IU/L)	LDH (IU/L)
Control	6	24 h	337.3±163.4[b]	417.2±247.5[a]	3 369.1±851.9[c]
	6	36 h	589.8±237.3[a]	744.5±317.6 [a]	3 623.2±907.1[c]
	6	48 h	713.3±191.8[a]	1 160.2±321.3 [a]	3 771.7±733.5[c]
DXR	6	24 h	140.5±58.5	148.8±110.6	3 162.5±1442
	6	36 h	347.3±89	340.5±139.4	3 468.7±815.7
	6	48 h	406.0±79	733.3±394.4	3 549.8±894.1

[a]$P<0.05$, [b]$P<0.01$, [c]$P>0.05$ *vs* DXR.

HA level

HA level was significantly higher in control group after preservation for 24, 36 and 48 h than in DXR group ($P<0.05$) (Table 2).

Table 2 Comparison of HA levels between two groups

Group	*n*	Term of storage	HA (ng/mL)
Control	6	24 h	43.1±17.0[a]
	6	36 h	91.2±19.8[b]
	6	48 h	143.7±23.2[a]
DXR	6	24 h	26.2±6.0
	6	36 h	44.2±7.8
	6	48 h	90.2±13.5

[a]$P<0.05$, [b]$P<0.01$ *vs* DXR.

Histology and immunohistochemistry for HSP 72

After cold storage for 24 to 48 h, hepatocytes in control group were swelling, ballooning, vacuolizing and partly autolyzing while the majority of sinusoidal endothelial cells (SECs) also became swollen, rounded and detached from basement membrane and hepatic sinusoids were narrowed. In DXR group, hepatocytes remained normal and few SECs appeared swollen, rounded or detached.

After cold storage for 24 to 48 h, some hepatocytes and SECs expressed HSP 72 in DXR group but not in control group.

Transmission electron microscopical analysis

After cold storage for 24 to 48 h, hepatocytes in control group showed swollen mitochondria, fatty dots, and while cellular swelling, rounding, detachment from the matrix and nuclear condensation were seen in part of SECs. In DXR group, hepatocytes remained normal and few SECs appeared swollen, rounded or detached.

DISCUSSION

The use of University of Wisconsin solution extended the time of organ cold preservation to 24 h in theory[15]. UW solution was designed to attenuate cell swelling, inhibit reactive oxygen intermediates (ROIs), offer substrates for synthesizing adenosine triphosphates (ATP) and prevent cells from absorbing ions of sodium and calcium[16,17]. But in the course of cold storage, cells remained to be injured in different degrees with the extension of preservation time. In the period of liver cold storage, hepatocytes and SECs were all injured, especially the latter[18,19].

During warm ischemia hepatocytes were the most vulnerable cells whereas SECs were less sensitive[20]. But hepatocytes were less damaged during cold preservation[21]. However, along with the extension of the time of cold storage, hepatocytes were also injured in different degrees. The mechanisms underlying hepatocyte injury during hypothermia storage were intracellular acidosis due to anaerobic glycolysis and lactate accumulation, drawback of protein synthesis and exhaustion of hepatin and ATP which lessen the ability to resist rewarm ischemia and reperfusion damage[21]. In morphology, changes of hepatocytes included swelling, ballooning and vacuolization. Although little loss of cell viability occurred after 24 h of storage in UW solution, the cellular functions were already injured[22]. In this study, histological results showed that hepatocytes were apparently damaged in control group after cold storage for 36 to 48 h. In contrast, the shapes of hepatocytes were normal in DXR group. In preservation solution, ALT and AST levels in DXR group were significantly lower than in control group ($P<0.05$). These data indicated that pretreatment with DXR could evidently protect hepatocytes.

During hepatic cold ischemia, SECs were most susceptible

to hypothermia injury. Injuries of SECs were due to angiogenic factors and proteases, resulting in digestion of fibronectin, a key molecule linking collagen to the sinusoidal lining cell membrane integrin[23]. In morphology, SECs became rounded, detached, and sloughed into the sinusoidal lumen[24-26]. These changes were more distinct along with the prolongation of cold storage[27]. But little loss of viability of SECs occurred after 24 h of storage in UW solution[28]. This study indicated that SECs in both groups were injured after 24 to 48 h of cold storage in UW solution, but the degree of injury was significantly attenuated in DXR group than in control group. The shape of SECs was normal after 24 h and a small quantity of SECs became rounded, and detached after 36 to 48 h in DXR group. But in control group, SECs were obviously rounded and detached after 24 h, and the morphological changes became more significant after 36 to 48 h. On the other hand, hyaluronic acid level was significantly higher in control group than in DXR group ($P<0.05$). Hyaluronic acid is a high-molecular-weight polysaccharide that could be rapidly and specifically degraded by SEC[29]. Hyaluronic acid level was a sensitive index of SECs' injury[30]. These results showed that pretreatment with DXR could protect SECs.

Cold storage of livers for more than 12 to 18 h carried the risk for graft failure[31-34] and post-transplantation infection[35]. In recent years, preconditioning has been used to prolong hepatic cold ischemia[6,36-38]. The liver graft was subjected to an acute sublethal stress and this preconditioning could offer resistance to subsequent lethal injury by inducing the expression of heat shock proteins (HSPs). One of the important functions of HSPs was to protect cells and organs from a wide variety of damages such as hypothermia, ischemia, and ROIs[39-41]. Cheng[42] reported that pretreated by Zinc and heat shock, the expression of HSP 72 was markedly elevated after rat livers were stored in UW solution for 24 h. It was also reported that rat kidneys were preserved well successively for 45 h in cold UW solution[43]. In our study, the protective effect of pretreatment of DXR on hepatic long-term cold storage injury might be attributed to induction of HSR and expression of HSP 72 in rat livers. HSR induced by DXR extended the time of hepatic cold storage to 48 h while morphological shape and functions of both hepatocytes and SECs remained commendable. The expressions of HSP 72 in hepatocytes and SECs were confirmed by immunohistochemical staining. It was clear that induction of HSP 72 in advance could make rat livers enter into stress state ahead of schedule and endure long-term cold ischemia injury afterwards.

In conclusion, these results demonstrate that pretreatment with doxorubicin could induce the expression of HSP 72 in rat livers. Thus pharmacological induction of HSR may be a successful method to prevent liver from long-term hypothermia preservation injury.

REFERENCES

1 **Belzer FO**, Kalayoglu M, D'Alessandro AM, Pirsch JD, Sollinger HW, Hoffmann R, Boudjema K, Southard JH. Organ preservation: experience with University of Wisconsin solution and plans for the future. *Clin Transplant* 1990; **4**: 73-77

2 **Bilzer M**, Gerbes AL. Preservation injury of the liver: mechanisms and novel therapeutic strategies. *J Hepatol* 2000; **32**: 508-515

3 **Jaeschke H**. Molecular mechanisms of hepatic ischemia-reperfusion injury and preconditioning. *Am J Physiol Gastrointest Liver Physiol* 2003; **284**: G15-26

4 **Serracino-Inglott F**, Habib NA, Mathie RT. Hepatic ischemia-reperfusion injury. *Am J Surg* 2001; **181**: 160-166

5 **Kang KJ**. Mechanism of hepatic ischemia/reperfusion injury and protection against reperfusion injury. *Transplant Proc* 2002; **34**: 2659-2661

6 **Redaelli CA**, Tian YH, Schaffner T, Ledermann M, Baer HU, Dufour JF. Extended preservation of rat liver graft by induction of heme oxygenase-1. *Hepatology* 2002; **35**: 1082-1092

7 **Wagner M**, Cadetg P, Ruf R, Mazzucchelli L, Ferrari P, Redaelli CA. Heme oxygenase-1 attenuates ischemia/reperfusion induced apoptosis and improves survival in rat renal allografts. *Kidney Int* 2003; **63**: 1564-1573

8 **Hiratsuka M**, Yano M, Mora BN, Nagahiro I, Cooper JD, Patterson GA. Heat shock pretreatment protects pulmonary isografts from subsequent ischemia-reperfusion injury. *J Heart Lung Transplant* 1998; **17**: 1238-1246

9 **Kume M**, Yamamoto Y, Yamagami K, Ishikawa Y, Uchinami H, Yamaoka Y. Pharmacological hepatic preconditioning: involvement of 70-kDa heat shock proteins (HSP72 and HSP73) in ischaemic tolerance after intravenous administration of doxorubicin. *Br J Surg* 2000; **87**: 1168-1175

10 **Yee SB**, Pritsos CA. Comparison of oxygen radical generation from the reductive activation of doxorubicin, streptonigrin, and menadione by xanthine oxidase and xanthine dehydrogenase. *Arch Biochem Biophys* 1997; **347**: 235-241

11 **Trost LC**, Wallace KB. Stimulation of myoglobin-dependent lipid peroxidation by adriamycin. *Biochem Biophys Res Commun* 1994; **204**: 23-29

12 **Lee EK**, Regenold WT, Shapiro P. Inhibition of aldose reductase enhances HeLa cell sensitivity to chemotherapeutic drugs and involves activation of extracellular signal-regulated kinases. *Anticancer Drugs* 2002; **13**: 859-868

13 **Huber SA**. Heat-shock protein induction in adriamycin and picornavirus-infected cardiocytes. *Lab Invest* 1992; **67**: 218-224

14 **Kamada N**, Calne RY, Wight DG, Lines JG. Orthotopic rat liver transplantation after long-term preservation by continuous perfusion with fluorocarbon emulsion. *Transplantation* 1980; **30**: 43-48

15 **Belzer FO**, Southard JH. Principles of solid-organ preservation by cold storage. *Transplantation* 1988; **45**: 673-676

16 **Lemasters JJ**, Thurman RG. Reperfusion injury after liver preservation for transplantation. *Annu Rev Pharmacol Toxicol* 1997; **37**: 327-338

17 **Southard JH**, van Gulik TM, Ametani MS, Vreugdenhil PK, Lindell SL, Pienaar BL, Belzer FO. Important components of the UW solution. *Transplantation* 1990; **49**: 251-257

18 **Urata K**, Nguyen B, Brault A, Lavoie J, Rocheleau B, Huet PM. Decreased survival in rat liver transplantation with extended cold preservation: role of portal vein clamping time. *Hepatology* 1998; **28**: 366-373

19 **Otto G**, Wolff H, David H. Preservation damage in liver transplantation: electron-microscopic findings. *Transplant Proc* 1984; **16**: 1247-1248

20 **Noack K**, Bronk SF, Kato A, Gores GJ. The greater vulnerability of bile duct cells to reoxygenation injury than anoxia. Implications for the pathogenesis of biliary strictures after liver transplantation. *Transplantation* 1993; **56**: 495-500

21 **Clavien PA**, Harvey PR, Strasberg SM. Preservation and reperfusion injuries in liver allografts. An overview and synthesis of current studies. *Transplantation* 1992; **53**: 957-978

22 **Lichtman SN**, Lemasters JJ. Role of cytokines and cytokine-producing cells in reperfusion injury to the liver. *Semin Liver Dis* 1999; **19**: 171-187

23 **Upadhya AG**, Harvey RP, Howard TK, Lowell JA, Shenoy S, Strasberg SM. Evidence of a role for matrix metalloproteinases in cold preservation injury of the liver in humans and in the rat. *Hepatology* 1997; **26**: 922-928

24 **McKeown CM**, Edwards V, Phillips MJ, Harvey PR, Petrunka CN, Strasberg SM. Sinusoidal lining cell damage: the critical injury in cold preservation of liver allografts in the rat. *Transplantation* 1988; **46**: 178-191

25 **Hansen TN**, Dawson PE, Brockbank KG. Effects of hypothermia upon endothelial cells: mechanisms and clinical importance. *Cryobiology* 1994; **31**: 101-106

26 **Marsh DC**, Lindell SL, Fox LE, Belzer FO, Southard JH. Hypothermic preservation of hepatocytes. Role of cell swelling. *Cryobiology* 1989; **26**: 524-534

27 **Fratte S**, Gendrault JL, Steffan AM, Kirn A. Comparative ultrastructural study of rat livers preserved in Euro-Collins or Uni-

versity of Wisconsin solution. *Hepatology* 1991; **13**: 1173-1180
28 **Clavien PA**. Sinusoidal endothelial cell injury during hepatic preservation and reperfusion. *Hepatology* 1998; **28**: 281-285
29 **Laurent TC**, Fraser JR, Pertoft H, Smedsrod B. Binding of hyaluronate and chondroitin sulphate to liver endothelial cells. *Biochem J* 1986; **234**: 653-658
30 **Reinders ME**, van Wagensveld BA, van Gulik TM, Frederiks WM, Chamuleau RA, Endert E, Klopper PJ. Hyaluronic acid uptake in the assessment of sinusoidal endothelial cell damage after cold storage and normothermic reperfusion of rat livers. *Transpl Int* 1996; **9**: 446-453
31 **Figueras J**, Busquets J, Grande L, Jaurrieta E, Perez-Ferreiroa J, Mir J, Margarit C, Lopez P, Vazquez J, Casanova D, Bernardos A, De-Vicente E, Parrilla P, Ramon JM, Bou R. The deleterious effect of donor high plasma sodium and extended preservation in liver transplantation. A multivariate analysis. *Transplantation* 1996; **61**: 410-413
32 **Ploeg RJ**, D'Alessandro AM, Knechtle SJ, Stegall MD, Pirsch JD, Hoffmann RM, Sasaki T, Sollinger HW, Belzer FO, Kalayoglu M. Risk factors for primary dysfunction after liver transplantation-a multivariate analysis. *Transplantation* 1993; **55**: 807-813
33 **Furukawa H**, Todo S, Imventarza O, Casavilla A, Wu YM, Scotti-Foglieni C, Broznick B, Bryant J, Day R, Starzl TE. Effect of cold ischemia time on the early outcome of human hepatic allografts preserved with UW solution. *Transplantation* 1991; **51**: 1000-1004
34 **Adam R**, Bismuth H, Diamond T, Ducot B, Morino M, Astarcioglu I, Johann M, Azoulay D, Chiche L, Bao YM. Effect of extended cold ischaemia with UW solution on graft function after liver transplantation. *Lancet* 1992; **340**: 1373-1376
35 **Nuno J**, Cuervas-Mons V, Vicente E, Turrion V, Pereira F, Mora NP, Barrios C, Millan I, Ardaiz J. Prolonged graft cold ischemia: a risk factor for early bacterial and fungal infection in liver transplant recipients. *Transplant Proc* 1995; **27**: 2323-2325
36 **Takahashi Y**, Tamaki T, Tanaka M, Konoeda Y, Kawamura A, Katori M, Kakita A. Efficacy of heat-shock proteins induced by severe fasting to protect rat livers preserved for 72 hours from cold ischemia / reperfusion injury. *Transplant Proc* 1998; **30**: 3700-3702
37 **Kiemer AK**, Gerbes AL, Bilzer M, Vollmar AM. The atrial natriuretic peptide and cGMP: novel activators of the heat shock response in rat livers. *Hepatology* 2002; **35**: 88-94
38 **Kiemer AK**, Kulhanek-Heinze S, Gerwig T, Gerbes Vollmar AM. Stimulation of p38 MAPK by hormonal preconditioning with atrial natriuretic peptide. *World J Gastroenterol* 2002; **8**: 707-711
39 **Leppa S**, Sistonen L. Heat shock response–pathophysiological implications. *Ann Med* 1997; **29**: 73-78
40 **Morimoto RI**, Santoro MG. Stress-inducible responses and heat shock proteins: new pharmacologic targets for cytoprotection. *Nat Biotechnol* 1998; **16**: 833-838
41 **Santoro MG**. Heat shock factors and the control of the stress response. *Biochem Pharmacol* 2000; **59**: 55-63
42 **Cheng Y**, Liu Y, Liang J. Zinc is a potent heat shock protein inducer during liver cold preservation in rats. *Chin Med J* 2002; **115**: 1777-1779
43 **Redaelli CA**, Tien YH, Kubulus D, Mazzucchelli L, Schilling MK, Wagner AC. Hyperthermia preconditioning induces renal heat shock protein expression, improves cold ischemia tolerance, kidney graft function and survival in rats. *Nephron* 2002; **90**: 489-497

Edited by Zhu LH and Wang XL **Proofread by** Xu FM

PO Box 2345, Beijing 100023, China
Fax: +86-10-85381893
E-mail: wjg@wjgnet.com www.wjgnet.com

World J Gastroenterol 2004;10(9):1379-1381
World Journal of Gastroenterology
Copyright ©2004 by The WJG Press ISSN 1007-9327

• BRIEF REPORTS •

Evaluation of effect of hybrid bioartificial liver using end-stage liver disease model

Qing Liu, Zhong-Ping Duan, Chun Huang, Chun-Hui Zhao

Qing Liu, Zhong-Ping Duan, Chun Huang, Chun-Hui Zhao, Artificial Liver Treatment and Training Center, Beijing Youan Hospital, Beijing 100054, China
Correspondence to: Qing Liu, Artificial Liver Treatment and Training Center, Beijing Youan Hospital, Beijing 100054, China. lqlq8@yahoo.com
Telephone: +86-10-63292211-2517
Received: 2002-08-06 **Accepted:** 2002-11-04

Abstract

AIM: To study the role of hybrid bioartificial liver (HBL) in clearing proinflammatory cytokines and endotoxin in patients with acute and sub-acute liver failure and the effects of HBL on systemic inflammatory syndrome (SIRS) and multiple organ dysfunction syndrome (MODS).

METHODS: Five cases with severe liver failure (3 acute and 2 subacute) were treated with HBL. The clinical signs and symptoms, total bilirubin (TBIL), serum ammonia, endotoxin TNF-α, IL-6 and prothrombin activity (PTA), cholinesterase (CHE) were recorded before, during and after treatment. The end-stage liver disease (MELD) was used for the study.

RESULTS: Two patients were bridged for spontaneous recovery and 1 patient was bridged for OLT successfully. Another 2 patients died on d 8 and d 21. The spontaneous recovery rate was 30.0%. PTA and CHE in all patients were significantly increased ($P<0.01$), while the serum TBIL, endotoxin,TNF-α, IL-6 were decreased. MELD score (mean 43.6) predicted 100% deaths within 3 mo before treatment with HBL. After treatment with HBL, four out of 5 patients had decreased MELD scores (mean 36.6). The MELD score predicted 66% mortalities.

CONCLUSION: The proinflammatory cytokines (TNFα, IL-6 and endotoxin)can be significantly removed by hybrid bioartificial liver and HBL appears to be effective in blocking SIRS and MODS in patients with acute and sub-acute liver failure. MELD is a reliable measure for predicting short-term mortality risk in patients with end-stage liver disease. The prognostic result also corresponds to clinical outcome.

Liu Q, Duan ZP, Huang C, Zhao CH. Evaluation of effect of hybrid bioartificial liver using end-stage liver disease model. *World J Gastroenterol* 2004; 10(9): 1379-1381
http://www.wjgnet.com/1007-9327/10/1379.asp

INTRODUCTION

About 80% ICU deaths may be attributable to progressive multiple organ dysfunction (MODS). MODS is also a major cause of death in patients suffering from severe hepatitis. The sequela of systemic inflammatory syndrome (SIRS) is MODS. Hybrid bioartificial liver (HBL) is a well-known liver support system that is close to native liver in function. In the present study our primary goals were to investigate the role of HBL in removing serum proinflammatory cytokines such as TNFa, IL-6, endotoxin and in blocking SIRS to MODS.

In this report, we used the validity of end-stage liver disease model as a disease severity index for patients with end-stage liver disease treated with bioartificial liver support system. The model was considered to be able to provide a reliable estimate of short-term survival over a wide range of liver diseases.

MATERIALS AND METHODS

Subjects

The Beijing Youan Hospital Ethics Committee approved the study and informed consent was obtained from all patients or their relatives. Five patients with severe hepatitis treated with HBL in our center from March, 2000 to June 2001 were involved in the study. Three of 5 patients were acute severe hepatitis and 2 of them were sub-acute hepatitis. All the 5 patients suffered from SIRS, 4 of them were complicated with 2-organ failure and only one patient were with 3-organ failure (Table 1). The criteria for severe hepatitis, SIRS and MODS were based on the recommendations of references 1-3[1-3].

HBL

HBL system consists of a bioreactor (Microgn1nc, Laguna Hills, CA with a pore size 0.2 μm, total fiber internal surface area 6 000 cm^2, external surface area 7 000 cm^2, volume 200 mL loaded with fresh isolated hepatocytes ($2\text{-}4\times10^{10}$), a single-use plasma circuit,and a machine to control the fluid flow through these components. At first, plasma exchange was achieved by a membrane separation method (PLASAUTO-IQ, Asahi, Tokyo). The amount of plasma removal was set at 3 000 mL. In the following HBL treatment (SYBIOL, U.S.A), patients' plasma was separated using a plasma separation system (COBE-Spectra,Lakewood,CO) and was then perfused through an HBL system. The plasma was separated at a rate of 70-100 mL/min and perfused through the bioreactor at a rate of 28-30 mL/min; flow rate of porcine cell suspension was 60 mL/min. After exchange of patients' plasma with porcine cells across the hollow-fiber membranes, patients' blood was returned to the superficial femoral vein. Evaluation of the viability of hepatocytes in circuit of porcine liver cells was done by cell membrane exclusion of trypan blue dye.

Clinical assessments

All patients were managed in a specialized intensive care unit and received standard supportive care. The following parameters were monitored before, during and after treatment: vital signs (blood pressure, heart rate, breath rate and SaO_2), hemodynamics (mean artery pressure, central venous pressure) and urinary output. Liver biochemistry (bilirubin, transaminases, Creatinine, BUN, serum ammonia, prothrombin activity (PTA)), cytokines TNTa, IL-6 (ELISA, Bangding Co) and endotoxin were analysed. The mental state of hepatic encephalopathy was graded into five stages. When the patients regained consciousness or hepatic encephalopathy decreased by I stage, the treatments was considered as effective.

MELD score assessment system

According to Kamath *et al.*, the score was multiplied by 10 and then rounded to the nearest integer. The formula for the MELD scores $3.8*\log_e$(bilirubin[mg/dL])+$11.2*\log_e$(INR)+$9.6*\log_e$ (creatinine[mg/dL]. We used on-line available worksheet to compute MELD scores (www.mayo.edu/int-med/gi/model/mayomodl.htm).

Statistical analysis

Statistical comparisons were carried out using chi-square and Student *t*-tests. A *P* value <0.05 was considered statistically significant.

RESULTS

Patients ‘response to treatment

All treatments were completed as scheduled. Each treatment lasted for 8-10 h and all were well tolerated. All patients remained hemodynamically stable throughout the treatment period. No gastrointestinal coagulopathy, fever, allergy and other severe adverse reactions were observed.

HBL treatment outcome

Gastrointestinal symptoms such as anorexia, nausea and fatigue were sighificantly improved in 4 out of 5 patients Three patients who suffered from hepatic encephalopathy (HE) experienced remarkable neurological improvement with reversal of the decerebrate state after HBL treatment. Two of 3 HE at grades III and II became respectively grades II and I, another one at grade IV regained consciousness. Four patients who were complicated with 2- organ failure recovered spontaneously, one died 8 and 21 d after HBL treatment. The patient who was complicated with 3-organ failure (liver, cardiovascular, and gastrointestinal coagulopathy) was successfully bridged until an organ became available for orthotopic liver transplantation 1 wk after HBL treatment. The spontaneous recovery rate was 40.0%.

The treatment with the PE lowered TBIL in all patients (from 23.08±12.50 mg/dL to 12.34±4.39 mg/dL). At the end of treatment TBIL was reduced about 50%. Post evaluation showed that TBIL had a significant difference before and after HBL treatment at 0, 24 and 72 h (P<0.05). No statistically significant improvement in albumin and blood ammonia levels noted (P<0.05). CHE and PTA were significantly increased in all patients at 0, 24, 72 h and at the end of HBL treatment (P<0.05-0.01). The serum chemistry changes are shown in Table 2.

A significant decrease in serum endotoxin levels was observed by the end of PE (P<0.05) and it was declined during the period of HBL treatment. By the end of HBL, endotoxin level was the lowest (P<0.001). TNF-α and IL-6 were reduced rapidly, the clearance rate of TNF-α was approximately 45% and IL-6 was 55% (P<0.001) (Figure 1).

Evaluation of effect of HBL with MELD

MELD was used for predicting the outcome of HBL before and after treatment (Table 3).

Table 1 General data of patients

No	Sex	Age(yr)	Diagnosis	Multi-organs failure	Outcome
1	Female	43	ALF, HBV	Liver, brain	Spontaneous recovery
2	Male	31	SALF, HBV	Liver, brain	Recovery spontaneous
3	Male	33	SALF, HBV and alcoholic liver disease	Liver, coagulopathy, cardiovascular	Orthotopic liver transplantation
4	Female	27	ALF, drug induced liver injury	Liver, brain	Death
5	Male	31	ALF, HBV	Liver, kidney	Death

ALF: acute liver failure, SALF: sub-acute liver failure, HBV: hepatitis B virus.

Table 2 Changes of partial biochemical indices pre- and post-treatment of HBL(mean±SD)

Item	TBIL (mg/dL)	NH_3(μg/dL)	ALB (g/L)	CHE (U/L)	PTA%
Pre-treatment	23.08±12.50	116.6±23.1	29.79±4.35	3 801.5±1710.6	17.25±10.11
Post-treatment at 0 h	12.34±4.39[b]	98.3±19.5	32.57±4.76	5 560.9±1067.6[a]	38.60±10.25[b]
Post-treatment at 24 h	14.10±6.08[b]	103.2±23.5	33.13±4.34	5 438.5±1024.3[a]	34.31±11.75[a]
Post-treatment at 72 h	17.24±8.34[a]	110.8±30.6	31.42±4.07	5 676.2±957.9[a]	35.20±9.78[b]

[a]P<0.05, [b]P<0.01, *vs* pre-treatment, TBIL: total bilirubin, NH_3: serum ammonia, ALB: albumin, CHE: cholinesterase, PTA: prothrombin activity.

Table 3 Changes of MELD score before and after treatment of HBL

Patients	Before-treatment						After-treatment					
	1	2	3	4	5	(mean± SD)	1	2	3	4	5	(mean±SD)
PTA%	22.4	21	18	11	14.37	17.35±4.7	40.2	43	45	30.1	18.2	35.3±20.87
INR	2.42	2.51	2.61	4.14	3.74	3.08±1.27	1.58	1.55	1.50	2.08	2.71	1.8±1.02
Creatinine (mg/dL)	13	16.9	7.9	16.6	42.4	19.36±15.3	5.9	5.0	4.3	8.9	35.2	11.8±13.1
Bilirubin (mg/dL)	20.4	17	15.1	22.2	40.46	23.03±10.1	20.4	17	15.1	22.2	40.46	17.4±12.66
MELD	41	41	41	47	48	43.6	34	33	32	39	45	33.6

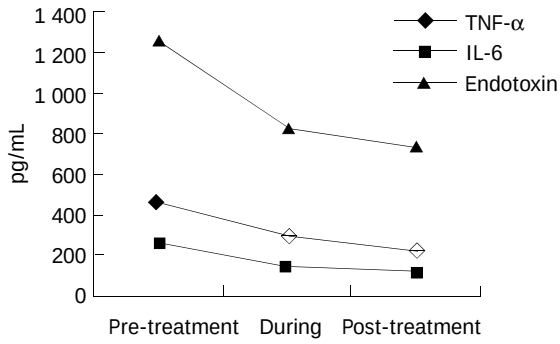

Figure 1 Change of cytokines and LPS in different points.

DISCUSSION

In the present study we demonstrated that the patients with severe hepatitis and hepatic failure might benefit from HBL for temporary liver support. HBL could maintain patients with hepatic failure alive, neurologically intact and metabolic state improved until a donor organ was available[4]. It could also allow the native liver to regenerate, thus avoiding liver transplantation. The study showed that TNF-α and IL-6 were reduced rapidly about 45% and 55% (P<0.001) after HBL treatment. The alteration of serum endotoxin levels was similar to TNFa and IL-6. Four of 5 patients responded to HBL treatment and 3 of them survived. Since the case number was limited, there were not enough data in our study to show that HBL could improve the survival rate of patients with multiple organ dysfunction. However the beneficial effect of HBL on the systemic concentration of cytokines was definite and the efficacy was not reached by drug treatment in such a short period. Just as Stephen described[5,6], a success liver support device was likely to depend on their ability to modify factors influencing liver cell death and regeneration and on the extent to which multi-organ failure could be prevented or reversed. Hybrid liver support devices replace the lost liver function through a combination of mechanical and biologic effects Mechanical parts use activated charcoal or plasma exchange before the hepatocyte bioreactor, which may not only provide a "protective" effect on the porcine hepatocytes from possible toxic effect of hepatic failure plasma, but also strengthen the effect of plasma detoxification. HBL treatment could remarkably improve SIRS signs and symptoms. Also it slowed down the progression from SIRS to MODS and protected MODS from further deterioration.

The mechanism of HBL to block the progression from SIRS to MDOS was to support failed liver. In our study, It was observed that CHE and PTA were significantly increased in all patients at 0, 24 and 72 h after HBL treatment (P<0.05-0.01). Plasma cholinesterase, an enzyme with a short half-life, is not usually changed by the substitution of clotting factors or by freshly frozen plasma and therefore is a good parameter of synthesis. Increased cholinesterase level in plasma may reflect improvement of liver synthesis function. The metabolic ability of liver for various nervous toxicity implicates liver detoxification function. Similar to the previous report, 3 patients with hepatic encephalopathy were improved by HBL treatment in our study, but it was different from previous report, in that the blood ammonia levels were not changed after HBL treatment. Impairment of central nervous system in hepatic encephalopathy is probably multifactorial in origin. Except ammonia, other neuroexcitatory factors like amino acid imbalance, mercaptans, phenols, fatty acids, GABA, and benzodiazepine, also play a role in hepatic encephalopathy. Therefore consciousness improvement may cause removal of other neuroexcitatory factors. There are two mechanisms blocking the progression from SIRS to MODS related to liver function improvement. First, liver is an amplifier of the systemic acute-phase reaction, proinflammatory cytokines enter the liver through the portal vein, eventually passing the smallest functional unit of the liver, the acnus. The special architecture of sinusoids ensures that cytokines in the liver primarily reach the nonparenchymal liver cells such as endothelial cells and kupffer cells. Because these cells express not only receptors of IL-1β, TNF-α and IL6, but also modulators of cytokines[7]. Also the most active cells howe the potential for the systemic response to the intrahepatic release of inflammatory cytokines. They might function as intrahepatic amplifiers of the systemic acute-phase reaction by liberating a second wave of proinflammatory cytokines which could enhance the effect of injuring agents and accelerate or maintain development of liver fibrosis[8]. Second, it has been found that LBP/CD14 is an endotoxin strengthening system. LBP is produced in liver. When under stress the production of LBP from liver would increase many times. Trace endotoxin binding to LBP and interacting with target cells would increase the sensitivity of target cells to endotoxin up to10 000 times and stimulate the synthesis and secretion of a large number of proinflammatory cytokines, mainly IL1B and TNFa[8]. Therefore the improvement in liver function is the basis for decreasing proinflammatory cytokine levels.

MELD is a reliable measure and predictive of short-term mortality risk in patients with end-stage liver disease[9].

REFERENCES

1 Fifth conference of national contagious disease and parasitic disease Guideline: prevention and treatment of virus hepatitis (draft). *Zhonghua Neike Zazhi* 1995; **34**: 788-791

2 **Qiu HB**, Zhou SX, Yang Y. Multiple organ dysfunction syndrom predictors of mortality and clinical therapetic strategies. *Linchuang Jjijiuy Yixue* 2001; **10**: 13-16

3 **Fry DE**, Pearlstein L, Fulton RL. Multiple system organ failure: the role of uncontrolled infection. *Arch Surg* 1980; **115**: 136-139

4 **Xue YL**, Zhao SF, Zhang ZY. Effects of bioartificial liver suppport system on acetaminophen-induced acute liver failure canines. *World J Gastroenterol* 1999; **5**: 308-311

5 **Zimminerman JE,** Knauus WA, Sun X, Wagner DP. Severity stratification and outcome prediction for multisystem organ failure and dysfunction. *World J Surg* 1996; **20**: 401-409

6 **Riordan SM**, Williams R. Acute liver failure: targeted artificial and hepatocyte-based support of liver regeneration and reversal of multiorgan failure. *J Hepatol* 2000; **32**(Suppl 1): 63-67

7 **Ramadori G**, Christ B. Cytokines and the hepatic acute-phase response. *Seminars In Liver Disease* 1999; **19**: 141-156

8 **Stange J**, Mitzner SR, Risler T. Molecular adsorbent recycling system: Clinical results of a new membrane- based blood purification system for bioartifical liver support. *Artificial Organs* 1999; **23**: 319-330

9 **Kamath PS**, Wiesner RH, Malinchoc M. A Model to predict survival n patients with end-stage Liver disease. *Hepatology* 2001; **33:** 467-470

Edited by Wang XL and Zhu LH **Proofread by** Xu FM

PO Box 2345, Beijing 100023, China
Fax: +86-10-85381893
E-mail: wjg@wjgnet.com www.wjgnet.com

World J Gastroenterol 2004;10(9):1382-1385
World Journal of Gastroenterology
Copyright ©2004 by The WJG Press ISSN 1007-9327

• BRIEF REPORTS •

Expression and significance of angiopoietin-2 in gastric cancer

Xiao-Dong Sun, Xing-E Liu, Jin-Min Wu, Xiu-Jun Cai, Yi-Ping Mou, Jun-Da Li

Xiao-Dong Sun, Xiu-Jun Cai, Yi-Ping Mou, Jun-Da Li, Department of General Surgery, the Affiliated Sir Run Run Shaw Hospital, Medical College, Zhejiang University, Hangzhou 310016, Zhejiang Province, China
Xing-E Liu, Jin-Min Wu, Center of Oncology, the Affiliated Sir Run Run Shaw Hospital, Medical College, Zhejiang University, Hangzhou 310016, Zhejiang Province, China
Correspondence to: Dr. Xiao-Dong Sun, Department of General Surgery, the Affiliated Sir Run Run Shaw Hospital, Medical College, Zhejiang University, Hangzhou 310016, Zhejiang Province, China. s.xiaodong@sohu.com
Telephone: +86-571-86090073 **Fax:** +86-571-86044817
Received: 2003-09-18 **Accepted:** 2003-10-12

Abstract

AIM: To investigate the expression and pathological factors of Angiopoietin-2 (Ang-2) in primary gastric cancers and adjacent normal tissues.

METHODS: The expression of Angiopoietin-2 and VEGF were studied in 72 primary gastric cancers and adjacent normal tissues from the same patients by semi-quantitative reverse transcriptase-polymerase chain reaction (RT-PCR) and immumohistochemistry.

RESULTS: Ang-2 was mainly expression in tumor cells. There were significantly difference between expression of Ang-2 in primary gastric cancer and in adjacent normal tissue samples (P=0.003). It was statistically correlation between Ang-2 and VEGF expression in tumors (P=0.0055). With regard to Ang-2 expression in tumors, there were significant difference between early stage and advanced stage (P=0.017), and significant difference between positive vascular involvement and negative vascular involvement (P=0.032). However, there was no significant difference between moderate-poor differential type and high differential type (P=0.908), between positive lymph node metastasis and negative lymph node metastasis (P=0.752), between positive serosal invasion and negative serosal invasion (P=0.764). The cases with expression of Ang-2 were increasing with advanced stage and vascular involvement.

CONCLUSION: The results manifested that Angiopoietin-2, coordinated with VEGF, play role in regulating tumor angiogenesis of gastric cancer.

Sun XD, Liu XE, Wu JM, Cai XJ, Mou YP, Li JD. Expression and significance of angiopoietin-2 in gastric cancer. *World J Gastroenterol* 2004; 10(9): 1382-1385
http://www.wjgnet.com/1007-9327/10/1382.asp

INTRODUCTION

Angiogenesis is required for the growth and metastasis of malignant tumor, and is defined as the sprouting of blood vessels from pre-existing vessels that migrate into the tumor and form a new vascular network. Many factors attend the process of angiogenesis. Recently, several studies have shown that, the expression of angiopoietin-2 (Ang-2) probably correlates to tumor angiogenesis[1,2]. However, the role and mechanism of Ang-2 in tumor angiogenesis still remain to be determined. Here, we investigate the expression and significance of angiopoietin-2 in gastric cancer.

MATERIALS AND METHODS

Materials

Reagents Trizol liquid, AMV reverse transcriptase, Oligd(T)$_{14}$, RNAsin, dNTP, Taq DNA polymerase were purchased from shanghai sangon biological engineering technology and service co.Ltd, PCR primers were synthesized by shanghai sangon biological engineering technology and service co.Ltd. N-18 and P-20, the monoclonal antibodies of Ang-2 and VEGF respectively, were purchased from santa cruz company.

Clinical data Total of 72 patients with respectable primary gastric cancer were analysed. There were 46 males and 26 females with primary gastric cancer. Age varied from 38 to 72 years, with a mean age of 53.5 years. Routine pathological diagnosis showed that 53 cases were adenocarcinoma, 19 cases were signet carcinoma. Of these 72 patients, 48 individuals had lymph nodes metastasis, and 26 others had no lymph node metastasis.

Methods

Detection of expression of Ang-2 AND VEGF Expressions of Ang-2 and VEGF were assessed in every gastric cancer sample and its adjacent normal tissue by semi-quantitative RT-PCR.

RNA extraction Total RNA was extracted by Trizol one step procedure, and suspended in DEPC-treated reverse osmosis-H_2O, and conserved at -70 ℃ for reverse transcription. RNA yield and purity were determined by standard UV spectrophotometric assay. The ratio of A_{260}/A_{280} is 1.80.

First strand cDNA synthesis A 5 μg of the total RNA was dissolved in 20 μL of a mixture containing 2 μL of 10× first-strand buffer, 20 μL of AMV reverse transcriptase, 2 μL of dNTP, 20 μL of RNAsin, 500 ng of Oligd(T)$_{14}$, and DEPC-treated reverse osmosis-H_2O. The reaction conditions were as following: at 42 ℃ for 60 min, at 95 ℃ for 5 min. The first strand cDNA was stored at -20 ℃ until use.

PCR amplification Primers of Ang-2, VEGF and β-actin were synthesized according to primer design principles, all primer sets used span an intron to control amplification of genomic DNA sequences. A 3 μL of the first strand cDNA were amplified in 20 μL volume. The primers of Ang-2 were yielded 921-bp product and as following: 5' -end primer: 5' -GGGGGAGGACTG GTGACAGCCACGG-3' ,3' -endprimer:5' -GAAATCTGCTGGC CGGATCATCAT-3' . Following an initial denaturation at 94 ℃ for 5 min, the samples were amplified by 30 cycles of denaturation at 94 ℃ for 30 s, annealing at 58 ℃ for 30 s, extension at 72 ℃ for 30 s, and ended by extension at 72 ℃ for 10 min. The primers of VEGF were yielded 356-bp product and as following: 5' -end primer: 5' -ACCATGAACTTTCTGCTCTCTTGG-3' , 3' -end primer:5' -CCGCCTTGGCTTGTCACATCTGCA-3' .Following an initial denaturation at 94 ℃ for 5 min, the samples were amplified by 28 cycles of denaturation at 94 ℃ for 30 s, annealing at 58 ℃ for 1 min, extension at 72 ℃ for 1 min, and ended by extension at 72 ℃ for 10 min. The primers of β-actin, which was

amplified with Ang-2 and VEGF as internal control, were yielded 644 bp product and as following: 5' -end primer: 5' -ACGTTATG GATGATGATATCGC-3' ,3' -end primer: 5' -CTTAATGTCACG CACGATTTCC-3' . PCR products were separated on 1.7% agarose gel , stained with ethidium bromide, and analysed with Quantity one 4.1.0 software. The ratios of Ang-2/β-actin, AEGF/β-actin were used to semiquantify the levels of Ang-2 and VEGF.

Immunohistochemical staining The immunohistochemical study of expression of Ang-2 and VEGF in gastric cancer and adjacent normal tissue was performed by the avidin-biotin-peroxidase technique using monoclonal antibody N-18 and P-20, as previously described[3,4]. Briefly, after formaldehyde-fixed paraffin-embedded tissue sections were deparaffinized in xylene and rehydrated in alcohol, they were incubated in 3 mL/L H_2O_2 to block endogeneous peroxidase activity. Each slide was incubated with normal horse serum for 20 min at room temperature, and then monoclonal antibody N-18 or P-20, the working dilution were 1:100 and 1:200 respectively, was incubated on the tissue section overnight at 4 ℃. After incubated in biotinylated mouse anti-goat IgG (the working dilution were 1:200) for 30 min at room temperature, each slide was rinsed in phosphate-buffered saline and was incubated in the avidin-biotin peroxidase complex for 40 min at 37 ℃. The peroxidase was visualized with 3-3' -diamino-benzidine-tetrahydrochloride solution and then counterstained with methyl green.

Expressions of Ang-2 and VEGF in primary gastric cancers and adjacent normal tissues were detected under microscopy.

Statistical analysis Results are calculated as mean±SD for each group. *t* test groups or *chisq* test was used to analyze the variables. Statistical analyses were performed with SPSS software, version 10.0.

RESULTS

Results of RT-PCR

Seventy-two primary gastric cancers and adjacent normal tissues from the same patients were examined for the expression of Ang-2 and VEGF by RT-PCR. In 72 cases of primary tumors, Ang-2 and VEGF were expressed in 46 (63.9%) and 48 cases (66.7%) respectively. However , in 72 adjacent normal samples, Ang-2 and VEGF were expressed in 10 (13.9%) and 16 (22.2%) respectively. The expression of Ang-2 in primary gastric cancer has significant differences from that in adjacent normal tissues (P=0.003), (Figure 1, Table 1).

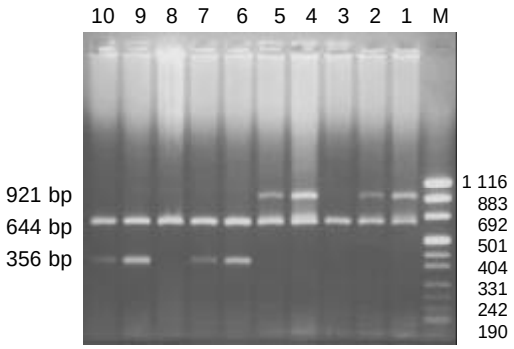

Figure 1 Semi-quantitative RT-PCR amplified products of Ang-2 and VEGF in primary gastric cancer and adjacent normal tissue 644 bp: internal standards, 921 bp: Ang-2 expression, 365 bp: VEGF expression, Lane-M: puc mix marker 8 (1116, 883, 692, 501, 404, 331, 242, 190, 147, 110, 67, 34, 26, 19) bp, Lanes 1-5: Ang-2 expression, Lanes 6-10: VEGF expression.

Meanwhile, in 46 cases of gastric cancers with Ang-2 positive expression, VEGF was coexpressed in 36 cases (78.26%), but 26 cases of gastric cancers with Ang-2 negative expression showed VEGF expression in 12 cases (46.15%). The expressions of Ang-2 and VEGF in the primary tumors were significantly correlated (P=0.0055), (Table 2).

Table 1 Expression of Ang-2 in primary gastric cancers and adjacent normal tissues detected by semi-quantitative RT-PCR

	Cases	Ang-2 (mean±SD)
Primary gastric cancers	72	0.497±0.393[a]
Adjacent normal tissues	72	0.088±0.224

a: P=0.003 *vs* adjacent normal tissues.

Table 2 Correlation between expression of Ang-2 and VEGF in 72 primary gastric cancer detected by semi-quantitative RT-PCR

Ang-2 expression (Cases)	VEGF expression (Cases)		P
	Positive	Negative	
Positive	36	10	0.0055
Negative	12	14	

Result of immunohistochemistry

Positive control included human placenta. Positive expression of Ang-2 and VEGF show brown staining in the cytoplasm of tumor or normal cells, Ang-2 was mainly expression in tumor cells (Figures 2,3).

Pathologic factors affecting expression of VEGF-C

Several pathological factors, including tumor stage, histological type, lymph node metastasis, serosal invasion and vascular involvement, were investigated to predicting expression of Ang-2 in gastric cancer. The results show that, in expression of Ang-2, there were significant difference between early stage and advanced stage (P=0.017), and significant difference between positive vascular involvement and negative vascular involvement (P=0.032). However, there was no significant difference between moderate-poor differential type and high differential type (P=0.908), no significant difference between between positive lymph node metastasis and negative lymph node metastasis (P=0.752), and no significant difference between positive serosal invasion and negative serosal invasion (P=0.764), (Table 3).

Table 3 Correlation between pathological factors and Ang-2 expression in 72 primary gastric cancer

Pathological factors	No. of cases	Ang-2 mRNA (mean±SD)	P value
Tumor stage			
Early stage	26	0.222±0.310	
Advanced stage	46	0.593±0.318	0.017
Histological type			
Moderate-Poor differential type	45	0.425±0.350	0.908
High differential type	27	0.203±0.290	
Lymph node metastasis			
Positive	48	0.413±0.346	0.752
Negative	24	0.490±0.450	
Serosal invasion			
Positive	43	0.404±0.327	0.764
Negative	29	0.334±0.459	
Vascular involvement			
Positive	46	0.640±0.335	0.032
Negative	26	0.272±0.298	

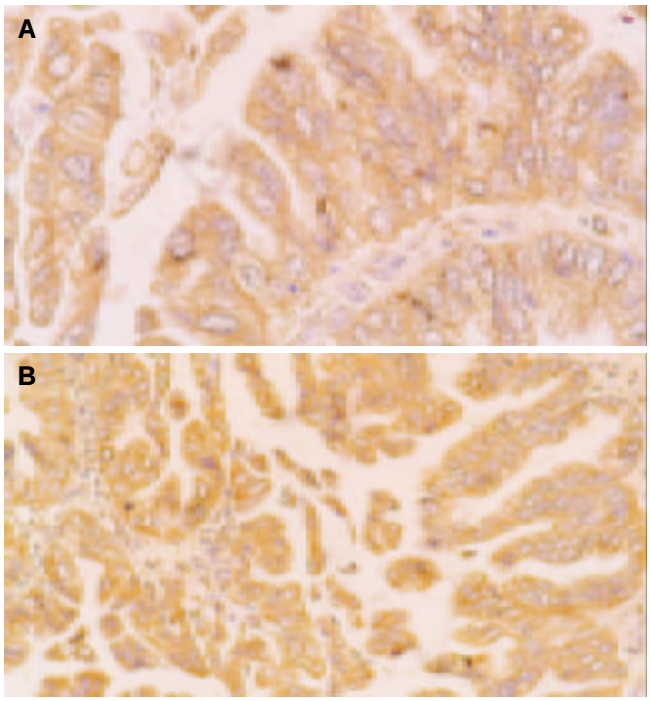

Figure 2 Expression of Ang-2 and VEGF in gastric cancer, A: Ang-2 positive expression in gastric cancer (×400), B: VEGF positive expression in gastric cancer (×400).

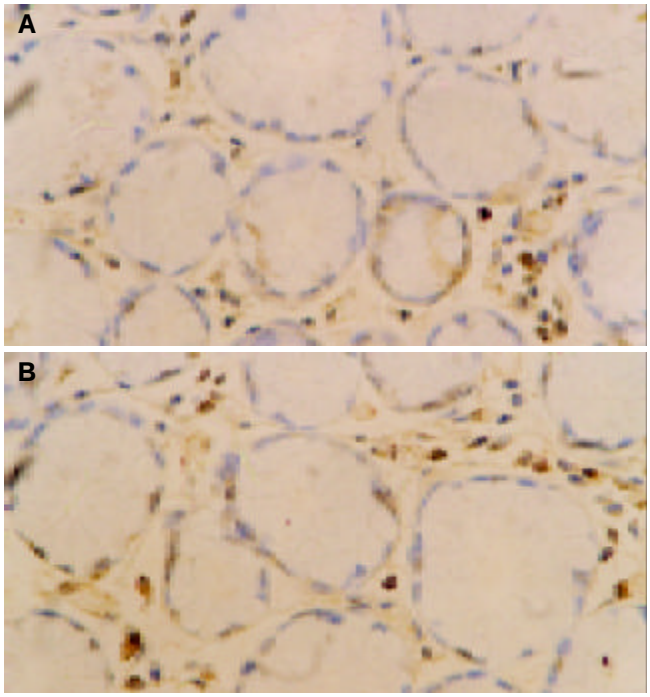

Figure 3 Expression of Ang-2 and VEGF in adjacent normal tissue, A: Ang-2 negative expression in adjacent normal tissue (×400), B: VEGF negative expression in adjacent normal tissue (×400).

DISCUSSION

Solid tumors could recruit blood vessels from the neighboring tissue by angiogenesis, and adequate blood supply could promote solid tumor growth to a clinically relevant size[5]. The ability of a tumor to induce angiogenesis could determine its rate of growth and its likelihood of metastasis[6-8]. It has been found angiogenesis is dependent on a tightly regulated balance between angiogenic promoters and inhibitors[9]. Numerous factors have been implicated in regulate angiogenesis, including growth factors and their receptors, a variety of proteases, adhesion receptors and ECM component[10,11].

Angiopoietins, novel endothelial factors, were found to be ligands for the endothelium-specific tyrosin kinase receptor Tie-2[12]. Angiopoietins (Ang) included Ang-1, Ang-2, Ang-3 and Ang-4, the best characterized were Ang-1 and Ang-2. Ang-1 and Ang-2 were soluble 70-ku factors, which consist of an amino-terminal coiled-coil domain and a carboxy-terminal fibrinogen-like domain[13,14].

Both of Ang-1 and Ang-2 could bind to the Tie-2 receptors. Ang-1 could bind to the Tie-2 receptor and activate it by inducing phosphorylation, and help to maintain and stabilize mature vessels by promoting interactions between endothelial cells and supporting cells[15-17]. Ang-2 could also bind to the Tie-2, but not activate phosphorylation. Ang-2 could block the action of Ang-1[18]. That is to say, Ang-2 was an antagonist of Ang-1 and induces the loosening of the interactions between endothelial and perivascular support cells and ECM, reducing vascular integrity and facilitating access to angiogenic induces[19,20]. Recent studies have shown that the expression pattern of Ang-2 is strongly associated with that of VEGF in the process of tumor angiogenesis, VEGF and Ang-2 seemed to play complementary and coordinated roles in the development of new blood vessels[21,22]. Angiopoietins were mainly produced by endothelial cells and pericytes, and their receptor Tie-2 was also expressed in endothelial cells and pertly in hematopoietic cells[23]. Ang-2 was selectively expressed in endothelial cells of tumors, ovaries, uterus and placenta, which are known to have extensive vascularization patterns[24-26].

The role and mechanism of Ang-2 in tumor angiogenesis have not been clarified. Some studies suggested that the production of VEGF and Ang-2 must be coordinated in development of tumor angiogenesis[27,28]. Ang-2 could produce destabilization and induce angiogenic response in the presence of VEGF, but lead to vessel regression in the absence of VEGF[13,29]. While other studies manifested that VEGF upregulates expression of Ang-1, but not Ang-2[30]. The expression of Ang-2 correlated with tumor size, but had no correlation with expression of VEGF[31]. Kuroda's results showed that upregulation of Ang-1, Ang-2 and Tie-2 is closely associated with the development of microvascular proliferation in psoriasis, and the angiopoietin-Tie-2 system might act coordinately with VEGF to promote angiogenesis[32]. Hatanaka's results suggested that tumor-produced IL-10 promotes stromal vascularization through expression of Ang-1, Ang-2 and Tie-2[33]. Angiopoietin-Tie-2 system, particularly Ang-2, played critical role in the vascularization of prostate carcinoma, breast cancer, colon cancer, astrocytoma, gastric carcinoma, *etc*[23,34-37]. Ang-2 expression was highest during the early stages of angiogenesis, perhaps reducing Tie-2 activity to allow the established vasculature to respond to angiogenic stimuli, consequently, Ang-2 expression was decreased and superseded by Ang-1 expression, perhaps activating Tie-2 and resulting in the stabilization and maturation of neovessel[13].

We studied the expression of Ang-2 in 72 primary gastric cancer and adjacent normal tissues by semi-quantitative reverse transcriptase-polymerase chain reaction (RT-PCR) and immumohisto-chemistry. The results showed that Ang-2 was mainly expression in tumor cells, and there were significantly difference in Ang-2 expression between primary tumor and adjacent normal tissue samples. The present study also clearly manifested that it was statistically correlated between Ang-2 and VEGF expression in tumors. The expression of Ang-2 was related with tumor stage and vascular involvement. Ang-2 overexpression by newly formed tumor blood vessels may lead to vessel destabilization and relative hypoxia, which could drive the release of VEGF, leading to robust angiogenesis[37].

REFERENCES

1 **Tanaka S**, Mori M, Sakamoto Y, Makuuchi M, Sugimachi K, Wands JR. Biologic significance of angiopoietin-2 expression in human hepatocellular carcinoma. *J Clin Invest* 1999; **103**: 341-345

2 **Yu Q**, Stamenkovic I. Angiopoietin-2 is implicated in the regulation of tumor angiogenesis. *Am J Pathol* 2001; **158**: 563-570

3 **Flens MJ**, Zaman GJ, van der Valk P, Izquierdo MA, Schroeijers AB, Scheffer GL, van der Groep P, de Haas M, Meijer CJ, Scheper RJ. Tissue distribution of the multidrug resistance protein. *Am J Pathol* 1996; **148**: 1237-1247

4 **Itsubo M**, Ishikawa T, Toda G, Tanaka M. Immunohistochemical study of expression and cellular localization of the multidrug resistance gene product P-glycoprotein in primary liver carcinoma. *Cancer* 1994; **73**: 298-303

5 **Folkman J**. Tumor angiogenesis. *Adv Cancer Res* 1985; **43**: 175-203

6 **Weidner N**, Semple JP, Welch WR, Folkman J. Tumor angiogenesis and metastasis–correlation in invasive breast carcinoma. *N Engl J Med* 1991; **324**: 1-8

7 **Weidner N**, Carroll PR, Flax J, Blumenfeld W, Folkman J. Tumor angiogenesis correlates with metastasis in invasive prostate carcinoma. *Am J Pathol* 1993; **143**: 401-409

8 **Macchiarini P**, Fontanini G, Hardin MJ, Squartini F, Angeletti CA. Relation of neovascularisation to metastasis of non-small-cell lung cancer. *Lancet* 1992; **340**: 145-146

9 **Mustonen T**, Alitalo K. Endothelial receptor tyrosine kinases involved in angiogenesis. *J Cell Biol* 1995; **129**: 895-898

10 **Hanahan D**, Folkman J. Patterns and emerging mechanisms of the angiogenic switch during tumorigenesis. *Cell* 1996; **86**: 353-364

11 **Risau W**. Mechanisms of angiogenesis. *Nature* 1997; **386**: 671-674

12 **Peters KG**. Vascular endothelial growth factor and the angiopoietins: working together to build a better blood vessel. *Circ Res* 1998; **83**: 342-343

13 **Maisonpierre PC**, Suri C, Jones PF, Bartunkova S, Wiegand SJ, Radziejewski C, Compton D, McClain J, Aldrich TH, Papadopoulos N, Daly TJ, Davis S, Sato TN, Yancopoulos GD. Angiopoietin-2, a natural antagonist for Tie2 that disrupts *in vivo* angiogenesis. *Science* 1997; **277**: 55-60

14 **Davis S**, Aldrich TH, Jones PF, Acheson A, Compton DL, Jain V, Ryan TE, Bruno J, Radziejewski C, Maisonpierre PC, Yancopoulos GD. Isolation of angiopoietin-1, a ligand for the TIE2 receptor, by secretion-trap expression cloning. *Cell* 1996; **87**: 1161-1169

15 **Papapetropoulos A**, Garcia-Cardena G, Dengler TJ, Maisonpierre PC, Yancopoulos GD, Sessa WC. Direct actions of angiopoietin-1 on human endothelium: evidence for network stabilization, cell survival, and interaction with other angiogenic growth factors. *Lab Invest* 1999; **79**: 213-223

16 **Witzenbichler B**, Maisonpierre PC, Jones P, Yancopoulos GD, Isner JM. Chemotactic properties of angiopoietin-1 and -2, ligands for the endothelial-specific receptor tyrosine kinase Tie2. *J Biol Chem* 1998; **273**: 18514-18521

17 **Suri C**, Jones PF, Patan S, Bartunkova S, Maisonpierre PC, Davis S, Sato TN, Yancopoulos GD. Requisite role of angiopoietin-1, a ligand for the TIE2 receptor, during embryonic angiogenesis. *Cell* 1996; **87**: 1171-1180

18 **Kampfer H**, Pfeilschifter J, Frank S. Expressional regulation of angiopoietin-1 and -2 and the tie-1 and -2 receptor tyrosine kinases during cutaneous wound healing: a comparative study of normal and impaired repair. *Lab Invest* 2001; **81**: 361-373

19 **Lauren J**, Gunji Y, Alitalo K. Is angiopoietin-2 necessary for the initiation of tumor angiogenesis? *Am J Pathol* 1998; **153**: 1333-1339

20 **Beck H**, Acker T, Wiessner C, Allegrini PR, Plate KH. Expression of angiopoietin-1, angiopoietin-2, and tie receptors after middle cerebral artery occlusion in the rat. *Am J Pathol* 2000; **157**: 1473-1483

21 **Stratmann A**, Risau W, Plate KH. Cell type-specific expression of angiopoietin-1 and angiopoietin-2 suggests a role in glioblastoma angiogenesis. *Am J Pathol* 1998; **153**: 1459-1466

22 **Holash J**, Wiegand SJ, Yancopoulos GD. New model of tumor angiogenesis: dynamic balance between vessel regression and growth mediated by angiopoietins and VEGF. *Oncogene* 1999; **18**: 5356-5362

23 **Etoh T**, Inoue H, Tanaka S, Barnard GF, Kitano S, Mori M. Angiopoietin-2 is related to tumor angiogenesis in gastric carcinoma: possible *in vivo* regulation via induction of proteases. *Cancer Res* 2001; **61**: 2145-2153

24 **Zagzag D**, Hooper A, Friedlander DR, Chan W, Holash J, Wiegand SJ, Yancopoulos GD, Grumet M. *In situ* expression of angiopoietins in astrocytomas identifies angiopoietin-2 as an early marker of tumor angiogenesis. *Exp Neurol* 1999; **159**: 391-400

25 **Wulff C**, Wilson H, Rudge JS, Wiegand SJ, Lunn SF, Fraser HM. Luteal angiogenesis: prevention and intervention by treatment with vascular endothelial growth factor trap(A40). *J Clin Endocrinol Metab* 2001; **86**: 3377-3386

26 **Otani A**, Takagi H, Oh H, Koyama S, Honda Y. Angiotensin II induces expression of the Tie2 receptor ligand, angiopoietin-2, in bovine retinal endothelial cells. *Diabetes* 2001; **50**: 867-875

27 **Takahashi Y**, Kitadai Y, Bucana CD, Cleary KR, Ellis LM. Expression of vascular endothelial growth factor and its receptor, KDR, correlates with vascularity, metastasis, and proliferation of human colon cancer. *Cancer Res* 1995; **55**: 3964-3968

28 **Woolf AS**, Yuan HT. Angiopoietin growth factors and Tie receptor tyrosine kinases in renal vascular development. *Pediatr Nephrol* 2001; **16**: 177-184

29 **Sato TN**, Tozawa Y, Deutsch U, Wolburg-Buchholz K, Fujiwara Y, Gendron-Maguire M, Gridley T, Wolburg H, Risau W, Qin Y. Distinct roles of the receptor tyrosine kinases Tie-1 and Tie-2 in blood vessel formation. *Nature* 1995; **376**: 70-74

30 **Hangai M**, Murata T, Miyawaki N, Spee C, Lim JI, He S, Hinton DR, Ryan SJ. Angiopoietin-1 upregulation by vascular endothelial growth factor in human retinal pigment epithelial cells. *Invest Ophthalmol Vis Sci* 2001; **42**: 1617-1625

31 **Holash J**, Maisonpierre PC, Compton D, Boland P, Alexander CR, Zagzag D, Yancopoulos GD, Wiegand SJ. Vessel cooption, regression, and growth in tumors mediated by angiopoietins and VEGF. *Science* 1999; **284**: 1994-1998

32 **Kuroda K**, Sapadin A, Shoji T, Fleischmajer R, Lebwohl M. Altered expression of angiopoietins and Tie2 endothelium receptor in psoriasis. *J Invest Dermatol* 2001; **116**: 713-720

33 **Hatanaka H**, Abe Y, Naruke M, Tokunaga T, Oshika Y, Kawakami T, Osada H, Nagata J, Kamochi J, Tsuchida T, Kijima H, Yamazaki H, Inoue H, Ueyama Y, Nakamura M. Significant correlation between interleukin 10 expression and vascularization through angiopoietin/TIE2 networks in non-small cell lung cance. *Clin Cancer Res* 2001; **7**: 1287-1292

34 **Wurmbach JH**, Hammerer P, Sevinc S, Huland H, Ergun S. The expression of angiopoietins and their receptor Tie-2 in human prostate carcinoma. *Anticancer Res* 2000; **20**: 5217-5220

35 **Currie MJ**, Gunningham SP, Han C, Scott PA, Robinson BA, Harris AL, Fox SB. Angiopoietin-1 is inversely related to thymidine phosphorylase expression in human breast cancer, indicating a role in vascular remodeling. *Clin Cancer Res* 2001; **7**: 918-927

36 **Ding H**, Roncari L, Wu X, Lau N, Shannon P, Nagy A, Guha A. Expression and hypoxic regulation of angiopoietins in human astrocytomas. *Neuro Oncol* 2001; **3**: 1-10

37 **Ahmad SA**, Liu W, Jung YD, Fan F, Wilson M, Reinmuth N, Shaheen RM, Bucana CD, Ellis LM. The effects of angiopoietin-1 and –2 on tumor growth and angiogensis in human colon cancer. *Cancer Res* 2001; **61**: 1255-1259

Edited by Xia HHX and Wang XL **Proofread by** Xu FM